Prodrug approaches to reduce treprostinil toxicity

Christina Picken

A thesis presented for the degree of

Doctor of Philosophy

University College London

UCL Institute of Cardiovascular Science

5 University Street, Rayne Building, London WC1E 6JF, United Kingdom

September 2018

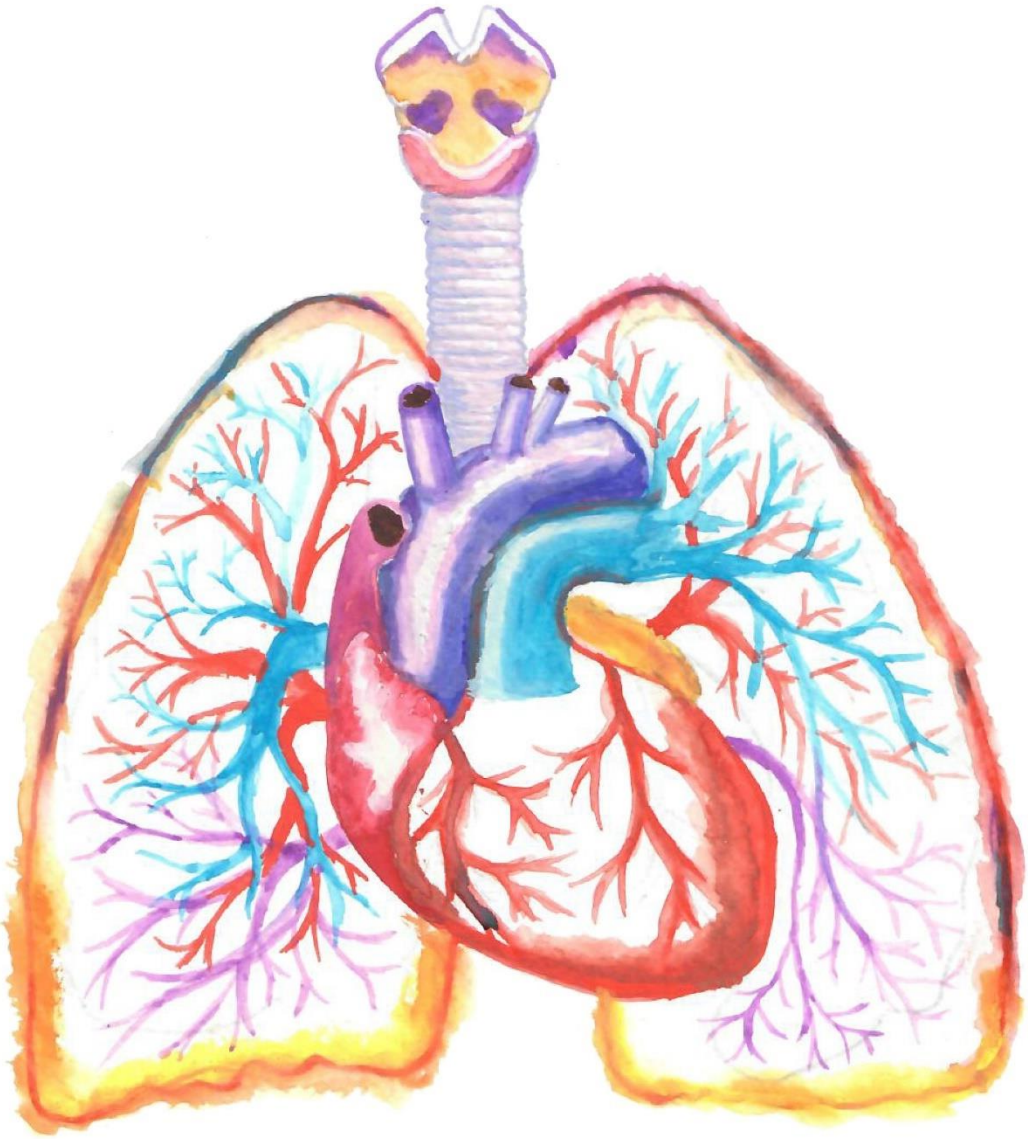

Plagarism Statement

This thesis describes work conducted at UCL Institute of Cardiovascular Science and School of Pharmacy between 03Oct14 and 28Sept18 under the supervision of Profs Lucie Clapp and Steve Brocchini. I certify that the research described is original and that any parts that were conducted as part of a collaboration are clearly indicated.

Christina Picken

_____ _____

(Signed) (Dated)

Acknowledgements

I am grateful to my supervisors, Profs Lucie Clapp and Steve Brocchini, for providing me the opportunity to work on such an applied and diverse project. Their guidance and support was crucial to the journey this work has taken. The passion they exude for their respective subjects has been a source of inspiration and I have learnt so much from being under their guidance. The freedom they permitted me during my project allowed me to carve my own path, learn from my mistakes and gain confidence in my work.

The project would not have been possible without the financial support of the BBSRC as well as United Therapeutics who not only part-funded the project and donated their compounds, but also offered the opportunity to gain experience in their labs during an internship. I wish to thank Prakash Sista for taking responsibility of my project and Hitesh Batra, Sudersan and Sri Tamala for their training, guidance and mentorship through out my stay. Their flair for chemistry was truly admirable and they taught me that with good lab planning and a positive team spirit, each reaction offered something to be learnt from.

I have been very fortunate to have had additional guidance from Peter Laing who as well as giving such a broad context to my fields of working, offered ideas, encouragement and endless positivity to my results. In addition I was also privelidged to have received a “brief history of treprostinil” from Brendan Whittle which gave precontext to my project setting. His enthusiasm for my project was most refreshing particularly when the project took unexpected directions.

My project took a welcomed but unplanned detour through more clinical aspects of treprostinil therapy and the work conducted as part of this would not have been possible without the assistance and patience of Mohammad Eddama, Costas Fragkos and Gerry Cochlan.

Working primarily in the School of Pharmacy, I received encouragement and help from many of the staff and colleagues that haunt it’s corridors. However, I am particularly grateful to John Malkinson for his advice and assistance in answering my many queries in the peptide synthesis work. Additional thanks go to Richard Angell for being my go-to organic chemistry guru, Emmanuel Samuel for his endless patience in helping me with the LCMS/MS, as well as Colin James for his assistance with the NMR.

The past four years would not have been worth it were it not for the friends I have made and memeories shared. I will forever be grateful for the mental coaching Jollie, Shen and Rijan were tasked with in introducing me to cell culture, as well as their patience as I bored them with curly arrow mechanisms each Friday morning. I owe many happy memories of this project to the Brocchini gang who are a continual source of genuine support, inspiration and hilarity. Even during the hardest parts of the past four years their ability to listen, break into song mid-sentence and get sucked into an off-topic debate, provided each day with a dose of necessary silliness.

Having the support and understanding of my family allowed me to give as much as I did to this project. So thank you to; Mumsy and Dadwa for putting up with my absentmindedness,

listening to my unintelligible rants, and providing me with a stream of Picken antics; Luigi for being my second brain, decision maker and sanity restorer (we are so sisters); and Bumper, who has followed my journey like a number one fan, cheered me on at every step and given much valued advice and insight.

Lastly, I owe any remaining sanity I possess to the Quandry of Quokkas; Laurie, Dave, and Lizzie. Your friendship, advice, thoughtfulness and outrageous dedication to a joke (and lil' Laurie) have made coming home each day a complete delight and I cannot thank you enough.

Research Dissemination

Publications

L. Shen, C. Picken, K. Von Kessler, P. Sista, L. H. Clapp., A Comparison Of The Pharmacological Profile Of Beraprost-315d With Esuberaprost And Beraprost: Role Of The Prostacyclin (IP) Receptor, PPARβ And Nitric Oxide In Rat Distal Pulmonary Arteries. American Thoracic Society 2016 International Conference, San Francisco, CA, USA, 2016.

C. Picken, M. Eddama, C. Fragkos, G. Coghlan, L. H. Clapp., Adverse events of prostacyclin mimetics in pulmonary arterial hypertension: A systematic review and meta-analysis. J. Clin. Med. 2019 (Under 2nd phase of review).

Presentations

“Meta-analysis of adverse events in prostacyclin mimetic therapy” – National Pulmonary Hypertension meeting – London, UK - 2017

“Novel N-acylsulfonamide treprostinil prodrug” - GP2A-JFB Medicinal Chemistry – Caen, France – 2018

“Oligoacetal-treprostinil for the localised treatment of pulmonary arterial hypertension” - EUCheMS chemical congress – Liverpool, UK – 2018

Poster Presentations

“Methods for the Conjugation of Treprostinil” – RSC Biological and Medicinal Chemistry Symposium – Cambridge, UK – 2016

“Targeting Polymer-Drug Conjugates for the Treatment of Pulmonary Arterial Hypertension” - ULLA summer school – Leuven, Belgium – 2017

“Polyacetal-treprostinil for the localised treatment of pulmonary arterial hypertension” – UK & Ireland controlled Release society symposium – Belfast, NI – 2018

“Novel approaches to target prostacyclin therapy to the lung” – UCL Graduate School – London, UK - 2018

Public Engagement and Further Outreach

“Destination known” – 3-minute thesis – SLMS, UCL – 2016

“Science for transformation” – Stall at Science4U outreach event – 2017

“Science for Discovery” – Stall at Science2U outreach event – 2018

“Helping PAH therapies to target inflammation” - 3-Minute Thesis Competition – UCL – 2018

“Chain Reactions” talk – Pint of Science Festival – London, UK – 2018

“Designer Slime” stall – The Green Man festival – 2018

“Novel approaches to target prostacyclin therapy to the lung” - Graduate School Research Poster Prize winner – 2018

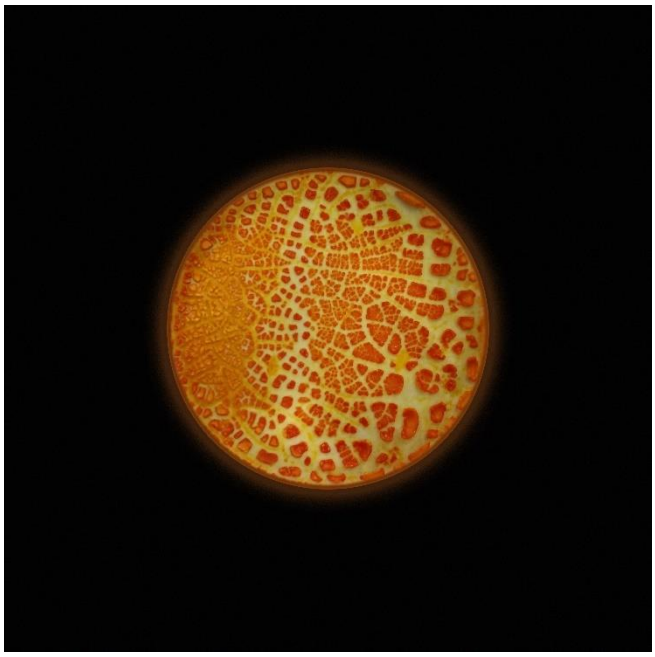

“Star Treatment” research photo entered into UCL Research images as Art competition – 2018

“Star Treatment” research photo featured on cover of Pharm^2 Magazine – 2018

Abstract

Pulmonary arterial hypertension is a chronic inflammatory condition of the peripheral pulmonary vessels which is thought to affect up to 52 in every million people. Vasoconstriction, proliferation and vascular remodelling mechanisms dominate which narrow and occlude pulmonary vessels, ultimately leading to right ventricular heart failure. Lung transplantation with all its associated complications remains the only cure. Prostacyclin mimetics are used as long-term therapy to slow disease progression and manage symptoms. Treprostinil is a clinically registered prostacyclin mimetic which is available in parenteral, oral and inhaled dosage forms, although the parenteral form provides the best treatment. Treprostinil shows some efficacy for PAH treatment, but is dose limited by adverse events that are a major burden to patients.

The aims of the project were to develop a prodrug strategy to increase the maximum tolerated dose of treprostinil. A meta-analysis was first conducted using clinical data for prostacyclin and treprostinil treatments to determine which adverse events caused the greatest impact on the dose of treprostinil that could be given. The meta-analysis was also designed to understand the likely mechanistic causes for the most limiting adverse events. The dose limiting adverse event causing the greatest limitation to dosing is the pain at the site of administration that is associated with subcutaneously administered treprostinil. Prostanoid EP2 and DP1 receptors for which treprostinil has potent affinity are present in the vasculature in the skin which gives rise to the swelling, flushing and pain upon exposure to high concentrations of treprostinil present in subcutaneous infusion

Although polymer-treprostinil prodrugs and their constituent components were examined, treprostinil N-acyl sulfonamide was first considered as a potential prodrug candidate. The N-acyl sulfonamide was evaluated because it has the potential to undergo subsequent enzymatic degradation in the liver to release active treprostinil. Although the *in vitro* activity of the prodrug treprostinil N-acyl sulfonamide was found to be less than treprostinil, there was concern from the industry collaborators about the stability of this prodrug version of treprostinil.

Since treprostinil is as an agonist, treprostinil N-acyl sulfonamide was also considered for a polyvalent strategy. Unfortunately linking treprostinil to a polymer without undue loss of activity did not appear to be feasible. So treprostinil was used as a monomer to be conjugated within a degradable polyacetal mainchain. Water-soluble polyacetals undergo accelerated degradation at mildly acidic pH values which may be present in PAH diseased tissue. Treprostinil was conjugated within the mainchain using divinyl ether ethylene glycol and poly(ethylene glycol) as co-monomers. Treprostinil oligoacetal was obtained and was found to degrade in acidic conditions. The use of treprostinil as a co-monomer for polyacetal synthesis requires further optimisation because the two secondary hydroxyl groups in treprostinil may not be reactive enough and better masking of the treprostinil carboxylic acid moiety during storage is required.

Developing a polymer-pendent drug conjugate strategy for the targeted release of treprostinil was also investigated. A targeting moiety, CAR peptide, was synthesised and investigated for the extent of specific localisation in disease cells over healthy cells. A treprostinil release linker based on tryptase which is an enzyme present in the PAH diseased lung was also examined in parallel. A method to prepare the tryptase substrate prodrug derivative of treprostinil on-resin was pursued. The method outlined shows promise in forming the treprostinil linker derivatives via a scalable route. It is envisaged that such treprostinil-linker adducts could be used in a polymeric conjugate or potentially in an antibody-drug conjugate.

Methods to derivatise treprostinil were identified highlighting routes that could be pursued further. Polymeric-derivatisation of treprostinil may be a promising strategy to overcome current existing limitations with prostacyclin mimetic therapies. It is hoped that the progress described in this thesis will aid and guide future investigations in polymeric derivatives of treprostinil.

Impact Statement

Adverse events caused by off-target effects limit the tolerability and efficacy of treatments for many diseases. For chronic, progressive diseases such as pulmonary arterial hypertension (PAH), the negative impact adverse effects from treatment on quality of life and not slowing disease progression can be a considerable burden for patients and their caregivers.

This CASE studentship funded by the BBSRC and Lung Biotechnology Ltd. (a subsidiary of United Therapeutics) focuses on improving the tolerability of the gold standard drug class for the treatment of PAH. Clinical data was consulted to understand the dose limiting adverse events associated with different therapies which were then interpreted in the context of different pharmacological behaviours. The understanding gained provided direction to develop a prodrug of treprostinil to reduce activity in healthy tissues while increasing drug exposure in the PAH lung. Much of the research described in this thesis focused on using polymeric prodrug strategies to improve the toxicity profile of treprostinil.

The impact of the work presented in this thesis is that the increased understanding of methods to chemically modify treprostinil as a prodrug to treat PAH can also be applied to related prostacylin mimetics. Furthermore, the approach for design and the concepts that were considered could be applied for therapies that are not inherently toxic but exert unwanted biological activity in healthy tissues which limits therapeutic efficacy. The intended net impact to optimise the effect of each dose while limiting adverse events could potentially reduce cost of treatment for chronic diseases such as PAH.

Contents

Figures

Tables

Schemes

Abbreviations

ACA	7-aminocoumarin-4-acetic acid
ADC-	antibody-drug-conjugate
AE	adverse event
Ahx	amino hexanoic acid
API	active pharmaceutical ingredient
β-NADP	beta-nicotinamide adenine dinucleotide phosphate disodium
BSA	bovine serum albumin
BTCA	benzyl-2,2,2-trichloroacetimidate
cAMP	cyclic adenosine monophosphate
CAR	CARSKNKDC peptide derivatives
$CHCl_3$	chloroform
$CDCl_3$	deuterated chloroform
CDI	1,1-carbonyl diimidazole
d^6-DMSO	deuterated dimethylsulfoxide
DBF	dibenzofulvene
DBU	1,8-diazabicyclo[5.4.0]-undec-7-ene
DCC	dicyclohexylcarbodiimide
DCE	dichloroethane
DCM	dichloromethane
DCU	1,3-Dicyclohexyl urea
Dde	N-(1-(4,4-dimethyl-2,6-dioxocyclohexylidene)ethyl)
DIPEA	diisopropylethyl amine
DMAP	4-(dimethylamino) pyridine
DMB	2,4-dimethyoxybenzaldehyde
DMF	dimethyl formamide
EDTA	Ethylenediaminetetraacetic acid
EA	ethyl acetate
EC	endothelial cell
ECM	extracellular matrix

EDCI	*N*-(3-dimethylaminopropyl)-*N*'-ethylcarbodiimide hydrochloride
EPR	enhanced permeation
ERA	endothelin receptor antagonists
FBS	fetal bovine serum
Fmoc	fluorenylmethyloxycarbonyl protecting group
FMPB	4-(4-Formyl-3-methoxyphenoxy)butyryl
FITC	fluorescein isothiocyanate
FTIR	fourier transform infrared
GPC	gel permeation chromatography
HATU	1-[Bis(dimethylamino)methylene]-1*H*-1,2,3-triazolo[4,5-b]pyridinium 3-oxid hexafluorophosphate
HBTU	*O*-(Benzotriazol-1-yl)-*N,N,N',N'*-tetramethyluronium hexafluorophosphate
HCl	hydrochloric acid
HEK	hamster embryonic kidney
HFIP	1,1,1,3,3,3-hexafluoropropanol
HOBt	1-hydroxybenzotriazole hydrate
HUVEC	human umbilical vascular endothelial cells
IPAH	idiopathic pulmonary arterial hypertension
IV	intravenous
MC	mast cell
MEM	minimum essential media
MeOD	deuterated methanol
MeOH	methanol
$MgCl_2$	magnesium chloride
MgO	magnesium oxide
MMP	matrix metalloproteases
MRM	multiple reaction monitoring
MTD	maximum tolerated dose
NADPH	nicotinamide adenine dinucleotide phosphate (reduced)
NEt_3	triethylamine

NHS	N-hydroxysuccimide
NMR	nuclear magnetic resonance
NO	nitric oxide
NYHA	New York Heart Association
OR	odds ratio
PAH	pulmonary arterial hypertension
PAP	pulmonary arterial pressure
*p*ABA	*para*-aminobenzyl alcohol
Pbf	2,2,4,6,7-pentamethyldihydrobenzofuran-5-sulfonyl
PBS	sodium phosphate buffer solution
PDC	polymer-drug conjugate
PDE-5i	phosphodiesterase inhibitors
PDI	polydispersity index
PEG	poly(ethylene glycol)
PenStrep	penicillin streptomycin
PGI_2	prostacyclin
PM	prostacyclin mimetic
PMA	phosphomolybdic acid solution
PMMA	polymethylmethacrylate
PPBS	potassium phosphate buffer solution
*p*TSA	*para*-toluene sulfonic acid
RBF	round bottom flask
RI	refractive index
RT	room temperature
SC	subcutaneous
SPE	solid phase extraction
SPPS	solid phase peptide synthesis
STAB	sodium triacetoxyborohydride
TBDMSCl	tert-butyl dimethylsilyl chloride
TEGDVE	triethylene glycol divinyl ether

TFA	trifluoroacetic acid
THF	tetrahydrofuran
TIS	triisopropyl silane
TLC	thin layer chromatography
T_{max}	Time to maximum concentration
TMOF	trimethylorthformate
TMS-OTf	trimethylsilyl trifluoromethanesulfonate
TNF-α	tumour necrosis factor alpha
TosCl-PNBP	4-toluene sulfonyl chloride - p-nitrobenzylpyridine
TRE-S	treprostinil N-acyl sulfonamide
UT	United Therapeutics Corp
PMA	phosphomolybdic acid
UV	ultraviolet radiation
VSMC	vascular smooth muscle cell
WHO	world health organisation
6MWD	6-minute walk distance

Chapter 1. Introduction

1.1 Pulmonary arterial hypertension

Pulmonary arterial hypertension is a rare but fatal inflammatory disease estimated to affect 10 million people worldwide. It is clinically defined as a sustained pulmonary arterial pressure (PAP) >25 mm Hg at rest, with a mean pulmonary-capillary wedge pressure and left ventricular end-diastolic pressure of less than 15 mmHg.[1] Pulmonary arterial hypertension (PAH) forms Group 1 of the classification system defined and updated at the World Pulmonary Hypertension Symposium, 2013.[2] Group 1 PAH includes idiopathic (IPAH), heritable, toxin/drug-induced PAH and PAH secondary to diseases such as connective tissue disease, congenital heart disease and human immunodeficiency virus (HIV) as well as persistent PAH of new-born infants. Regardless of the underlying cause, all PAH types are characterised by vasoconstriction as well as vascular smooth muscle cell (VSMC), endothelial cell (EC) and fibroblast proliferation causing remodelling of the distal pulmonary arteries.[3]

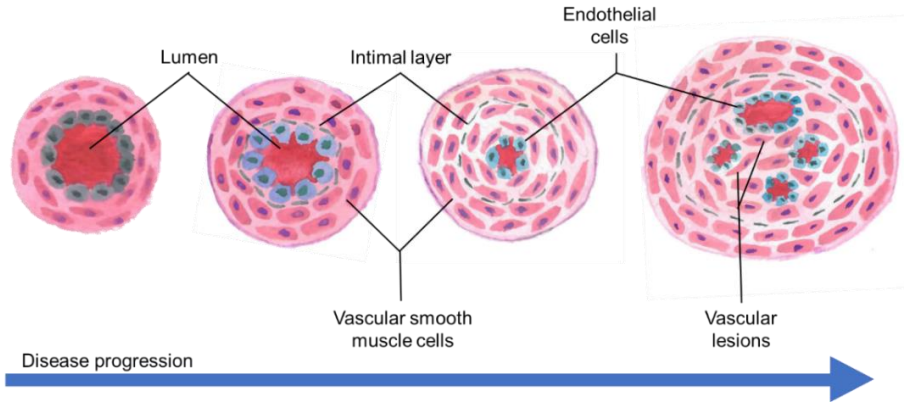

Figure 1-1. Change in vascular smooth muscle cells during progression of pulmonary arterial hypertension. (i) The endothelial cells become dysregulated and small pulmonary arterials become muscularised; (ii). Large pulmonary arteries become muscularised (medial hypertrophy) and the vessel contracts, narrowing the lumen; (iii) Smooth muscle cells proliferate and infiltrate the intimal layer (neointimal formation) narrowing the lumen further, and resulting in occlusion of vessels; (iv) Severe remodelling of arteries forming plexiform lesions within the vessels.[4]

Pulmonary arterial hypertension effects females disproportionately at a ratio of 2:1 compared to males, although the prognosis if often better for women.[5] Mean age of patients with PAH was 36 ±15 for the National institute of health (NIH) registry between 1981 -85.[6] The mean age has increased to 50 years in the years since 1993, as PAH in elderly patients is better recognised.

In the initial stages of PAH, patients are often asymptomatic and only as the disease progresses do patients present with breathlessness and fatigue when performing everyday tasks (e.g. climbing the stairs). Owing to its rarity, the time taken from initial contact with a general practitioner to referral for PAH investigation is often over 3 years.[7] The diagnostic procedure for PAH involves catheterisation of the pulmonary artery to calculate pulmonary

arterial pressure (PAP) and vascular resistance (PVR). As the disease progresses, the vessels become narrower, more fibrotic and are under a higher pressure with higher resistance (**Figure 1-1**).[8] The increased pressure puts strain on the right ventricle of the heart which becomes less elastic and more fibrotic in response. As a result of these effects on the heart, PAH patients ultimately die of right ventricular heart failure or sudden cardiac death.[9]

As well as haemodynamic parameters, the severity of disease is determined using functional read outs, such as 6-minute walk test and patient-reported outcomes such as Borg-dyspnea score. Disease severity is stratified by the World Health Organisation/New York Heart Association (WHO/NYHA) classification increasing from class I to IV which is used to guide treatment strategies. NYHA class uses the symptoms experienced by patients to classify heart function. Class I, patient experiences no limiting symptoms during physical activity; Class II, patients experience some limitations when performing physical activities; Class III, patients experience marked limitations during even normal activities but are comfortable at rest; Class IV, patients experience discomfort even at rest. Disease severity is measured and assessed through the clinical measure 6-minute walk distance (6MWD). The 6MWD test is performed by calculating distance walked on a flat surface in 6 minutes. As well as at initial diagnosis, these methods allow for less invasive monitoring of patient health and effects of lifestyle and therapeutic interventions.

1.1.1 Pathophysiology of PAH

Endothelial changes are the earliest understood step to initiate PAH[10], and although the underlying mechanism in IPAH is unknown, there is evidence that mitochondrial malfunction could play a role.[11] In all PAH cases, endothelial damage caused by a variety of factors, including sheer stress, genetic factors and hypoxia are considered to be initiators of the disease. In healthy tissues, the endothelial cell layer lining small vessels is known to regulate vascular function. In PAH tissue, however, their phenotype changes and cells release growth factors and cytokines. The dysfunction facilitates vasoconstriction, thrombosis and inflammatory cell infiltration.[12] VSMCs become proliferative and anti-apoptotic which leads to their infiltration through the medial layer and into the intima.[13] Alterations in the phenotype of endothelial and VSM cells, where thromboxane and endothelin are released causes constriction of the vessel and a characteristic increase in PAP because of a high pulmonary vascular resistance occurs.[1] In response to the inflammatory environment created, angiogenesis is stimulated.[14] However, vessel growth occurs in a disordered fashion which leads to vascular remodelling and the formation of plexiform lesions.[15] This further disrupts the vessel haemodynamics and eventually leads to vascular pruning where the distal pulmonary arteries become completely occluded and lose function and/or undergo necrosis.[16] This process puts more strain on the right ventricle of the heart causing hyperplasia, hypertrophy and fibrosis of cardiac muscle cells, eventually leading to right heart failure and ultimately death.[17]

1.1.2 Extracellular matrix remodelling (ECM) and associated enzymatic changes

Within PAH tissue, the dysregulation of growth factors, enzymes, cell surface receptors, nuclear receptors and chemokines have been reported.[16,18] Cell proliferation is promoted via changes to the extracellular matrix (ECM) brought about in part by matrix metalloproteases (MMPs), elastases and proteases. Specifically, MMP 2 and 9 are upregulated in PAH, which drives proliferation by releasing extracellular matrix (ECM) proteases. During remodelling, serine elastase activity is also increased which degrades the ECM,[19] as well as heparinase, responsible for the cleavage of heparan sulfate chains on the cell surface.[20] As a result of the mast cell accumulation and activation during chronic inflammation,[21] tryptase and chymase are also released into the surrounding tissue.[22,23]

Mast cells are present at varying densities throughout the body but can migrate and accumulate in sites of chronic inflammation.[24] Their pathogenic roles include immune modulation, pro-inflammation, pro-fibrotic and surprisingly anti-inflammation. Mast cells are granulated, and each granule contains a cocktail of enzymes including tryptase and chymase, histamine, cytokines such as TNF-α, vasoconstrictors including thromboxane and prostaglandin D_2, platelet activating factors and reactive oxygen species. Whereas many inflammatory cells release or produce most of the contents of a mast cell, tryptase and chymase are entirely specific to mast cells. Furthermore, there are two types of mast cells (MCs); in addition to the other contents listed, MC_T are found only in the lung, and contain only tryptase (Hence, T) whereas MC_{TC} which are associated with connective tissue, contain tryptase and chymase (hence, TC). Therefore, wherever chymase is present, tryptase is there too, but not vice versa. Upon activation of the mast cells, the granule contents are released into the surrounding tissue.

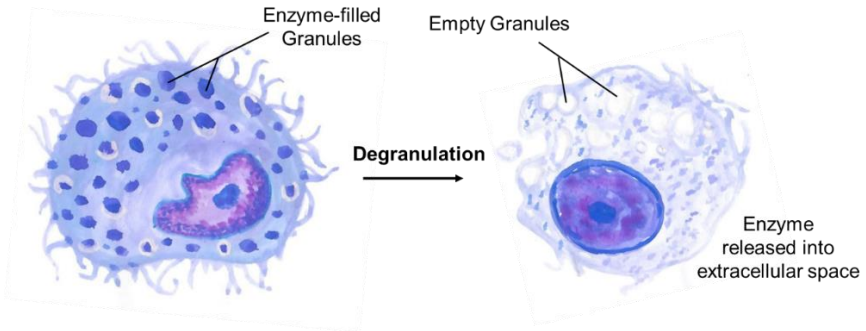

Figure 1-2. Mast cell degranulation. Enzymes are stored within granules in the mast cells. Upon stimulation, the mast cell undergoes degranulation, releasing the enzymes into the extracellular compartment.

The lung tissue contains two types of mast cells; MC_T is found in the lung parenchyma which is rich in mast cells; and MC_{TC} are found surrounding the pulmonary blood vessels, associated with connective tissues.[25] Mast cells populations have been shown to increase in fibrosis, notably chronic obstructive pulmonary disease and idiopathic pulmonary fibrosis (IPF). In IPF

patients, mast cell numbers have been reported to increase,[26] particularly in the lung parenchyma and in fibrotic bundles compared to healthy tissues.[27] Tryptase-positive mast cells in IPF have also been detected in their degranulated state.[26] It should be noted however, that another study has shown an increase in mast cell density but not in total mast cell number.[28]

PAH is an inflammatory, fibrotic disease[29] so it is highly possible that MCs are involved with the progression of PAH. Increased chymase has been detected in vascular lesions with intimal fibrosis, suggesting a role in tissue remodelling in PAH.[30,31]

Because PAH is such a complex disease, a variety of animal models are used to replicate the different features of the disease. However these models indicate different levels of MC involvement.[30] None-the-less, in human tissue, chymase- and tryptase- positive mast cells have been shown to accumulate in the lung parenchyma and the adventitia of small blood vessels.[32] Furthermore, in hypoxic conditions, MCs were implicated in the muscularisation of peripheral vessel[33], and activated perivascular MCs were upregulated in the tissues of IPAH.[34] Price et al. found that the MC increases are found in both IPAH as well as PAH associated with coronary heart disease.[35]

An increase in chymase and mast cells was found in a rat monocrotaline model of PAH with an aorto-cavel shunt. Tissue remodelling was attenuated and haemodynamic improvements were observed when the rats were treated with mast cells inhibitors.[36] Mast cell accumulation was also associated with a supra-coronic aortic band model of left heart disease.[37,38] The movement of MCs was investigated in the days after hypoxia exposure. Accumulation began in the pre-alveloar regions after 4 days which migrated to the pulmonary vasculature with further hypoxia exposure.[39] Hypoxia-induced mast cell accumulation has been reported by others, which increases the chymase and trypase production.[22,34,40]

Once released the contents of the mast cell granules have been shown to play an important role in initiating hypoxic pulmonary vascular modelling.[31,41] It is well understood that a number of the inflammatory markers released from MC granules are implicated in remodelling pathways.[42] Tryptase has been shown to split collagen I which stimulates the proliferation of smooth muscle cells, and thus likely to contribute to PAH pathobiology.[43]

The role of mast cells in fibrosis and PAH is still not elucidated and is a topic of debate,[44] however the accumulation of mast cells within the PAH tissue is evidenced. A role of enzymes in chronic inflammation and PAH is established which changes the phenotype of cells.[4,16,42] The extracellular matrix is degraded which stimulates pro-inflammatory, pro-thrombotic, proliferative and fibrotic pathways, ultimately driving remodelling and the progression of PAH.[42]

1.1.3 The cancer hypothesis in PAH

Proliferative and pro-inflammatory mechanisms, glycolytic respiration and tissue remodelling are all characteristic features of cancer. The parallel between PAH and cancer in relation to the pathways implicated and pathophysiological features has been highlighted.[45] The hallmarks of cancer were highlighted and described by Hanahan and Weinberg[46] and have

since been used to describe many facets of PAH.[45] Although treatment strategies differ between cancer and PAH, the delivery and targeting of therapies may share similar approaches. A downside to PAH treatments is that as an orphan disease, fewer attempts to treat and understand PAH have been made compared to cancer. On the other hand, the similarities between the diseases may suggest that PAH treatments can benefit from the research and lessons learnt in the cancer field.

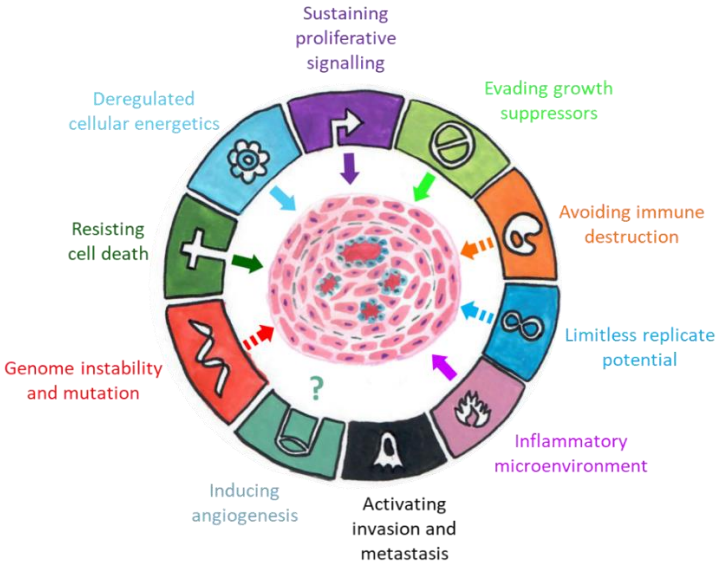

Figure 1-3. Hallmarks of cancer, originally described by Hanahan and Weinberg[46] and later compared to PAH by Bouchater et al., from which this is adapted.[45] Half of the cancer features overlap with PAH and only one the activation and invasion of metastatis is not seen in PAH. The bold arrow indicates a high degree of similarity between cancer and PAH and a dashed arrow indicates a low similarity.

Similar to the rapid cell growth characteristic of cancer, as PAH smooth muscle cells proliferate rapidly[47] and gas exchange becomes less efficient, oxygen is used up faster than it can be provided, particularly in the fibrotic regions.[48] Under stimulation by growth factors and pro-proliferative agents, cells switch to an anaerobic glycolytic pathway for respiration and thus survival.[16] Employing glucose as the energy source, cells can continue proliferating and developing, producing lactate as a by-product.[49] In areas of poor vascularisation and inefficient gas exchange, the lactic acid builds up, in a process known as lactic acidosis. The high concentration of lactic acid causes an increase in acidity which can reach pH 6.0.[50]

1.1.4 PAH-Implicated pathways

The complexity of PAH combined with an unknown underlying cause means that the main implicated pathways are multiple and much debated.[4,29,51] It is well understood that an imbalance in vasomediators resulting in increased vasoconstrictors (thromboxane, endothelin) and decreased vasodilators (nitric oxide, prostacyclin) is involved in the disease progression.

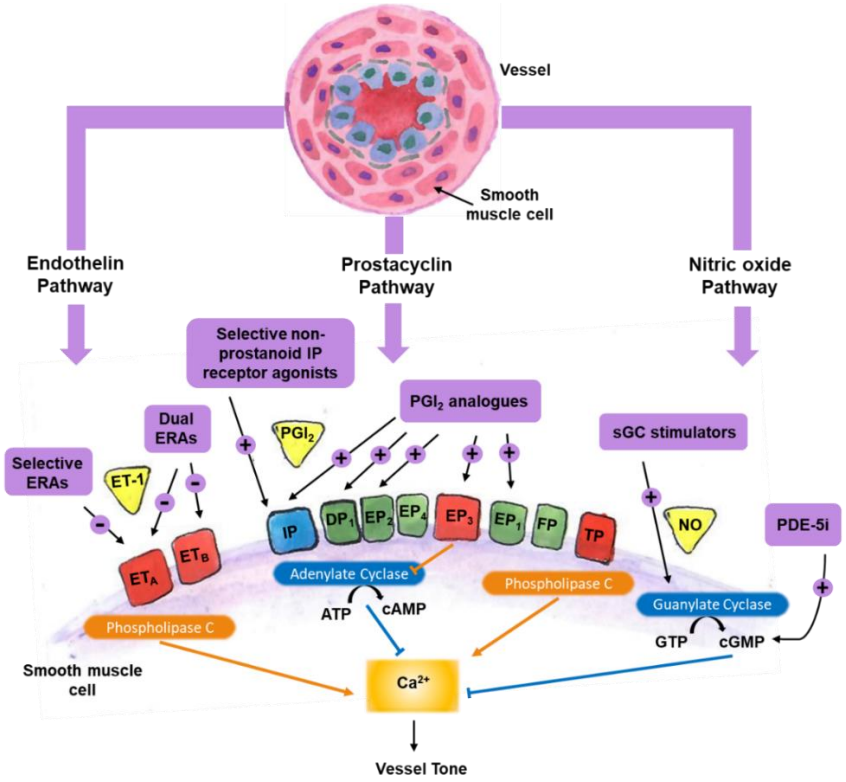

Figure 1-4. The endothelin, nitric oxide (NO) and prostacyclin pathways involved in the pulmonary arterial hypertension in smooth muscle cells and their targeting for therapeutic benefit. The yellow triangles indicate the endogenous vasomediators. Endothelin-1 (ET-1) is an agonist of the ET_A and ET_B receptors which activates phospholipase C and increases intracellular calcium. An increase in calcium leads to a constriction of the vessel. Inhibiting the endothelin pathway can be achieved by use of selective and dual endothelin receptor antagonists (ERAs) Phospholipase C can also be activated by agonism of the EP_1, FP and thromboxane (TP) receptors. Prostacyclin (PGI_2) and selective agonists are active at the prostacyclin (IP) receptor. Prostacyclin analogues also have affinity for the IP receptor as well as other prostanoid receptors; The agonism of IP, DP_1 and EP_2 receptors activates adenylate cyclase which converts adenosine triphosphate (ATP) to cyclic adenosine monophosphate (cAMP). An increase in cAMP inhibits the mobilization of calcium (Ca^{2+}) causing a vasodilatory response. Some prostacyclin (PGI_2) analogues have affinity at the EP_3 receptor which inhibits the activation of adenylate cyclase, resulting in the increased mobilization of calcium. The EP_1 receptor can be activated by prostacyclin analogues causing a vasoconstrictive effect. NO activates guanylate cyclase which converts guanosine triphosphate (GTP) into cyclic guanosine monophosphate (cGMP) which inhibits the mobilization of calcium, resulting in vasodilation. Guanylate cyclase can also be activated by soluble guanylate cyclase (sGC) stimulators or the removal of cGMP can be inhibited by phosphodiesterase-5 inhibitors (PDE-5i) which extends the inhibition of calcium mobilization. Orange lines indicate vasoconstrictive effects and blue lines indicate vasodilating effects. Image adapted from Lang and Gaine.[52]

Endothelin Pathway

Endothelin-1 is a 21-amino acid peptide produced in endothelial (and smooth muscle) cells which activates its two native receptors (ET_A and ET_B) to activate phospholipid C which mobilises calcium. An increase in calcium results in heightened proliferative and vasoconstrictive effects.[53] During PAH, production of endothelin-1 is increased leading to disease progression.[54] Therefore, the therapeutic use of endothelin receptor antagonists (ERAs) was designed to block the actions of endothelin by competitively binding to its receptors which prevent the downstream effects and slow disease progression. Clinically,

bosentan, macitentan, and ambrisentan are endothelin antagonists used in the treatment of PAH.

Nitric Oxide (NO)

Within healthy tissues, a whole host of vasoactive mediators implicated in a variety of mechanistic pathways control the activity of the vasculature. Within PAH, vasodilators NO and prostacyclin are down-regulated which allows for vasoconstrictive mechanisms, involving endothelin and thromboxane to dominate. NO is synthesised in endothelial cells by the conversion of L-arginine to L-citrulline by endothelial nitric oxide synthase enzyme. NO acts locally on smooth muscle cells and platelets to activate guanylate cyclase which causes an increase in cyclic guanosine monophosphate (cGMP) which prevents calcium being mobilised and ultimately results in antiproliferative, anti-platelet and vasorelaxation effects. An increase in arginase is also thought to be responsible for the decrease in NO.[55,56]

Phosphodiesterase pathway

The phosphodiesterase-5 (PDE-5) enzyme is responsible for the inactivation of cyclic guanosine monophosphate (cGMP), the compound responsible for activating vaso-protective mechanisms, including vasodilation and antiproliferative.[57] Upregulated in PAH, driving disease progression by reducing the downstream effects of NO which in itself activates guanylate cyclase to produce cGMP. The action of PDE-5 is a therapeutic target to inhibit using PDE-5 inhibitors (PDE-5is). Inhibitors such as sildenafil and tadalafil have been shown to improve functional class, the 6-minute walk distance (6MWD) and decrease pulmonary arterial pressure.[58,59] PDE-5 inhibitors are often used in combination without classes of PAH treatment.[60]

Prostacyclin

Prostacyclin (PGI_2) (**1)**, is a vasoactive compound first identified by Sir John Vane for which he was later awarded the Nobel Prize. Prostacyclin is derived from arachidonic acid metabolism in the endothelial and smooth muscle cells of vascular tissue by the action of cyclooxygenase-2 and PGI_2 synthase enzymes. PGI_2 is the natural ligand for the G-protein coupled IP receptor, found on the surface of platelets, endothelial cells (ECs) and vascular smooth muscle cells (VSMCs). The structure of prostacyclin contains a vinyl ether which is susceptible to acid-mediated hydrolysis converting it to a less stable compound in less than 3 minutes in blood. Owing to its chemical instability, PGI_2 cannot be stored so can only exert its action locally.[61] Upon binding to the IP receptor, the G_s protein becomes activated and initiates an intracellular cascade of reactions resulting in elevated concentrations of intracellular cyclic adenosine triphosphate (cAMP). Increased concentration of cAMP causes the activation of protein kinase A which decreases intracellular calcium ions, leading to vasodilation as well as the inhibition of VSMC proliferation and platelet aggregation.[62]

In healthy patients, the relative concentrations of PGI_2, and resulting outcomes, are in balance with other members of the prostaglandin family which maintain optimal vascular tone.

However, in PAH patients, there is a significant decrease in PGI_2 synthase expression as well as a down regulation of the IP receptor[63,64] enhancing the effect of vasoconstrictive mechanisms and progressing the disease further. Introducing exogenous prostacyclin to agonise the IP receptor or transfer of the IP receptor gene into animal models of PAH have been shown to ameliorate disease progression.[65] This mechanistic understanding has driven the development of prostacyclin mimetic (PM) therapies to agonise the PGI_2 pathway in the treatment of PAH.

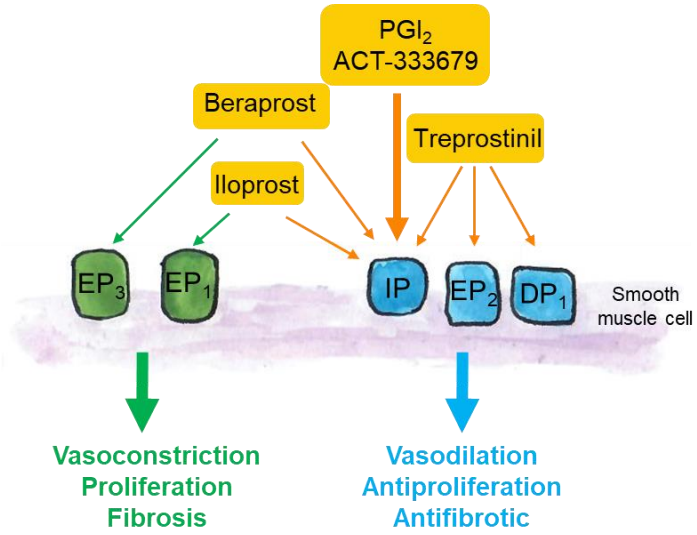

Figure 1-5. Different prostacyclin mimetics have different prostanoid receptor affinity profiles and are able to activate therpeuically beneficial receptors (Blue) and receptor which aid disease progression (Green).

As well as the IP receptor, other prostanoid receptors exist which possess very similar structures. Despite the similar binding domains of the receptors, the intracellular couplings can vary to stimulate different intracellular proteins. The Gs protein is coupled to the IP, EP_2, EP_4 and DP_1 receptors, leading to cAMP generation, a decrease in intracellular calcium promoting a vasodilatory effect. Alternatively, the prostanoid receptors, such the EP_1, EP_3 and TP receptors, may be coupled to a G_q or G_i protein which have the opposite effect by raising intracellular calcium levels. Many synthetic IP receptor agonists have been developed and several have reached the market. As a result of the similarities between prostanoid receptors, IP receptor agonists are not entirely specific and possess varying affinity towards the different receptors.[29] Successful prostanoid mimetics used in the treatment of PAH include Iloprost (**2**), Beraprost (**3**), Treprostinil (**4**) and selexipag (**5**), the prodrug of ACT-333679 (**6**) which all have affinity and potency at the IP receptor with varying additional selectivity to other prostanoid receptors. ACT-333679 is unique in that its structure is not based on that of prostacyclin and does not activate other prostanoid receptors so is considered a non-prostanoid, highly selective IP receptor agonist.

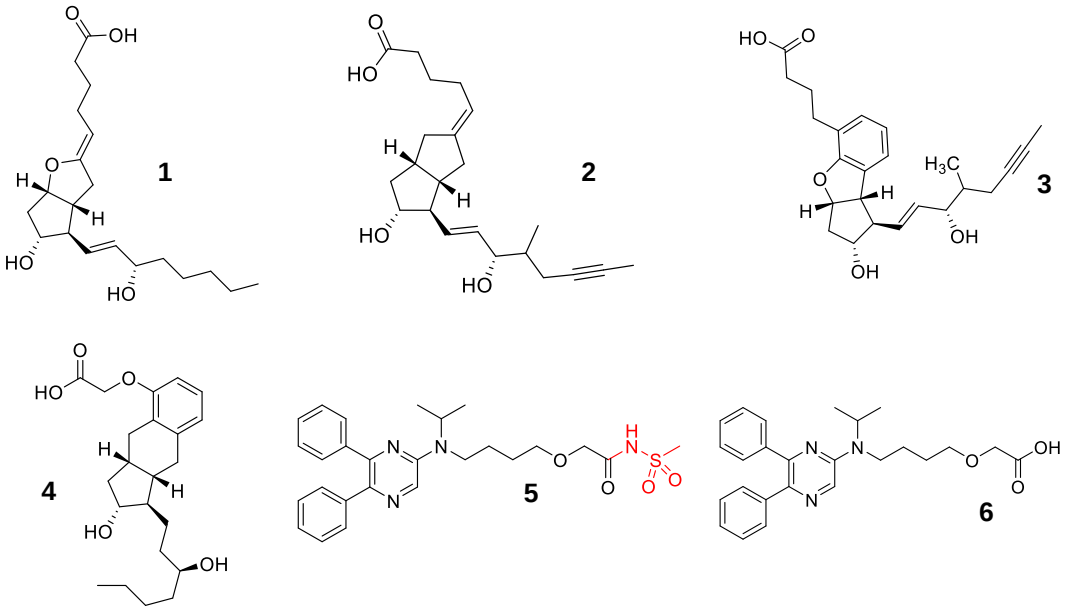

Figure 1-6. Prostacyclin mimetics used in the treatment of pulmonary arterial hypertension (PAH). Prostacyclin (and Epoprostenol) 1; Iloprost 2; Beraprost 3; Treprostinil 4; Selexipag prodrug 5; Selexipag metabolite, ACT-333679, 6. Red shows the cleavable moiety to release active agonist.

1.2 Prostacyclin and Mimetic Therapies

Epoprostenol (Same structure as 1) is synthetically produced PGI_2 and was the first prostacyclin receptor agonist therapy to be approved for the treatment of PAH in the USA in 1995. It has a systemic half-life of less than 3 minutes in the blood, mostly due to the susceptibility of the vinyl ether to hydrolysis[66] which drastically limits the potential of the drug due to the difficulty surrounding administration. Due to the lability of the vinyl ether, epoprostenol 1 needs to be continuously infused intravenously *via* a portable pump[67] and the drug formula cassette needs to be kept cold by the use of a cooling pouch which needs to be changed every ~12 hours.[68] Despite the cumbersome delivery device, risk of sepsis and associated risks with jamming of the pump,[67] epoprostenol 1 is considered the gold standard treatment for late stage PAH. It has shown to significantly improve 6MWD and haemodynamic parameters, and is still the only treatment available shown to improve survival.[69]

To minimise the issue of poor stability, epoprostenol sodium (Veletri®) was reformulated in 2008 for use with a diluent containing L-arginine at pH 11-13 by addition of sodium hydroxide to achieve thermostabililty.[70,71] The presence of L-arginine is thought to improve NO bioavailability as well as adding to the basic nature of the diluent. This formulation reduced the acid-catalysed degradation and negated the need for cooling of the dose pack.

Intravenous administration of bioactive compounds *via* a catheter provides an instant increase in drug plasma concentration and with continuous infusion can be tuned to supply a constant dose over time minimising the peak and trough concentration variations. Although epoprostenol 1 is efficacious in treating PAH, the chronic nature of PAH requires an easier

method of therapy delivery. The central catheter delivery requires healthcare professionals to insert, maintain and remove which as well as being inconvenient for the patient. Not only is this a costly way to administer the drug, but the the risk of infection is high (particularly in tropical climates) with severe outcomes. Lastly, the device is bulky to carry around. Together all of these issues, have a significant impact on quality of life.[72]

Despite its biological relevance in PAH and its efficacy in the clinic, the instability of epoprostenol 1 *in vivo* means administration by any route other than central IV line is not viable for long-term use. Nebulised epoprostenol has been used off-label in critically ill or paediatric patients with PAH in pre, during or post cardiac surgery.[73] Epoprostenol sodium is reconstituted in glycine buffer at pH 10.2 - 10.8 and delivered *via* ventilation mask or endotraceal mask fitted to a ventilator continuously over a period of hours.[74,75] The system must avoid direct sunlight as epoprostenol is light sensitive.[68] Whilst a suitable option for hospitalised patients, it is not easy for patients to adopt over a long period of time and maintain a degree of independence. Attempts to overcome stability of epoprostenol have carved an evolutionary path of PGI_2 mimetic therapies. Initially PGI_2 therapy was given by continuous IV infusions, which then led to the development of subcutaneous, inhalable and oral for formulations before arriving to the present day in the beginning of the nanomedicine revolution.[76] Recent formulations trialled in academia and industry involve liposome encapsulations,[77,78] polymer prodrugs[79] and slow release nanoparticles.[80]

1.2.1 Parenteral Therapies

Treprostinil 4 was approved as a PAH treatment by the FDA in 2002. Its stable tricyclic benzindene structure is based broadly on the prostanoid structure without possessing the labile vinyl ether. Formulated as the sodium salt, treprostinil **4** has a neutral pH, is stable at room temperature and has a systemic half-life of 4 hours in blood.[81] *In vitro*, 91 % of treprostinil was shown to bind to unspecified proteins in human plasma.[82] Treprostinil 4 is metabolised in the liver mainly by the CYP2C8 enzyme[66] and 79% is excreted as several urinary metabolites none of which possess any biological activity.[83,84] Initially selected for its potent IP receptor agonist properties, treprostinil 4 has since been shown to have activity at the EP_2, DP_1 and peroxisome proliferator-activated receptors (PPAR) β receptors, which may contribute to drug efficacy in slowing disease progression.[62] In addition to potent activity at the IP receptor, treprostinil 4 is 10-fold more active at the DP_1 (venodilating) and EP_2 receptors (vasodilating).[85]

Marketed as Remodulin®, treprostinil 4 was developed as a subcutaneous formulation for continuous infusion without the need for pack-cooling. This was intended to give patients more freedom to continue daily routines with reduced risk of serious catheter related infections.[86,87] Furthermore, the reliance on healthcare professionals and hospital time was reduced, as insertion of the SC line can be carried out by trained patients. Remodulin® was approved for subcutaneous infusion matching the constant dosing provided by IV with 100 % absolute bioavailability yet with a less invasive entry route and reduced risk of infection. Despite this, slight biurnal fluctuations in treprostinil concentrations in the blood are still prevalent

throughout the day and if terminated (e.g. from a pump malfunction), blood drug concentration decreases rapidly with a half-life of 3 hours.[88] Treatment with Remodulin® in PAH patients over 12 weeks improved 6MWD by 16 m ($p = 0.006$).[89] The cost of Remodulin® treatment for patients using 60-69 ng/kg/min exceeds $142,350 per year.[90]

Although patients receive a relatively constant dose of treprostinil and experience improvements in the symptoms of PAH, the adverse events at the site of administration are a major limitation. Patients reported significant adverse events related to the injection site that include, swelling burning sensations, vasodilation of the local vasculature and most significantly, pain.[89] It is recommended that the infusion site is maintained for as long as possible before changing and non-opiate analgesics are prescribed to manage the infusion site pain.[82] In addition the pump is cumbersome and inconvenient for everyday living[91]. Although not common, infusion pump malfunctions can occur which results in a decreased tolerated dose, restricting a patient's progress and can cause serious side effects including death.

To alleviate the site pain, Remodulin was reformulated and approved for intravenous infusion administration in 2004. Owing to the inconvenience of IV administration and the risk of catheter infections, it is used as an alternative to epoprostenol as a second line treatment for patients presenting group III and IV PAH or for those who have been hospitalised.

The benefits of continuously infused parenteral therapy, either SC or IV is that a near constant dose can be maintained. Although there are slight variations resulting in changes in metabolism between activity during the day and resting fast states in the night, the fluctuations are kept to a minimum. Because of the 100% bioavailability of these routes, cost of treatment is optimised to utilise all the active pharmaceutical ingredient available. The direct route of administration results in higher doses being tolerated than for non-parenteral routes.

Despite the efficacy of parenteral PM therapy, the restrictions discussed, including wearing a continuous pump and demanding maintenance requirements, are burdening for patients for long-term therapy.

1.2.2 Inhaled therapies

The next generation of therapeutics introduced were designed to widen the therapeutic window to overcome the systemic effects with the introduction of inhalable treatments directed towards the diseased tissue. Nebulised prostacyclin mimetics are a non-invasive and self-administered dosage form which provides a titratable and localised dose to the target organ. Once administered, the active pharmaceutical ingredient (API) is absorbed through the alveolar membrane and diffuses into the pulmonary capillaries where it arrives directly at the pulmonary vasculature at a rate dependent on diffusion across the alveolar tissue.[92] Re-dosing is required multiple times a day via a hand-held nebuliser, depending on the active analogue used.

Inhaled iloprost 2 was first approved in 2004 by the FDA under the trade name Ventavis.[93,94] Iloprost is a PGI_2 analogue stable at room temperature and physiological pH.[95] Non-invasive delivery was first achieved by aerosol inhalation. Bioavailability of iloprost entering the vascular compartment is approximately 80% with the maximal concentration reached within 5 minutes.[96] Although iloprost has a half-life of 20-25 minutes when administered intravenously,[97] in the airways the half-life is decreased to 6.5–9.4 minutes owing to rapid β-oxidation.[98] As a result, 6-12 inhalations per day are required to maintain concentrations of iloprost that maintain clinical benefit.[99] As well as the inconvenience to patients, this made treatment disproportionately expensive for the efficacy achieved. Inhalation time has been reduced from 15 to 4 minutes per dose by use of ultrasonic nebulisation for particle formation.[100] Pharmacologically, Iloprost 2 is a potent IP receptor agonist, with an inhibition constant (Ki) of 3.9 nM. Although iloprost has low affinity for EP_2, EP_3 and DP_1, it has the most potency at the EP_1 receptor with Ki at 1.1 nM.[62] Activation of the EP_1 receptor leads to an increase in intracellular calcium which leads to vasoconstriction,[101] working against the vasorelaxation brought about by IP agonism.[85] Although inhaled iloprost is used clinically, improving haemodynamics and exhibiting fewer adverse events,[95] its utility in the clinic as a first line treatment could be hindered by its conflicting pharmacological character.

Treprostinil 4 was formulated into an inhaled nebulised form of the sodium salt and marketed as Tyvaso®. In 2009, Tyvaso® received FDA approval for treatment of PAH in patients with class III symptoms.[102] When treprostinil was first used clinically on a compassionate basis in only three patients, an improvement in functional class was achieved with no reported adverse events,[103] although this was not reflected in the results of Tyvaso in the pivotal clinical trial.[104] An increase in 6MWD and measure of quality of life was reported, but not improvement in functional class or time to clinical worsening. In addition, adverse events including coughing and flushing were experienced, which in 7 patients (out of total 115) receiving inhaled treprostinil, resulted in its discontinuation. In an open-label trial comparing inhaled iloprost and inhaled treprostinil, the maximal vasodilatory effect measured by PVR was experienced later (18 ±2 min *versus* 8 ±1 min, mean ± standard error of the mean (SEM), $p<0.0001$) and for a longer time period (>1 hour, $p<0.0001$) with treprostinil *versus* iloprost which returned PVR to baseline after 40 minutes.[105]

The bioavailability of Tyvaso® is determined to be 64% and 72% for the respective single doses, 18 and 32 µg.[102] Tyvaso® is a longer acting prostacyclin analogue than iloprost with a potentially more desirable receptor affinity profile, (EP_2 affinity, which dilates bronchial smooth muscle in airways).[106] The pharmacokinetics are still limited, requiring 4 doses during waking hours; 3 breaths approximately every 4 hours.[102] The nebuliser is not a hand-held device and requires, power to operate, addition of an ampoule of Tyvaso® formulation and distilled water and daily cleaning.[107]

Inhalable PM therapies achieve greater therapeutic effect with smaller doses compared to parenteral delivery although they have a lower maximum tolerated dose.[108–110] Inhaled and

oral PM therapies are often prescribed as part of a dual therapy strategy with PDE-5is or ERAs. For treprostinil, it is as part of dual therapy that Tyvaso® was approved by the FDA in 2009.[102] Approval of Tyvaso® in Europe is yet to be granted. Administration requires a handheld portable nebuliser which is not as discrete as inhalation devices used by asthma patients. The short residence time of the drug in the alveolar region and its rapid metabolism means multiple doses each day are required. Between doses, large fluctuations in drug blood concentrations are experienced which are thought to exacerbate adverse events such as flushing, and headache.

1.2.3 **Oral prostacyclin mimetics**

Being the most patient-compliant method of drug administration, the first oral PM was long-awaited. Oral therapy does not require difficult and time-consuming drug administration. Unlike subcutaneous and inhalable formulations, additional training is not necessary for patients to deliver their treatment. Furthermore, the oral tablet option allows for discrete administration in any setting which is less burdening for the patient.

Beraprost 3 was the first oral prostacyclin mimetic developed which received approval in Asia in 2003. In the Arterial Pulmonary Hypertension and Beraprost European Study (ALPHABET), an improvement in symptoms and exercise capacity (6MWD) were observed.[111] Functional class and haemodynamic measurements did not show improvements after 12 weeks. A further study demonstrated improvements in 6MWD at early time points within the 12 month trial but efficacy was attenuated after 6 months.[112]

Treprostinil diolamine (7) was approved by the FDA (2013) as the first orally available prostacyclin therapeutic for use in the USA. The alternative diolamine salt of treprostinil 7 is administered in an osmotic, laser-drilled tablet which becomes hydrated after ingestion and slowly releases active treprostinil from the laser-drilled hole at a near zero order release rate. Patients are prescribed a starting dose of 0.25 mg twice daily which is titrated incrementally dependant on patient tolerance. The bioavailability of the oral formulation is 17% so greater concentrations are administered than enter the blood stream.

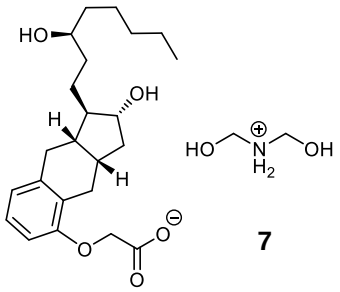

7

Figure 1-7. Structure of treprostinil diolamine salt 7 used in the oral formulation orenitram®.

Following the first approvals for oral PMs, 2015 saw the first global approval (USA, Canada, EU, Japan) of selexipag (**5**), a pro-drug of the active compound, ACT-333679 (**6**).[62] Marketed

as Uptravi, selexipag is a non-prostanoid, selective IP agonist.[113] The half-life of the inactive pro-drug form is 1-2 hours which is hydrolysed by hepatic enzymes to the active metabolite, which has a half-life of 7-8 hours. The increased lifetime in the blood is attributed to the 99% binding to plasma proteins such as albumin and α-acid glycoprotein.

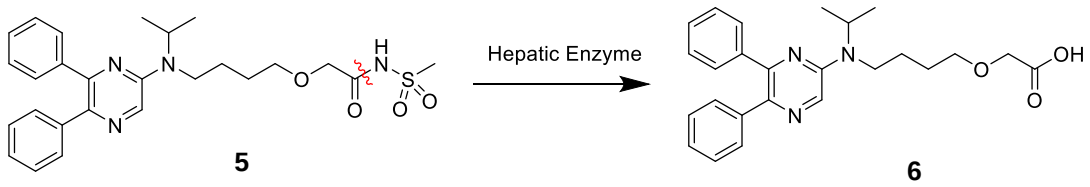

Figure 1-8. The structure of selexipag (**5**), the pro-drug which cleaves to release active compound ACT-333679 (**6**)

When developing a series of potential prostacyclin receptor agonists, it was found that using the N-acyl sulfonamide derivative (5) of what was later termed ACT-333679 (6), exhibited a 130-fold lower affinity than its parent acid at the human IP receptor in radioligand binding studies (Ki 20 nM verses 260 nM). Furthermore, when measuring inhibition of platelet aggregation at the same receptor, the IC_{50} of the N-acyl sulfonamide derivative, was 26-fold greater compared to its parent acid.[114,115] Following the observation of hepatic degradation of N-acyl sulfonamide 5 to release the acid, turned what was first an unexpectedly inactive structure into selexipag 5, the first globally approved prodrug formulation for PAH.[116]

Selexipag (5, tradename UPTRAVI®) is the most recent orally administered IP receptor agonist, and the only pro-drug to be granted FDA approval for the treatment of PAH.[117] Compared to other prostacyclin mimetics (PMs) used to treat PAH, the selexipag structure is not derived from prostacyclin and is therefore considered a non-prostanoid agonist.

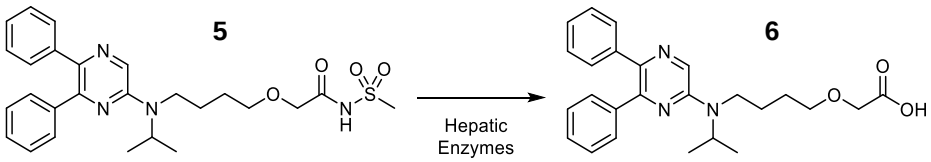

Figure 1-9. The conversion of selexipag (**5**) to ACT-333679 (**6**) by carboxylesterases found in hepatocytes of rats, dogs, monkeys and humans, as well as the blood plasma of rats.

1.2.4 Summary of current PM therapy

Synthesis of prostacyclin in the pulmonary vessels of PAH patients is significantly reduced leading to the dominance of vasoconstrictive and proliferative pathways to drive the disease.[63] The disruption of the prostacyclin pathway is considered a key mechanism involved in the pathobiology of PAH.[29] Therapeutic restoration of prostacyclin levels has been shown to slow disease progression, improve functional class and ameliorate symptoms.[118]

Prostacyclin can be used in patients with all stages of PAH, but is specifically recommended in patients with class III or IV PAH.[119] Clinical benefit of prostacyclin therapies are proven

although, only epoprostenol has been shown to increase survival in a placebo-controlled and randomised trial.[120] Prostacyclin therapies are limited to the maximum tolerated dose which restricts the efficacy of treatment to the tolerability of the adverse events. Patients would benefit in two ways if adverse events were overcome; (i) pain and discomfort of treatment would be removed, increasing quality of life (ii) greater concentrations of treatment could be administered, increasing efficacy.

Many attempts to overcome adverse events associated with current therapies have been made. Improvements to current formulations have been investigated to reduce adverse events. Oral treprostinil 7 was developed for twice daily dosing but patients who split the dose into trice daily achieved a steadier drug-blood concentration throughout the day.[121] Unfortunately adverse events were not reduced.[122] Subcutaneous infusions are recommended to be moved every 2-3 days, but to reduce the pain, are generally left in for 2-3 weeks without increased infection.[123] Furthermore, delivery of capsaicin to the infusion site by use of a patch was also shown to decrease site pain.[124] Ideas to reformulate the PMs have also been investigated as will be discussed in the following section.

1.2.5 Ongoing Research into Prostacyclin Therapies

Preclinical research by industry and academic groups is being undertaken to address the drawbacks of PMs. Examples include the introduction of new molecules to the drug class,[125,126] and assessing the benefits of cross-class combinations of PAH therapies alongside the application of nanomedicine approaches in the delivery of known drugs.[77,90,127,128] Following successful and titratable release of prostaglandin E_1 from encapsulating nanoparticles,[129,130] the sodium salt of beraprost (3) was similarly encapsulated into slow releasing particles.[131] The nanoparticles were made from either racemic or isotactic polylactic acid (PLA) and PEG-PLA block co-polymers using iron chloride to help trap the hydrophobic drug into the hydrophobic polymer. Experimentation of rhodamine S nanoparticles in a monocrotaline and hypoxia model of PAH showed that in treated rats, accumulation occurred more in diseased tissue than control tissue and occurred even more so than free rhodamine over a period of 5 days. Furthermore, monocrotaline-treated rats, intravenously injected with nanoparticles containing 20 µg /kg of beraprost once a week for 21 days, experienced a similar reduction in right heart hypertrophy as rats treated daily with 100 µg /kg oral dose of free beraprost sodium. A formulation which requires less frequent administration without compromising clinical efficacy has potential for clinical translation.

Liposomal nanoparticles have been employed to encapsulate Iloprost (2) to improve pharmacokinetics.[78] Iloprost 2 was encapsulated in various cationic PEG_{2000}—lipid block co-polymers via thin film rehydration methods to produce liposomes with 59% average encapsulation efficiency. The rate of iloprost 2 release was determined by measuring the ability of the supernatant to dilate the rat pulmonary artery using a myograph. The ability to relax pre-constricted small pulmonary arteries was measured using the empty liposome, iloprost encapsulated liposomes and free iloprost. These experiments showed that the use of

liposomes allowed the same extent of vasodilation to occur with half the amount of iloprost compared to free drug ($p < 0.001$).

Liposomes have also been employed for the pulmonary delivery of treprostinil pro-drugs in rats with hypoxia-induced PAH.[80,132] Cationic alkyl ester derivatives of treprostinil pro-drugs are encapsulated into PEG-lipid nanoparticles by surfactant molecules which after inhalation, slowly diffuse out into the alveolar cavity and cross the tissue into the pulmonary vasculature. The peak concentration measured is lower than that obtained by inhalation of free treprostinil and the release is sustained for a longer period of time.[133] The liposomal approach has been shown to achieve sustained release of treprostinil 4 using a non-invasive delivery method direct to the target organ. Unfortunately, liposomal prostacyclin is expensive to be manufacture on large scale and difficult to sterilise. Maintaining stability and characterising liposomal prostacyclin are also major bottle-necks limiting the clinical translation of liposomal approaches.

An alkylated prodrug derivative of treprostinil has similarly been incorporated into a liposomal delivery system for a nebulised delivery system. The drug is called INS1009, compound 8, in **Figure 1-10**.[134] A 16-carbon linear alkyl chain was conjugated to treprostinil 4 acid group forming an ester bond that was designed to be hydrolysed by esterases. The alkyl treprostinil prodrug was combined with 1,2-distearoyl-*sn*-glycero-3-phosphoethanolamine-N-[methoxy(polyethylene glycol)-2000 to encapsulate the prodrug within a liposome. Upon intratracheal administration to dogs, a localised reduction in PAP was observed. A similar effect of PAP was observed with guinea pigs and additionally, no cough respiratory tract irritation or emesis was observed.[134] In a phase I single dose study in humans, patients were administered either inhaled treprostinil or inhaled liposomal nanoparticle INS1009 prodrug.[135136] Blood plasma concentrations of the prodrug were extended compared to free treprostinil although a 30% reduction in total treprostinil exposure was observed. The lower measure of treprostinil indicates 30% of the prodrug in INS1009 is cleared before converting to treprostinil. Adverse events between the two groups were similar although details of adverse events were not reported. No further developments into phase II trials have been reported, so it is likely that the pharmacokinetic improvement did not outweigh the negligible decrease in adverse events and thus, clinical development of INS1009 for PAH was terminated.

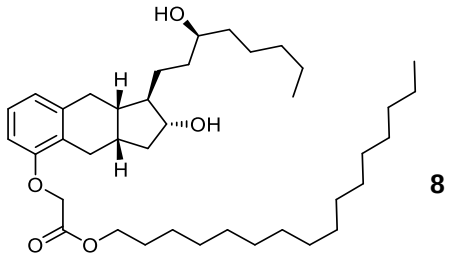

8

Figure 1-10. Structure of the prodrug treprostinil 8 used in INS1009 formulation.[134]

Slow-release formulations delivered directly into the lung would potentially require less frequent administration and achieve localised drug release in the lung. Once treprostinil **4** diffuses into the bloodstream it is free to activate systemic receptors, reducing the intended effect to reduce unwanted systemic activation of prostanoid receptors. For treprostinil **4** to have optimal effect in the treatment of PAH, its target receptors in the lung will need to be activated preferentially over systemic receptors.

In 2012, a collaboration between United Therapeutics (UT) and Ascendis was initiated to develop a PEGylated treprostinil. Four treprostinil **4** molecules were conjugated to a 4-arm PEG of 40 kDa with the intention of later being released from the coonjugate.[137] The structure utilised the TransCon system developed by Ascendis but the exact conjugation method was not disclosed. It is presumed that treprostinil was likely to have been conjugated through the acid based on the expected lack of specificity between the two secondary hydroxyls. The prodrug was developed as a subcutaneous formulation which would reduce pain at the site of administration with an extended half-life to facilitate a once daily dosing regimen. In 2015 a press release was published announcing the study termination.[138] Despite "favourable pharmacokinetic effects", the tolerability was still an issue. The activity of treprostinil at any of the receptors that it has potent affinity for (IP, EP_2, DP_1), is expected to be reduced upon conjugation to the PEG structure. The reported adverse events after administration likely resulted from premature degradation of the ester bond in the subcutaneous hypodermis environment before permeation into the circulation. Carboxylesterases are ubiquitous in the body so enzymatic cleavage is likely to be rapid,[139,140] which may have degraded the compound more rapidly than expected.

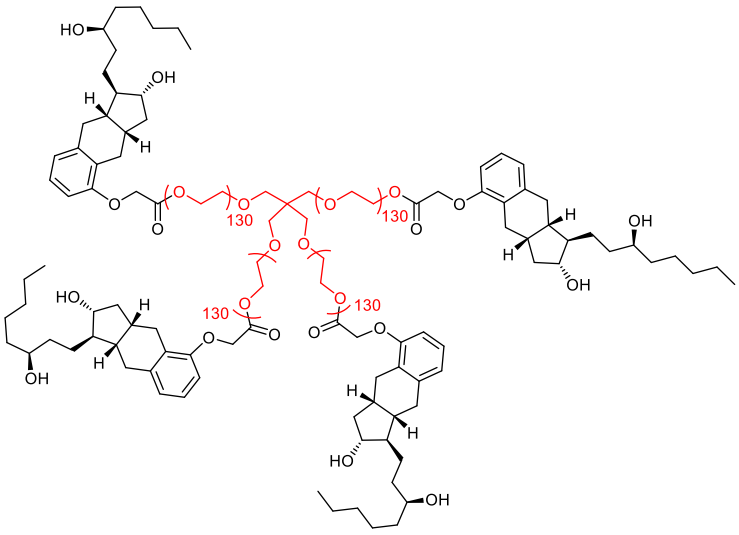

Figure 1-11. Proposed structure of 40 kDa 4-arm PEG with a treprostinil conjugated at each terminal. Ester bonds have been drawn although the exact conjugation method has not been revealed.

In late 2017, UT announced it had initiated a collaboration with Corsair Pharma with the aim of developing a transdermal patch for the delivery of treprostinil using a prodrug derivative which has reduced activity upon administration but once in the blood stream is transported to

the liver where is it converted to active treprostinil.[343] No further details have been released about the treprostinil prodrug structure or its pharmacokinetic profile.

1.3 Therapeutic Potential of Treprostinil (4)

Treprostinil is a stable analogue of prostacyclin and the only prostacyclin mimetic available to be given *via* four routes of administration; subcutaneous infusion, intravenous infusion, inhaled and oral routes.[141] All PMs are designed as IP receptor agonists, and all but selexipag exhibit affinity at other prostanoid receptors.[62] Treprostinil **4** is unique in that its efficacy is likely to be mediated through multiple targets, including the EP_2 receptor.[62,142,143] The affinity exhibited by treprostinil for the EP_2 receptor was first considered to be an off-target effect although it now has to be considered as a therapeutic target.[144] The IP receptor is downregulated in PAH and the EP_2 receptor has been shown to increase in expression, making the latter receptor a particularly relevant therapeutic target in PAH (**Figure 1-12**).[29]

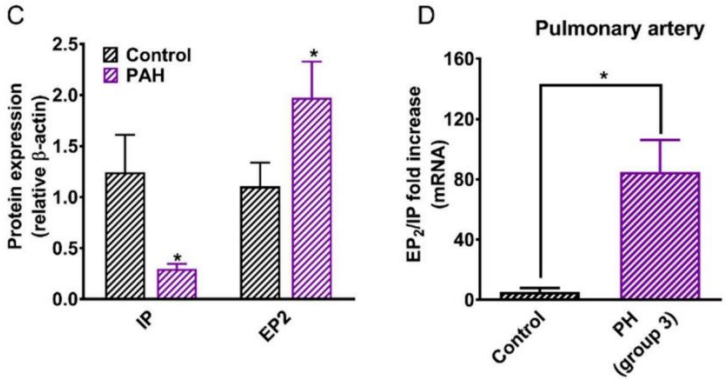

Figure 1-12. The relative changes in expression of IP and EP_2 receptors in human pulmonary arterial smooth muscle cells derived from patients with pulmonary arterial hypertension and controls. Reported by Patel and colleagues.[142]

Treprostinil (4) is a benzindene derivative possessing an aryl acid and two hydroxyls; one cyclic and one as part of the alkyl chain.[145] Early structure activity relationship studies using a platelet inhibition assay to determine activity concluded that the acid was necessary for receptor binding and activity is reduced 10-fold by its derivatisation to a methyl ester.[145] Furthermore, the presence and stereochemistry of the hydroxyls are also required for anti-platelet activity.

Parenteral delivery of PMs remains the most effective treatment for alleviating symptoms and increasing disease severity measurements including 6MWD. In later stages of disease or if a patient's health rapidly declines, the patient is often moved to subcutaneous infusions until their condition stabilises. Although there are many PM options for early stage PAH (non-PM therapies as well as treprostinil in oral and inhaled forms), there is no substitute for subcutaneous treprostinil in late stage disease other than IV infusion.

Within the clinic, a universal maximum concentration that patients reach does not exist. Instead, patients are encouraged to reach and maintain the highest dose they can tolerate

before adverse events cannot be withstood. The therapeutic window is narrow, so most patients will experience adverse events when taking treprostinil. Despite the clinical benefits of treprostinil 4, adverse events still limit the maximum tolerated dose. Treprostinil therapy is hindered by toxicity at the site of injection as well as adverse events induced by systemic activation.[146]

1.4 Methods of drug optimisation

Improving the pharmacokinetics and altering the biodistribution of an active pharmaceutical ingredient can improve efficacy and patient tolerability.[147] A treatment can be improved to some degree by a judicious choice of formulation and route of administration. It is also possible to modify the drug structure to produce analogues with more optimal solubility, permeability and biodistribution while preserving sufficient biological activity.

Drug compounds can also be covalently conjugated to small moieties such as an amino acid, or to large biologics including antibodies, proteins such as albumin, or polymers. Alternatively, drugs can be non-covalently encapsulated in larger structures such as hydrogels, polymeric nanoparticles or within particles such as liposomes, vesicles or nanoerythrosomes. Sustained-release formulations of PMs have been investigated, some of which reached phase I trials.[136,137] Only one pro-drug PM, selexipag (5), has been approved for the treatment of PAH.[116]

1.4.1 Prodrug Approach

A commonly employed method to improve pharmacokinetics of a drug molecule is to temporarily modify the structure to reduce its activity and enhance its pharmacokinetic properties.[148] Covalent modification of an active drug to a small functional moiety to form prodrug, which then undergoes an *in vivo* reaction to regenerate the active drug, is a strategy used in ~20% of all newly approved small molecule drugs entering the market.[148] Prodrugs are often used to decrease activity in non-specific tissues and allow for the distribution of the prodrug to a select tissue before the prodrug moiety is cleaved and the active drug released.

Many different prodrug moieties have been examined. Hydrophilic pro-moieties such as sugars and phosphoesters can increase the solubility of a drug.[149] Alkyl prodrugs (eg. methyl or propyl esters) can increase drug permeation, such as tafluprost for delivery to the eye for glaucoma treatment.[150]

The reaction of a pro-drug to form the active drug molecule is dependent on the prodrug structure and the conditions required to cleave it. Some bonds require a chemical interaction to cleave the pro-drug (e.g. pH, redox), whereas other moieties require enzymatic degradation. A summary of the physiological conditions required to cleave commonly employed prodrug structures is listed in **Table 1-1**.

Table 1-1. Structures of a selection of prodrug structures in the clinic and their cleavage conditions.

Prodrug	Property	Cleavage conditions	Indication	Ref
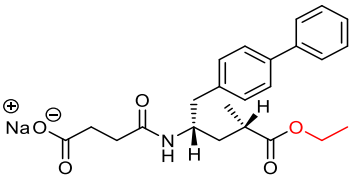	Increased lipophilicity and permeability	Esterases	Heart failure	151
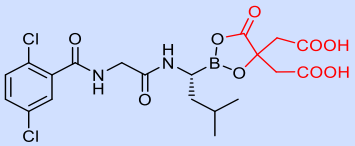	Increased stability of the boronic acid	Hydrolysis in physiological conditions	Multiple myeloma	152
9 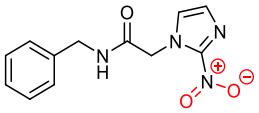	Generates radical species	Reduced by nitroreductases	Chagas disease in children	153
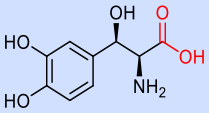	Improved brain permeability	Decarboxylation catalyzed by L-aromatic-amino-acid decarboxylase	Neurogenic orthostatic hypotension	154
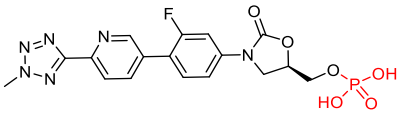	Improved solubility	Plasma or intestinal phosphatases	Acute skin infections	155

Depending on the medical application, the release site and rate for generating the active drug can in principle be tailored. For instance, 5-aminosalicylic acid is an oral anti-inflammatory agent used for the treatment of inflammatory conditions of the gastrointestinal tract (GIT) such as Crohn's disease, ulcerative colitis and irritable bowel disease.[156] To increase specificity to the GIT, 5-aminosalicylic acid is administered in the inactive prodrug form, balsalazide. When in the colon, bacterial enzymes cleave balsalazide by azoreduction to release the active parent compound 9 where it is able to locally interact in the inflamed colon (**Table 1-1**).

Protein binding prodrug

Another strategy to increase the circulation lifetime of bioactive compounds includes exploiting interactions with circulating proteins, such as the case of alkylated insulin (Levermir®) an approved treatment for the management of diabetes which exhibits a longer half-life owing to enhanced albumin binding.[157] Albumin, which makes up 55% of the proteins in blood, interacts with neonatal Fc receptors which extends its half-life to 19-21-days. Drugs such as warfarin, diazepam and ibuprofen are able to bind to albumins and remain in the circulation longer than for other small molecules.[158] α-Tocopherol is able to bind to albumin through hydrophobic interactions and has been considered in the conjugation of bioactive compounds to extend their half-lives.[159,160] The concept of conjugating treprostinil 4 to a protein binding moiety such as α-tocopherol could increase the half-life of treprostinil to reduce the frequency of

administration, although the distribution of drug across the body would still be wide spread. Treprostinil therapy is limited by its systemic exposure, so by only increasing half-life leaves the challenge of optimising biodistribution to the lung yet to be solved.

1.4.2 Polymer drug conjugates

Prostacyclin mimetics, like most small molecule drugs, exhibit short half-lives owing to their susceptibility to be renally excreted, metabolised and distributed to non-diseased tissues which is a result of their small size.[161] To compensate, delivery strategies have included the conjugation of small drugs to large macromolecules, including, proteins, polymers and nano particles.[162] Conjugation of a drug to a polymer can be used to mask activity, similar to a prodrug approach will additional macromolcular properties. In contrast, multiple drug compounds may be conjugated to a polymer whilst preserving the drug activity, to enhance activity using a polyvalent approach. In addition to either approach, the conjugation of other molecules may be desired to aid solubility or conjugate localisation.

Conjugation of drugs to polymers, known as polymer drug conjugates (PDC), have been designed and investigated with different water-soluble polymers and drugs.[163–166] Polymer conjugation has seen most success in the conjugation of proteins by poly(ethylene glycol) (PEG) in a process termed PEGylation. PEG is simple in design, easy to synthesise and obtain commercially with a variety of functional groups and exhibits a narrow molecular weight distribution.[167,168] Since 1990, at least nine PEG-protein conjugates have received FDA approval, involving therapeutic proteins such as enzymes, antibodies, growth factors and cytokines.[168] The PEG chains provide steric shielding of the protein to reduce immunogenicity, increase biological half-life which results in decreasing the frequency of dosing. For instance, when interferon-α2b (Intron® A) was PEGylated with a 12 kDa PEG molecule the resulting conjugate, PegIntron®, possessed a longer half-life than Intron® A.[169] Following intravenous administration in humans, the serum concentration of Intron A rapidly decreased to untraceable amounts within 24 hours, whereas PegIntron® was detectable at a maximal sustained concentration for 48 to 72 hours.[170] PegIntron® is dosed once weekly rather than once every other day for the non-PEGylated interferon (Intron®). The less frequent dosing also reduced the frequency of side effects suffered by the patient. The size of PEG has been shown to exhibit direct correlation with lifetime by avoiding renal excretion[171] and other PEGylated proteins have also become first line treatments (e.g. PEG-Granulocyte colony stimulating factor (PEG-GCSF)) used to treat non-Hodgkins lymphoma.

The concept of conjugating low molecular weight drugs to polymers was proposed by Ringsdorf in 1975 (**Figure 1-13**),[172] which consisted of a polymer containing water solubilising pendant chains, targeting moieties and drug conjugated by a biodegradable linker.

The first polymer-drug conjugate in Phase 1 trials for the treatment of cancer in 1994 (HPMA copolymer- doxorubicin (Dox) (FCE28068, PK1)).[173] Since then, the progression into the clinic of polymer-drug conjugates derived from a cytotoxic agent has been more hindered than for

the PEG-protein conjugates.[174] Polymer conjugates of low molecular weight drugs generally require that the drug be released from the polymer. PEG-proteins do not require release of the protein. For the case of cytotoxic drugs, and any drug with off-target effects, the site and specificity of release of the drug from the polymer is an important feature.

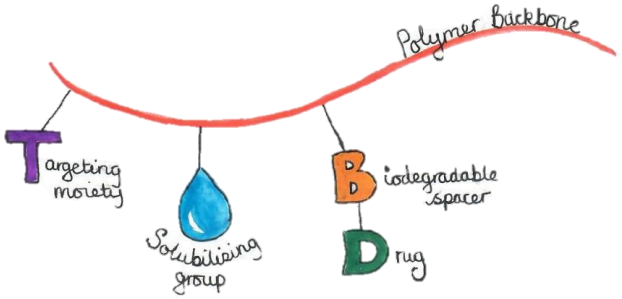

Figure 1-13. Ringsdorf model of a multifunctional polymer proposed as a method to achieve site-specific delivery of drug compounds. The structure contains a hydrophilic polymer back bone with targeting moieties conjugated in a pendant fashion. The drug is also conjugated to the polymer *via* a biodegradable linker.

In the case of oncology, conjugation of drugs to macromolecules exploit tissue permeability gradients where diseased tissue can often be more permeable than healthy tissue.[175] Permeability is often associated with angiogenesis and inflammation in cancer.[176] Within malignant tissue, especially in rapidly growing tumours, there may also be decreased lymphatic drainage which can aid to retain a molecule after tissue uptake. These combined effects are known as the enhanced permeability and retention effect (EPR) and may also partially explain why macromolecules initially extravasate into malignant tissue.[175–177] Retention is established by the prolonged circulation time of a polymer drug conjugate to allow for extravasation into more permeable tissues by diffusion. The accumulation of macromolecules into permeable vasculature by the EPR effect results in passive targeting of malignant and often inflammed tissues.[177–179] Given that endothelial disruption and inflammation are key features of PAH, it is possible to imagine targeting therapeutics to the PAH lung but exploiting the EPR effect.[180,181]

The covalent conjugation of a drug to a polymer often causes the drug activity to be reduced, owing to the steric hindrance that the relatively large polymer provides.[164] Drug cleavage is required from the polymer to restore activity and thus the polymer drug conjugate can be considered a polymeric prodrug; temporarily exploiting the properties of macromolecules to extend circulatory life time and passive targeting of permeable vessels.[166]

The choice of polymers utilised also deserve consideration as the polymer must be water soluble to facilitate fluid-like interactions with physiological media.[182] The polymer must also be inert, *i.e.* must not evoke a biological response such as toxicity or immunogenicity. Metabolism or excretion must be defined and accumulation of the polymer within cells should not occur. Particularly for hydrophobic drug compounds, the polymer must contain a hydrophilic backbone to facilitate fluid-like interactions with physiological media.

Both biodegradable and non-biodegradable polymers have been employed for polymer drug conjugates.[165] An historical advantage has meant non-biodegradable polymers have received more attention which has led to their dominance in the clinic over biodegradable options. Biodegradable polymers for drug conjugates offer alternative materials, with less chance of bioaccumulation as well as the opportunity to conjugate the drug through the polymer mainchain.[183,184] The most successful polymers employed for conjugation are poly(ethylene glycol) (PEG) and poly(2-(N-hydroxypropylmethacrylamide)) (pHMPA).[165]

Table 1-2. Polymer-drug conjugates being clinically investigated [185] DOX = doxorubicin; CPT = camptothecin

Polymer	Conjugate	Linker	Clinical Status
HPMA	HPMA-copolymer-DOX PK1; FCE28068	Peptidyl	Phase II
	HPMA copolymer-DOX-galactosamine PK2; FCE28069	peptidyl	Phase I
	HPMA copolymer-paclitaxel PNU166945	Ester	Phase I/ discontinued
	HPMA copolymer-camptothecin MAG-CPT	Ester	Phase I / discontinued
	HPMA copolymer malonato-platinate	Malonate	Phase I
	HPMA copolymer-DACH-platinate, AP5346 ProlindacTM	Aminomalonate	Phase II
PGA	PGA-camptothecin CT-2106	Amide	Phase I/II
	PGA-paclitaxel Xyotax™	Ester	Phase III
Dextran	Oxidised dextran-DOX AD70, DOX-OXD	Schiff Base	Phase I discontinued
	Carbomethyldextran-exatecan DE-310	Amide	Phase I
Dextrin	Cyclodextrin-camptothecin IT-101	Amide	Phase I
PEG	PEG-camptothecin Pegamotecan	Ester	Phase II discontinued

PEG is a popular choice in polymer-drug conjugate mainly owing to its FDA approval.[186] PEG is usually terminally conjugated and thus is limited in the number of drug molecules conjugated per polymer chain, although attempts to increase loading by forming multi-arm and branched PEG chains has been conducted.[187–189] More recently, the inert nature of PEG has been called into question as anti-PEG antibodies have been identified in patients treated with macromolecules with PEGylated surfaces.[190–192] The role and clinical implication of the antibodies is unknown[190] and the observation has not deterred PEG conjugates from entering the clinical setting.[193]

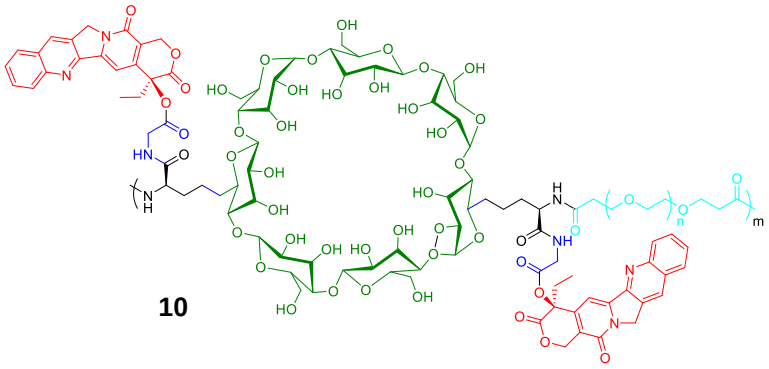

10

Figure 1-14. Monomer of camptothecin (CPT) – cyclodextrin – PEG (CDP) conjugate which increases the solubility of CPT by 3-fold. Number of PEG monomers, n (average) = 77 and PEG M_w is 3400. Number of CDP-CPT monomer per drug polymer, m (average) = 18 ±5 and M_w is 85 ±23 kDa.

One example of harnessing macromolecular attributes for a drug delivery is the conjugation of naturally occurring camptothecin (CPT) which is used in the treatment of cancer (**10**).[194] Camptothecin promotes apoptosis of tumour cells, but its low solubility and unstable structure limits its potential in the clinic. The cytotoxic nature of CPT is a significant problem as it is not tissue specific and exerts its effects in healthy tissue as well. Conjugation to a cyclodextrin-based linear polymer via an ester bond to a glycine linker increased the hydrophilicity and solubility by 3-fold. Furthermore, the increased molecular weight prevented excretion by renal filtration, extending systemic half-life. Compared to free CPT, enhanced biodistribution to tumour tissue is observed which is a result of the enhanced permeation and retention (EPR) effect,[195] where small aggregates accumulate in tumours. Despite the acid catalysed esterolytic cleavage of CPT from the polymer (between CPT and glycine linker) not being tumour specific, pre-clinicial trials showed the accumulation of the conjugate in the tumour tissue resulted in a greater proportion of CPT release in the tumour, meaning a higher maximum tolerated dose could be achieved with reduced systemic toxicity.[196,197]

Clinically, polymer-drug conjugates have had limited success in cancer owing to minimal improvements in therapeutic outcome.[185] Off-target effects have been reduced but improvements in survival have not been achieved. Without specific mechanisms for the release of the cytotoxic agents used in cancer, release can occur prematurely, and even small concentrations released in healthy tissues can cause serious off-target effects.

1.4.3 Targeting therapeutic approaches

One of the most significant drawbacks of prostacyclin therapies for PAH is the lack of specificity towards the lung tissue as synthetic prostacyclin and its analogues are active at prostanoid receptors (including EP_1, EP_2, EP_3, EP_4, DP_1 receptors) expressed in the vasculature throughout the body.[62,85] The activation of prostanoid receptors on the systemic endothelial cells (ECs) and vascular smooth muscle cells (VSMCs) is understood to be the major cause of the characteristic side effects such as diarrhoea, flushing and nausea and gives rise to the risk of systemic hypotension, lowering blood pressure at higher doses.[198]

These factors conspire to limit the maximum dose resulting in a narrow therapeutic window for many of the prostacyclin therapies.

Pulmonary delivery

The targeting of therapies to the PAH diseased lung can potentially be achieved by delivering pharmaceuticals *via* the pulmonary route. Pulmonary delivery has long been used to deliver therapeutic gases (e.g. nitrous oxide and ethers for anaesthetic).[199] Methods to impart properties suitable for inhalation to drug compounds has received much attention in the form of nebulised drugs and drug powder formulations.[200] Localised pulmonary delivery has been shown in to induce the same therapeutic effect at lower concentrations.[201]

The lung is designed to facilitate absorption from the alveoli into the blood stream and as a result possesses an efficient mechanism to ensure foreign particles do not enter the alveoli. Thus, pulmonary delivery is restricted to particles between 2-5 μm and limited by the rapid clearance of particles from the lung by entrapment by mucociliary escalator or macrophage uptake.[202] Many inhaled therapeutics have been successful, such as asthma therapies which deliver steroids to the airway receptors.

The delivery of therapies which achieve a steady concentration by sustained release has been harder to achieve clinical success.[92] Particles which reside in the alveolar regions, avoiding detection of clearance mechanisms, have been investigated. Steady release of drugs over time from the particles has been demonstrated *in vitro* and *in vivo* but none have entered phase II trials.[200,201,203] One possible limitation is the fate of the particle carrier once the drug has been released. The accumulation of such particles in the alveoli have been linked to inflammatory responses such as granulomas,[204] and inducing molecular pathways associated with inflammation, oxidative stress and fibrosis;[205–207] all of which key characteristics of the PAH lung.[51]

Delivery of PAH agents *via* the pulmonary route although offers direct organ targeting, was considered likely to exacerbate the inflammatory response and so for this reason, the pulmonary route was ruled out for this PhD project.

Active targeting

Since Ehrlich first developed the concept of the ‘magic bullet’,[208] where drugs would be designed to be systemically delivered yet carry out their effect exclusively at the target site, much research has been focused on achieving this concept. Understanding the environment established within a diseased tissue and how it contrasts to normal tissues has been a key objective in designing responsive conjugates for achieving localised delivery of drug molecules. The expression of different antigens and enzymes vary for different cell types and this complementary binding can be exploited to target cell/tissue/organ.

Clinically, active targeting approaches are best exemplified with the conjugation of drug compounds to antibodies (**Figure 1-15**), forming antibody drug-conjugates (ADC).[209]

Exploiting the body's natural system for distinguishing between different tissues and cells, ADCs can be designed for a specific antigen found in the target tissue.

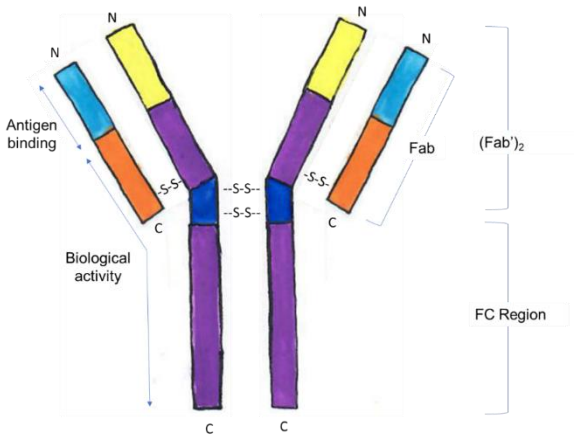

Figure 1-15. General structure of an antibody, showing the Fab chains, the FC region and the hinge region, coloured dark blue. The tail-like Fc region is responsible for interacting with cell surface receptors which extends its biological half-life The chains are oriented and aligned with N-termini at the top and C-termini at the bottom. Chains are held together by disulfide bridges between the thiols of cysteine residues in the protein structure. Only the light blue regions are the site of antigen specific binding.

Many of the ADCs investigated clinically have been in development for the treatment of cancer.[210] Highly cytotoxic drug molecules are covalently linked to antibodies which are targeted to specific epitopes overexpressed by tumour cells. This localises the cytotoxic compounds at the tumour sites where they are released. As important as choosing the antibody, is identifying a suitable releasable linker, which must exhibit stability in the blood plasma to allow for the ADC to get to its target without premature release of the drug. Once internalised by the cell or the tissue site, the linker must be degraded (either hydrolytically, oxidatively or enzymatically) to release the cytotoxic compound. It has been suggested that the withdrawal of ADCs BR96-DOX 11 and Mylotarg® were a result of poor linker stability.

Table 1-3. Features of a selection of antibody-drug conjugates (ADCs) clinically approved or under clinical review. AcBut = 4-(4-acetylphenoxy)butanoic acid

ADC[ref]	Antibody	Drug	Linker bond	Indication	Stage
Brentuximab vedotin (Adcetris®)[211]	Anti CD30	Monomethyl Auristatin E	Valine-citrulline amide bond	Hodgkin's lymphoma, systemic anaplastic large cell lymphoma (ALCL)	Approved (2011)
inotuzumab ozogamicin (Besponsa®)[212]	Anti-(CD)-22	calicheamicin	Hydrazone AcBut	relapsed/ refractory acute lymphoblastic leukemia (ALL)	Approved (2017)
gemtuzumab ozogamicin (Mylotarg®)[213]	Anti-CD33	calicheamicin	Hydrazone AcBut	CD33-positive acute myeloid leukemia (AML)	Approved (2000), withdrawn (2010), reapproved (2017)
Trastuzumab emtansine (Kadcyla®)[214]	Anti-HER2	emtansine (DM1)	thioether	HER2 metastatic breast cancer	Approved (2015)
(IMMU)-110 (hLL1-DOX)[215]	Anti-CD74	Doxorubicin	Hydrazone	Multiple myeloma	Phase I/II
Lorvotuzumab mertansine (IMGN901)[216]	Anti CD56-	Maytansine (DM1)	Disulfide	Multiple myeloma, solid tumours	Phase I/II (2009) Discontinued (2013)

Conjugation of antibodies to single drug molecules as for emtansine (**Figure 1-16**) or to drug carriers such as drug-polymers or nanoparticles,[217] have proven their targeting ability in preclinical trials. However, in the almost 20-year period since the first market entry, only three more ADCs have successfully been clinically registered.[218,219] Reasons for the ADCs not reaching the market include; non-specific release of drug, lack of specific antigen binding after conjugation to drug, insufficient expression of antigen on target cell and insufficient amount of drug released from ADC.

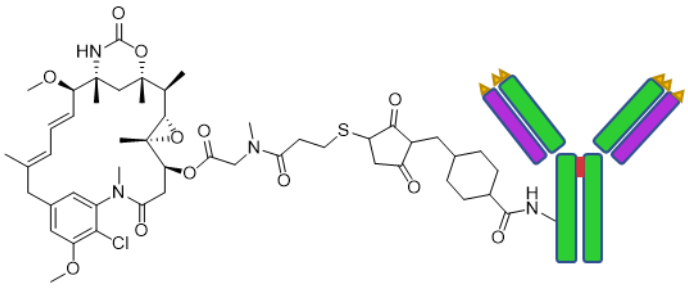

Figure 1-16. Antibody-emtansine conjugate for the targeting and delivery of drug to tumour tissue.

Additionally, the use of antibodies as targeting agents have limitations in respect to their stability. As with all proteins, the 3D-conformation is vitally important, as biological activity is dependent on the tertiary structure of the antibody. Modifying an antibody with a drug-linker, especially with hydrophobic drugs, can result in a greater propensity for protein aggregation. The interactions between the polypeptide chains in an antibody are also sensitive to temperature, pH, oxidative stress and the solvent they are exposed to. The stability of antibodies is limited between a narrow range of optimum conditions which limits the modification and reaction types employed to conjugate the drug.[220] Conjugation of drug compounds can destabilise the structure further which adds to the instability of ADCs which results in a propensity to aggregate upon storage.[221]

Methods to overcome the limitations of antibody targeting have led to the investigation of antibody-fragments (Fabs) as targeting motifs. Antibodies carry out many functions (antigen binding, neonatal Fc receptor binding, aggregation) so their structure is an amalgamation of all the parts necessary to carry out each function. The antigen binding region is relatively small compared to the whole antibody. To harness only the binding functionality, antibodies have been proteolytically cleaved by specific enzymes (e.g. pepsin) to obtain the Fab, which could then be used to conjugate to drug.[222–225] In more commercial settings, the Fabs can be generated recombinantly.[226]

The specificity of peptide-protein interactions, such as that of endothelin to its receptors, is a result of a small amino acid sequence with the large protein. The specificity possessed by the peptide has inspired investigations to find small peptide moieties which selectively bind to a protein target for use as a targeting moiety.[227,228] The use of a highly specific peptide can

circumvent the limitations associated with antibodies by removing any non-essential binding structures. In addition, without a tertiary structure, many peptide targeting moieties are stable and less prone to aggregation.

A downside to the smaller peptidic targeting is rapid clearance from the circulatory system by renal excretion.[161] Peptides have a greater ability to permeate tissues more rapidly, which is less possible with macromolecules. In addition, peptides are susceptible to proteolysis by circulating enzymes.[229] The circulation time can be extended by conjugating the target peptide to a macromolecule.[230] Using a targeting peptide in a polymer drug conjugate may allow active targeting of the pulmonary vasculature to cause localised accumulation of prostacyclin mimetics and restrict their exposure at the IP receptors located elsewhere.

Targeted polymer drug conjugate

The design of a polymer drug conjugate can include; (i) a hydrophilic polymer backbone to increase solubility; (ii) drug bound by a biodegradable linker and: (iii) a moiety which actively targets the desired tissue. As discussed in 1.4.4, the release of the drug compound in the desired tissue relies on the polymer derivative getting into the tissue. The passive diffusion of polymeric structures even aided by the EPR effect is often not sufficient enough to achieve great enough drug concentrations to reach the therapeutic dose. In such instances, active targeting structures may be better employed within the PDC.

Methods to achieve active targeting have employed antibodies and targeting peptides to localise the conjugate and subsequent pay-load release to the desired tissue. The inclusion of targeting moieties as ligands on polymer-drug conjugates have been employed to target various tissues (**Table 1-4**).

Table 1-4. Targeting moieties used in the preclinical trials, including antibodies, peptides and peptidic linkers.

Conjugates	Targeting moiety	Target	Ref
Anti-CD20 Multivalent HPMA Copolymer-Fab' Conjugates	Anti-CD20	B-lymphocyte antigen	231
SP5-52-Lipo-Dox	SVSVGMKPSPRP	Tumor Blood Vessels of Lung Cancer	232
P-(Esbp)-DOX	DITWDQLWDLMK	E-selectin	233
HPMA copolymer-PGE1 conjugates	Gly-D-Asp8	Cathepsin K in bone	234
PAMAM-Ac-FITC-LCTP	RCPLSHSLICY	Lung cancer	235

A targeted-polymer drug conjugate approach for the delivery of treprostinil **4** to PAH would combine many of the approaches discussed so far. The design of such a construct requires consideration of the drug conjugation site, the linker and targeting moiety to be employed, the polymer structure, polymer molecular weight and synthetic route to prepare a polymer treprostinil conjugate.

Only limited information on the PEG-treprostinil conjugates is publicly accessible and no information on using a targeting moiety to target any of the prostacyclin mimetics has been described. Therefore, the design of a target treprostinil polymer conjugate will require investigation into the individual components before a conjugate can be prepared.

Site-specific Implantation

A strategy used to overcome a lack of specificity to the diseased tissue and to avoid large systemic exposure is to physically place or implant the drug in the desired tissue or organ using a device or insert. For example, to help prevent a foreign body response and localised inflammation, drug eluting stents designed to slow the progression of restenosis are coated with a layer of a polymer-loaded with an anti-proliferative compound that is slowly released at the site of stent implantation at the vascular wall achieving a localised anti-proliferative effect.[236,237] A drug-eluting stent is known as a combination device as it has a structural function in addition to drug release.

Patients who have stents inserted are at a greater risk of stent-induced thrombosis, must also take a systemic anticoagulant therapy as a preventative measure.[238] The effect of these treatments on non-target tissues carries the risk of adverse events so localising the anti-proliferative drug release to the site of stent insertion using a drug-eluting stent further reduces the risk of coronary infarction or embolism.[238] Investigations into the formulation of the stent coating, where and how the drug should be loaded, *i.e.* either a homogenous drug layer or loading drug into reservoirs in the stent structure[239] and how to modify the rate and time period of release, have been described.[240]

1.4.4 Drug Linker

Methods to conjugate drug molecules to macromolecules (**Figure 1-17**) must allow linker function to increase blood circulation lifetimes, alter biodistribution, regulate cellular uptake, modify the drug release profile and to reduce unwanted activity e.g. at the administration site. Drug-conjugation can in principle be accomplished using linkers that are either degradable (releasable) or non-degradable (non-releasable).

Figure 1-17. Basic structure of a drug conjugate; where the carrier (C) represents either a polymer or targeting moiety, B represents the biodegradable linker and D represents a drug.

Linker degradation and subsequent drug release can be accomplished by hydrolysis which occurs by one of two mechanisms; auto hydrolysis (catalysed by acid) and enzymatic.[241] Alternatively, in the case of polymer drug conjugates that are inherently active, a non-releasable linker is desirable.

Hydrolytic Cleavage

Non-enzymatic degradation of esters, carbonates and carbamates occur at a slow rate at biological pH (~7.4) but increase with decreasing pH. The linkers employed are often acid-sensitive[242] and many features of linker structure can influence degradation rates.[243]

The use of acid-sensitive linkages has been described to localise release at a tumour site and also within a lysosome for drugs requiring uptake by a cell. Both sites are acidic environments. Acid-labile bonds that have been used include acetals, orthoesters, hydrazones, imines and cis-aconitryl bonds[241] (**Table 1-5**). One example is the hydrazone-linked doxorubicin conjugate 11, investigated for the tumour-specific release of doxorubicin. Following administration, the conjugate is designed to be stable in healthy tissues at pH 7.4, preventing drug release. Upon antibody binding to the tumour, the conjugate is internalised into lysosomes where the pH is lower (~5.5). The bond is cleaved, releasing the cytotoxic payload into the tumour cells. The conjugate exhibit activities similar to free doxorubicin at 1/8th of the dose equivalent and extended the lifetime of tumour-inoculated mice.[244]

Table 1-5. Examples of acid-labile drug linkers employed in pre-clinical investigations. Dox=doxorubicin; mAb = monoclonal antibody; PEG = poly(ethylene glycol); BSA = bovine serum albumin.

Structure	Bond	Description	Ref
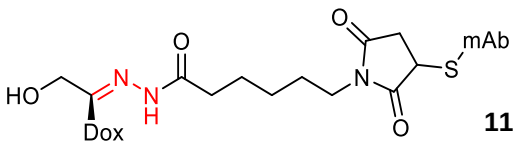 **11**	Hydrazone	Antibody doxorubicin conjugate conjugated by hydrazone	245
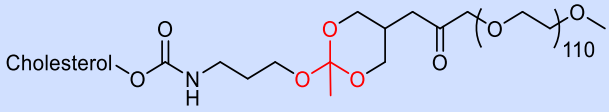	Orthoester	PEGylated cholesterol conjugated by ortho ester	246
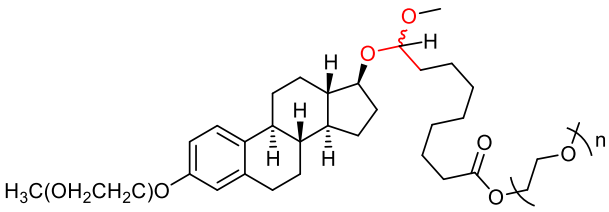	Acetal	Estradiol conjugated to PEG *via* acetal bond	247
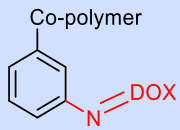	Imine	Polymer-bound doxorubicin conjugated by aromatic imine	248
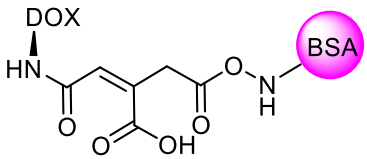	*Cis*-acetonitryl	Doxorubicin conjugated to bovine serum albumin *via* *cis*-acetonitic bond	249

Recently, a silyl di-ether linker was used in an antibody-drug conjugate (**Figure 1-18**) which claimed to possess a slow release degradation profile which could be altered by modification of the silicon side chains to alter the degradation rate.[250] *In vitro* results showed no drug release in solution at pH 7.4, while 80 % of the conjugated drug was released over 72 hours in solution at pH 5. Unlike linkers such as orthoesters, silyl di-ethers do not require strict anhydrous conditions for their synthesis and storage, which make them more practical.

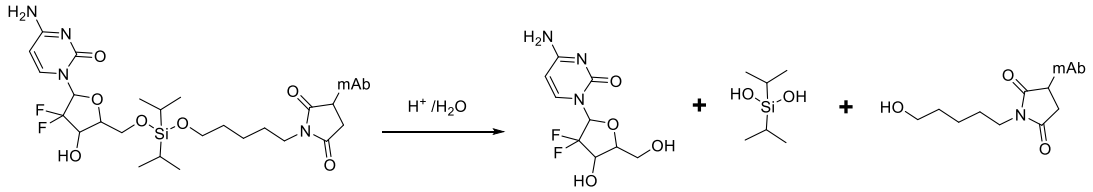

Figure 1-18. Acid sensitive degradation of silyl ether antibody conjugate prodrug to release gemcitabine

Acid degradation offers a simple approach to target drug release in PAH given the acidic nature of the hypoxic lung.[50,251] However, there is limited literature on the exact pH of the pulmonary environment and how localised that environment is. One concern would be that release would be triggered in tissues (such as muscles) by lactic acidosis caused by exercise or in areas of unrelated inflammation.

Enzyme Degradation

Some esters as well as amide bonds (present in peptidyl linkers) are not susceptible (or are weakly so) to non-enzymatic hydrolysis and so require the presence and action of esterases or proteases and peptidases respectively, for drug release. Less specific enzymes cleave their respective bonds providing there is minimal steric hindrance and the compound is hydrated. More specific enzymes require a particular peptide sequence in the linker for cleavage to occur. The specificity of enzymatic degradation can be altered to control and optimise drug release rate and site by careful selection of peptide linker. For example, doxorubicin has been conjugated to HPMA *via* a peptidyl linker specific for cleavage by cathepsin, Gly-Phe-Leu-Gly.[173] Employment of the peptide linker resulted in cathepsin-dependant release which achieved a 4-7 fold increase in doxorubicin concentration in the tumour compared to treatment with free drug.

The upregulation of enzymes and metalloproteases in PAH is understood to occur, so employment of enzyme degradable linkers to activate treprostinil holds potential. Lytic enzymes which are disease-specific may not offer a cleavage method that is easily exploitable. For example, the enzyme matrix metalloprotease (MMP) 9 cleaves its substrate within the chain, between the two amino acids leucine and threonine.[252] Such an enzyme does not facilitate a method of conjugation of a drug that can be released upon enzyme cleavage. Therefore, an exploitable enzyme would need to cleave a peptidyl chain at the terminus of the recognised substrate sequence.

To assist in cleavage, a drug molecule can be bound to its conjugate via a self-immolating spacer molecule to allow release after enzymatic cleavage[253,254] (**Figure 1-19**). Self-immolative spacers can undergo an intramolecular reaction upon a linker reaction or cleavage to release free drug.

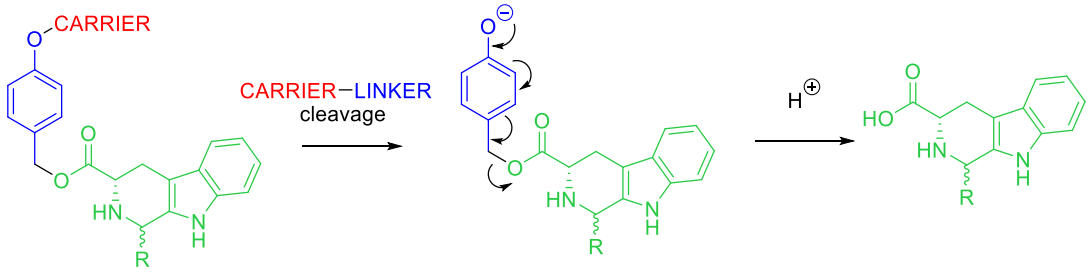

Figure 1-19. Example structure of a Tripartite conjugate undergoing 1,6-elimination to cleave a carboxylic acid terminated drug molecule.[255] involving drug, linker and carrier. Green representing the drug; blue the linker and red the carrier.

Polyvalent approach

An established but less investigated route to utilise a polymer drug conjugate is to employ a polyvalent approach. Polyvalency takes its inspiration from bacterial interactions and antibody binding by conjugating multiple drug molecules to a macromolecule such as polymers, in a manner which retains receptor potency.[256] Upon binding of a carrier-bound ligand to a receptor, the other ligands attached to the conjugate are then in close proximity of other receptors which using a co-operative approach to increase the likelihood of forming a binding interaction with other bound-ligands.[257] Furthermore, some ligand targets are activated by receptor clustering, which can be induced by the polyvalent approach.[256]

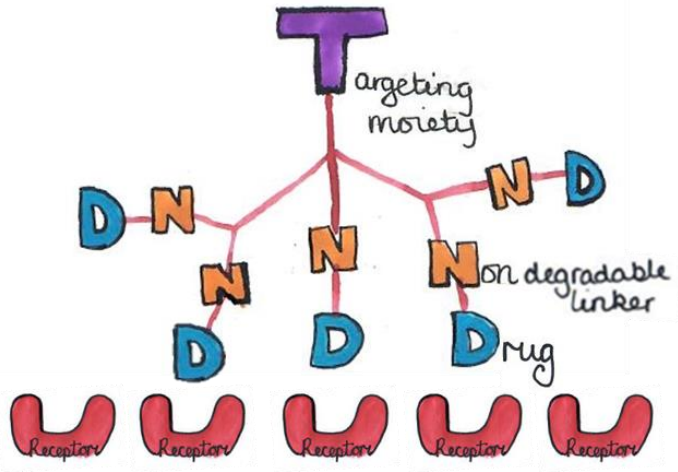

Figure 1-20. Structure of a polyvalent approach which possesses multiple non-cleavable drug molecules on the same structure. The drugs are conjugated without the intention of release as a polyvalent approach requires the drug structures to be active upon conjugation. As the first drug ligand bind to the receptor, other ligands are in close proximity to other receptors which uses a co-operative binding effect in increase lreceptor activation. A targeting moiety can be employed to localise receptor binding.

Drug delivery using polyvalency aims to achieve greater receptor activation by using co-operative binding. Such an approach has been attempted using polymers and liposomes as a carrier and is appropriate to consider when agonism of surface receptors is required.[257] The polyvalent concept for drug delivery has been hypothesised and investigated preclinically, but is yet to demonstrate clinical efficacy.[257,258] A limitation of a polyvalent approach is that it does not necessarily ensure effects are exerted in the correct tissues. A targeted polyvalent carrier may guide the conjugate to the desired site but could become quite complicated to design if a prodrug version was required so that activity was not present when the drug is administered.

1.5 The Project

Prostacyclin mimetic therapy is used clinically to treat PAH in patients that do not respond to initial therapeutic approaches, usually oral. Clinical benefit is established but does not ultimately inhibit disease progression. Furthermore, the burden on patients is considerable owing to the adverse events. Chemical modification of active pharmaceutical agents is a common strategy to optimise therapy efficacy. The project was formed as part of a collaboration with Lung Biotechnology (Silver Spring, USA) who invest heavily in the PAH field and continue to seek new strategies for therapeutic improvements. Through the collaboration, treprostinil 4 sample was donated from their parent company United Therapeutics. Therefore, our approach focused on the improvement of treprostinil use, although the similarities in structure between treprostinil, beraprost and iloprost and to a lesser extent, selexipag, mean that many approaches could be applied to other prostanoid structures.

Treprostinil 4 has proven to be a successful drug clinically, and its multiple mechanisms elucidated, might mean that it offers wider benefits over other single mechanism PAH treatments. Despite a desirable agonist profile (i.e. IP, EP_2, DP_1), treprostinil suffers (like all PMs) from poor specificity for the lung, which causes adverse events and limits the maximum tolerated dose and thus, the efficacy of the treatment. Overcoming the adverse events and increasing tolerability has served as motivation for many attempts to reformulate treprostinil.

1.5.1 Strategies for consideration

Pulmonary Delivery

Delivery of PAH agents such as treprostinil 4 *via* the pulmonary route offers a method of direct organ targeting.[201] Treprostinil and iloprost are available in nebulised form which achieve localised therapeutic effects to the pulmonary vasculature over the systemic circulation.[259,260] The limitation with treatment is the frequency and complexity of the dosing regimen. Furthermore, inhaled treprostinil is less efficacious than parenteral delivery and is therefore delivered as dual therapy.[261] Suggested improvements to decrease the burden of treatment on patients include a portable delivery system and a sustained release formulation to reduce dosing frequency.[262]

Chemical approaches to develop a sustained delivery system could potentially utilise nanotechnologies to create inhalable particles which slowly releases treprostinil over time. The particle would need to exhibit properties to avoid premature clearance from the airways and achieve the correct particle dimensions to enter the alveoli. Treprostinil would be released from the particle allowing it to dissolve and diffuse across the alveolar epithelial cell layer. The particle would then require degradation to facilitate transportation across the epithelial cells to enter the blood stream to be excreted.

The use of nanotechnologies in the lung is applied with caution as many particles have been associated with inducing inflammatory and fibrotic responses.[263] The delivery of nanoparticles to the lung which is affected by an uncontrolled inflammatory pathway initiated in PAH was considered too likely to exacerbate the problem. The occlusion and muscularisation of the small vessels in PAH results in poor transfer of molecules across the alveolar membrane. Requiring a clearance mechanism which relies on the pathways affected by the disease may limit therapy to patients with less progressed PAH. For the reasons discussed, development of a treprostinil formulation delivered by the pulmonary route was ruled out.

Pulmonary Vascular Stent

The localised delivery of agents to the vasculature by insertion of a stent is an attractive concept for treating pulmonary arterial hypertension. Stents are usually used in the coronary arteries,[236] although the insertion of a stent into the pulmonary artery may also be possible. It remains standard practice for patients with suspected PAH to undergo right heart catheterisation for diagnosis.[8] The procedure is invasive and associated with risks, although may offer an opportunity to deliver a drug-releasing implant. Similar to a drug-eluting stent for the prevention of restenosis, a treprostinil-eluting stent could be hypothesised. Unlike the stents currently in the clinic, the stent would not be required for structural purposes, only to release drug in the pulmonary tissue. Treprostinil 4 could be conjugated to a polymer which could then be utilised to coat a stent inserted into the pulmonary artery. Overtime, treprostinil would be released from the polymer and transported into the smaller pulmonary vessels. After total treprostinil 4 had been released from the stent, the stent no-longer holds a purpose. To facilitate a second dose, a second stent would require insertion. Therefore, the stent would need to be biodegradable.[240] Furthermore, the rate of degradation of the stent structure would ideally match the total drug release rate to reduce the time the patient is not receiving a localised drug dose before the next stent is inserted.

A limitation with biodegradable stents is their difficulty in tracing to determine their structure integrity.[240] The main limitation with any insertable device particularly of those which are embedded into the vasculature is the issue in removing them should adverse events occur.[264] Once inserted, the dose and release rate of the drug from the stent is not tuneable. Non-tuneable delivery of treprostinil presents a limitation as PAH patients respond to and tolerate different doses of PMs. Therefore, realistically the dose provided by such a structure would be a baseline dose and more traditional forms of therapy would likely be required. Furthermore,

the drug eluting stent has a fixed dose of therapeutic so would require re-insertions, each of which, causes damage to the artery and imposes the additional risk, cost and burden associated with insertion. For a chronic illness repeated stent insertion did not seem like a better tolerated or less costly, in terms of both time and clinical resources, alternative. The risks associated with inserting a stent into the damaged vasculature of the PAH lung precluded further consideration to examine developing a treprostinil-releasing stent.

Protein binding prodrug

A technique to optimise the systemic lifetime of bioactive compounds includes exploiting interactions with circulating proteins, such as the case of albumin bound paclitaxel an approved treatment for breast, lung and pancreatic cancer.[265] Albumin, makes up 55% of the proteins in blood which makes it an attractive protein to exploit. An alkyl-drug conjugate which binds to albumin could evade clearance by exploiting the abundance of albumin proteins in the blood. By interacting with neonatal Fc receptors, albumin exhibits an extended half-life to 19-21-days. Drugs such as warfarin, diazepam and ibuprofen are able to bind to albumins and remain in the circulation longer than for other small molecules.[158] α-Tocopherol is able to bind to albumin through hydrophobic interactions and has been considered in the conjugation of bioactive compounds to extend their half-lives.[159,160] The concept of conjugating treprostinil **4** to a protein binding moiety such as α-tocopherol could increase the half-life of treprostinil to reduce the frequency of administration, although the distribution of drug across the body would still be wide spread. Furthermore, treprostinil is 90% bound to blood proteins following administration,[266] so an enhanced protein binding derivative may not best exploit the protein binding potential. A method to develop an albumin binding prodrug of treprostinil was therefore not considered further.

Polyvalent approach

A pro-drug conjugate with treprostinil (4) could act as a slow releasable depot and reduce administration site pain and the number of daily doses, however the systemic effects would not be avoided as once treprostinil is released, the activity of treprostinil is no longer local as the circulatory system will distribute the free drug to receptor targets systemically, which will also lead to rapid elimination.[267] In contrast, non-degradable drug polymer conjugates are designed to maintain drug activity upon conjugation via a stable bond designed not to undergo degradation *in vivo*. Non-degradable conjugation of treprostinil would require activity at the IP, EP_2 and DP_1 receptors to be maintained after conjugation but if achieved, localised accumulation of treprostinil in PAH tissue could reduce side effects in the systemic vasculature.

Treprostinil (4) displays a 10-fold decrease in activity when the carboxylic acid is derivatised to an ester, so conjugation through the acid would to be expected to reduce treprostinil activity even further. Although a polyvalent approach might mask this reduction in activity, there would be a need to ensure that treprostinil could also be conjugated with the carboxylic acid groups intact. This leaves conjugation through the hydroxyl groups as other options which are also

required for receptor binding. An alternative route might be to pursue a method of treprostinil derivatisation through parts of the molecule less vital to receptor binding, such as alkylation of the aromatic ring.

Should it be possible to prepare polyvalent treprostinil structures that had some activity, then there would still be the side effects to contend with, e.g. site of administration pain. This could be overcome using a pro-drug approach by employing a degradable protecting group to deactivate the polyvalent treprostinil moieties. Presumably, if treprostinil were conjugated via the aromatic ring then the carboxyl terminus could be derivatised so the activity of treprostinil is restored upon site-specific degradation. A polyvalent strategy would require a prodrug version of a polyvalent treprostinil drug (**Figure 1-21**).

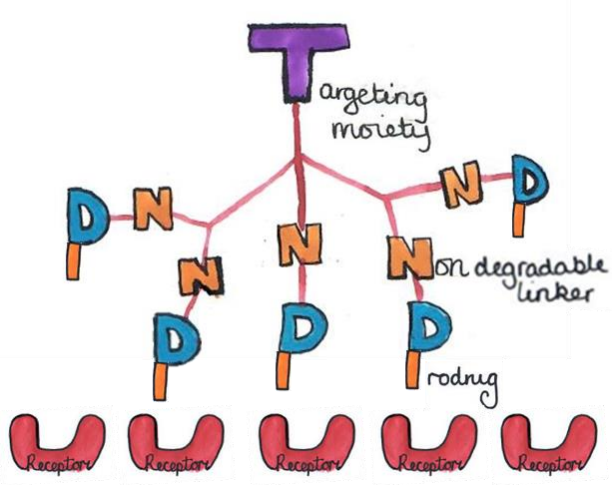

Figure 1-21. Basic structure of a permanently conjugated treprostinil 4 molecule with reduced activity by virtue of a degradable carboxylic acid protecting group

Such an approach would require many separate considerations; validation of a polyvalent approach for treprostinil therapy; macromolecular structure type, size and material; choice of prodrug masking group; conjugation of treprostinil to maintain activity; and finally combining the ideas to synthesise the final compound. Completion of such a venture without any prior results to act as a starting point is is likely beyond the scope of a single PhD project. None-the-less, initial investigations into a polyvalent approach were considered, described in Appendix 8.3.

Antibody targeting

Antibody-drug conjugates offer a method of targeting which has achieved some clinical success.[268] The targeting of treprostinil 4 to the lung using an antibody specific to an antigen expressed exclusively in the pulmonary vessels in PAH can be envisaged. Treprostinil 4 could be conjugated by a cleavable linker which is specific to the PAH lung so that once the ADC binds within the pulmonary vessels, treprostinil is released. The localised delivery of treprostinil would result in a localised therapeutic effect. To achieve such a compound both the antibody and linker require consideration. As described earlier, ADCs have received much attention but

only 4 have entered the clinic in the past 20 years.[219] Finding an antibody for a verified target in PAH and then obtaining and derivatising the structure for an antibody drug conjugate has taken industrial teams decades to achieve so such an approach is likely beyond the scope of a PhD project.

Prodrug

Formation of prodrug derivatives of active pharmaceutical agents is a common procedure used to temporarily impart properties to a drug which can later be modified by a chemical or enzymatic reaction to reveal the active drug.[148,269] A prodrug form of treprostinil 4 could be imagined which would exhibit reduced activity upon administration and once absorbed could then be converted to treprostinil by either hydrolytic or enzymatic degradation. Ideally, the cleavage mechanism, the site of cleavage and the rate of cleavage should be tailored to facilitate prodrug conversion in the PAH lung to achieve site specific drug release.[148,149,270]

A treprostinil prodrug could conceivably have limited activity upon SC administration to reduce local adverse events. The mechanism by which treprostinil is released from the pro-drug structure could be imagined to be degraded by a systemic mechanism to facilitate a slow release and thus, less frequent dosing. Alternatively, the cleavage mechanism could be designed to exhibit specificity for the PAH diseased lung. The limitation of a prodrug approach for the localisation of treprostinil in the treatment of PAH is the non-specific permeation of small molecules into tissues which may still exert prostanoid receptor agonist effects if cleaved.

Polymer drug conjugate

Another prodrug strategy for treprostinil 4 could be to design a polymer-drug conjugate.[165] As previously described, PEG-treprostinil derivatives have been investigated that have shown some activity and degradation preclinically, but failed to reduce adverse events in clinical trials, likely owing to premature release of treprostinil. The suboptimal results published do not suggest that all polymer-drug conjugates will be unsuccessful. None of the published attempts utilised a disease specific degradation mechanism. The choice of the drug linker is a key feature of polymer conjugate design. Therefore, polymer-treprostinil conjugate employing a disease specific linker can be envisaged to improve upon current treprostinil therapy and previous polymeric-treprostinil approaches.

The conjugation of treprostinil 4 to a polymer would be expected to remove treprostinil activity by the act of conjugation. In addition, the macromolecular size of the conjugate is expected to reduce clearance rates to extend biological duration of action. Polymer-drug conjugates are available in a variety of configurations, but it could be imagined that treprostinil could be covalently conjugated to a linear polymer either as a pendant or terminus moiety or within the polymer backbone. For both concepts, a linking moiety is required for treprostinil. The linker must be cleavable. Incorporation of treprostinil within a polymer backbone, requires that the degradable element can be formed either during polymerisation or reside within a monomer.

Polymer conjugation offers many opportunities that can be modified; the choice in polymer, drug loading, conformation of polymer (i.e. linear, branched, dendritic), site of treprostinil conjugation, and size of the conjugate. Furthermore, targeting can be achieved either by careful design of a cleavable treprostinil-conjugation bond or by employing targeting moieties.

1.5.2 Project Aims

The aim of this project is to develop prodrug strategies for treprostinil **4** with the view to reducing the adverse events associated with the use of PMs in the treatment of PAH. Prodrug derivatives reduce the activity of the parent compound and can be optimised to exhibit more favourable biological half-lives and distribution profiles. A benefit of the prodrug strategy is that the cleavage of the prodrug drug, to release active drug, can be tailored to the disease environment, localising the site of drug exposure.

It is hypothesised that a method of reversibly conjugating treprostinil 4 can be developed in a manner that reduces the activity of treprostinil but will degrade to release active treprostinil either (i) once in the systemic circulation or (ii) by a mechanism specific to the disease to localise the activity of therapy. A well-designed prodrug strategy has the potential to decrease adverse events, increase the maximum tolerated dose and reduce the dosing frequency.

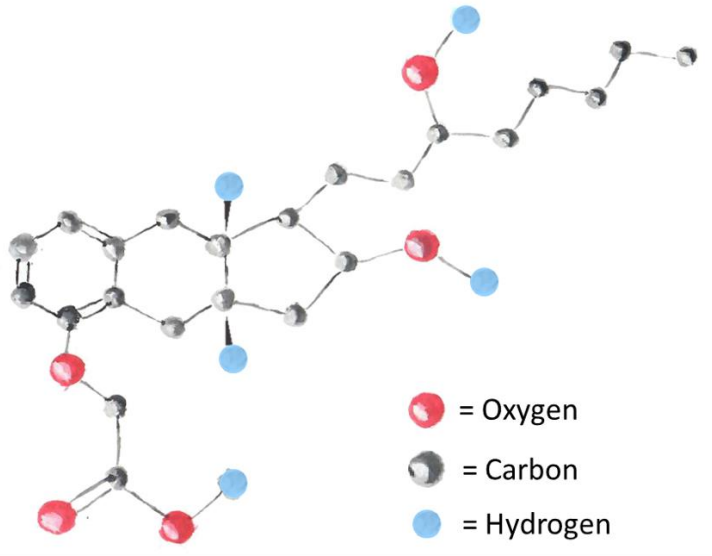

Figure 1-22. Structure of treprostinil **4**, to which this project is focused on improving the delivery for the treatment of pulmonary arterial hypertension (PAH).

Initially, the limitations in current prostacyclin therapies will be quantified using trial data reporting adverse events in the published literature. A meta-analysis of combined data will allow for trends to be identified. Adverse events specific to each prostacyclin mimetic and their biological profiles will be determined. Moreover, the adverse event profiles will and analysed to consider the role in which administration route plays in the differences in tolerability. The results of the meta-analysis will be used to establish the qualities required of a prodrug derivative of treprostinil to overcome adverse events associated with the current formulations.

Chapter 2. Meta-analysis on the adverse events of prostacyclin mimetics.

2.1 Introduction

Pulmonary arterial hypertension (PAH) is a rare but life threatening inflammatory remodelling disease of the small (< 500µm) pulmonary arteries.[271] Pulmonary vascular resistance progressively increases, ultimately leading to right ventricular failure. The aetiology of the disease is unknown, but pulmonary vessels from PAH patients show reduced expression of prostacyclin (PGI_2) synthase leading to reduced levels of prostacyclin as well as downregulation of its classical target, the IP receptor.[272] One consequence of the loss of prostacyclin signalling is promotion of vasoconstriction of the pulmonary circulation. To circumvent a defective prostacyclin pathway, PAH patients are therapeutically targeted by the administration of synthetic prostacyclin (epoprostenol 1) or its stable analogues, such as iloprost 2, treprostinil 4, and beraprost 3. More recently, selexipag 5, a selective IP receptor agonist with a structure not based on prostacyclin, has been approved for PAH treatment.[273] Described collectively as prostacyclin mimetics (PMs, **Figure 1-6**), these agents are able to bind to and activate prostacyclin's native receptor (IP) promoting vasodilatory, anti-proliferative and anti-thrombotic effects, which are likely to contribute to their clinical benefit.[85,144,274–277] However, administration of PMs are associated with adverse events (AEs) in patients, including headache, jaw pain, nausea, diarrhoea, cough, flushing and in the case of subcutaneous formulations, site pain. In general patients that tolerate higher doses derive most benefit, however in a number of patients the maximum tolerated dose is well below the optimal treatment dose.[72]

PMs are also known to activate other prostanoid receptors. Some could contribute to therapeutic efficacy (DP_1, EP_{2+4}), because they couple to Gs and increase cAMP, whilst others may have a negative impact (EP_{1+3}, TP) because they oppose the biological effects of IP receptor activation through activation of Gi and Gq inhibiting cAMP generation and/or raising calcium levels.[85] Different compounds in this drug class have varying affinities for the above mentioned prostanoid receptors, including the IP receptor which may introduce variance in their overall activity (**Table 2-1**). The different receptor affinities of the PMs might therefore be expected to translate clinically to different efficacies, adverse events and tolerability in patients. For example, selexipag and its active metabolite, ACT-333679 has no reported biological activity at other prostanoid receptors.[278] Consequently, it might reasonably be expected to be associated with fewer adverse events.[198,279]

Table 2-1. Binding affinity at human prostanoid receptors (K_i /nM), split into therapeutically beneficial receptors (blue) and therapeutically disadvantageous (green). ND = not determined.

Prostacyclin mimetic[ref]	IP	EP_2	EP_4	DP_1	EP_1	EP_3	TP
Epoprostenol[62]	2	ND	ND	ND	>100	10-40	ND
Iloprost[280]	3.9±0.6	1172±159	212±27	1016±63	1.1±0.3	208±26	6487±29
Treprostinil[280]	32.1±0.2	3.6±0.3	826±116	4.4±0.4	212±56	2505±263	NC
Selexipag[281]	260±20	>10000	>10000	>10000	>10000	>10000	>10000
ACT-333679 (Selexipag metabolite)[281]	20±1	5800	4900	2600	>10000	>10000	>10000
Beraprost[282]	16	>3300	>3300	>3300	>3300	110	>3300

To overcome adverse events and improve the patient's quality of life, a variety of PM formulations have been developed which allow for dosing *via* different administrative routes (**Table 2-2**). Treprostinil **4** and iloprost **2** are available *via* more than one route. Different routes of administration possess inherent limitations and will vary the impact of quality of life for a patient. Additionally, different administrations expose different tissues to the PM which has the potential to cause localised adverse events. The different activity profiles, drug formulations and administration routes of the collective PMs (including synthetic epoprostenol sodium, iloprost, treprostinil sodium, treprostinil diolamine **7**, beraprost sodium, and selexipag), could potentially translate into different clinical responses with varying tolerability. Therefore, the common practice of describing adverse events as "prostanoid" is too generalised to help guide either patients and doctors when choosing therapies or medicinal and formulation scientists when designing new therapies.

Table 2-2. The different clinically approved prostacyclin mimetics are available in different formulations for delivery by different routes of administration.

Prostacyclin mimetic	Route of administration	Description
Epoprostenol	Intravenous	***Flolan*®; Epoprostenol sodium in glycine buffer diluent**
		***Veletri*®; Epoprostenol sodium in sodium chloride diluent**
Iloprost	Intravenous	***Ilomedin*®;** aqueous solution of iloprost trometamol
	Inhaled	***Ventavis*®; Nebulised iloprost trometamol**
Beraprost	Oral	**Beraprost sodium**; Beraprost sodium tablet
Treprostinil	Subcutaneous	**Remodulin®**; Treprostinil sodium in sodium chloride diluent delivered by ambulatory infusion pump *via* catheter under skin
	Intravenous	**Remodulin®**; Treprostinil sodium in glycine diluent delivered by ambulatory infusion pump *via* central venous catheter
	Inhaled	**Tyvaso®**; treprostinil sodium nebulised by portable nebuliser
	Oral	**Orenitram®;** Treprostinil diolamine, extended osmotic release tablet
Selexipag	Oral	**Uptravi®**; Prodrug form, film coated tablet

The primary aim of this thesis is to explore strategies to improve the side effect profile of treprostinil therapy for the treatment of PAH. In order to target the most efficient method to achieve a better tolerated treprostinil therapy, the limitations of current therapies needed to be identified. Although a recent review has qualitatively explored the sources and management of different adverse events,[72] the present analysis sought to investigate the effect quantitatively, using data gathered systematically from published randomised clinical trials.

The primary objective of this systematic review and meta-analysis is to examine the tolerability of PMs. It was hypothesised that the different PMs and routes of administration would affect the AE profile and so this was explored. Furthermore, to appreciate the clinical benefit in the context of adverse effects, relevant outcome measures including: 6MWD, Borg score; haemodynamic parameters; discontinuation and fatalities were meta-analysed.

2.2 Results

2.2.1 Study characteristics

Initial searching highlighted 1802 papers which decreased to 297 after application of the RCT filter and search criteria (**Figure 2-1**). An abstract review identified 35 papers as relevant which

when reviewed in full outlined 15 papers of interest, published between 1990 and 2013, to be analysed. All studies included were multicentre trials. Included studies had a median trial length of 12 weeks, ranging between 8-156 weeks. Patients were given PMs via continuous SC infusion (treprostinil), continuous IV infusion (treprostinil, epoprostenol), repeated daily inhalation (treprostinil, Iloprost) or daily oral administration (beraprost, treprostinil, selexipag).

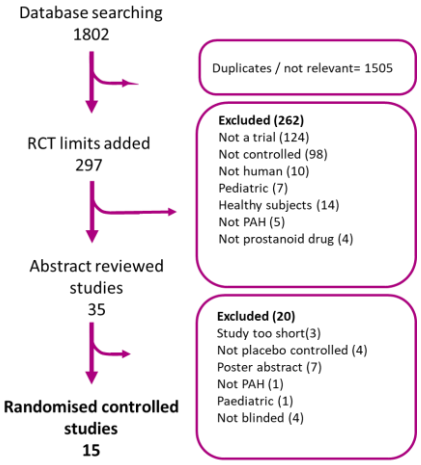

Figure 2-1. Flow diagram of the selection process for identifying relevant trials.

Assessment of the quality of the included papers show relatively high study quality except for a high risk in "other bias" owing to a potential conflict of interest by funding sources (**Figure 2-2**). The high percentage of unclear risk arises from a majority of blinded studies not specifying whether the endpoint assessors were also blinded or not and the treatment of missing data due to high attrition rates. The Barst study for beraprost was a 12-month trial and although outcome data could be obtained after 12 weeks, adverse events were not.[112] Data obtained for adverse event analysis were cumulative data over a 12-month period. Selexipag data from the GRIPHON trial was also obtained after 26 weeks for outcome data but after the end of the trial for adverse event data.[283] This may exaggerate odds ratios for these trials. However, a majority of trials also found that most events occurred in the titration period at the beginning of trials, so we believe the trials to still be comparable.

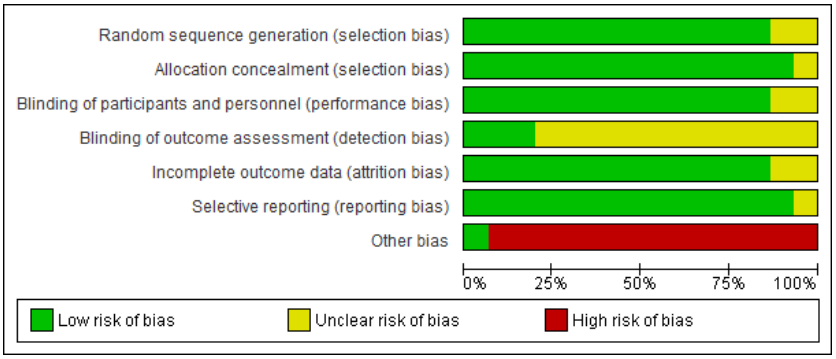

Figure 2-2. Assessment of bias results for the combined trials.

2.2.2 Patient characteristics

Within the studies, a total of 3541 patients were included in the meta-analysis; 1857 treated with PMs and 1684 given placebo. Patients enrolled were mostly female (76%) and of a similar age (mean = 46 years, standard deviation (SD) = 7). The aetiology of PAH of the patients were idiopathic PAH (66%) diagnosed with mostly class II (25%) or class III (68%) PAH. Within individual trials, adjustments for age, gender and disease severity between placebo and treatment cohorts were made. In all but one trial, patients were receiving non-specific therapy, including seven in which patients were also receiving PAH-specific treatment in the form of an ERA and/or a PDE-5i, described as combination therapy. Where necessary, clinical trial reports were referred to obtain data not published in the journal articles. All but one trial reported adverse events. A brief description of the trials basic characteristics is shown in **Table 2-3**.

Maximum daily doses were collected from published trial methods and supplementary materials. When maximum doses were given as per administration, the value was multiplied by the number of administrations per day. Where actual mean doses achieved for subcutaneous and intravenous administrations were not reported, estimates were calculated based on the mean doses reported per kilogram, by multiplying by the average worldwide weight (62kg).[284] To consider the effects of the varying bioavailabilities of the different PMs and different routes of administration, we multiplied the daily dose by the reported bioavailabilities, taken from the packet inserts for each treatment. To obtain a single value, the two reported bioavailabilities for the two doses available for inhaled treprostinil (Tyvaso) were averaged.[128] The dosing information for each trial is shown in **Table 2-4**.

Table 2-3. Summary of trial and patient characteristics. NYHA = New York Heart Association functional class; ERA = endothelin receptor antagonist; PDE-5i = phosphodiesterase -5 inhibitor.

	Study	Drug	Administration	Study length /weeks	Background therapy	Pre-trial therapy	Treatment patients	Control patients	%NYHA class III	% female	Mean age /y
1	Simonneau et al. 2002	Treprostinil	Subcutaneous	12	adjunctive therapies**	30 days no prostanoids	233	236	81	81	44.5
2	McLaughlin et al. 2003	Treprostinil	Subcutaneous	8	none	conventional therapy	15	9			
3	Rubenfire et al. 2007	Treprostinil	Subcutaneous	8	none	Patients must have been receiving epoprostenol therapy for 3 months	14	8	41	86	45.5
4	Hiremath et al. 2010	Treprostinil	Intravenous	12	none	conventional therapy	30	14	95	61	32
5	McLaughlin et al. 2010	Treprostinil	Inhaled	12	Bosentan	bosentan 3 months	115	120	98	81	54
6	Tapson et al. 2012	Treprostinil	Oral	16	PDE-5i and/or ERA	PDE-5 inhibitor and or ERA for 3+ months at a stable dose for 1 month, no prostanoids	174	176	74	82	51
7	Jing et al. 2013	Treprostinil	Oral	12	none	no specific treatments	233	116	66	73	39.4
8	Tapson et al. 2013	Treprostinil	Oral	16	PDE-5i and/or ERA	PDE-5 inhibitor and or ERA for 3 months + at a stable dose for 1 month, no prostanoids	157	153	73	78	54
9	Barst et al. 2003	Beraprost	Oral	52	none	conventional therapy	60	56	47.4	85.3	42
10	McLaughlin et al. 2006	Iloprost	Inhaled	12	Bosentan	bosentan 4 months	34	33	94	79	50
11	Galie et. Al. 2002	Beraprost	Oral	12	none	Not prostanoid treatment for 1 month	65	65	50.8	61.5	45.5
12	Simonneau et al. 2012	Selexipag	Oral	17	ERA and or PDE-5i	Stable dose ERA and PDE-5i for 12 weeks	33	10	60.5	81.4	54.6
13	Sitbon et al. 2015	Selexipag	Oral	156	ERA and or PDE-5i	Stable dose ERA and PDE-5i for 12 weeks	582	574	52.5	79.8	48.1
14	Olschewski et al. 2002	Iloprost	Inhaled	12	none	conventional therapy	101	102	58.6	67.5	52

Table 2-4. Dosing information for each trial. PM = prostacyclin mimetic; BD = two dosings daily; QD = four dosing; * = Mean number of inhalations achieved during trial; + = weight based on international average (59 kg).

Trial	Administration route	PM	Dose per administration	Daily Dosing regime	Bio-availability[ref]	Daily dose /mg
Simonneau et al. 2002	Subcutaneous	Treprostinil	9.3 ng/kg/min	Continuous	1[82]	0.830+
McLaughlin et al. 2003	Subcutaneous	Treprostinil	13 ng / kg/min	Continuous	1[82]	1.161+
Rubenfire et al. 2007	Subcutaneous	Treprostinil	32.2 ng/kg/min	Continuous	1[82]	2.875+
Hiremath et al. 2010	Intravenous	Treprostinil	72 ng/kg/min	Continuous	1[82]	4.769+
McLaughlin et al. 2010	Inhaled	Treprostinil	50 µg	9 inhalations QD	0.78[102]	1.404
Tapson et al. 2012	Oral	Treprostinil	-	-	-	-
Jing et al. 2013	Oral	Treprostinil	3.4 mg	BD	0.17[285]	1.156
Tapson et al. 2013	Oral	Treprostinil	3.1 mg	BD	0.17[285]	1.054
Simonneau et al. 2012	Oral	Selexipag	583 µg	BD	0.49[113]	0.571
Sitbon et al. 2015	Oral	Selexipag	950.4 µg	BD	0.49[113]	0.931
Galie et al. 2002	Oral	Beraprost	80 µg	QD	0.6[286]	0.192
Barst et al. 2003	Oral	Beraprost	71 µg	QD	0.6[286]	0.170
McLaughlin et al. 2006	Inhaled	Iloprost	26.8µg	5.6 inhalations*	0.8[93]	0.120
Olschewski et al. 2002	Inhaled	Iloprost	4.8 µg	7.5 inhalations*	0.8[93]	0.029
Rubin et al. 1990	Intravenous	Epoprostenol	7.1 ng/kg/min	Continuous	1[287]	0.634

2.2.3 Adverse Events

2.2.3.1 Overall, drug type and route of administration

Nine adverse events were significantly increased compared to placebo. Site pain, jaw pain, flushing and headache demonstrated the highest ORs associated with PM therapies (OR 8.7, 4.8, 4.0, 3.6, respectively), although heterogeneity between the results in each subgroup was present, ranging from 0 to 82%, indicating poor agreement in the overall result.

Sub group analysis was performed with respect to PM drug type and administration route. A summary of the results is shown in **Table 2-5** and **Table 2-6**. In brief, the likelihood of site pain was only increased in patients receiving parenteral (IV and SC) treprostinil vs. placebo[89,288–290] (OR = 8.7; 95% CI: 1.6, 45.9; I^2 = 79%). The high heterogeneity (I^2 = 79%) indicates that there is considerable variability in the likelihood of site pain between trials. Furthermore, of the parenteral routes, site pain was most associated with the subcutaneous route of administration (OR =17.5; 95% CI: 11.1, 27.1; I^2 = 0%). Thirteen studies[89,112,127,283,289–295] recorded headache as a common side-effect associated with PM therapies (OR = 3.6; 95% CI: 2.4, 5.4; I^2 = 82%). Although headache was not associated with any particular PM drug type, the strongest association was observed with intravenous treprostinil[290] (OR = 6.0; 95% CI:1.1, 31.5; I^2 not calculated) but in contrast, was not significantly measured for subcutaneous therapy. Vomiting was reported in eight studies[89,127,283,288,289,291,294] and showed a significant increase in patients given PM treatment vs. placebo but again there was significant heterogeneity between studies (OR = 2.5; 95% CI: 1.4, 4.7; I^2 = 79%). Sub-group analysis with regard to vomiting did not reveal any association with PM drug type but was most common with the intravenous route of administration (OR = 6.0; 95% CI: 1.1, 31.5; I^2 not calculated) and was not significantly increased by subcutaneous administration (**Table 2-5**).

Table 2-5. Table showing likelihood of experiencing adverse events during trial period associated with prostacyclin mimetic therapy as meta-analysed by each mimetic (treprostinil, beraprost, iloprost and selexipag). OR = odds ratio; NS = non-significant; CI = confidence interval.

Adverse Event	Overall OR CI I^2, p value	Treprostinil OR CI I^2, p value	Beraprost OR CI I^2, p value	Iloprost OR CI I^2, p value	Selexipag OR CI I^2, p value
Site pain	8.7 (1.6, 45.9) 79%, 0.003	8.7 (1.6, 45.9) 79%, 0.003	-	-	-
Flushing	4.0 (3.0, 5.3) 19%, 0.259	4.4 (2.7, 7.1) 30%, 0.02	5.3 (2.3, 12.1) 49%, 0.16	3.7 (1.8, 7.4) 0%, 0.886	2.7 (1.7, 4.1) 0%, 0.675
Jaw Pain	4.6 (3.6, 5.8) 0%, 0.571	4.0 (2.9, 5.6) 0%, 0.421	8.7 (2.0, 37.2) 50%, 0.159	4.2 (1.6, 10.8) 0%, 0.885	5.0 (3.4, 7.3) 0% 0.356
Headache	3.6 (2.4, 5.4) 82%, 0.000	3.3 (1.6, 6.8) 88%, 0.000	NS 87%, 0.006	2.4 (1.0, 5.7) 49%, 0.161	3.9 (3.0, 5.0) 0%, 0.406
Pain in extremity	2.7 (1.7, 3.5) 0%, 0.480	3.3 (2.2, 4.9) 0%, 0.421	-	NS - , -	2.4 (1.7, 3.5) 0%, 0.354
Diarrhoea	2.6 (2.0, 3.4) 46%, 0.039	2.7 (1.9, 3.9) 47%, 0.079	3.1 (1.4, 7.3) 36%, 0.213	NS - , -	3.1 (2.4, 4.1) 0%, 0.698
Vomiting	2.5 (1.4, 4.7) 79%, 0.000	2.6 (1.1, 6.1) 79%, 0.000	-	-	2.4 (1.7, 3.4) - , -
Arthralgia	1.5 (1.1, 2.2) 0%, 0.788	NS 0%, 0.628	-	-	NS - , -
Nausea	2.2 (1.7, 2.8) 41%, 0.060	2.0 (1.3, 3.0) 63%, 0.012	3.4 (1.7, 6.7) 0%, 0.451	NS 0%, 0.588	2.2 (1.7, 2.9) 0%, 0.386
Peripheral Oedema	NS 59%, 0.024	2.1 (1.2, 3.8) 18%, 0.297	NS - , -	NS 0%, 0.889	NS - , -
Fatigue	NS 50%, 0.062	NS 0%, 0.726	3.6 (1.1, 11.8) - , -	NS - , -	NS - , -
Cough	NS 68%, 0.005	NS 68%, 0.042	-	2.0 (1.2, 3.5) 0%, 0.042	NS 0%, 0.376
Upper respiratory tract infection	NS 6%, 0.382	NS 0%, 0.486	0.5 (0.2, 1.0) - , -	NS - , -	NS 0%, 0.726
Dyspnea	NS 57%, 0.030	NS 59%, 0.046	-	NS - , -	0.7 (0.5, 1.0) - , -

The likelihood of diarrhoea was increased in patients as reported in twelve studies[89,112,127,128,283,289–292,294–296] (OR = 2.6; 95% CI: 2.0, 3.4; I^2 = 46%). Analysis by different drug types revealed a decrease in heterogeneity for the selexipag group (OR = 3.1, 95% CI: 2.4, 4.1, I^2 = 0%), indicating that the results for each selexipag trial are consistent with one another. Diarrhoea was more likely in patients treated with oral PM therapies (OR = 3.3; 95% CI:2.7, 4.0; I^2 = 0%) and not significantly associated with inhaled therapies. Nausea was associated with thirteen studies[89,112,127,128,283,289–296] with moderate heterogeneity (OR = 2.2; 95% CI: 1.7, 2.8; I^2 = 41%). When analysed by drug type, the magnitude was greatest for patients taking beraprost (OR = 3.4; 95% CI: 1.7, 6.7; I^2 = 0%) and was non-significantly associated with iloprost therapy. Eleven studies recorded flushing as an adverse event [112,127,128,283,289,291–296]. Meta-analysis calculated a strong significant increase in OR with limited heterogeneity (OR = 4.0; 95% CI: 3.0, 5.3; I^2 = 19%). Sub-group analysis showed the greatest association with beraprost (OR = 5.3; 95% CI: 2.3, 12.1; I^2 = 49%) and inhaled therapy (OR = 4.7; 95% CI: 2.0, 11.1; I^2 = 26%) compared to the least association with selexipag (OR = 2.7; 95% CI: 1.7, 4.4; I^2 = 0%) and no significant increase for subcutaneous administration. The thirteen studies[89,112,127,128,283,289–296] reporting jaw pain showed a significant association with PMs vs. placebo (OR = 4.6; 95% CI: 3.6, 5.8; I^2 = 0%). This association was greatest for treatment with beraprost (OR = 8.7; 95% CI: 2.0, 37.2; I^2 = 50%) and oral PMs (OR = 5.1; 95% CI: 4.0, 6.7; I^2 = 0%) and lowest for treprostinil (OR = 4.0; 95% CI: 2.9, 5.6; I^2 = 0%) and inhaled administration (OR = 2.7; 95% CI: 1.2, 6.0; I^2 = 14%). Data shown in **Table 2-6**.

Table 2-6. Likelihood of developing each adverse event during trial period associated with prostacyclin therapy as meta-anlaysed by different routes of administration (subcutaneous and intravenous infusion, inhaled formulation and oral tablet/capsule) Odds ratios of adverse events as meta-analysed by route of administration. AE = adverse event; OR = odds ratio; CI = confident interval; NS = non-significant.

AE	Overall OR CI I^2, p value	SC OR CI I^2, p value	IV OR CI I^2, p value	Inhaled OR CI I^2, p value	Oral OR CI I^2, p value
Site pain	**8.7** (1.6, 45.9) 79%, 0.003	**17.5** (11.1, 27.1) 0%, 0.915	**0.7** (0.2, 3.6) - , -	-	-
Flushing	**4.0** (3.0, 5.3) 19%, 0.259	**1.3** (0.2, 7.4) - , -	-	**4.7** (2.0, 11.1) 26%, 0.26	**4.0** (2.9, 5.5) 27%, 0.226
Jaw Pain	**4.6** (3.6, 5.8) 0%, 0.571	**3.1** (1.6, 6.2) 0%, 0.929	NS - , -	**2.7** (1.2, 6.0) 14%, 0.313	**5.1** (4.0, 6.7) 0%, 0.700
Headache	**3.6** (2.4, 5.4) 82%, 0.000	NS 59%, 0.088	**6.0** (1.1, 31.5) - , -	**2.4** (1.0, 5.7) 49%, 0.161)	**5.4** (3.5, 8.2) 73%, 0.001
Pain in extremity	**2.7** (1.7, 3.5) 0%, 0.480	NS - , -	**13.0** (1.5, 112.3) - , -	NS - , -	**2.7** (2.1, 3.6) 0%, 0.418
Diarrhoea	**2.6** (2.0, 3.4) 46%, 0.039	**1.8** (1.2, 2.9) 0%, 0.915	NS - , -	NS 0%, 0.474	**3.3** (2.7, 4.0) 0%, 0.659
Vomiting	**2.5** (1.4, 4.7) 79%, 0.000	NS 12%, 0.322	**6.0** (1.1, 31.5) - , -	-	**2.5** (1.4, 4.7) 85%, 0.000
Arthralgia	**1.5** (1.1, 2.2) 0%, 0.788	-	-	-	**1.5** (1.1, 2.2) 0%, 0.788
Nausea	**2.2** (1.7, 2.8) 41%, 0.060	NS 65%, 0.091	NS - , -	**1.7** (1.0, 2.9) 0%, 0.766	**2.6** (2.2, 3.2) 0%, 0.433
Peripheral oedema	NS 59%, 0.024	**3.8** (1.5, 9.6) - , -	- 	NS 0%, 0.889	NS 45%, 0.141
Cough	NS 68%, 0.005	-	NS - , -	**2.4** (1.6, 3.5) 0%, 0.537	NS 0%, 0.668

The eight studies[127,283,289–291,293–295] reporting pain in the extremity showed significant and homogenous association with PM treatment (OR = 2.7; 95% CI: 1.7 3.5; I^2 = 0%). Pain in extremities was mostly associated with intravenous administration of PMs (OR = 13.0; 95% CI: 1.5, 112.3; I^2 not calculated) but was not significantly associated with subcutaneous and inhaled administrations. Arthralgia was reported in four of the studies[127,283,291,294] featuring only

oral treprostinil and selexipag, and showed a strong increase in OR in the treatment groups with no heterogeneity (OR = 1.5; 95% CI: 1.1, 2.2; I^2 = 0%). Seven studies[89,112,127,283,291,293,296] reported peripheral oedema although on meta-analysis this was not more frequent with active therapy when compared to placebo (OR = 1.3; 95% CI: 0.8, 2.1; I^2 = 59%). However, on sub-group analysis the likelihood of peripheral oedema was only significantly increased for patients treated with treprostinil (OR = 2.1; 95% CI: 1.2, 3.8; I^2 =18%). Subcutaneous administration, which only included treprostinil treatment, was also the only administration route associated with an increase in peripheral oedema (OR = 3.8; 95% CI: 1.5, 9.6; I^2 not calculated).

Fatigue was reported in seven trials[127,128,283,291,293,294] although no significant difference in incidence between placebo and treatment groups with significant heterogeneity was detected (OR = 1.2; 95% CI: 0.8, 1.8; I^2 = 50%). When analysed by PM drug type, heterogeneity was eliminated and a significant increase in OR of fatigue in patients treated with only beraprost was observed (OR = 3.6; 95% CI: 1.1, 11.8; I^2 not calculated). Seven trials reported cough as a side effect,[128,283,290,291,293,295,296] which when meta-analysed, showed no significant difference between treatment and placebo groups (OR = 1.5; 95% CI: 0.9, 2.6 I^2 = 68%). Sub-group analysis only revealed a significant increase in the combined OR of cough for patients taking inhaled PMs (OR = 2.4; 95% CI: 1.6, 3.5; I^2 = 0%) and iloprost (OR = 2.0; 95% CI: 1.2, 3.5; I^2 = 0%). Despite showing no significant correlation in the overall meta-analysis, when compared by PM types, a decreased likelihood for upper respiratory tract infection (URTI) was shown only to be associated with beraprost treatment (OR = 0.5; 95% CI: 0.2, 1.0; I^2 not calculated). A similar decreased association was found for patients experiencing dyspnoea when treated with selexipag (OR = 0.7; 95% CI: 0.5 to 1.0; I^2 not calculated).

2.2.4 Efficacy Outcomes

2.2.4.1 6-MWD, Borg score, haemodynamics and quality of life score

Study interventions were overall effective at increasing 6MWD by 16.3 m (95% CI: 13.0, 19.7; I^2 = 90%). Significant improvements were greatest for intravenously administered drugs (treprostinil and epoprostenol, WMD = 72.4 m; 95% CI: 8.4, 136.4; I^2 = 0%). In comparison, orally administered PMs showed an increase of 15.3 m (95% CI: 11.1-19.5; I^2 = 93%). Overall, patient-reported Borg score was decreased by PM therapies to a limited extent (SMD=-0.3 95% CI: -0.4, -0.1). By subgroup analysis, this was significant for only beraprost[112,292] (SMD = -0.4; 95% CI: -0.6, -0.1; I^2 = 0%). The largest decreased Borg score was measured in trials using intravenous PMs (SMD = -1.0; 95% CI: -1.6, -0.3; I^2 not calculated) although was also observed with oral therapies (SMD = 0.3; 95% CI: -0.6, -9.1; I2 = 0%) but not significantly for subcutaneous and inhaled therapies. Patients receiving monotherapy only[89,128,288,290,293] were also associated with a decreased Borg score (SMD = -0.4; 95% CI: -0.6, -0.1; I^2 = 32%). Four trials monitored quality of life which was increased overall (SMD = 0.2; 95% CI: 0.1, 0.3; I^2 = 0%). When analysed by route of administration, this was only significant for inhaled therapies (SMD = 0.3; 95% CI: 0.1, 0.6; I^2=9%). Mixed venous saturation improvements were shown for inhalation therapies[89,112,288,295,296] (WMD = 2.1; 95% CI: 0.1, 4.0; I^2 not calculated) although a similar non-significant increased trend was observed for subcutaneous (WMD = 2.4; 95% CI: -0.6, 5.4; I^2 = 57%) and oral (WMD = 4.7; 95% CI: -2.2, 11.6; I^2 = 0%) therapies. Data for continuous outcome variables are shown in **Table 2-7** and **Table 2-8**.

Table 2-7. Standardised mean difference of clinical outcomes as meta-analysed by different prostacyclin mimetics (treprostinil, beraprost, iloprost , selexipag and epoprostenol).

	Overall SMD (CI) I^2, p value	**Treprostinil SMD** (CI) I^2, p value	**Beraprost SMD** (CI) I^2, p value	**Iloprost SMD** (CI) I^2, p value	**Selexipag SMD** (CI) I^2, p value	**Epoprostenol SMD** (CI) I^2, p value
6MWD	1.1 (0.6, 1.7) 98%, 0.000	1.2 (0.9, 1.6) 90%, 0.000	0.9 (0.0, 1.7) 90%, 0.002	0.4 (0.2, 0.7) 0%, 0.690	NS 98%, 0.000	NS -, -
Borg Dyspnea score	-0.3 (-0.4, -0.1) 36%, 0.133	NS 60%, 0.040	-0.4 (-0.6, -0.1) 0%, 0.356	NS -, -	NS -, -	-
Quality of Life Score	0.2 (-.1, 0.3) 0%, 0.391	NS 62%, 0.106	NS -, -	NS -, -	-	-
Mixed venous saturation	NS 99%, 0.000	NS 99%, 0.000	NS -, -	0.3 (0.0, 0.6) -, -	NS	-
Right arterial pressure	NS 99%, 0.000	NS 99%, 0.000	NS 0%, 0.875	NS -, -	1.0 (0.2, 1.7) -, -	-
Heart rate	NS 72%, 0.003	0.40 (0.22, 0.58) - , -	NS -, -	NS 55%, 0.136	NS -, -	NS -, -
Cardiac index	NS 99%, 0.000	NS 99%, 0.000	NS 49%, 0.161	-	1.1 (0.4, 1.9) -, -	-

Table 2-8. Standardised mean difference (SMD) of clinical outcomes associated with prostacyclin mimetic therapy as meta-analysed by route of administration. SC = subcutaneous; IV = intravenous; CI = confidence interval; 6MWD = 6-minute walk distance; NS = non-significant odds ratio.

	Overall SMD (CI) I^2, p value	**SC SMD** CI I^2, p value	**IV SMD** CI I^2, p value	**Inhaled SMD** CI I^2, p value	**Oral SMD** CI I^2, p value
6MWD	1.1 (0.6, 1.7) 98%, 0.000	1.1 (0.6, 1.7) 47%, 0.152	0.6 (0.1, 1.1) 0%, 0.584	NS 96%, 0.000	1.4 (0.4, 2.4) 99%, 0.000
Borg Dyspnea score	-0.3 (-0.4, -0.1) 36%, 0.133	NS 17%, 0.300	-1.0 (-1.6, -0.3) -, -	NS 41%, 0.193	-0.3 (-0.6, -0.1) 0%, 0.459
Quality of Life Score	0.2 (0.1, 0.3) 0%, 0.391	NS -, -	-	0.3 (0.1, 0.6) 9%, 0.293	NS -, -
Mixed venous saturation	NS 99%, 0.000	NS 99%, 0.000	-	0.3 (0.0, 0.6) -, -	NS 0%, 0.588
Right arterial pressure	NS 99%, 0.000	NS 99%, 0.000	-	NS -, -	NS 99%, 0.027
Heart rate	NS 72%, 0.003	0.4 (0.2, 0.6) -, -	NS -, -	NS 55%, 0.136	NS 57%, 0.126
Cardiac index	NS 99%, 0.000	NS 99%, 0.000	-	-	NS 66%, 0.052

2.2.4.2 Fatalities and discontinuation from adverse events

Discontinuations due to adverse events were monitored in 11 trials, and occurred in 10 trials.[87,111,112,127,128,283,290,293,297,298] Common adverse events leading to discontinuation were headache, nausea, jaw pain, diarrhoea, and vomiting. Compared to placebo, patients were significantly more likely to discontinue therapy in trials involving orally administered PMs[89,112,127,128,283,288,289,292,293,297] (OR = 2.1; 95% CI: 1.5, 3.0; I^2 = 0%) and was not significantly associated with subcutaneous, intravenous or inhaled administrations. An increased trend was seen for all three of the oral PM trials analysed, although when considering PM type, this reached significance for only selexipag (OR = 2.2; 95% CI: 1.5, 3.3; I^2 not calculated). Mortality was reported in 12 studies but OR could not be calculated for 2, in which no deaths were reported. Therefore, 10 studies were included in the analysis. Although the overall OR was not significant, the intravenous PM group, including treprostinil and epoprostenol, had significantly fewer fatalities in the treatment group than the placebo group during the trials (OR = 0.2; 95% CI: 0.1, 0.9; I^2 = 0%). A similar non-significant trend was observed for inhaled therapies. When analysed by separating into PM type, PMs were not associated with any significant change in likelihood of fatality, lung transplant, rescue therapy and right ventricular heart failure, during the period of observation. Results are shown in **Table 2-9** and **Table 2-10**.

Table 2-9. Different prostacyclin mimetics (treprostinil, beraprost, iloprost, selexipag, epoprostenol) possess different likelihoods of affecting various measures of clinical efficacy as measured by odds ratio.

	Overall OR (CI) I^2, p value	**Treprostinil OR** (CI) I^2, p value	**Beraprost OR** (CI) I^2, p value	**Iloprost OR** (CI) I^2, p value	**Selexipag OR** (CI) I^2, p value	**Epoprostenol OR** (CI) I^2, p value
Discontinuation from adverse event	NS -, -	NS 74%, 0.002	NS -, -	NS -, -	2.2 (1.5, 3.3) -, -	NS -, -
Clinical deterioration	0.4 (0.2, 0.8) 47%, 0.080	NS 65%, 0.036	-	NS -, -	0.3 (0.2, 0.5) 0%, 0.440	-
Fatalities	NS 12%, 0.334	NS 0%, 0.511	NS -, -	NS -, -	NS -, -	NS -, -
Lung transplant	NS 0%, 0.870	NS 0%, 0.610	-	-	NS -, -	-
Rescue therapy	NS 0%, 0.695	NS 0%, 0.488	NS -, -	NS -, -	NS -, -	-
Right ventricular heart failure	NS 0%, 0.485	NS 0%, 0.380	NS -, -	NS -, -	-	-

Table 2-10. The effect of route of delivery by which prostacyclin mimetics are administered on the likelihood of clinical efficacy as measured by odds ratio.

	SC OR CI I^2, p value	**IV OR** CI I^2, p value	**Inhaled OR** CI I^2, p value	**Oral OR** CI I^2, p value
Discontinuation from adverse event	NS 89%, 0.000	NS 46%, 0.175	NS 0%, 0.703	2.1 (1.5, 3.0) 0%, 0.743
Clinical deterioration	NS 88%, 0.004	- 	NS -, -	0.4 (0.3, 0.5) 0%, 0.485
Fatalities	NS -, -	0.2 (0.1, 0.9) 0%, 0.785	NS 0%, 0.863	NS 0%, 0.691
Lung transplant	NS -, -	- 	- 	NS 0%, 0.712
Rescue therapy	NS 0%, 0.866	NS -, -	NS -, -	NS 0%, 0.448
Right ventricular heart failure	NS -, -	- 	NS 4%, 0.309	NS 36%, 0.211

2.2.4.3 Publication bias and heterogeneity analysis

The presence of publication bias was investigated using two methods; Begg's test; Egger's test. Publication bias arises when not all studies conducted are reported. Usually, the results or conclusions of unpublished studies differ from those published. A plot of effect size against sample size allows for a funnel plot to be analysed. The narrower and more symmetrical the plot the more consistent the data is and therefore it is less likely that publication bias exists. The Begg's test subtracts the pooled estimate of effect size by each value of effect size and divides by the standard error of the deviation. The adjusted effect size is correlated with the meta-analysis weight using Kendall's rank correlation coefficient. The Egger's test is a measure of regression of study difference. The log of the odds ratio divided by standard error (difference/SE) is plotted by one divided by standard error (1/SE) and whether the intercept passes through zero is set as the null hypothesis. A p-value less than 0.05 indicates publication bias.

No publication bias was detected for 6MWD (SMD and WMD), Borg score (SMD and WMD), mixed venous saturation (SMD and WMD), right atrial pressure (SMD and WMD), cardiac index (SMD and WMD), heart rate (SMD and WMD), fatalities, rescue therapy and discontinuation due to adverse events using funnel plot symmetry as well as Begg's and Egger's tests. However, these results are only backed up by funnel plots for Borg score, heart

rate and discontinuation. Heterogeneity was not attributed to differences in percentage of patients with class III IPAH, gender or mean age for 6MWD (SMD and WMD), borg score (WMD), fatalities, rescue therapy and discontinuation due to adverse events. Data is shown in **Table 2-11**.

Table 2-11. Meta-regression analysis was carried out to determine the effect of age, gender or aetiology on the outcomes measured.

	Meta-regression	Coefficient	Standard error	p-value
Clinical deterioration	Mean age	0.0590	0.2755	0.8440
	% female	0.1150	0.2858	0.7140
	% IPAH	0.0092	0.1605	0.9580
Adverse event discontinuation	Mean age	0.0236	0.1938	0.9090
	% female	0.0279	0.1082	0.8090
	% IPAH	0.0897	0.0789	0.3190
Fatalities	Mean age	0.0033	0.0620	0.9600
	% female	0.0548	0.0465	0.2920
	% IPAH	0.0217	0.0312	0.5170
6MWD (WMD)	Mean age	0.5621	0.7830	0.491
	% female	0.5230	0.6427	0.437
	% IPAH	0.0094	0.4465	0.984
6MWD (SMD)	Mean age	0.0600	0.6275	0.364
	% female	0.0378	0.0396	0.364
	% IPAH	0.0300	0.0290	0.328
Borg (WMD)	Mean age	0.1440	0.0881	0.350
	% female	0.0729	0.0666	0.472
	% IPAH	0.0606	0.0577	0.485
Borg (SMD)	Mean age	0.0511	0.0266	0.306
	% female	0.6314	0.0329	0.306
	% IPAH	0.0368	0.0260	0.392
Rescue therapy	Mean age	0.1580	0.1148	0.262
	% female	0.0084	0.1104	0.944
	% IPAH	0.0828	0.0680	0.310

2.3 Discussion

The likelihood of experiencing an adverse event within the trial period was explored in this meta-analysis. It was anticipated that the administration route chosen would have some inherent adverse events associated, independent of the compound being administered. For example, subcutaneous catheter would be expected to induce pain and discomfort. To eliminate the inherent effect of each administration, the pain reported for each trial was interpreted as a ratio between the proportion of treatment receiving and placebo receiving groups, by use of the odds ratio. This allowed for a value of the likelihood of an adverse event to be ascribed to each trial and groups of trials, thus removing any inherent effect associated to administration route.

This meta-analysis investigated the effects of different PMs, and route of administration on the likelihood of various side effects in the treatment of PAH. Using subgroup analysis, different trends were identified to help indicate the underlying cause. Here it is demonstrated that the adverse event rate continues to limit dose optimisation in all treatments targeting the IP receptor. Altering the route of administration and the receptor selectivity of PMs, does appear to change the side effect profile, but not to significantly reduce or prevent their overall incidence. The parenteral route of administration is considered the least patient compliant, which was reinforced by our analysis, showing the greatest likelihood of adverse events. However, they were associated with the fewest types of adverse events, and intravenous administration was the only route to decrease the patient Borg Dyspnea score and risk of mortality. On the other hand, oral administration is considered the most convenient form of administration but was found to be associated with the widest variety of adverse events, even in patients treated with a selective IP receptor agonist.

2.3.1 Main findings

The associated AEs significantly increased in PM therapy compared to placebo include; site pain, headache, jaw pain, nausea, vomiting, diarrhoea, nausea, cough, peripheral oedema and arthralgia, although their likelihoods varied greatly, depending on treatment (

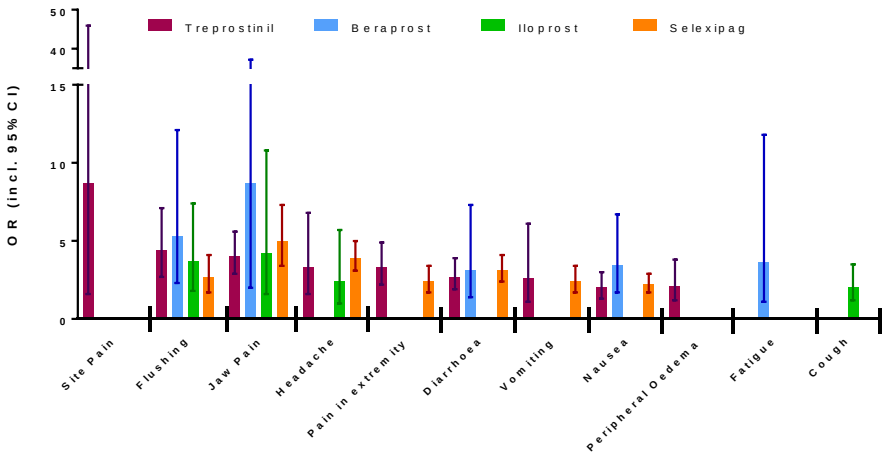

Figure 2-3). Treprostinil, (DP_1, EP_2 and IP agonist) displayed the greatest number of adverse events and was responsible for the most strongly drug associated adverse event, with site pain increasing nine-fold in the treatment group versus placebo. This finding is consistent with other published literature[90] and is in line with clinical reports.[299] Beraprost (IP and EP_3 agonist) showed the least number of AEs but was associated with the largest likelihood of flushing, jaw pain and nausea. Selexipag (selective IP agonist) was associated with the highest likelihood of headache. Only inhaled iloprost (EP_1 and IP agonist) increased likelihood of cough and, despite previous reports,[300] showed no significant increase of gastrointestinal AEs than placebo. Inhaled treprostinil also reported cough, however the analysis between PM type combines the effect of all treprostinil treatments.

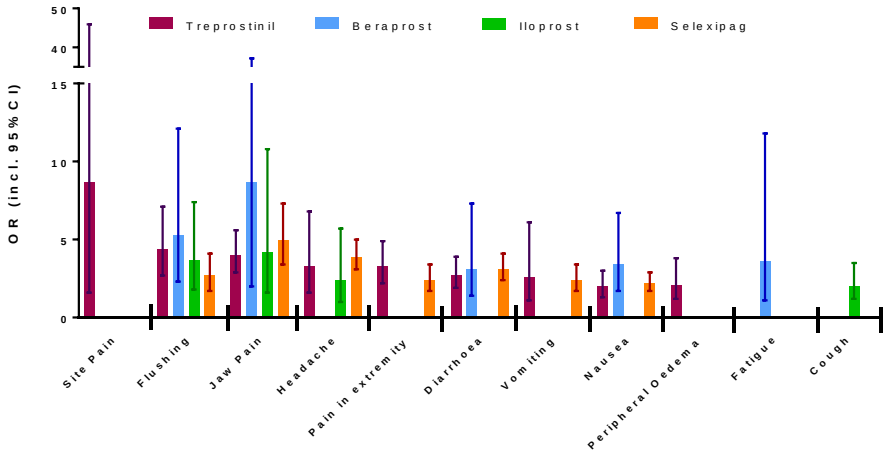

Figure 2-3. Likelihood of developing each adverse event during trial period associated with prostacyclin mimetics (treprostinil, beraprost, iloprost and selexipag) as determined by odds ratio.

In regard to the route of administration, there was association between intravenous administration of PMs and pain in extremities, headache and vomiting. Cough was exclusively associated with inhaled therapies, although flushing, jaw pain, headache, nausea and cough were all significantly increased. Orally administered PMs were associated the greatest number of different AEs, including; flushing, jaw pain, headache, pain in extremities, vomiting, arthralgia and nausea. Adverse events associated with epoprostenol therapy could not be quantified and were therefore not included in the analysis but were described as photosensitivity, loose stools, jaw pain and cutaneous flushing when patients lay on their left side.

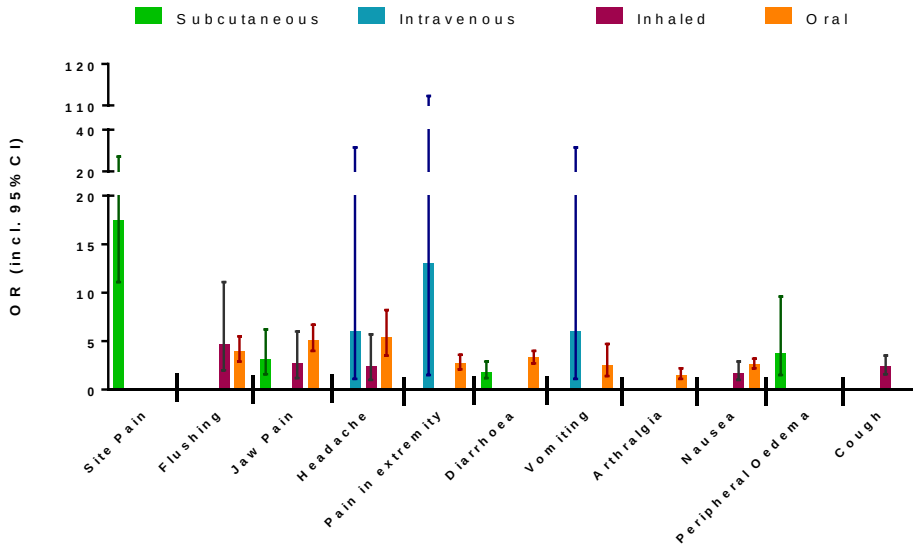

Figure 2-4. Likelihood, measured by odds ratio, of experiencing each adverse event during trial period associated with prostacyclin mimetic therapy as analysed by route of administration (subcutaneous infusion, intravenous infusion, inhaled therapy and oral tablet/capsule).

The increased likelihood of nausea associated with oral route of administration may be attributed to local effects consequent to the route of administration. Gastrointestinal (GI) adverse events may be ameliorated by drug administration strategies. For example, selexipag is administered in its inactive pro-drug form. After absorption and metabolism to its more active form, ACT-333679, it can activate IP receptors with a 10 fold higher potency.[278,281] The pro-drug form was expected to achieve steady blood concentrations and reduce GI AEs,[279] which, in contrast to the selexipag trial reports, may explain the lower likelihood of nausea in patients taking selexipag than other PMs. Conversely, no reduction in vomiting and diarrhoea compared to active PMs was observed, which suggests a systemic underlying mechanism.

Cutaneous flushing was increased in patients taking inhaled and oral PM therapy (

Figure 2-4). Compounds such as nicotinic acid are known to cause flushing by activating the DP_1 receptor, which is found in abundance in the skin. [301–303] The promiscuous activity of some PMs at different prostanoid receptors, makes it possible for the flushing effect experienced in PAH therapies to be in part driven by the DP_1 receptor. Upon inhalation and subsequent exhalations of PMs, they may come into contact with the skin surrounding the mouth, leading to a flushing effect. Flushing effects were prevalent for the treprostinil group, which has the most potent DP_1 activity, but less prevalence for the selexipag group, which has no reported DP_1 activity.[62] Conversely, oral beraprost and selexipag are also associated with flushing, despite having little or no potency at the DP_1 receptor (beraprost; K_i>10 μM and selexipag metabolite; Ki = 2.6 μM).[278,280] Treatment with epoprostenol reportedly causes cutaneous flushing when patients lay on their left side. Affinity of epoprostenol at the DP1 receptor has not been established, owing to the instability of epoprostenol. This opens the possibility that

the IP receptors drive the effect but might combine with the DP_1 receptor to produce a greater effect. Furthermore, the low association of facial flushing with subcutaneous administration, which achieves near-constant blood concentrations, could also suggest flushing to be associated with DP_1 and/or IP receptor agonism in response to fluctuations of drug in the blood, or might indicate receptor desensitisation. Affinity for epoprostenol at the IP and EP_2 receptors are established (**Table 2-1**). Treatment with epoprostenol is associated with photosensitivity, which is implicated with the EP_2 receptor,[304] although this effect is not reported in other PMs notably treprostinil, a potent EP_2 agonist.

Treprostinil is the only drug in this analysis to be administered parenterally, and hence, was the only PM to be associated with site pain. Additionally, treprostinil was the only PM to show an increase in peripheral oedema, which is particularly likely when administered subcutaneously. This may be a consequence of the vasculature in the skin being rich in IP, DP_1, EP_2 and EP_4 receptors, all of which are linked to inflammatory reactions within the skin and to which treprostinil will bind with variable affinity. Furthermore, activation of EP_2 receptors induce skin irritation upon UV exposure.[304,305] Whether this is a unique side-effect to treprostinil is unknown, although could be further investigated with subcutaneous administration of other PMs. Our results suggest that on-going trials into prodrug formulations[306] and implantable pumps[307] for treprostinil are likely to possess a significant reduction in pain at the implantation site due to the reduction in skin tissue contacting active drug.

There is considerable interest and clinical need for upfront combination therapies and clinical evidence suggests a clear benefit to combination PAH therapy.[308–310] This meta-analysis shows ERAs and PDE-5i given alongside PMs were associated with increased headache and vomiting.

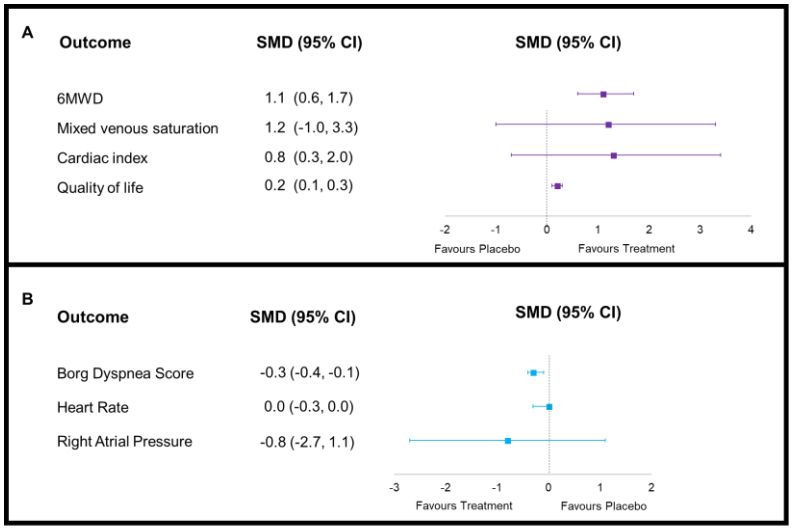

Figure 2-5. Forrest plots of overall meta-analysed outcome data for prostacyclin mimetic therapy as determined by standardised mean difference (SMD), where A) an increased value favours treatment and B) a decreased value favours treatment. CI = confidence interval; 6MWD = 6-minute walk distance

Patient experience was interpreted using patient reported outcomes. The decrease in Borg score suggest patients experienced symptomatic relieve overall during the trials. However, the decrease was modest and when analysed by sub group by PM type, was only significant for patients receiving beraprost. Orally administered PMs were associated with a modest improvement; however, the most significant change was seen for those administered intravenously. Quality of life scores were measured using one of two questionnaires (Minnesota Living with Heart Failure Questionnaire or EuroQol visual-analogue scale) and showed an increase with inhaled therapies but not oral PMs, which is considered the administration route with the least patient burden. Limited changes in quality of life scores indicate that the benefits associated with more favourable treatment options are still hindered by treatment impact on day-to-day living.

Discontinuation of treatment due to AEs is an indicator of tolerability. Our study found no overall significant increase in likelihood of discontinuation with PM therapies. However, selexipag was associated with a greater tendency for discontinuations, reported to be caused by headache, diarrhoea and nausea in these trials.[283] When analysed by administration route, oral PMs also showed an increased likelihood of discontinuation. This may suggest a mechanism dependant on route of administration. As selexipag is a selective IP agonist, these results may further suggest that discontinuation in some cases may also be caused by adverse events driven by the IP receptor.

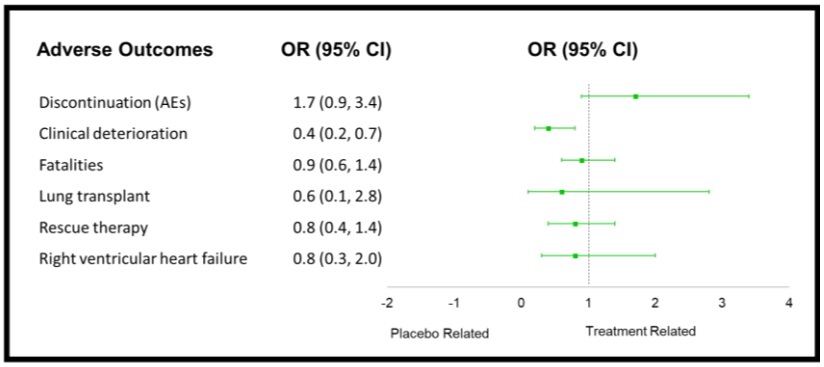

Figure 2-6. Forest plot showing the overall changes in efficacy measures of prostacyclin mimetic therapy as determined by odds ratio (OR).

6MWD is a cheap, easy and well-tolerated, standardised test to measure symptomatic improvement. Indeed, most of the therapies included gained approval based upon their ability to improve walking distance. 6MWD was reported for all the studies included in this analysis. PM therapy is effective at improving 6MWD in patients compared to placebo controls. This effect was greater for IV, consistent with previous meta-analysis.[311] Although debates surrounding its validity as a measure of disease severity,[312313] it was found that PMs improved 6WMD by 16.3 m, less than previously calculated,[69,314,315] and less than the reported minimal important distance (33 m)[316] or distance associated with clinical benefit (41.8 m).[317] The relevance in using 6MWD has recently been under question.[318] Although some trials have shown improved survival outcomes with improved 6MWD,[319] others have shown no correlation

between 6MWD and survival rates and long-term outcomes such as time to clinical worsening.[313] Furthermore, a relationship between baseline 6MWD has been shown to be a better marker predictor of mortality than change in 6MWD.[320]

A statistical difference in mortality between treatment and placebo group was only found for intravenously administered PMs. However, the few deaths reported, short trial periods and the intervention of rescue therapy, limits the accuracy of this trend

All treatments were effective at improving exercise proficiency although none avoided the burden of adverse events. Sub-group analysis identified that administrative route had as much effect on the type and severity of AE reported as the PM type and a greater effect on quality of life improvements. The variation in AEs with different administration route indicates that a many of the effects are caused by local activation of receptors. Other AEs were similar across all administration routes, indicating that the systemic exposure of drug is the cause. Surprisingly, selectively activating the IP-receptor did not alter the AE profiles, implicating the IP receptor is predominantly driving the AEs.

2.4 Secondary meta-analysis: Treprostinil

The main limitation with the analysis conducted is the inability for drug compounds, i.e. treprostinil, to be analysed by individual route of administration, additional to the drug compound. Therefore, the analysis conducted includes an average of either all treprostinil data, regardless of the administrative route or all therapies of one administrative route (i.e. “oral” subgroup includes beraprost, oral treprostinil and selexipag). Therefore, a secondary meta-analysis was conducted focusing only on treprostinil trials. Analysis of treprostinil trials provides an opportunity to explore the effect of administration route of one compound which would more accurately quantify the administration effect. The secondary investigation into treprostinil was carried out to explore the following aims;

1) To better compare the effects of administration route on adverse event data
2) To retrospectively compare the results with the general trends identified in the prostacyclin mimetic analysis.
3) To explore the effect of an IP selective agonist and prodrug formulation on AE outcomes.

2.4.1 Results

Selecting only the trials involving treprostinil, a total of 1684 patients were enrolled in these studies; 891 were treated with treprostinil and 793 given placebo, additional to any predefined background therapy. Patient groups were comparable in terms of patient characteristics and within individual trials were adjusted for age, gender and disease severity between placebo and treatment cohorts. The aetiology of the majority of patients was idiopathic, familial or associated PAH and were in NYHA class III. In half of the trials patients were receiving non-prostanoid PAH-specific treatment concomitantly, ERAs or PDE-5i. An overview of the trial

characteristics is shown in **Table 2-12**. The primary end point was 6MWD in all but one trial where 6MWD was observed but the time to clinical worsening was the primary end point. Other outcome measures reported included Borg score, haemodynamic effects, clinical worsening and fatalities. All trials reported adverse events and where available, the clinical trial report was referred to in order to obtain unpublished information.

Table 2-12. Summary of treprostinil trial and patient characteristics. 6MWD = 6-minute walk distance; IPAH = idiopathic pulmonary arterial hypertension; NYHA = New York Heart association functional class; Specific therapy includes endothelin receptor antagonists and phosphodiesterase 5-inhibitors; Non-specific background therapy includes oxygen, oral vasodilators, calcium channel blockers, anticoagulants and digoxin.

Trial	Administration Route	No. treatment	No. Placebo	Primary end point	Background Therapy	Eitology (IPAH : disease associated PAH)	NYHA Class	Length of study /weeks
Simonneau 2002	Subcutaneous	233	236	6MWD	Non Specific	IPAH (58%) / Disease associated (42%)	II/III/IV	12
McLaughlin 2002	subcutaneous	17	9	6MWD	None	IPAH (73%) / Disease associated PAH (27%)	III / IV	8
Rubenfire 2007	Subcutaneous	14	8	time to clinical deterioration	Specific	IPAH (73%), Disease associated PAH (27%)	I, II, III	8
Hiremath 2010	IV	30	14	6MWD	Non Specific	IPAH (95%) / Disease associated PAH (5%)	III / IV	12
McLaughlin 2010	Inhaled	115	120	6MWD	Specific	IPAH (56%) / Disease associated PAH (44%)	III / IV	12
Jing 2012	Oral	151	77	6MWD	None	IPAH (75%) / Disease associated PAH (25%)	I/II/III	12
Tapson 2012	Oral	174	176	6MWD	Specific	IPAH (66%) / Disease associated PAH (34%)	I/II/III/IV	16
Tapson 2013	Oral	157	153	6MWD	Specific	IPAH (65%)/ Disease associated PAH (35%)	II/III/IV/ unknown (2)	16

2.5 Adverse Events

A meta-analysis of the likelihood of each adverse event was carried out to establish whether there was in significant increase in adverse events as a direct result of treprostinil, or if the route of administration also played a role in the events recorded. Overall, there were 19 side effects reported, out of which nine were significantly related to treprostinil (site pain, flushing, jaw pain, headache, pain in extremity, diarrhoea, vomiting, peripheral oedema, nausea) and the remaining 10 were not (dizziness, upper respiratory tract infection, insomnia, abdominal pain, arthralgia, fatigue, palpitations, chest pain, dyspnoea, cough). In terms of magnitude, the presence of any adverse event was ten times more likely in the treprostinil over placebo [OR 10.3, (95% CI: 1.1, 92.8), p = 0.038; I^2 = 51 %, p = 0.128] while site pain, flushing, jaw pain and headache were most the most likely AEs associated with treprostinil therapy (OR 8.7, 4.4, 4.0, 3.3, respectively). However, heterogeneity was invariably present ranging from 0 to 88 %.

2.6 Sub group analysis

To further investigate the effect of administration route on the overall likelihood of adverse event, the trial data was split into individual administration routes. Intravenous administration was significantly associated with headache, extremity pain and vomiting (OR = 6.0; 95% CI: 1.1, 31.5; I^2 = Not calculated), (OR = 6.0; 95% CI: 1.5, 112.3; I^2 = Not calculated), (OR = 13.0; 95% CI: 1.1, 31.5; I^2 = Not calculated), respectively. Flushing was most significantly attributed to inhaled treprostinil (OR = 20.6; 95% CI: 2.7, 157.9; I^2 = Not calculated). Unsurprisingly, the greatest odds ratio was seen for site pain associated with subcutaneous administration (OR = 17.5; 95% CI: 11.1, 27.4; I^2 = 0%). Jaw pain, diarrhoea and peripheral oedema were also increased by subcutaneous treprostinil. Patients receiving oral treprostinil experienced the most types of adverse events including flushing (OR = 4.6; 95% CI: 3.2, 6.6; I^2 = 0%), headache (OR = 6.5; 95% CI: 3.4, 12.4; I^2 = 76%), pain in extremities (OR = 3.1; 95% CI: 2.0, 4.8; I^2 = 7%), diarrhoea (OR = 3.6; 95% CI: 2.7, 4.9; I^2 = 0%) and nausea (OR = 3.0; 95% CI: 2.2, 4.0; I^2 = 8%).

Table 2-13. Likelihood of developing each adverse event during trial period associated with treprostinil therapy as analysed by each route of administration. AE = adverse event; OR = Odds ratio; NS = not significant.

AE	Overall OR	p-value	No. studies	Oral	Inhaled	Intravenous	Subcutaneous
Any event	10.3 (1.1-92.8) 51%, 0.128	0.038	3	26.2 5.1, 135.4 0%,	-	NS -,- -	-
Site pain	8.7 1.6, 45.9 79%, 0.003	0.011	4	-	-	NS -,- -	17.5 11.1, 27.4 0%
Flushing	4.4 2.7, 7.1 30% 0.222	< 0.0001	5	4.6 3.2, 6.6 0%	20.6 2.7, 157.9 -	-	NS -,- -
Jaw Pain	4.0 2.9, 5.6 0%, 0.421	< 0.0001	7	4.9 3.3, 7.4 0%	NS -,- -	NS -,- -	3.1 1.6, 6.2 0%
Headache	3.3 1.6-6.8 88%, 0.0001	0.001	7	6.5 3.4, 12.4 77%	-	6.0 1.1, 31.5 -	NS -,- 59%
Pain in extremity	3.3 2.2, 4.9 0%, 0.412	< 0.0001	5	3.1 2.0, 4.8 7%	-	13.0 1.5, 112.3 -	NS -,- -
Diarrhoea	2.7 1.9, 3.9 47%, 0.079	< 0.0001	7	3.6 2.7, 4.9 0%	NS -,- -	NS -,- -	1.8 1.2, 2.9 0%
Vomiting	2.6 1.1, 6.1 79%, 0.0001	0.024	7	NS -,- 90%	-	6.0 1.1, 31.5 -	NS -,- 12%
Peripheral Oedema	2.1 1.2, 3.8 18%, 0.297	0.013	3	NS -,- 0%	-	-	3.8 1.5, 9.6 -
Nausea	2.0 1.3, 3.0 63%, 0.012	0.002	7	3.0 2.2, 4.0 8%	NS -,- -	NS -,- -	NS -,- 65%

Table 2-14. Non significant likelihoods of developing each adverse event during trial period associated with treprostinil therapy as analysed by each route of administration. AE = adverse event; OR = Odds ratio; NS = not significant.

AE	Overall OR	p-value	No. studies	Oral	Inhaled	Intravenous	Subcutaneous
Dizziness	NS -,- 0%, 0.625	0.172	7	NS -,- 53%	NS -,- -	NS -,- -	NS -,- 0%
Upper respiratory tract infection	NS -,- 0%, 0.486	0.923	4	NS -,- 0%	NS -,- -	-	NS -,- -
Insomnia	NS -,- 0%, 0.919	0.131	3	NS -,- 0%	-	NS -,- -	NS -,- -
Abdominal pain	NS -,- 0%, 0.693	0.579	3	NS -,- -	-	-	NS -,- -
Arthalgia	NS -,- 0%, 0.628	0.129	3	NS -,- 0%	-	-	-
Fatigue	NS -,- 0%, 0.726	0.159	4	1.5 1.0, 2.2 0%	NS -,- -	-	-
Palpitations	NS -,- 72%, 0.028	0.595	3	NS -,- 79%	NS -,- -	-	-
Chest pain	NS -,- 3%, 0.357	0.948	3	NS -,- -	NS -,- -	NS -,- -	-
Dyspnoea	NS -,- 59%, 0.046	0.830	5	NS -,- 87%	NS -,- -	NS -,- -	NS -,- -
Cough	NS -,- 68%, 0.042	0.372	3	NS -,- -	2.8 1.7, 4.9	NS -,- -	-

2.6.1 Discussion

The analysis highlighted the same nine adverse events associated with PM therapy as significantly related to treprostinil treatment; site pain, flushing, jaw pain, headache, pain in extremity, diarrhoea, vomiting, peripheral oedema and nausea. Adverse events which were reported but not found to be significant either at meta-analysis or sub-group analysis level, suggests the cause is a direct consequence of the administration and not specific to treprostinil therapy.

Patients receiving intravenous administration of treprostinil received the greatest dose, yet patients experienced minimal site pain, presumably because fewer tissues were exposed to treprostinil entering the circulatory system. In the earlier period of intravenous PM therapy, catheter-related complications caused by infection, were common with IV administration,

particularly in tropical environments although indwelling catheters have improved over the years to minimise the risk. Such events were described in the trial but not included in our statistical analysis. However, it is well understood that intravenous infusion is the least convenient method of drug delivery due to the reliance on the healthcare professionals and the risk of serious infection without maintenance procedures.

The localised pain when treprostinil is subcutaneously administered appears to be a reaction of treprostinil with localised tissue. The role of prostanoid receptors such as EP_2, EP_4 and DP_1 in the swelling, irritation and inflammation of skin has been documented.[304,305] The increase in flushing associated with only inhaled treprostinil is likely explained by the nebuliser of Tyvaso. It is possible that during inhalation and the subsequent exhalations, the skin surrounding the mouth and nose are exposed to small particles of active drug. Treprostinil is a known DP_1 receptor agonist found in skin which has been implicated in heat and flushing reactions.[305] It seems plausible that the flushing effect seen in patients taking inhaled treprostinil is mediated by the local activation of DP_1 receptors, which treprostinil activates at a 10-fold lower concentration than the IP receptor [280]. The significant but weaker association between oral treprostinil and flushing might be explained by this theory if residual treprostinil remains on the skin of fingers after capsule administration which is further spread by touching other areas. However, as oral and inhaled treatments are both associated with fluctuating drug blood-concentrations, the variance in drug concentrations experienced between dosings may also contribute to the prevalence of flushing. Thus, when a steady concentration is maintained by continuous infusion, flushing is reduced.

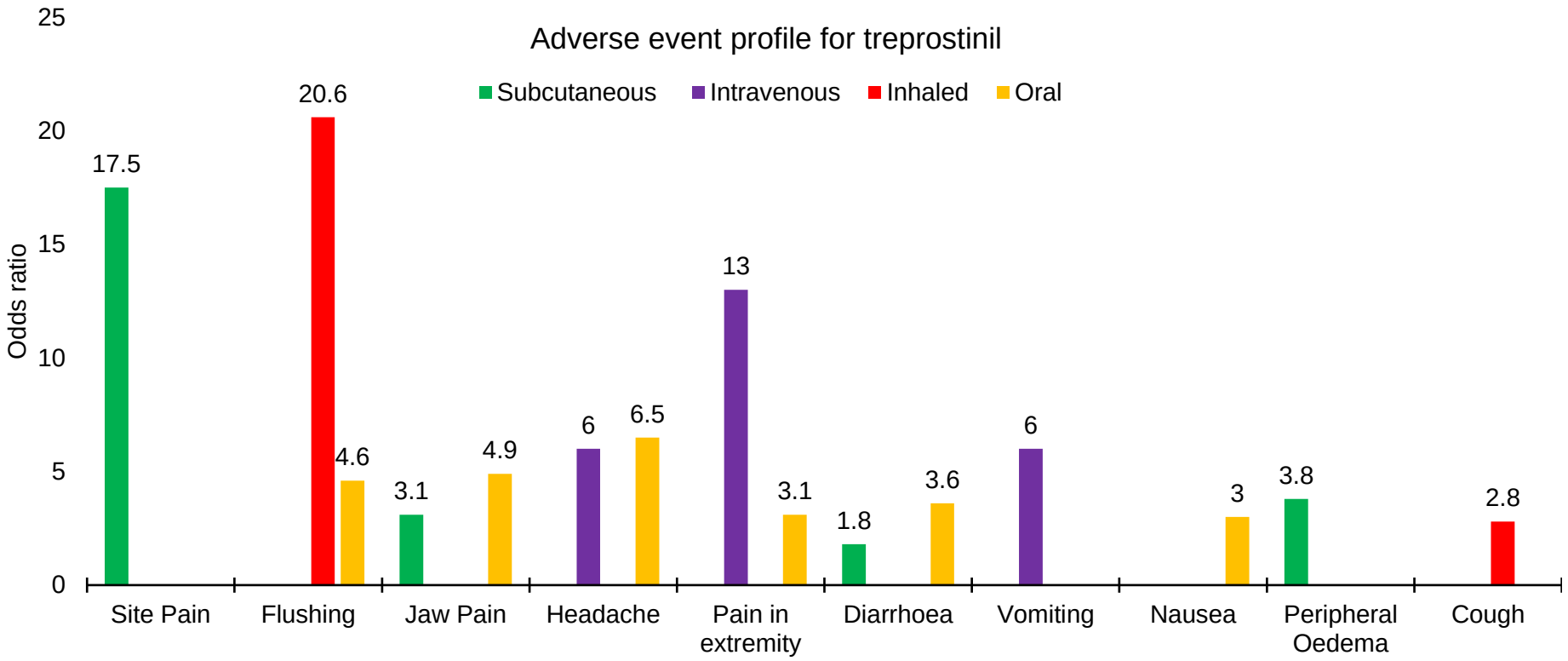
Adverse event profile for treprostinil
Subcutaneous
Intravenous
Inhaled
Oral
Odds ratio
25
20
15
10
5
0
17.5
20.6
4.6
3.1
4.9
6
6.5
13
3.1
1.8
3.6
6
3
3.8
2.8
Site Pain
Flushing
Jaw Pain
Headache
Pain in extremity
Diarrhoea
Vomiting
Nausea
Peripheral Oedema
Cough

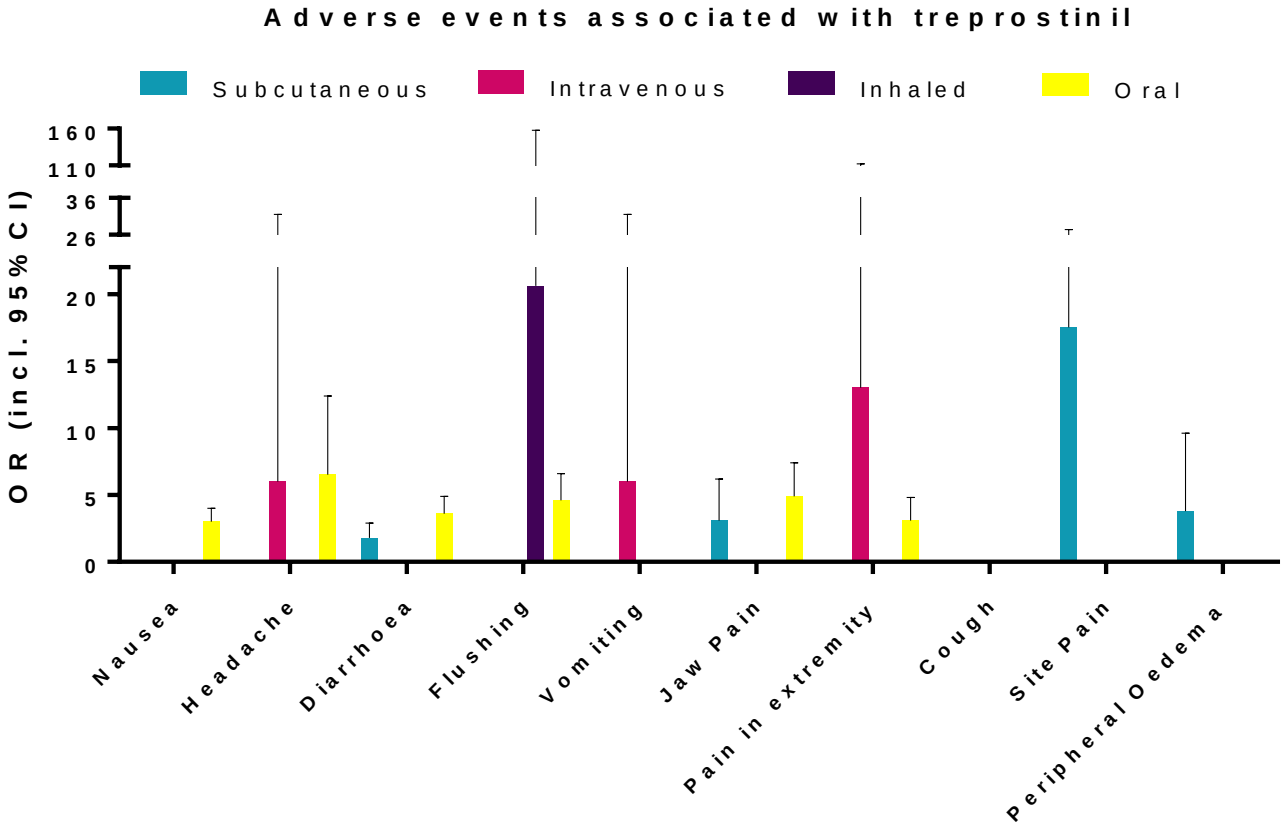

Figure 2-7. Adverse event profile for treprostinil as analysed by routes of administration

Of the treprostinil therapies, only oral administration significantly increased cases of nausea suggesting that the local interaction of treprostinil with the gastrointestinal tract results in nausea. However, the association of nausea with selexipag treatment suggest that a systemic action also contributes, as the stomach tissue is exposed to the less active prodrug. Selexipag does have affinity for the IP receptor in its prodrug form, so nausea may be a result of the relative concentrations of selexipag prodrug and treprostinil released from the osmotic capsule found within the stomach. If the rate of absorption into the blood stream is comparable to the dissolution or capsule release time, then the short residence time may reduce local activation of prostanoid receptors. Interestingly, the trend for vomiting does not match that of nausea as vomiting was not associated with oral treprostinil but was with selexipag.

Diarrhoea and jaw pain show a similar pattern in that they are both associated with SC and oral treprostinil. This overlap rules out the possibility that high doses or fluctuating drug blood concentrations explain the side-effects. In the case of diarrhoea, direct activation of local receptors is also rejected. This suggests that both events are caused by systemic exposure of treprostinil, which is backed up by the lack of association when given by inhalation. Both adverse events were reported with high OR for IV administration but were not found to be significant, which may be a result of IV administration being represented by only one trial.

Only intravenous administration caused a significant increase in vomiting. With similar systemic exposure, bioavailability and final mean daily dose, it is surprising that this trend was not also seen for subcutaneous administrations. This may be a result of the rate of dose escalation. IV trial patients were initiated onto treprostinil at 3 times the starting concentration as the SC trial[89] and yet had the lower incidence of vomiting. For IV infusion, the dose was increased by 8 ng/kg/min per week with a maximum permitted dose of 100 ng/kg/min, with patients tolerating a mean dose of 72 ng/kg/min.[290] The Simonneau SC trial did not however specify a dose increase rate but the maximum dose was less than a quarter of the IV trial, at 22.5 ng/kg/min. Another SC trial[288] not included in this study, shared a similar initiation dose range at the IV trial (2.5-5.0 ng/kg/min) but had a maximum allowed dose of 20 ng/kg/min. One of the SC trials differed in its design as it involved a weaning period from epoprostenol, onto treprostinil. [87] The dose of treprostinil at transition was reported at 25.3 ng/kg/min and the mean maximum dose tolerated by patients was 32.2 ng/kg/min. Although the mean daily doses are comparable, with a maximum of 4.8-fold difference, IV is administered at a greatest dose, so it is possible that the dose crosses a concentration threshold which induces vomiting systemically.

Extremity pain was increased in trials involving both IV and oral treprostinil, although to a greater extend with the former. It is unlikely that fluctuating drug blood concentrations are the cause, as IV achieves steady-state concentrations. Systemic exposure of treprostinil or the difference in achieved daily dose may provide an explanation, although in these cases, it might be expected that subcutaneous administrations may also be associated with increased extremity pain. Only one SC trial is included in the sub-group analysis as only one trial reported

extremity pain.[87] Being an unexpected adverse event in early treprostinil trials, it is possible that the adverse event was experienced more than it was reported.

Interestingly, only one SC treprostinil trial reported increased peripheral oedema, whilst IV did not report any cases. IV and SC are given in similar concentrations with the same bioavailability (**Table 2-4**). The only difference being the tissue in which SC treprostinil comes into contact with. However, the subcutaneous tissues exposed to treprostinil, are not local to the extremities where peripheral oedema occurs. Peripheral oedema is considered a nervous effect associated with EP_3 signalling through binding of PGE_2.[305] Treprostinil has poor affinity for the EP_3 receptor,[62] but the combined observation of peripheral oedema with treprostinil therapy as well as the ability for treprostinil to bind high affinity of treprostinil at the EP_2 receptor may suggest a similar mechanism to induce peripheral oedema.

2.6.2 Comparison with prostacyclin mimetics

The primary analysis including all prostacyclin mimetics was hindered by the averaging of the treprostinil effects for all administration routes. With the added understanding of how route of administration effects the likelihood of treprostinil side effects, by splitting the treprostinil trials by their routes of administration, it is possible to better compare the prostacyclin therapies without conflation and averaging the effect of treprostinil.

Although it was possible in the first meta-analysis to determine the effect of subcutaneous treprostinil (only drug to be given *via* subcutaneous infusion), the effect of inhaled or oral treprostinil were conflated with other drugs administered *via* that route. With the further analysis into treprostinil, it is possible to compare between the different oral and inhaled therapies and determine the effect of a prodrug formulation on adverse events.

Compared to the combined calculated odds ratio for inhaled therapies, including treprostinil and iloprost, when inhaled treprostinil was analysed separated, fewer AEs were reported. The combined analysis highlighted jaw pain (OR = 2.7), headache (OR = 2.4) and nausea (OR = 1.7) to be associated with inhaled therapy. However, none of these adverse events were significantly associated with inhaled treprostinil and in the case of headache, no incidences were reported. As a composite of all administration routes, treprostinil was not associated with cough and was mildly associated with flushing. Consistent with clinical reports,[321] when only inhaled treprostinil is considered, cough was significantly associated with therapy (OR = 2.8), similar to that of iloprost. Analysis of inhaled treprostinil revealed a strong significant association with flushing (OR = 20.6), indicating flushing is primarily a treprostinil effect (**Figure 2-8**).

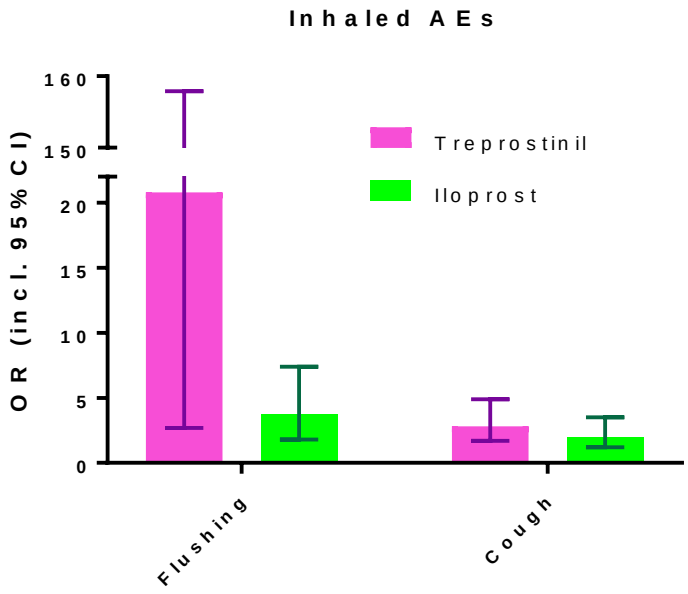

Figure 2-8. Comparison between inhaled treprostinil and iloprost in their association in inducing flushing and cough in PAH patients as measured by odds ratio.

Beraprost, selexipag and treprostinil are all offered as an oral formulation. Whereas beraprost and treprostinil are administered in their active form, selexipag is not. Selexipag prodrug exhibits weak IP binding affinity (K_i = 260 nM) until it is metabolised by the liver after absorption from the GI tract (K_i = 20 nM). Therefore, it would be expected for the GI-tract related AEs to be less likely in patients taking selexipag. However, only a modest decrease in likelihood was observed.

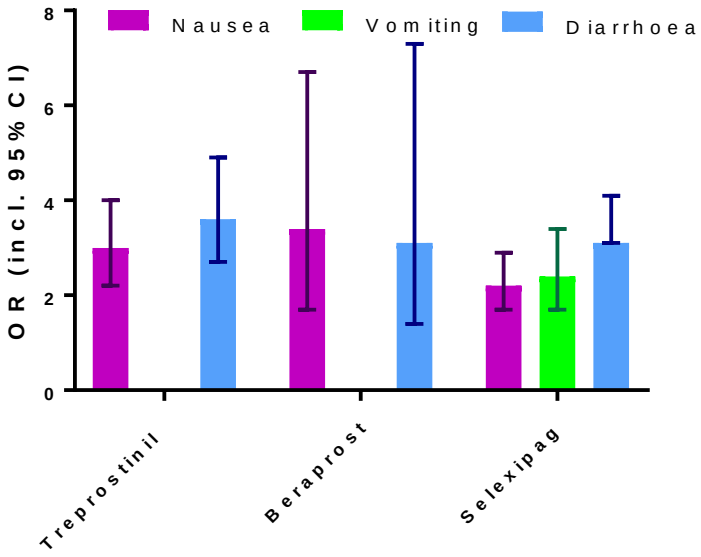

Figure 2-9. Comparative likelihoods of GI-related adverse events in oral prostacyclin mimetics therapies (treprostinil, beraprost and selexipag), as determined by odds ratio.

The overall analysis determined headache to be the most likely AE for oral therapies, when this is split into the different oral therapies it is clear that this is most likely to be an effect of treprostinil (**Figure 2-10**). Beraprost is less likely to induce headache and selexipag is least likely. Treprostinil is an agonist of the EP_2 receptor which regulates blood pressure. Both beraprost and selexipag exhibit poor affinity for the EP_2 receptor which might explain the increase in headache with treprostinil.

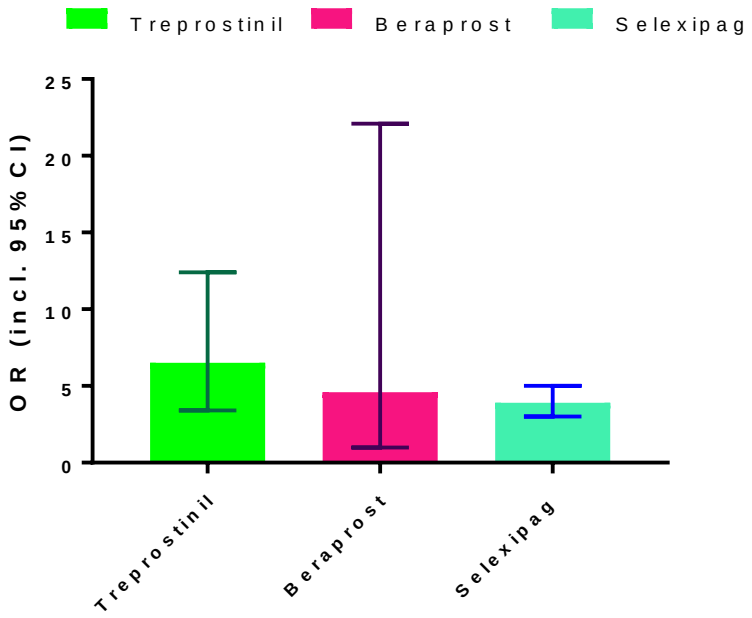

Figure 2-10. The relative likelihood of headache associated with oral prostacyclin mimetic therapies (treprostinil, beraprost and selexipag) as determined by odds ratio.

Pain in extremities was most significantly associated with intravenous and not subcutaneous treprostinil although was associated to a lesser extent with oral therapies. When analysed by the different oral therapies, a similar likelihood was identified for oral treprostinil and selexipag (**Figure 2-11**). As selexipag is an IP selective agonist, is could be assumed that the extremity pain is driven through the IP receptor. However, no extremity pain was noted for beraprost, an IP and EP_3 agonist, or any other drug types.

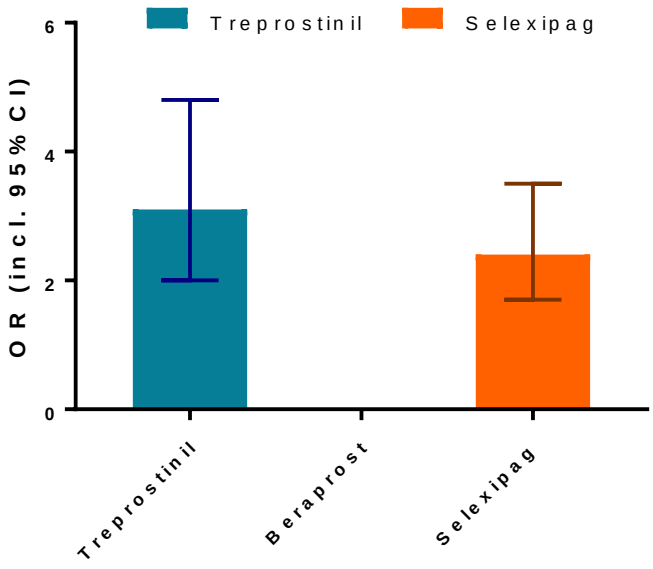

Figure 2-11. Comparative likelihood of inducing extremity pain for oral prostacyclin mimetic therapies (treprostinil, beraprost, selexipag) as determined by odds ratio.

Similar to the comparison of oral therapies, inhaled treprostinil can be compared with inhaled iloprost as only inhaled delivery of iloprost was included in the original analysis. Flushing is mostly associated with inhaled and oral PM therapies (OR = 4.7 and 4.0, respectively) which is thought to be a result of activating the prostanoid receptors in the skin surrounding the face (**Figure 2-12**). However, the similar trend for inhaled and oral PMs identified by meta-analysis hides the trend.

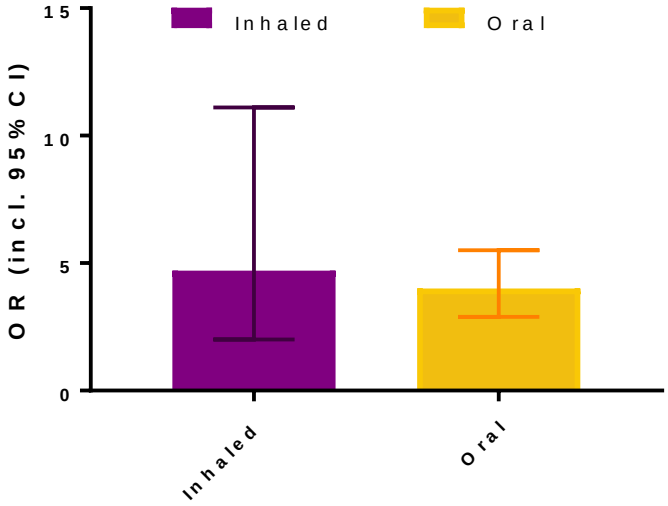

Figure 2-12. Comparison of likelihood of experiencing flushing for all prostacyclin mimetics (treprostinil, iloprost, selexipag and beraprost) delivered as analysed by inhaled and oral routes.

When analysed by the different drug types, flushing is more than four times more likely for inhaled treprostinil than for any other treatment (**Figure 2-13**).

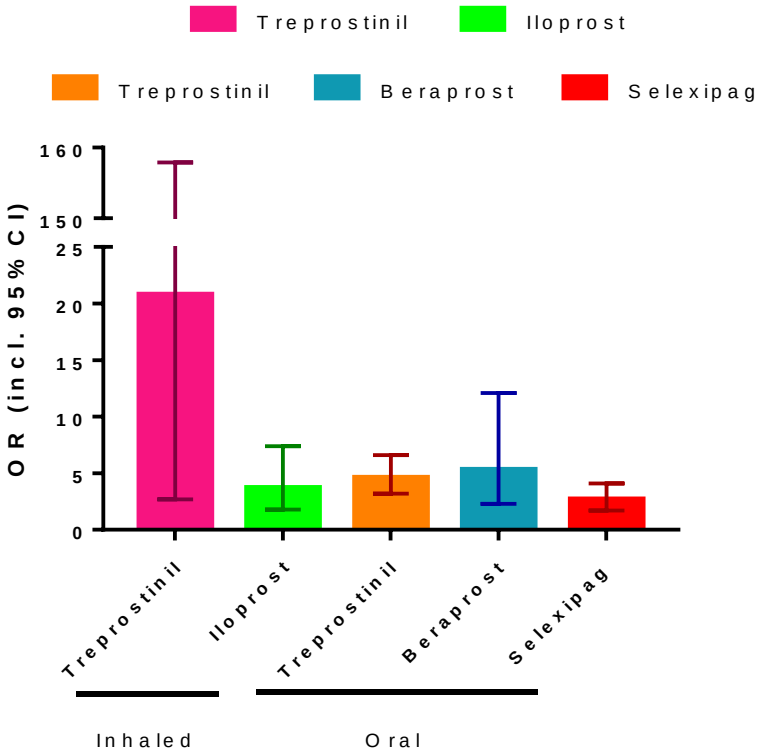

Figure 2-13. Relative likelihoods of patients experiencing flushing during trial periods as analysed by odds ratio of each individual inhaled and oral prostacyclin mimetic therapies. Inhaled treprostinil is most associated with reports of flushing.

Whereas selexipag has been granted global approval, beraprost is only approved in Japan and south Korea. Oral treprostinil (Orenitram®) has FDA approval but has not been granted approval from European Medicine Agency. This decision lies on the unfavourable risk:benefit:cost ratio. It is likely that the increased likelihoods of side effects experienced with treprostinil may relate to its potent activation of EP_2 and DP_1 receptors. Indeed the antiproliferative effects of treprostinil in human pulmonary artery smooth muscle cells isolated from PAH patients is largely driven by the EP_2 and not the IP receptor, via a mechanism involving PPAR gamma activation.[142,272] This could be of particular importance when the IP receptor is downregulated, as is known to occur in PAH.[47,277] Comparison of trial data between treprostinil and selexipag show no considerable difference in likelihood of AEs, indicating that achieving IP receptor selectivity does not reduce AEs in the patient. As will be discussed in future chapters, attempts to improve treprostinil therapy by employing a pro-drug approach have been investigated, however by extrapolating the treprostinil and selexipag, this data suggests that a pro-drug approach which releases treprostinil systemically, is expected to exhibit a major benefit in reducing site pain and increasing half-life but not in alleviating systemically induced adverse events. For a marked decrease in systemic adverse events an element of tissue targeting will be required.

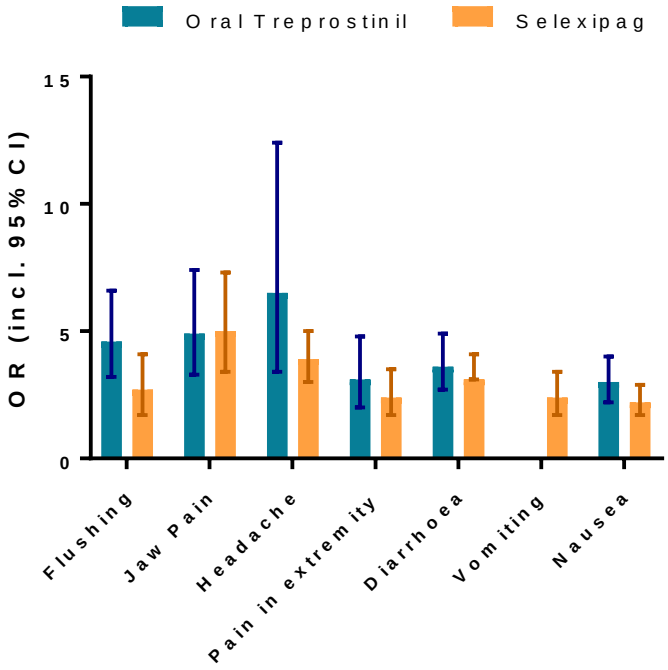

Figure 2-14. Comparison of likelihoods of experiencing adverse events during trial periods associated with selexipag, a selective IP receptor agonist administered as a prodrug, and oral treprostinil.

2.6.3 Strengths and Limitations

Previous meta-analyses have included all types of PAH treatment or focused on survival and outcomes.[315,322–324] To our knowledge, this is the first meta-analysis of the PM class, firstly to

include selexipag, and secondly to explore the effect of different IP receptor agonists and route of administration on the adverse event profile. We collected data from 15 blinded, placebo-controlled, randomised clinical trials and analysed their reported results. After thesis submission and following advice from reviewers, one trial was removed from the analysis as it only provided outcome data.[297] The quality of the trials overall was acceptable, and data was collected to the best of our abilities. The aim was to focus on the patient experience of PM therapy, so the approach included data on AEs reported as well as patient-reported outcomes, Borg score and quality of life scores. By including secondary analysis of the treprostinil subset, direct correlation between AE profiles and PM types with multiple administration routes could be drawn. Nonetheless, our analysis is not without limitations; most studies were funded by the drug manufacturer which may be a source of reporting and publication bias OR was used to report likelihood of events which does not take trial duration into consideration.[310] Inconsistent reporting of 6MWD and Borg score (mean vs. median, SD vs. SE) was overcome by assuming data to be normally distributed and converting medians and interquartile ranges to means and SE, respectively. For one study,[283] discontinued patient data was reported as a zero change in 6MWD, which potentially hides negative effects. During review of a manuscript detailing this work, one reviewer noted that for one trial,[283] the adverse event data for the total trial period was used when the three month titration phase data was available in the supplementary information, and would have been a better comparison with the other shorter trials. Although the secondary analysis of treprostinil increased the depth of the investigation, reducing the group sizes decreases the sensitivity of the meta-analysis, so caution is advised when drawing trends and conclusions from meta-analyses with limited samples.

2.6.4 **Conclusions**

The purpose of this analysis was to gain understanding of the limitations of current prostacyclin therapies. The underlying causes of adverse events were suggested as a way of identifying methods to mitigate them. In summary, it was identified that treprostinil was limited by pain experienced at the site of injection administration and flushing which are primarily local effects. The remaining adverse events, with lower likelihoods are likely a result of systemic exposure of treprostinil. Selective IP receptor agonism did not avoid side effects. A prodrug strategy for oral delivery did not significantly reduce AEs relating the GI tract, presumably because the effects are systemically induced. In conclusion, this investigation identifies two approaches by which treprostinil therapy could be improved:

No.	Limitation	Strategy
1	Site pain	Reduce activity upon subcutaneous administration of treprostinil using prodrug strategy
2	Systemic Exposure	Achieve targeted therapy or release localised to the diseased pulmonary tissue

The following work described within this chapter, the thesis will focus on contributing ideas, strategies and suggestions in achieving one, or both, of the aims identified in this chapter.

Chapter 3. Treprostinil N-acyl sulfonamide prodrug strategy.

3.1 Introduction

Prodrug derivatives can optimise the properties of an active pharmaceutical ingredient (API) to be better suited for use in a medicine. Solubility, biological stability, adsorption, metabolism, activity, excretion and release site are all factors which can be altered by introducing a prodrug strategy. Pro-drugs are derivatives of an API which are conjugated to other chemicals that serve to temporarily mask the activity of the API. Upon administration, the masking group is cleaved to convert the structure into that of the original API, thereby reactivating it.

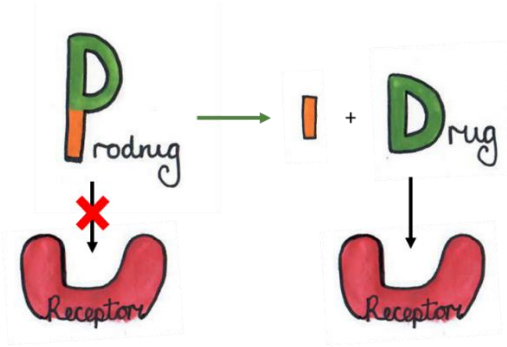

Figure 3-1. Concept of prodrug approach. Prodrug moiety changes property of drug structure which can hinder its ability to bind to its receptors. Upon degradation, the prodrug moiety is cleaved to release drug compound which is able to interact with receptors.

Over the past 2 decades, prodrugs have made up ~20% of all new small molecule approvals.[148] A variety of masking prodrug head groups have been described such as alkyl esters, acetyl groups, sugars, amino acids, phosphoesters and alkyl ethers (**Figure 3-2**). Depending on the API and the pro-drug group employed, structural properties can be optimised to best achieve the necessary efficacy.[148] Esterification and amidation of a carboxylic acid have been employed to reduce the polarity of compounds to allow for better permeation into tissues or cells.[325,326] The former type of chemical modification can in many instances be readily reversed by endogenous cell esterases. Increasing hydrophobicity of polar moieties, for example, by esterification of carboxylic acids, can increase permeation and bioavailability for oral and ocular formulations.[150,327] Additionally, carboxylic acids and hydroxyl moieties have been conjugated to sugar structures and phosphoesters, respectively, to increase aqueous solubility.[149,328] Amino acid conjugation can also increase systemic lifetime and allow for prolonged released.[329–332] For example, the amide-conjugated alanine derivative of brivanib, **12** (BMS-540215) exhibits increased bioavailability and solubility in aqueous media as compared to its parent API.[331] This can reduce dosing frequency and smooth peak and trough fluctuations in drug-blood concentration between dosings.[333]

Degradation of the pro-drug to release the API can be triggered by either chemical or enzymatic means. Most chemical release mechanisms rely on hydrolysis although oxidation has also been used.[334] Enzymatic mechanisms that rely on endogenous enzymes include oxidoreductases like CYP450 and DT-diaphorase as well as hydrolytic enzymes like carboxylesterase and β-glucuronidase, which are able to cleave the masking group of a prodrug structure.[148] Prodrug strategies have been used in a wide variety of therapeutic areas including hypertension, antibiotics, gastric ulcers, coagulation anti-inflammatories and cancer.[148,335] Prodrugs encounter different environments before reaching their intended system, tissue or cell of degradation, so stability requires consideration of the route of administration. Furthermore, the degradation must be sensitive enough for efficient release of the active drug.

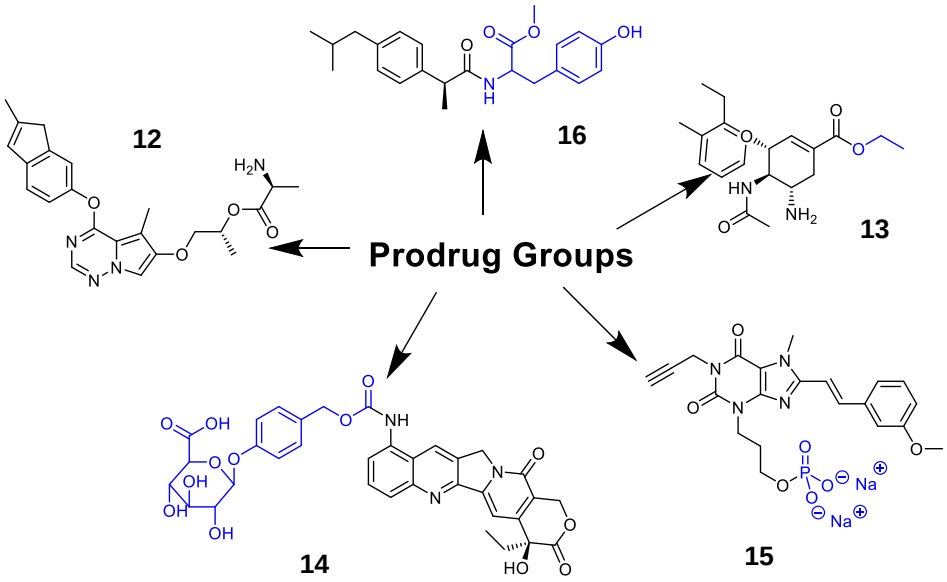

Figure 3-2. Different prodrug groups (highlighted in blue) used to temporarily modify properties of drug compounds. Compound **12** is Brivanib alaninate, the L-alanine ester of anticancer drug, Brivanib. Compound **16** is the tyrosine-conjugated derivative of non-steriodal inflammatory drug, dexibuprofen. Compound **13** is the ethyl ester derivative of antiviral Oseltamivir. Compound 15 is the phosphate ester of adenosine A_{2A} antagonist, MSX-2; Compound **14** shows conjugate of 9-aminocamptothecin and glucuronidic acid linked by carbamate spacer.

Prodrugs of treprostinil have been made with several different strategies having been described in published literature and patents.[79,80,132,134,306,336,337] However, no treprostinil-derived prodrugs have so far been developed for clinical use. It is well established in the few early structure-activity relationship studies conducted on treprostinil, that removing or derivatising the acid group, or even moving its position around the treprostinil benzindene ring, drastically decreases the anti-platelet effects of treprostinil.[145] Therefore, reversibly derivatising the acid group would decrease the activity, suitable for a pro-drug strategy.

Previous attempts were made by United Therapeutics to make a 5kDa poly(ethylene glycol) (PEG) conjugate of treprostinil which had prolonged cardiovascular actions *in vivo* when delivered *via* the pulmonary route.[338] When administered (3 mg) *via* intratracheal instillation to

a hypoxia-induced rat model of PAH, a 5 mmHg decrease in pulmonary arterial pressure was observed over 5 hours, compared to free treprostinil and iloprost, which produced more transient effects. Following publication in 2000, no further advances were made to pursue preclinical or clinical testing. Although no information on tolerability of treprostinil-PEG has been described, it is known that pulmonary exposure to nanoparticles can cause inflammation so are not suitable for the treatment of chronic inflammatory diseases.[263]

As described in Chapter 1, PEGylated-treprostinil conjugates and treprostinil prodrugs have been pursued previously without achieving the primary goal of reducing site pain upon administration of the subcutaneous infusion. [134,135,306,339]Without knowing the linker structure employed for PEG-treprostinil, it is not possible to accurately assess the underlying reason for the site pain. However, given the size of the PEG structure in relation to the appended APIs, and the specificity and conformation of the binding pocket of the IP and EP_2 receptors,[340,341] it is reasonable to assume the conjugate exhibits negligible inherent activity. Such a large conjugate would hinder interaction at the receptor binding domains. Therefore, the activity at the administration site is likely a result of premature release of treprostinil. Esterases are ubiquitous throughout the body so it's possible that the 4-star-PEG-treprostinil is a substrate for carboxylesterases found in the subcutaneous compartment. Although other acid-labile linkers have been investigated for conjugation to treprostinil,[342] it is likely that those structures would also lead to premature release of treprostinil in a bolus subcutaneous formulation.

The N-acyl sulfonamides, moiety (**Figure 3-3**) is considered a common bioisostere of the carboxylic acid since carboxylic acids are susceptible to rapid metabolic degradation either by glucuronidation or acyl-CoA thioester formation.[344] For example, the anti-inflammatory agent, tolmetin, is rapidly metabolised to an acyl-coenzyme A thioester intermediate in rats.[345] With similar volume, size and charge, N-acyl sulfonamides offer drug candidates a structure with similar physical properties to their parent acid with reduced metabolic degradation. By means of the acidic proton (highlighted in red in **Figure 3-3**) with similar pKa as the carboxylic acid derivative, drug activity is usually preserved.[346]

Figure 3-3. Structure of N-acyl sulfonamide

The use of sulphonamides as bioisosteres is indicative that receptor interaction is not usually hindered. However, some compounds such as TIPP-703 and venetoclax display different yet favourable receptor activities (**Figure 3-4**). Unlike other sulphonamides, which are acid labile,[347] the nitrogen-carbon bond of N-acyl sulfonamide requires enzymatic cleavage by carboxyl esterases to degrade the N-acyl sulfonamide bond.[346] Interestingly, when exposed to hepatic enzymes of rat microsomes, which contain cytochromes P450, monooxygenases

and uridine glucuronide transferases, Asunaprevir **18** was not metabolised to its acid derivative.[348]

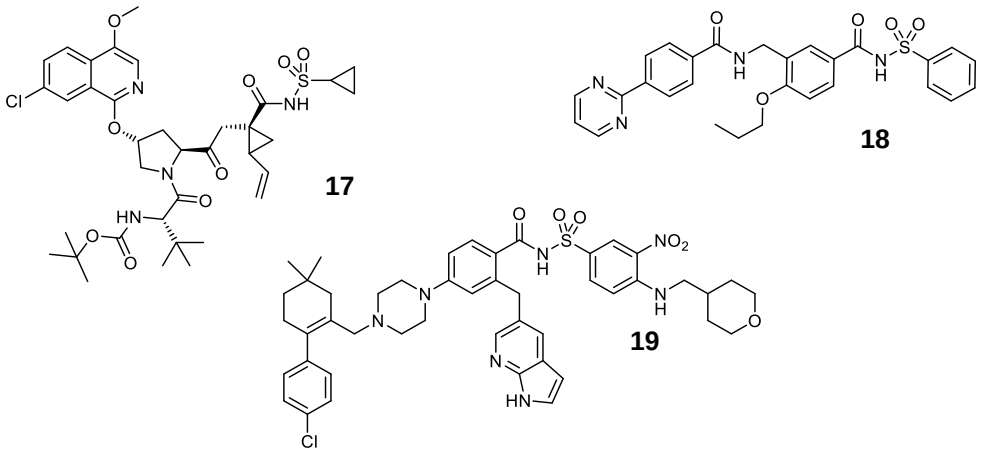

Figure 3-4. Examples of N-acyl sulphonamides as bioisosteres of clinical interest. Asunaprevir, **18** which is in development for the treatment of hepatitis C; N-acyl sulfonamide derivative of TIPP-703 which is a pan agonist of the peroxisome proliferator-activated receptors (PPARs), **19**; and venetoclax **20** for the treatment of chronic lymphocytic leukaemia.

As discussed in Chapter 1, selexipag is the only prodrug strategy used to treat PAH. Selexipag **5** is stable in blood plasma and as determined in healthy volunteers, has a terminal half-life of between 0.7 and 2.3 hours, depending on the dose received. Once exposed to the carboxyesterases of the liver, the N-acylsulfonamide is cleaved to release ACT-333679 (6) into the blood stream with a terminal half-life of 9.4–14.2 hours. [349] In the blood, the drug is able to act on IP receptors found throughout the body.[274] Whilst this does not reduce the likelihood of systemic adverse events, it has the potential to reduce local adverse events at the in the gastrointestinal tract as well as achieving a steady release of active drug in the blood owing to albumin binding.[350] By increasing the half-life, blood concentrations do not fluctuate so rapidly, so the number of dosing administrations per day can be reduced. Although, the 28-fold reduction in activity of prodrug 5 potentially results in a reduction of local effects in the GI tract before absorption, our meta-analysis indicates that GI related AEs are systemically induced.

The significantly reduced activity of the N-acyl sulfonamide at the IP receptor indicates that the carboxylic acid interaction with the receptor binding pocket is highly size dependent. Although the structures of ACT-333679 6 and treprostinil **4** are not analogous, interactions with the IP receptor are thought to be similar. Therefore, an N-acyl sulfonamide derivative of treprostinil 4 is hypothesised to exhibit similar prodrug properties. Furthermore, a prodrug formulation of treprostinil would substantially reduce the local adverse events associated with administration. Learning from previous prodrug ideas in the literature, requiring metabolism by hepatic enzymes would avoid premature treprostinil release in the subcutaneous tissue. N-acylsulfonamide have been shown to exhibit slow degradation rates which, if the biological half-life of the pro-drug is suitable, will result in a slow release of active drug over time.[351]

As described in Chapter 2, treprostinil therapy is associated with a range of adverse events. The most prevalent and hindering being administrative site pain upon subcutaneous delivery.[352] To overcome this limitation, masking the activity of treprostinil via a pro-drug derivative was pursued. Previous attempts at devising prodrug formulations have been centred around acid degradability which have all been limited by the premature release of treprostinil leading to activation of prostanoid receptors in the subcutaneous tissue.

The most recently approved drug introduced to the PAH market, selexipag, utilises an N-acyl sulfonamide pro-drug approach. We hypothesised that the similarly derivatised treprostinil, would avoid site pain upon administration to the subcutaneous tissue by expressing reduced IP receptor activity until degradation by hepatic enzymes. Removing activity at the IP receptor may also indicate a reduction in activity at other prostanoid receptors (notably the EP_2 and DP_1) receptors. The primary aim was to investigate N-acyl sulfonamide treprostinil as a prodrug.

The following objectives were set:

1.) To prepare treprostinil N-acyl sulfonamide (**21**).
2.) To determine the *in vitro* activity of treprostinil *N*-acyl sulfonamide **21** to induce cAMP elevation in a cell line expressing the IP receptor.
3.) Determine the cleavage of N-acyl sulfonamide treprostinil **21** with hepatic enzymes to release free treprostinil 4

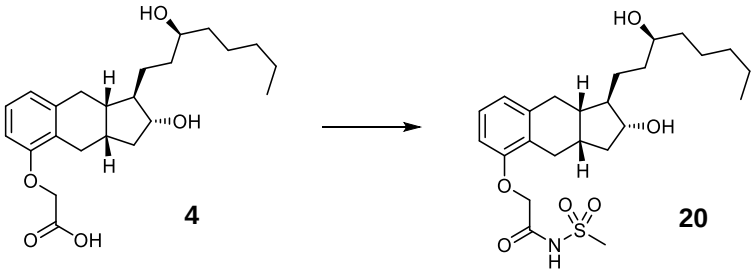

Scheme 3-1. Proposed conversion of treprostinil 4 to its *N*-acyl sulfonamide **21**

3.2 Results and Discussion

3.2.1 Design of synthesis

Knowing the importance of the acid functional group of treprostinil for its IP receptor activity, it was hypothesised that an acyl sulfonamide derivative of treprostinil would have reduced activity. A sulfonamide prodrug moiety was similarly utilised in selexipag. The reduced activity of treprostinil acyl sulfonamide **21** would potentially be beneficial at the injection site as it would be expected to induce less severe pain and swelling. Preparation of treprostinil acyl sulfonamide **21** essentially involves the formation of an amide bond at the treprostinil carboxylic acid. There are many routes to form an amide bond from a carboxylic acid. A widely used method is to increase the electrophilicity of the carbonyl by using coupling agents to

activate the acid for nucleophilic attack by an amine.[353] This is commonly utilised in peptide synthesis, to link amino acids together.

3.2.2 Treprostinil Synthesis

Treprostinil **4** was successfully synthesised following a published method[354] during a 3-month placement with United Therapeutics & Lung Biotechnology in Silver Springs, Maryland, USA (**Scheme 3-2**). The purpose for preparing treprostinil **4** was to learn about the synthetic routes that are used to prepare treprostinil **4** commercially as well as the common intermediates that could potentially be used in a prodrug strategy.

Two methods **Scheme 3-2** are used by United Therapeutics for preparing treprostinil 4. Route i shows the FDA approved route and route ii is an improved synthesis which uses the controlled epinepherine derivative as the chiral reagent to couple the two starting materials. During the placement both synthetic routes were followed and the stereomeric purities of both products were compared. Complete synthesis, isolation and characterisation (details provided in appendix section 2) took over 2 months to yield 67.8 mg of pure treprostinil **4**.

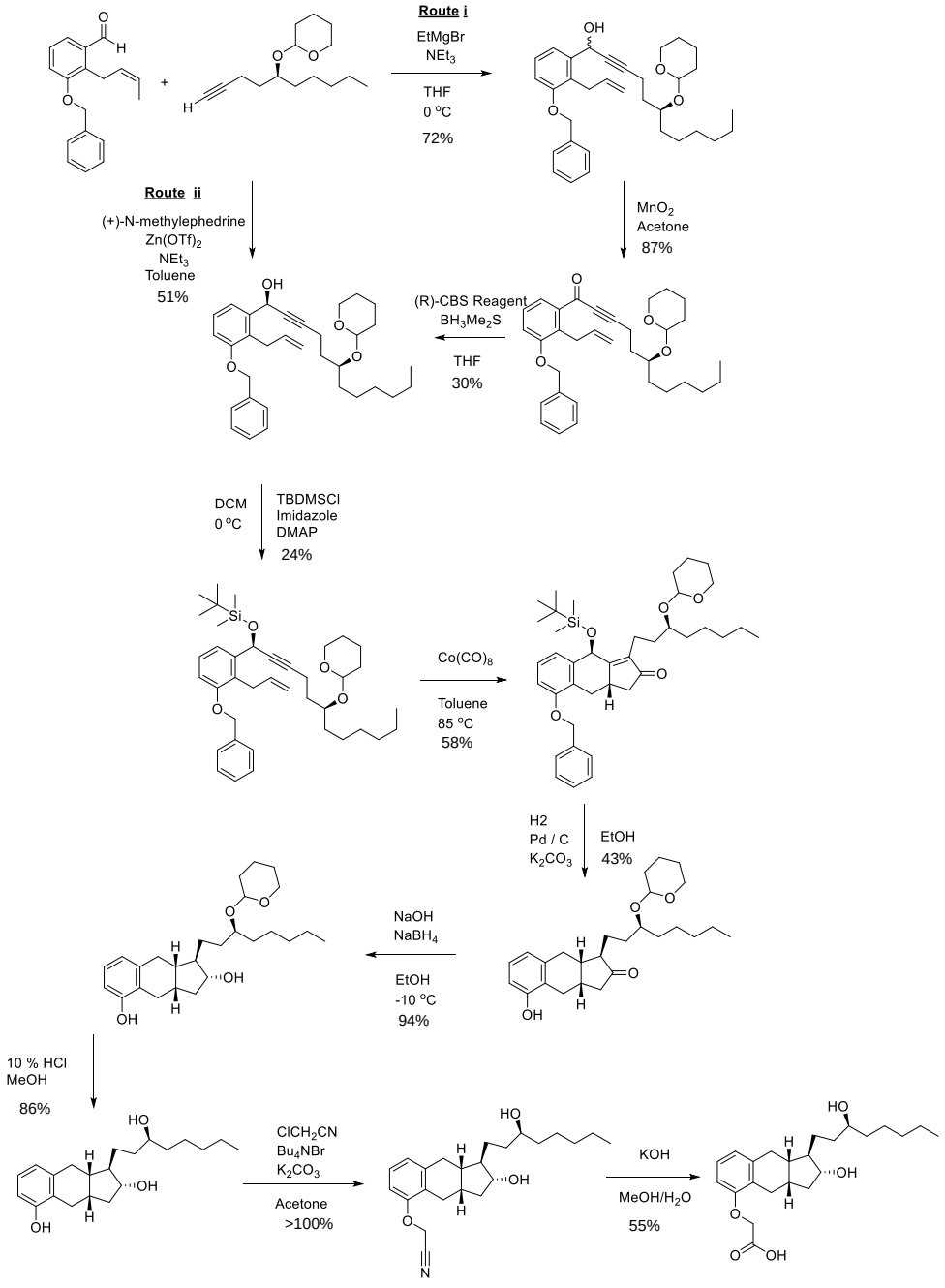

Scheme 3-2. Two synthetic routes to achieve treprostinil **4**; route i uses a Grignard reagent to couple the aldehyde and alkyne to form a racemic product. The hydroxyl is converted to a ketone which is subsequently converted back with defined stereochemistry. Route ii achieves the same compound with defined stereochemistry of the hydroxyl in one step using a chiral epinephrine-derived chiral reagent.

A certain amount of purified treprostinil **4** was pledged towards the project saving time and money. Appreciating the complexity of synthesis, cost, and the generosity of UT to provide material, treprostinil **4** was used sparingly and small reaction scales (5-50 mg) were employed.

The carboxylic acid in treprostinil **4** is a phenoxyacetic acetic acid. Considering the cost and limited supply of treprostinil **4** , a model phenoxyacetic acetic acid **22** was used to examine reaction conditions for preparing acyl sulfonamide derivatives. Clearly the use of a model phenoxyacetic acid **22** does not possess the two hydroxyls that are present in treprostinil **4**. Use of a model compound generally carries some risk that its properties (e.g. solubility, reactivity) will vary compared to the parent compound, treprostinil **4**. However, to preserve the supply of treprostinil **4**, it was necessary to use phenoxyacetic acid **22** for synthetic studies.

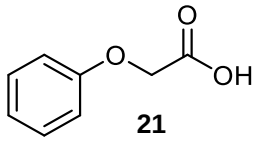

21

Figure 3-5. Structure of phenoxyacetic acid **22** which possesses the same acid moietyas treprostinil and was therefore selected as a suitable model drug.

N-(methylsulfonyl)-2-phenoxyacetamide

Initial reactions aimed to modify the phenoxyacetic acid **22** to the N-acyl sulfonyl derivative, by coupling to methyl sulfonamide **25** (**Scheme 3-3**). Several methods were attempted **Table 3-1**, mainly utilising known coupling reagents to make amides and esters.[355] Of the coupling agents that were examined, carbodiimides were the most widely used.

Table 3-1. Attempted reactions for formation of N-acyl sulfonamide using model drug, phenoxyacetic acid **22**. ^{t}BOK = potassium *tert*-butoxide; CDI = carbonyldiimidazole; DBU = 1,8-Diazabicyclo[5.4.0]undec-7-ene; THF=tetrahydrofuran; DCM=dichloromethane

Model drug	Conditions	Solvent	Scale (mg)	Reaction time	Temp	Outcome	Ref
39	Methane sulfonyl chlroide, tBOK	THF	30	1 hours	0 C	Change in TLC to lower Rf but when worked up minimal methylene resonance was not detected by ^{1}H NMR.	356
22	**25**, CDI (**36**)	THF	100	16	RT		
22	**25**, CDI (**36**), DBU (**31**)	THF	200	48 hours	RT → 67 → RT	TLC indicated reaction progess but 1H NMR showed only 20% product.	357,358
22	**25**, EDCI (**34**), DMAP (**32**),	DCM	50	16 hours	RT	Additional TLC spot but starting acid still present. 1H NMR confirmed 50% conversion.	359
22	**25**, CDI (**36**), DBU (**31**)	THF	200	90 hours	RT → 67 → RT	Starting material still detected on TLC. Work up showed impure product by ^{1}H NMR which was purified by crystallisation from $CHCl_3$	357,358
22	Thionyl chloride, **25**	DCM	100	3 hours	80 C	TLC revealed starting acid was still present and no new product spots	
22	Thionyl chloride, **25**	THF	100	3 hours - overnight	70 C - RT	TLC showed presence of starting acid and subsequent NMR confirmed that minimal (<20%) reaction had occurred.	

These reagents activate the acid carbonyl by replacement of the electron donating acid hydroxyl with an electron withdrawing carbodiimide generated intermediate **23**. Carbodiimides possess two weakly basic nitrogens which render the central carbon susceptible to nucleophilic attack by a carboxylic acid. The O-acylisourea generated, is susceptible to rapid nucleophilic attack by any nucleophiles present. In the presence of amines, the desired amide is generated. However, the reaction solution possesses multiple nucleophiles which facilitates several other possible reaction routes. In the presence of excess acid, the symmetrical anhydride is formed which can be subsequently cleaved to form one equivalent of the desired methane sulfonamide. The high reactivity of the O-acylisourea makes it able to undergo an irreversible, undesired rearrangement to form the N-acylurea, particularly in the presence of weak nucleophiles.

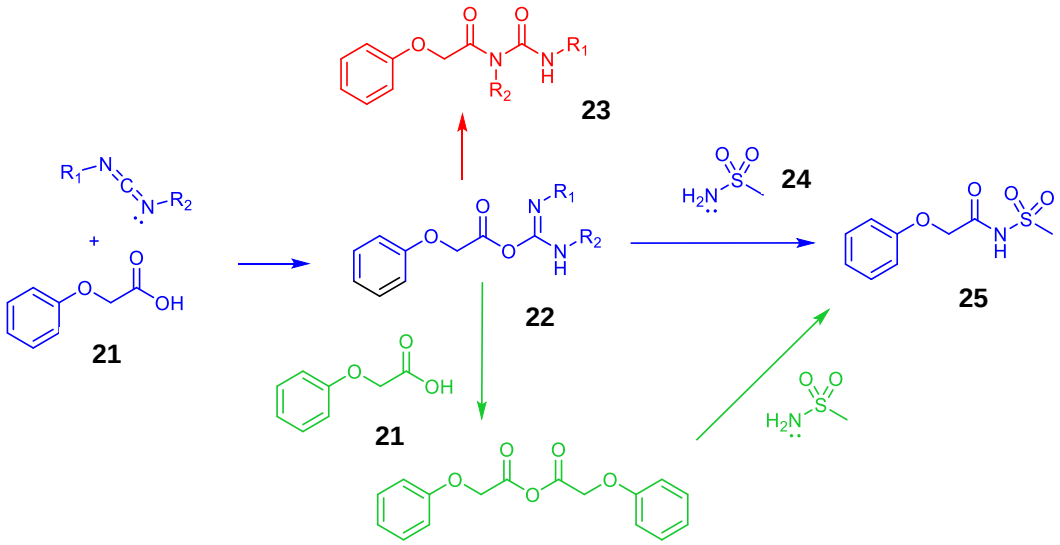

Scheme 3-3. BLUE: Proposed conversion of phenoxyacetic acid to the N-acylsulfonamide derivative **26**, *via* the O-acylisourea **23**. DCC: R_1, R_2 = cyclohexane; DIPC: R_1, R_2 = isopropyl; EDCI: R_1 = ethyl and R_2 = dimethylaminopropyl; GREEN: Alternative method of sulfonamide formation via anhydride; RED: Formation of N-iso-acylurea **24** resulting from unwanted side reaction of carbodiimides.

To reduce the propensity for the N-iso-acylurea formation **24**, additives are added to diminish the activity of the O-acylisourea **23** by two mechanisms; (i) N-hydroxy additives (**Figure 3-6**) protonate the O-acylisourea **23**, preventing the intermolecular reaction, and (ii) they form the active ester which is less reactive. Formation of N-hydroxy additives is favoured in the presence of tertiary amine.

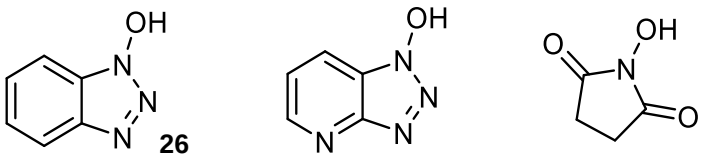

27 **28**

Figure 3-6. N-hydroxy additives to enhance coupling efficiency and avoid N-acylurea formation; HOBt **27**, HOAT **28**, N-hydroxysuccinimide NHS **29**.

The formation of the active ester is especially necessary for the coupling of weak or hindered nucleophiles such as alcohols and aromatic amines. For such reactions, a catalyst is employed. Nucleophilic bases (**Figure 3-7**) are added to form the active ester which possess electron withdrawing properties. The carbonyl of the active ester is exceptionally electrophilic which facilitates attack by weak nucleophiles. Although 1-hydroxybenzotriazole hydrate (HOBt) **27** is an effective catalyst, it is costly and explosive.[360] In certain cases, DBU **31** has been shown to increase rate of reaction more than DMAP **32** or HOBt.[361] This is attributed to its ability to act as a nucleophilic base in a similar manner to that of DMAP or HOBt.

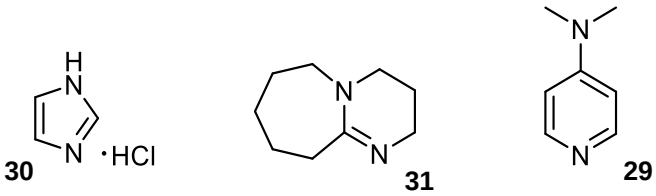

30 **31** **29**

Figure 3-7. Amide coupling catalysts; imidazole chloride **30**, 1,8-Diazabicyclo[5.4.0]undec-7-ene (DBU) **31**, 4-(dimethylamino)pyridine (DMAP) **32**.

EDCI **34** is a carbodiimide which gives a water soluble by-product (**33**).[355] This simplifies the extraction during work up. Other carbodiimides (DCC, DIC) produce ureas of varying solubility which can be difficult to remove completely. Using EDCI **34** in the presence of catalytic DMAP **32**, coupling of sulfonamide **25** with phenoxyacetic acid **22** using EDCI **34** was attempted,[362] resulting in incomplete conversion to the desired sulfonamide derivative **26** Complete depletion of phenoxyacetic acid **22** spot was not observed and ^{1}H NMR confirmed a 1:1 ratio of acid **22** methylene (4.58 ppm) and sulfonamide **26** methylene (4.68 ppm). The coupling reaction was repeated, leaving the acid **22** to undergo reaction with EDCI **34** for longer (18 hours) which achieved a 9:1 ratio of sulfonamide product **26** to starting acid **22** as determined by ^{1}H NMR spectroscopy. Purification by basic liquid extraction yielded the desired acyl sulfonamide **26** in 33% yield.

EDCI **34** was purchased as the hydrochloride salt. Upon the result that EDCI **34** yields lower coupling product in the presence of additional base, it was thought that EDCI **34** may need to be deprotonated to allow the tertiary amine to deprotonate the intermediate species. Following this hypothesis, the EDCI-mediated reaction was repeated on a 50 mg scale, with the addition of triethylamine to neutralise the hydrochloride salt. A TLC spot with R_f at 0.86 was seen (similar to the product spot of the previous reaction, R_f = 0.94) but the phenoxyacetic acid **22** was not consumed after 5 days. ^{1}H NMR did not show the presence of any sulfonamide product **26**; no shift in methylene resonance or methyl singlet was observed.

An additional attempt was conducted in the same manner, with the addition of N-hydroxylsuccinimide (NHS) **29** to avoid formation of N-acylurea **24**. NHS **29** was added to the

solution at the same time as acid **22** and stirred for 30 minutes before addition of the sulfonamide **25** to allow for the NHS-ester to form. TLC revealed six product spots and the ^{1}H NMR spectrum, following basic workup with sodium carbonate, confirmed the absence of sulfonamide product **22**, NHS-ester or EDCI **34**.

Based on these results, it is likely that the protonation of EDCI **34** is required for the EDCI-mediated coupling (**Scheme 3-4**). It is possible that the ammonium side chain facilitates protonation of the imide which helps to drive the nucleophilic attack by sulfonamide **25**.

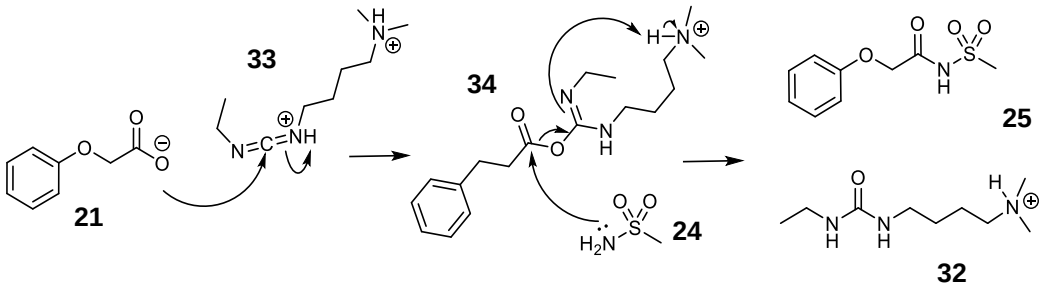

Scheme 3-4. Mechanism for the N-(3-Dimethylaminopropyl)-N′-ethylcarbodiimide hydrochloride (EDCI) **34** mediated amide coupling of phenoxyacetic acid **22** and methane sulfonamide **25** to form N-acyl sulfonamide derivative **26**.

The model acyl sulfonamide **26** was also prepared using carbonyl diimidazole (CDI) **36** as the coupling agent. CDI **36** was used for the synthesis of selexipag 5.[115,363] Whilst not a carbodiimide, the coupling with CDI **36** proceeds in a similar manner. The sp^{3} nitrogens on the imidazole rings in CDI **36** are slightly basic and can serve to deprotonate the phenoxy acetic acid **22** resulting in the formation of the mixed anhydride imidazolide intermediate **38** (**Scheme 3-5**). Imidazole is liberated as a result. Acyl imidazole **37** formation through the nucleophilic attack of the displaced imidazole is driven by the evolution of CO_2 (**Scheme 3-5**). The innocuous by-products generated by CDI-mediated couplings make their employment for amide couplings favourable-for pharmaceutical applications.

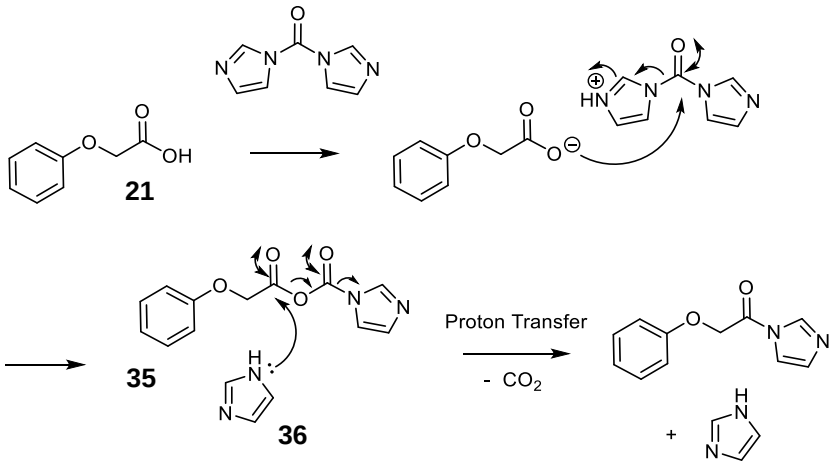

Scheme 3-5. Mechanism of amide formation between phenoxyacetic acid **22** and methane sulfonamide **25** mediated by 1,1-carbonyldiimidazole (CDI) **36**. Attack of the imidazole into the anhydride intermediate **37** is driven by carbon dioxide evolution to form the acyl imidazole **38**.

Upon addition of a nucleophile to the acyl imidazole **38**, the imidazole is substituted for the nucleophile.[364] The nucleophilic nature of both reactions means anhydrous conditions and protocols must be adhered to. Although the acyl imidazole **38** serves to activate the carbonyl and make it more susceptible to nucleophilic attack, reactions rates of hindered and weak nucleophiles, such as methane sulfonamide **25** can be slow. CDI-mediated coupling was carried out between phenoxyacetic acid **22** and methane sulfonamide **25** in the absence of DBU **31** and no coupling product could be detected by ^{1}H NMR after 16 hours. In such cases, catalysts are employed (**Scheme 3-6**).

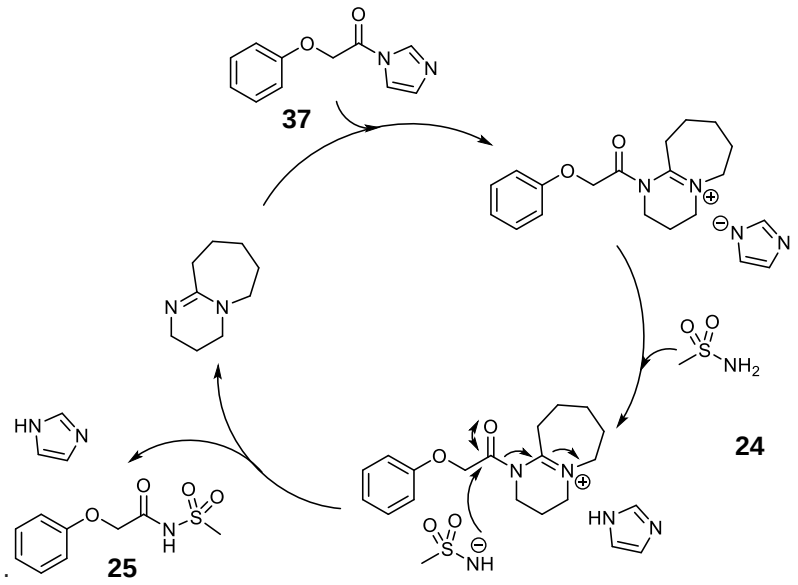

Scheme 3-6. Mechanism of 1,8-Diazabicyclo[5.4.0]undec-7-ene (DBU) catalysis of carbonyldiimidazole (CDI)-mediated amide coupling. Once acyl imidazole **38** is formed, DBU **31** displaces the imidazole which facilitates nucleophilic attack of methane sulfonamide **25** to form N-acyl sulfonamide **26**. DBU catalyst **31** is regenerated during displacement which can undergo reaction with further molecules of acyl imidazole **38**.

Following previous protocols, the CDI-mediated coupling of phenoxyacetic acid **22** and methane sulfonamide **25** was carried out on a 200 mg scale in the presence of DBU **31**. Varying from the previous DBU-free protocol, the reaction was heated to 67 ^{o}C. The reaction was difficult to track by TLC as only a slight shift down the TLC plate was observed from the R_f of phenoxyacetic acid **22** (R_f = 0.43) and N-acyl sulfonamide **25** (R_f = 0.35). However, a colour change from brown to green when stained with phosphomolybdic acid (PMA) was observed upon reaction progression. Following liquid extraction to remove base, unreacted acid **22** and CDI, crystals were observed in $CDCl_3$ during ^{1}H NMR spectroscopy of the crude sample. Purification was therefore carried out by repeat crystallisation from chloroform to yield N-acyl sulfonamide **25**, which was a white powder.

An alternative method to circumvent possible formation of N-acylurea **24** was to form the primary amide via a mixed anhydride (**Scheme 3-7**) followed by reaction with a methane sulfonyl halide (**Scheme 3-8**). Amination of phenoxyacetic acid **22** into its respective primary amide **39** was successfully achieved by treatment with ammonium chloride by activation of the

acid using ethyl chloroformate.[365] Reaction progression was monitored by TLC, showing an increased R_f value which stained mauve with ninhydrin and did not stain with bromocresol green. ^{1}H NMR spectroscopy showed a shift in methylene resonance of 0.04 ppm. Spiking the NMR sample with the starting phenoxyacetic acid **22** confirmed the presence of two different methylene proton environments, suggesting the reaction had occurred.

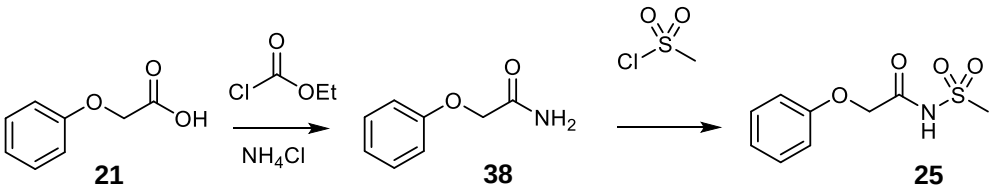

Scheme 3-7. Conversion of carboxylic acid **22** to primary amide **39** which can then displace chloride of methane sulfonyl chloride to form **26**.

Based on clean TLC and NMR spectra, 2-phenoxyacetamide **39** was taken to the next step without further purification. Coupling to methane sulfonyl chloride was attempted under basic conditions in the presence of 1,4,7,10,13,16-hexaoxacyclooctadecane (18-crown-6).[356] The pKa of a primary amide such as **39** is ~25,[366] and owing to the ability of the nitrogen electrons to resonate into the sulfonyl groups, possesses limited nucleophilicity. Alternative bases, such as DMAP **32** and sodium hydride, are also reportedly used for nucleophilic reactions of primary amides which may have helped this reaction succeed.[367,368] However, the transfer of such conditions to an analogous reaction with treprostinil **4** was anticipated to be unsuccessful owing to the presence of the secondary alcohols. Furthermore, the carbodiimide synthetic route had proved successful and the transfer to treprostinil **4** seemed the next logical step.

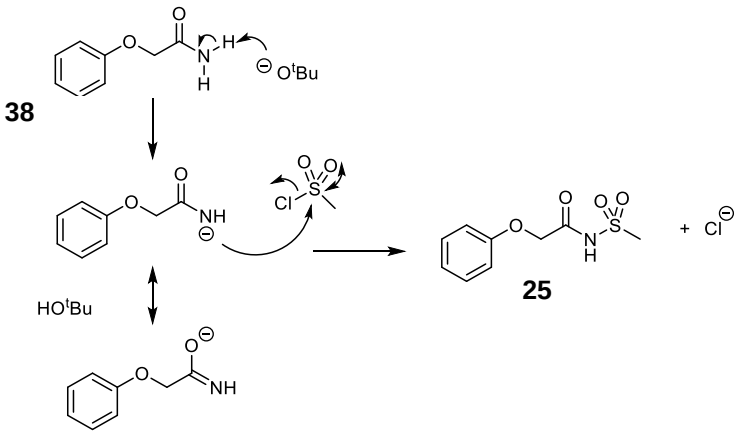

Scheme 3-8. Reaction of primary amide **39** with sulfonyl chloride to form N-acylsulfonamide derivative **26** by displacement of chloride ion.

There are many methods and reagents available for amide coupling all of which have their own advantages and disadvantages (i.e. cost availability, ease of handling, activity, solubility, ease of removal). Although the synthesis of **26** could have been optimised further, a method of synthesis was identified with the reagents available. It was considered more worthwhile to transfer the conditions identified and lessons learnt over to the derivatisation of treprostinil than to optimise the model coupling further.

N-acyl sulfonamide treprostinil

The synthesis of N-acyl sulfonamide treprostinil **21** using the CDI **36** conditions identified for derivatising phenoxyacetic acid **22** were then explored. On a 50 mg scale, treprostinil **4** was coupled to methane sulfonamide in the presence of CDI **36** and DBU **31**. After 18 hours, TLC revealed 6 PMA-staining spots, including the starting material treprostinil. ^{1}H NMR spectroscopy of the crude sample without work up revealed only the treprostinil **4** carboxyl methylene resonance, indicating the reaction had not occurred. HPLC analysis confirmed an absorbance with the same retention time as treprostinil **4**.

Treprostinil **4** (50 mg) was then treated to the EDCI **34** and DMAP **32** conditions found to be successful with phenoxyacetic acid **22**. TLC conducted after 48 hours revealed 7 spots of which, one corresponded to treprostinil 4. After liquid extraction from both acidic and basic aqueous layers, the TLC still possessed 6 UV active compounds. A preparative TLC was carried out using 10% methanol in ethyl acetate and each band collected by extraction into methanol. The signal to noise ratio for all fractions was low and none of fractions possessed both the methyl resonance and treprostinil resonances. The reaction was thus considered unsuccessful.

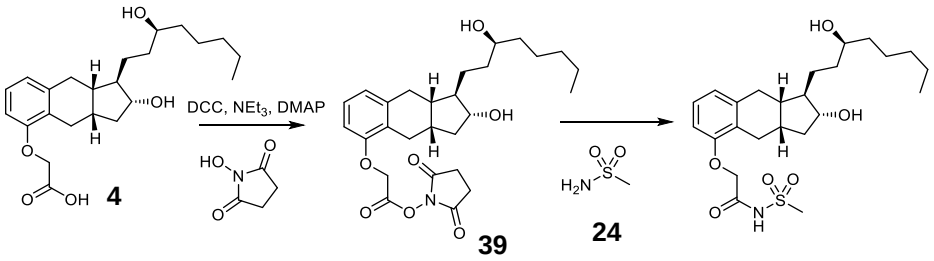

Figure 3-8. Proposed N,N'-Dicyclohexylcarbodiimide (DCC)-mediated formation of treprostinil-N-hydroxysuccinimide (NHS) ester, which is then displaced by methane sulfonamide to form N-acyl sulfonamide treprostinil **21**. NEt_3 = triethylamine; DMAP = 4-(dimethylamino)pyridine **32**.

One further attempt was made to pre-form the treprostinil-NHS ester **40** which could then be treated with methane sulfonamide **25** to achieve the desired sulfonamide **21**. On a 5 mg scale in DMF, treprostinil 4 was treated with DCC, NHS and triethylamine in the presence of DMAP **32** catalyst. To minimise the possibility of the interference of the secondary alcohols with the activated carbonyl, methane sulfonamide **25** was added after 15 minutes. Following 16 hours of stirring at RT, TLC detected 9 spots, including mostly starting material. The crude reaction mixture was analysed by ^{1}H NMR which did not show any shift in resonance corresponding to the carboxyl methylene of treprostinil.

For work described in appendix 8.3, other derivatives of treprostinil were attempted to be made however, with limited success (**Table 3-2**). In light of this, as well as the contrast between the successful sulfonamidations of the phenoxyacetic acid **22**, and the unsuccessful attempts for that of treprostinil 4, it was concluded that the problem was a feature of coupling treprostinil 4. The number of spots formed for each reaction indicated that a variety of unwanted reactions were occurring, despite no observable differences in the solubility between phenoxyacetic acid

22 and treprostinil 4. The main difference appeared in the presence of the hydroxyl groups of treprostinil 4. Although secondary alcohols are less nucleophilic that their primary counterparts, they are still capable of attacking electrophiles, particularly when in the presence of an activated carbonyl, such as the O-acylisourea activated carbonyl of treprostinil formed during coupling reactions (**Figure 3-9**). To avoid possible competing side reactions, it was hypothesised that the treprostinil 4 hydroxyl groups will need to be protected before coupling to sulfonamide **25** so a suitable protecting group was sought

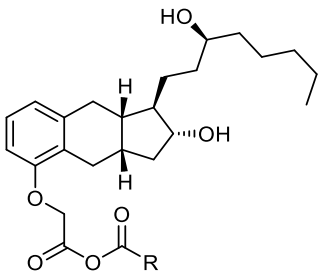

Figure 3-9. O-Acylisourea derivative of treprostinil formed as an intermediate during carbodiimide or carbodiimidazole coupling reactions. Where R = isopropyl, imidazole, cyclohexyl or ethyl groups.

.

Table 3-2. Unsuccessful attempted reactions to protect Treprostinil (4). At either carboxyl acid (COOH) terminus or both COOH and hydroxyl termini (OH). Dmob = dimethoxybenzyl alcohol; K_2CO_3 = potassium carbonate; MeI = methyl iodide; DIPC = diisopropyl cardodiimide; EDCI = N-(3-Dimethylaminopropyl)-N′-ethylcarbodiimide hydrochloride; DMAP = 4-(dimethylamino)pyridine; BzBr = benzyl bromide; Cs_2CO_3 = caesium carbonate; DCC = N,N'-dicyclohexylcarbodiimide; NHS = N-hydroxysuccinimide; BTCA =benzyl-2,2,2-trichloroacetimidate MeOH = methanol; $CDCl_3$ = deuterated chloroform; DCM = dichloromethane; THF = tetrahydrofuran; ^{t}BuOH = tert-butanol; RT = room temperature; TLC = thin layer chromatography.

Protecting group	Treprostinil moiety	Conditions	Solvent	Scale (mg)	Time	Temp	Outcome
Methyl esterification	COOH	K_2CO_3, MeI	MeOH	5	20 mins	RT	No reaction (TLC)
Dmob esterification	COOH	DIPC, Dmob	$CDCl_3$	2	2 hours	0 - RT	No reaction by NMR
Triethylene glycol esterification	COOH	DIPC, Triethylene glycol	$CDCl_3$	2	6 days	RT	Conversion of treprostinil but many spots - difficult to isolate.
Dmob esterification	COOH	EDCI, Dmob, DMAP	DCM	2	3 days	0 - RT	TLC conversion of trep, terminated
Tribenzylation	OH + COOH	BzBr, Cs_2CO_3	NaH	50	7 days		No reaction
Benzyl esterification	COOH	DCC, NHS, benzyl alcohol, DMAP	DMF	5	5 days	RT	Prep TLC, LCMS peak
Tribenzylation	OH + COOH	BTCA, triflic acid	DCM	10	5 days	RT	No reaction
Tribenylation	OH + COOH	BTCA, triflic acid	THF	10	17 hours	RT	negligable benzylation
Esterfication	COOH	Di-tert-butylcarbonate, DMAP,	^{t}BuOH	20	48 hours	RT	Many spots by TLC, difficult to isolate by prep TLC

The possibility of forming a cyclic ketal bond between the two hydroxyls was considered, however this would form an unfavourable 9 membered ring, so was not anticipated to be straight forward. Therefore, methods to cyclise the hydroxyl groups together were abandoned. Alternative commonly employed hydroxyl protecting groups are shown in **Table 3-3**.

Table 3-3. Commonly employed hydroxyl protecting groups. TBAF = tetra-n-butylammonium fluoride; DBU = 1,8-Diazabicyclo[5.4.0]undec-7-ene.

Protecting group	Structure	Cleavage conditions[369]
tert-Butyldimethylsilyl ether (TBDMS)	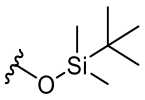	**Fluoride:** TBAF, hydrofluoric acid, Lithium aluminium hydride **Acid:** Dowex 50W-X8, sulfuric acid, trifluoroacetic acid **Base:** Lithium aluminium hydride,
Alkyl ether (^{t}butyl)	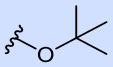	**Acid:** 4 *N* hydrochloric acid, Trifluoroacetic acid, formic acid[353],
Benzyl ethers	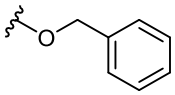	Hydrogen/palladium on carbon, sodium/ammonia, Iron chloride + acetic acid
Acetal (tetrahydropyran)	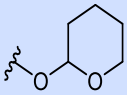	**Acid:** 0.01 *N* hydrochloric acid, acetic acid, pH 5
Acyl groups	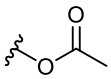	Potassium carbonate/methanol, DBU, lipase enzyme

Ester and amide formation using coupling agents such as diicarbodiimides and uronium salts require basic conditions[353] so hydroxyl protecting groups that are stable to base were sought. However, in the presence of the free acid of treprostinil 4, acid labile protecting groups are not appropriate as the treprostinil acid could cleave an acid labile protecting group prematurely.

Protection of treprostinil 4 hydroxyls has been described in published patents,[79,370,371] however, all methods describe simultaneous protection of the acid. The acid protecting group is then replaced with either an amine or ester bond. Although this gave confidence that the hypothesis of requiring hydroxyl protection was correct, only the silyl ethers were reported which did not give much information on the relative reactivity of the hydroxyls.

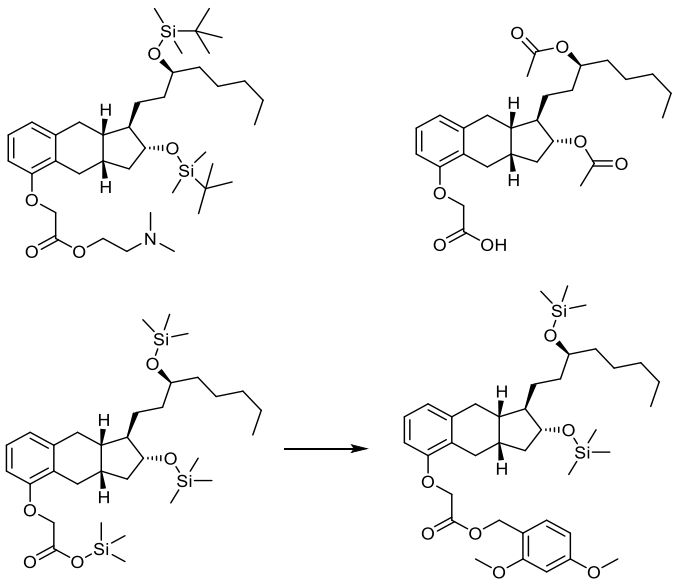

Figure 3-10. Protected treprostinil structures within the patent literature.[79,370–372]

Several attempts to protect either only the hydroxyls or both the hydroxyls and the acid of treprostinil **4** simultaneously were attempted **Table 3-4** which were largely unsuccessful. For the future ester and amide formation reactions using coupling agents such as diicarbodiimides in basic conditions as well as considering work described in **Appendix 8.3** hydroxyl protecting groups that are stable to base were sought.

Table 3-4. Summary of attempted reactions to protect the hydroxyl groups of treprostinil 4. TBDMS(Cl) = tert-butyl dimethyl silyl (chloride); DMAP = 4-(Dimethylamino)pyridine; BTA = N,O-Bis(trimethylsilyl)acetamide; BzBr = benzylbromide; NaH = sodium hydride; ^{t}BuOK = potassium tert-butoxide; Cs_2CO_3 = caesium carbonate; BTCA =benzyl-2,2,2-trichloroacetimidate; DCM = dichloromethane; DMF = dimethyl formamide; THF = tetrahydrofuran; DMSO = dimethylsulfoxide; RT = room temperature; TLC = thin layer chromatography (using silica)

Intended protecting group	Conditions	Solvent	Scale (mg)	Time	Temp	Result
Silylation	TBDMSCl, DMAP, Imidazole	DCM	50	48 hours	0 - RT	**Unsuccessful:** No change by TLC. Degraded or no reaction.
Trisilylation	BTA	DMF	50	16 hours	0 - RT	**Partial success:** One pot methane sulfonamide coupling
Trep benzylation	BzBr, NaH	THF	10	16 hours	RT	**Unsuccessful:** by TLC
Trep benzylation	BzBr, ^{t}BuOK	DMSO	10.2	2 hours	RT	**Unsuccessful:** multiple products
Trep tribenzylation	BzBr, NaH	THF	50	7 days		**Unsuccessful:** No reaction
Trep tribenzylation	BzBr, Cs_2CO_3	THF	20	6 days	reflux	**Partial success:** Multiples products including dibenzylated treprostinil
Trep tribenzylation	BTCA, triflic acid	DCM	10	5 days	RT	**Unsuccessful:** No reaction
Trep tribenzylation	BTCA, triflic acid	THF	10	17 hours	RT	**Unsuccessful:** negligable benzylation
TBDMS ether	TBDMSCl, imidazole	DMF	50	16 hours	0 - RT	**Partial silylation** Free acid may cleave silyl groups

Following guidance from the patent literature, the synthesis of tri-silyl protected treprostinil was carried out using tert-butyl dimethylsilyl chloride (TBDMSCl). The stability of the silylated ester was anticipated to be poor, however masking of the acid head group was required for the stability of the silyl ethers. The reaction was carried out on treprostinil **4** (50 mg) under basic conditions and using DMF as solvent which is thought to drive coupling reactions.[373] TLC showed no change in the R_f value from starting treprostinil. In hindsight, it is possible that the TLC plate was acidic enough to cleave the silyl groups and this could have been investigated by running a 2D TLC. With retrospect, alumina could have been used as a neutral TLC alternative.

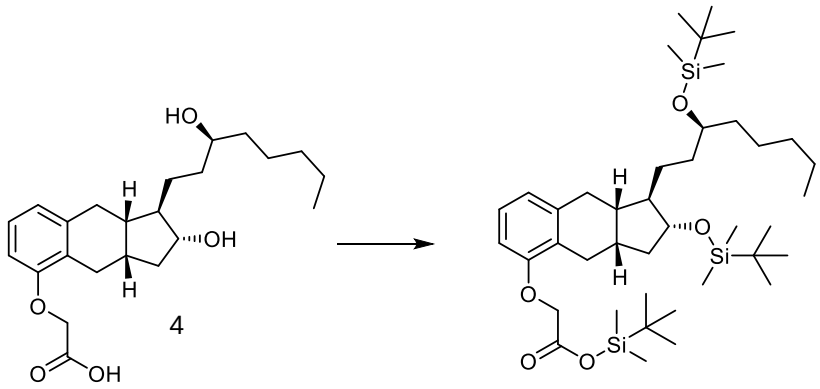

Scheme 3-9. Trisilylation of treprostinil 4 to form silyl ethers at the hydroxyls and a labile silyl ester at the acid using tertiary butyl dimethyl silyl chloride (TBDMS).

The trisilylation of treprostinil **4** was repeated with three equivalents of TBDMSCl. Separation between ethyl acetate and aqueous layers during liquid extraction was poor and although ^{1}H NMR showed resonances at 0.1 and 0.9 corresponding to the silylated groups, the resolution was poor and further extraction only reduced the sensitivity of ^{1}H NMR analysis. The lability of the silyl ethers and the issues experienced during isolation led to the termination of efforts on the silylation reaction.

The isolation of the silylated treprostinil presented an opportunity for degradation, so using a different patented procedure, the trimethylsilyl ether and ester bonds were formed and the ester reacted with a more stable nucleophile in a two-step, one-pot reaction. Following the success of the EDCI **34** reaction with phenoxyacetic acid **22**, it seemed reasonable to attempt the same coupling with treprostinil 4, assuming the hydroxyls were silylated. A more reactive silylating agent N,O-bis(trimethylsilyl)acetimidate **41** was employed for the trimethylsilyl (TMS) protection of treprostinil **4** on a 50 mg scale in DMF (**Scheme 3-10**). After 12 hours, EDCI **34** and DMAP **32** were added to the solution mixture. After cooling for 30 minutes, methane sulfonamide **25** added and the reaction left for 3 days.

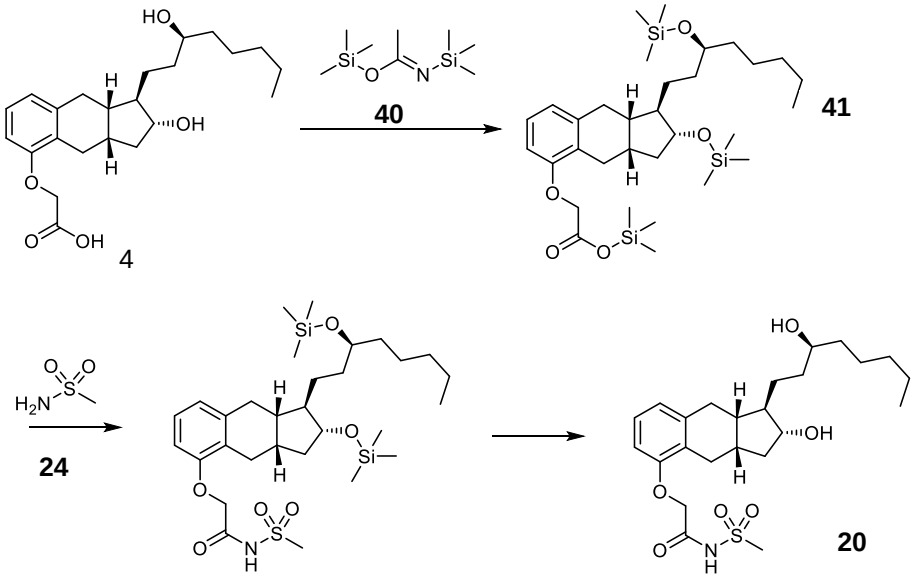

Scheme 3-10. Trisilylation of treprostinil 4 *in situ* with N,O-bis(trimethylsilyl)acetimidate (BTSA) **41** before cleavage and coupling of carboxylic acid with methane sulfonamide **25** with EDCI coupling agent **34** to form silylated N-acyl sulfonamide derivative. Cleavage of silyl ethers forms the desired N-acyl sulfonamide treprostinil derivative **21**.

TLC revealed treprostinil **4** was present but with an additional spot with higher R_f = 0.8). The solution was run through analytical HPLC column (mobile phase = 10-90% acetonitrile/ water over 20 minutes) to identify reaction progression. The HPLC chromatogram showed a peak at 13.3 minutes, different from that of treprostinil **4**. The ^{1}H NMR spectrum (**Figure 3-11**) suggests that N-acyl sulfonamide **21** was present, based upon the shift in methylene resonance from 4.6 to 4.7 ppm, and the presence of a singlet at 3.8 ppm, corresponding to the sulfonamide resonance, compared to treprostinil **4**. No TMS groups were observed which could mean that the protection did not occur, or silylated product **42** was produced, but silyl groups were subsequently cleaved during work up. A total yield of 12 mg (20%) of N-acyl sulfonamide treprostinil **21** was produced, greater than that of the EDCI-coupling of phenoxyacetic acid **22** (4%). Additionally, the reaction appeared by TLC to form over 6 compounds, indicating that the reaction was involved with multiple unwanted side reactions. For any commercial application, the loss of treprostinil 4 must be kept to a minimum and unwanted side reactions are a source of inefficiency. For this reason, a more reliable synthetic route was sought.

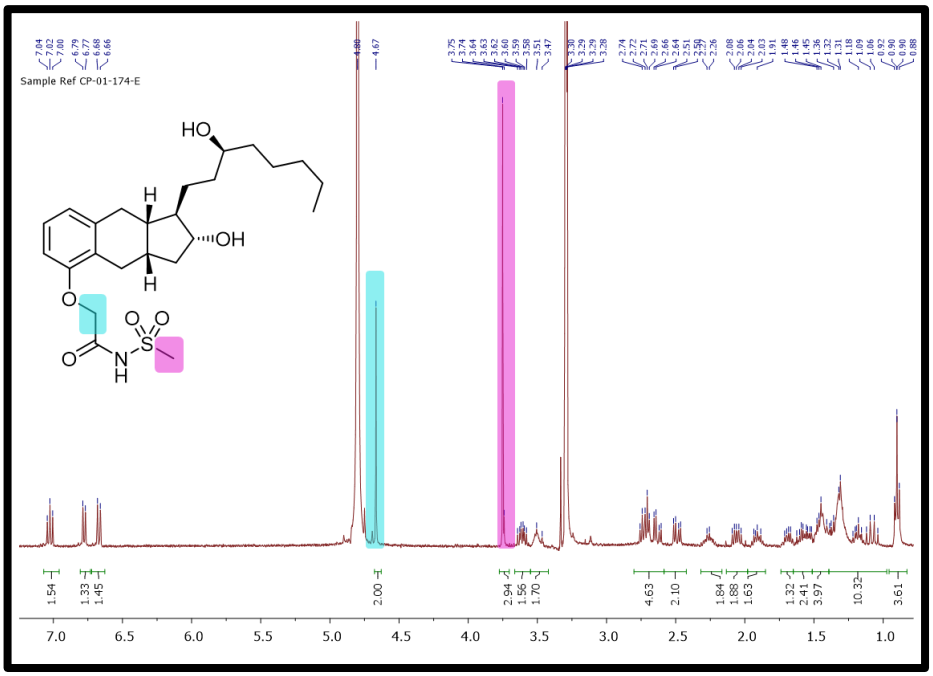

Figure 3-11. ^{1}H NMR of *N*-acylsulfonamide treprostinil **21** derived from trimethylsilane-treprostinil formed in a one-pot, two-step reaction. Blue shows the shifted methylene resonance and pink shows the presence of the sulfonamide methyl resonance

Hydroxyl-benzylation (**Scheme 3-11**) is a protecting group strategy used in the synthesis of treprostinil 4 (**Scheme 3-2**) and is robust to both acid and base conditions. Benzylation of treprostinil 4 *via* a base catalysed mechanism was explored, using benzyl bromide (**Scheme 3-11**).

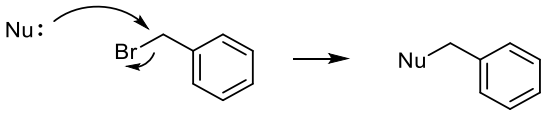

Scheme 3-11. Benzylation of nucleophile by nucleophilic displacement of bromide. Base is often employed to deprotonate the nucleophile.

Owing to the electron withdrawing effects of bromine, the benzylic carbon is subject to nucleophilic attack by alcohols and amines. The benzylation of treprostinil 4 (10 mg) was attempted with four equivalents of benzyl bromide in the presence of potassium tertiary butoxide. TLC revealed the presence of 6 spots including those with R_f values of treprostinil and benzyl bromide. Carrying out benzylations in the presence of sodium hydroxide was carried out on a small scale (10 and 50 mg), but TLC revealed only treprostinil and benzyl bromide.

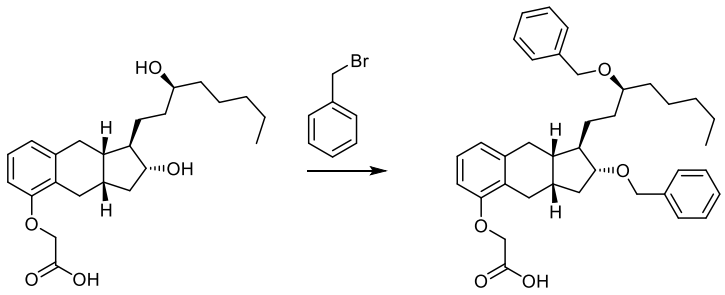

Scheme 3-12. Proposed benzylation of treprostinil hydroxyls by base-mediated nucleophilic displacement of bromide ion.

One final attempt was made to achieve the di-benzylated treprostinil. Treprostinil 4 (20 mg) in THF was treated to 3 equivalents of benzyl bromide in the presence of a weaker base caesium carbonate. The reaction TLC showed 5 spots and a sample was analysed by LCMS. As well as the treprostinil mass ion, the dibenzylated hydroxy-ether product ion was detected $[M+H]^+$ 571.3 m/z. The number of product spots in the TLC indicated that the reaction was only partially successful.

It was hypothesised that removing the possibility of interference from the acid group of treprostinil 4 would increase the success of the hydroxyl resonances. Despite the inefficiency of the proposed synthetic route (**Scheme 3-13**), methods to protect treprostinil were expected to have been previously explored and elucidated by UT and the sulfonamide coupling step was considered the novel and important step. Therefore, any route to allow sulfonamide coupling to be investigated was considered acceptable in the meantime and if deemed necessary, the protecting group strategy could be optimised post-hoc.

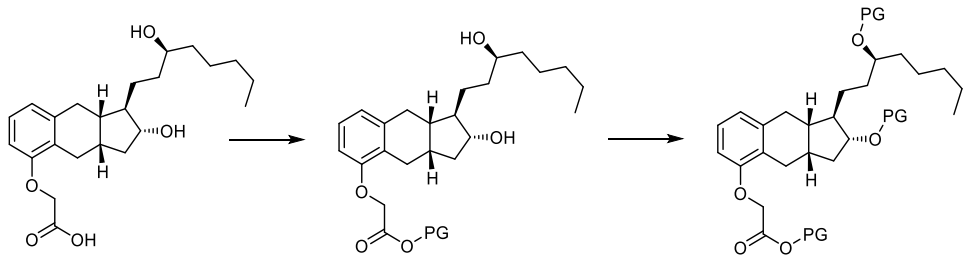

Scheme 3-13. Proposed synthetic route to protect hydroxyl groups of treprostinil **4**. Protecting the acid of treprostinil **4** and then subsequent protection of the alcohols. PG = protecting group.

Fischer esterification was employed by refluxing treprostinil 4 in anhydrous ethanol with an acid catalyst for 16 hours. The excess of solvent statistically results in ethanol attacking the π* orbital of the carbonyl bond, and further acidification of the intermediate hydroxyl, by proton transfer, eliminates water, leaving the ethyl ester. The build-up of water in the reaction solution prevents completion of the reaction. To circumvent hydrolysis of formed ester, several measures were taken; i) ethanol was dried over molecular sieves prior to reaction; ii) A large excess of ethanol was used; iii) reaction solution was dried over sodium sulfate towards the

end of reaction; iv) The solution was neutralised before reaction solvent was concentrated *in vacuo*.

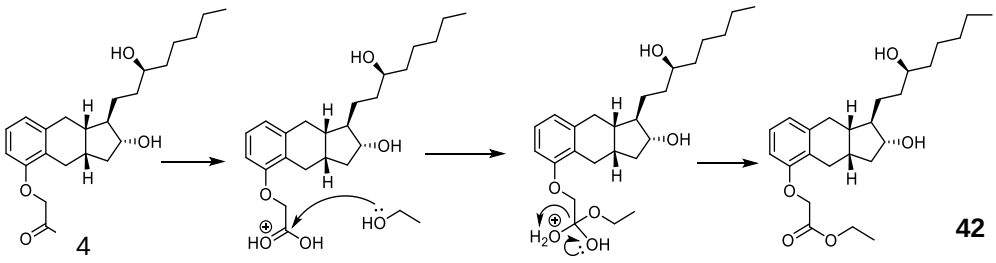

Scheme 3-14. Proposed mechanism for the acid-catalysed Fischer esterification of treprostinil 4 to form the ethyl ester derivative **43**.

Fischer esterification was monitored by TLC (determined by UV/PMA stain). Trace remaining treprostinil **4** was removed by base (K_2CO_3) extraction and the ^{1}H NMR spectrum (**Figure 3-12**) showed the expected ethyl resonances at δ 4.23 and 1.27 ppm corresponding to the ester CH_2 and CH_3, highlighted orange and green in **Figure 3-12** respectively ($CDCl_3$). By comparison to the ^{1}H NMR spectrum of starting treprostinil **4** in $CDCl_3$, the methylene resonance also shifted from δ 4.66 to 4.58 ppm. Treprostinil ethyl ester **43** was afforded as a dry white powder in 88% yield.

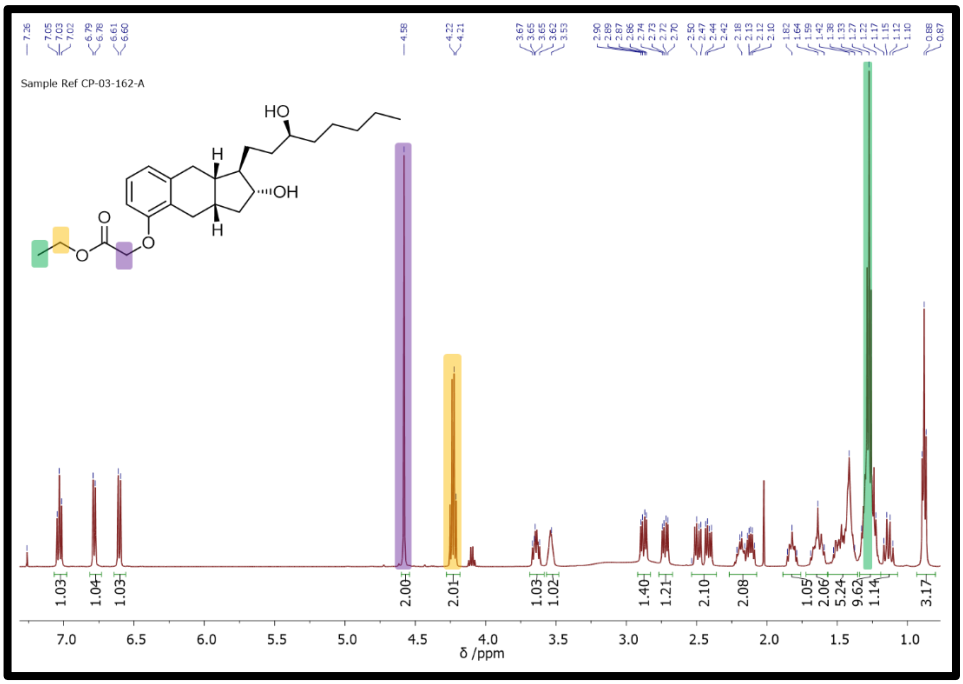

Figure 3-12. ^{1}H NMR spectrum of treprostinil ethyl ester **43** showing a shift in methylene resonance in purple, and the presence of the ester methylene and methyl resonances in yellow and green respectively.

With the treprostinil ethyl ester **43** in hand, hydroxyl group protection was attempted using acid-catalysed nucleophilic substitution of benzyl-2,2,2-trichloroacetimidate **44** (BTCA) in the presence of trimethylsilyl trifluoromethane sulfonate (TMS-OTf).[374,375] Under these conditions

multiple spots were detected by TLC (UV/PMA detection). A preparative TLC was conducted, and the fractions extracted in methanol then analysed by NMR. None of the compounds separated contained both benzyl aromatic and treprostinil resonances.

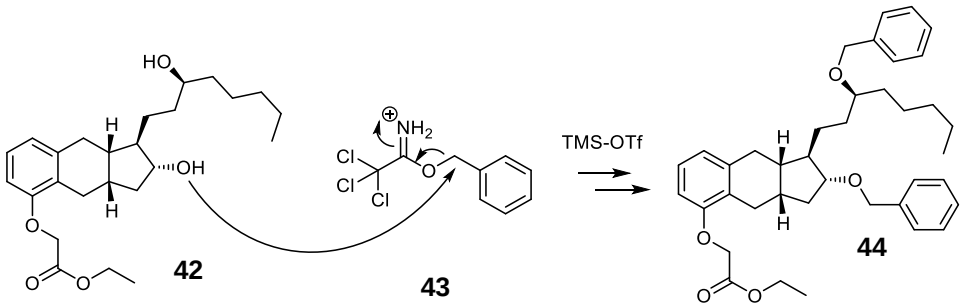

Scheme 3-15. Proposed mechanism for the benzylation of treprostinil ethyl ester **43** with benzyl-2,2,2-trichloroacetimidate (BTCA) **44** to form the bis-benzylated ethyl ester product **45**. TMS-OTf = trimethylsilyl trifluoromethanesulfonate.

Benzyl protection of treprostinil free acid 4 using BTCA **44** in the presence of TMS-OTf in both DCM[376] and THF[377] were both unsuccessful. Reagents were insoluble in DCM so additional THF was added to the reaction to aid solubility. In both cases TLC showed predominately the presence of treprostinil **4** after 5 days. ^{1}H NMR of the crude reaction product showed less than 10% benzylation, as determined by the benzyl methylene resonance. Owing to the steric hindrance and lack of nucleophilicity of the treprostinil **4** hydroxyl moieties in an acidic environment, treatment of treprostinil ethyl ester **43** with two equivalents of BTCA **44** could not displace the trichloroacetamide to form the benzyl ethers of **45**.

The neutral benzylation agent, 2-benzyloxy-1-methylpyridinium triflate **46** (dubbed the Dudley reagent) offered an alternative method for benzylation (**Scheme 3-16**).[378] Neutralisation of the positively charged pyridinium ion weakens the benzylic C-O bond to make the carbon more susceptible to nucleophilic attack by even weak nucleophiles, which ultimately drives the benzylation reaction. The hydroxypyridinium intermediate **48** is slightly acidic but the addition of magnesium oxide to the reaction mixture neutralises the intermediate as it forms, converting it to the N-Methyl-2-pyridone, **47**. The Dudley reagent **46** has been used successfully to protect secondary,[379] tertiary[380] and hindered hydroxyls.[381] Reactions are known to progress well when trifluoromethyl benzene solvent is employed,[382] particularly when reagents are poorly soluble in toluene, such as treprostinil. Trifluoromethyl benzene has a boiling point 60 ^{o}C higher than DCM, so it is able to facilitate reaction conditions with higher operating temperatures.[383] Trifluoromethyl benzene has been reported to offer benefit to selective benzylation reactions compared to toluene. For example, the benzylation of a glucose derivative does not proceed in the presence of toluene solvent but achieves a yield of 93% when carried out in trifluoromethyl benzene.[378]

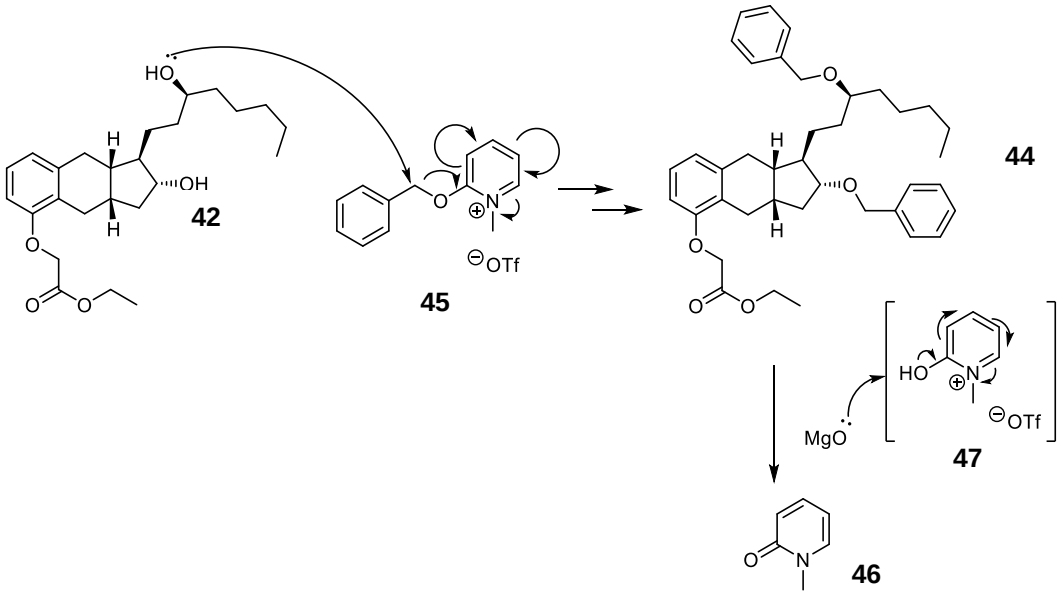

Scheme 3-16. Benzylation of secondary alcohols of treprostinil ethyl ester **43** using N-methyl pyridinium triflate **46** (Dudley reagent). Magnesium oxide **47** (MgO) is present to neutralise hydroxypyridinium by-product **48**. The reaction was conducted in trifluoromethyl benzene solvent and refluxed for 24 hours.

The benzylation of treprostinil ester **43** using the Dudley reagent **46** was investigated on a 280 mg scale. After heating in trifluoromethyl benzene at 83 ^{o}C for over a 24-hours, TLC indicated reaction success by the consumption of starting material **43** spot. Additionally, a product spot with higher R_f was seen, which is consistent with the reduced polarity expected of benzylated ester **45**. The presence of a single TLC product spot suggested formation of either the mono or bis, but not a mixture of both the benzylated treprostinil derivatives.

The heterogenous reagent magnesium oxide was removed by filtration and the filtrate dried *in vacuo* to yield 451 mg (>100%) of crude benzylated ester **45**. ^{1}H NMR analysis of the crude product **45** showed the presence of the benzyl groups at 7.42 – 7.16 ppm which integrated to 10 protons, as well as showing resonances corresponding to the benzyl resonances; doublet of doublets at 4.55 – 4.39 ppm and a singlet at 4.49 ppm, which indicated there had been a successful bis-benzylation of treprostinil ethyl ester **43**. A shift in the methine protons (highlighted in pink and purple in **Figure 3-13**) from 3.53 and 3.65 ppm, to 3.38 and 3.50 ppm was observed, indicating that the benzyl groups had attached to the alcohol moieties, as desired.

With the treprostinil 4 carboxylic acid and hydroxyl groups protected as shown in structure **45**, purification by chromatography was expected to be simpler. With reduced polarity, less interaction occurs with the polar solid phase and better partitioning between stationary and mobile phases results. Reduced solid phase interaction reduces the broadening of the product band of compound and increases the resolution of the product which reduces the likelihood of overlapping product with impurities. The increased resolution facilitated isolation by automated

chromatography through normal phase silica in two batches to yield bis-benzyl ester **45**, as a clear oil which forms a crystalline structure upon cooling, in 49% total yield.

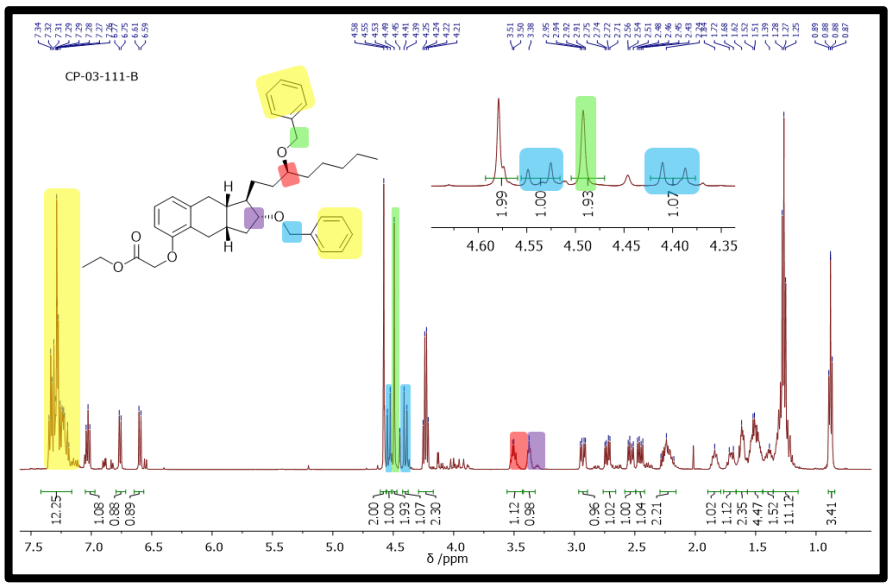

Figure 3-13. ^{1}H NMR spectra of bis-benzyl treprostinil ethyl ester, **45**

Subsequent ester hydrolysis of bis-benzyl treprostinil ethyl ester **45** was carried out using basic hydrolytic conditions using lithium hydroxide to afford a 64% yield of *bis*-benzyl treprostinil acid **49**, a clear oil.

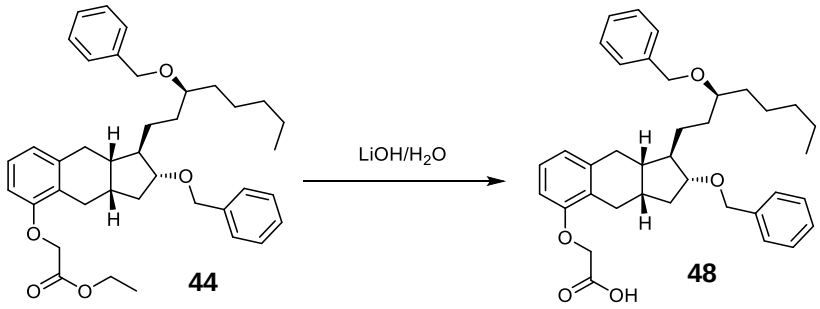

Scheme 3-17. Ester hydrolysis of bis-benzyl treprostinil ethyl ester **44** to form bis-benzyl treprostinil **49** using lithium hydroxide (LiOH)

Hydrolysis was monitored by TLC, showing a reduction in Rf value, from 0.71 to 0.0 as the reaction progressed. The presence of the acid group was confirmed by bromocresol staining forming a yellow TLC spot. There were no ^{1}H NMR resonances for the ethyl ester methylene or methyl protons. A downfield proton at δ 9.26 ppm was consistent with being the exchangeable carboxylic acid proton. The resonance corresponding to the α-carbonyl methylene protons shifted from 4.75 to 4.60 ppm (highlighted in pink in **Figure 3-14**). The IR spectra showed a change in absorption from 1759 to 1732 cm^{-1} consistent with ester having been hydrolysed to a carboxylic acid. The addition of the OH absorption at 2858 cm^{-1} is also consistent with ester hydrolysis having occurred.

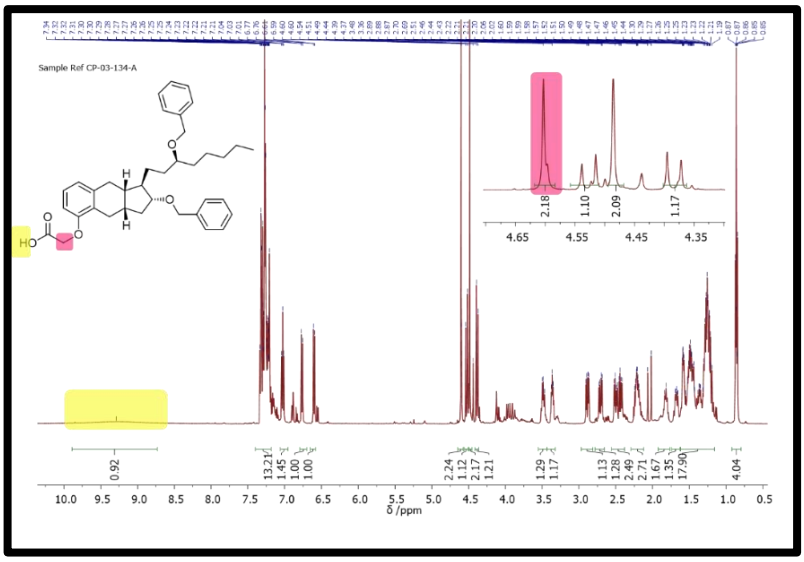

Figure 3-14. ^{1}H NMR spectra of bis-benzyl treprostinil **49** following ester hydrolysis. A shift in methylene resonance is observed (shown in pink) and the acidic proton (shown in yellow) is also present.

As each protection/deprotection is associated with yield loss, it was hoped a route to the bis-benzyl treprostinil **49** could be achieved without the protection and subsequent deprotection of the acid. Having found suitable conditions to protect the hydroxyl groups of treprostinil ester **43** with the Dudley reagent **46**, the same benzylation conditions was trialled for treprostinil **4** on a 50 mg scale. TLC showed the absence of treprostinil **4** spot (R_f = 0.1) and the presence of a new spot with higher R_f (0.4) after 18 hours. After filtration to remove magnesium oxide **47**, the concentrated filtrate was acidified and extracted from aqueous layer in DCM to retain treprostinil 4 for comparison to afford a yellow/brown gel-like material. The ^{1}H NMR spectrum showed the presence of three methylene resonances; one singlet for the treprostinil α-methylene protons; one singlet for the benzyl methylene attached via ether to the alkyl chain of treprostinil 4; and one doublet of doublets corresponding to the two environments of the benzyl methylene protons forming the cyclic ether. The doublet of doublets forms from the two distinct environments of the two methylene resonances as a result of the confined freedom of rotation associated with being bound to a cyclic structure with multiple stereocentres, also seen in spectra of bis benzyl ester **44** and bis-benzyl acid **49** formed by ester hydrolysis. The direct benzylation was carried out to investigate the route, and a large supply of bis-benzyl treprostinil **49** had already been synthesised through the ester protection-deprotection route, so the direct benzylated product was not purified further.

The successful direct benzylation of treprostinil **4** eliminates the esterification and ester cleavage steps. The diagnostic resonance upon benzylation is a shift in methine resonance 0.1 ppm upfield. Although the final bis-benzyl treprostinil **49** formed by direct benzylation of treprostinil **4** was not purified and a yield cannot be determined and compared, the acid work up should have retained all the treprostinil **4** starting material. No remaining methane resonance corresponding to treprostinil **4** were detected. The TLC and the lack of treprostinil

4 detected by ^{1}H NMR suggests that the coupling was complete. The direct benzylation was meant to serve as proof that the esterification could be circumvented for the formation of the *N*-acyl sulphonamide as below.

As described earlier, an efficient method to couple methane sulphonamide **25** to the free acid was optimised on phenoxyacetic acid **22**. The conditions which proved successful were coupling agents EDCI **34**, reported by Pelletier,[384] and CDI **36**, reported by Nakamura.[115] In the case of CDI **36**, the catalyst DBU **31** was necessary for coupling, and catalytic DMAP **32** assisted EDCI **34** coupling, however, the presence of triethylamine or addition of NHS **29** prevented the product forming.

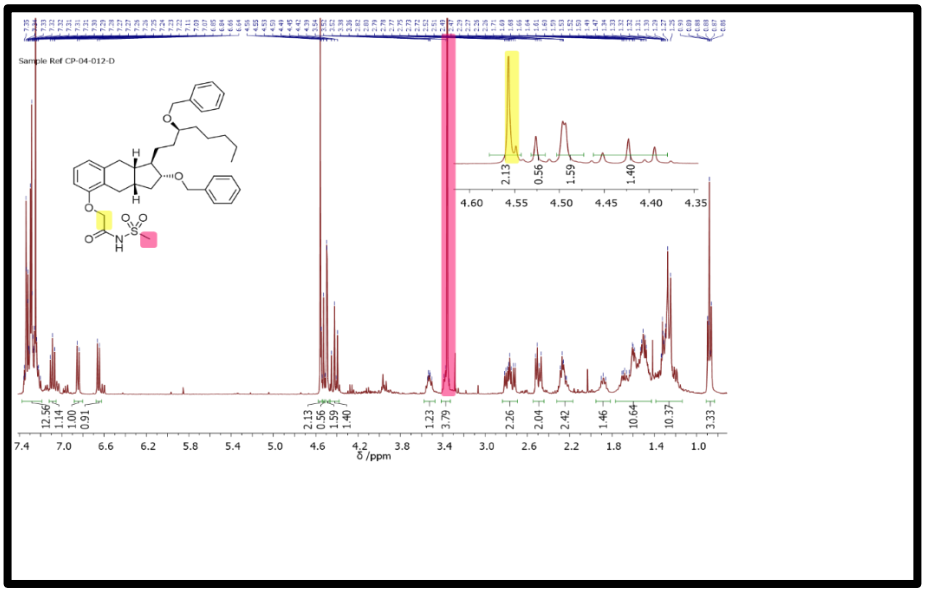

Figure 3-15. ^{1}H NMR spectra of bis-benzyl N-acyl sulfonamide treprostinil **21** showing the shifted methylene resonance highlighted yellow and the additional methyl resonance of the sulfonamide group in pink.

The successful conditions for forming the *N*-acyl sulfonamide derivative of phenoxyacetic acid **22** were then employed for *bis*-benzyl treprostinil **49** on a 50 mg scale. CDI **36**/DBU **31** conditions in refluxing THF proved successful giving a 21% isolated yield of bis-benzyl treprostinil N-acyl sulfonamide **50** after purification over a silica column. Interestingly, a greater yield of 46% for bis-benzyl treprostinil N-acyl sulfonamide **50** was achieved by employing EDCI **34**/DMAP **32** when carried out on a smaller 20 mg scale. The isolation of bis-benzyl acylsulfonamide treprostinil **50** required three runs of column chromatography to achieve good separation. Initially, automated separation of the product was conducted on normal phase silica with mobile phase 20% ethyl acetate/hexane increasing to 100% over 13 column volumes with a flow rate of 3 mL/min. Apart from an initial peak at the void volume, no peaks were distinguished. An increase in absorbance was measured but it remained across the entire spectrum. The column was purged manually with 50% ethyl acetate/methanol and all fractions were collected. The column was repeated but with the same outcome. With the concentrated collected fractions, a manual column was run using mobile phase 50-100% ethyl

acetate over 4 column volumes. Separation was achieved although some overlap of the compound spots were observed by TLC. For purity, only clean fractions were collected and combined to afford colourless oil so the isolated yield of 47% is not optimised. ^{1}H NMR showed the presence of a singlet at 3.38 ppm corresponding to the sulfonyl methyl singlet. There was also a small downfield shift for the α-carbonyl methylene protons of 0.02 ppm, although a greater shift had been anticipated. However, mass spectroscopy confirmed the product mass of $[M+H]^+$ 468 m/z. The neglibable shift in methylene resonance is possibly a result of the similar pKa of the acid and N-acyl sulfonamide acidic protons.

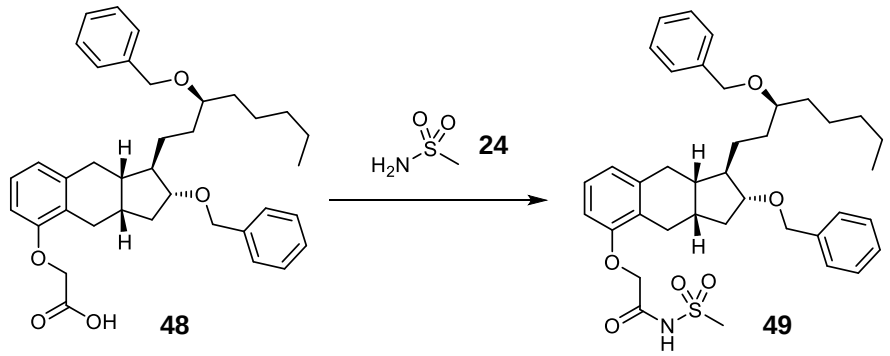

Scheme 3-18. Coupling of bis-benzyl treprostinil **49** to methyl sulfonamide **25** to form bis-benzyl N-acylsulfonamide treprostinil **50**.

Debenzylation was first attempted by treating bis-benzyl N-acyl sulfonamide **50** with $AlCl_3$. These conditions were examined because of an earlier observation when attempting to acylate the bis-benzyl protected-treprostinil ethyl ester **44** which resulted in the unwanted removal of the benzyl groups (Appendix 8.3). Although $AlCl_3$ is reported by others to cleave ethers and alkylated aromatic amines,[385] debenzylation was not successful.

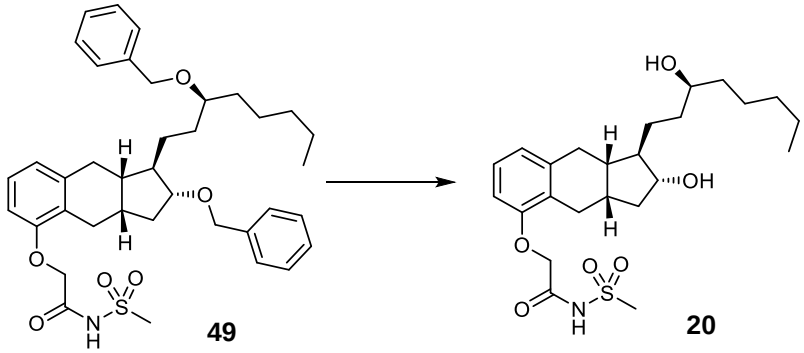

Scheme 3-19. Debenzylation of bis-benzyl N-acyl sulfonamide treprostinil **50** to form desired product N-acyl sulfonamide treprostinil **21**.

Hydrogenation is widely used for debenzylation, so was conducted using hydrogen and palladium on carbon. There are restrictions that prohibit hydrogen storage at UCL, so it was not possible to use a hydrogen balloon to purge and run the reaction. One effective method to

generate hydrogen *in situ* was to use purpose-designed glassware, known as “CO-ware” **Figure 3-16**.

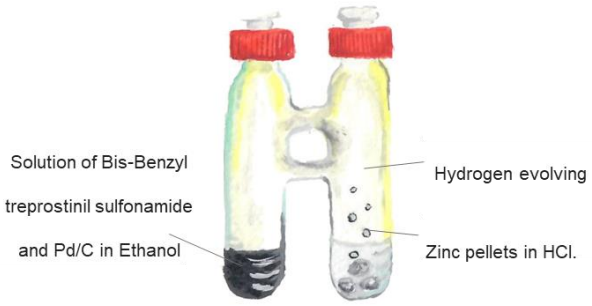

Figure 3-16. Reaction of the reductive cleavage of benzyl ethers using the two-chamber "CO-ware" glassware. HCl = 4 M hydrochloric acid; Pd/C = palladium on carbon.

The CO-ware consists of two chambers which are linked by a bridge near the top, above the solvent levels. In one chamber, HCl and zinc undergo reaction to form hydrogen which passes *via* the bridge to the second chamber where the hydrogenation reaction mixture is stirred. In our hands, reaction times for the small scale reactions were generally no longer than standard hydrogenation reactions although larger scale reactions required longer time periods.

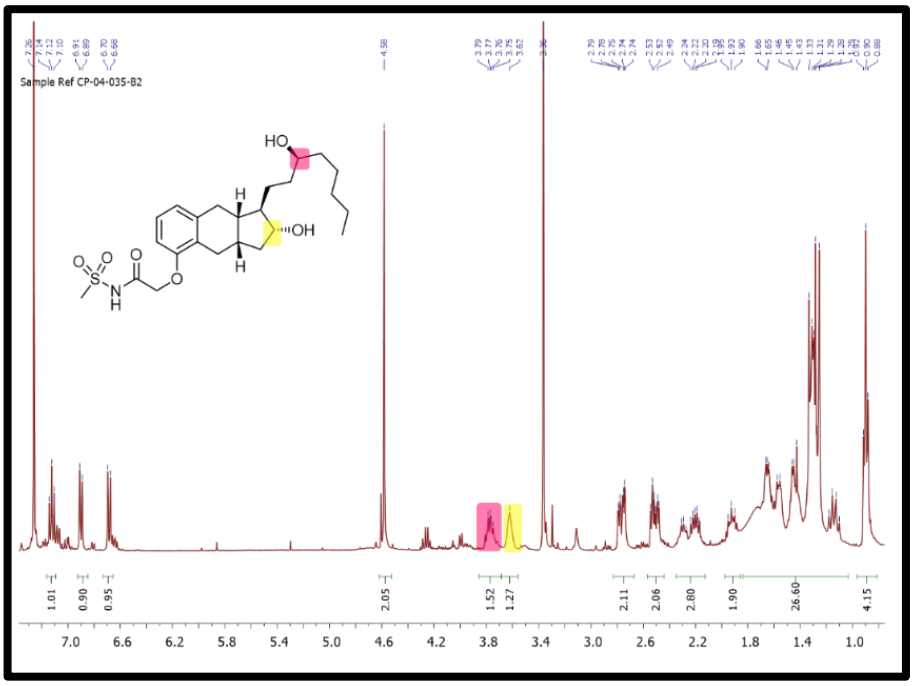

Figure 3-17. ^{1}H NMR spectra of desired product N-acyl sulfonamide treprostinil **21** following hydrogenation of the hydroxyl-protecting benzyl group. No benzyl groups are detected and a shift in the methine resonance shown in yellow and pink was observed.

N-acyl sulfonamide treprostinil **21**, named TRE-S, was ultimately synthesised (**Scheme 3-20**) but required protection of the hydroxyl groups. Original synthesis of N-acyl sulfonamide

treprostinil **21** was limited by the need to protect and deprotect both the carboxyl and hydroxyl groups (Shown in blue). However, a route was found to protect the hydroxyl groups without the need for esterification (shown in red). It also became apparent that the coupling reactions using methane sulfonamide were not efficient in their yields. These factors thus limited options for scaling up the preparation of TRE-S **21**.

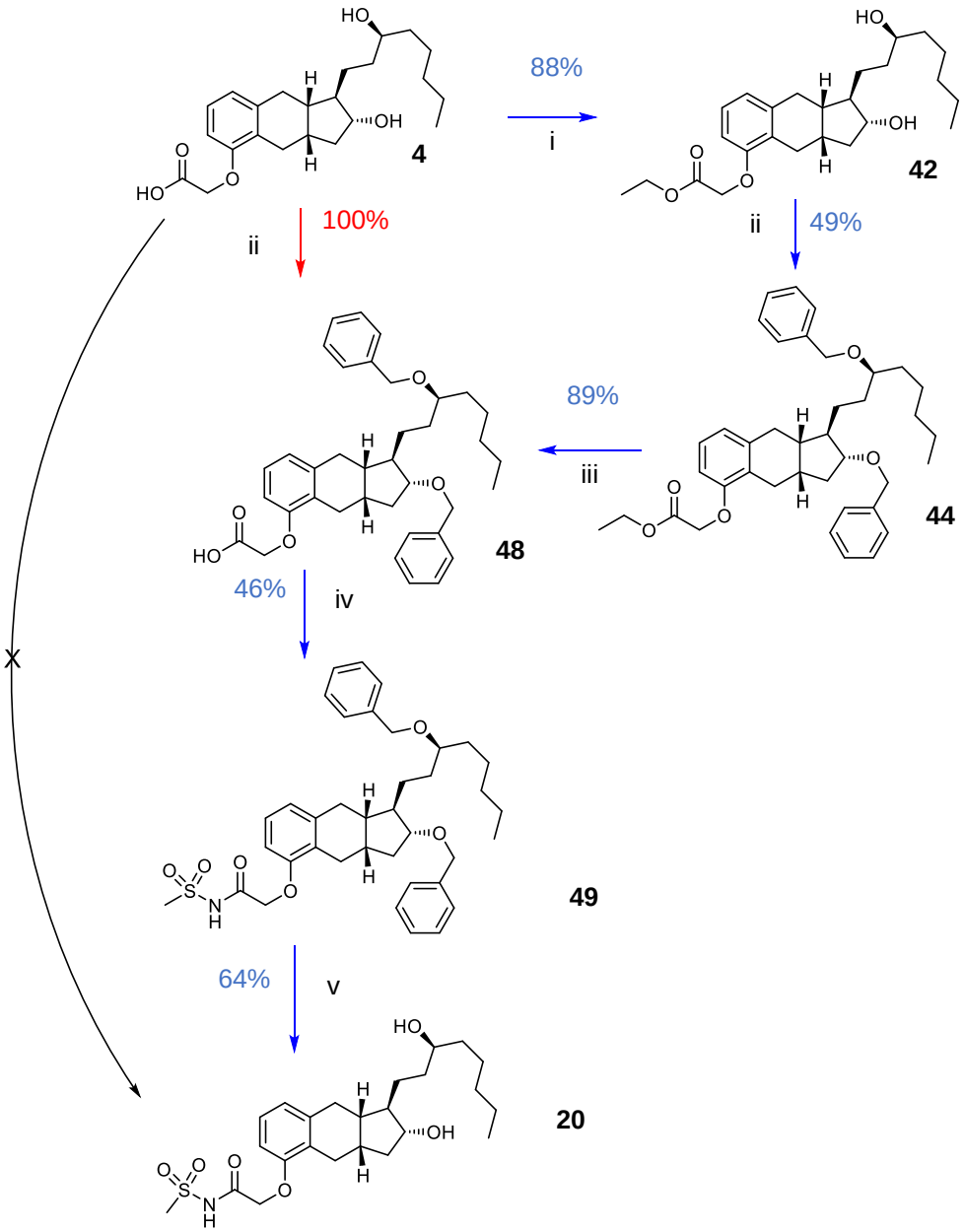

Scheme 3-20. Scheme of the final synthesis of N-acylsulfonamide treprostinil **21** from treprostinil, 4 by two different methods to achieve the bis-benzylated treprostinil acid **49**. Isolated yields (labelled in blue) are reported. Yields reported in red were not isolated but are based on thin layer chromatography progress. i) Ethanol, sulfuric acid, 86 ^{o}C ii) Dudley reagent, magnesium oxide, trifluoromethyl benzene; iii) Lithium hydroxide, methanol/tetrahydrofuran'water, 18 hours; iv) carbonyldiimidazole, methane sulfonamide, diisopropylethylamine, dichloromethane; Palladium/carbon, hydrogen (zinc/HCl), ethanol.

Following the longer blue route in **Scheme 3-20** showing the isolated yields, the total yield for TRE-S **21** was 11%. Negating the need to esterify by benzylating treprostinil directly to form intermediate **44** is thought to improve the overall yield of synthesis. No treprostinil **4** was detected by TLC or ^{1}H NMR spectroscopy indicating 100% conversion, although isolation was not carried out. Recalculating the yield *via* the red route, using an optimistic yield of 100%, gives an overall yield of 29%. The step with the lowest yield *via* this route is the sulfonamide coupling which suggests further optimising is possible. However, the need to protect also contributes to the remaining losses, so a route to N- acyl sulfonamide treprostinil **21** which circumvents the need to protect was therefore sought.

3.2.3 Triol intermediate

During the synthesis of treprostinil 4 , a precursor triol intermediate **51** undergoes reaction with the chloroacetonitrile **52** in acetone, using potassium carbonate base and butylammonium iodide as iodide metathesis reagent to give treprostinil **4** after nitrile hydrolysis in methanol/water with potassium hydroxide (**Scheme 3-21**). The precursor triol **51** undergoes alkylation at the phenolic hydroxy without undergoing reaction at either of the secondary hydroxyls. There is no need to protect the secondary alcohols in the precursor triol intermediate **51**. It was hypothesised the triol precursor 51 could be used to prepare the treprostinil acyl sulfonamide **21**.

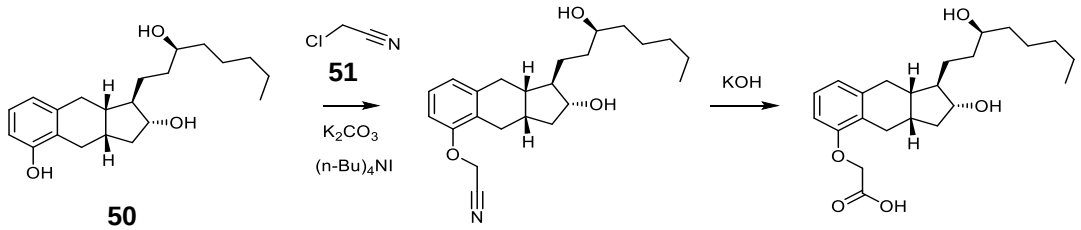

Scheme 3-21. Last steps of treprostinil synthesis taking the triol to treprostinil.

Before triol **51** was requested from UT, an attempt was made to obtain the triol **51** from treprostinil **4** by aryl ether cleavage. Ethers are relatively chemically stable bonds but are also known to undergo cleavage when exposed to strong acid in the presence of a nucleophile. The resonance of oxygen's electrons into the aromatic ring upon phenol formation was thought to aid the likelihood of cleavage. Model compound phenoxyacetic acid **22** was treated with one equivalent of hydroiodic acid in dimethyl sulfoxide on a 100 mg scale. Monitoring by TLC after one hour showed the spot for starting acid **22** as well as additional spots with higher R_f. The reaction solution was worked up by liquid extraction in ethyl acetate and analysed by ^{1}H NMR spectroscopy. The spectrum revealed the presence of the methylene resonance as well as no shift in aromatic proton resonances, deeming the reaction unsuccessful. Improvements to the ether cleavage could have been made by using acidic solvent and heating the reaction.[386] However, soon after the benzindene triol intermediate **22** was kindly donated by United Therapeutics.

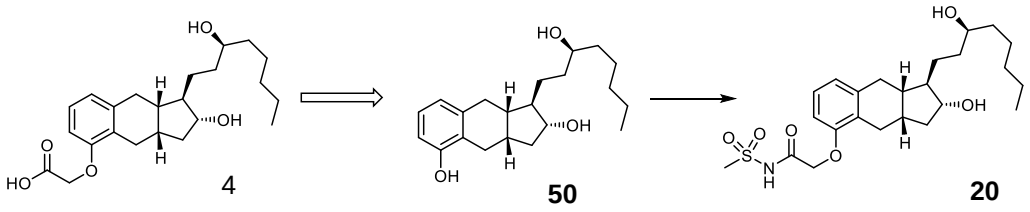

Scheme 3-22. Proposed conversion of treprostinil triol precursor, **51**, to TRE-S **21**.

Bromoacetyl bromide **53** (**Scheme 3-24**) was selected to be used in place of chloroacetonitrile **52** to make the treprostinil acyl sulfonamide **21**. Reaction of treprostinil triol **51** was first examined with triethylene glycol (TEG) with the intention of forming the ester. Forming the ester allowed for a test reaction with a primary nucleophile without the interference of resonance, such as that of methane sulfonamide **25**. Reaction with a bromo acetyl bromide **53** and triethylene glycol were allowed to react in the presence of 1 equivalent of triethylamine for 30 minutes producing bromoacetyl ester **54** as a colourless oil (yield 73 %).The reaction of the bromo ester **54** with the triol precursor **51** was based upon the conditions used by Kokotos et al,[387] which required acetone reflux at 58 ^{o}C in the presence of potassium carbonate for 4 hours. The displacement of the chloride ion in the treprostinil synthesis, required the formation in the iodo derivitave *in situ* by addition of t-butylammonium iodide. Such activation was not required in the synthesis of the prodrug derivatives as the bromine intermediates (**54** and **55**) were employed.

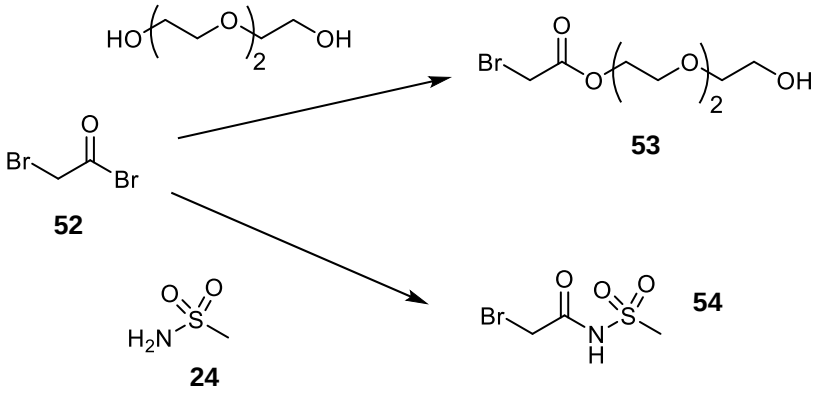

Scheme 3-23. Formation of prodrug precursors. Displacement of acyl bromide of **53** with trietheylene glycol forms bromo triethyleneglycol ester **54** and bromide substitution with methane sulfonamide **25** forms bromo-N-acylsulfonamide **55**.

A higher R_f for the esterified triol **56** was expected, similar to the properties possessed by the ethyl ester treprostinil derivatives. After 4 hours TLC showed the presence of a new product spot (R_f = 0.58) and only a faint spot corresponding to the starting triol **51** (R_f = 0.48). Multiple spots were visible with R_f less than 0.17, so purification was expected to be easy by column chromatography. The reaction was filtered to remove potassium carbonate and the filtrate concentrated to afford a brown oil. Column chromatography was carried out but neither of the high R_f compounds were the desired TEG esterified treprostinil **56**. A mobile phase with higher

polarity was used to elute and isolate the more polar compounds. Surprisingly, TEG ester treprostinil **56** was isolated as the compound with the lowest R_f. ^{1}H NMR spectroscopy confirmed the presence of the methylene proton at 5.83 ppm and the presence of the methyl ether singlet at 3.33 ppm. A downfield shift in the resonance corresponding to the methylene protons of TEG originally neighbouring the hydroxyl was observed, from 3.48 to 4.28 ppm, upon ether formation.

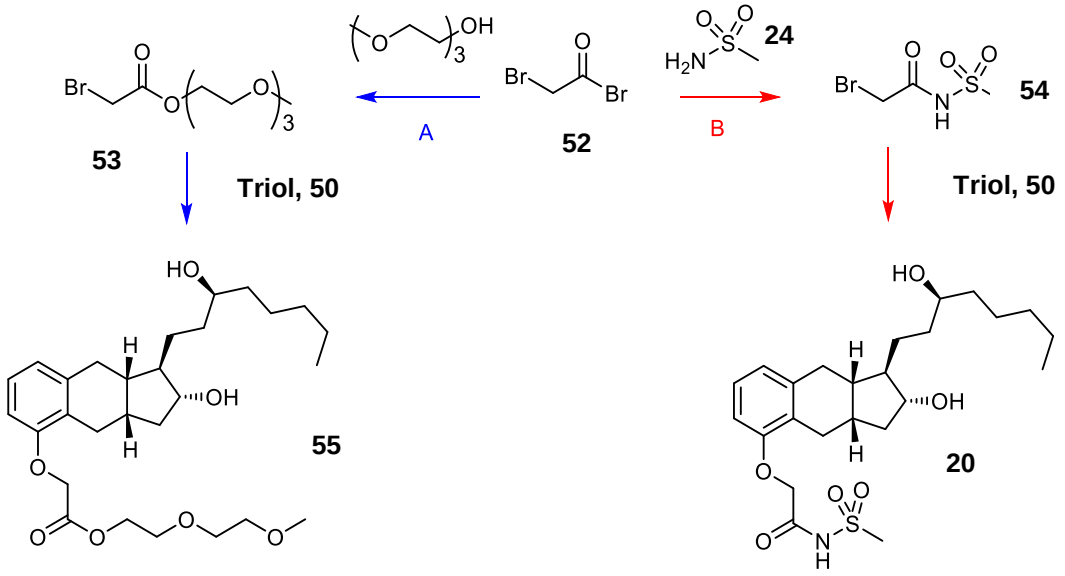

Scheme 3-24. Synthesis of treprostinil prodrugs (**21** and **56**) using triol intermediate **51** and prodrug derivatives (**54** and **55**) of bromoacetyl bromide (**53).**

Nucleophilic substitution at the acyl bromide **53** under basic conditions with triethylamine were not sufficient for the formation of bromo *N*-acyl sulfonamide **55**. It was necessary to conduct the reaction in refluxing toluene in the absence of base for 5 hours then cooling on ice to induce crystallisation to obtain the desired bromo acyl sulfonamide **55** at a yield of 24%. Reaction of the desired bromo acyl sulfonamide **55** with triol **51** was not achieved using the mild potassium carbonate conditions used to synthesise treprostinil TEG ester **56**.

In a similar manner to the synthesis of treprostinil **4**, [388] nucleophilic displacement of the halide was expected to be aided by the addition of an iodide phase transfer agent. The reaction was repeated with the addition of tetrabutylammonium iodide, but no reduction in the product spot nor increase in a product spot observed after 72 hours. Conditions described by Oslund et al.,[389] employ much stronger bases, such as sodium hydride, for the substitution of bromine by weak or hindered nucleophiles, such as phenolic hydroxyls. Following the unsuccessful attempts with mild bases, sodium hydride was employed.

The reaction between treprostinil triol **51** and bromo acyl sulfonamide **55** was completed in the presence of two equivalents of sodium hydride base in DMF. Since the reaction was conducted at a small scale (20 mg), care was taken to ensure excess NaH was not added to reduce the likelihood of deprotonating either of the secondary alcohols. Tracking by TLC indicated the

reaction was not complete after 30 minutes so additional sodium hydroxide (1.1 equivalents) was added until the reaction progressed to completion. The N-acyl sulfonamide treprostinil **21** was isolated by column chromatography to afford a clear oil in 20% yield. ^{1}H NMR spectroscopy confirmed the presence of a methylene carbonyl at 4.58 ppm as well as a singlet methyl peak at 3.36, consistent with the treprostinil-derived sulfonamide **21**.

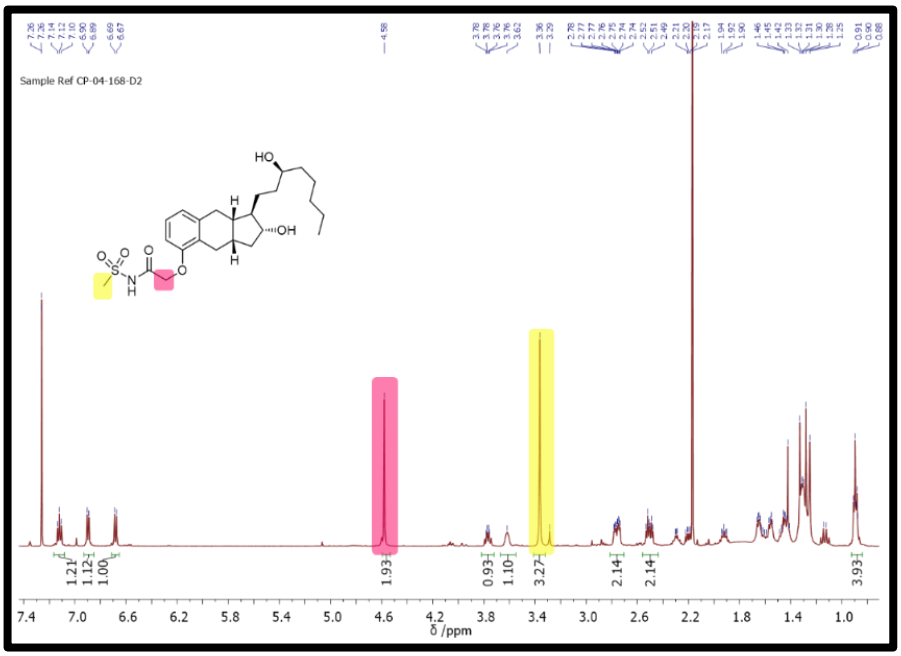

Figure 3-18. ^{1}H NMR spectrum of N-acylsulfonamide treprostinil **21**, synthesised *via* the triol intermediate **51**. Resonance in pink shows the methylene resonance and that in yellow shows the methylene resonance of the sulfonamide.

Unlike the bromo ester **54**, the bromo N-acyl sulfonamide **55** has an acidic sulfonamide proton. Once deprotonated, the negative charge resonates through the carboyl and sulfonyl bonds. This increases electron density at the bromomethyl carbon rendering it less susceptible to nucleophilic attack. Additionally, an extra equivalent of base is required as the sulfonamide proton (highlighted red in **Figure 34**) is the most acidic proton, so the second equivalent deprotonates the phenol.

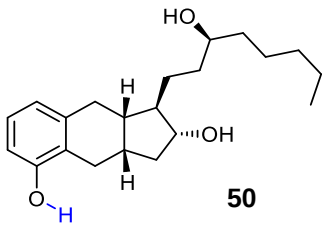

50

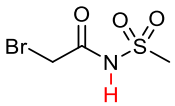

54

10.36 3.96

Figure 34. Triol **51** and bromosulfonamide **55** with their respective pKas

The requirement of a strong base such as sodium hydride to alkylate the phenol of triol **51** with the alkyl bromide **55** which possesses an additional acid proton may explain why the

treprostinil 4 synthesis utilises a two-step approach; the first reaction of triol **51** with chloroacetonitrile **52**, followed by hydrolysis to obtain the acid. A feasible, alternative route might be to obtain the acid in one step using a halo-acetic acid (**Scheme 3-25**). However, the milder, two-reaction route is preferred, suggesting that there is a downside when scaling up to using strong bases such as sodium hydride (NaH) in the presence of acids. Indeed, whilst investigating routes to a polyvalent structure (described in Appendix, Section 3) we observed multiple TLC spots upon treating treprostinil ethyl ester **43** with NaH, indicating there was some degradation. It is hypothesised that the methylene becomes deprotonated and forms a ketene intermediate structure of treprostinil, which may explain the low yield of the triol reaction with methane sulfonyl bromide.

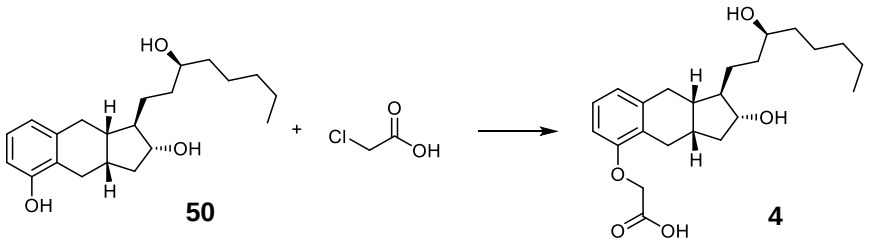

Scheme 3-25. Proposed alternative route to treprostinil **4** from triol **51** using chloroacetic acid.

Treprostinil N-acyl sulfonamide **21** from both the triol **51** and treprostinil 4 methods were both compared. ^{1}H NMR spectra show overlapping resonances ($CDCl_3$) as shown in **Figure 3-19**.

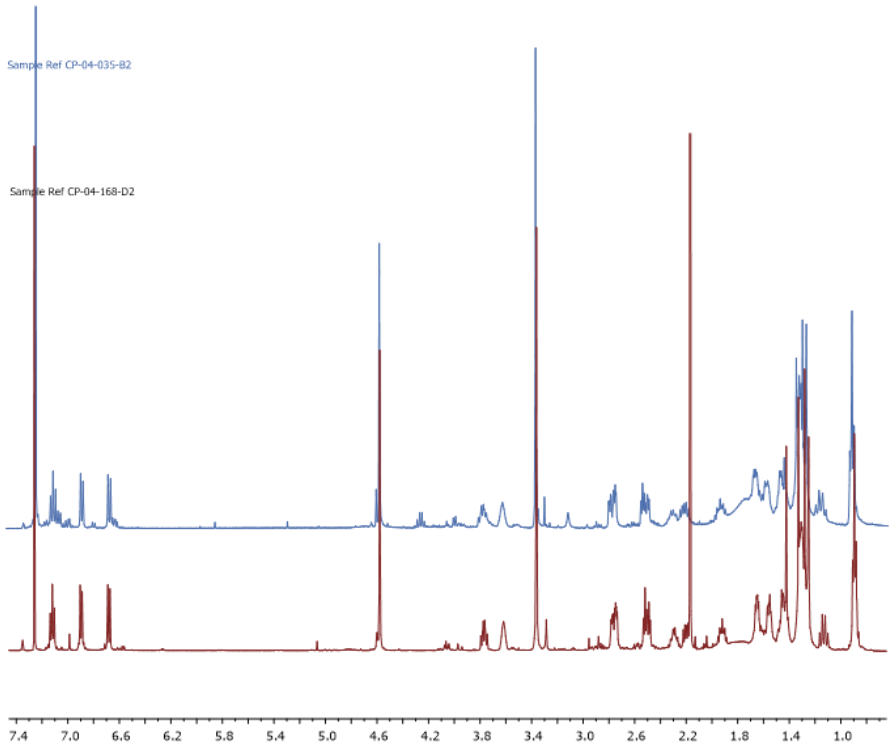

Figure 3-19. Comparison of ^{1}H NMR spectra of the two N-acyl sulfonamide treprostinil compounds **21** formed from treprostinil **4** (blue) and triol **51** (red).

Treprostinil 4 and both samples of N-acyl sulfonamide treprostinil **21** were analysed by RP-HPLC for comparison. The HPLC system used is able to detect 3 wavelengths simultaneously. A short wavelength of 217 nm was used to detect for compounds with higher sensitivity. A higher wavelength of 254 nm was used to detect for fluorescent compounds.

The predicted increase in solubility suggests that TRE-S **21** would have a shorter retention time than treprostinil **4**. Both N-acyl sulphonamides **21**, regardless of their synthetic route should elute at the same time, although surprisingly this was not the case (**Figure 3-20**). Treprostinil **4** has a retention time of 19.7 minutes. Treprostinil-derived sulfonamide **21** had a retention time of 16.6 minutes and was present at a 70% purity as determined by relative peak area using 217 nm wavelength view. In comparison, the triol-derived sulfonamide **21** had fewer impurities and had a slightly extended retention time of 18.6 minutes.

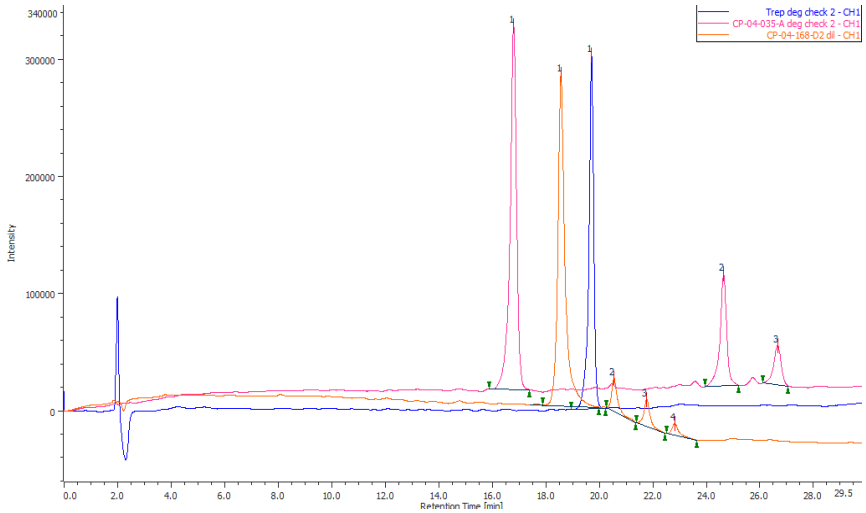

Figure 3-20. HPLC traces for treprostinil **4** and the two TRE-S compounds **21**; one derived from treprostinil **4** and the second via the triol **51**.

A possible explanation for the difference in retention times is that the samples were run several months apart, between which, the column had been run by multiple users with various compounds. A solution was made combining the two TRE-S compounds together in acetonitrile (0.25 mM) which was analysed by HPLC. The compounds eluted together after 18 minutes, with no distinction between the two products. Thus, the two expected TRE-S compounds appear to be the same, still without the presence of treprostinil.

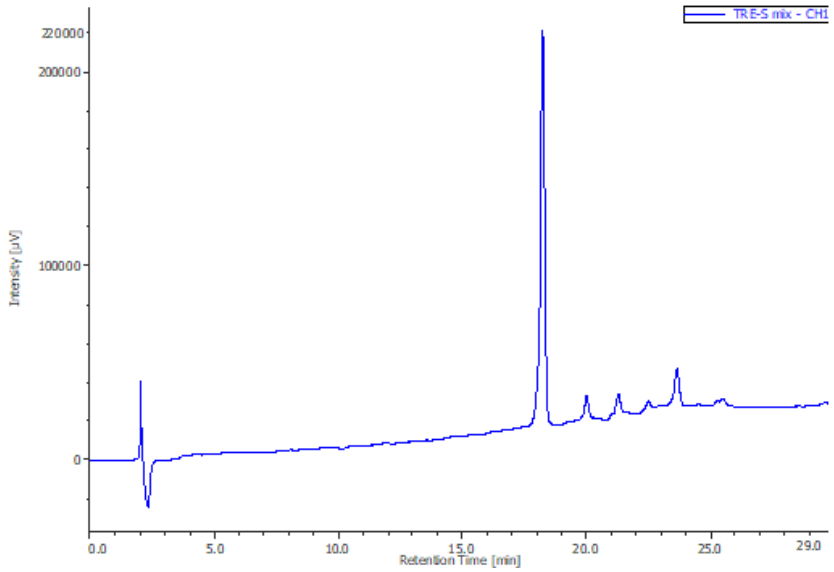

Figure 3-21. Elutogram of the combined TRE-S **21** compounds. No distinction between the products by HPLC absorbance confirms structure similarity and indicates that the product of the TRE-S synthesis using treprostinil or triol, is the same.

The accurate mass of both compounds were the same although interestingly, the triol **51**-derived acyl sulfonamide **21** was detected in the negative mode ($[M-H]^-$ 466 m/z), similar to

the N-acyl sulfonamide phenoxyacetic acid compound **26**, whereas the treprostinil derived sulfonamide **21** was detected in the positive mode ($[M+H]^+$ 468 m/z).

Notably, all sulfonamides (except triol **51**-derived *N*-acyl sulfonamide **21**) were characterised as their $[M-H]^-$ ion, although the LCMS/MS detected the compounds most sensitively as their positive $[M+H]^+$ ion. To investigate whether this was a result of the formic acid added to the LCMS/MS system, the mobile phase buffer was changed to ammonium acetate and the samples re-run. However, the detection was still more sensitive in positive mode.

The N-acylsulfonamide treprostinil **21** structure derived from treprostinil 4 *via* the TMS protected intermediate isolated by HPLC during an investigation into the hydroxyl-protection was retrospectively compared against the ^{1}H NMR spectra of the known N-acylsulfonamide structures **21**. Interestingly, the methylene resonance and the proposed methyl resonances do not overlap with the confirmed structures of N-acylsulfonamide treprostinil **21**. Although analysis of the TMS-derived sample was carried out in a different deuterated sample (MeOD), the resonances share fewer similarities that would be expected. The sample of the TMS-derived sample could not be located so unfortunately no re-analysis could be carried out.

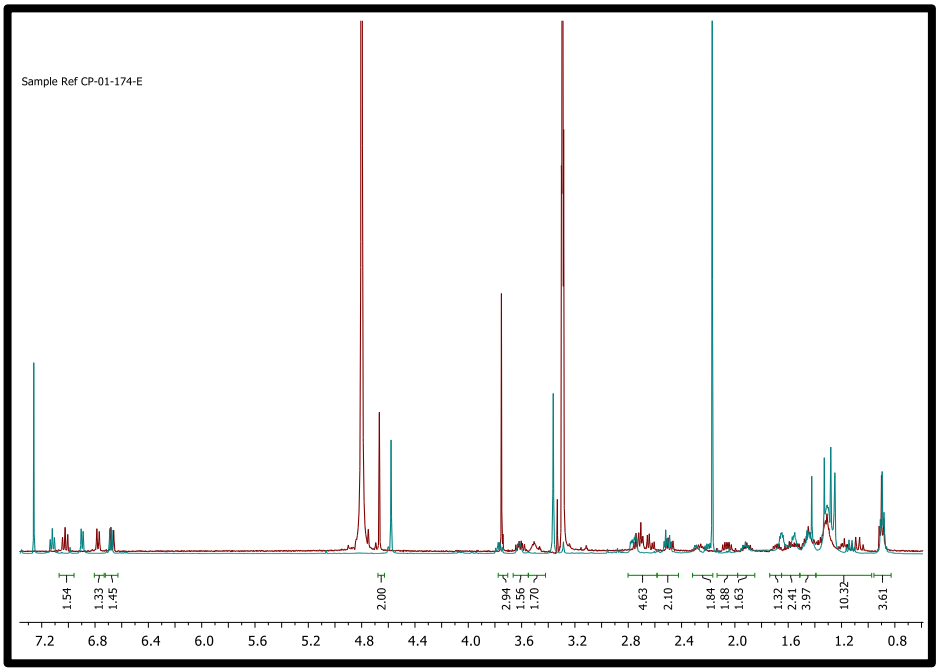

Figure 3-22. ^{1}H NMR spectra comparing the treprostinil 4 derived *N*-acylsulfonamide **21** (Red) and the trimethylsilyl ether-derived isolated product (Blue). Neither methylene or methyl resonances overlap.

In this section, among many attempts, three methods to obtain N-acylsulfonamide treprostinil **21** were described, all with similar overall yields. Two of the methods described produce consistent characterisation. Derivatising treprostinil 4 *via* an acid and hydroxyl protection route and derivatising the trial intermediate, although similar yields were achieved for the two methods of making *N*-acyl sulfonamide treprostinil **21**, the triol **51** method took significantly less time and resources. One-pot derivisation from treprostinil *via* the TMS-protected product

gave as great a yield of product **21** compared to the other two methods, despite the many side reactions which seemed to occur by TLC. However, there are inconsistencies with the product as it was not fully characterised and unfortunately post-hoc analysis was not an option. With two synthetic routes outlined for the synthesis, of *N*-acyl sulfonamide treprostinil **21**, the compound was taken forward to investigate its biological activity.

3.2.4 In vitro evaluation of treprostinil-sulfonamide 21

An effective pro-drug is required to be stable upon storage and when administered, which will degrade to release the active compound at the target site. The pro-drug should have reduced activity in comparison to the parent drug. Selexipag 5 had a 10-fold decrease in activity at the IP receptor in comparison to its metabolite, ACT-333679 6, as measured by cAMP generation.[390] Selexipag 5 was stable when incubated in human blood plasma (although not in rat plasma owing to the many esterases present), but was degraded in a time-dependant manner when incubated in both human and rat hepatic microsomal assays.[115] The stability and degradation of TRE-S **21** was investigated using selexipag 5 as a comparative control.

The anti-proliferative and vasodilatory effects of prostacyclin mimetics (PMs) is established to be dependent on cAMP,[276] although not exclusively.[272] Upon binding of PMs to the IP receptor, a cascade of intracellular mechanisms is initiated which cause adenylate cyclase to convert ATP to cAMP. The stimulation of cAMP generation results in a vasodilatory, anti-proliferative and anti-thrombotic response.[62] The dependence of the pathway on cAMP makes it an ideal indicator of pathway activation.[391] The activity of the PMs was measured comparatively in their ability to stimulate cAMP generation in a stable cell line, HEK-298.

To increase the sensitivity of comparative cAMP generation and reduce the effects of other receptors, cells stably transfected to over-express the IP receptor were used. Once generated, cAMP has a half-life of approximately 1 hour and the time course of cAMP generation with treprostinil has previously been carried out, showing levels to peak at between 15-30 mins in normal human arterial smooth muscles.[276]

The concentration-dependent response of treprostinil was evaluated over the range 0.01 to 1000 nM in HEK-293 cells exposed to the agonist for 15 mins. Intracellular cAMP levels began to be elevated at concentrations above 0.01 nM of treprostinil. The log concentration causing 50% of the maximal response (log EC_{50}) was calculated from the fit to be of -9.2, which equates to an EC_{50} value of 0.6 nM. This is very similar to the EC_{50} (1.9 nM) value for cAMP generation reported in CHO cells expressing the IP receptor,[85] but 10-fold lower than that (reported EC_{50} 8.2 nM) in normal human pulmonary arterial smooth muscle cells.[276] This may simply reflect the different nature of the cell systems reflect differences in the expression of the IP receptor and/or activity of the phosphodiesterase enzymes that break-down cAMP. In contrast to treprostinil, the response of TRE-S had a 30-fold lower potency at elevating cAMP compared to treprostinil (EC_{50} was 18nM), where cAMP levels did not start to become elevated until above the 1 nM concentration. Therapeutically, treprostinil is administered to patients to

achieve drug-blood concentrations between 10-40 nM. As shown in **Figure 3-23**, at 10nM, TRE-S exhibits a 11.5-fold decrease in activity compared to treprostinil, and for 100 nM, a 1411-fold decrease. The difference in EC_{50} of TRE-S and its metabolite (30-fold) is greater than that of selexipag and ACT-333679 (15-fold difference) as measured using a similar cAMP assay.[278]

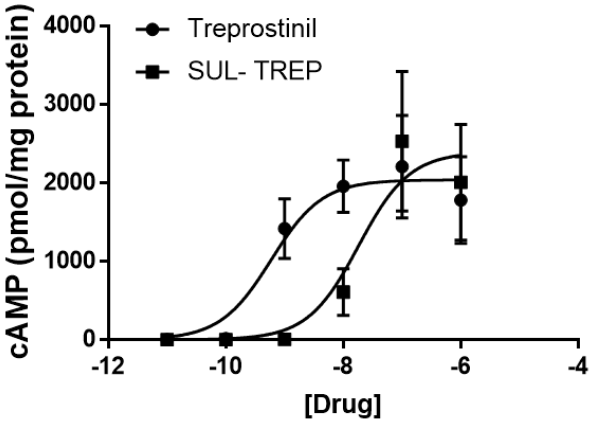

	Treprostinil	SUL- TREP
Bottom	~ 1.351e-016	~ 2.113e-016
Top	2039	2395
LogEC50	-9.226	-7.739
EC50	5.943e-010	1.825e-008

Figure 3-23. Concentration–response relationship of intracellular cyclic AMP changes induced by the treprostinil pro-drug, TRE-S **21** compared with treprostinil. HEK-293 cells, stably transfected with the human IP receptor, were grown in minimum Earle's medium containing 9% serum and treated with treprostinil drugs for 15 mins over the concentration range of 0.01-1000nM. Cyclic AMP was extracted from cells and normalised to protein content. Data are presented as mean ± S.E.M. (n=4) and points fitted using the sigmoidal-curve fitting routine in GraphPad Prism where the Hill slope has been set to 1. The table gives the min (Bottom) and max (Top) and the log of the EC_{50} values for the two curves shown.

3.2.5 Prodrug degradation

The reduced potency of TRE-S 21 at the IP receptor suggests there is potential to avoid adverse events experienced upon administration of treprostinil 4. The prodrug degradation drastically effects the utility of the prodrug. To evaluate the utility of TRE-S 21 as a prodrug, the stability in blood plasma and its enzymatic degradation profile was assessed.

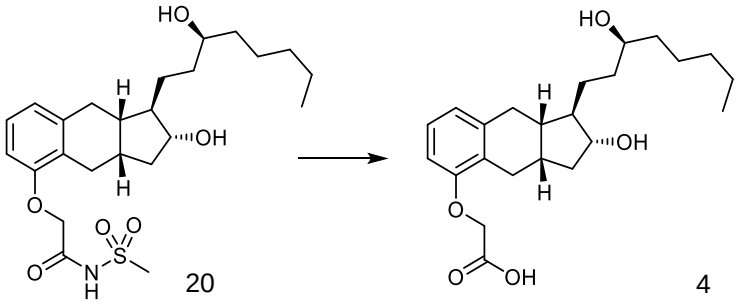

Scheme 3-26. Proposed degradation of TRE-S **21** to treprostinil **4** by carboxylesterases found in hepatic microsomes.

Enzymatic degradation of selexipag **5** (**Error! Reference source not found.**) to ACT-333679 6 metabolite was reported to occur by the action of carboxylesterases. Enzymatic activation of selexipag was evaluated using hepatic microsomes *in vitro*.[392] To investigate whether treprostinil sulfonamide 21 was broken down in a similar manner, the same type of assay was used. Selexipag **5** was used as a positive control. A general microsome protocol[393] was followed with recalculated concentrations to match that reportedly employed by Nakamura.[115]

The liver is rich in metabolic enzymes and is the site of most drug metabolism so stability and degradation are often determined *in vitro* using hepatocytes.[393] Enzymes responsible for drug degradation are stored on the endoplasmic reticulum of cells. By isolating particles of the endoplasmic reticulum, known as microsomes, its associated enzymes are isolated and from soluble enzymes in the spuernatant and retained. Using the microsomes in the presence of pharmaceutical compounds, offers a method to determine profiles of drug degradation and prodrug activation by intracellular, non-soluble enzymes. Removing the issue of cellular uptake, analysis of each assay requires only a quenching and protein precipitation step to prepare the samples for analysis by HPLC. For analysis by LCMS(/MS), buffer salts must also be removed.

Microsomes are a specific fraction of homogenised hepatic cells which contain a high level of non-aqueously soluble enzymes. Collected from several samples of one species and pooled together, the fraction aims to represent the enzymatic activity of a generalised population of that species. Degradation of TRE-S 21 was evaluated in rat microsomes, in a similar manner to that reported for selexipag 5,[115] owing to their known activity for the degradation of selexipag 5 and their affordable cost and availability. Microsomes were supplied as a concentrated suspension with 20 mg/mL of protein. For the assay, total protein concentration was diluted to 0.53 mg/mL.

A nicotinamide adenine dinucleotide phosphate (NADPH)-generating system was included in the assay to replenish enzyme activity. Enzymes utilise NADPH as a co-factor so without the regeneration of NADPH, concentrations of NADPH decrease, reducing enzymatic activity. The enzyme glucose-6-phosphate dehydrogenase removes protons from glucose-6-phosphate, and in doing so, converts $NADP^+$ into NADPH. The inclusion of this enzymatic reaction in the

assay replenishes the NADPH which is consumed by enzymatic activity by the microsomes and thus, maintains the activity of microsomes over time. $MgCl_2$ is also included to stimulate CYP activity.[394] NADPH can be added directly to the system but without replenishing the NADPH concentration, the enzyme activity is expected to reduce over time as NADPH becomes depleted

Potassium phosphate buffer (PPBS) at pH 7.4 was used to dilute the microsome solution and all constituents of NADPH regenerating system, except the magnesium chloride. The buffer concentration described by all protocols[115,393–395] was 100 mM, approximately 10 times the concentration of buffer salts than used for isotonic cell preparations. The higher phosphate concentration is required to maintain CYP(3A) activity. All solutions were prepared prior to each assay and stored on ice prior to combining. Protocol variations exist about the order of addition. Most protocols indicated that following aliquoting of the microsomal suspension into assay vials labelled for each time point, the vials should be pre-incubated for 5 minutes. However, whether the NADPH-regenerating system or the study drug is added in this step varies between different protocols. The microsomal enzymes were expected to have some activity before NADPH is spent, which would affect the drug concentrations even within the pre-incubation period. For this reason, the NADPH-regenerating system was added in the preincubation step and the addition of pro-drug (TRE-S **21** or selexipag **5**) marked the beginning of the timed incubation. Selexipag **5** was run as positive control for the carboxylesterases and indomethacin was run as a positive control for the PY450 enzyme, which served as an indicator that the microsomes were active.[396] At designated time points, the samples were quenched by addition of ice cold organic solvent (150 µL) which precipitates proteins, then the sample was vortexed and centrifuged at 4 ^{o}C at 14 000 g for 10 minutes to remove proteins and the supernatants collected. A negative control was determined for each concentration by addition of the quenching solution to the microsome and NADPH-regenerating solution before the drug compound which was immediately vortexed and centrifuged to remove the proteins.

Selexipag was reported to have been run in the microsome assay at 10 µM and quantified at 10 minutes. Clearly, more time points were conducted in order to calculate a rate of degradation but the 10-minute starting point was a reasonable place to initiate a pilot microsome study. The study assay was designed to test selexipag at 10-fold above and below the 10 µM concentration (1 µM and 100 µM) and samples would be analysed at 5, 10 and 20 minutes. Using these parameters, the assay was run following the protocol described by Ackley et al.[393] A vial was prepared for each concentration and time point, which contained PBS (271 µL), NADPH-generating solution (18 µL) and rat microsomes (8 µL). After 5 minutes of preincubation, the respective concentration of selexipag was added (3 µL) to achieve a final concentration of 1, 10 or 100 µM. At each time point, ice cold methanol (150 µL) was added to the solution which was then vortexed, centrifuged and the supernatant retained (200 µL).

The samples were analysed by HPLC measuring UV absorbance at 217 nm using a UV detector and the analysing standards of selexipag and ACT-333679 (100 fm – 100 µM) immediately after. An isocratic mobile phase was emplyed of 55% acetonitrile/water spiked with 0.1% TFA over 20 minutes. Each sample was analysed in duplicate. Detectable absorbances were only observed for 100 µM standards and for assay samples originally containing 100 µM selexipag (**Table 3-5**). No observable absorbances were shown for lower concentrations.

Table 3-5. Absorbance of selexipag were only detectable for samples containing 100 µM of selexipag initially. A decrease in selexipag is observed, however, concentrations seems to rise after 20 minutes.

Selexipag concentration 100 µM	Incubation time /minutes	1st Analysis		2nd Analysis	
		Retention time of peak	AUC	Retention time of peak	AUC
100	5	9.4	753	9.3	807
	10	9.3	71	9.4	76.7
	20	9.3	174	9.3	173

Without a standard curve, the concentration of selexipag cannot be determined. Providing the value after 5 minutes is true, a decrease in selexipag concentration is observed, although concentrations increase after 20 minutes. The increase in concentration sheds doubt on the values obtained after 10 or 20 minutes; possibly an error during the sample preparation or an instrumental error.

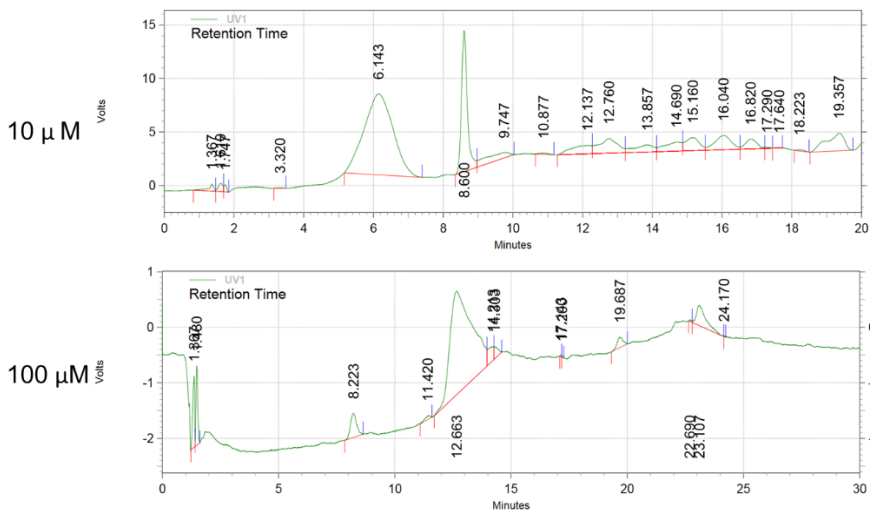

Figure 3-24. Low UV absorbance of selexipag standards.(10 and 100 µM) was observed as analysed by HPLC using isocratic mobile phase 55% acetonitrile/water. At 10 µM, two absorbances are present but both at a very low absorbance. At 100 µM, only one peak was observed, with a different retention time which was less resolved. The same mobile phase was used but to be sure that selexipag was given enough time to elute, the analysis was run for a further 10 minutes.

As shown by the low absorbance of selexipag in (**Figure 3-24**) it appeared UV detection was not sensitive enough to determine the presence of any remaining prodrug in the assay supernatant. This was surprising considering the article reporting selexipag 5 degradation in microsomes used HPLC.[115] The authors were contacted, who could not confirm the extinction coefficient of selexipag 5 but revealed that in more recent studies they had utilised LCMS/MS to quantify degradation. Based on the results obtained and the guidance from the authors LCMS/MS was pursued as a prodrug detection method.

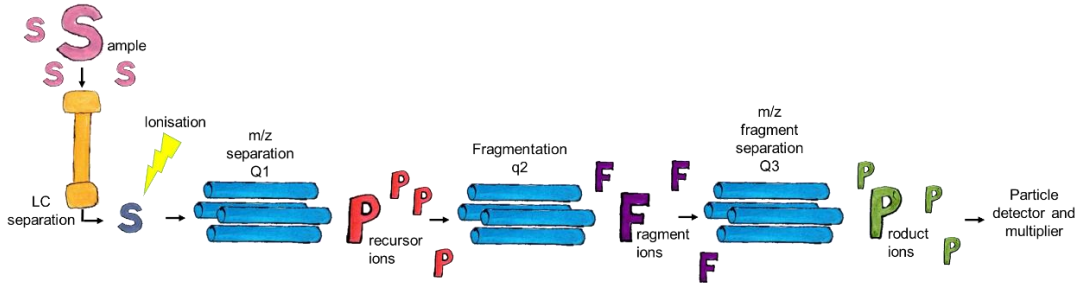

Figure 3-25. Principle of liquid chromatography tandem mass spectrometry. Following injection, the sample is separated by column chromatography. The eluent is ionised which is accelerated towards the first of the three blue quadrupole. The specified precursor ions (red) are identified and permitted into the fragmentation quadrupole where they are further fragmented and enter the third qudrupole. Product ions result which are detected and quantified.

In LCMS/MS, the sample is separated into its different compounds by LC on a RP-column. Following separation, the separated samples are channelled to the MS which selects ions with the specified full ion mass. Once isolated, the mass ions are further fragmented into smaller ions. The most abundant ion, as well as the total mass ion, can both be used to quantify the amount of analyte in the sample.

To determine the fragment ions an optimisation MS process was developed. A standard solution of each compound (selexipag, TRE-S and papaverine) was prepared and a full scan of each sample was conducted. Ions can be identified as either their positive ion, using positive mode, or the negative mass ion, using negative mode. Based on the acidic nature and stability as a negative ion, the sulfonamide compounds (selexipag **5** and TRE-S **21**), were expected to be detected in their negative $[M-H]^-$ state. By analysis on the LCMS/MS, a more sensitive detection was observed using the positive ion detecting mode.

The mass ion was identified for each drug compound; 497.01 m/z for selexipag and 467.6 m/z for TRE-S. Using the mass ion as the precursor ion, the sample was analysed to detect for the fragments produced from the precursor ion. Agilent Optimiser software was used to vary the collision energy and fragmentor voltage value to identify the method which produced the most sensitive detection of fragments. The most abundant ion (302.1 m/z for selexipag and 337.2 m/z for TRE-S), was used to quantify the amount of compound present. Following product-ion identification, a multiple reaction monitoring (MRM) method was created which uses the same solvent system and selectively detects for the specified ions identified in the MS.

Once the fragments had been identified, an LC method measuring total ion count was determined which would identify each product peak without overlap. Gradient methods appeared to show considerable baseline shifts and therefore an isocratic solvent of 55% acetonitrile/water both spiked with 0.1% formic acid, was employed. Using the fragments ions, a standard concentration curve could be plotted. Whilst investigating a suitable protocol to be sure enzymatic activity was occurring and could be detected, initial studies only included selexipag **5**. Therefore, a selexipag standard concentration curve was analysed and plotted (**Figure 3-30**).

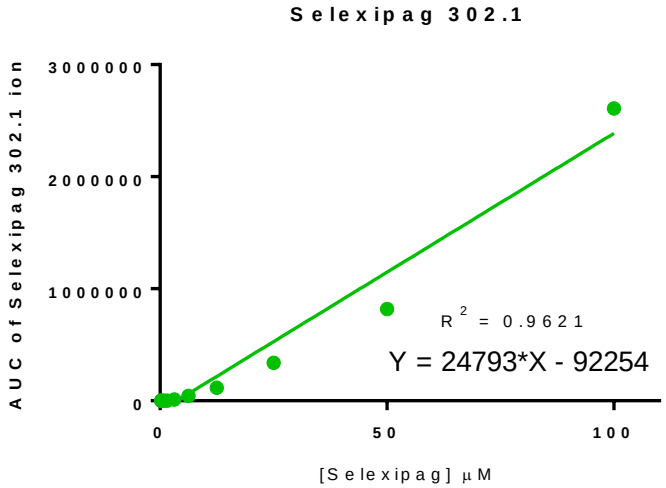

Figure 3-26. Plot of known concentrations of selexipag standards vs. the quantity of selexipag-derived ions with mass 302.1 m/z, as measured by area under the curve (AUC) using LCMS/MS.

Both the selexipag study[115] and microsome protocol for LCMS/MS analysis[393] made no mention of any further purification of samples, so supernatants (20 µL) were analysed directly by LCMS/MS.

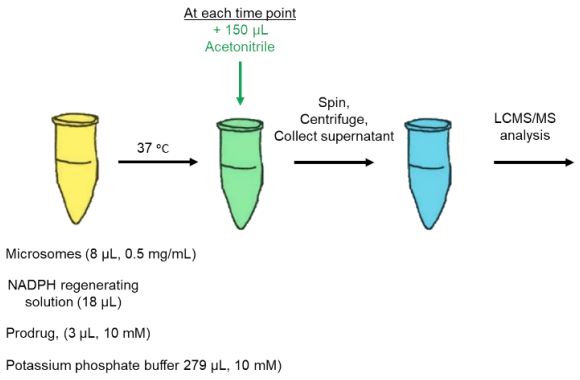

Figure 3-27. Microsome assay used to investigate rate of degradation of prodrug by hepatic enzymes. Nicotinamide adenine dinucleotide phosphate (NADPH) regenerating solution includes glucose-6-phosphate, glucose-6-phosphate

dehydrogense, β- nicotinamide adenine dinucleotide phosphate disodium salt, magnesium chloride. Samples were analysed by tandem LCMS

The data were analysed by the amount of the 302.1 m/z fragment ion of selexipag, which was converted to concentrations using the standard curve in **Figure 3-26**. The concentrations were plotted versus time for each concentration (**Figure 3-28**). The data for the 10 µM sample after 5 minutes shown in **Figure 3-28**. A looked spurious, with a total concentration of 666 µM (60-times greater than the concentration added). This outlying data point was removed (**Figure 3-28** B). The calculated concentration for the assay run at 1 µM was determined to be 3µM, three times greater concentration than the total. The concentration did not change over 20 minutes. A decrease in selexipag was observed for the 10 µM assays between 10 and 20 minutes. The concentrations expected for the 100 µM within the first 10 minutes was much lower than expected, given the reported half-life of selexipag.

All time points for 100 µM assays were lower than the initial concentration although however, a lower concentration was observed after 5 minutes than expected based. An explanation for the detection of selexipag at greater concentrations than added into the assay, was not developed.

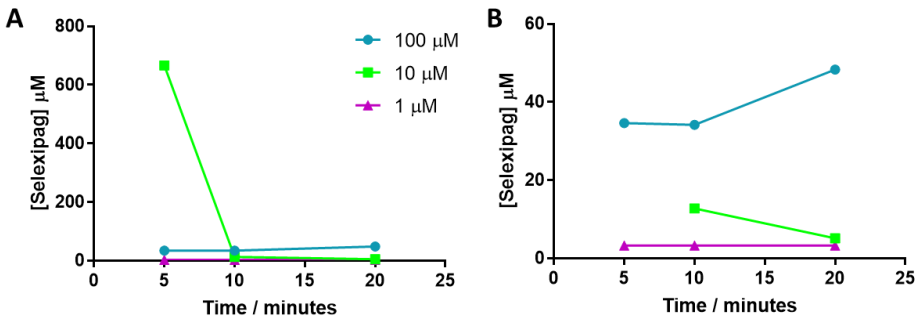

Figure 3-28. Quantification of selexipag **5** in the microsomal assay over time. The assay was run using concentrations of selexipag 5 at 1, 10 and 100 µM over a 20-minute period. Concentrations were determined using liquid chromatography mass spectroscopy/mass spectroscopy using multiple reaction monitoring searching for the conversion of product ion (467 →302 m/z. **A)** shows the concentration of selexipag determined in the samples. The concentration calculated for the 10 µM sample after 5 minutes is 60 times greater than that the amount of selexipag added into the sample and on this scale other trends cannot ber determined. Therefore, **B)** shows the same data on a smaller scale, excluding the spuriously high concentration determined for the 10 µM sample after 5 minutes.

The first assay was run as a pilot study to try to gather information such as time frame, concentration and whether the enzyme activity was verified. The study was limited by few time points and enzyme activity was still doubted. The trends shown in the data were inconsistent between HPLC (**Table 3-5**) and LCMS/MS analysis (**Figure 3-28**) which may have been a result of degradation upon freeze-thaw cycles. The source of the inconsistencies was not determined. Possible sources of error include; experimental error, instrumental error and lack of enzyme activity. The assay was repeated in duplicate and to obtain a better understanding of the changes in selexipag 5 concentration over time, the assay was conducted over a longer

time frame and a sample for the initial time point was also included. To exclude instrumental error upon analysis by LCMS/MS an internal standard was added to the quenching solution.

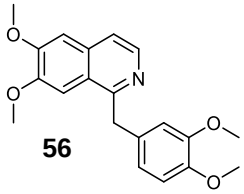

56

Figure 3-29. Structure of papaverine 57 used as a standard to compare concentrations of prodrugs against. The structure consists of stable bonds and only the $[M+H]^+$ ion forms by protonation of the nitrogen.

To eliminate any instrumental error, a standard (papaverine **57**) was added to each sample and a ratio between the standard and selexipag peak was calculated. Papaverine **57** (shown in **Figure 3-29**) is a common LCMS standard with a stable structure that primarily forms the $[M+H]^+$ ion. Without many smaller fragments, papaverine is detected cleanly with sharp, well-resolved resonance, minimising interference with other ions present. Before analysis, an optimiser was run to identify the most abundant ion for papaverine, 324.1 m/z.

A new standard curve was ploted which quantified the ratio between the most abundant selexipag and most abundant papaverine ions detected in the LCMS.

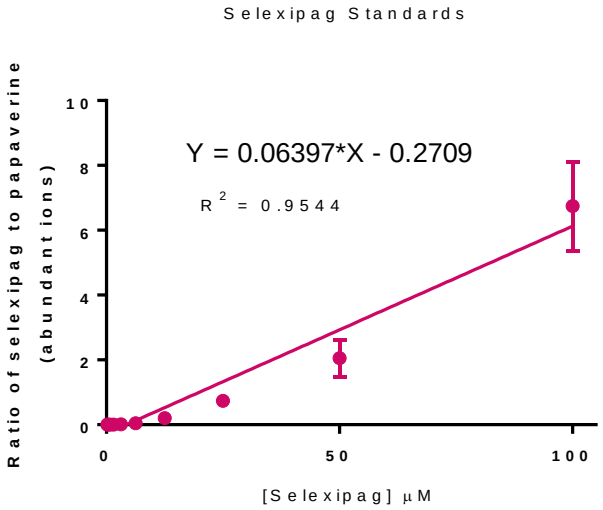

Figure 3-30. Standard curve of selexipag 5 quantified as the area under the curve for the selexipag product ion (302.4 m/z) chromatogram as a ratio of the product ion 324 of papverine.

The assay was repeated using the same procedure over a longer time frame to better determine the change in selexipag 5 concentrations over time. Each sample was run in duplicate to identify any outlying results. Samples were quenched using methanol spiked with

papaverine (1 ng/mL) then prepared and analysed using the same LCMS/MS method developed.

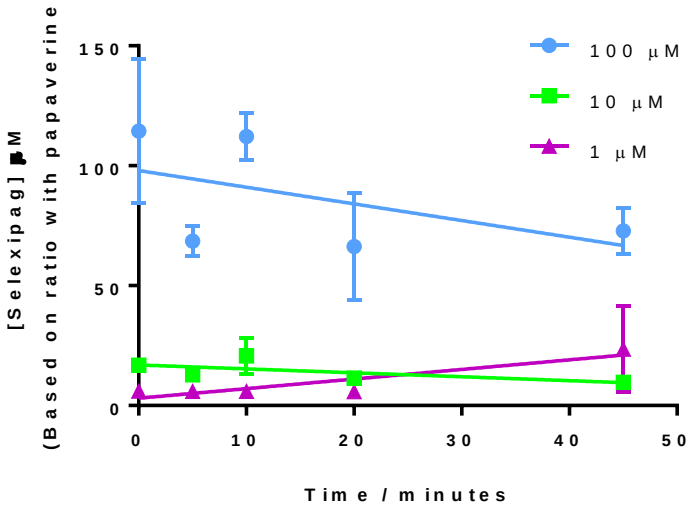

Figure 3-31. Concentrations of selexipag 5 detected in the microsomal assay. The assay was run at 100, 10 and 1 μM, and quenching aliquotes at time points between 0-45 minutes. A decreasing trend was visible for 100 and 10 μM although values for 100 μM varied. An outlying value for selexipag 5 concentration in the 1 μM microsome solution after 45 minutes skewed the data to show an increasing trend. For all values, starting selexipag 5 concentration detected were greater than the amount of selexipag 5 introduced into the microsomal assay.

A consistent decreasing trend was observed for the 100 μM and 10 μM assays. Variability was still present in the samples, particularly at the higher concentration of 100 μM. The 45-minute time point at 1 μM for one of the duplicates was spuriously high (41 μM) which skews the trend in a positive direction. The decreasing rate of concentrations was lower than expected which called into question the level of activity. Selexipag was run as a comparator control for the TRE-S which would be run when the assay method was established, but confirmation of the enzyme activity was not provided using selexipag. Therefore, a second positive control for enzyme activity was sought.

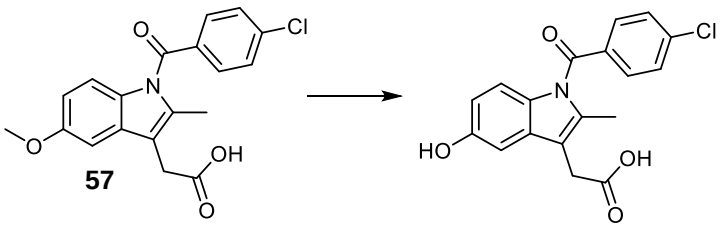

Scheme 3-27. Metabolism of indomethacin **58** to its O-desmethyl derivative which is mediated by CYP enzymes found in hepatic microsomes.

To be certain of enzymatic activity, a positive control for the CYP enzyme was added. Indomethacin **58** is a cyclooxygenase (COX) inhibitor which is rapidly metabolised to its *O*-desmethyl derivative by CYP enzymes (**Scheme 3-27**).[396,397] For this reason, indomethacin **58** can be employed as a positive control to confirm enzyme activity in microsome assays. Furthermore, indomethacin **58** is detected by MS in the positive mode, similar to selexipag. Indomethacin **58** controls were run in parallel with selexipag with few time points. An optimisation protocol was run in a similar fashion to selexipag **5**, TRE-S **21** and papaverine to identify the most abundant product ion for indomethacin, 138.9 m/z. Following collection of these data, it was decided that the assay would be repeated without the 100 µM concentration, using the assay constituent concentration described by Nakamura and colleagues for selexipag degradation.[115] The assay was conducted using the revised concentrations of assay constituents, described in **Table 3-6**.

Table 3-6. Comparison of the two assay protocols employed for microsome degradation of prodrugs. Initially, a general protocol for microsomal degradation of pharmaceutical agents was followed. The details of the assay utilised to report degradation of selexipag was considered for further degradation attempts. NADP = Nicotinamide adenine dinucleotide phosphate; $MgCl_2$ = anhydrous magnesium chloride.

Assay parameter	Old assay[115]	New Assay[390]
Total volume	300 µL	500 µL
NADP	1.3 mM	2.5 mM
Glucose-6-phosphate	3.3 mM	25 mM
Glucose-6-phosphate dehydrogenase	0.4 U/mL	4 U/mL
$MgCl_2$	3.3 mM	10 mM
Microsomes	0.53 mg/mL	0.4 mg/mL

Although the same column is used for both HPLC and LCMS/MS the sensitivity of the mass spectrometer to salts, proteins and lipids is greatly increased. Accumulation of precipitated proteins or salts can be severely damaging to the MS system. Precipitation with acetonitrile only removes large proteins and not all the salts, thus, a more extensive work-up procedure was required.

Liquid-liquid extraction is known to be time consuming and inaccurate, so a more practical method was sought. Solid phase extraction (SPE) is a simpler, yet more expensive method to remove salts, proteins and lipids from samples. SPE products exist specifically for the purpose of preparing biologically derived samples for analysis by MS. Various SPE products are available and we utilised one which could be utilised to remove salts and proteins using a syringe attachment that did not require a vacuum manifold. Oasis HLB Prime cartridges were employed which as advised in their brochure can prepare samples in a 3-step procedure.

The addition of an extra step adds the potential for more inaccuracy and the work up needed to be verified to ensure that the drug compounds were interacting with the solid phase as expected. Prodrug losses in the wash step need to be minimised and the recovery from the

solid phase in the elution step needed to be determined. To test the efficacy and recovery of the SPE work-up, known concentrations of selexipag (390 nM, 6.25 µM and 100 µM) were prepared in water. Three samples of each concentration split were used (**Figure 3-32**). The first sample (300 µL) was analysed by LCMS/MS without any work up; a second sample (300 µL) was filtered through the SPE cartridge; and the third sample was filtered through the cartridge and then rinsed with MeCN (450 µL). The samples were analysed by LCMS/MS in MRM mode detecting for papaverine and selexipag ions. Peak areas vs. concentrations for each of the three samples were plotted (**Figure 3-33**). A separate series of concentrations were prepared in PPBS to check for the removal of buffer salts. The presence of buffer salts would quickly be identified as precipitate would accumulate on the ion source.

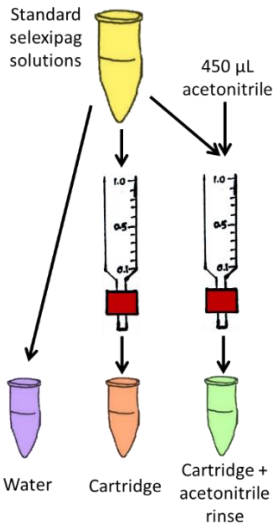

Figure 3-32. Verification of cartridge method to isolate selexipag solution whilst removing salts and lipids.

Passing the aqueous selexipag 5 solution through the SPE cartridge resulted in a 56-88% loss in concentration peak area. Upon flushing through the sample with MeCN, approximately 96% of the sample was recovered. Samples made in PPBS were also detected at levels comparable to the water samples. No salt precipitate formation was visible on the ion source, indicating buffer salts had been removed successfully. This indicated that the SPE cartridges would be suitable for the work up the microsome samples without compromising the concentrations of the prodrug.

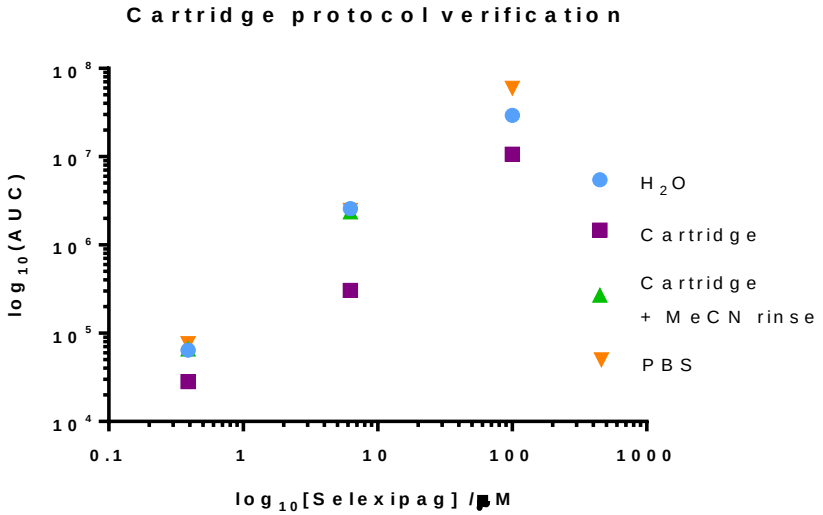

Figure 3-33. Log_{10} plot of the detected peak areas for selexipag concentration during each step of the solid phase extraction (SPE) cartridge procedure as detected by LCMS/MS (MRM mode = searching for 497^{+} ion. Selexipag 5 concentration plotted as log_{10}.; Blue = selexipag sample in water; Orange = selexipag in potassium phosphate buffer solution (PPBS); Purple = aqueous selexipag solution filtered through cartridge; Green = filtered through cartridge and then flushed with acetonitrile (MeCN). Similar concentrations are detected in water as in PPBS. After filtering with SPE cartridge selexipag concentration is reduced (purple) which is recovered by additional rinse of acetonitrile.

In discussion with the cartridge suppliers, it was suggested that an additional step be included to the cartridge protocol. The suggestion was based on the mixture of aqueous solvent (PPBS) and organic solvent (acetonitrile) in the supernatant added to the cartridges. Having established that the drug interacts well with the cartridge layer and no salts are entered onto the column, plus the cost of each cartridge (£4 per single-use cartridge), the amended cartridge protocol was employed.

Samples were assumed to contain a mixture of buffer salts, enzyme proteins and membrane lipids, as well as prodrug and active drug metabolite. Supernatant from the assay (500 µL) was immediately loaded onto the SPE cartridge by syringe. A solution of 5% methanol in HPLC-grade water (500 µL) was then added to wash the sample. In this step, the aqueous solvent should facilitate a better interaction of the drug and prodrug compounds with the solid phase and dissolve any salts which will be flushed through the column. Into a new vial, the small organic compounds were eluted from the solid phase by addition of MeCN (500 µL) spiked with papaverine (1 ng/µL). The filtrate from this step is retained for LCMS/MS.

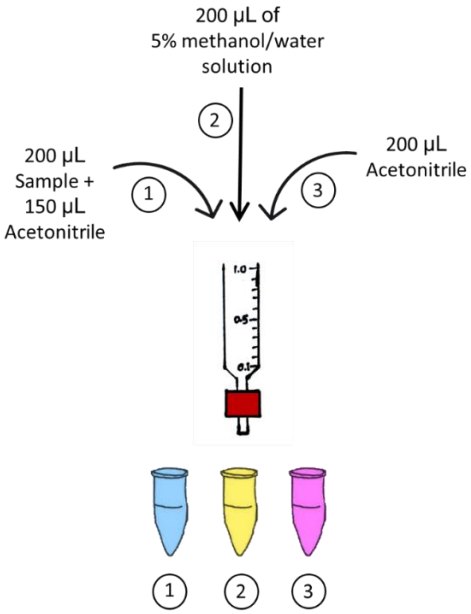

Figure 3-34. Method employed to prepare samples for liquid chromatography mass spectroscopy (LCMS). At each time point, microsomal solution is quenched with acetonitrile (150 µL) and loaded onto the solid phase extraction (SPE) cartridge and the supernatant retained. Salts are flushed through with washing with 5% methanol/water solution (200 µL) and the supernatant retained separately. Hydrophobic drug components, including selexipag 5 and TRE-S 21, are eluted by flushing SPE cartridge with acetonitrile (200 µL). Supernatant (3) collected for analysis by LCMS.

The assay was run as before only using the cartridge protocol once the microsome assay supernatant had been collected. The standards were treated in the manner to provide a direct comparison. To prevent residual salts reaching the MS ion source, solvent eluted during the first minute from the LC was sent to waste rather than to the MS. As all compounds are eluted after 1.5 minutes only residual salts were directed to waste.

Unfortunately, the TRE-S 21 standards did not show any sensitivity significant above baseline, so a standard curve could not be plotted. However, the TRE-S concentrations determined in the samples were sensitively detected and showed a decreasing trend over time, suggesting first-order kinetics. When plotted against time an exponential curve is determined.

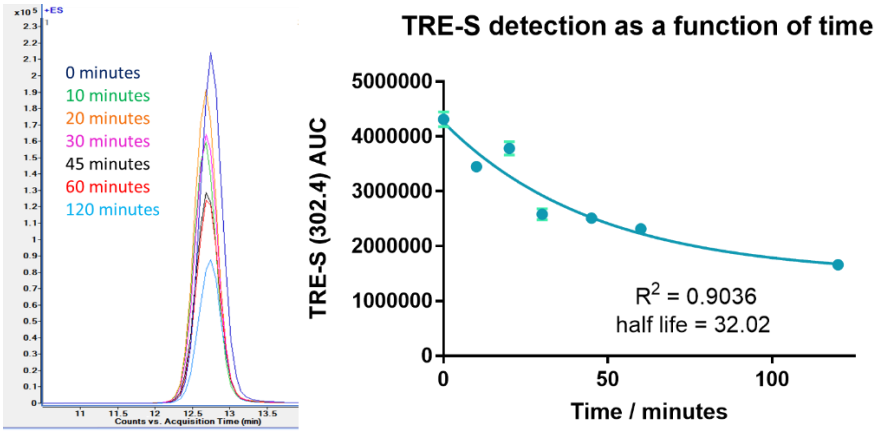

Figure 3-35. Quantification of TRE-S product ion 302.4 in microsomal solution at different time points. A shows the ion count chromatogram and B shows the integration of each curve plotted as a function of time.

Surprisingly, analysis of selexipag and indomethacin in the same experiment showed negligible concentration even in the initial timepoints. Concentrations around baseline were detected for even the most abundant ions. The negligible concentrations of indomethacin and selexipag detected (**Figure 3-36**.) the data was not analysed and plotted.

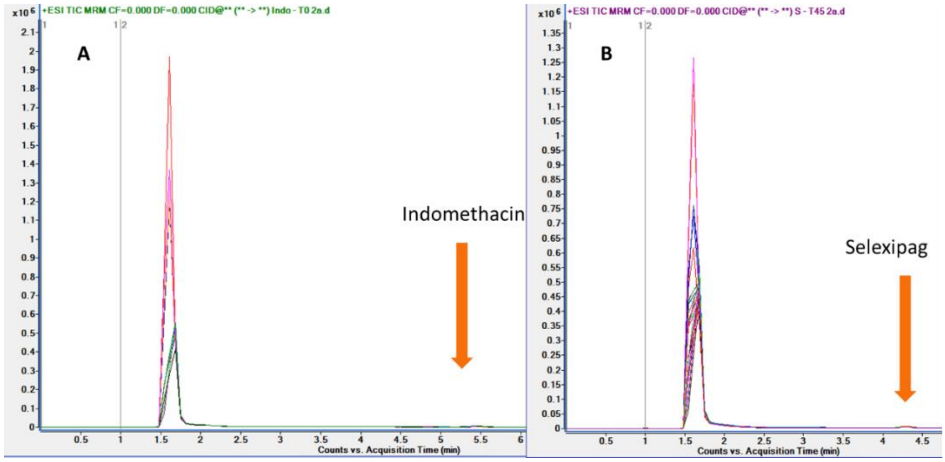

Figure 3-36. Total ion count spectra for samples containing **A**) indomethacin or **B**) selexipag. Both samples contain papaverine standard. Detection was negligible.

The data shown in **Figure 3-36** (**A** and **B**) were collected during the final weeks of experimental lab work and although promising data from TRE-S run in duplicate was obtained (**Figure 3-35**), the detection of selexipag 5 and indomethacin was unexpectedly insensitive (**Figure 3-36**). During discussions with our industry collaborators, United Therapeutics (UT), they confirmed that treprostinil sulfonamide 21 had been also synthesised, but *via* a different route utilising an unknown di-protected treprostinil. The sulfonamide degradation had been evaluated using a microsome assay by a contract research organisation (CRO).

The microsome protocol used by UT was similar to both the standard protocol[393] and the method used to report selexipag 5 degradation,[115] however several minor differences were identified. The method employed by UT used a different system to regenerate the enzyme. Instead of including an enzyme system to generate NADPH, their protocol added NADPH directly. The end result of NADPH presence is theoretically the same so is potentially unlikely to feature as the underlying cause for the failed attempts. Whether the NADPH-generating enzyme was functioning as expected was not determined. Instead of aliquoting time points out, the assay used by UT was carried out in one solution and at each time point aliquots removed, quenched with ice cold acetonitrile. Solutions were centrifuged to pellet the proteins and the supernatant frozen at -80 ^{o}C until analysis. There was no mention of an extraction procedure to remove salts, so a solvent divert method (sending the eluted solvent to waste initially) was probably used. It is not thought the differences in the microsome assay protocol described in this chapter and used by UT account for the ambiguous results shown in **Figure 3-28**, **Figure 3-31**, **Figure 3-36**. The data obtained for TRE-S indicates that there was enzyme activity in the assay (**Figure 3-35**) and the recovery of sample from the SPE cartridge was verified so it is likely that the LCMS/MS method requires further optimisation to increase sensitivity. A great deal of effort was committed to optimise the microsome assay. Since UT have confirmed that microsomes do cause sulfonamide cleavage of TRE-S 21 to treprostinil 4, further work to optimise the microsome assay was postponed. Furthermore, it was also recently revealed that UT conducted a functional assay of receptor activation, with a difference in specific activity values when compared to the assay used in this work.

HPLC analysis of the TRE-S 21 sample was run to determine if treprostinil 4 or other degradation products were present. A slow gradient was employed to avoid any overlapping of the TRE-S and treprostinil peaks and a treprostinil standard was run immediately afterward for comparison (**Figure 3-37**). Analysis of treprostinil 4 standard produced an absorbance with retention time 19.7 minutes. The TRE-S 21 sample produced a peak after 16.8 minutes with no absorbances at or around 19.7 minutes which suggest the presence of treprostinil.

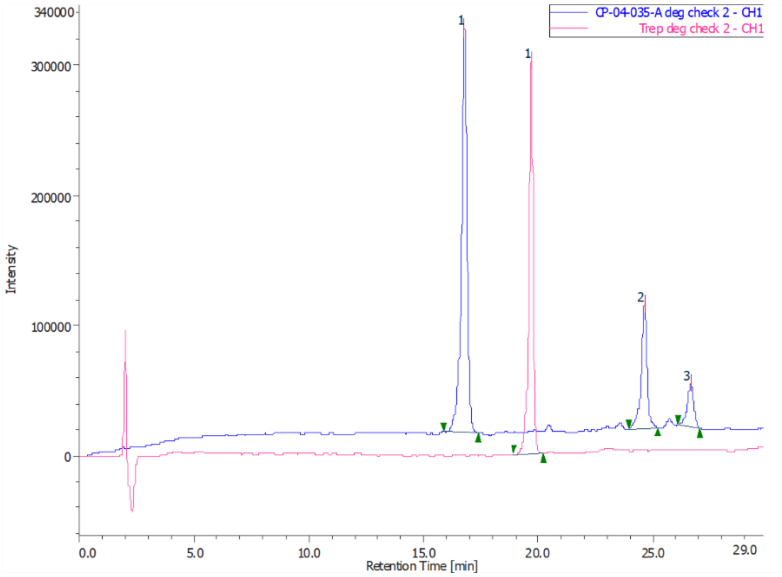

Figure 3-37. Comparison of the HPLC elutograms of the TRE-S **21** sample used in the cAMP assays and treprostinil **4**, run consecutively. No indication that TRE-S **21** had degraded to treprostinil **4** was presented.

This suggested that no degradation had occurred and the 100-fold difference in activity between treprostinil 4 and TRE-S 21 that had been determined (**Figure 3-23**) is accurate. The variation between the company calculated activity and that reported in this work may be a result of the different cells used and a different assay used to determine activity. The decreased activity of TRE-S 21 suggested it to be an encouraging structure for prodrug formulation.

.

3.2.6 **Strengths and limitations**

This work offers a method of enhancing treprostinil therapy for PAH using pro-drug approach. Although the *N*-acyl sulfonyl derivatisation of treprostinil required a 5-step synthesis, the final structure was achieved using two different coupling agents. We were fortunate to obtain a precursor intermediate which permitted the synthesis in two-steps. The samples of treprostinil and benzindene triol were used sparingly and a cheaper model was used where possible to obtain reaction conditions.

Despite our best efforts, this study was not without limitations. In our quest to economise on treprostinil and benzindene triol use, small scale reactions were employed which are inherently associated with considerable error and difficulty in controlling reaction conditions which made synthesis more challenging. Work up of reactions was challenging and often resulted in loss of compound. Consequently, the results from the early, small-scale reactions (<20 mg) are

less reliable and should be interpreted with more caution. The complexity of mechanistic pathways in PAH and PM therapy is well appreciated and thus is yet to be fully understtod. Therefore, it is not possible to accurately predict whether TRE-S will reduce adverse events induced by other receptors in other tissues. What is demonstrated is a decrease in IP receptor binding for TRE-S. Despite our best and continuous attempts to conduct a microsomal assay, it remains to be determined whether TRE-S is metabolised to active treprostinil in a similar manner to selexipag. Several protocols were consulted, and methods attempted, however the coherent data was not obtained.

Activity was tested and shown to reduce at the IP receptor but activity at the DP_1 and EP_2 receptors was not investigated. Treprostinil is a potent agonist of both receptors and has recently been shown to act principally through the EP_2 receptor which is upregulated in the PAH arteries. The IP receptor agonism is a known and established concept, whereas the role played by the EP_2 receptor has been identified but is not yet widely recognised. Thus, the IP receptor agonism of TRE-S was tested first with the intention of testing other receptors should time permit, which it unfortunately did not. For any continuing studies on the prodrug TRE-S, the activity at all active receptors should be investigated.

3.2.7 **Conclusion**

In conclusion the N-acyl sulfonamide derivative of treprostinil (TRE-S) **21** was synthesised *via* two routes. The reduced activity of the TRE-S prodrug compared to treprostinil *per se*, having a more favourable ratio than licensed prodrug Selexipag (as shown in IP-expressing HEK cells), suggests that the N-acyl sulfonamide is a suitable pro-drug structure for further investigation towards clinical development. With reduced IP receptor activity, it is hypothesised that the present treprostinil prodrug strategy will translate clinically to a reduction in side effects and adverse events experienced upon administration. The requirement for enzymatic degradation by enzymes specific to the liver suggests that release of TRE-S in the subcutaneous tissue will not lead to premature release of free treprostinil.

An additional advantage over Selexipag, which is a pure IP-receptor agonist, is that treprostinil additionally and predominantly activates EP_2 receptors to achieve its therapeutic effects. Thus, one could conceive of the combined use of Treprostinil prodrug *with* Selexipag, providing a more broadly-based, potentially synergistic pharmacotherapy of PAH, additionally allowing dose-sparing of Selexipag to ameliorate its gastric side effects.

A particular advantage of the present strategy is that it potentially avoids the release of free treprostinil upon parenteral administration. A reduction in adverse events would therefore be expected in IV infusion or sc depot modes of administration. In the case of infused treprostinil (Remodulin), injection site pain is the most prevalent AE for treatment. Likewise, local injection-site reaction may have been a factor in the termination of previous attempts to develop a PEGylated pro-drug of treprostinil as a subcutaneous depot.[138] Moreover, the ‘delivery ratio’ of the present prodrug (wherein 75% of the prodrug substance is treprostinil) is

markedly better than the PEGylated form (where this was less than 4%),[79] i.e. a potential 18-fold advantage for dosing purposes (i.e. lesser, more manageable, volume of injectate or infusate), depending on efficiency and rate of release of free treprostinil systemically.

Chapter 4. Treprostinil as a co-monomer

4.1 Introduction

Polymer conjugation has been a successful clinical strategy to extend circulation time for proteins that rapidly clear from the body following administration (e.g. protein conjugation to poly(ethylene glycol), termed PEGylation). While conjugation of low molecular drug molecules to polymer structures have been evaluated clinically, particularly using cytotoxic molecules in the treatment of cancer, they have been less successful in achieving clinical registration.

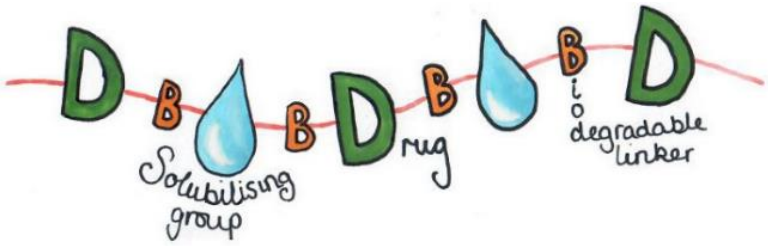

Figure 4-1. Proposed concept of incorporating a drug (D) along the mainchain of a polymer mainchain *via* biodegradable elements (B). For hydrophobic drugs, solubilising monomers or functions are included within the design.

The overall strategy of conjugating toxic low molecular weight drugs to polymers is to impart macromolecular properties to low molecular weight actives. For example, macromolecules are able to remain in the blood compartment to avoid systemic distribution, which can be one strategy to increase the maximum tolerated dose of a drug. Tissue uptake at diseased sites can occur by passive (e.g. enhanced permeability and retention (EPR)) or active targeting. Upon conjugation of a small drug molecule to a polymer, biological activity is reduced. Therefore, a challenge for the polymer conjugation of drugs is the need to release the intact drug to restore biological activity. One way to conjugate a drug to a polymer is to use the drug as a co-monomer to become incorporated into the polymer mainchain (**Figure 4-1**).

Subcutaneous (SC) administration of treprostinil **4** is an effective prostacyclin therapy associated with significant site pain at the injection site which negatively impacts patients' quality of life.[72,299] Site pain limits the maximum tolerated dose (MTD) of treprostinil reducing the potential for therapeutic benefit.[398] As discussed in **Chapter 3**, polymeric derivatives of treprostinil **4** have been examined.[79,306,338,339,399] However the major limitation with previous treprostinil-polymer derivatives for subcutaneous delivery has been that persistent site pain has not be alleviated. Conjugation of a drug to a polymer often reduces the activity and toxicity of a drug. Pain is likely the result of either free treprostinil **4** in the preparation or premature release of treprostinil within the hypodermis prior to diffusion into circulation. An improved strategy would be to design a polymeric pro-drug with either a faster diffusion rate (smaller polymeric structure) or a slower drug release rate (more stable or site-specific conjugation bond).

As a potential co-monomer, treprostinil **4** possesses two secondary alcohols and one carboxylic acid. Acid degradable elements were limited to these moieties if treprostinil **4** was to be used without further derivatisation. The water solubility of treprostinil is influenced by the acid group which is deprotonated at physiological pH (>10 mg/mL). Therefore, conjugation through the treprostinil acid could potentially compromise solubility of oligomers during polymer degradation. Acid labile, biomedical degradable polymers include poly(ortho esters) and polyesters, although these polymers have been investigated for implant applications rather than as water-soluble polymers for drug conjugation.

Biomedical polyesters are typically used for implants (e.g. microsphere or devices fabricated from poly lactic-co-glycolic acid (PLGA)) rather than for soluble applications such as for drug-polymer conjugation as described here. Previous treprostinil-polymer conjugations have utilised ester bonds which are enzymatically labile by the ubiquitous esterases in the body. This results in non-specific conjugate degradation. Furthermore, depending on co-monomer composition, if both hydroxyl groups were to participate in a polymerisation, esterification of treprostinil into a polymer mainchain could result in a hyperbranched structure. Such a structure would have the advantage of reduced viscosity, however structural heterogeneity would be high and maintaining solubility could be challenging. Although no difference in the reactivity between the hydroxyls was observed from the hydroxyl protection reactions (**Chapter 3**), it is possible that in a polymerisation reaction, one hydroxyl group might be favoured requiring relatively harsh conditions or coupling reagents to give polymeric material.

During chronic inflammation in pulmonary tissue of the PAH lung, the environment becomes acidic as a result of lactic acidosis which occurs in the hypoxic tissues.[251] Therefore, a polymer-drug strategy could be applied to release treprostinil in the diseased lung tissue. Reduced toxicity upon subcutaneous administration and through systemic exposure of the drug could potentially be achieved.

Drug-linkers were described in **Chapter 1**, although not all are suitable as the biodegradable element within a polymer backbone. For polymerisation, a biodegradable element must possess characteristics outlined in **Table 4-1**. In addition to the limitations described above, polyesters as water soluble polymers may not be sensitive enough to the hydrolytic conditions at mildly acidic pH that can exist in some diseased tissues. Poly(ortho esters) require highly anhydrous synthetic conditions using hydrolytically labile and often chemically complex cyclic monomers.[400]

Table 4-1. Criteria for conjugation linkers

Requirements of polymer conjugation bond
Must facilitate incorporation of treprostinil *via* the mainchain in a linear polymer
Must be sensitive to acid hydrolysis
Must be stable at physiological pH
Must be soluble or facilitate incorporation of soluble monomers
Must not require specialised equipment for synthesis.

Acetal bonds undergo hydrolysis in acidic environments and remain broadly stable at physiological pH. Water-soluble polyacetal co-polymers derived from drug monomers have been studied (**Table 4-2**).[401,402] Although they are hydrolytic, the dry conditions required for formation are less stringent than that of poly(ortho esters). Polyacetals are more simple molecules to make than poly(ortho esters) as they have two oxygens at the hydrolytically labile carbon instead of 3 oxygens that are present in poly(ortho esters). Polyacetal structures are described which possess drug monomers in the form of diols as well as solubilising diol monomers which under reaction with divinyl ether compounds form a tert-polymer (**Scheme 4-6**).[401,402] Smaller polymers are isolated when drug monomers are included than without. Polyacetals are acid labile and display a pH dependent degradation profile that correlates with decreasing pH.

Table 4-2. Mainchain polyacetal structures reported in the literature which utilise diol drug compounds as co-monomers. PEG = poly(ethylene glycol).

No.	Polyacetal structures in the literature	Description	Ref
58	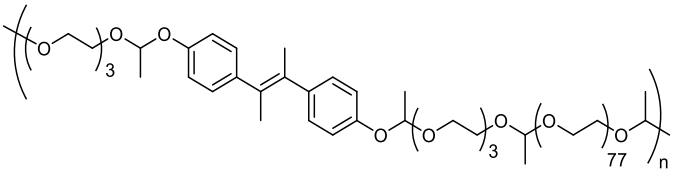	Mainchain incorporation of diethylstilboestrol (DES) in poly(PEG-DES acetal)	402
60	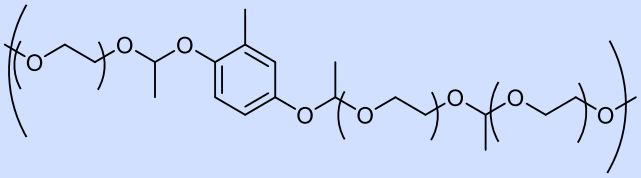	Mainchain incorporation of methylhydroquione into PEG polyacetal	401
59	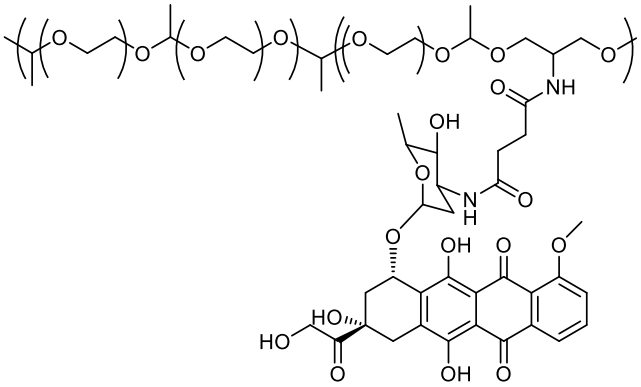	Pendantly conjugated Doxorubicin to poly(PEG acetal) mainchain	403
61	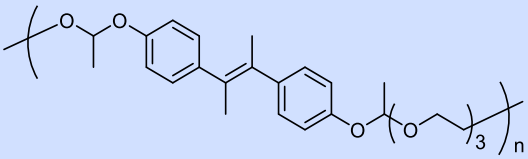	Polyacetal of DES	402

Polyacetals can be prepared by the acid catalysed condensation of a diol and aldehyde such as acetaldehyde **63** (**Scheme 4-1**). A mole of water by-product is formed which must be removed to achieve a high degree of polymerisation and avoid acetal degradation. Water can be removed by distillation, but the high boiling point limits the choice of solvent used and makes removal challenging.

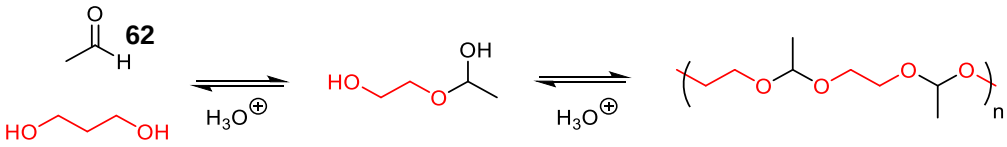

Scheme 4-1. Polyacetal formation by condensation reaction between aldehyde and diol which forms water as a by-product. To achieve a high degree of polymerisation, the water must be removed by distillation of water.

Acetal exchange reactions can be conducted using pre-formed acetals derived from a low molecular weight alcohols (eg. methanol) which have a lower boiling point (**Scheme 4-2**). The acid catalysed reaction is an equilibrium, so to drive the reaction and avoid the reverse

degradation, anhydrous conditions are employed and the alcohol is removed by distillation as the polymer form formation. Without complete removal of the hydroxyl condensation product, acetal degradation makes reproducibility of the polymer product challenging.

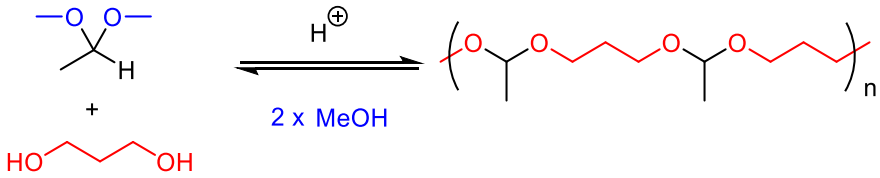

Scheme 4-2. Polyacetal formation with pre-made acetal structures, displacing methanol. The methanol by product must be removed from the reaction mixture by distillation to drive polymerisation.

In the 1980s, Heller devised an alternative method to form acetals without forming a by-product by the reaction of a alcohol and vinyl ether (**Scheme 4-4**).[404] Conjugation is acid catalysed which occurs presumably by protonation of the vinyl ether allowing hydroxy addition to form the acetal without generation of a hydroxylic by-product that must be removed.

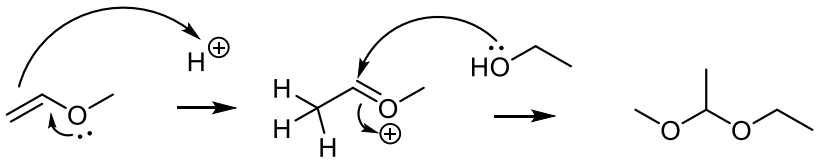

Scheme 4-3. Mechanism for acetal formation from the acid catalysed reaction of a vinyl ether with an alcohol.

The formation of polyacetals can be conducted using bis-functional monomers; containing an alcohol and vinyl ether, known as an A-B monomer (**Scheme 4-4**). Since each monomer possesses a 1:1 ratio of each polyacetal precursor moiety, addition of any number of A-B monomers in an acidic, anhydrous environment will result in polyacetal formation. Limitations of this method involve synthesising a highly pure monomer and preventing spontaneous polymerisation during work-up and storage. Alternatively, two monomers can be employed; one containing two hydroxyls, and one containing the two vinyl ethers (Scheme 4-5). The structures are described as A-A and B-B monomers.

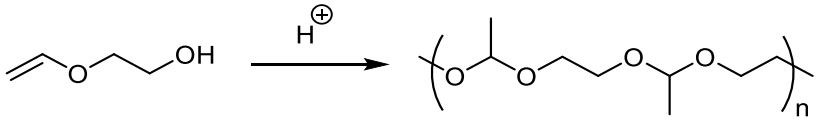

Scheme 4-4. Mechanism for polyacetal formation from the acid catalysed polymerisation of an A-B type monomer with both vinyl ether and hydroxyl functionalities. Provided the monomer is pure and anhydrous reaction conditions are employed, polymerisation would be expected to occur in the presence of an acid catalyst.

A potential limitation of using vinyl ether-based monomers to prepare polyacetals is the need to avoid the presence of water in the reaction. The presence of water at acidic pH can hydrolyse vinyl ethers to an alcohol. Loss of stoichiometric equivalence would result in dead

chain ends to terminate polymer growth. Additionally, although the polymerisation is catalysed by acid, the presence of water in an acidic environment also causes acetal degradation *in situ*. Thus, despite successful polyacetal formation, if water is present in the polymerisation reaction, acetal degradation can occur before it is possible to isolate the polymer.

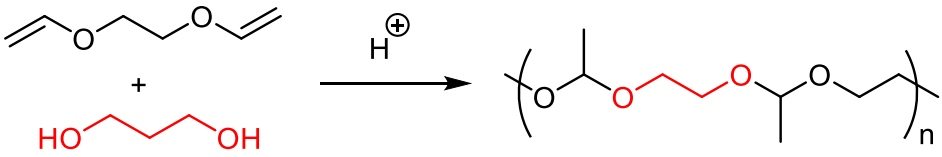

Scheme 4-5. The formation of a polyacetal by step growth polymerisation using an A-A and B-B monomers. One monomer has two vinyl ethers and the other monomer has two hydroxyl moieties. No by-products are produced during polymerisation, but the monomers must be pure and added in exact 1:1 stoichiometry to achieve a high degree of polymerisation.

Since polyacetal formation is a step polymerisation reaction, it is critical to maintain a 1:1 stoichiometry if A-A and B-B monomer system is being used. As monomers form dimers and then oligomers and eventually polymer chains, the number of reactive end groups decreases. If a 1:1 monomer stoichiometry is not maintained, then polymer growth will be inhibited.

To improve solubility, many polyacetals previously described include PEG diol as an A-A monomer.[402,403,405] Low and moderate molecular weight poly(ethylene glycol) (PEG) diols (400 to 3400 Da) have been used as a co-monomers for making water-soluble polyacetals.[402,403,405] Although many monomeric diols possess solubilising properties, PEG is a water soluble non-ionic diol which is generally, but not always,[192,406] considered non-toxic and biocompatible, especially at molecular weights above ~400 Da.[407] Many PEG derived molecules have been used as excipients in widely used parenteral, oral and topical healthcare products.[167] PEG is also utilised clinically in polymer protein conjugates[408–410] and PEG toxicity has been extensively evaluated.[168,411]

PEG molecular weight is often chosen to be large enough to reduce number of acetal bonds and therefore the number of aldehyde molecules released upon degradation, but also small enough to facilitate a reasonable amount of drug loading.

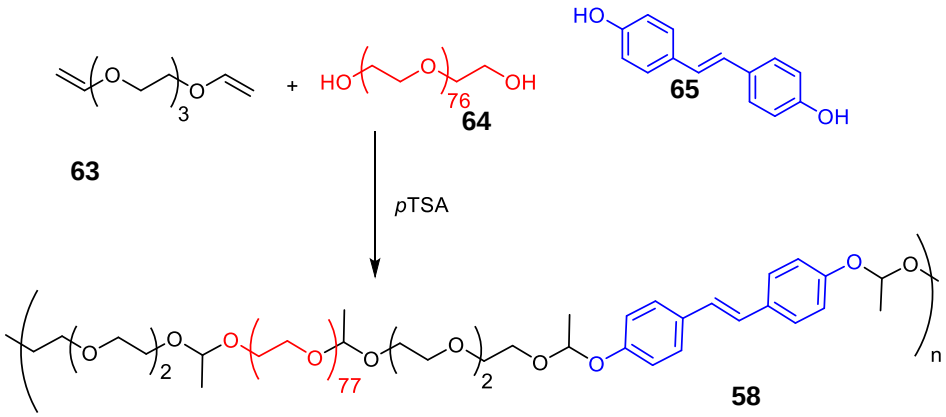

Scheme 4-6. Synthesis of polyacetal **59** containing diethylstiboestrol **66** (DES). Poly(ethylene glycol)$_{3400}$ **65** was employed as a co-monomer to aid solubility of hydrophobic DES and the polymerisation was conducted in the presence of triethylene glycol divinyl ether **64** under acidic conditions using *para*-toluene sulfonic acid (pTSA).

Use of PEG diol macromonomers requires consideration of the polydispersity of PEG, which is often narrow, but not homogenous. The preparation of monodisperse, discrete PEG molecules of low–molecular weight is challenging thus, they are expensive to purchase. If the PEG is not mono-dispersed, then maintaining 1:1 stoichiometry from the outset of the polymerisation is difficult. Diol and divinyl ether monomers must be pure and anhydrous, otherwise polyacetal formation can be difficult to reproduce.

Once a drug polymer is localised in the tissue, release of the drug is required. Degradation of acetal bonds is achieved by acid hydrolysis. The pH-dependent degradation make polyacetals an attractive delivery system for drug release in acidic environments such as chronically inflamed tissues. Involving the degradable element in the mainchain of a drug polymer allows for fast clearance of monomers once the drug has been released which avoids issues of polymer accumulation in the disease tissue.

Hypothesis

Owing to the two secondary alcohols present in treprostinil **4** it was reasoned that treprostinil could be incorporated into a polyacetal along the mainchain to overcome the limitations of continuous dosing and site pain associated with subcutaneous. An acetal structure would hopefully maintain an acceptable rate of diffusion from the hypodermis into circulation exhibiting a slow enough rate of degradation at physiological pH. If treprostinil forms part of the mainchain of an oligomeric (or polymeric) acetal, little activity from the bound treprostinil is expected, so such a structure would theoretically reduce site pain.

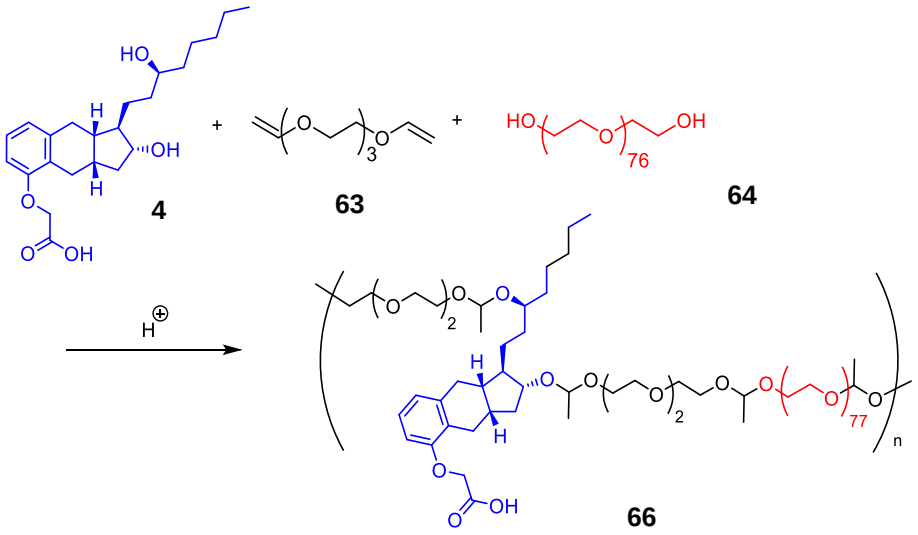

Scheme 4-7. The proposed ter-polymerisation of treprostinil 4 and poly(ethylene glycol)$_{3400}$ (65) as A-A monomer and triethylene glycol divinyl ether (64) as the B-B monomer. The step growth polymerisation product 67 was expected to incorporate treprostinil in the main chain *via* acid-degradable acetal bonds.

To prepare a treprostinil **4** containing polyacetal structure with a viscosity suitable for injection, large molecular weight polymers are not desirable. To minimise the possibility of hydrolysis in the subcutaneous compartment, a high enough rate of diffusion from the subcutaneous tissue into circulation is required. Therefore, small oligomeric polyacetals were sought.

To begin to determine the potential of an acetal treprostinil macromolecule the following aims were:

- To use treprostinil 4 as a co-monomer by utilising the secondary alcohols to prepare a polyacetal copolymer with treprostinil in the mainchain.
- To investigate and compare the degradation profiles of a treprostinil polyacetal at physiological and acidic pH values.

4.2 Results and Discussion

To overcome the activity of treprostinil at the site of subcutaneous infusion, it was hypothesised that a soluble drug conjugate of treprostinil 4 which could diffuse into the blood stream would reduce pain. Poly- or oligoacetals which incorporate treprostinil 4 into the mainchain can undergo degradation in an acidic environment such as what may exist in the inflamed tissue of the PAH lung[251,412,413] to release treprostinil 4. A common synthetic route to prepare drug containing acetal macromolecules is to allow the diol containing drug to act as a co-monomer with a water solubilising PEG$_{3400}$ 65 and triethylene glycoldivinyl ether 64 in the presence of an acid catalyst. In this chapter, methods to link treprostinil 4 to an acetal macromolecule were explored. The intended product from the acetal polymerisation with treprostinil was poly(PEG-treprostinil acetal) 67 (shown in **Figure 4-2**).

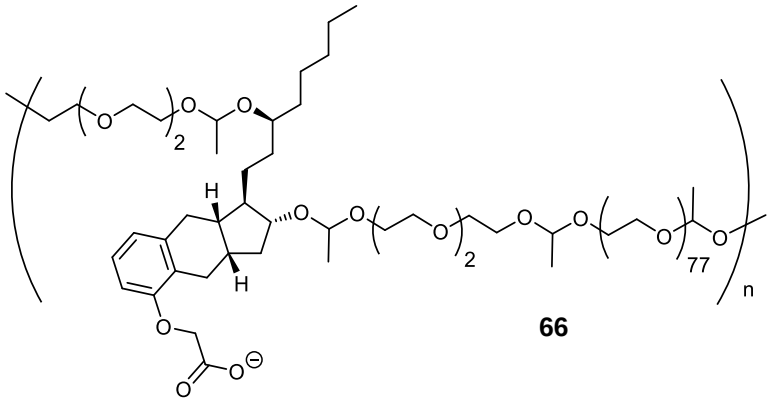

66

Figure 4-2. Proposed structure of the expected polymerisation product, polyacetal(PEG-Trep) 67.

In the presence of a diol acting as an A-A monomer and a divinyl ether acting as a B-B monomer, polyacetal formation can result via a step-polymerisation mechanism (**Scheme 4-10**). Inclusion of treprostinil 4 as a diol A-A monomer offers the opportunity for inclusion into an acetal oligomer or polymer by reaction with a divinyl ether B-B monomer. Addition of each monomer in a 1:1 ratio will result in a homopolymer (**Scheme 4-8**), which often results in reduced solubility.[402] Furthermore, with small oligomers forming early on in the step polymerisation, cyclisation products are possible (**Scheme 4-9**). Cyclisation is less of a problem when longer monomers are included in the synthesis at the two termini at each end of the monomer are less likely to interact. Therefore, additional water-soluble diols such as PEG macromonomers are included as a co-monomer.

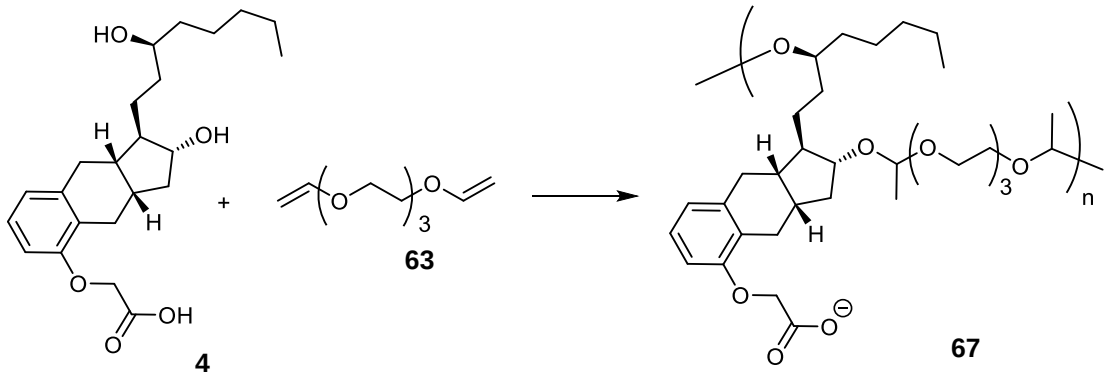

4 **63** **67**

Scheme 4-8. Possible polymerisation product **68** using treprostinil as the A-A monomer and triethylene glycol divinyl ether **64** as the B-B monomer. Such drug polymers often exhibit poor polymerisation.[402]

The reactivities of the two secondary hydroxyls in treprostinil 4 appear to be poor. As discussed in **Chapter 3** in the context of hydroxyl protection, the treprostinil hydroxyls were weakly nucleophilic in S_N2 displacement reactions of benzyl bromide in mild basic conditions. A similar result was observed when attempting to benzylate the hydroxyls of treprostinil ethyl ester by the triflic acid catalysed nucleophilic attack of benzyl-2,2,2-trichloroacetimidate **44** (BTCA). Attempts to achieve the protected hydroxyls were more successful when the acid was protected, although treprostinil acid **4** was successfully benzylated when the highly reactive

Dudley reagent was employed in neutral conditions (**Chapter 3**). It was anticipated that the reactivity of the treprostinil hydroxyls could differ from a primary alcohol derived from PEG in the formation of an acetal macromolecule containing treprostinil 4 in the mainchain such as the proposed structure 67.

Whilst the rate of acetal formation at the PEG termini was expected to be fast, the rate of acetal formation at the treprostinil hydroxyl termini was expected to be relatively slower. With differing rates of acetal formation, it was anticipated that the rates could be manipulated by stepwise addition of the two diol monomers; treprostinil and PEG_{3400}. One strategy is to add the treprostinil monomers and divinyl ether monomers together to form bis-functional treprostinil-vinyl ether intermediates to which PEG can later be added. However, the intermediate dimers, such as **69** possess the potential to cyclise (**Scheme 4-9**). Without any evidence to indicate the relative differences in rate of acetal formation, the preliminary reaction was carried out by simultaneous addition of treprostinil and PEG.

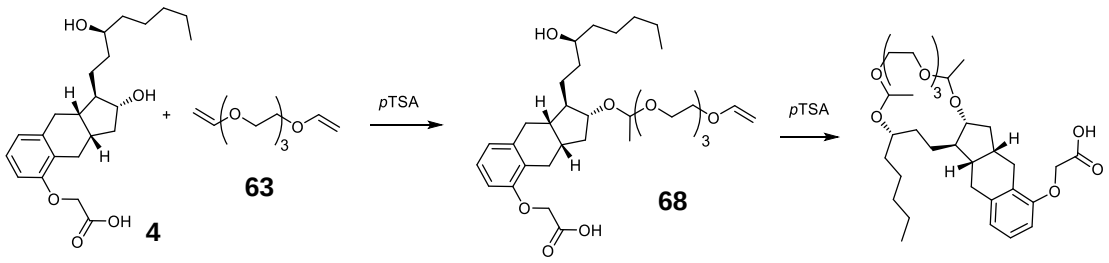

Scheme 4-9. Possible cyclisation of reactive acetal dimer formed as an intermediate when pre-forming treprostinil reactive monomers for polymerisation by addition of PEG. The cyclisation product is non-reactive and less likely to form when longer chain monomers are present as the likelihood of the vinyl ether and hydroxyl moieties of the same molecule reacting is reduced.

PEG_{3400} 65 was chosen as the solubilising diol macro co-monomer. The number of acetal bonds in the polymer should be low owing to the release of acetaldehyde **63** upon degradation. Unnecessary acetal bonds, which serve only to link solubilising PEG monomers together, can be avoided by using longer PEG chains. Using PEG_{3400} 65 in a 1:1 molar ratio with treprostinil **4**, theoretically reduces the possibility of two PEG chains neighbouring each other and achieves a treprostinil 4 percentage incorporation of 9%, which is a similar drug loading to other drug acetals.[402] Guided by work previously reported by Vincent and colleaugues, triethylene glycol divinyl ether 64 (TEGDVE) was utilised as the divinyl monomer. [401–403,414] In addition to being hydrolytically labile, vinyl ethers are susceptible to homolytic fission when exposed to UV radiation, so light sensitive conditions were employed.

An additional challenge in the formation of a treprostinil-containing polyacetal is the presence of the treprostinil acid moiety. Although several compounds have been linked to a polyacetal (**Table 4-2**) either within the mainchain or in a pendant fashion, none have possessed a free acid moiety. Acetals bonds are degraded in the presence of acid and water so to prevent self-degradation by the treprostinil acid, scrupulous anhydrous conditions must be employed, and neutralisation is required to isolate the polymer as the carboxylate salt.

4.2.1 Polyacetal synthesis

Polymerisation by acetal formation between diols and divinyl ethers occurs by a step growth polymerisation mechanism (**Scheme 4-10**). Step growth polymerisations rapidly consume monomer to form dimers which then undergo reaction to form oligomers that grow in a step wise fashion to form polymeric material. Typically, as the polymerisation progresses, the viscosity increases, and the number of chain ends decreases. The fast rate of monomer consumption in addition to the slow rate of larger polymer formation make tracking the reaction progression by monomer consumption irrelevant.

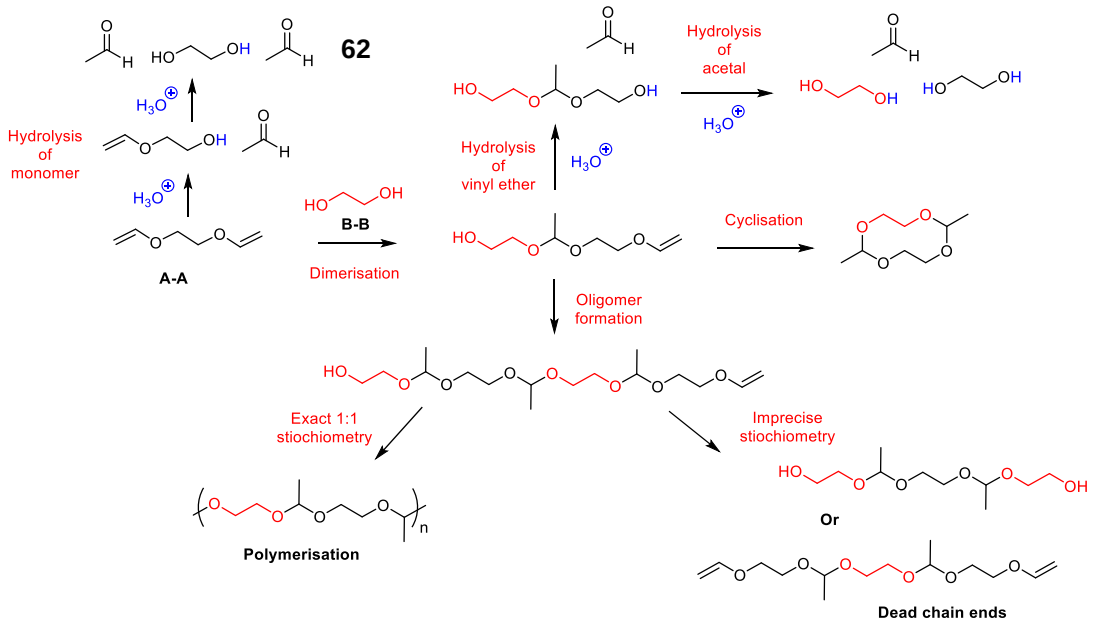

Scheme 4-10. Possible outcomes of polyacetal formation during step-growth polymerisation of A-A divinyl ether and B-B diol monomers. Hydrolysis of the vinyl ether moieties results in dead chain ends and produces acetaldehyde **63** as by-product. For complete polymerisation, the ratio of vinyl ether to hydroxyl moieties must equal 1:1. Imprecise stoichiometry of the monomers will result in dead chain ends and prevent chain growth.

Possible side reactions include the cyclisation of small intermediate oligomers, which is most likely with smaller chains. High concentration of reagents in the reaction solution with continuous stirring can prevent intramolecular reactions occurring. To prevent the formation of dead-chain ends by vinyl ether hydrolysis, the acetal polymerisation reactions were carried out in anhydrous conditions removing traces of water from PEG_{3400} 65 and hydrated *p*TSA by azeotropic distillation with toluene using Dean-Stark apparatus (**Figure 4-3**).

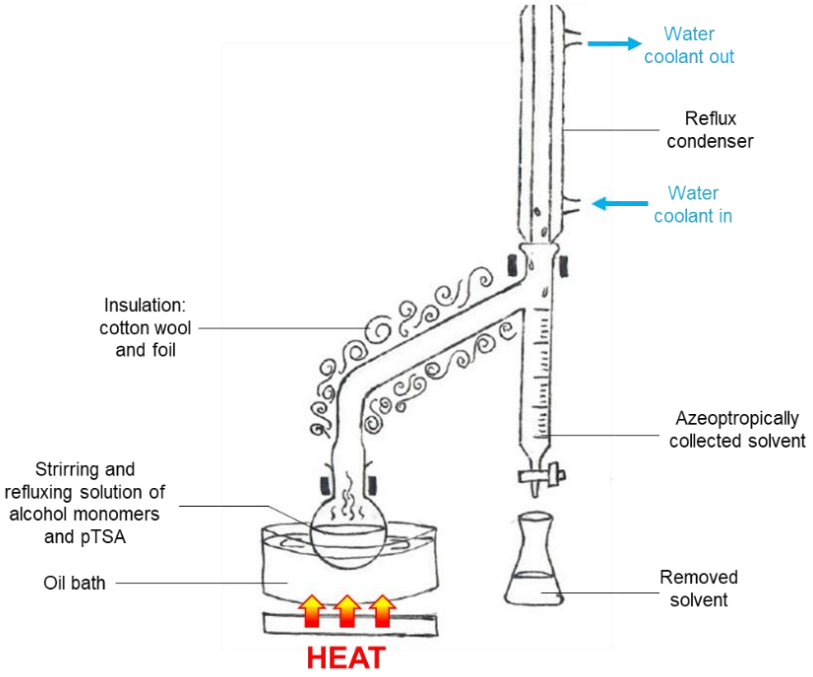

Figure 4-3. Image of the Dean-Stark apparatus used to dry acid and PEG_{3400} before polymerisation.

After distillation of toluene, the Dean-Stark apparatus was removed and the reaction solution, containing PEG_{3400} **65**, treprostinil derivative (when used) and pTSA, was dissolved in anhydrous tetrahydofuran (THF) and the TEGDVE **64** was added slowly. When polymerisation results, the solution can become viscous and in the case of high molecular weight polymerisation, a gel-like solid is formed. Excess solvent is sometimes required to keep the reaction solution stirred. For the treprostinil **4** and treprostinil ethyl ester **43** containing polymers, a cloudiness was observed after 2-3 hours. Acid was neutralised by addition of triethylamine and polymers were isolated by precipitation into hexane. All monomers and expected products are insoluble in hexane so its choice as a precipitation solvent collects all components from the reaction mixture. Hexane precipitation does not offer the opportunity for reaction purification or removal of by-products, such as the catalytic acid salt. However, it does provide information on the whole reaction mixture, so following previous protocols,[402,403,405] polymerisation reaction mixtures were precipitated into hexane. Once collected under reduced pressure the polymers were dried under vacuum. To reduce the chance of degradation during storage, all polymerisation products were neutralised during work up, dried and stored at -20 °C.

After dying in vacuum, the isolated products were characterised by ^{1}H NMR to determine the degree of acetal formation and in the case of drug polymers, the percentage of treprostinil incorporation. Deuterated water, with potassium carbonate to prevent degradation, was used as a solvent for NMR spectroscopy. Gel permeation chromatography (GPC) was used to estimate the polyacetal molecular weight characteristics by measuring refractive index. The weight distribution, known as the polydispersity index (PDI) is calculated as a ratio between

weight average molecular weight and the number average molecular weight, M_w/M_n. A value closer to one indicates uniformity of the molecular weight. Molecular weight characteristics were estimated by GPC using poly(methyl methacrylate) (PMMA) calibrants.

Poly(PEG acetal)

Anticipating lower reactivity of the treprostinil hydroxyls compared to the PEG hydroxyls, poly(PEG acetal) 70 was first synthesised to be certain that the conditions described in the literature resulted in polyacetal formation (**Scheme 4-11**).

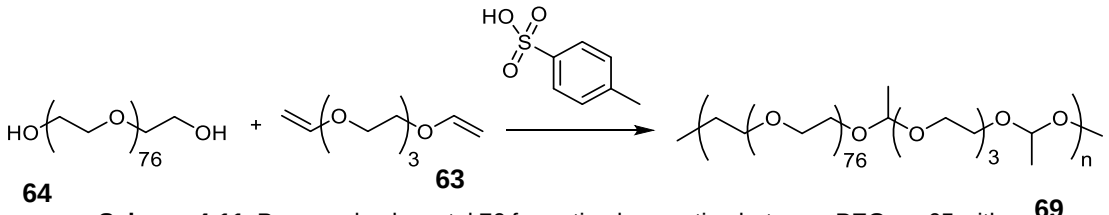

Scheme 4-11. Proposed polyacetal 70 formation by reaction between PEG_{3400} 65 with triethylene glycol divinyl ether 64 in the presence of *para*-toluene sulfonic acid (pTSA).

Polymerisation of PEG_{3400} **65** with TEGDVE **64** to form poly(PEG acetal) **70** (**Scheme 4-12**) was carried out on a 3 g scale. Analysis by ^{1}H NMR spectroscopy (**Figure 4-4**) shows the acetal methine and methylene resonances in a 1:3 ratio; a quartet at 4.77 ppm integrating to 2 protons (highlighted in pink), and a doublet at 1.25 ppm integrating to 6 protons (highlighted in green). The PEG proton resonances between 3.45-3.74 ppm have a combined integration of 340 protons. Each PEG chain has an average of 77 repeat units, each with 4 methylene resonance thus 308 protons. Each TEGDVE monomer has 3 ethylene glycol repeat units so a total of 12 methylene resonance. The total expected number of protons is 320 and the total seen in the ^{1}H NMR spectrum is 340. Comparing the ratio between one PEG chains to every two acetal bonds, indicates PEG was fully incorporated into a polyacetal mainchain.

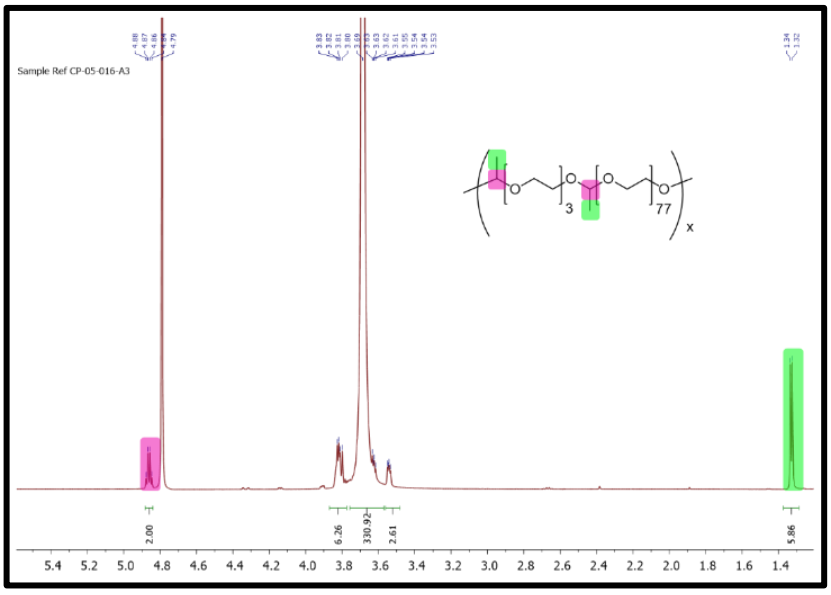

Figure 4-4. ^{1}H NMR spectra of Poly(PEG acetal) **70**. The acetal resonances are detected in the expected 1:3 ratio between the methine (highlighted in pink) and the

methyl resonance (highlighted in green). The ratio of acetal resonances to PEG resonances indicate a high degree of PEG incorporation into the polycetal mainchain.

Poly(PEG acetal) **70** was analysed by GPC running DMF with 5 mM NH_4BF_4 additive, and the elutogram (**Figure 4-5**) estimated a weight average molecular weight (Mw) of 48 kDa (compared to polymethyl methacrylate (PMMA) standards) with a polydispersity index (PDI) of 2.0. A Mw of 48 kDa is consistent with a degree of polymerisation of 13 PEG 65 units. The ^{1}H-NMR and GPC data gave confidence that polyacetal formation with treprostinil 4 as co-monomer could occur.

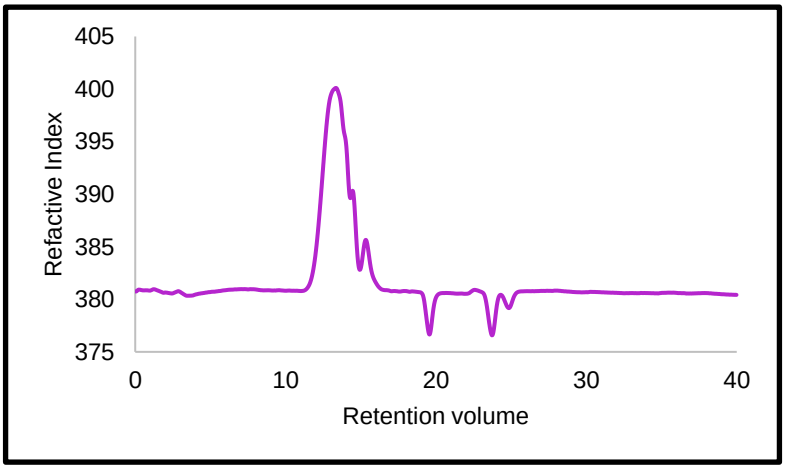

Figure 4-5. Gel permeation chromatography elutogram of poly(PEG acetal) **70** displaying a molecular weight of 48 kDa (PDI = 2.0). The GPC was conducted in DMF using PMMA calibrants at 70 °C.

Oligo(PEG-treprostinil acetal)

A 1:1 molar ratio of treprostinil 4 to PEG_{3400} **65** was used to prepare the treprostinil polyacetal 67 (**Scheme 4-12**). TEGDVE 64 was added dropwise to the dry THF solution of acidified diols (65 and 4) over 5 minutes and left to stir while shielding from light. The viscosity of the solution increased to form a gel-like solid consistent with polyacetalisation having occurred. The polymer was isolated after 3 hours by first adding more THF to the solution. Erroneously the neutralisation of the reaction mixture was conducted after precipitation into hexane had been initiated. Therefore, the neutralisation occurred during the precipitation, by addition of triethylamine (5 equivalents) to the remaining polymer solution and a further 2 equivalents to the hexane mixture. The precipitate was collected and dried.

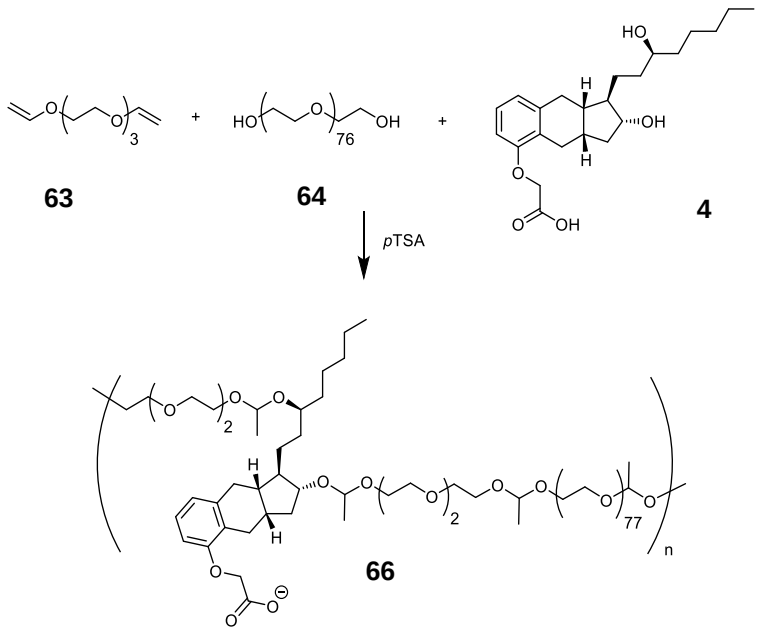

Scheme 4-12. Proposed acetal forming reaction between triethylene glycol divinyl ether 64 and diols; poly(ethylene)glycol$_{3400}$ 65 and treprostinil 4. Based on previous studies using diol drugs,[401–403,405,415] the poly(PEG-Treprostinil acetal) 67 was expected. *p*TSA = *para*-toluene sulfonic acid.

^{1}H-NMR can be used for end-group analysis for relatively low molecular weight polymers. ^{1}H-NMR can also provide an estimate of the relative incorporation of monomers in a co-polymer. Initial analysis of the ^{1} H NMR was carried out using phase and baseline correction functions within the analysis software (**Figure 4-6**) to obtain better resolution between the acetal methine (highlighted blue in **Figure 4-7**) and the water resonance. This was achieved using phase correction which skewed the baseline (**Figure 4-6**). The spectrum indicated a ratio of 1:2 for one aromatic treprostinil and acetal methine proton, which suggested treprostinil **4** had been incorporated as predicted into the oligoacetal macromolecular mainchain. On this basis, degradation assays were conducted without further purification.

Only upon re-analysis of the ^{1}H NMR data during the write up, did it become apparent that using the software analysis correction functions provided an inaccurate insight into the reaction success. Using the integrations calculated from **Figure 4-6**, a ratio of 2:14 was found for the acetal methine and methyl peaks, respectively. The acetal resonances cannot exist in a ratio other than 1:3. Thus, it was assumed that the conclusion of full treprostinil **4** incorporation into the main chain was not an accurate interpretation of the true polymerisation product. Using this insight, the raw ^{1}H NMR data was re-analysed without using phase correction functions. However, by this point the degradation assays were completed with impure samples. Without time or sample to repeat the assays, the data obtained originally was retrospectively analysed to account for the updated structure analysis.

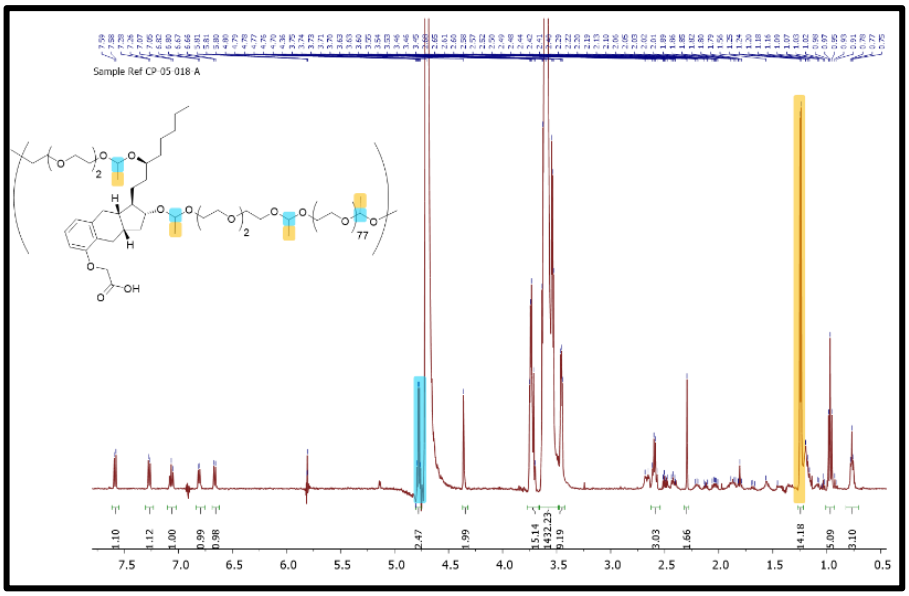

Figure 4-6. ^{1}H NMR spectrum of the product obtained from the attempted polyacetal polymerisation with poly(ethylene glycol)$_{3400}$ **65**, triethenylene glycol divinyl ether **64** and treprostinil **4**. To distinguish between the acetal methine proton peak (highlighted in blue), phase correction functions within the Mestrenova software were employed. This indicated a 1:2 ratio between treprostinil **4** and acetal groups. However, this skewed the integration of the acetal methine (blue) and methylene (yellow) resonances away from the possible 1:3 ratio. Therefore, this spectrum is not an accurate representation of the relative proton environments in the isolated product.

Similar to that of the poly(PEG acetal) 70, the ^{1}H NMR spectra for the polymerisation product, expected to be poly(PEG-treprostinil acetal) 67 showed the presence of a doublet at 1.25 ppm corresponding to the methyl of the acetal (highlighted in orange) and a quartet corresponding to the neighbouring lone acetal proton at 4.78 ppm (highlighted in blue). Treprostinil 4 resonances were observed at their expected chemical shifts but owing to the overlap of PEG resonances no shift could be observed for the methine protons (highlighted red) on the hydroxyl carbons expected to have undergone reaction.

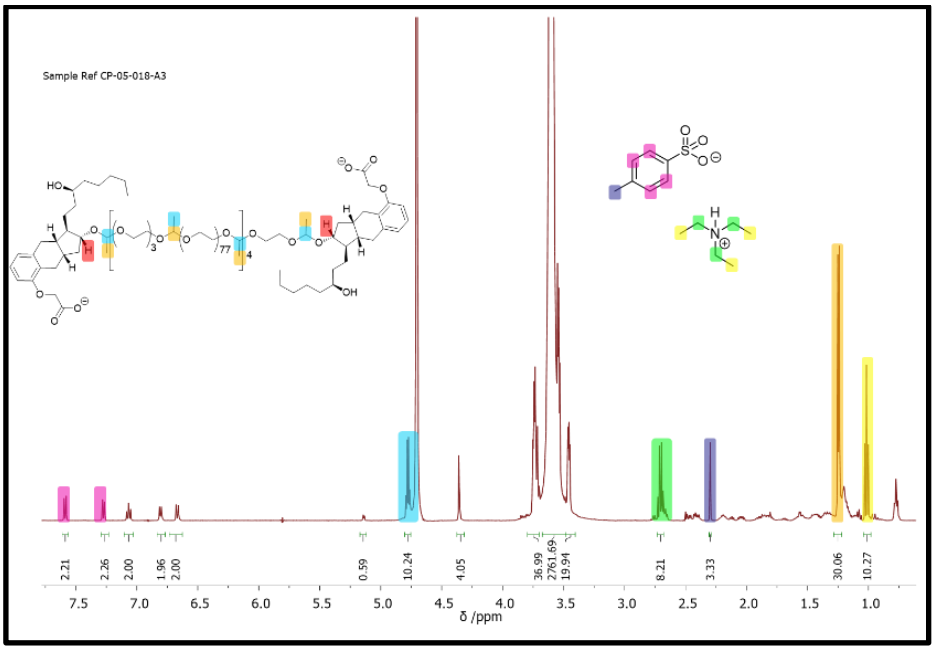

Figure 4-7. ^{1}H NMR spectrum of oligo(PEG-Treprostinil acetal) 71 in D_2O formed from polymerisation reaction. Acetal methine (blue) and methyl (orange) resonances are present in the expected ratio of 1:3. The *p*-toluene sulfonic acid (pink and purple) is present in equal ratio to the tritheylamine resonances (green and yellow) indicating neutralistaion. Although treprostinil resonances are present, the diagnostic methine resonances (red) are located under the PEG resonance at 3.5 ppm.

The ratio of acetal methine:methyl resonances fit the expected ratio of 1:3 although the resolution is less clear than the spectrum for poly(PEG acetal) 70 (**Figure 4-4**). Notably, the acetal resonance of treprostinil acetal (highlighted in blue, in **Figure 4-7**) is less distinguished from the water peak, which makes integration less accurate. The ratio of integration between the acetal methine resonance and an aromatic doublet (6.7 ppm) resonance of treprostinil is 1:5, which can occur when two PEG groups are present in a repeat unit. As PEG_{3400} 65 has been shown to undergo acetal formation (polyacetal 70), and the treprostinil hydroxyls probably possess reduced reactivity compared to the PEG 65 hydroxyls. Therefore, it is possible that the PEG 65 rapidly formed acetal bonds with the TEGDVE **64** to form oligo(PEG acetal) chains which then react with treprostinil 4 at the oligomer terminus (**Figure 4-8**). With a treprostinil at the terminus, two PEG chains and five total acetal bonds, three vinyl ethers would be required. Thus, ending the oligomer with the reactive vinyl ether (**Figure 4-8**). Vinyl ethers are highly reactive so are unlikely to remain intact in the presence of the PEG 65 primary alcohols. Therefore, a terminal vinyl ether suggests that it possesses a dead chain end. However, no acetal, or aldehyde resonance was detected by ^{1}H NMR, although it might be expected that if vinyl ether degradation had occurred, the acetaldehyde 63 was removed during isolation.

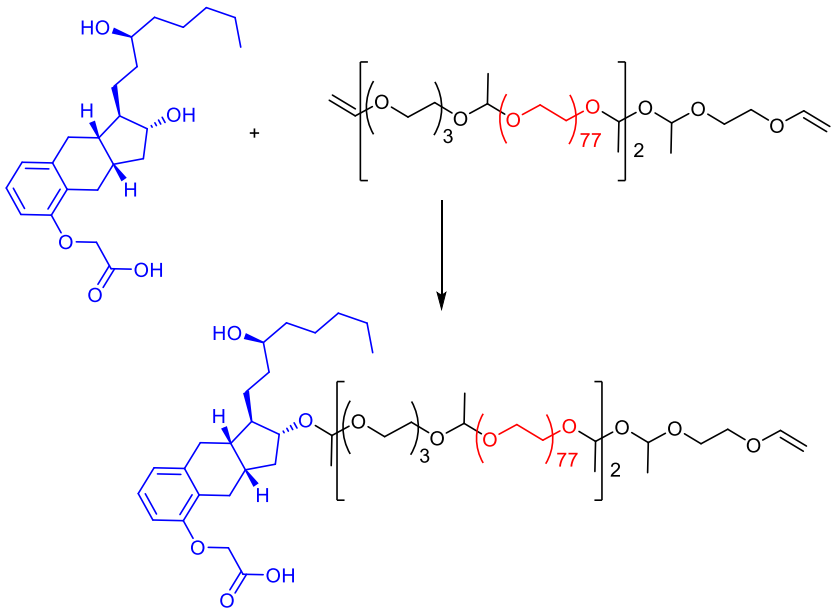

Figure 4-8. Formation of the proposed structure of polymerisation product based on the ratio of one aromatic treprostinil **4** peak to 5 acetal methine resonances visible in the ^{1}H NMR spectrum. With 5 acetal bonds, the sequence ends in a triethylene glycol divinylether monomer **64**. However, neither the vinyl ether proton peaks or the peaks corresponding to the degradation product, acetaldehyde **63** were visible, which lead to the conclusion that this was not the structure of the product isolated.

The lack of terminal vinyl ether resonances visible in the ^{1}H NMR spectrum suggests that perhaps two treprostinil 4 groups are present per oligomer at each terminus, with four PEG chains and ten acetals in total (**Figure 4-9**). An oligomer possessing treprostinil 4, PEG 65 and TEGDVE 64 with ratio 1:2:3 (**Figure 4-8**) would have an expected M_w of 7.4 kDa, and an oligomer 71 with double the PEG and treprostinil groups (**Figure 4-9**) would possess a M_w of 15 kDa.

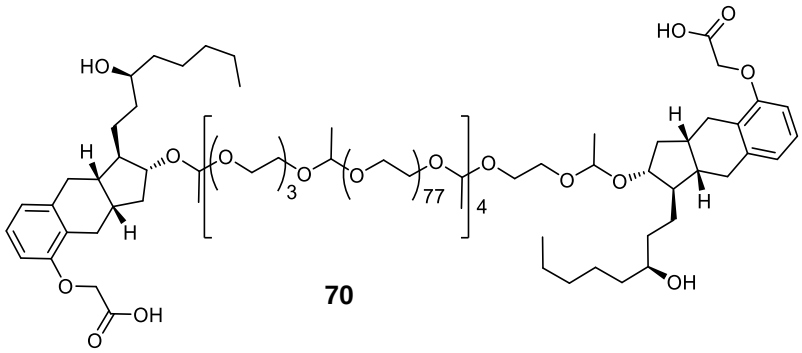

70

Figure 4-9. Proposed structure of the isolated product from the polymerisation reaction using treprostinil 4 as a co-monomer. Treprostinil 4 end groups are likely as their presence reduced the degree of acetal formation expected. The ratio of treprostinil 4, PEG 65 resonances indicates 5 acetal bond which would leave a terminal vinyl ether, which is not observed. Therefore, the structure must possess treprostinil at each terminus in oligo(PEG-treprostinil acetal) 71, which is supported by the M_w of 17 kDa estimated by gel permeation chromatography.

The GPC of oligoacetal 71 (**Figure 4-10**) estimated a modest M_w of 17 kDa (based on PMMA calibrants), supporting the ^{1}H NMR interpretation of a bis-treprostinil oligomer 71. The M_w is considerably less than the M_w 43 kDa measured for poly(PEG-DES acetal) 59,[402] implying treprostinil is a less efficient monomer than DES. While the PDI of oligoacetal 71 at 1.8 is comparable to other poly(PEG-drug acetals)[402,403,405] the GPC displays several multiple peaks, suggesting many oligomeric species are present.

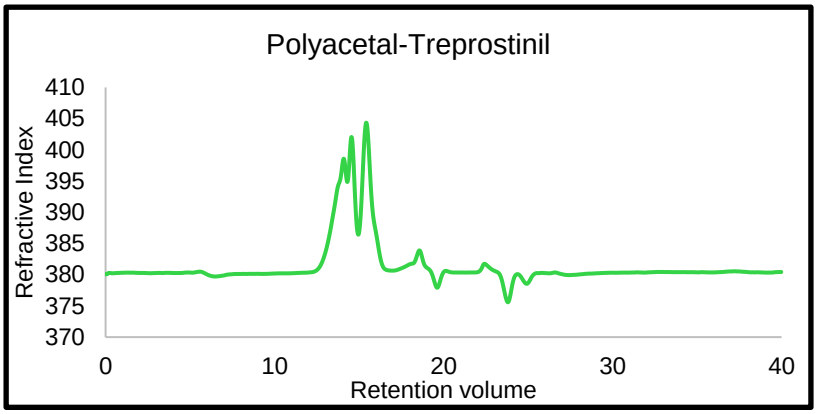

Figure 4-10. Gel permeation chromatography elutogram of poly(PEG-treprostinil acetal) 71 displaying a molecular weight of 17 kDa (PDI = 1.8). The GPC was conducted in DMF using PMMA calibrants at 70 °C. The numerous peaks indicate a heterogeneous product.

Based upon the predicted oligo(PEG-treprostinil acetal) 71, the theoretical inclusion of treprostinil 4 is 5% $wt_{treprostinil}/wt_{polymer.}$ The expected polyacetal 67 included treprostinil 4 within the mainchain with a 1:1:2 ratio of treprostinil, PEG and TEG, respectively. Theoretical inclusion of treprostinil 4 based upon full polymerisation would be 9%.

Determination of the oligomer structure does not account for all the PEG protons detectable in the ^{1}H NMR spectra.

Total TEG/PEG protons in the oligo(PEG-trep acetal):

= ((77 PEG repeat units x 4 protons per repeat unit) x 4 PEGs per oligomer) + (12 TEG protons x 5 TEGs in the oligomer)

= 1232 TEG/PEG protons

Total PEG protons in spectra = 2818 protons

Remaining PEG protons = 21818 – 1232 = 1586 protons

protons per monomer = (1586/4)/77 = ~5 PEG chains worth remaining.

Mass % of soluble treprostinil 4 in a sample

= (390.5 × 2)/ [(390.5 × 2) + (3400 × 9) + (202.25 × 5) + 172.2 + 101.19

= 781 / (781 + 30600 + 1011.25 + 172.2 + 101.19)

= 2.4% $wt_{treprostinil}/wt_{sample}$.

The conclusion that treprostinil 4 incorporation is limited to one or two treprostinil compounds per oligomer, in the context of a successful polymerisation of PEG, may suggest poor dissolution of the oligomer 71 during the reaction. Whilst not an issue in the formation of polyacetal 70, the reaction solution for poly(PEG-treprostinil acetal) 67 formed a highly viscous gel after 3 hours. The lack of fluid behaviour may have hindered the possibility of the chain ends interacting to form larger polymers, resulting in the isolation of smaller oligomer chains. However, it is unlikely that oligomers would result in a viscous material. A gel-like material is usually consistent with the formation of high molecular weight polymer. One possible explanation is that a polyacetal compound with a greater degree of polymerisation formed initially, but degraded upon isolation, which is made plausible considering the error in delayed neutralisation.

Oligomer 71 formation may be explained as a function of the hydroxyl reactivity. If the treprostinil 4 molecules were incorporated as terminal groups, this may indicate a difference in the reactivity of the two hydroxyls, as only one hydroxyl is able to either form or maintain an acetal bond. Unfortunately, no diagnostic resonances are visible to confirm or reject this interpretation that a terminal treprostinil 4 selectively conjugates through one hydroxyl.

Treprostinil 4 was added in a 1:1 ratio with PEG 65, although only 27% of the total treprostinil expected is accounted for by ^{1}H NMR spectroscopy (**Figure 4-7**). Furthermore, HPLC (**Figure 4-11**) was conducted on an aqueous solution of the polymer sample isolated (5 mg/mL) and showed no free treprostinil 4 (retention time of treprostinil 4 is 9.6 minutes). The presence of treprostinil was measured by UV absorbance at 217 nm, following previous treprostinil detemination.[354] This was initially interpreted as there was no free treprostinil 4 present in the polymeric solution. Free treprostinil 4 which was not accounted for in the ^{1}H NMR spectrum (**Figure 4-7**) would have been expected to be isolated during precipitation in hexane.

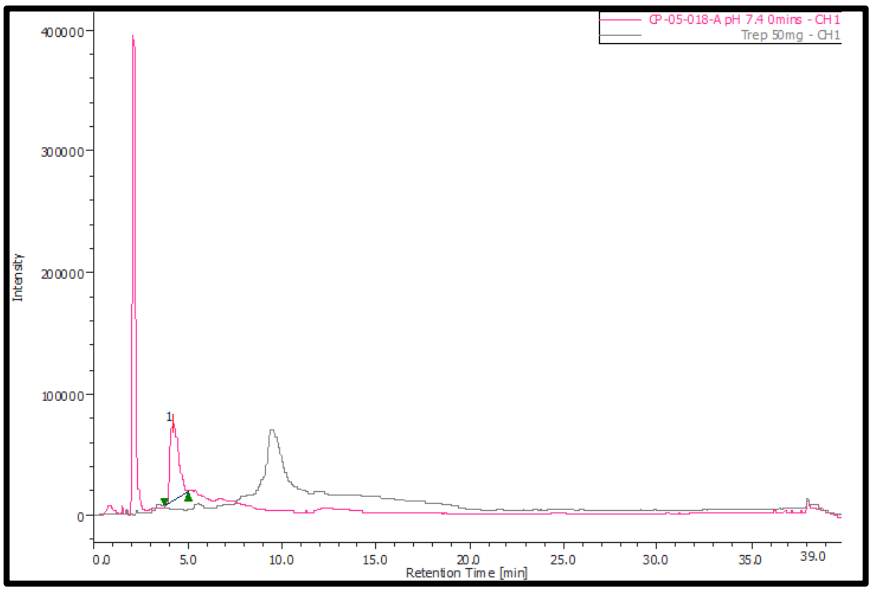

Figure 4-11. Overlapping HPLC chromatograms of the oligomeric product **71** in pH 7.4 buffer (pink) and a sample of treprostinil 0.5 mg/mL (grey). No treprostinil absorbance is observed in the polymer solution.

Based on the weight of treprostinil added to the reaction compared to the total weight of all polymer-forming reagents added, theoretical percentage of treprostinil, either conjugated or non-conjugated, is 9%. The maximum amount of total treprostinil visible in the ^{1}H NMR was calculated to be 2.4%, which suggests that the 6.6% of the treprostinil added is unaccounted for. The NMR solvent used was deuterium oxide in the presence of potassium carbonate, an aprotic base not detected by ^{1}H NMR analysis. Its presence was included to reduce *in situ* degradation of the acetal bonds but would have also aided solubility of any unconjugated treprostinil. Furthermore, when analysed by HPLC in buffer at pH 7.4, the chromatogram of oligo(PEG-treprostinil acetal) **71** showed no evidence of treprostinil. Therefore, it is unlikely that the treprostinil unaccounted for had precipitated.

Treprostinil, PEG_{3400} and p-toluene sulfonate triethylamine salt are all insoluble in hexane, owing to the high polarity and charge. Therefore, it is expected that all of the reagents present in the reaction mixture were isolated by precipitation into hexane. The delayed neautralisation of the polymerisation solution may have meant that protonated treprostinil was added into hexane which may have exhibited solubility given the large volume of solvent. Following the initial incorrect interpretation of the ^{1}H NMR, the hexane layer was discarded.

The ^{1}H NMR spectrum of oligomer **71** (**Figure 4-7**) shows the pair of downfield aromatic doublets visible at 7.35-7.68 ppm corresponding to the presence of residual *p*TSA in a molar ratio of 2:13 with PEG. The triplet and quartet at 0.99 and 2.57 ppm, respectively, indicate that triethylamine is also present in equal equivalents to pTSA so it's likely that they are present as the salt which precipitated out in hexane. To help ascertain whether the pTSA is present in a protonated or deprotonated form, an independent ^{1}H NMR of pTSA in D_2O with and without the addition of excess potassium carbonate base was conducted. However, no shift in the aromatic resonances was observed.

Oligo(PEG-treprostinil ethyl ester acetal)

Use of a drug co-monomer with a free carboxylic acid and secondary hydroxyls for incorporation into a polyacetal has not been previously described. In principle the treprostinil free acid **4** is capable of catalysing the degradation of acetal bonds, although this was not attempted. Treprostinil **4** solubility in toluene was poor even in the protonated form and required heating to over 50 °C. With residual toluene in the reaction solution at room temperature, it was assumed that a protonated treprostinil **4** would aid solubility and thus the solution was acidified. The secondary hydroxyls may contribute to a lower degree of polymerisation. In addition to the concern about the difference in the treprostinil hydroxyl reactivity, there was concern that the treprostinil **4** carboxylic acid would catalyse degradation during polyacetal synthesis.

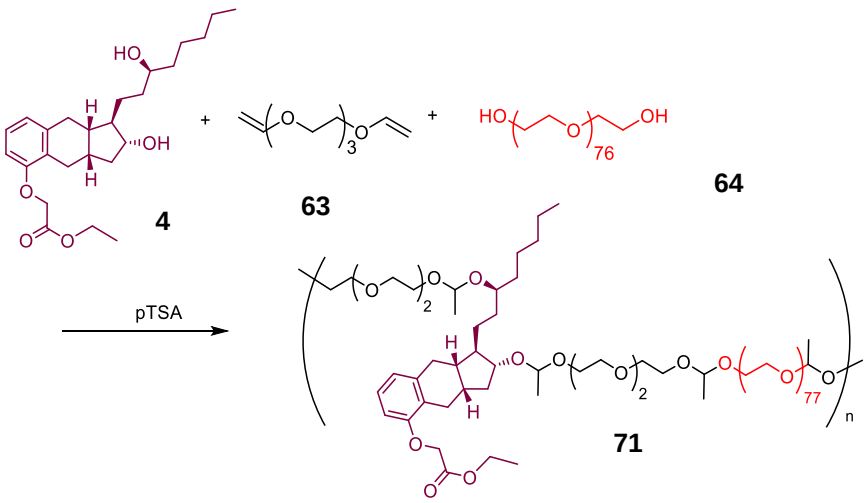

Scheme 4-13. The proposed synthesis of poly(PEG-treprostinil ethyl ester acetal) **72** formed by the ter-polymerisation using treprostinil ethyl ester **43** as a co-monomer. The success of the polymerisation was investigated in the absence of treprostinil acid. pTSA = *para*-toluene sulfonic acid.

To investigate the effect of the free acid on acetal formation, the polymerisation was repeated using treprostinil ethyl ester **43** as a co-monomer (**Scheme 4-13**). The reaction was carried out with 50 mg treprostinil ethyl ester **43**, using 0.03 equivalents of pTSA catalyst and more than 4 times the amount of solvent as used for treprostinil 4 to aid solubility. Upon addition of the divinyl ether 64, the reaction solution soon became cloudy. The solution was neutralised by addition of 16 equivalents of triethylamine. After precipitation and drying, GPC (**Figure 4-12**) indicated the average molecular weight as 8 kDa, corresponding to approximately two PEG_{3400} **65** chains per structure, with a narrow PDI of 1.1. ^{1}H NMR showed the presence of treprostinil ethyl ester **43**, acetal and PEG **65** protons in a ratio of 1:4:5088, indicating a low conversion of acetal. The 5088 PEG **65** methylene protons correspond to 15 units of macromonomer PEG **65** for every one treprostinil ethyl ester **43** and **4** acetals. Therefore, only 2 of the 15 PEG **65** chains detected in the NMR have undergone acetal formation. The expected structure of poly(PEG-treprositnil ethyl ester acetal) **72**, was not obtained.

Table 4-3. ^{1}H NMR spectrum of polymerisation product in the attempt to form polyacetal(PEG-treprostinil ethyl ester) **72**. Only small quantities of treprostinil ethyl ester **43** were present compared to the PEG **65** protons. Additionally, the *p*ara-toluene sulfonic triethylammonium salt was present and unreacted vinyl ether chains were also obtained. Where R is any number of PEG_{3400} macromonomers.

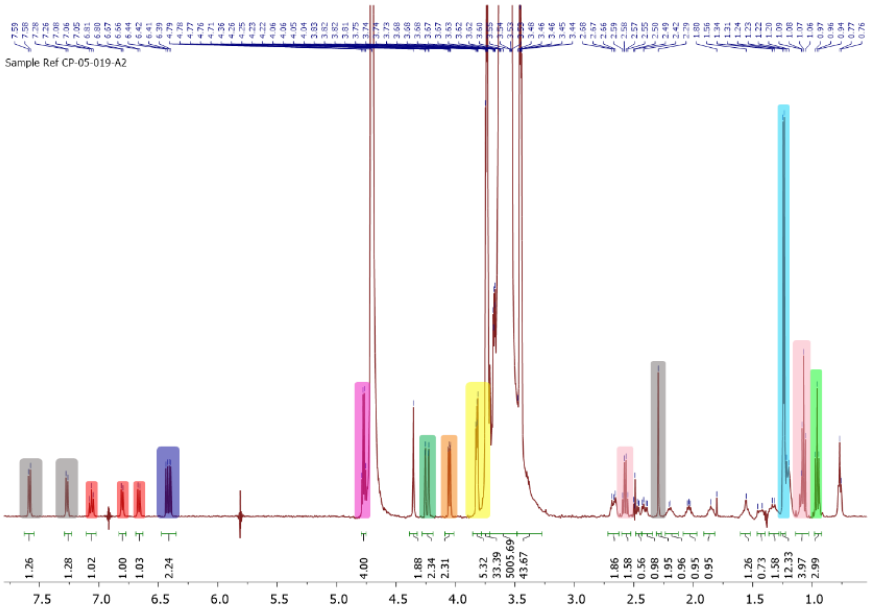

Proton environments identified

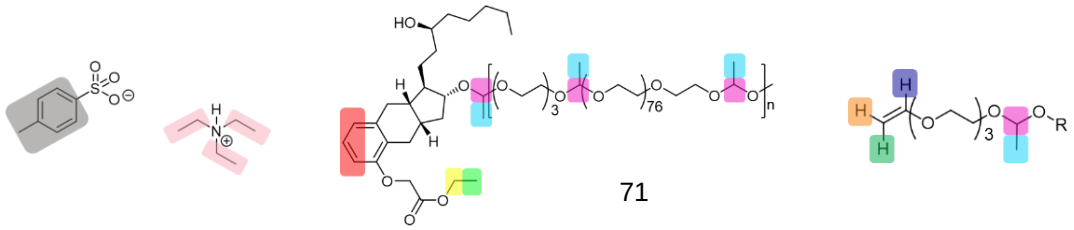

71

The ^{1}H NMR spectrum (**Table 4-3**) showed the ethyl ester moiety of treprostinil ethyl ester **43** remained intact during the reaction, as concluded by the presence of the methylene resonance (highlighted in yellow) and the terminal methyl resonance of the ester (highlighted green). The treprostinil aryl carbonyl methylene peak is not observed as it lies under the broad peak for the PEG **65** methylene protons. Treprostinil ethyl ester **45** exhibits poor solubility in water compared to its free acid parent compound. Therefore, the detection of treprostinil ethyl ester **43** resonances suggests they are included within the acetal structure.

To prevent any degradation in the deuterium oxide solvent during ^{1}H NMR analysis, potassium carbonate was added. Interestingly, the vinyl ether moiety was detected in its intact form, rather than the degraded acetaldehyde product **63**. Ordinarily, vinyl ethers undergo hydrolysis in the presence of primary alcohols and mildly acidic water, which implies that in the presence of treprostinil ethyl ester, only a proportion of the vinyl ethers underwent nucleophilic addition. The poor acetal forming reactivity of treprostinil ethyl ester **43** also supports the interpretation that the treprostinil **4** secondary alcohols are only modestly reactive for incorporation into a

polyacetal using the reaction conditions which have been tried. Furthermore, interference of the treprostinil acid **4** in acetal formation is also ruled out.

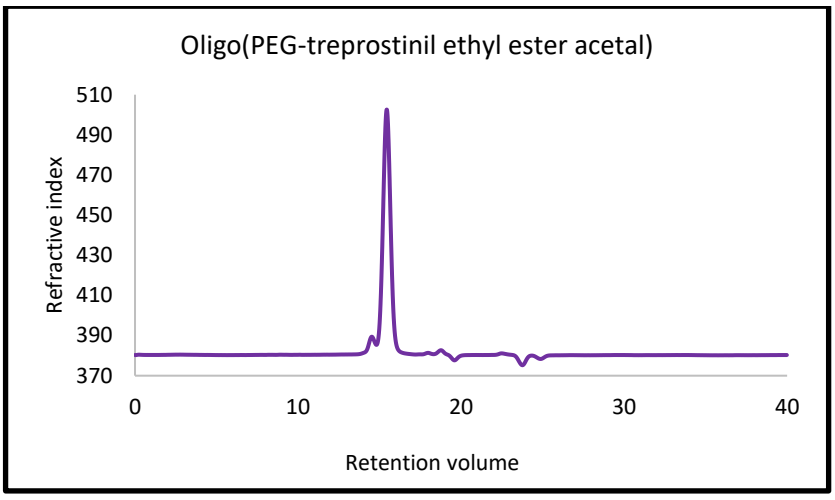

Figure 4-12. Gel permeation elutogram for the product of the acetal polymerisation reaction of treprostinil ethyl ester **43** and poly(ethylene glycol)$_{3400}$ **65** Only a small degree of acetal formation occurred with an average M_w of 8 kDa corresponding to only two PEG chains. The small M_w resulted in a narrow polydispersity index (1.1)

Low efficiency for acetal formation using the treprostinil ethyl ester **43** may also be caused by its poor solubility in the reaction solution. During the reaction, a cloudy solution was formed upon addition of treprostinil ethyl ester **43**, which remained slightly pearlescent until work-up. Solubility was also a factor which could be investigated further through optimising the solvent system used to better suit treprostinil ethyl ester **43**. Despite the unsuccessful reaction, the detection of unreacted vinyl ethers is consistent to the anhydrous conditions employed.

4.2.2 Degradation

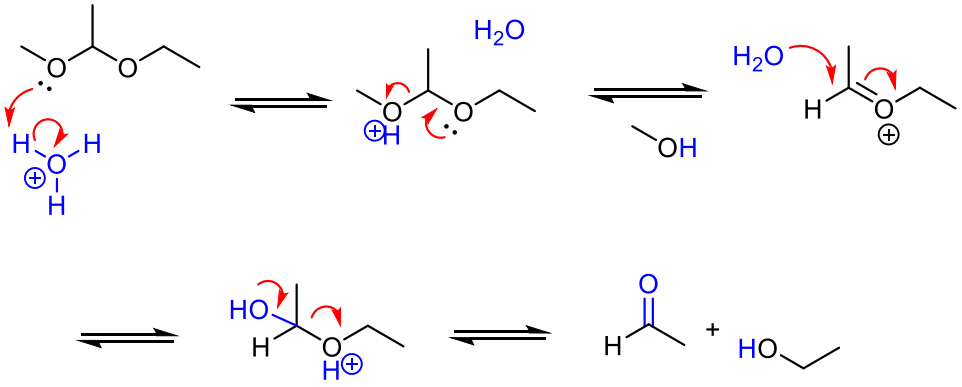

Scheme 4-14. Mechanism of acetal degradation. Acid catalysed mechanism for acetal hydrolysis is driven by protonation of one of the acetal oxygens to allow facile nucleophilic attack by water to cleave the acetal into two moles of alcohol and a mole of aldehyde **63**.

Polyacetals are known in the literature to exhibit pH dependent degradation.[401–403,405,416] In the presence of protons, an acetal oxygen becomes protonated (**Scheme 4-14**). This drives the donation of electrons from the neighbouring acetal oxygen resulting in the formation of an

alcohol and an alkylated aldehyde intermediate. Water attacks the carbonyl by nucleophilic additional to form a hemiacetal which again donates electrons to facilitate the production of an alcohol and acetaldehyde. One limitation is the formation of 1 mol acetaldehyde upon degradation which may cause issues relating to its toxicity.

Several studies have shown that polyacetals are hydrolytically stable at physiological pH and degrade at reduced pH to release drug. Degradation of the acetal bonds is acid catalysed with the release of the hydroxyl monomers as diols. For every vinyl ether derived acetal bond, one mole of acetaldehyde is also produced upon acetal hydrolysis. Acetaldehyde, the metabolite to ethanol, is a known carcinogen but has also shown to stimulate prostacyclin release in tissues and cells by stimulating prostacyclin synthase.[417,418]

The hypoxic conditions formed in chronic PAH causes a switch in metabolism from oxidative phosphorylation to glycolysis, resulting in an acidic tissue.[49] To evaluate pH dependent degradation, oligomers were incubated in aqueous environments at different pHs and the amount of treprostinil released over time was quantified. Oligo(PEG-treprostinil acetal) 71 were evaluated in buffers adjusted to pH 7.4 and 6.6-5.5 to mimic physiological and acidic, diseased tissue respectively. Following previous studies,[402,405] oligomer degradation studies were conducted using a concentration of 5 mg/mL at 37 °C with gentle agitation. The concentration of free treprostinil was analysed by HPLC at time points during the study.

An initial degradation study was conducted at pH 7.4 and 5.5. An aqueous solution (1 mL) of oligo(PEG-treprostinil acetal) **71** (5 mg/mL) was analysed by HPLC at designated time points without neutralising the sample. To prevent further acid-mediated degradation during elution, the mobile phase comprised only acetonitrile (30% to 80% gradient) and water without any TFA. The UV absorbance of the eluted sample was analysed at 217 nm using a UV detector, which is sensitive enough to detect most pi bond electrons. Time points were taken between 0 and 48 hours, and any free treprostinil was expected to elute at approximately 9.6 minutes (**Figure 4-14**). No change in the HPLC was observed at pH 7.4 (**Figure 4-13 A**). In contrast at pH 5.5, the chromatograms changed with time with a broad peak for treprostinil appeared by the end of the study (**Figure 4-13 B**).

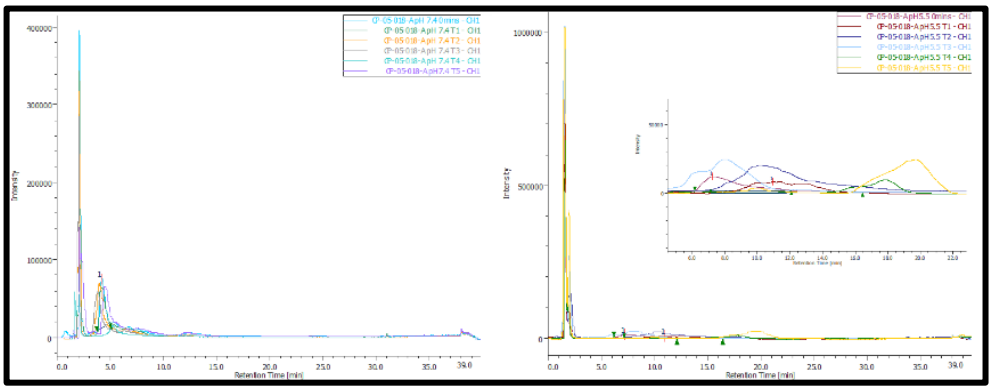

Figure 4-13. HPLC chromatograms of oligo(PEG-treprostinil acetal) **71**, incubated at A) pH 7.4 and B) pH 5.5. No treprostinil was detected at pH 7.4 whereas absorbances

were detected for the oligo(PEG-treprostinil acetal) **71** at pH 5.5. The retention time of the peaks changed with time.

The solubility of treprostinil sodium salt used for parental delivery is 10 mg/mL.[266] For the subcutaneous formulation, each 1mL of solution contains 4.0 mg sodium chloride, 3.0 mg metacresol, 6.3 mg sodium citrate. Despite the solubility of treprostinil, direct analysis of the degradation mixture at pH 5.5 did not unambiguously show treprostinil (**Figure 4-13**), even for treprostinil standards (**Figure 4-14**). Furthermore, real time monitoring of the degradation, without a quenching step, meant measurements could only be taken when the HPLC apparatus was free, i.e. not during analytical run time. Therefore, the run time of the HPLC (40 minutes) limited the frequency of analysis.

Even with quantifiable treprostinil peaks, the absence of the TFA-buffer in the mobile phase created an inconsistent peak shape for the treprostinil standards (**Figure 4-14**) in comparison to when standards are run in a TFA-spiked mobile phase (**Figure 4-16**).

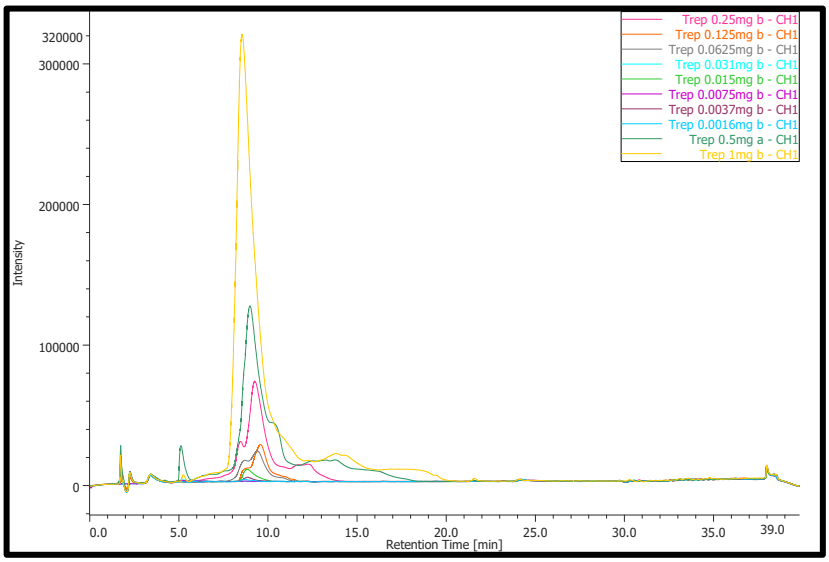

Figure 4-14. HPLC chromatograms of treprostinil standards run in the absence of TFA. Peaks have multiple shoulders and are slightly inconsistent.

The remaining sample solutions were incubated for a total of 6 days whilst the data was being analysed and interpreted. Consulting previous protocols,[402] a method to quantify drug compound by liquid-liquid extraction was investigated. Neutral treprostinil (free acid) is soluble in ethyl acetate whereas PEG_{3400} was still insoluble after vortexing and sonication in ethyl acetate. Therefore, ethyl acetate was considered suitable for extraction of unconjugated treprostinil. For each of the remaining oligomer solutions, 880 µL was extracted with an equal volume of ethyl acetate (3×) which were combined, washed with brine, dried by passing through a glass pipette plugged with cotton wool and magnesium sulfate and the filtrate dried over a stream of air. The residue was dissolved in acetonitrile (150 µL) and analysed by HPLC

using steeper TFA-spiked solvent gradient (40-90% acetonitrile/water) and shorter analysis time (11 minutes).

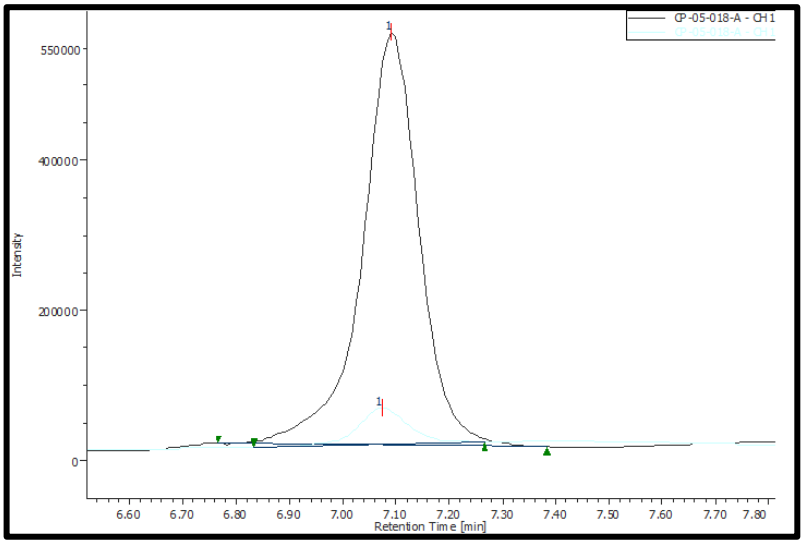

Figure 4-15. HPLC chromatograms for treprostinil detected in pH 7.4 (turquoise) and pH 5.5 (black) oligomer samples after 6 days. The samples were extracted using ethyl acetate and analysed using trifluoroacetic acid-spiked acetonitrile (40-90%) and water over 11 minutes

For the two different pHs (7.4 and 5.5), the amount of treprostinil detected varied drastically (**Figure 4-15**). Using a treprostinil calibration curve and the shortened HPLC analysis method (**Figure 4-16**), the peaks were better resolved and allowed for quantification of the treprostinil in each sample.

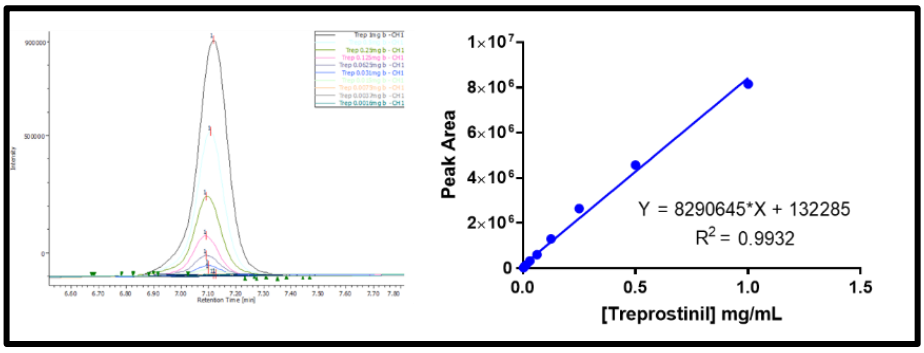

Figure 4-16. Analysis of treprostinil standards using mobile phase spiked with trifluoroacetic acid (TFA) is absorbed with better resolution and sensitivity than without TFA. A) HPLC chromatograms for treprostinil standards using TFA-buffered mobile phase and shorter method. B) Treprostinil concentrations were used to plot a standard curve.

Using the HPLC standard curve determined for treprostinil using a TFA-spiked mobile phase (**Figure 4-16**), the peak areas of treprostinil detected by working up the degradation assay after 6 days were converted to concentration of treprostinil.

Table 4-4. The conversion of peak area to concentrations of treprostinil **4** extracted from the degradation assay at pH 7.4 and 5.5. AUC, area under the curve as analysed by HPLC.

pH	AUC	Concentration µg/mL	% drug released from total drug in sample
7.4	322611	4	0.48
5.5	4135539	85	10.0

With a differing amount of treprostinil released for the neutral and acidic solutions, the reaction was repeated using the extraction method using a pH more relevant to inflamed tissue (pH 6.6).[251,412,413] A method of neutralising the test solutions before extracting the lipophilic components with ethyl acetate has been used in previously reported studies.[402] However, the pKa of treprostinil acid (pKa 4.5)[419] means treprostinil solubility in the organic layer is only facilitated at lower pH values. At neutral pH, treprostinil is expected to be in its deprotonated form rendering it poorly soluble into the organic layer. Therefore, neutralisation of acidic solutions would prevent treprostinil from partitioning effectively into an organic extraction solvent. Unfortunately, acidification during extraction would be expected to degrade acetal bonds further resulting in an increased concentration of treprostinil being extracted to cause an over estimation of polymer degradation. Thus, the oligo(PEG-treprostinil acetal) solutions were worked up directly at the pH of the buffer used for each degradation experiment. For this reason, the liquid extraction was carried out at each time point as quickly as possible. The reconstituted solutions were stored at -20 °C until all samples had been collected and then thawed before HPLC analysis

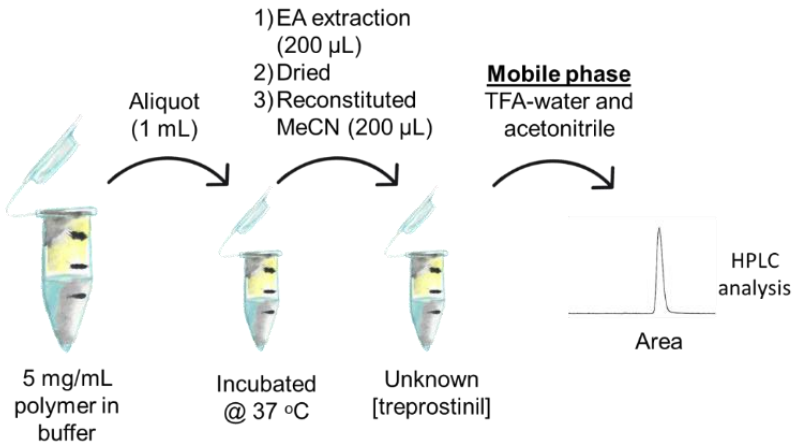

Figure 4-17. Method for extraction of treprostinil 4 from degradation assay samples. Once a solution of oligo(PEG-treprostinil acetal) **71** has been made up at 5 mg/mL, aliquots of 1 mL are portioned immediately which are then incubated at 37 °C. At each time point, the solution is extracted with ethyl acetate (EA; 200 µL ×3) which is then

dried under a stream of air and reconstituted in acetonitrile (MeCN). The sample is analysed by HPLC using a TFA-spiked acetonitrile/water mobile phase.

A further consideration of the known poor solubility of treprostinil **4**, was the possibility of treprostinil aggregation or precipitation upon release from the oligomer. Thus, removal of an aliquot from the degradation experiment for the first time point and an aliquot for the last time point may contain differing proportions of insoluble treprostinil **4**. To reduce this effect and attempt to achieve an equal concentration of treprostinil **4** and oligomer for each time point, once the treprostinil oligoacetal **71** solutions in the respective buffers for each pH were prepared for the degradation study, the solutions were immediately aliquoted into vials of equal volumes designated for each time point (**Figure 4-17**). A 10 mL degradation solution was prepared with oligo(PEG-treprostinil acetal) **71** at a concentration of 5 mg/mL in buffers at pH 7.4 and 5.5. At each hour between 0 and 6 hours, a sample (1 mL) was taken and worked up as already described by extraction in 200 µL ethyl acetate (×3) which was washed with brine and dried over magnesium sulfate, and then reconstituted in 200 µL of solvent. A solvent of water, acetonitrile and methanol solution (5:2:1) was chosen which minimised the organic content and facilitated sample dissolution. The calibration curve obtained by dissolving treprostinil **4** in acetonitrile and analysing using TFA-mobile phase, shown in **Figure 4-16** was used to determine treprostinil **4** content for each sample. A mix of dissolving solvents was designed to solubilise treprostinil **4** using a primarily aqueous solution to maximise interaction with the HPLC column.

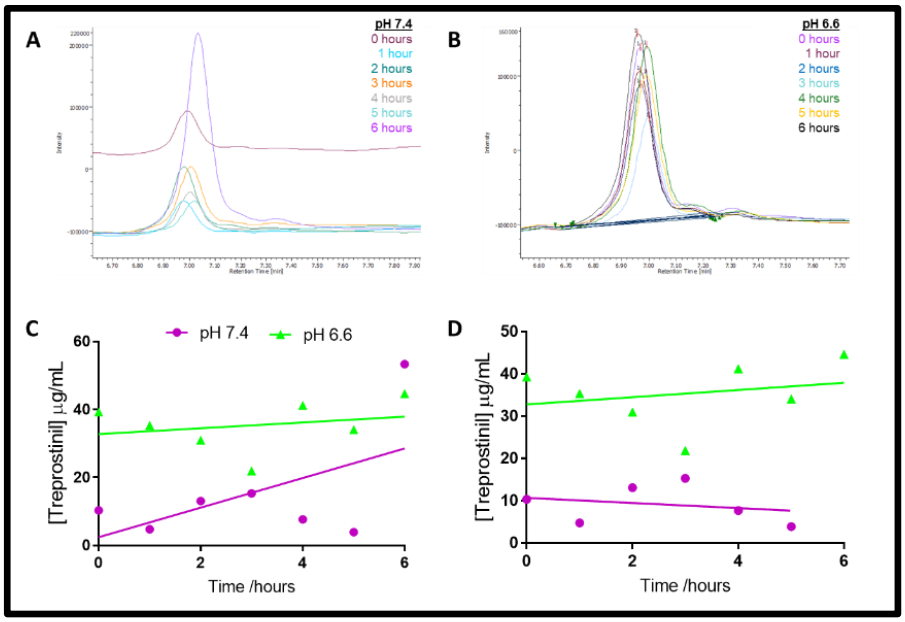

Figure 4-18. Release of treprostinil from oligo(PEG-treprostinil acetal) **71** over time when incubated at pH 7.4 (purple) and pH 6.6 (Green). Treprostinil was extracted into ethyl acetate from aliquots of aqueous sample and reconstituted into solvent mix of water/acetonitrile/methanol (5:2:1). The HPLC absorbances of treprostinil extracted from pH 7.4 (Graph A) and pH 6.6 (Graph B) The first sample to be analysed possessed a baseline greater than all other points; C) The integration of each peak was plotted as a function of time to each pH. A spurious data point was calculated

after 6 hours at pH 7.4, which was erroneously not washed with brine after extraction; D) The data was re-plotted without the spurious data point to observe the more consistent trend.

The degradation experiment was conducted once appeared to show a difference in degradation between pH 7.4 and 6.6. Variability was observed although, on average, greater concentrations of treprostinil were detected in the more acidic aqueous buffer. Surprisingly, the gradient of the data collected at pH 6.6 was shallower than expected and amount of treprostinil collected over time remained fairly constant. One spurious result was detected after 6 hours at pH 7.4 (**Figure 4-18 C**), but when removed from the data set (**Figure 4-18 D**), no overall change in treprostinil concentration was overserved over 6 hours. During the extraction of the sample at 6 hours in pH 7.4 buffer, the brine organic layer wash layer was erroneously skipped before filtering through the magnesium sulfate, which when analysed produced a much higher absorbance than expected. Interpretation of the effect of missing the brine step, may suggest that extracted treprostinil located in the ethyl acetate layers is subsequently lost to the aqueous layer upon brine wash. The slight variation in data observed could be due to the extraction process, particularly the drying step, or instrumental error (i.e. varying amounts of sample being collected by the autosampler for analysis). To mitigate any instrumental error an internal was added to the solvent used to dissolve the dried extracted treprostinil.

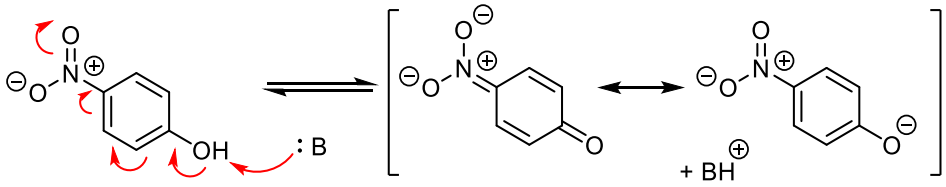

Scheme 4-15. Para-nitrophenol and the resonant forms of the deprotonated form. Upon deprotonation the UV absorbance changes.

An internal standard was added to the reconstituting solvent to reduce variability. The presence on an internal standard would identify if the variability was an instrument error (e.g. inaccuracies in the autosampler volume) and if so, allow for exact quantification by quantifying the ratio of treprostinil to internal standard. Initially, *p*-nitrophenol (**Scheme 4-15**) was investigated as an internal standard in the solvent mix of acetonitrile, water and methanol. Several dilutions were made to achieve a concentration of *p*-nitrophenol that remained in the detectable range when detected at 217 nm. When re-analysing the solution of *p*-nitrophenol after 24 hours, the solution was noticeably more yellow and the absorbance at the same concentration had increased in intensity and slightly increased retention time. The concentration of the day-old sample was diluted by a factor of 20, and the absorbance was still greater than the original sample analysed the day before (**Figure 4-19**). The change in absorbance it likely a result of p-nitrophenol becoming deprotonated (**Scheme 4-15**). The resonance forms of the deprotonated forms result in greater UV activity resulting in larger absorbances detected. The requirements of an internal standard are that they produce a

consistent measurement for the sample of interest can be compared against. Based on the variation in absorbance observed over time, *p*-nitrophenol was not a suitable internal standard.

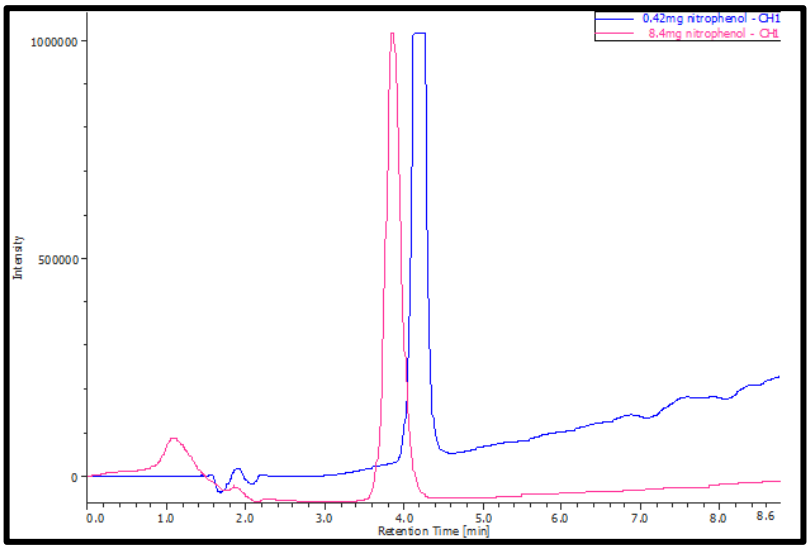

Figure 4-19. Comparison of HPLC chromatograms of *p*-nitrophenol. When freshly prepared at 0.84 mg.mL (pink), *p*-nitrophenol elutes after 3.9 minutes with an absorbance within the detectable limit. After 24 hours, a diluted solution (0.42 mg/mL) has a longer retention time and absorbance increases above the detectable limit (blue).

With a similar structure to treprostinil **4**, phenoxyacetic acid **22** was investigated as an internal standard by measuring absorbance at 217 nm. Without resonances involving the π-bond electrons of the aromatic ring, phenoxyacetic acid showed reproducible absorbance over time. As an internal standard, phenoxyacetic acid **22** in acetonitrile had a retention time of 3.6 minutes which was sufficiently different from treprostinil with a retention time of 7.1 minutes (**Figure 4-20**). Baseline resolution between the two compounds was achieved while being sufficiently long enough to elute after the solvent peak. Therefore, acetonitrile was used for the reconstitution step.

A standard curve of treprostinil was made using treprostinil concentrations made by serial dilution in MeCN of 0.5 mg/mL – 2 µg/mL (**Figure 4-20**). Each concentration solution was diluted in a stock solution of 1 mg/mL phenoxyacetic acid 22 in acetonitrile and 20 µL injected and analysed in duplicate by HPLC. The treprostinil peak areas were analysed as a ratio to the internal standard and plotted against concentration. The small amount of drug release observed in the preceding degradation studies (**Figure 4-18**) when compared to other polyacetals described in the literature suggests the hydrolysis is not occurring at a comparable rate.

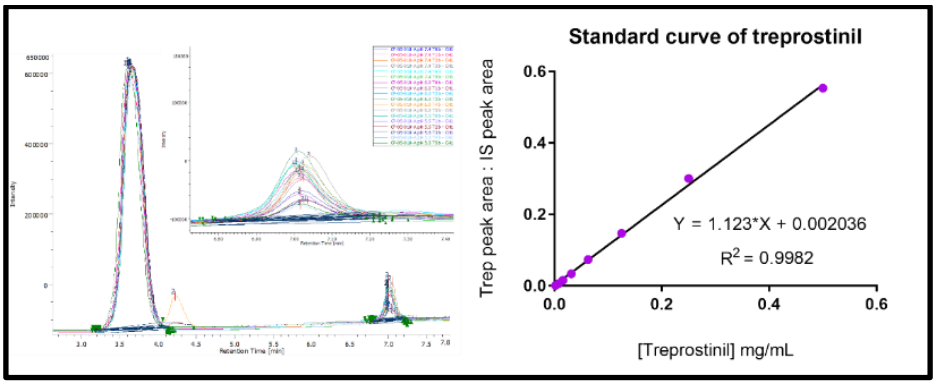

Figure 4-20. Results of the standard treprostinil **4** concentrations when analysed in the presence of internal standard, phenoxyacetic acid **22**. A) Comparison between the area of treprostinil absorbance and that of phenoxyacetic acid 24 removes any variation as a result of instrumental error. B) A plot of the ratio versus concentration of treprostinil **4** produces a reliable standard curve.

The effect of oligoacetal **71** dilution on hydrolysis rate was then investigated. In addition, it was necessary to investigate whether the small concentrations of treprostinil detected were a result of slow oligoacetal degradation or an inefficient extraction process. Therefore, alongside the extraction process, the change in weight of the polymers was monitored by GPC. A solution of the oligomer product was made up at 2.5 mg/mL in buffers at pH 7.4, 6.0 and 5.5 and aliquots were portioned in duplicate. To preserve the sample, a smaller aliquot size of 400 µL was used instead of 1 mL. At timepoints 0-24 hours, two aliquots were removed from incubation; one was flash frozen in an acetone/dry ice bath and stored at -20 °C before lyophilisation and GPC analysis; and the other sample was worked up as usual by triple ethyl acetate extraction (200 µL), reconstituted in phenoxyacetic acid **22**/acetonitrile solution and analysed by HPLC. Peak areas were multiplied by 2 to standardise the data obtained from a 2.5 mg/mL solution of oligo(PEG-treprostinil acetal) **71** to previous and future data obtained at 5 mg/mL and shown in **Figure 4-21**.

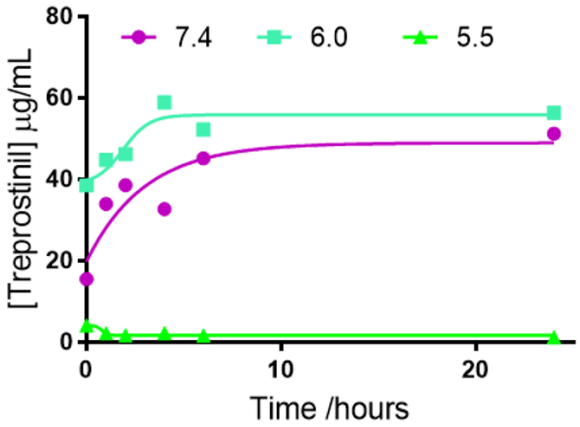

Figure 4-21. Treprostinil released from oligo(PEG-treprostinil acetal) **71** over 24 hours when incubated at 37 °C in buffers at pH 7.4, 6.0 and 5.5. Treprostinil was slowly released at pH 7.4 and 6.0 but no treprostinil was detected at any time point from the pH 5.5 buffer.

Peak area was plotted as a ratio between that of treprostinil **4** and phenoxyacetic acid **22** and converted to concentration using the standard curve in **Figure 4-20**. Surprisingly, the lowest concentrations of treprostinil **4** were detected for the most acidic buffer, which seemed to slightly decrease over 24 hours (**Figure 4-21**). The pH of the buffer used was reconfirmed to be pH 5.5, suggesting that perhaps the samples vials had been mixed up. However, upon consulting the raw data, the same values were obtained. Furthermore, the lack of an identified trend (**Figure 4-22**), implied an error occurred during the assay preparation. The gradient over 24 hours was similar to the previous data over 6 hours and so it was concluded that the concentration of the oligomer solution was not reducing the rate of degradation.

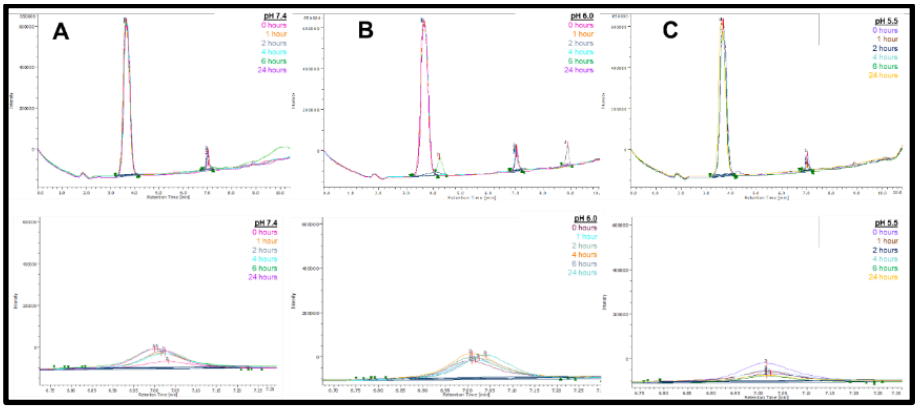

Figure 4-22. Chromatograms showing treprostinil **4** release from oligo(PEG-treprostinil acetal) **71** solution in aqueous media (2.5 mg/mL) over time in different pH environments. Top row shows full scan and bottom row is the treprostinil absorbance. The assay was conducted in three different pH buffers, shown in each column; A) pH 7.4; B) pH 6.0; C) pH 5.5

GPC analysis was carried out by a colleague for a preliminary investigation and only time points at T_0 and $T_{6\ hours}$ were analysed. No detectable change was observed over 6 hours for either the neutral and acidic environments. Data for pH 7.4 and pH 5.5 shown in (**Figure 4-23**). This provided reassurance that the low concentrations of treprostinil detected by HPLC were accurate. In a published study, degradation of poly(PEG acetal) as calculated by molecular weight loss, achieved 60% over 100 hours at pH 5.5.[405] The disparity in degradation properties between poly(PEG acetal) and oligo(PEG-treprostinil acetal) provided further evidence that treprostinil must be present within the oligomer in order to alter behaviour.

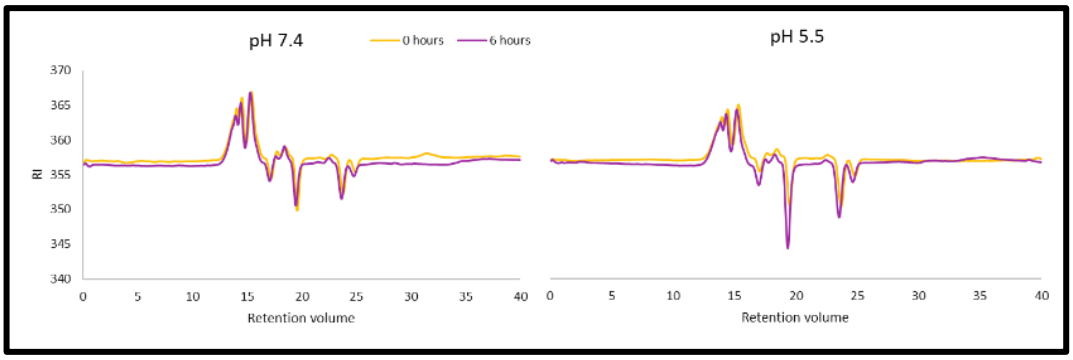

Figure 4-23. GPC traces showing degradation of oligo(PEG-treprostinil acetal) **71** after 6 hours at pH 7.4 and 5.5. RI = refractive index

Evidence of minimal degradation was determined by the concentration of treprostinil extracted as well as the GPC weight of the oligoacetal **71** structure after 6 hours. Thus, an investigation was carried out to investigate if the minimal degradation exhibited at pH 5.5 was reproducible. Fresh citrate buffer was made, and the assay repeated at 5.mg/mL in pH 5.5 only (**Figure 4-24**).

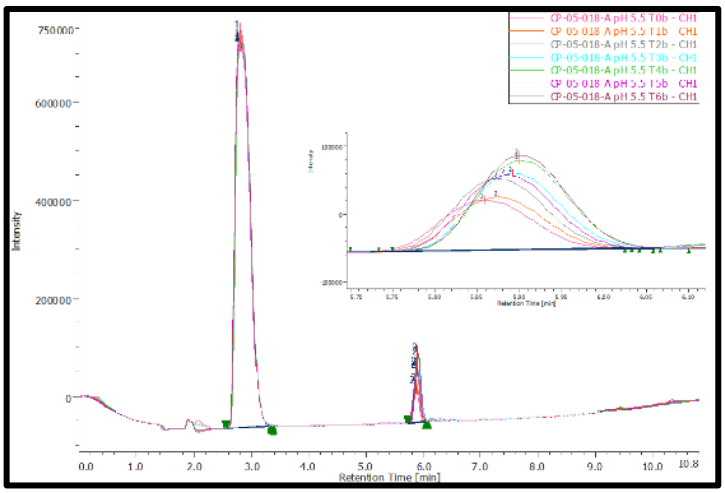

Figure 4-24. Repeat degradation of oligo(PEG-treprostinil acetal) **71** conducted at pH 5.5, extracting treprostinil from the aliquots at each time point using ethyl acetate. The absorbance of treprostinil detected was more sensitive and followed a consistent trend in concentration over time that the previous attempt did not.

The concentrations of treprostinil released from oligo(PEG-treprostinil acetal) **71** in buffer at pH 5.5 over 24 hours were calculated using the standard curve in **Figure 4-20**. The repeated assay data (**Figure 4-24**) was compiled with the previous data obtained for pH 7.4 and 6.0 (**Figure 4-21**) to determine if a trend could be identified. Degradation occurred at a greater rate at pH 5.5 than of pH 6.0 and 7.4.

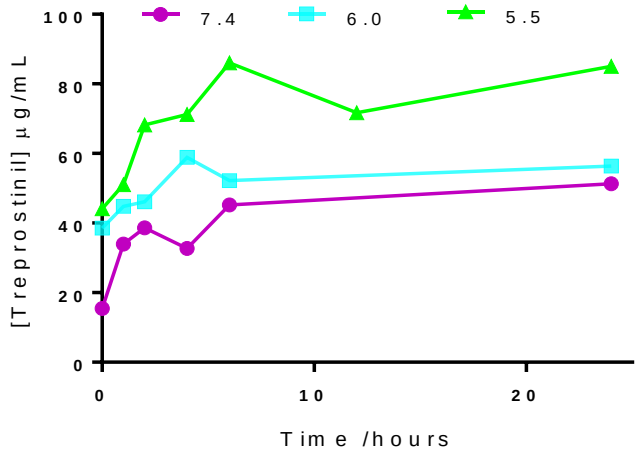

Figure 4-25.Plot of concentration of treprostinil **4** over 24 hours when incubated at different pHs. Following a poorly sensitive result for pH 5.5 previously, the degradation assay was repeated at pH 5.5 and combined with the original data for pH 7.4 and 6.0. Concentration of treprostinil **4** showed pH-dependent nature, with more treprostinil **4** detected at lower pHs.

Liquid-liquid extractions can be inefficient if there are solutes that can partition into both liquids, although was considered necessary based on earlier data (**Figure 4-13**) which suggested that direct analysis of the aqueous oligo (PEG-treprostinil acetal) **71** solution to determine the extent of treprostinil release was insensitive. While considering the limitations of extraction, each extraction and dissolution step was carefully controlled. Liquid-liquid extractions are made less accurate when carried out on a small scale, such as extraction from a 200 µL sample. Drying of the ethyl acetate layer was achieved by passing a stream of air over the liquid and was harder to control. Fluctuations in the air flow rate meant a consistent stream of air was not always achieved. It is not inconceivable that the solution splashed, altering the amount of treprostinil left as a residual solid. To reduce any effect the drying process had on treprostinil concentrations, a different method of drying was sought. Removal of ethyl acetate solvent was attempted using a vacuum centrifuge.

With the overlapping concentrations of the previous results for pH 7.4 and 6.0, the degradation study was repeated using only pH 7.4 and 5.5 using returning to the higher oligomer concentration of 5 mg/mL. The original higher concentration was anticipated to have fewer errors in detection. Each aliquot contained a volume of 500 µL.

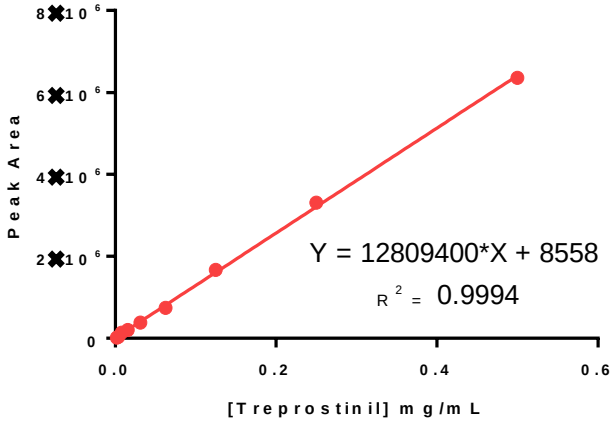

Figure 4-26. Standard concentration curve of treprostinil using the peak area of treprostinil absorbance directly. The wrong internal standard was used which maxed out the detector so a ratio between treprostinil and internal standard could not be used.

The dried, extracted samples and treprostinil standards were erroneously reconstituted in a solution of *para*-nitrophenol in a 5:2:1 solution of water, acetonitrile and methanol (0.42 mg/mL) instead of the phenoxyacetic acid solution (1 mg/mL in acetonitrile). The absorbance for *p*-nitrophenol reached above the maximum absorbance so a ratio between treprostinil could not be accurately determined. Therefore, the AUC of the treprostinil absorbance was directly plotted (**Figure 4-26**).

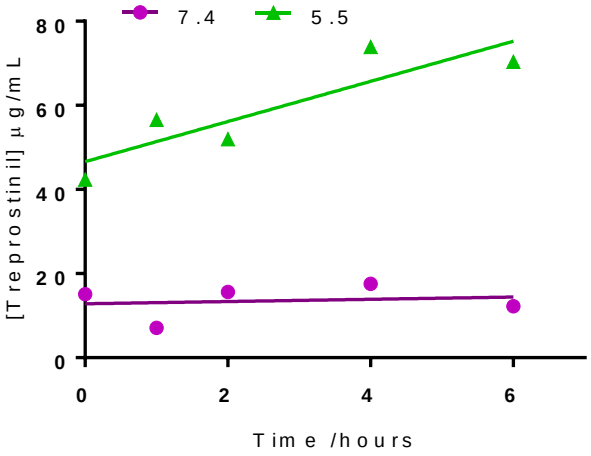

Figure 4-27. A plot of treprostinil concentration extracted from solutions of oligo(PEG-treprostinil acetal) in buffers at pH 7.4 and 5.5 over 6 hours. A greater concentration of treprostinil was detected when incubated at pH 5.5 than at pH 7.4. Using vacuum centrifugation to dry the samples produced less varied concentrations of treprostinil.

Using a larger volume and vacuum method of drying produced less varied results which follow a clear and defined trend over 6 hours. A baseline level of treprostinil is detected at all time points in buffer at pH 7.4, which does not increase over a 6-hour period. Consistent with published reports, at pH 5.5 the amount of treprostinil increases over time. The discrepancy between the initial relative concentration of treprostinil in solution may suggest some

degradation occurs immediately although is most likely a result of the different solubility of treprostinil at different pHs and is discussed later.

In order to describe the in context of the maximum amount of treprostinil released from the oligomer product, a solution (500 mL, 5mg/mL) was exposed to a TFA environment, shown in an earlier ^{1}H NMR investigation to degrade the acetal bonds. The oligomer solution was heated to 50 °C for 2 hours. After 1 hour at RT a precipitate was visible. Extraction with ethyl acetate appeared to remove the precipitate and the sample was prepared for HPLC in acetonitrile (200 µL) with phenoxyacid acid internal standard.

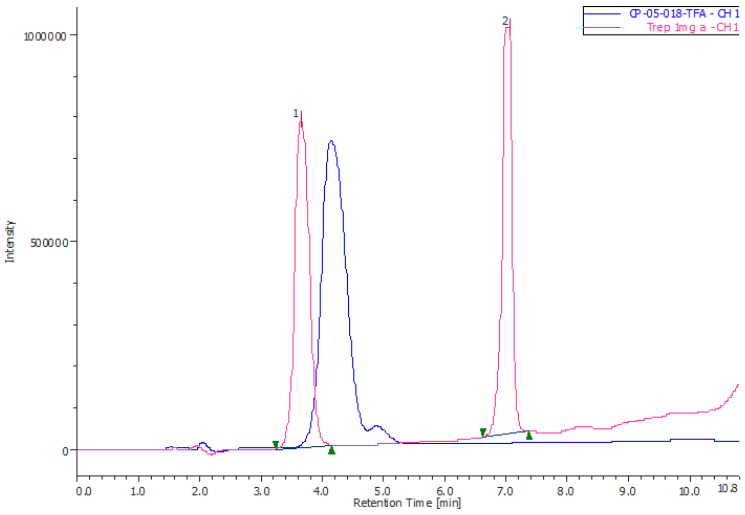

Figure 4-28. HPLC chromatogram of TFA-degraded oligo(PEG-treprostinil acetal) **71** (blue) compared to standard sample of treprostinil **4** (red). Both samples were prepared with phenoxyacetic acid internal standard.

Surprisingly, no absorbance corresponding to the retention time of treprostinil was observed. Although the height of the phenoxyacetic acid HPLC absorbance was comparable to that in the treprostinil standard, the width, and hence the integrated area was larger. Interestingly, when consulting the ^{1}H NMR spectra of oligo(PEG-treprostinil acetal) before and 60 minutes after incubation with TFA, as well as the acetal resonances being removed, so is the methylene resonance, highlighted in **Figure 4-29**, providing further evidence that treprostinil is unstable in strong acid.

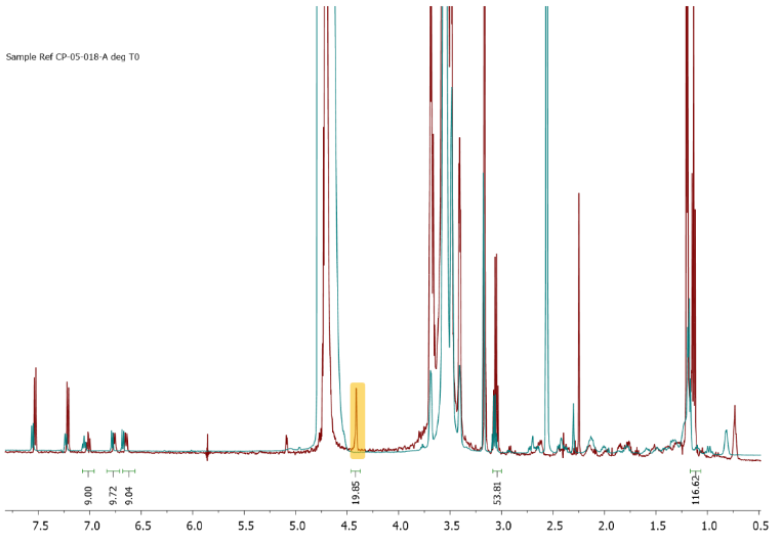

Figure 4-29. Overlapping ^{1}H NMR spectra of poly(PEG-trep) before (In red), and after incubation with TFA in D_2O (in blue).

It was queried whether the acidified treprostinil was eluting at the same retention time as phenoxyacetic acid **22**, so the reaction was repeated without the addition of internal standard. Upon addition of acetonitrile (200 µL) a cloudy solution formed which was solubilised by addition of methanol (200 µL). Interestingly, no absorbance was observed, indicating that the treprostinil had either not been extracted or solubilised sufficiently.

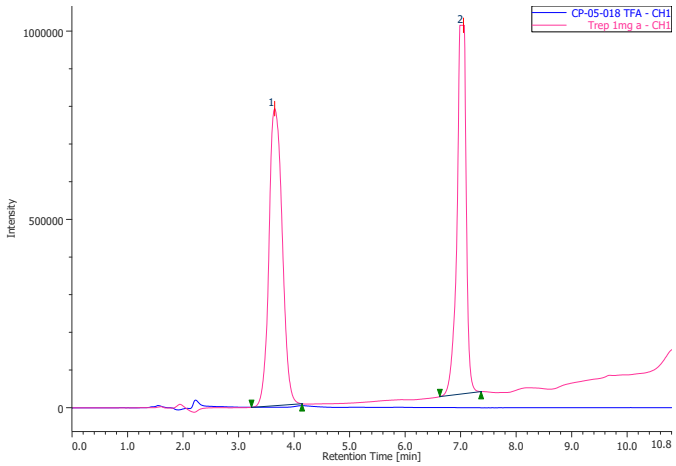

Figure 4-30 Overlapping chromatograms of treprostinil standard with phenoxyacetic acid (pink) and the elutogram of the sample extracted from oligo(PEG-treprostinil acetal) incubated with trifluoroacetic acid (blue).

The presence of strong acid may have been enough to cleave the aromatic ether, however the 2-hydroxyacetic acid cleaved would still likely possess a methylene resonance in the same region of the ^{1}H NMR spectrum. Furthermore, formation of the triol compound (**51**) does not fit the observation of poor solubility in either ethyl acetate (during extraction) or acetonitrile (during resolubilising).

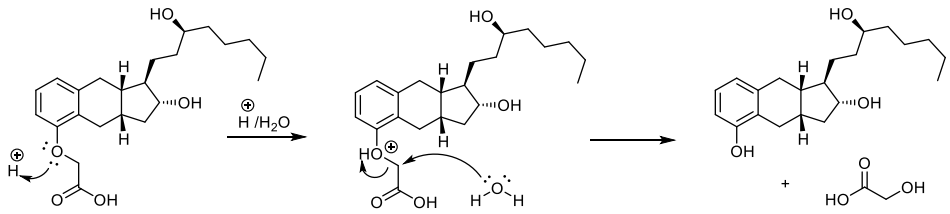

Scheme 4-16. Proposed mechanism of acid catalysed ether cleavage, degradting treprostinil **4** to form the triol intermediate **51**.

An alternative method was used to quantify the maximum amount of treprostinil 4 in released from a sample of oligomeric product. Oligo(PEG-Treprostinil acetal) **71** (5 mg/mL), was incubated in a similar fashion in HCl (0.155 M), a pH 1 buffer used to mimic the degradative environment of the stomach. The change in treprostinil **4** concentration was analysed over 3 hours. Sample aliquots (200 µL) were extracted, dried by a passing stream of air and reconstituted in phenoxyacetic acid spiked acetonitrile (200 µL). Samples were analysed by HPLC to quantify the amount of treprostinil present. Peak areas were converted to concentration using the phenoxyacid acid standard curve (**Figure 4-20**).

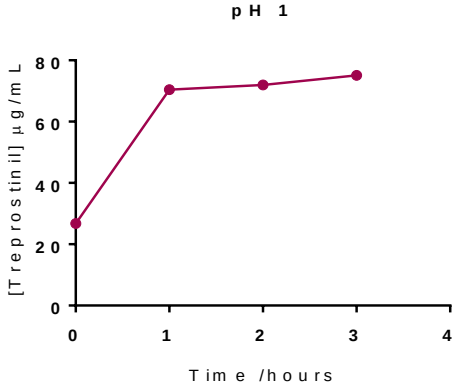

Figure 4-31. Plot of concentration of treprostinil **4** detected over 3 hours when incubated at pH 1 and extracted into ethyl acetate.

The concentration of treprostinil **4** was observed to plateau after 1 hour which suggests that a maximum concentration, which can be extracted and detected, is reached. Therefore, this can be interpreted as the maximum amount of treprostinil **4** in a given sample. Conversion of the average peak area for hours 1-3 indicate that every 1 mL of oligomeric solution at concentration 5 mg/mL, 73 µg (1.4%) is treprostinil. Using 73 µg/mL as the maximum, previous data could be reanalysed in the context of the maximum amount of treprostinil possible.

Most of the data from the two studies which were conducted using the extraction method (**Figure 4-25** and **Figure 4-27**) were combined to analyse duplicate data to try to better understand assay reproducibility. The data obtained from the first extracted assay conducted at pH 7.4 and 6.6 was not used because of the variability in the concentrations over time. Several differences in the assay design set limitations in the overall trends observed. First, between the studies two different methods to dry the samples were used (air drying and

vacuum filtration), although the concentrations should not be altered, only variability. Second, only data obtained from buffer 7.4 and 5.5 and data obtained up to 6 hours, are duplicated. Lastly, the volumes of the aliquots worked up differ. The first study used an aliquot volume of 500 µL and the second 400 µL. The volume of ethyl acetate used to extract (200 µL) was kept constant. Although the volume of sample extracted from was taken into consideration when calculating concentration of treprostinil **4**, the effect the differences has on the partition of treprostinil into the organic layer cannot be discounted. As previously discussed, the first study used a dilute concentration of 2.5 mg/mL where all other studies were conducted at 5 mg/mL. The peak area was multiplied by a factor of two to standardise the result for comparison with other data.

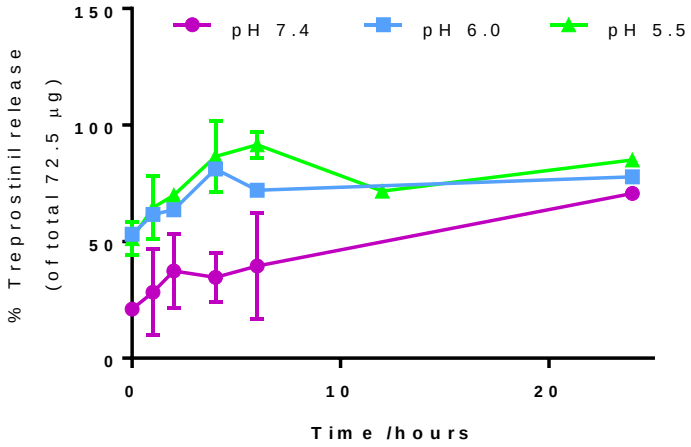

Figure 4-32. Combined data showing the pH-dependant release of treprostinil **4** from oligo(PEG-treprostinil acetal) **71**, as a percentage of the total treprostinil **4** released at pH 1.

Treprostinil **4** release from oligo(PEG-treprostinil acetal) appears to occur in a pH-dependent fashion. Almost 100% of treprostinil was released after 6 hours when incubated in pH 5.5 buffer, whereas the concentration increase of treprostinil at pH 7.4 was much lower for the first 6 hours. The one aliquot analysed after 25 hours was comparable to treprostinil release from lower pH buffers. With only one repeat for each of the incubations after 25 hours, a limitation is met in drawing any conclusions. The study would benefit from repeated measurements.

A base-level of treprostinil is detectable even at the initial time point at pH 7.4. The concentration of treprostinil released over a 24 hour period increases negligibly which implies that oligo(PEG-treprostinil acetal) is stable. Therefore, the detection of treprostinil **4** at the first time point suggests that some treprostinil was either never incorporated into the acetal of had prematurely degraded upon storage.

One of the noticeable features of the degradation assays is the varying concentrations detected for at the initial time point. One limitation of the assay is the time lag between addition of the polymer to the buffer and aliquoting into an extraction solvent. Approximately 20 seconds are given to facilitate dissolution and efficient mixing by vortexing, and the preparation

is conducted as rapidly as possible. The premature degradation of acetal bonds to release treprostinil during the sample preparation is expected to be more pronounced in highly acidic buffers and less so at pHs which exhibit little acetal degradation. The results obtained (**Figure 4-32**) show a much greater difference in concentration than might be expected based on reported results.[402]

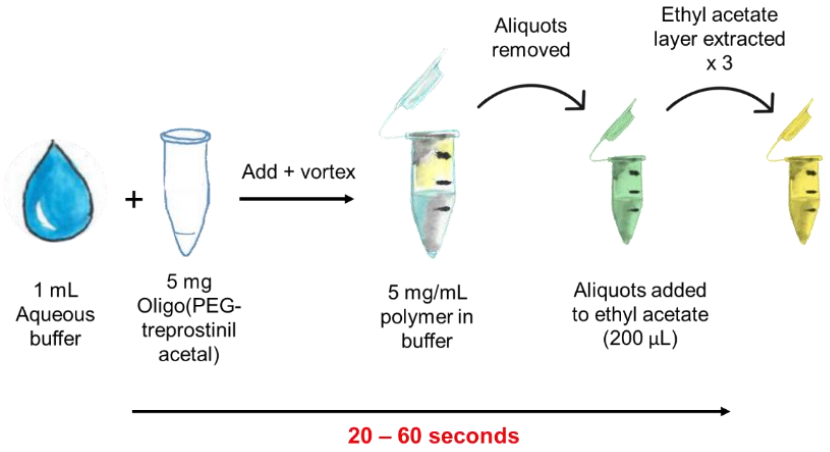

Figure 4-33. Process of preparing assay sample for initial time point. Following dissolution of oligo(PEG-treprostinil acetal) **71** in aqueous buffer (5 mg/mL) by vortexing, the first aliquot is removed and added to a prepared vial containing ethyl acetate (200 µL). The extraction solutions are vortexed and allowed to separate and the extraction repeat three time total. The combined organic layers are then prepared for HPLC. Between the addition of polymer to aqueous buffer and the final extraction, approximately one minute passes which when acidic buffers are used may be enough time to degrade the acetal and release treprostinil.

The difference in treprostinil **4** concentration at the initial time points when incubated in different buffers may be a result of the treprostinil acid group. At low pH values the treprostinil acid is protonated and in an environment with higher pH will exist in the deprotonated form. At different pHs, treprostinil will have different interactions with its solvent meaning the concentrations in each layer of an extraction conducted at different pH values will possess different concentrations of treprostinil. At high pH, the acid exists in the deprotonated, anionic form which facilitates stronger interactions with the polar aqueous phase and interact weakly with the ethyl acetate layer. At lower pH values, treprostinil exists as the cationic protonated form which with its reduced polarity interacts weakly with the aqueous phase and is more soluble in the ethyl acetate layer. Poor extraction of treprostinil is expected to occur at pH above 4.5, when the partition coefficient of treprostinil favours the aqueous layer over the organic layer.

The extraction step was deemed important to ensure all treprostinil released was quantified. The first degradation assay suggested poor solubility of treprostinil in aqueous solution as direct analysis by HPLC showed minimal amount of treprostinil **4**. However, when extracted 24 hours later, a much greater concentration was obtained. An extraction method using ethyl acetate was successfully employed by Tomlinson and colleagues to quantify the hydrophobic hormone drug, diethylstilboestrol from poly(PEG-DES acetal) 59. Extraction allows for

treprostinil to be solubilised but carries its own limitation in the variation in extraction at different pHs. Additionally, following extraction the drying and reconstituting of the organic layer introduces variability in the results, as determined by the differing results for duplicate samples.

It was expected that the limitation of the varying partition coefficients as well as the large variation in results could be overcome by removing the extraction step. A degradation study was designed which used samples prepared as before, except at each time point, the sample is neutralised by addition of ammonium phosphate buffer to further prevent degradation. After which free treprostinil would be solubilised by addition of an equal volume of acetonitrile to the neutralised degradation solution. Samples would be collected and frozen before analysis, without removing the polymer. To prevent degradation during analysis on the column, mobile phases would be used without TFA buffer.

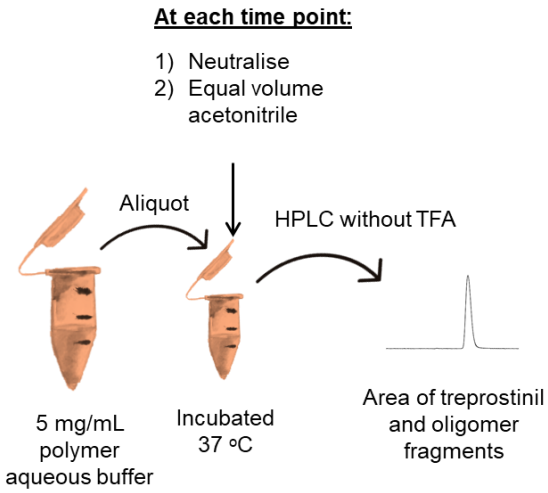

Figure 4-34. Proposed method of analysing degradation of oligo(PEG-treprostinil acetal 71 without the need to extract samples at each time point. A solution of oligo(PEG-treprostinil acetal) 71 in aqueous buffers at varying pH at 5 mg/mL would be prepared. Aliquots would be prepared and incubated at 37 °C. At each time point a sample will be neutralised by the addition of ammonium phosphate buffer and diluted by a factor of 2 by the addition of acetonitrile. Samples can then be frozen until HPLC analysis. To prevent degradation during analysis, HPLC mobile phase will we used in the absence of trifluoroacetic acid.

As mentioned previously, the presence of treprostinil 4 in initial samples may suggest degradation had occurred in the 4 months since original synthesis, despite the neutralisation of the acid and storage at -20 °C. Indeed, the initial amount of treprostinil detected at pH 7.4 increased over time. Therefore, an investigation was conducted to establish the extent of any premature degradation. To avoid the issues surrounding the extraction which had been identified, oligo(PEG-treprostinil acetal) 71 was dissolved in MeCN at 5 mg/mL and analysed directly by HPLC in the absence of TFA using the original method employed for the direct analysis of the aqueous degradation (**Figure 4-13**). One broad absorbance was observed with a retention time of 14.3 minutes, marginally earlier and much broader than that of a treprostinil standard used for comparison, with absorbance after 14.4 minutes.

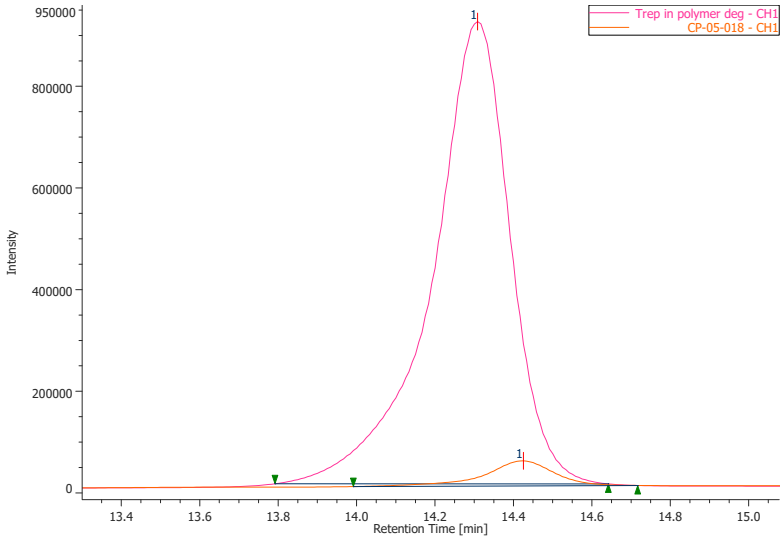

Figure 4-35. HPLC chromatograms comparing absorbance of oligo(PEG-treprostinil acetal) 73 after 4 months of storage at -20 °C (shown in pink) and the absorbance of a treprostinil standard (orange). A larger, broader resonance is observed.

Assuming the absorbance corresponds to only treprostinil, the concentration detected is greater than that obtained from the pH 1 degradation data by 174% (**Figure 4-36**). The concentration of treprostinil detected, accounts for 2.5% of the weight of the whole sample, which matches the amount of treprostinil calculated to be present in the ^{1}H NMR spectrum. Which indicates that the oligo(PEG-treprostinil acetal) has fully degraded, at least at the termini where treprostinil was estimated to be conjugated.

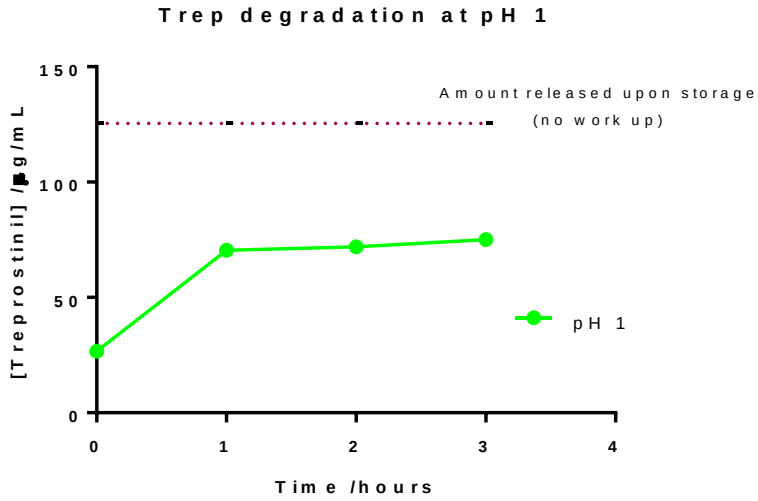

Figure 4-36. Treprostinil **4** release measured by HPLC over 3 hours when incubated in buffer at pH 1 (shown in green), in the context of the amount of treprostinil **4** detected in the stored sample of oligo(PEG-treprostinil acetal) 71 when dissolved in acetonitrile and analysed by HPLC directly. Degradation was measured only once and the corresponding treprostinil **4** concentration indicated by the purple dashed line. Oligo(PEG-treprostinil acetal) 71 had degraded upon storage to release the same amount of treprostinil detected by ^{1}H NMR after synthesis. Despite maximum degradation occurring at pH 1, indicated by the plateau, the concentration extracted is less than total treprostinil 4 released upon storage when analysed directly.

Degradation upon storage had been confirmed and the greater amount of treprostinil measured than the total amount extracted from buffer at pH 1 provided further evidence that the extraction method was limited for the quantification of treprostinil. Both a new method of accurately quantifying degradation and a new batch of oligo(PEG-treprostinil acetal) were required.

Repeat synthesis was anticipated to give an opportunity to implement lessons learnt from the first synthesis, including; using a larger volume of reaction solvent, neutralisation of the reaction before precipitation, removal of the acid salt before storage. Optimising the synthesis was anticipated to achieve a better degree of polymerisation with a higher average molecular weight polymer, narrower PDI and exhibit greater stability upon storage. In more recent descriptions of polyacetal formation in the literature,[420] precipitations were carried out in diethyl ether twice, re-dissolving in THF, and then lyophilised from water to remove traces of acid.

Consideration was given to the mechanism by which the step growth polymerisation occurs, specifically the effect of the stoichiometry between the divinyl ether and diol monomers. When stochiometric amounts of vinyl ether and alcohol groups are not employed dead chain ends can arise. With more of one reactive monomer than the other, conjugation of the oligomers is inhibited, preventing larger chains from forming. The use of polydisperse PEG chains means the stoichiometry is estimated based upon the reported average molecular weight. Achieving stochiometric amounts of vinyl ether is therefore impossible but can overcome by addition of an underestimation of vinyl ether. After sufficient time for small oligomers to form, small amounts of vinyl ether are titrated in. The conjugation of oligomers to form polymers is deemed complete by an increased viscosity. The intended neutralisation before exposure work-up was anticipated to preserve a higher degree of oligomerisation.

The synthesis was repeated using the same batches of materials. Variations included using rotary evaporation for drying the PEG and acid, addition of more solvent, as well as using the recommended equivalents of pTSA (0.03 eq). The scales were also varied and the ratios of monomers were kept constant. An increase in viscosity was not observed. ^{1}H NMR confirmed minimal acetal formation.

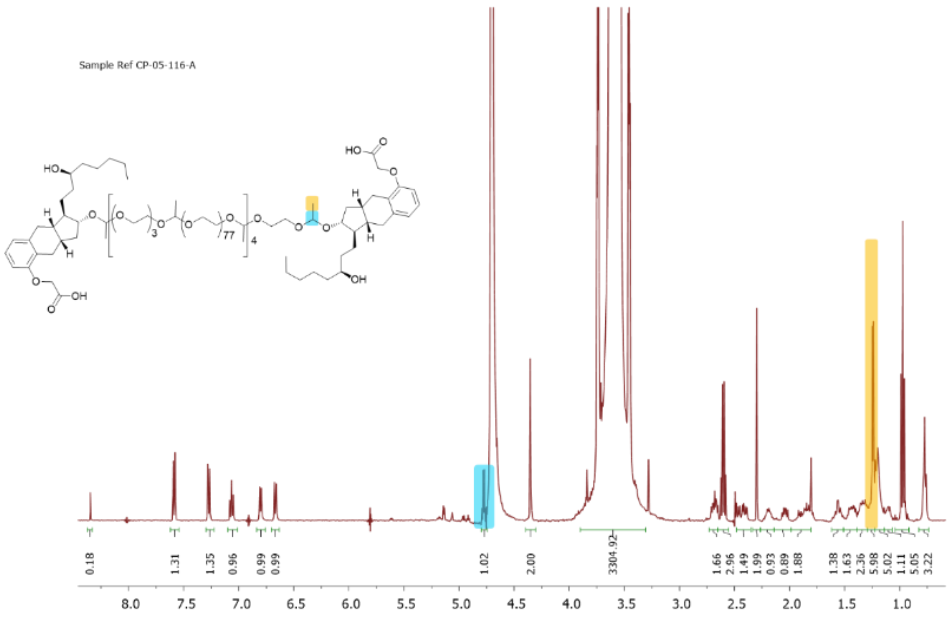

Figure 4-37. ^{1}H NMR spectrum of a repeat attempt to synthesise oligo(PEG-treprostinil acetal) **71**, using the same procedure proven successful before. The ratio of acetal methine resonances (blue) compared to the PEG resonances indicate that minimal acetal formation has occurred.

A repeat of the first reaction was attempted on the same scale as before. To avoid the issue of the reaction becoming too viscous, anhydrous THF was only slightly increased above the original reaction (4 mL vs. 3mL). The purity of the vinyl ether was confirmed by NMR and 90% of the calculated amount added. Based on the reaction time of the first reaction, the reaction was left for 3 hours to form the oligomers. Addition of a further 5% did not alter the viscosity. Two more portions of 5% were titrated in without affecting the reaction progression. It was feared that an excess of vinyl ether would result in chain ends. Addition of a diol would offer the opportunity to conjugate the chains together. Although any diol compounds can be used, to keep the characterisation easy, A solution of PEG 3400 and pTSA.H_2O in toluene was dried by azeotropic removal of water using rotary evaporation. Under argon, anhydrous THF was added and 10% of PEG 3400 was added to the reaction mixture. Although a subtle increase in viscosity was observed initially, no further change was seen after 24 hours stirring. The only remaining difference with the first reaction is the equivalents of catalytic acid. Despite being catalytic, the reaction may progress slowly in its absence. Addition of pTSA monohydrate would introduce competing water into the reaction so as an alternative the pyridinium salt was added. Pyridinium toluene sulfonate salt is a weak acid, employed for catalysing polyacetal formation.[415,421] Without the bound water molecule, it does not require drying so carries less risk of driving polyacetal degradation. In total, 5 repeats were carried out with each repeat consuming treprostinil and time, yet no indication that polymerisation had occurred was given.

Several attempts were carried out to accurately study the degradation of oligo(PEG-treprostinil acetal) 71 and quantify the treprostinil released. Through the iterations, a method was created to quantify treprostinil by extraction of the aqueous solution and subsequent HPLC analysis.

Using this method, it was shown that the stability of oligo(PEG-treprostinil acetal) 71 at pH 7.4 is consistent over a period of 24 hours, with 19% amount of treprostinil released. Comparatively, at pH 6.0 higher concentrations of treprostinil are detected, although the concentration measured after 24 hours is similar to the value at pH 7.4 for the same time point. When oligo(PEG-treprostinil acetal) 71 was incubated at pH 5.5, the rate increases sharply to over 80% release over 5 hours.

Incorporation of poorly soluble diol drugs into polyacetal mainchains has been reported previously,[401–403,405,416] however, none possessing an additional acid group. In comparison to literature reports, the treprostinil release from the oligo(PEG-treprostinil acetal) occurs at a faster rate than larger polyacetals which incorporate hydrophobic drugs in the main chain. The reported degradation of poly(PEG-DOX acetal) **59** achieved 65% of DOX release in 96 hours,[402] comparable to the 60% Mw reduction of poly(PEG acetal) over 100 hours in the same acidic conditions.[405] Release of DES from poly(PEG-DES acetal) **59** was measured at 85% after 100 hours in pH 5.5 buffer, and deemed completely degradation after 145 hours. In contrast, oligomeric treprostinil was fully degraded after 6 hours at pH 5.5. The consistency of the degradation rates for mainchain polyacetals of similar loading and Mw, suggests that the type of alcohol contributing to the acetal bond plays a minimal role in the degradation. The slightly faster degradation rate of poly(PEG-DES acetal) **59** may be explained by the phenolic acetal formed. Phenolic hydroxyls resonate into the aromatic ring which weakens the oxygen bond into the acetal and make better leaving groups which ultimately increase the rate of hydrolysis. Extrapolating of the trend for hydroxyl stability affecting acetal degradation, it would be expected that an acetal bond comprised of a secondary alcohol might have increased stability. However, conjugation to treprostinil revealed a faster rate of degradation. The size difference between an oligomer of M_w 17 kDa in comparison to a 43 kDa polymer, previously described,[402,414] will have a smaller volume and therefore a larger proportion of the structure will interact with the solvent. Additionally, as opposed to the mainchain incorporation of DES in poly(PEG-DES acetal) **59** the ^{1}H NMR suggests treprostinil is most likely conjugated at PEG-acetal termini.

Although pH 5.5 was investigated, pH 6.0 is more relevant in the context of the chronically inflamed tissue of PAH patients. Thus, the degradation at pH 6.0 was investigated. After 6 hours, 40% of treprostinil had been released, which did not show much further release after 24 hours. The reported degradation of poly(PEG acetal) at the similar pH of 6.5 showed 20% degradation after 100 hours. When DES was incorporated within the back bone, 30% of DES had been released after 100 hours at pH 6.5.

4.2.3 **Polysilylethers**

The difficulty in producing a polyacetal polymer of oligomer, demonstrates the poor reactivity of the treprostinil hydroxyls in an acid environment. The reactivity of nucleophiles is often increased by the presence of a base which can deprotonate either the nucleophile or the intermediate formed. To overcome the poor reactivity of treprostinil hydroxyls, a base

catalysed polymerisation of treprostinil to form an acis-cleavable linker may be better suited. Based on work published by DeSimone and colleagues (**Chapter 1**, **Figure 1-18**),[250] we designed a PEG-treprostinil polymer which was hypothesised to degrade in an acid environment. Instead of using the linker to conjugate two structures in a pendant fashion, we looked at utilising the linker in a similar method to the polyacetal, to link the drug into the polymer mainchain via the alcohols.

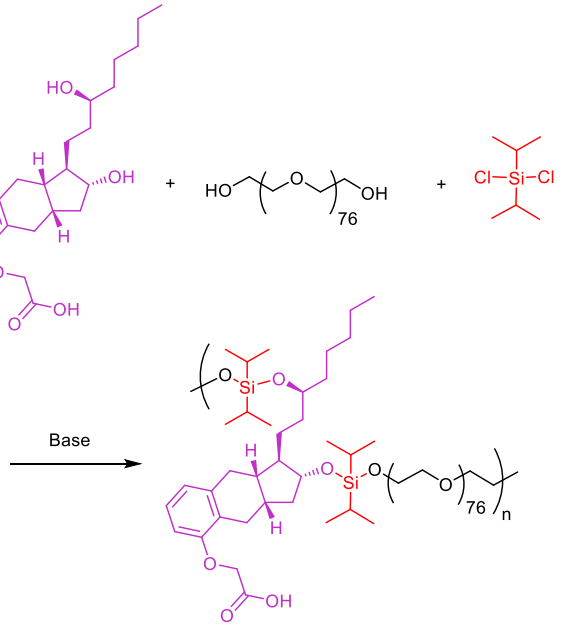

Scheme 17. Proposed reaction for the incorporation of treprostinil monomer into a polymer backbone using silyl ethers as the biodegradable element. The reaction is conducted under basic conditions which was expected to facilitate nucleophilic substitution of the chloride ions by the treprostinil hydroxyls.

Polymerisation is carried out by a substitution reaction, where the chloride is displaced by nucleophiles including the hydroxyl groups of PEG and treprostinil. Although the nucleophilicity of treprostinil alcohols is weak, their reactivity at chlorinated silyl groups has been published and proven in our hands (**Chapter 3**).

Reactions were kept anhydrous to minimise hydrolysis of the dichloroisopropyl silane which is susceptible to nucleophilic attack by water. Trace water bound to PEG was removed by azeotropic removal of toluene using dean-stark apparatus and anhydrous solvents were used. Following the same procedure as for the polyacetal, the alcohol species was stirred in the presence of the catalyst, in this case, pyridine, and the polymerising agent was added slowly with vigorous stirring. Much like polyacetals, silyl ethers are susceptible to acid degradation. The requirement of base catalyst for silyl ether formation removes the problem of self-degradation *in situ* provided enough base is added to deprotonate the acid group.

Silyl ether polymerisation was attempted using treprostinil as a co-monomer with PEG in a 1:1 ratio. To confirm the silyl ether is polymer can be formed, a drug free polymerisation was attempted using only PEG_{3400} as the control. In the case of polysilyl-PEG, no visual change

occurred upon addition of dichloroisopropylsilane. However, the polysilyl-treprostinil-PEG reaction became cloudy immediately upon addition of diisopropylsilyl chloride. The reaction was stirred for 18 hours to allow enough time for the reaction to proceed. The polymerisation reaction solution was precipitated by addition into cold hexane.

The ^{1}H NMR of both compounds was inconclusive. In addition to the treprostinil hydroxyl methine resonances residing under the PEG peak, so did the silyl methine. Therefore, no diagnostic resonances for the reaction could be observed. GPC using PMMA calibrants estimated the PEG silyl compound to be 10 kDa, consistent with a trimerization. Based on the lack of polymerisation, the GPC of the treprostinil silyl ether was not conducted.

The polysilyl ether treprostinil was attempted as a pilot reaction in the final days within the lab to test the hypothesis that a basic polymerisation would facilate polymerisation of treprostinil. Polymerisation of PEG_{3400} and treprostinil through silyl ether bonds was unsuccessful as determined by the low molecular weight estimated by GPC. The ^{1}H NMR does not provide clear diagnostic resonances upon formation of the silyl ether which limits the information obtained. The reactivity of the hydroxyls may require a stronger base in stoichiometric amounts or longer reaction times. In future attempts, these factors could be considered.

4.3 Strengths and limitations

Treprostinil was incorporated into an oligomeric acetal conjugate of 17 kDa, containing two terminal treprostinil moieties This is the first drug monomer used in polyacetal conjugation featuring an acid moiety. Anhydrous conditions were employed and verified by the isolation of intact vinyl ethers. Upon polymerisation with treprostinil, the polyacetal signals appeared less sharp than the control polyacetal. Upon contribution of the hydroxyl oxygen to the acetal bond, a down field shift in the neighbouring methine proton peak would have been expected. Unfortunately, the methine proteins bound to the trep hydroxyl could not be seen in the NMR due to the overlapping chemical shift with the PEG signal. Incorporation of treprostinil into the acetal oligomer was inferred by the small amount of treprostinil detected at neutral pH and a pH-dependant increase in treprostinil detection over time. Methods to accurately quantify treprostinil were considered. Extraction into ethyl acetate proved more successful than direct analysis of the aqueous system. Clinically, the use of acetal biodegradable elements are limited by the release of acetaldehyde product, although this may provide an additional therapeutic benefit as acetaldehyde induces prostacyclin synthesis.

None-the-less, this work was not without limitations. It should be highlighted that suitable quantities of treprostinil were not immediately available and as a result the work described in this chapter was conducted in the last months of the project. Upon confirmation that enough treprostinil was available, the tert-polymerisation was conducted. The limitations of treprostinil-conjugated oligoacetals are proven evident. Successful polyacetal synthesis between A-A and B-B monomers is inherently intricate owing to the strict stoichiometry required to achieve full polymerisation. Using polydisperse PEG monomer further complicated the synthesis as stoichiometric quantities cannot be achieved.

Although an oligoacetal was isolated, treprostinil was not incorporated into the mainchain as expected, which produced a similarly low Mw oligomer when repeated with the ethyl ester derivative, suggesting acetal formation was hindered by the poor reactivity of the hydroxyls. The viscosity of the reaction solution indicated a higher degree of polymerisation than that obtained, potentially suggesting acetal degradation upon isolation. An error was made which meant the neutralisation of the product was not conducted until after precipitation into hexane had been initiated, providing a time window for degradation to occur.

Although the oligomer was formed initially, the problems surrounding reproducibility were also demonstrated. Furthermore, despite efforts to deprotonate residual acid, degradation occurred upon storage at -20 °C. Due to the system available, GPC characterisation of polymers was carried out using PMMA standards, which decreases the accuracy of measured characteristics of PEG-based polymers, although provided an estimate for the oligomeric structure to be determined. Although ^{13}C NMR analysis often show broad peaks for polymers, it may have been possible for changes in the methine carbons neighbouring the acetal to confirm treprostinil inclusion upon polymerisation. Direct HPLC analysis of an aqueous solution of oligo(PEG-treprostinil acetal) **71**, following synthesis, did not indicate the presence of

treprostinil. However, HPLC using an extraction method after 2 weeks from the date of isolation, shows the presence of treprostinil, which suggests not all treprostinil was incorporated in the oligomer. The extraction method detected treprostinil by HPLC more sensitively than directly from the aqueous assay solution. Despite the improvement, the extraction was inherently limited by the solubility of treprostinil in aqueous solutions above pH 4. Furthermore, the partition coefficient of treprostinil in buffers of different pH was expected to vary. However, the neutralisation of the aliquots was anticipated to hinder the extraction of treprostinil into ethyl acetate and the acidification was expected to further degrade the acetal bonds, skewing any data obtained. Therefore, no adjustments were made to standardise the pH of the buffers before extraction.

pH-dependent degradation was observed although the analysis would benefit from additional repeats conducted over a longer time period. Results from the degradation profile were varied and although efforts were made to reduce losses, including using vacuum centrifugation to dry the samples. Limitations with the work up were present and attempts were made to overcome them. An optimised protocol to study the degradation was designed, although its efficacy could not be put to test owing to the lack of reproducibility of the polymerisation. The demonstrated inherent issues surrounding reproducible synthesis, highlighted the issues this approach has commercially. Thus, an investigation into oligoacetal treprostinil conjugates was not continued further.

4.4 **Conclusion**

Treprostinil was successfully incorporated into an oligoacetal. The relatively poor reactivity of the two treprostinil hydroxyl groups limited polymerisation, though one hydroxyl placed the treprostinil moiety at the oilogmer termini. Degradation was observed to be pH-dependent. The rate of treprostinil release was greater than that reported in the literature for DES, which is likely a result of the small oligomer formed and terminal treprostinil groups. Compared to the release profiles of other therapeutics reported in the literature (DES and DOX), we observed that the position of the secondary alcohols on a hydrophobic drug compound (such as treprostinil) can affects the degradation of the acetal bonds. Limitations in the degradation assay protocol were identified and methods were proposed to produce more reproducible degradation data. Although the study would benefit from optimised storage results and repeat degradation analysis, the inability to reproduce the polymerisation hindered this. An explanation into the poor reproducibility of the synthesis was not determined.

Clinically, the small oligomer obtained is expected to have a faster rate of permeation from the subcutaneous tissue into the circulation with a longer residence time in the blood compartment than free treprostinil. The stability observed at pH 7.4 indicates minimal treprostinil release in healthy organs and a slow degradation of oligomer poly(PEG-treprostinil acetal) at pH 6.0 suggests that oligomer **71** would exhibit a greater release of treprostinil in acidic tissues than those at physiological pH.

The polymerisation of treprostinil using a silyl ether approach was expected to be successful owing to the basic conditions employed preventing *in situ* degradation. One attempt was made to form poly(PEG treprostinil silyl ether) which was unsuccessful. For future attempts, a longer reaction time and stronger base would be expected to aid polymerisation. Another approach is to derivatise each treprostinil diol such that a diacetal treprostinil monomer with more reactive polymeric functionality (e.g. amine) could be used for making a treprostinil containing acetal polymer. In this scenario, the treprostinil monomer would possess the acetal degradable elements and polymerisation could be better controlled using monomers that could be purified as solids (e.g. diamino-diacetal treprostinil and diacids).

Treprostinil-drug conjugates have the potential to reduce both site pain and systemic site pain as well as increasing systemic half-life. Mainchain incorporation of other diol drugs offers a method to easily synthesise a polymer drug conjugate with high drug loadings. Treprostinil as a monomer has several limitations (i.e. secondary alcohols and an acid) which for polyacetals prevents polymerisation. Further investigations are required to determine a strategy to optimise treprostinil as a monomer for a polymerisation which possesses degradation sensitive to the PAH lung.

Chapter 5. Targeting of drug release

5.1 Introduction

The practice of administering neutral synthetic polymers along with bioactive-compounds (drugs, proteins, genes and peptides) is used widely to alter distribution, biorecognition and site specificity of accumulation.[162–164,422–424] The basic concept of polymer drug conjugates was proposed by Ringsdorf (**Figure 5-1**).[425] The structure includes a hydrophilic polymeric structure which is able to actively target the disease site and result in localised accumulation. The drug is conjugated *via* a biodegradable linker which is stable in healthy tissues and also specific to the disease site. Conjugation forms a prodrug derivative with reduced activity which upon reaching the disease site results in release of the active drug.

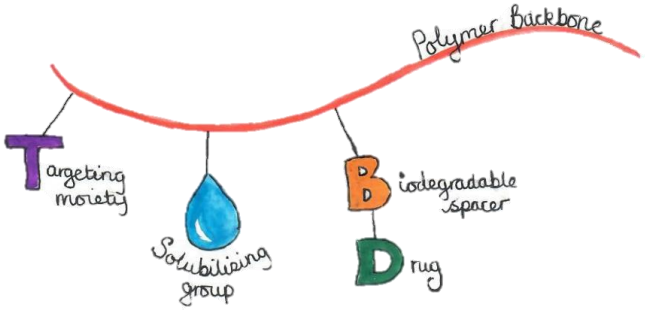

Figure 5-1. Generic structure of polymer drug conjugate proposed by Ringsdorf, which consists of a polymer backbone with solubilising groups, targeting moieties and drug molecules conjugated by a biodegradable linker.[425]

A majority of polymer-drug conjugates explored and approved to date are designed to exploit enhanced permeation and retention (EPR) effects of malignant tissue. While it has been possible to increase the maximum tolerated dose of cytotoxics and achieve greater tumour uptake of drug in preclinical models, there has been little clinical improvement in mortality.

The EPR effect is a feature of chronically inflamed tissue such as that of the PAH lung and PAH therapies are limited by lack of specificity for the disease tissue. To overcome the limitations of PM therapy, a drug-polymer conjugate was sought which would avoid site injection toxicity at the same time achieving localised release of treprostinil in the diseased pulmonary vasculature. Such a treprostinil polymer conjugate requires consideration of (i) the targeting moiety to localise a treprostinil polymer-drug conjugate to the lung, (ii) the linker used to conjugate treprostinil to the polymer and (iii) the water-soluble polymer to be used.

For i) the conjugate is required to be located in the pulmonary tissue outside the cell where the IP, EP_2 and DP_1 receptors are located. The conjugate must not accumulate in other tissues. For ii) the linker must be stable in serum until the target tissue is reached and then must be cleaved in the extracellular compartment of the pulmonary vessels to release treprostinil.

Two general approaches to target a polymer-treprostinil conjugate to the PAH lung; addition of an active targeting moiety to the polymer as well as the use of PAH specific linkers to conjugate treprostinil to the polymer.

5.1.1 Active Targeting Approach

Targeting of drug compounds is best exemplified by the antibody drug conjugates in the clinic. Exploiting the natural targeting method our immune systems utilise to protect us from disease, antibodies can be conjugated to drug compounds to allow for targeted drug delivery. Antibodies which compliment a variety of disease expressing antigens can be produced efficiently using recombinant methods. Employing a suitable linker for the conjugation of the antibody and a potent drug molecule offers a method to localise drug compounds and their effects at the desired site.[426]

Several antigens upregulated in PAH were considered for potential use as a targeting moiety for a polymer-drug conjugate (**Table 5-1**). Within PAH, the expression of pro-inflammatory markers, growth factors and mediators of vascular remodelling are increased. One such growth factor is vascular endothelial growth factor (VEGF) which is responsible for mediating angiogenesis, shows increased expression in the plexiform lesions of human PAH vessels above basal.[427,428] The exact role of VEGF is still not elucidated as evidence in conflicting,[429,430] which makes it a poor protein to target. Within the vascular lesions, production of hypoxia-inducible factor-1 is also upregulated, driving anaerobic respiration, vascularisation and proliferation. Targeting of intracellular HIF-1 has the potential to be hindered by the expression in non-disease cells.[431–433]. However, HIF-1 is also expressed in a variety of other cells including macrophages, drenditic cells and lyphmocytes. Platelet (P-) and Endothelial (E-) selectins as well as intracellular cell adhesion molecule-1 (ICAM-1) are all detected in greater quantitites in patients with PAH than in healthy patients,[434–438] however in their soluble forms. Therefore, targeting proteins released into the circulatory system, would not achieve pulmonary localisation.

Table 5-1. Summary of changes in expression of the following possible antigens in PAH and controls. PAH – pulmonary arterial hypertension.

Proteins upregulated in PAH	Pros	Cons
Hypoxia induible factor-1	Increased in PAH within plexiform lesions[427,439]	Also present in macrophages,[431] drendritic cells[432] and lymphocytes[433]
intracellular adhesion molecule 1 (ICAM)	Increased expression in plasma of children with PAH[440]	Basally expressed in all endothelium[441] Exisits in soluble forms in plasma so present systemically[440]
Vascular endothelial growth factor (VEGF)	Increased expression in plexiform lesions of PAH vasculature[427,428]	Conflicting evidence of role in PAH[429,430] – not recommended for therapeutic applications[442]
P-selectin	Increased levels of soluble P-selectin[434,435]	Soluble release means systemically expressed.
E-selectin	Increased in endothelium in PAH and released in soluble form[438,443] Increased by microparticles released from PAH tissue[444]	Present in hematopoietic tissues[435,436]

As described in **Chapter 1**, antibodies have achieved success in the clinic although wide spread use of ADCs has been hindered by limitations. The recombinant production of the chosen antibody and reproducable modification to synthesise the final ADCs is very expensive.[445] In addition, toxicity can still be problem as a result of the bystander effect,[446] and through non-specific uptake and subsequent release of cytotoxic compounds in healthy tissues.[219,268] The ability of ADCs to initiate immunogenic responses in patients has also been reported.[219] From a production view point, the biggest issues with employing antibodies as targeting moieties is their limited stability and and their propensity to aggregate which presents a limitation on the long-term storage of ADCs.[221,222]

The antigen binding region is relatively small compared to the whole antibody. To harness only the binding functionality, antibodies have been metabolised by enzymes to release the fab chain, which could then be used to form a stable targeted-drug conjugate.[222,223] The quest for stable and potent binding moieties has led investigations further to develop peptides which can bind to specific targets and assist in drug localiseation using peptide-drug conjugates.[445]

Over 60 therapeutic peptides have entered the market,[447] although in the context of interacting with therapeutic targets, rather than targeting moieties for the delivery of drug molecules. However, the precise nature of peptides used endogenously and therapeutically demonstrate

the potential targeting abilities that peptide possess. The use of peptides as targeted drug carriers has been explored preclinically, with one having completed phase II trials.[448] ANG1005 (formerly, GRN1005) is the conjugated product of the brain-permeating peptide Angipeptin-2 which targets tumour expressing receptor, lipoprotein protein 1, and the cytotoxic drug, paclitaxel.[449] Combining the targeting and permeating abilities of the peptide allows for paclitaxel accumulation in metastasised brain tumours, which are notoriously difficult to treat.[448]

Peptidic targeting moieties offer several advantages over ADCs, including, stablilty, cost, easier synthesis and modification. Peptides can be made synthetically so do not require extraction and purification from biological sources which makes them easier and cheaper to manufacture.[445] Furthermore, their simplified structure is expected to reduce the adverse events associated with ADC conjugates, described above.

Employing targeting peptides in polymer drug conjugates combines the targeting ability of peptides with the longer circulation times and reduced systemic distribution of macromolecules.[164,450] In addition, greater drug loadings are often tolerated. Owing to the size ratio between polymer and targeting peptide, multiple targeting moieties are often required on each polymer chain to maintain binding affinity.

Pre-clinically, an E-selectin targeting peptide (namely, Esbp) has been evaluated as a targeting moiety for polymer drug conjugate. When Esbp peptide and fluorescein were conjugated to a poly(hydroxypropyl methacrylate) backbone, binding to TNF-α activated vascular endothelial cells was increased 7-fold compared to a scrambled peptide polymer derivative.[233] Esbp was then incorporated into a doxorubicin (DOX) containing HPMA to form the polymer drug conjugate P-Esbp-DOX (**Figure 5-2**).[451] When admisitered in a single IV dose (15 mg/kg DOX equivalent dose) to mice with 3LL foot pad tumour, tumour growth was inhibited for 27 days, compared to a non-targeted polymeric DOX. Furthermore, following a single injection (45 mg/kg DOX equivalent) of P-Esbp-DOX in mice inoculated with a B16–F10 lung metastasis model, survival was greater than 50% after 120 days. In comparison, mice treated with the scrambled peptide drug polymer did not survive beyond 44 days. When a second dose of P-Esbp-DOX was given, survival was increased to 80% after 95 days. When conjugated with a visualising agent, IR783, P-Esbp was shown to accumulate in metastatic tissues.

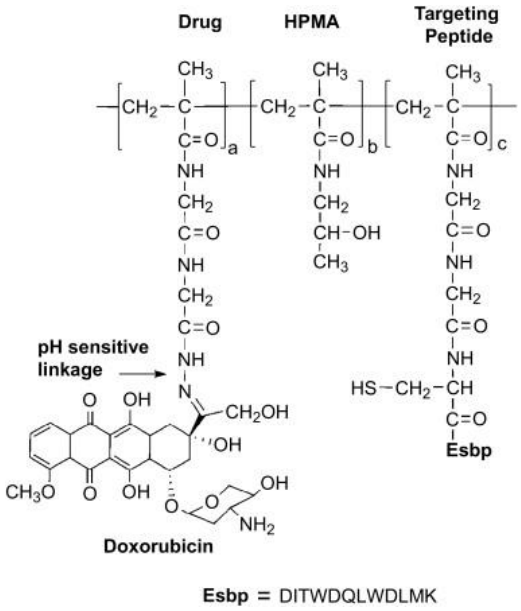

Figure 5-2. Structure of E-selectin binding polymer shown preclinically to reduce colonic tumours. The backbone is made up of non-biodegradable methacrylate monomers. A majority of which are hydroxypropyl methacrylate to aid solubility. The targeting moiety, Esbp, is selective for E-selesctin and is conjugated through a gly-gly-cys linker. The presence of the thiol is necessary for thioester rearrangement to facilitate the conjugation of Esbp, post-polymerisation. Doxorubicin is conjugated to a gly-gly linker *via* pH sensitive hydrazine linker.[233]

Similar to the Esbp targeting moiety, a peptide has been described which appears to exhibit selective binding to inflamed tissues.[452] The 8 amino acid peptide, namely CARSKNKDC (CAR), (**10**) was found to exhibit selective binding in wounded vasculature[452] including in the pulmonary tissue of a sugen/hypoxia mouse model of PAH which replicates the remodelling and altered haemodynamic aspects of PAH.[453] Determined in a tendon wound model, phage binding of sequences where the basic amino acid side chains of CAR were exchanged for neutral side chains resulted in a loss of binding.[452] Binding studies indicated that CAR is a ligand for heparin and heparan sulfate expressed on the surface of cells[452] which become altered due to an increased release of heparanase, an enzyme that degrades polymeric heparan sulfate.[454] PAH is associated with an increased expression in genes encoding heparanase enzyme and a heparan sulfate (HS) moiety, IdoA2S-GlcNS, to which heparanase is resistant to.[455] The IdoA2s-GlcNS moiety is the likely receptor for CAR peptide which mediates cell endocytosis by micropinocytosis. which increases cellular internalisation.

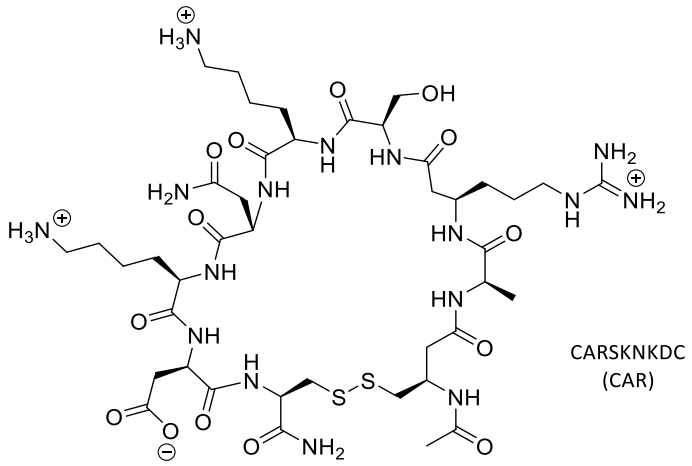

Figure 5-3. Structure of CAR peptide which exhibits selective binding for inflamed tissue, including lung tissue in an experimental rat model of pulmonary arterial hypertension.[453]

Co-administration of CAR (3 mg/kg) sublingually with intravenous imatinib, a broad spectrum tyrosine kinase inhibitor, (5 and 20 mg/kg), increased the localisation of therapeutic action as measured by an 8% reduction in right ventricular systolic pressure after 1 hour compared to no change when given imatinib alone.[456] Furthermore, CAR peptide has been conjugated to liposomes and nanoerythosomes (vesicles derived from red blood cells) as surface targeting moieties which have aided in the specificity of drug release.[77,457,458] The half-life of CAR-liposomal fasudil was 34-fold higher than that of plain fasudil, and resulted in a 35-40% decrease in mean pulmonary arterial pressure with no change to the mean systemic arterial pressure.[458] Some concern was raised about the lack of interest shown by the scientific community in the 4 years since the CAR publications but we sought to verify the results to determine its suitability as a targeting moiety.

The homing properties reportedly possessed by the CAR peptide offer a potential method to target a polymer-treprostinil conjugate to the inflamed PAH lung. The high dose of CAR employed may be required to overcome rapid clearance which is often experienced with small peptides or a result of the poor bioavailability when administered sublingually. Conjugation onto a polymer for subcutaneous delivery may offer a route to overcome these limitations. We sought to confirm the CAR binding findings by labelling CAR with fluorescein and visualising the binding to inflamed endothelial cells (HUVEC) *in vitro,* employing TNF-α to stimulate an inflammatory response. The possibility of using the CAR peptide targeting moiety to aid localisation and thus, promoting localised drug release was envisaged.

5.1.2 **Passive Targeting**

Drug delivery at a target site can be achieved by a passive targeting approach, employing a disease-specific drug release mechanism. Particularly for toxic drugs or drugs which exhibit many off-target affects, the premature release of the drug compound results in off-target effects and negates the purpose of the conjugate. Only once the conjugate has reached the

site of release, must the linker be cleaved to release the active drug with a potent therapeutic response.[218,459]

As well as pro-inflammatory markers, disease-mediating enzymes are also upregulated in PAH, which might serve as a targeting strategy. By nature, enzymes exhibit specific activity for a unique structure of sequence of amino acids, for example ribozymes in the translation of RNA into the respective proteins for which they code.[460] For metabolic enzymes, this activity involves a cleavage step, which depending on the enzyme and substrate, can occur at different bonds along a primary amino acid sequence. For example, the precursor for atrial natriuretic peptide is synthesised endogenously as a chain of 126 amino acids with low activity.[461] It is cleaved between a specific serine and threonine bond by the protease corin to release the active 28 amino acid carboxyl terminus atrial natriuretic peptide which reduces blood volume.[462] As well as endogenous enzyme substrates, many enzymes have been shown to possess specificity for exogenous peptidic substrates.[463] Many peptide substrates are commercially available conjugated to a chromophore which releases a coloured compound upon cleavage by the respective enzyme. Chromogenic substrates are often used in either bench top or *in vitro* assays to quantify the amount of enzyme present in a system (e.g. cell culture or tissue isolation).[464]

The conjugation of a drug to the substrate in place of a chromophore to form an enzymatically degradable peptide prodrug can be envisaged. Such a prodrug linker could be employed to link a drug to a polymer-drug conjugate which would exhibit minimal receptor activity upon administration and systemic circulation. Upon interaction with the specific enzyme located at the target site, the linker is cleaved to release the active drug compound.

Tissue remodelling is a distinctive feature of PAH which implicates many pathways and mechanisms to drive the changes seen in this disease. As part of the pro-inflammatory mechanism, mast cells have been shown to accumulate around the small blood vessels of adult patients with PAH and in monocrotaline treated rats with induced PAH.[31,37,40] Mast cells characteristically contain enzyme-filled granules which when stimulated degranulate to release the enzymatic contents. Within the granules two mast cell specific, serine proteases, tryptase and chymase, are released. Tryptase and chymase have unknown endogenous substrates but are known to cleave exogenous substrates at the N-terminus.[463] Both tryptase and chymase are thought to drive progression of PAH, even in the early stages of disease.[34,465] Tryptase stimulates collagen 1 synthesis and fibroblast proliferation,[39] while chymase is implicated in development of bleomycin-induced lung fibrosis[30], the mechanism for which is likely to involve activation of MMPs.[466]

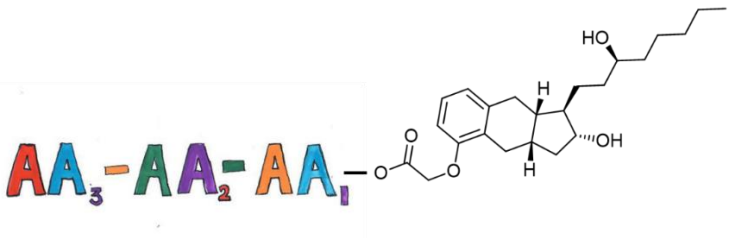

Figure 5-4. Proposed concept of employing peptidic substrates for tryptase and chymase as a linker which would be cleaved in the pulmonary arterial hypertensive lung.

We hypothesised that the specific nature and locality of tryptase and chymase as well as their N-terminal substrate cleavage point, make their substrates suitable prodrug appendages to achieve PAH specific drug release in the pulmonary tissue (**Figure 5-4**). We sought to investigate CARSKNKDC as a targeting moiety and tryptase substrates as an enzyme degradable linker which could be later employed on a polymeric structure. Thus, we aimed to:

- Obtain and test the utility of CAR as a homing peptide in pulmonary arterial smooth muscle cells with tumour necrosis factor alpha (TNF-α) induced inflammation.
- Develop a method to synthesise a prodrug comprised of treprostinil bound to the C-terminal of a peptidic substrate for tryptase and chymase.

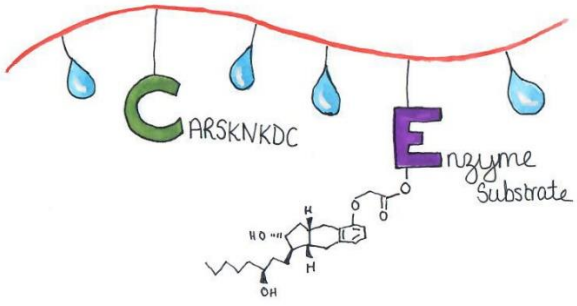

Figure 5-5. Proposed Polymer drug conjugate which features CARSKNKDC as a targeting moiety and an enzyme substrate linker to conjugate treprostinil *via* the aryl acid.

5.2 Results and Discussion

The design of a successful polymer-drug conjugate (PDC) necessitated consideration of method to target localisation of treprostinil in the pulmonary vessels. For any drug conjugate, moieties to be considered include; tissue or cell to be targeted, drug to be released, suitable linker to carry and release drug, strategy to target the desired tissue and polymer system employed to optimise pharmacokinetics and dynamics of PDC.[242,267,467] Targeting of the drug to a tissue can be achieved directly using an active targeting moiety, where the entire PDC possesses specificity to the target tissue; or indirectly by achieving site specific drug release where the PDC itself does not exhibit any specific affinity for the target tissue. The approaches are not mutually exclusive and thus, both approaches were pursued.

Exploiting the EPR effect does not completely avoid systemic exposure and therefore, targeting moieties can also be employed to increase localisation. The prostanoid receptor target for treprostinil exists on the surface of platelets, vascular endothelial and smooth muscle cells. Therefore, prostanoid receptor binding would be advantaged by the localisation of polymer drug conjugates in the pulmonary tissue. Targeting of the extracellular compartment is less explored than internalised target, although the extracellular environment is has been proven to cleave proteolytic ADC linkers to achieve desired therapeutic effects.[468,469] Several antigens to which an antibody could target are presented in PAH (**Table 5-1**), however the issues associated with extracting, conjugating and purifying led our attention to small targeting peptides. CARSKNKDC (CAR) was identified as a potential moiety which could be incorporated into the design of a polymer drug conjugate.

The importance of the drug releasable linker even in targeted therapies such as antibody drug conjugates is established.[459] The requirement for a linker to be stable during storage, injection, circulation and releasable at the desired site of action is just as necessary for the design of polymer-drug conjugates.[470] From the earliest efforts to develop PDCs, it is clear the linker is a key feature in the design of any conjugate or pro-drug structure.[470] In the case of treprostinil, release is required at the surface of endothelial cells, platelets and smooth muscle cells where prostanoid receptors are located. Previous linkers investigated for the polymeric conjugation of treprostinil[79,138,339,399] have consisted of esters which are labile to ubiquitous carboxylesterases. As discussed in **Chapter 3**, premature release of treprostinil was exhibited and thus the conjugates were unsuccessful in reducing site pain. Upon the successful design of a treprostinil linker which achieves PAH specific release, the potential to be employed on a varied of structures, including; prodrug conjugates, antibody drug conjugates, polymer drug conjugates, dendritic drug conjugates is opened.

The expected benefit to patients of a treatment option which localised treprostinil to the lung is expected to not only increase quality of life, but also increase the efficacy of treatment by raising the maximum tolerated dose. Therefore, both a strategy for actively directing a conjugate to the lung and a strategy to selectively release the drug at the disease site were pursued. A targeting peptide was identified, synthesised and tested. Enzyme specific peptides were designed, synthesised and modified for a peptidic prodrug conjugation of polymer and treprostinil.

5.2.1 Tissue targeting with CAR peptide

Following reports of the disulfide cyclised peptide sequence CARSKNKDC[452,453] the sequence was investigated as a method to target a polymeric conjugate. To be certain of the specificity of CAR peptide towards PAH, it was desirable to conduct some assays to verify its utility, before attempting to include CAR in a larger conjugate.

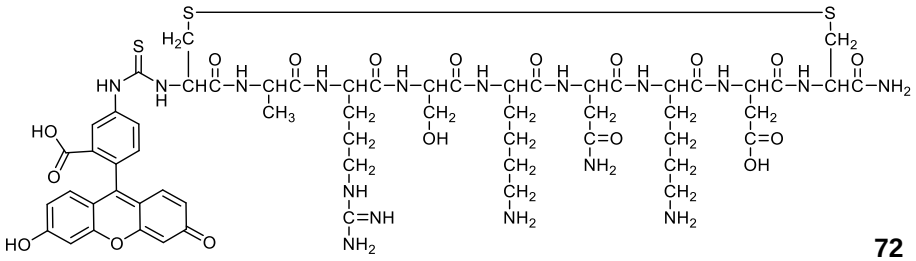

72

Figure 5-6. Structure of fluorescein (FITC)-conjugated disulfide cyclised CARSKNKDC peptide which has been shown to possess specific binding and uptake in cells in an inflammatory state.[452,453]

As reported in the original literature, CAR was conjugated with FITC **75** to aid the visualisation of the CAR peptide **73** homing in the intended site. Chromophores by nature possess delocalised electrons which denote their colour. The delocalised or conjugated system often renders the molecule hydrophobic, which is associated with increased non-specific binding.[471] The non-specific accumulation of fluorescein-labelled conjugates in cells and tissues is particularly prominent when the ratio of fluorescein to the substrate or peptide is increased.[472] In testing the homing ability of CAR peptide, a small chromophore would be ideal to limit non-specific binding. However, FITC **75** is a common chromophore used in tissue visualisation studies. Furthermore, the original CAR papers used FITC **75**, so to verify their results, the same FITC chromophore was employed here to synthesise **73**.

In terms of conjugation, both the amine and carboxyl terminus of the peptide were accessible to conjugation and had been described previously.[77] The disulfide cyclisation is a feature of the phage display method used to identify CAR peptide. Cyclic peptides exhibit greater stability than their linear counterparts.[473] The disulfide link is subject to reductive conditions to form the two thiols so reductive conditions should be avoided. Conjugation to a polymer should be carefully considered as the presence of two lysine amines and carboxylic acid additional to the terminal groups hinders the potential for controlled amide bond formation. In negotiation with several companies offering quotes for the peptide, it seems that the FITC conjugation was an expensive step in an already expensive purchase. Therefore, rather than ordering FITC-Ahx-CARSKNKDC-NH_2 **73**, as the original CAR papers suggest, a non-FITC conjugated precursor which contained lysine masking groups was settled on as a compromise. Such a structure would allow for the solution-phase FITC conjugation and subsequent lysine deprotection to obtain the desired structure in a two-step reaction. No by-products would be formed in the FITC conjugation and only the protecting group would require removal from the peptide. The intermediate would also be available for conjugation to other structures, *via* the terminal amine.

FITC conjugation to cyclised CAR

Initial strategies utilised a bespoke-made CAR peptide **74**. Cyclisation was accomplished by disulfide bond formation between the two cysteines. The N-terminus was unprotected for further conjugation and as described in the literature, the C-terminus was amidated. With the

exception of lysine, the side chain residues (alanine, arginine, serine, asparagine, aspartic acid were unprotected. To ensure site-specific conjugation to the N-terminus amine, lysine sidechains were protected with 1-(4,4-dimethyl-2,6- dioxacyclohexylidene)ethyl (Dde) groups. Alternative protecting groups considered were allyloxycarbonyl (alloc) and 1-(4,4-dimethyl-2,6-dioxocyclohex-1-ylidene)isovaleryl (ivDde) groupswhich are both orthogonal protecting groups stable to the conditions employed by the manufacturers to couple the amino acids and isolate the peptide.

Table 5-2. Considered protecting groups for amines of lysine side chains. Alloc = allyloxycarbonyl; Dde = N-(1-(4,4-dimethyl-2,6-dioxocyclohexylidene)ethyl); ivDde = 1-(4,4-dimethyl-2,6-dioxocyclohex-1-ylidene)isovaleryl; TFA = trifluoroacetic acid; AcOH = acetic acid; NMM = N-methylmorpholine; $CHCl_3$ = chloroform; DMF = dimethylformamide; NMP = N-methyl-2-pyrrolidinone; DCM = dichloromethane; $Pd(Ph_3P)_4$ = palladium-tetrakis(triphenylphosphine).

Lysine protecting group	Structure	Stable conditions	Deprotection conditions
Alloc	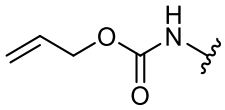	Piperidine TFA Hydrazine	3 eq. $Pd(Ph_3P)_4$ in $CHCl_3$/AcOH/NMM (37:2:1)
Dde	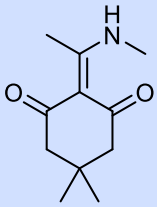	Piperidine TFA	2% hydrazine in DMF or 20% hydroxylamine /15% imidazole in NMP/DCM (5:1)
ivDde	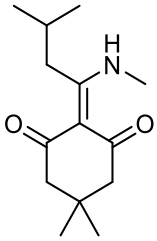	Piperidine TFA	2% hydrazine in DMF or 20% hydroxylamine /15% imidazole in NMP/DCM (5:1)

Protection with an alloc group forms an allyl carbamate and is cleaved catalytically with either palladium or tin. The presence of trace metal was however of concern for later evaluation in biological assays, so alloc- and allyl-based protection groups were not considered to be suitable at this stage. Dde and ivDde groups are both removed by treatment of 2% hydrazine (**Scheme 5-3**). During Fmoc removal steps Dde can migrate to other amine side chains which can be problematic in the synthesis of large peptides.[474] The hindered nature of ivDde was thought to provide an alternative to Dde as it would circumvent these drawbacks making it more robust but harder to cleave.[475] In the case of CARSKNKDC, only two lysine groups were present, both of which required protection so the benefits of ivDde would not be utilised and a struggle in removing the protecting groups was anticipated. Therefore, lysines were protected with the more easily cleaved Dde groups (**Figure 5-7**).

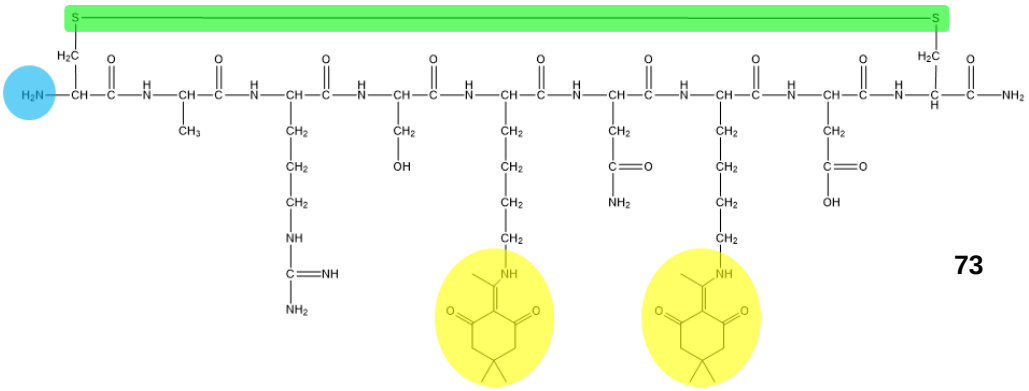

Figure 5-7. Structure of disulfide cyclised H-CARSK(Dde)NK(Dde)DC-NH_2 **74**. Yellow indicates the 1-(4,4-dimethyl-2,6- dioxacyclohexylidene)ethyl (Dde) groups, blue shows the free amine terminus and the green highlights the disulfide link.

Fluorescein conjugation to the terminal amine (highlighted blue in **Figure 5-7**) was conducted using fluorescein isothiocyanate **75** under basic conditions (**Scheme 5-2**).[476] Isothiocyanates are readily reactive owing to the electrophilic carbon, so anhydrous conditions were employed. The carbon of an isothiocyanate is electrophilic owing to the electronegativity of the heteroatoms sulfur and nitrogen. The nucleophilic free amine of the peptide will attack the isothiocyanate carbon breaking the carbon-nitrogen π-bond resulting in the formation of a thiourea adduct **77** (**Scheme 5-1**).

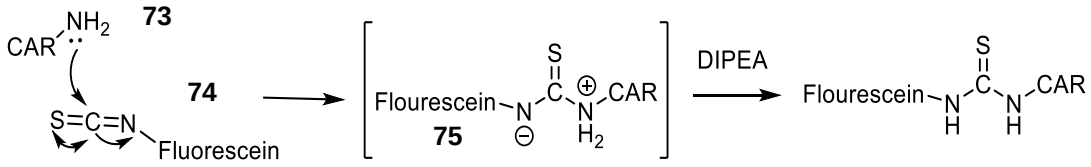

Scheme 5-1. Mechanism for the nucleophilic addition of CAR amine **74** into fluorescein isothiocyanate **75** to form thiourea product **77**.

Non-nucleophilic base, diisopropylethylamine (DIPEA), was employed to deprotonate the trifluoroacetate salt the peptide is supplied as. A slight excess of FITC 75 was used to ensure complete consumption of the peptide and to account for possible side reactions of FITC 75 with water or other nucleophile contaminants. The reaction was monitored by RP-TLC and completion of the reaction was indicated by the formation of a fluorescent spot with an increased R_f value (0.15 versus. 0.59). A sample of the reaction (0.5 mL) was dried and the triethylamine hydrochloride salt was precipitated addition of THF. A pale precipitate was filtered through a cotton wool plugged pipette.

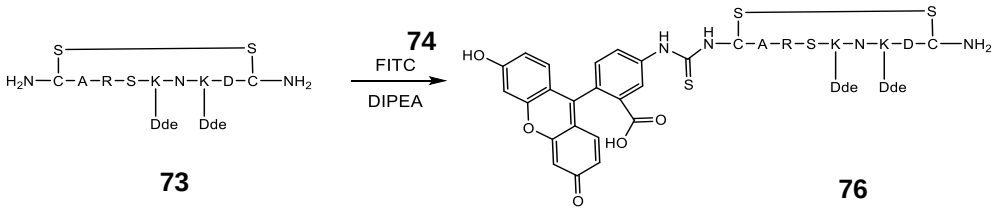

Scheme 5-2. Fluorescein isothiocyanate (FITC) **75** conjugation of cyclised CARSKNKDC **74** with 1-(4,4-dimethyl-2,6- dioxacyclohexylidene)ethyl (Dde) lysine side chain protecting groups, in the presence of diisopropylethylamine (DIPEA).

Whilst all the CAR amines were protected, attempts were made to purify FITC-CAR(Dde) 77 before deprotection of the Dde protected lysine side chains. Isolation of FITC-CAR(Dde) **77** was attempted using automated RP-chromatography with acetonitrile and water as the mobile phase. However, despite multiple attempts, resolution between the different components was not obtained. Eluted fractions were analysed by HPLC. Compared to retention time of the starting CAR(Dde) 74 at 6.2 minutes, the HPLC trace of the reaction solution contained no starting peptide and the presence of a new and large absorbance at 14.8 minutes. The longer retention time indicates an increase in lipophilicity consistent with the expected FITC conjugation in the desired product 77. The presence of salts in the solution was not deemed a problem for HPLC analysis when aqueous solvents are employed, so attempts to remove the salt were not repeated for subsequent samples.

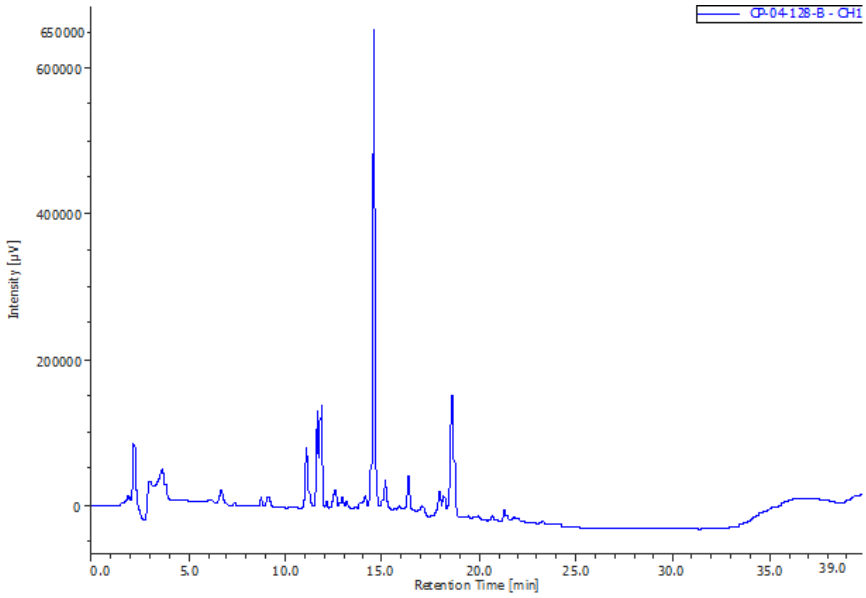

Figure 5-8. Chromatogram of suspected FITC-CAR(Dde) **77** analysed by HPLC using a gradient of 10-60% acetonitrile/water over 22 minutes. An attempt to isolate the product was attempted using automated RP- column, however all components of the crude mixture eluted together.

The reaction was repeated on a 20 mg scale and after 18 hours the mixture split into two portions. The first was dried and the residue dissolved in THF to facilitate removal of

triethylamine hydrochloride salt by precipitation. The yellow solution was filtered through cotton wool but resulted in a very pale filtrate. The cotton wool was flushed through with a 50% methanol/water solution. Both fractions were dried over air and analysed by ^{1}H NMR spectroscopy (δ^{6}-DMSO) but no peptide resonances were observed in the spectra.

The remaining sample of reaction solution was also dried. Redissolution in acetonitrile formed a precipitate which was filtered off through cotton wool. Serial flushing of the cotton wool with different solvents into different vials was conducted. A RP-TLC of each vial was conducted in 40% acetonitrile/water. Most product was located in the first acetonitrile flush (vial 1). It was decided that the reaction would be carried forward with impurities still present.

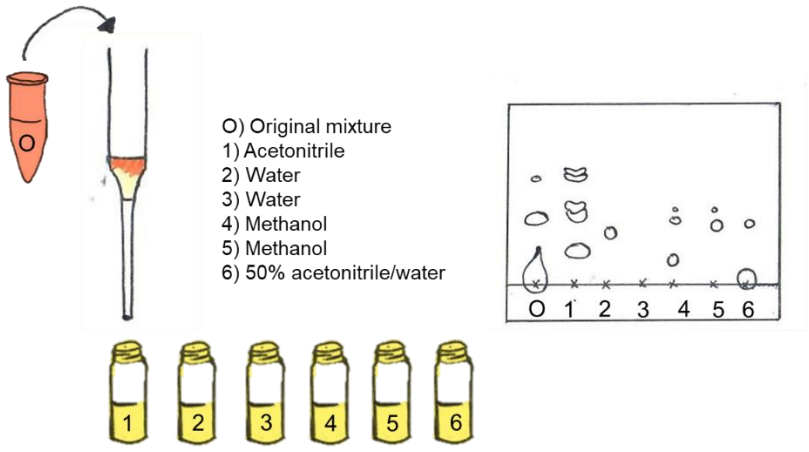

Figure 5-9. A sample of the cloudy solution in which fluorescein conjugation of CARSK(Dde)NK(Dde)DC-NH_2 had been attempted was filtered through a cotton wool plugged pipette. A series of solvents were passed through the pipette to solubilise any compounds removed by filtration or interaction with the cotton. The filtrate of each flush was collected and analysed by thin-layer chromatography (40% acetonitrile/water). Most product was obtained in the first fraction in acetonitrile.j

A trial deprotection of the Dde groups of the starting CAR(Dde) **74** was attempted using hydrazine hydrate 78 on a 2 mg scale (**Scheme 5-3**). Tracking by RP-HPLC from the starting material showed a decrease in retention time from 10.4 minutes to 8.2 minutes, which was consistent with an increase in polarity expected for lysine deprotection.

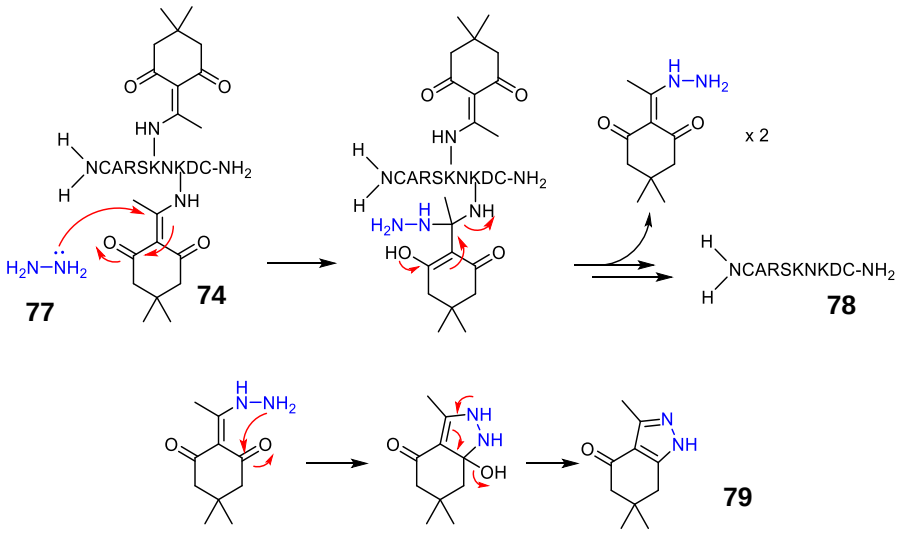

Scheme 5-3. Deprotection of lysine protecting group, 1-(4,4-dimethyl-2,6-dioxacyclohexylidene)ethyl (Dde) of cyclised CARSKNKDC **75** with hydrazine **78** to release the free amine peptide **79**, forming a pyrazole side product **80**.

The reaction solution was dried under a stream of air and the crude residue was analysed by ^{1}H NMR spectroscopy. The spectra showed a change in the resonance corresponding to the methyl group of the Dde group from a doublet at 2.57 ppm in the starting CAR(Dde) **74** to a broad singlet at 2.46 ppm (labelled pink in **Figure 5-10**). This suggested a reaction at the alkene had occurred (**Scheme 5-3**). Additionally, a singlet at 2.39 ppm, corresponding to the four identical protons on the Dde cyclohexyl ring before treatment with hydrazine **78**, was split into two different singlets at 2.36 and 2.71 ppm. This suggested that the Dde structure was no longer symmetrical and the downfield shift is consistent with the formation of the pyrazole group **80**. This evidence suggested that the reaction had occurred as desired but still contained the pyrazole by-product, **80**. Successful conditions for forming free amine CAR **79** by Dde removal of CAR(Dde) **74** were verified so the conditions were transferred to FITC-CAR(Dde) **77** without further purification.

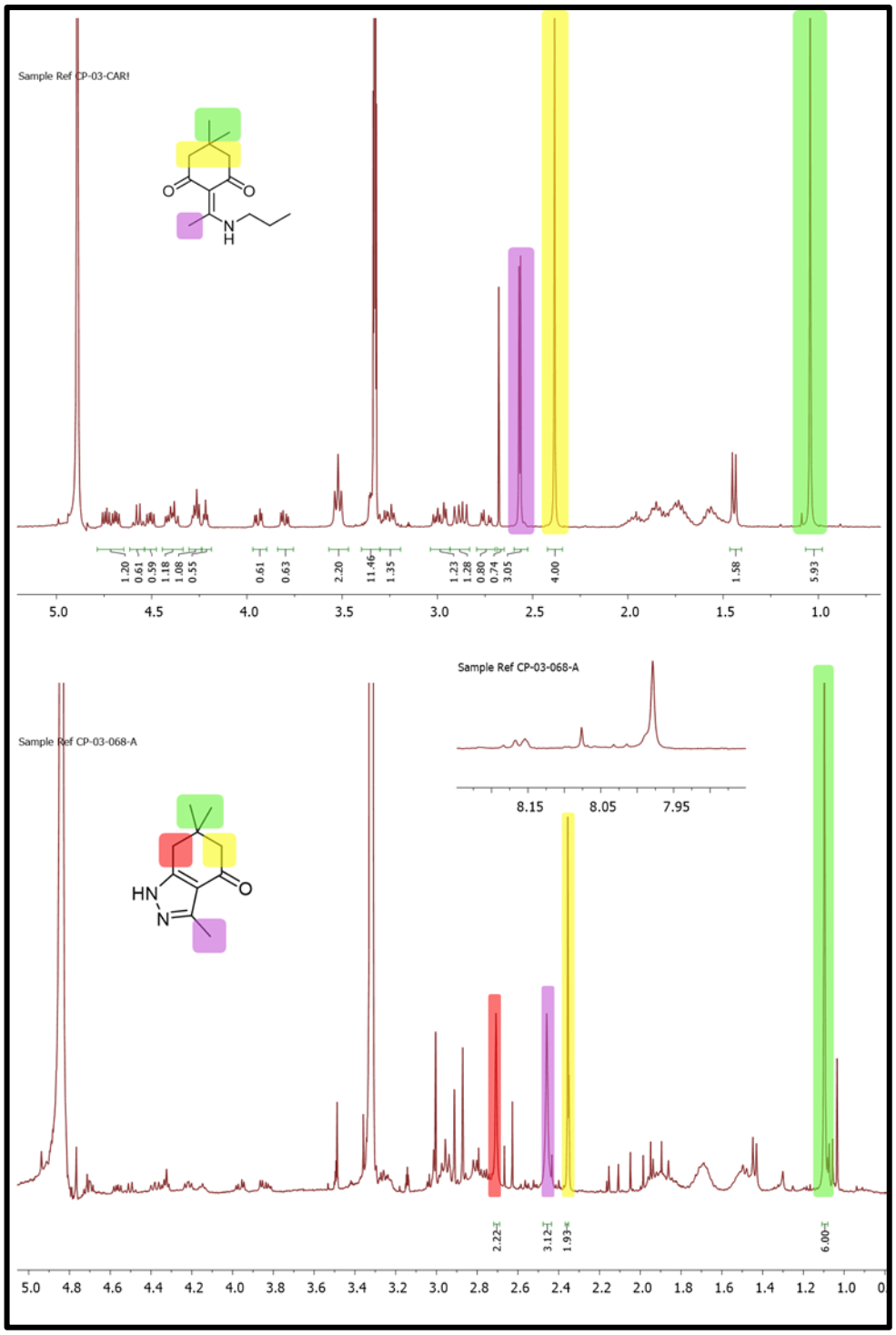

Figure 5-10. ^{1}H NMR spectrum of cyclised CAR 79 before and after 1-(4,4-dimethyl-2,6- dioxacyclohexylidene)ethyl (Dde) cleavage by hydrazine hydrate 78 showing the presence of pyrazole by-product 80.

A small sample of FITC-CAR(Dde) 77 was then allowed to react with hydrazine hydrate 78 to remove the Dde groups. The reaction was monitored by HPLC. Impure starting material 77 was used so to be able to achieve better separation of peaks on the HPLC chromatogram, a slower gradient than previously used for the deprotection of the starting CAR(Dde) 74 was employed.

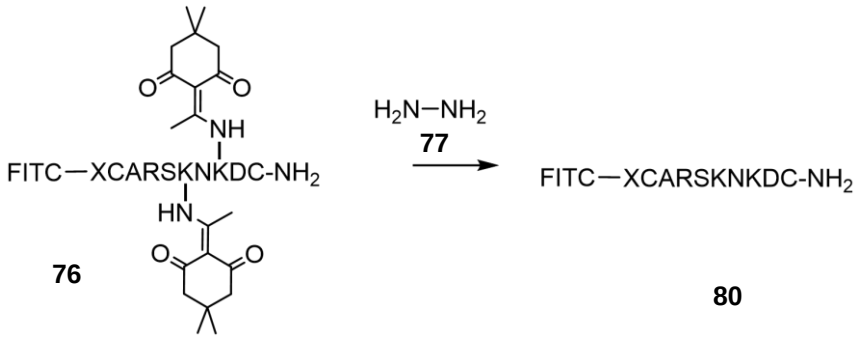

Scheme 5-4. Deprotection of lysine 1-(4,4-dimethyl-2,6- dioxacyclohexylidene)ethyl (Dde) groups of FITC-CARSKNKDC **77** to the lysine side chain product 81 by hydrazine hydrate 78.

The reaction was monitored by HPLC using a solvent gradient 25-50 acetonitrile/water over 15 minutes and then retaining 50% acetonitrile for a further 15 minutes. Treatment of the FITC labelled peptide **77** with hydrazine hydrate **78** resulted in the formation of a new HPLC absorbance at 7.0 minutes and decrease of the starting peptide **77** absorbance at 15.1 min. The change in the HPLC elutogram was consistent with the decrease in retention time observed for the deprotection of the starting CAR(Dde) 74.

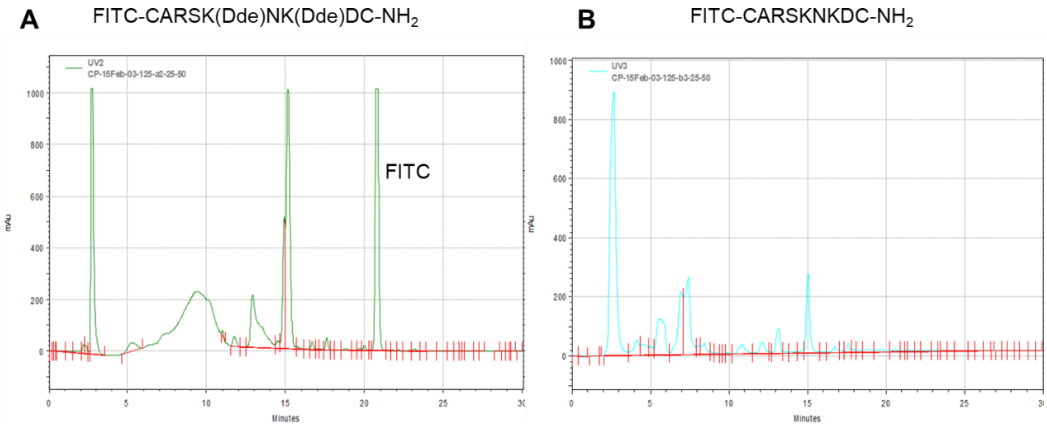

Figure 5-11. Comparison of chromatographs obtained of FITC-CARSK(Dde)NK(Dde)DC-NH_2 **77** before (A) and after (B) treatment with hydrazine hydrate to afford free amines of FITC-CARSKNKDC-NH_2. **81** Peptide were analysed by HPLC using 25-50% acetonitrile/water mobile phase.

The hydrazine **78** deprotection of FITC-CAR(Dde) **77** was again conducted on a 5 mg scale in acetonitrile. Upon addition of hydrazine hydrate **78**, a precipitate was formed and collected by filtration through cotton wool. The filtrate was retained, and precipitate flushed with water and the filtrate collected. Both solutions were analysed by HPLC (**Figure 5-12**), using a solvent gradient 40-70% acetonitrile/water over 15 minutes and plateauing at 70% for 15 minutes. The peptidic product was found in the first acetonitrile solution (A). Flushing with water released very little compound as indicated by the much smaller scale.

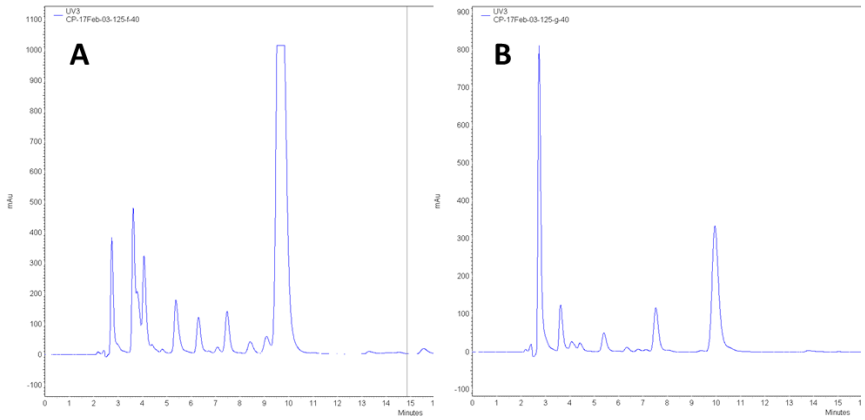

Figure 5-12. HPLC elutograms of filtered FITC-CAR peptide **77** upon treatment of hydrazine hydrate **78**. (A) shows filtrate in acetonitrile and (B) shows water soluble precipitate.

It was questioned whether the difficulty in isolating the deprotonated FITC-CAR **81** was a result of the presence of FITC **75** or residual impurities from the FITC-conjugation step (**Scheme 5-2**). For this reason, an attempt was made to remove residual impurities. FITC-CAR(Dde) **77** (20 mg) was dissolved in acetonitrile and a drop of trifluoracetic acid added to form the triethylamine salt. The triethylammonium trifluoroacetate salt precipitate formed was filtered through cotton wool. Upon addition of hydrazine hydrate **78** fumes were observed, and a precipitate formed. After 10 minutes the solution was filtered through cotton wool and the filtrate collected. The precipitate was flushed with water and both filtrates analysed by HPLC. (**A** and **B** of **Figure 5-13**, respectively). An unidentified peptide product was observed by increased absorbance at 217 nm in the acetonitrile layer which produced a sharp peak at 5.3 minutes. The aqueous flush fraction also contained a peak at 4.5 minutes but with a reduced intensity (25%, as shown by the different scales).

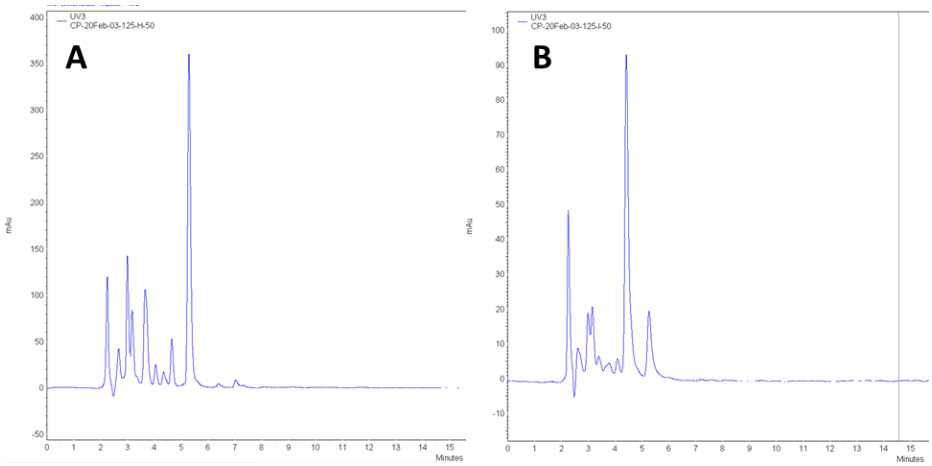

Figure 5-13. HPLC elutograms of reaction with FITC-CAR 75 with hydrazine hydrate 78 following triethylamine salt removal with trifluoroacetic acid. The reaction was filtered through cotton wool with acetonitrile and the filtrate retained (A). The precipitate collected was flushed through with water and analysed (B).

The main hindrance experienced during the synthesis is the small scale of the reactions undertaken which eliminated the possibility of analysis by ^{1}H NMR or by multiple techniques. Therefore, after several unsuccessful attempts to isolate the product by precipitation and dissolution in different solvents, fractions obtained thus far were analysed by TLC to confirm the presence of possible products (**Figure 5-14**). The fractions which contained the visibly orange product with were then pooled together and isolation by automated RP column chromatography attempted. However, separation of the peaks was not achieved as determined by TLC, which showed the same compounds in all the fractions.

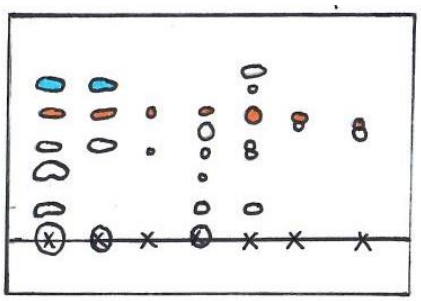

Figure 5-14. All fractions retained from FITC-CAR(Dde) deprotection with hydrazine hydrate until this point were analysed by simultaneous thin layer chromatography employing 50% acetonitrile/water, represented as an accurate drawing of the TLC observed. Purification of small quantities was challenging and combining relevant fractions was anticipated to increase sensitivity of detection. All fractions contained the orange compound and so were combined for further purification.

Employing a shallower solvent gradient (from 12-80% acetonitrile in the first run to 5-40% acetonitrile over double the time) facilitated partial separation by collection of compounds into one of two populations. The two slightly overlapping peaks on the chromatogram were both UV active allowing for detection, however the compounds with a shorter retention time

possessed a spot which was coloured yellow in white light on a TLC plate (R_f =0.35). The fractions obtained from the automated RP chromatography were split into two populations (**Figure 5-15**); those containing the yellow spot and those with a lower Rf without the yellow spot. Owing to the overlapping retention times, compounds thought to be side products appearing at different Rfs were also unavoidably collected. The pooled fractions were dried by lyophilisation and analysed by ^{1}H NMR spectroscopy. Both spectra showed the presence of FITC 75 resonances but a lack of resonances observed corresponding to the peptide 74, indicating the peptide was still bound to the stationary phase. Repeat flushing using methanol, acetonitrile and water did not isolate the peptide, as determined by ^{1}H NMR spectroscopy.

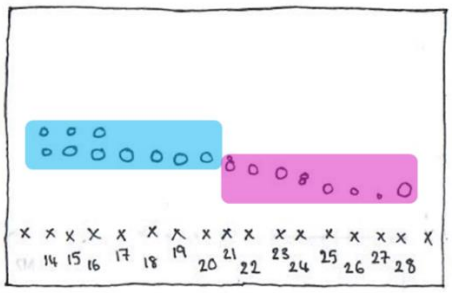

Figure 5-15. Accurate drawing of the thin layer chromatogram observed showing fractions from column chromatography of pooled fluorescein-XCARSKNKDC reaction mixtures. Separation achieved was poor and to maintain reasonable concentrations for ^{1}H NMR spectroscopy, the fractions were split into two populations labelled in blue and purple.

FITC-conjugation of the pre-made peptide **74** was achievable and easy to deprotect as determined by tracking of the reaction using TLC. HPLC indicated both reactions went to completion, although the isolation the peptides proved problematic. Purification of both the FITC **75** conjugation (**Scheme 5-2**) and Dde removal steps (**Scheme 5-4**) proved problematic as it was difficult to determine the location of the peptidic compound because of the small scales employed. An alternative method of deprotection has been reported using imidazole and hydroxylamine.[477] However, it was assumed that the issue in purification would remain. At the time, only analytical HPLC columns were available which made separation attempts tedious. Loading high concentrations of reaction mix onto the column made UV detection virtually impossible as for all wavelength monitored, the concentration was too high and the signal was off scale preventing accurate resolution and measurement. Additional to this, too high loading would result in poor dissolution and the impure product would exhibit poor column interaction and the risk on precipitation on the column. Upon seeking advice from colleagues, the opportunity to synthesise the desired peptide by solid phase peptide synthesis (SPPS) was presented.

Solid phase peptide synthesis of FITC-CAR

SPPS allows for a controlled stepwise conjugation of amino acids. Choosing the correct side chain and N-terminal protecting groups, conjugation can preferentially be conducted. Furthermore, reaction on the solid phase allows for easy removal of excess reagents and unconjugated by-products by simple filtration after each step. With the use of an automated system, a short peptide such as CAR peptide could be synthesised within 24 hours, followed by a FITC **75** conjugation and a cyclisation step (**Figure 5-16**). In light of the struggle encountered with solution phase work-up, SPPS was considered simpler and predictable. For this reason, synthesis of CAR peptide on-resin from its constituent amino acids was pursued. The variety of different protecting groups, coupling reagents and the number of unwanted side reactions possible (Described earlier in **Chapter 3**, **Scheme 3-3**), necessitates a thorough plan for SPPS synthesis (**Figure 5-16**).

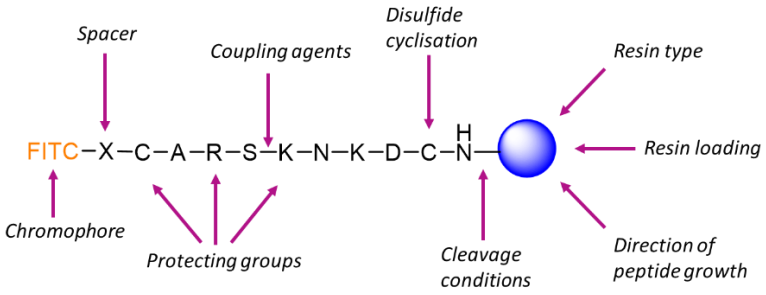

Figure 5-16. Considerations for synthesis of FITC-XCARSKNKDC using solid phase peptide synthesis.

N-terminal growth of peptides using Fmoc-protected amino acids was employed as it is a robust, reliable and widely used methodology for peptide synthesis and had previously been reported to be possible with CAR peptide **73**.[478] The literature reportedly synthesised CAR on a polystyrene (PS) resin with surface PEG chains and terminated with a peptide amide linker (PAL).[452,479] Polystyrene is a cost-efficient resin matrix which can be used on small to large scale. PS has good swelling properties in organic solvents but for long sequences can facilitate peptide aggregation. Polar supports, such as polyethylene glycol (PEG) are better for such peptides and so to combine both properties, PEG-PS composites are often employed. A comparable resin for the synthesis of CAR peptide **73** was sought.

PAL-Novasyn® TentaGel® resin fitted the resin description employed in the literature and consists of: (a) a core copolystyrene with mesh size 100-200 for organic swelling; (b) an outer layer of water soluble PEG chains to aid swelling and interactions with the solvent; and (c) an aminomethyl-dimethoxyphenoxyvaleric acid terminal peptide amide linker (PAL) which will conjugate to the carboxylic acid of the first amino acid, cysteine (**Scheme 5-5**). Upon TFA-catalysed cleavage of the peptide from the PAL-resin, the primary amide derivative of the peptide carboxyl terminus 103 would be generated (**Scheme 5-5.**). The loading for PAL-Novasyn TG resin was 0.22 mmol/g which is low for a standard resin but will facilitate potential cyclisation of the thiols, whilst on resin which will be easier to purify than cyclisation in solution.

Complete coupling with 100 mg of resin, will yield a maximum of 0.022mmol of product. For the desired peptide with molecular mass 1523 g/mol, this will result in a maximum of 34 mg of product.

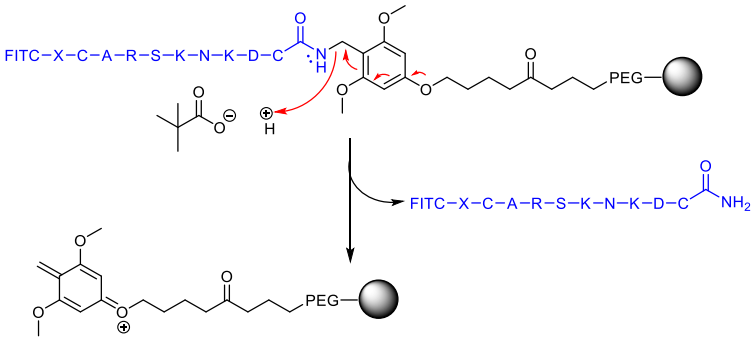

Scheme 5-5. Proposed mechanism for acid-mediated peptide cleavage from peptide amide linker (PAL) resin to form a primary amide on the peptide C-terminus, 81.

Fmoc-amino acids, except cysteines, were employed possessing acid-sensitive side chain protecting groups so deprotection could occur during the final resin cleavage step. Disulfide-linked peptides (highlighted blue in structure **74**) exist in nature, for example in the hormones oxytocin and somatostatin (**Figure 5-17**) and also between keratin strands in hair follicles. However, their synthesis is often very sensitive to the oxidation technique, peptide structure, and solvent employed during the disulfide bond formation leading to peptide cyclisation.

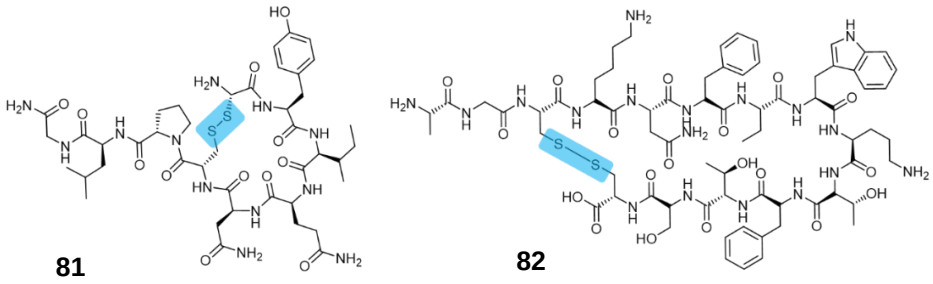

Figure 5-17. Structure of naturally occurring disulfide linked cyclic peptide hormones; oxytocin 82 and somastatin 83 Disulfide bonds are highlighted in blue.

Anticipating a need to explore cyclisation both on- and off-resin, an orthogonal thiol protecting group was sought. The ideal protecting group would be stable to peptide formation and resin cleavage conditions and be removed by conditions which all other protecting groups and resin linker would be stable to. The thiol protecting group, acetamidomethyl (Acm), was employed for cysteine protection as it is stabile to 95% TFA and will cleave and be simultaneously oxidised to the disulfide in the presence of oxidising agents such as iodine.

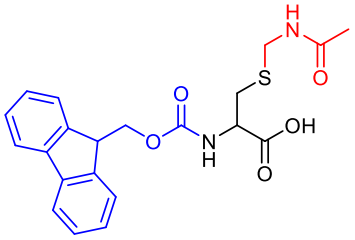

Figure 5-18. Structure of Fluorenylmethyloxycarbonyl-(Acetamidomethyl) Cysteine.

On resin FITC 75 conjugation at the N-terminus undergoes a cyclisation during acid-mediated resin cleavage which cleaves the last amino acid (**Scheme 5-6**).[480] To prevent this a long enough spacer can be introduced which does not readily form the cyclisation product. An aminohexanoic acid (Ahx) spacer was included in the sequence at the N-terminus (denoted X in **Scheme 5-7**) to aid on-resin conjugation in later steps.

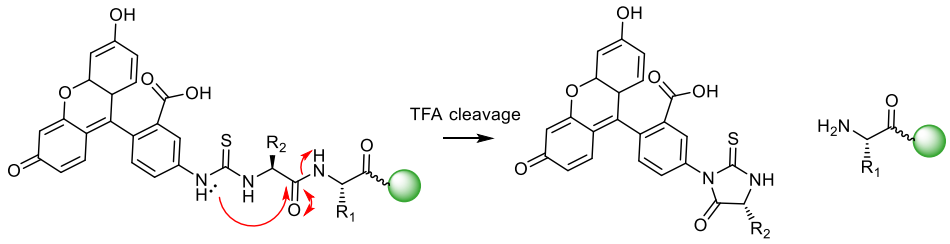

Scheme 5-6. Possible cyclisation upon acid-mediated resin cleavage of N-terminal Fluorescein-conjugated amino acid resulting in removal of cyclised conjugate of fluorescein and terminal amino acid.

The coupling to form CAR peptide 84 was carried out in quintuplet using 100 mg resin per vessel. As recommended for all polystyrene resins, the resin was swollen in dichloromethane (DCM) and reaction was carried out in DMF using an automated synthesiser. Coupling using HBTU and DIPEA is most widely employed, so these conditions were examined first. Amino acids were added to the resin in order of the carbonyl terminal amino acid to the amine-terminal amino acid (**Scheme 5-7**). The resin was treated with 5 equivalents of both the first amino acid (Fmoc-Cys(Acm)-OH) (**Figure 5-18**) and HBTU and 10 equivalents of DIPEA. The coupling reaction was conducted twice for each amino acid before removal of the Fmoc group on the growing peptide on the resin. Fmoc deprotection was conducted using a solution of 40% piperidine in DMF. Although Fmoc is labile to piperidine, it is stable to DIPEA owing to the hindered tertiary amine. The final automated step involved deprotection of the Fmoc group after the coupling of the Ahx amino acid 105 of resin-bound CAR peptide 84.

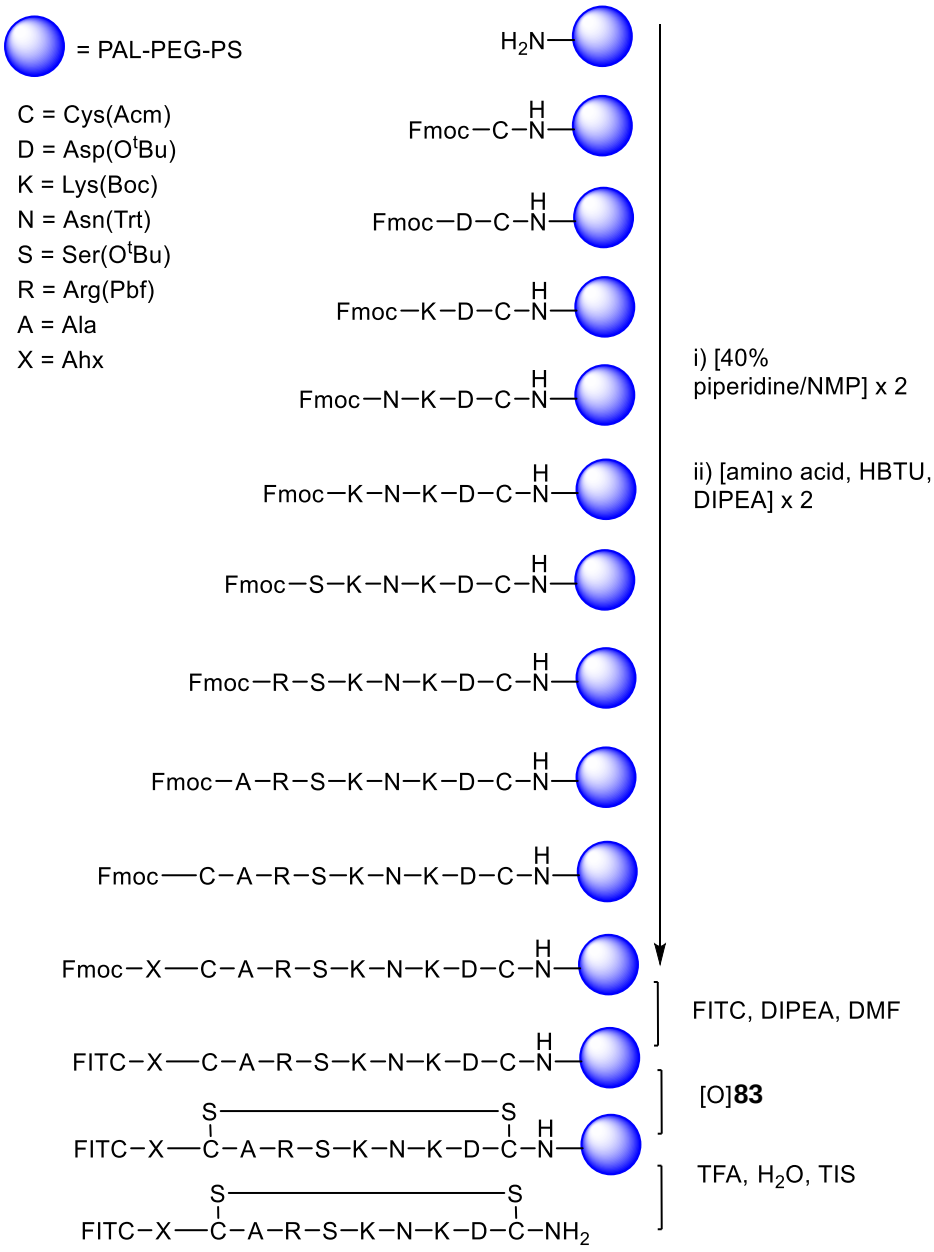

Scheme 5-7. Proposed fluorenylmethyloxycarbonyl (Fmoc)-protected solid phase peptide synthesis (SPPS) of Fluorescein-XCARSKNKDC from corresponding amino acids. The process is automated up until the formation of 84 which is Fmoc-deprotected using piperidine to render the free amine terminus. Fluorescein isothiocyanate (FITC) is then reacted and the cysteine thiols are deprotected and cyclised. TFA = trifluoroacetic acid; TIS = triisopropyl silane; water. Pbf = 2,2,4,6,7-pentamethyldihydrobenzofuran-5-sulfonyl; O^{t}Bu = tertiary butyl ester; Boc = tert-butyloxycarbonyl; Trt = trityl; PAL-PEG-PS = peptide amide linker-poly(ethylene glycol)-polystyrene; NMP = N-methylpyrrolidinone; DIPEA = diisopropylethylamine; DMF = dimethylformamide; [O] = oxidising agent. HBTU =3-[Bis(dimethylamino)methyliumyl]-3H-benzotriazol-1-oxide hexafluorophosphate.

Confirmation of a free terminal amine of **84** was checked with the Kaiser test which involves treating a sample of beads with ninhydrin **85.** Primary amines form an imine compound when treated with ninhydrin (**Scheme 5-8**). The imine is hydrolysed to form a primary amine **86** and aldehyde. The primary amine formed **86** can react with another molecule of ninhydrin **85** to

from an imine-bridging conjugated dimer **87** which results in the solution exhibiting an intense blue colour.

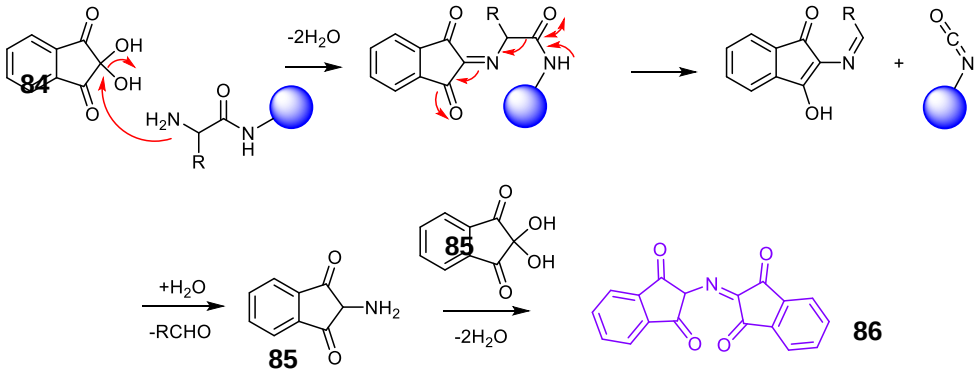

Scheme 5-8. Reaction between primary amine of amino acid on resin solid support and ninhydrin **85** to produce a solution of blue dimer **87** *via* primary amine intermediate **86**. In the absence of a resin-bound amine the reaction cannot proceed and the solution remain colourless.

The resin bound peptide **84** was then conjugated to FITC **78** in DIPEA/DMF and an aliquot of the reaction cleaved from the resin using standard TFA procedure. After drying, HPLC analysis confirmed the presence of one product with the mass of the desired linear CAR(Acm) peptide **89** as the $[M+2H]^{2+}$ ion with mass of 834.3 m/z.

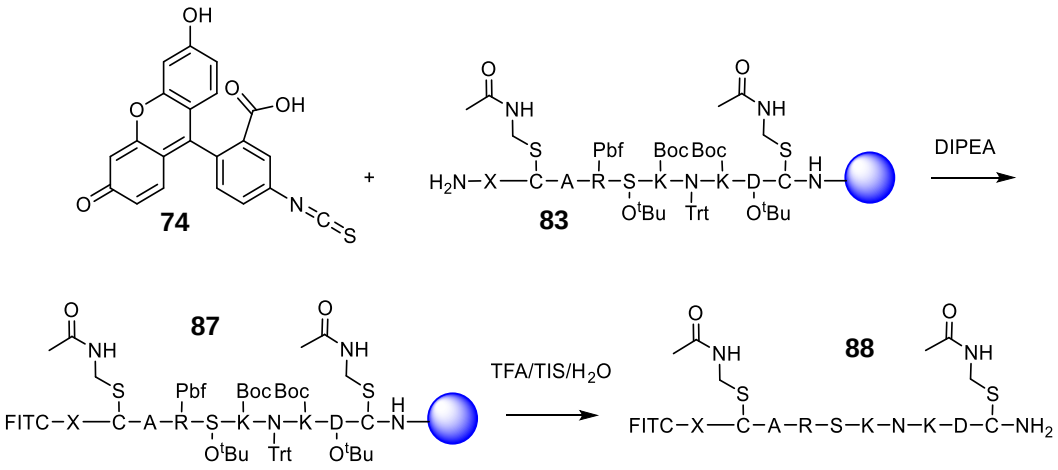

Scheme 5-9. Isolation of linear fluorescein-CARSKNKDC peptide with acetamidomethyl thiol protecting groups **89**. On resin fluorescein isothiocyanate **75** (FITC) conjugation of fluorenylmethyloxycarbonyl (Fmoc) depotected resin bound peptide, **84**. Followed by resin removal and global deprotection of all side chains other than cysteine acetamidomethyl (Acm) thiol protecting group of 88 to form amidated fluorescein-conjugated CARSKNKDC peptide **89**. TFA = trifluoroacetic acid; TIS = triisopropyl silane; Pbf = 2,2,4,6,7-pentamethyldihydrobenzofuran-5-sulfonyl; O^{t}Bu = tertiary butyl ester; Boc = tert-butyloxycarbonyl; Trt = trityl; DIPEA = diisopropyl ethylamine.

One reaction vessel was retained and cleaved using standard conditions to obtain linear FITC-CAR(Acm) **89**. The peptide was purified by preparative HPLC and the eluted fractions collected. The fractions were analysed by analytical HPLC and the pure fractions combined.

The solvent was removed by lyophilisation to yield FITC-CAR(Acm) **89** as an orange glassy solid.

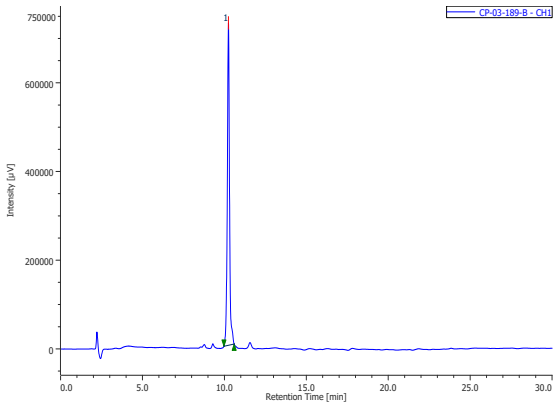

Figure 5-19. Chromatogram of FITC-Ahx-C(Acm)ARSKNKDC(Acm) **89** following purification by preparative high performance liquid chromatography.

Disulfide bonds form between thiols under oxidative conditions. The pKa of a thiol is approximately 5 units lower than the corresponding alcohol (pKa_{SH} = ~8.5 pKa_{OH} = ~15), making thiols weakly acidic.[481,482] As a result, in mild oxidative conditions, thiols can oxidise to form disulfide bonds. Thiol oxidation can be achieved on resin and off resin, post- or during thiol protecting group removal. Depending on the peptide, solution, and concentration, disulphide bonds can form mono-cyclic peptides, dimerization of peptides, polymers or a combination of all three.

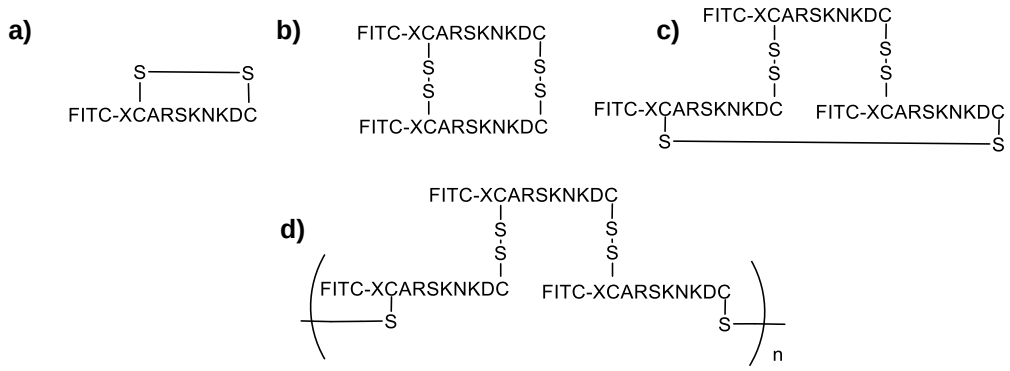

Figure 5-20. Possible cyclisation products, a) monocylised peptide, b) sidulfide CAR peptide dimer c) cyclisation of tripeptide and d) polymerisation by disulfide bond formation.

Cys(Acm) is known to oxidise faster in polar protic solvents, such as water and methanol, compared to organic aprotic solvents such as DCM and chloroform ($CHCl_3$).[483] In rare circumstances, migration of Acm groups (shown in red in **Figure 5-18**) to other side chains including Ser, has been reported.[484] Different conditions including thallium or mercury salt oxidation, presence of acid, trifluoroethanol /chloroform solvent mixtures, are employed to circumvent side reactions and encourage the formation of the desired product. In this case, the disulphide mono-cyclic peptide was sought.

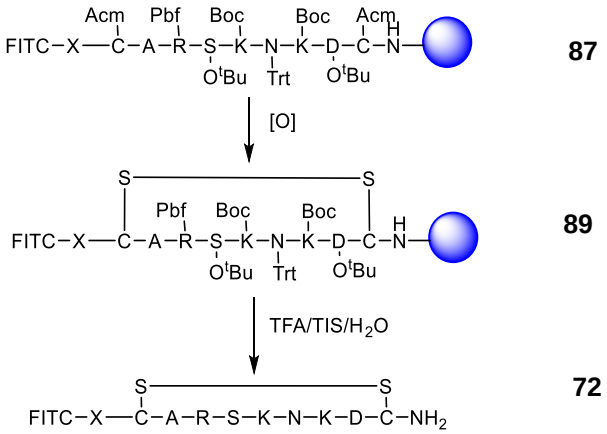

Scheme 5-10. Proposed on-resin cyclisation of fluorescein conjugated CARSKNKDC 88 (FITC-CAR) to form the disulfide bridge of 90, followed by deprotection of the side chains and removal of the resin to form 73. TFA = trifluoroacetic acid; TIS = triisopropyl silane; water. Pbf = 2,2,4,6,7-pentamethyldihydrobenzofuran-5-sulfonyl; O^{t}Bu = tertiary butyl ester; Boc = tert-butyloxycarbonyl; Trt = trityl

Cyclisation with iodine

Iodine is known to oxidise free and Acm-protected thiols. Iodine cyclisation of resin bound peptide 88 was attempted twice; once using DIPEA in DMF on a 22 µmol scale, the other using ammonium acetate in DMF on a 4.4 µmol scale. Both reactions were left for 1 hour before rinsing and drying and removing from resin. The dry yellow solid formed had a mass greater than that expected which suggested that the product was impure and either resin-bound impurities or residual acid may be present. Oxidation of the Acm groups to achieve the disulfide bond in the presence of DIPEA produced multiple products observed by HPLC. The reaction with ammonium acetate buffer following the method employed by Nishino,[485] showed fewer products by HPLC, with one main resonance at 14.3 minutes (**Figure 5-21**).

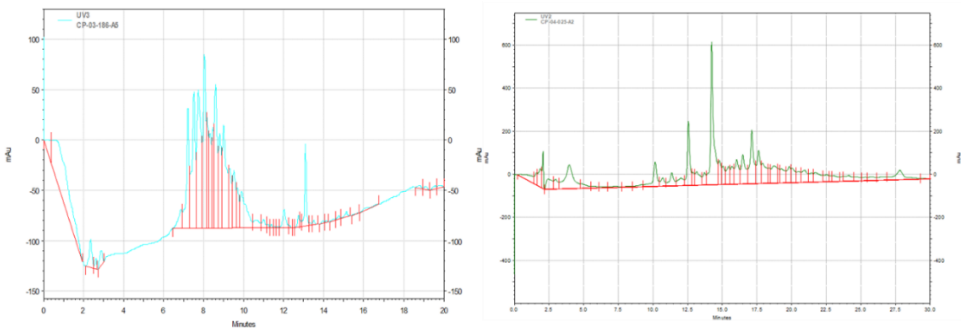

Figure 5-21. Chromatograms of peptide **88** products after cyclisation attempts. The chromatograms show the products formed after on resin cyclisation, A) in the presence of diisopropylethylamine (DIPEA) and B), in the presence of ammonium acetate buffer.

The sample obtained from the cyclisation in the presence of ammonium acetate was analysed by LCMS. However, the UV absorbance was less defined, and no spectral signal was detected corresponding to either the unclycised peptide (Mr = 1521 m/z) or the expected product (Mr = 1523 m/z) or its associated salts (**Figure 5-22**).

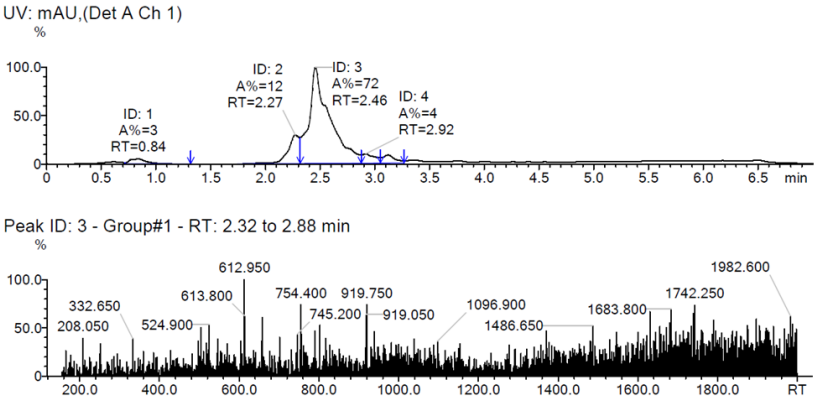

Figure 5-22. LCMS chromatograph of the product obtained following on-resin cyclisation of FITC-CARSKNKDC by simultaneous remocal of (Acm) groups and oxidation of the cysteinyl thiols. The mass spectrum of the main peak did not show any of the uncyclized starting material, expected cyclised product with mass 1523 m/z or its associated salts.

Cyclisation with thallium

Heavy metals are known to bind to the polystyrene mesh, which despite repeated washings become liberated in the acidic conditions of resin cleavage to contaminate the cleaved peptide. Although the use of heavy metals with resin-bound reactions is avoided, thallium had been reported to achieve successful on-resin cyclisations, so was used to examined to investigate if cyclisation of CAR 88 could be achieved. Cyclisation using thallium trifluoroacetate[486] was carried out on a 4.4 µmol scale in DMF for 1.5 hours. The peptide was isolated by cleaving from resin before analysis by HPLC. Multiple resonances were observed indicating unsuccessful cyclisation (**Figure 5-23**).

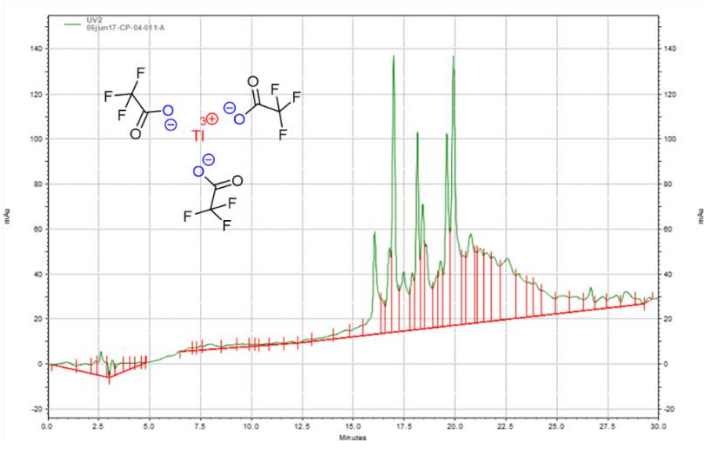

Figure 5-23. The chromatogram showing the result of on resin cyclisation of **88** using thallium trifluoroacetate (shown in inset).

Forming the disulfide bond with the peptide bound to the resin was expected to be easier to purify owing to the ability to rinse away side-products and unreacted reagents. However, HPLC traces revealed multiple products were being formed, thus making it difficult to isolate. Despite the low resin loading, this is likely a result of the proximity of peptides to their neighbour, enabling dimer, trimers and polymers to form. The separation of the different peptide

compounds by HPLC was anticipated to be difficult and time consuming using an analytical column, so before purification was attempted, off-resin cyclisations were trialled.

Linear FITC-conjugated CAR peptide **89** obtained previously was used to attempt the simultaneous deprotection and oxidation cyclisation of the cysteine thiols to form desired peptide **73**. Unlike the on-resin attempts, the side chain protecting groups of amino acids other than cysteine in peptide **89** are not present. To prevent intermolecular disulfide bonds forming, the reactions were run in dilute solvent systems which kept the concentrations low and minimised interaction between peptides.

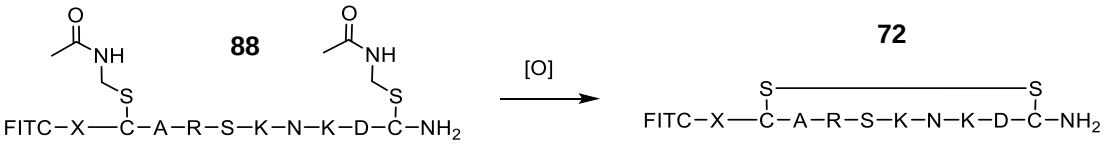

Scheme 5-11. Proposed cyclisation of linear Fluorescein (FITC)-CAR(Acm) **89** to form disulfide bond of **73** through cysteine thiols.

Off-resin cyclisation with iodine

A sample of the linear FITC-CAR(Acm) 89 was used to oxidise the thiols in solution. The cyclisation was attempted on a 1.2 mg scale using 60 equivalents of iodine in MeOH/H_2O (8 mL).[487] The reaction was left for 24 hours and analysed by HPLC. In comparison to linear FITC-CAR(Acm) 89 which has a retention time of 10.2 minutes, the product of the cyclisation either exhibited no interaction with the column and was eluted at the void volume or was not isolated during work-up (**Figure 5-24**).

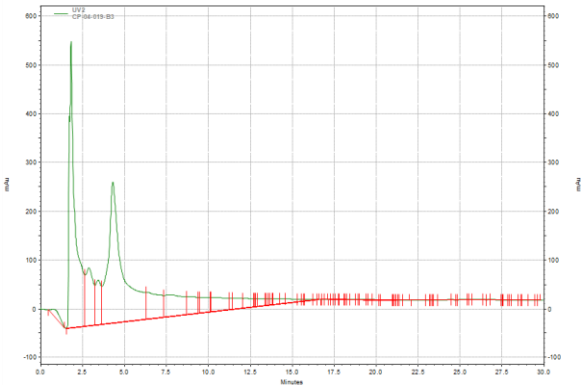

Figure 5-24. Chomatogram of the peptide following off resin cyclisation using iodine. No peak was observed, suggesting the peptide had been lost during wor-up.

Cyclisation with Acm-protected thiols was not as straightforward as anticipated and multiple products were forming, presumably by the close interaction of peptide chains on resin allowing for reactions between different chains. An alternative strategy was sought which would allow for thiol deprotection without simultaneous disulfide bond formation. Synthesis of CAR-peptide **91** was performed using trityl-protected cysteine which is deprotected with mild acid to expose free thiol groups which can be oxidised under milder oxidative conditions. The reaction was

carried out using automated peptide synthesis on a 100 mg scale in duplicate. FITC **75** was conjugated as described before and was deemed successful by a clear result upon Kaiser test, suggesting full conjugation of amine terminus forming FITC-CAR(trt)-Resin **91** had been formed.

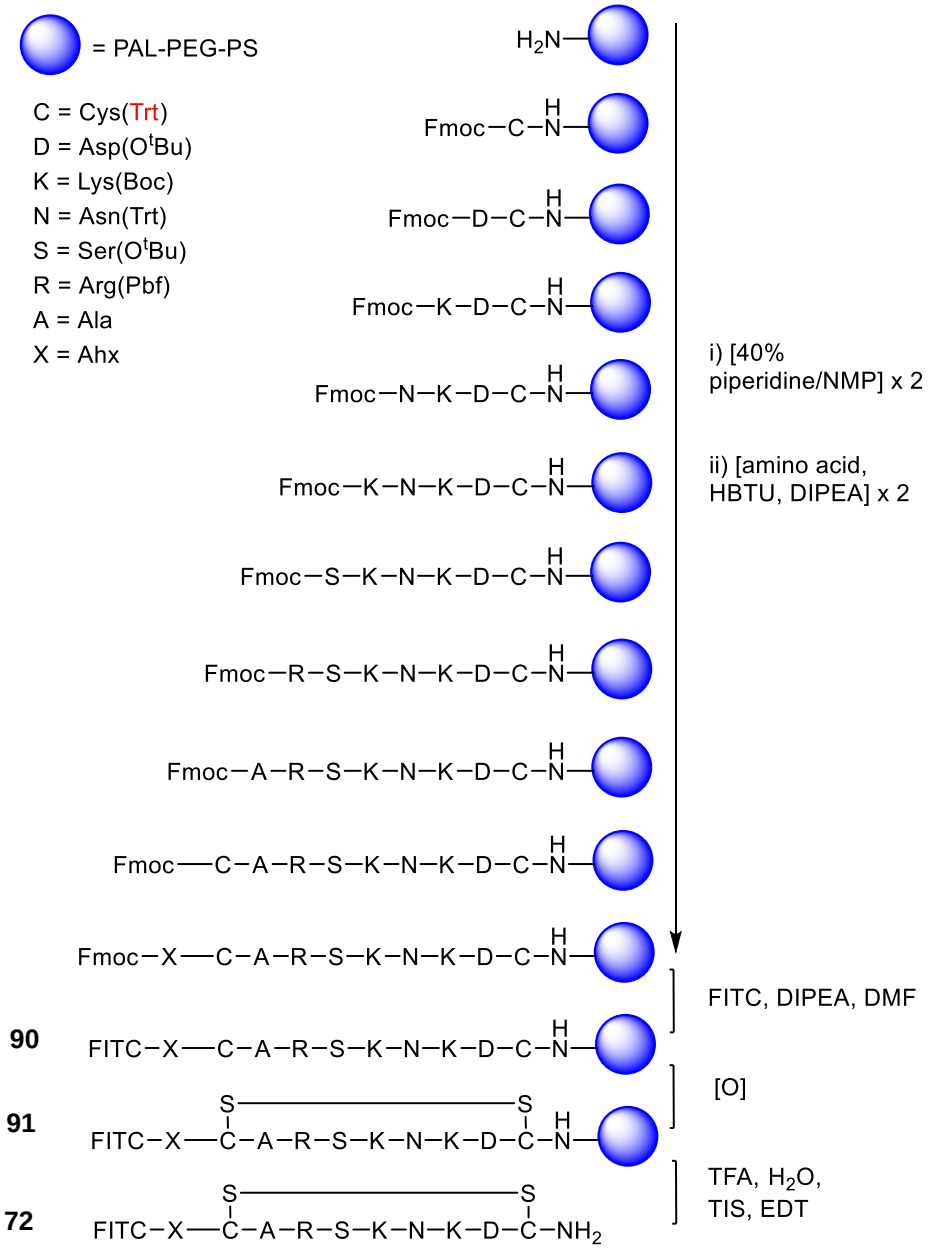

Scheme 5-12. Proposed synthesis of fluorescein-XCARSKNKDC-NH_2 **73** by employing tritylated cysteine (Cys(Trt)) for solid phase peptide synthesis. TFA = trifluoroacetic acid; TIS = triisopropyl silane; EDT = ethane dithiol; Pbf = 2,2,4,6,7-pentamethyldihydrobenzofuran-5-sulfonyl; O^{t}Bu = tertiary butyl ester; Boc = tert-butyloxycarbonyl; Trt = trityl; PAL-PEG-PS = peptide amide linker-poly(ethylene glycol)-polystyrene; NMP = N-methylpyrrolidinone; DIPEA = diisopropylethylamine; DMF = dimethylformamide; [O] = oxidising agent. HBTU =3-[Bis(di-methylamino)methyliumyl]-3H-benzotriazol-1-oxide hexafluorophosphate.

On resin cyclisation of the FITC-CAR **92** using trityl protecting groups for cysteine thiols was attempted to investigate whether a more labile cysteine-protecting group results in more efficient cyclisation to achieve desired peptide **73** (**Scheme 5-13**).

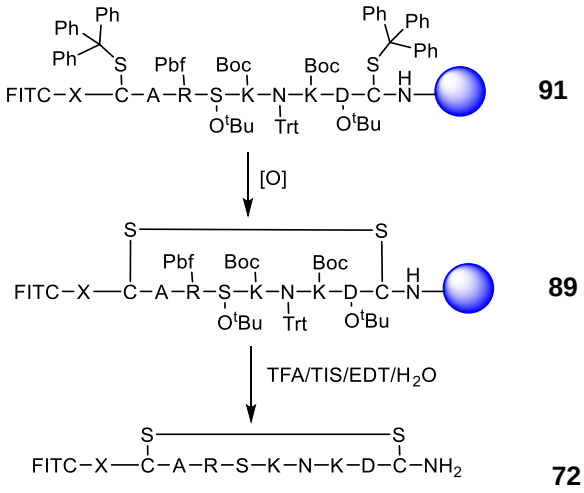

Scheme 5-13. Proposed on-resin cyclisation of fluorescein conjugated CARSKNKDC **92** (FITC-CAR) to form the cyclised peptide **73**. The trityl-protected thiols are simultaneously deprotected and cyclised by oxidation to form the cyclised peptide **90**. The remaining side chain protecting groups are removed during the resin cleavage step to form desired peptide **73**. TFA = trifluoroacetic acid; TIS = triisopropyl silane; EDT = ethane dithiol; Pbf = 2,2,4,6,7-pentamethyldihydrobenzofuran-5-sulfonyl; O^{t}Bu = tertiary butyl ester; Boc = tert-butyloxycarbonyl; Trt = trityl; [O] = oxidising agent.

Iodine oxidation of fully protected peptide **92** was conducted on a 2.2 µmol scale in the presence of DIPEA in DCM which possesses better resin swelling properties so was thought to result in fewer intermolecular disulfide bonds. After two hours, the resin was washed, dried and cleaved. HPLC analysis of the peptide product showed multiple absorbances.

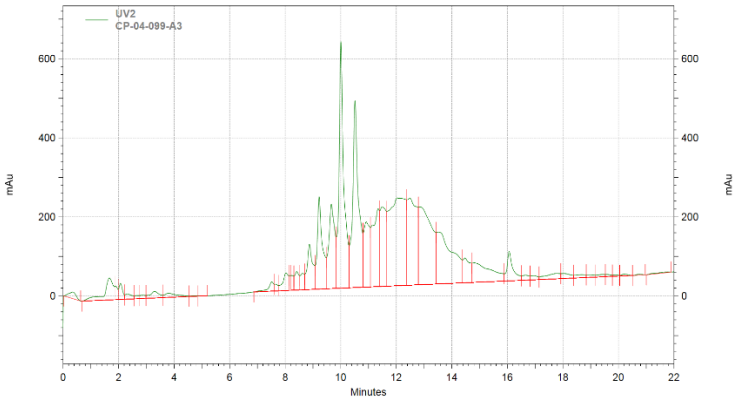

Figure 5-25. High performance liquid chromatogram showing multiple compounds are formed following on resin cyclisation of fluorescein conjugated XCARSKNKDC peptide **92** (FITC-CAR) with trityl protected cysteine thiols using iodine.

Iodine oxidation of FITC-CAR(Trt) **92** was carried out again on the same scale but in DMF without the presence of a base. HPLC analysis of the cleaved product obtained showed many absorbances, with no obvious major product (**Figure 5-26**).

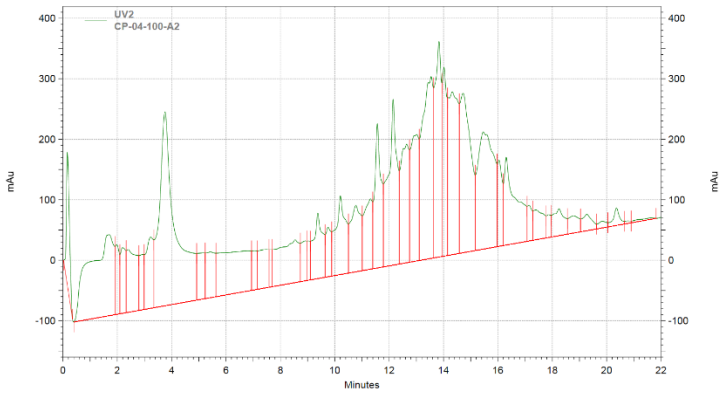

Figure 5-26 Chromatogram of the products formed following on resin iodine cyclisation of the trityl-protected cysteines of fluorescein-XCARSKNKDC **92** (FITC-CAR). Multiple products were detected.

Although cyclisation using thallium is undesirable for reasons explained earlier, the cyclisation of FITC-CAR(trt) **92** using thallium trifluoroacetate **93** was performed out of curiosity as to whether the cyclised product **73** could be obtained by on-resin cyclisation techniques.

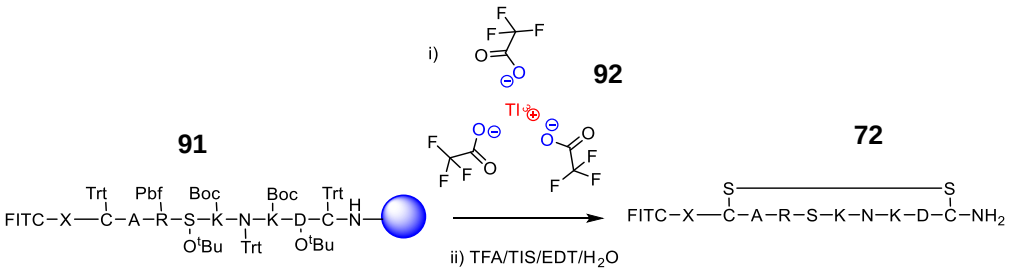

Scheme 5-14. Proposed conversion of fluorescein conjugated XCARSKNKDC (FITC-CAR) **92** to form desired peptide **73**, using thallium trifluoroacetate **93** to form the disulfide bond. TFA = trifluoroacetic acid; TIS = triisopropyl silane; EDT = ethane dithiol; Pbf = 2,2,4,6,7-pentamethyldihydrobenzofuran-5-sulfonyl; OtBu = tertiary butyl ester; Boc = tert-butyloxycarbonyl; Trt = trityl;

Protected FITC-CAR(Trt)-Resin **92** on a 2.2 µmol scale was treated with thallium trifluoroacetate **93** in DMF for 2 hours. HPLC of the resin-cleaved product showed one main resonance at 11.2 minutes (**Figure 5-27**). The identity of the compound corresponding to the main absorbance was not investigated as it was known that the thallium **93** mediated oxidation was not viable for the synthesis of a biologically relevant compound. The result however, indicated that it was possible to form one product predominantly.

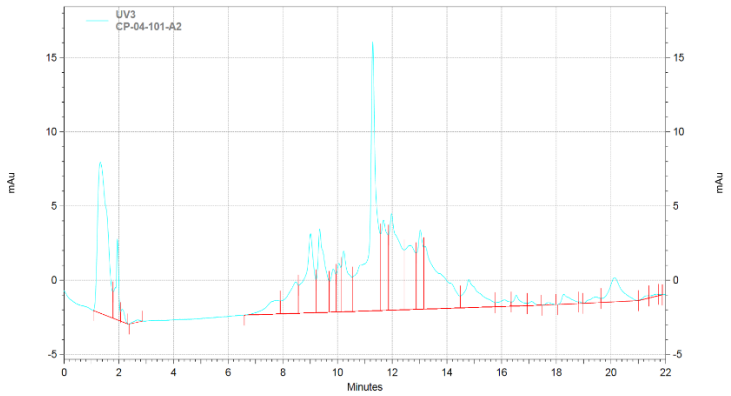

Figure 5-27 Chromatogram of the product isolated from resin following on resin cyclisation of fluorescein conjugated XCARSKNKDC **92** (FIC-CAR) *via* disulfide bond formation between the two trityl-cysteines with thallium trifluoroacetate **93**. Although multiple resonances were observed, one peak dominated.

Meanwhile, investigations were conducted on the solution phase cyclisation of triyl CAR peptide **94**. The remaining resin bound protected FITC-CAR(Trt) **92** was cleaved from the resin using TFA in the presence of triisopropyl silane (TIS), water and ethane dithiol. Treatment of TFA with trityl groups as well as all other side chains, results in removal of the protecting groups and exposure of the amino acid side chain. The presence of ethane dithiol was employed to maintain the reduced state of the trityl-cleaved cysteine thiols and prevent alkylation of the thiols. Once cleaved and lyophilised, the free thiols can be oxidised to form a disulfide bond.

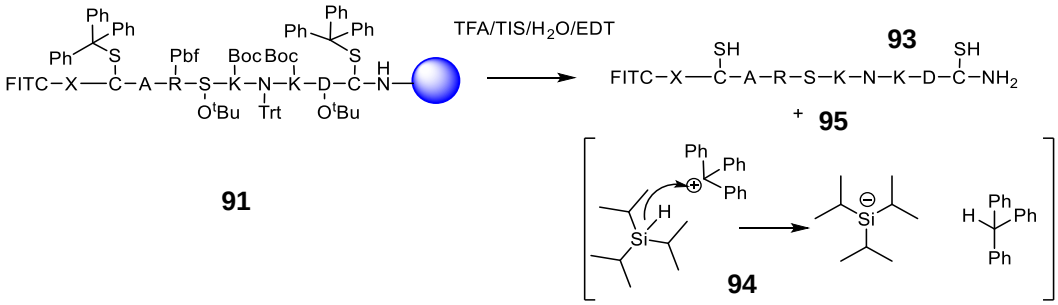

Scheme 5-15. Resin removal and removal of amino acid side chains of fluorescein conjugated CARSKNKDC 92 (FITC-CAR) in the presence of trifluoroacetic acid (TFA), triisopropyl silane **95** (TIS), ethane dithiol (EDT) and water. Removal of cysteine trityl protecting groups results in peptide with free thiols **94** and trityl cation **96** which is sequestered by TIS **95**. Pbf = 2,2,4,6,7-pentamethyldihydrobenzofuran-5-sulfonyl; O^{t}Bu = tertiary butyl ester; Boc = tert-butyloxycarbonyl; Trt = trityl;

Oxidation of unprotected thiols can be governed by thermodynamic or kinetic control. Formation of the kinetically most favourable product is often achieved with iodine. The addition of an iodine solution to the peptide stirring in an organic-aqueous mixture produces a permanent yellow colour when oxidation is complete.

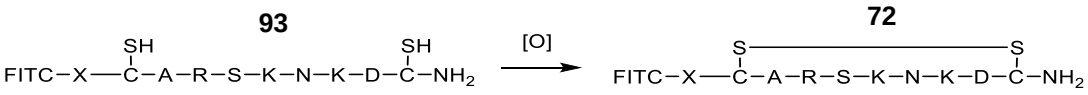

Scheme 5-16. Proposed solution phase cyclisation of fluorescein conjugated CARSKNKDC (FITC-CAR) thiol **94** to form desired cyclised peptide **73**.

Thermodynamic oxidation can be carried out by oxygen. Using atmospheric air is the simplest method, requiring dissolution and stirring of the peptide in a volatile aqueous buffer solution such as ammonium bicarbonate. The slow reaction and dilute concentration used reduces intermolecular reactions and facilitates the cyclisation of peptides. Depending on the peptide sequence, the reaction time varies and can be catalysed by the addition of activated charcoal. Alternative oxidising conditions such as potassium ferricyanide, can also be employed. A 16 mg sample of FITC-AHx-CARSKNKDC **93** was oxidised by dissolution in deaerated ammonium bicarbonate solution (1 M, 32 mL) and stirred at RT for 16 hours. The reaction was monitored by HPLC using a mobile phase 10-60% acetonitrile/water over 20 minutes. The first HPLC sample was analysed after 2 minutes of reaction initiation (**Figure 5-28**).

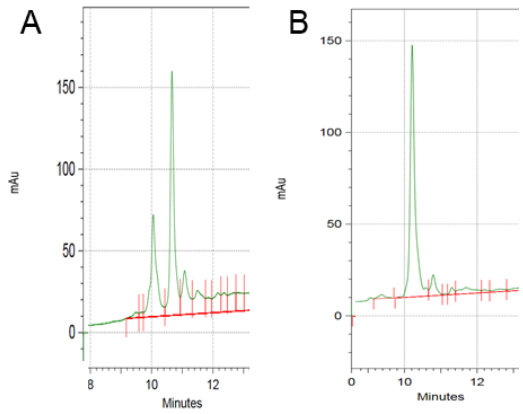

Figure 5-28. Two chromatograms of the air oxidation of the two cysteine thiols to form a disulfide linked, cyclised product. A) is taken immediately after the reaction was initiated and B is following 16 hours. The absorbance at 10.6 decreases as that at 10.2 minutes increases.

Oxidation of thiol FITC-CAR **94** with air and ammonium bicarbonate was deemed complete by HPLC after 16 hours without the need for catalysis. Purification of expected cyclised peptide **73** was carried out by preparative HPLC and the product-containing fractions were dried *in vacuo* to yield a dry orange powder which contained mostly ammonium carbonate salt, as determined by ^{1}H NMR spectroscopy. Upon dilution of the product in water, methanol, acetonitrile, DMSO or various combinations, a red precipitate remained, usually on the glass surface. The yellow solution was run on an analytical HPLC column but did not show any absorption after 20 minutes. Only addition of acetic acid in water solubilised the precipitate. The salt was removed by preparative chromatography. The eluted product was collected in fractions which were checked for purity by analytical HPLC before combining pure fractions.

The solvent was then removed *in vacuo* to yield cyclised FITC-CAR 73 as an orange oil with molecular mass 1523.6 g/mol as confirmed by MS.

Binding of CAR peptide to HUVECs

The selective binding of FITC-CAR had previously been shown *in vitro,* using chinese hamster ovarian cells (CHO-K) and in an in vivo monocrotaline PAH model in rats.[452,453,456] The binding site of CAR was shown to be dependant on the presence of heparan glycan chains on the cells surface. When a CHO-K cell line with defective glycosaminglycan biosynthesis, pgsA-745, was incubated with a CAR-expressing phage, a 50-fold decrease in binding was observed compared to the CHO-K cells.[452] Furthermore, when CHO-K cells were pretreated with heparanase I and III, binding was reduced by 80%. However, this was not measured comparing relative binding in a healthy state versus inflammatory state. To investigate utility of CAR peptide as a disease targeting moiety for the treatment of PAH, an *in vitro* assay was designed to test and compare CAR peptide binding in endothelial cells in a control and pro-inflammatory state.

To extend this concept, CAR binding was measured using an endothelial cell line, human umbilical venous endothelial cells (HUVECs). TNF-α is an inflammatory mediator upregulated in many inflammatory diseases including cancer, irritable bowel disease, depression. Proinflammatory TNF-α is released from a variety of cells, including smooth muscle cells and fibroblasts to induce an inflammatory response.[488] TNF-α is a pro-inflammatory cytokine which by inducing numerous signalling cascades, leads to adhesion of leukocytes, migration of transendothelial cells, vascular leaks as well as promoting thrombosis in vascular endothelial cells.[489] In addition, TNF-α has been implicated in contributing to the pathobiology of PAH, as evidenced in several *in vitro* and *in vivo* models.[490–495] Mechanisms for TNF-α participation in PAH have been investigated. TNF-alpha reduces expression of bone morphogenetic protein type-II receptor (BMPR-II) which is heavily implicated in the progression of PAH. [496] The mechanism is thought to involve an upregulation of NOTCH II signalling, a known pro-inflammatory pathway. Furthermore, TNF-α activates the transcription factor nuclear factor-kappa B (NF-κB) which is a central driver in inflammatory mediated diseases.[497] Antagonism of TNF-α is considered a therapeutic approach for such inflammatory diseases.[498] TNF-α antagonism using recombinant TNF-α receptor II:IgG Fc fusion protein (rhTNFRFc) was shown to attenuate mean pulmonany arterial pressure and remodelling in a monocrotaline-induced PAH model in rats.[499]

Owing to the vast mechanistic changes induced by its presence, TNF-α is used to stimulate controlled inflammatory states, both *in vitro* and *in vivo*. To mimic an aspect of the inflammatory response in PAH, TNF-α was used to initiate an inflammatory cellular response in the binding assay.

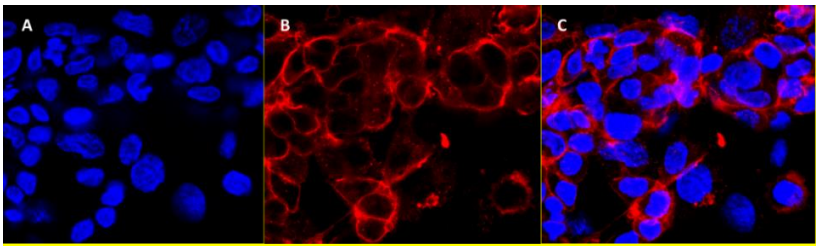

Figure 5-29 Fluorescence image of cultured human umbilical vein endothelial cells. Nuclei are stained blue using DAPI and the endothelial marker, CD31, is visualised in red.

Initially, the FITC-CAR **73** was added to the solution using the concentration reported in the literature (10 μM) as a preliminary investigation into whether fluorescence of the FITC-CAR could be detected. Cultured HUVECs were treated with FITC-CAR (10 μM) in diluted in endothelial cell media in the absence or presence of TNF-α (10 μg/mL) for 24 hours. After staining of the nucleus and fixing of the cells, the slides were analysed by fluorescent microscopy within 48 hours. Excitation and emission wavelengths of 525 nm and 495 nm were used for fluorescein, and 358 nm and 461 nm were used for DAPI.

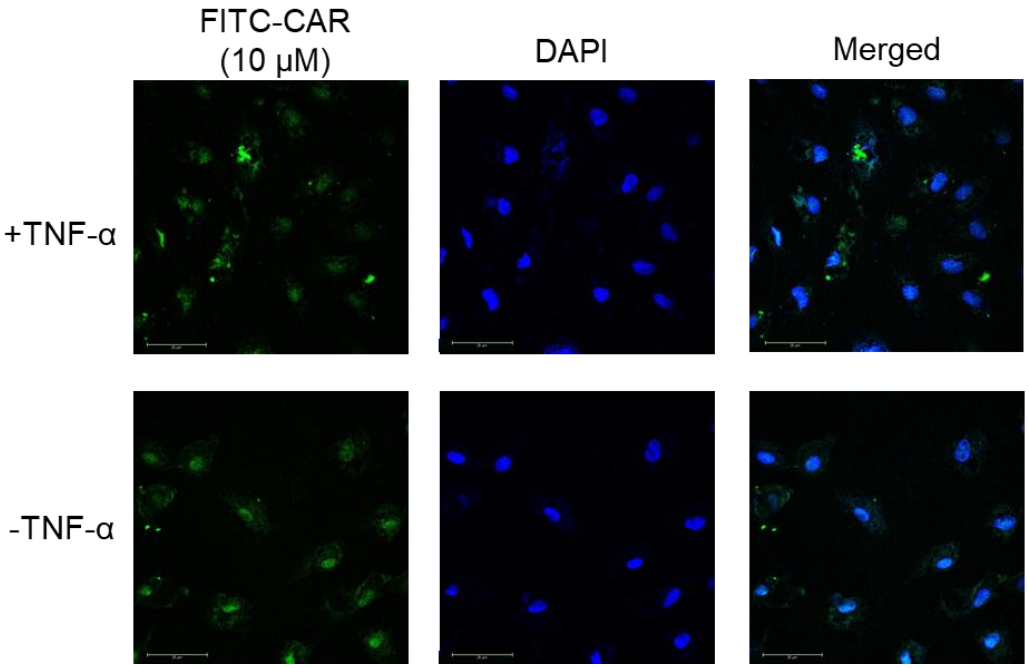

Figure 5-30. Fluorescence microscopy of human umbilical vein endothelial cells (HUVECs) treated with Fluorescein-labelled cyclised CARSKCNKDC peptide (FITC-CAR). HUVECs were treated with FITC-CAR at 10 μM for 24 hours in the presence and absence of TNF-α. FITC-CAR was observed near nuclear regions suggesting internalisation and particularly in the absence of TNF- α, co-localised with DAPI, potentially suggesting oversaturation.

FITC-CAR **73** was visible by fluorescence microscopy and appeared to be localised in the nucleus. By eye, there appeared to be limited difference in the amount of accumulation of FITC-CAR between healthy and inflamed cells and it was questionable whether the

concentration used was oversaturating the cells with FITC-CAR. To investigate this, the reaction was repeated using 10-fold decreasing concentrations of FITC-CAR **73**.

A 10-fold decrease in concentration (1 μM) was used and showed a decrease in the binding of FITC-CAR, showing preference in HUVECs exposed to TNF-α, acting as a surrogate for the inflammation. In comparison to the 10 μM reaction, the CAR-FITC did not seem to accumulate in the nuclear regions and also showed the cytosolic vacuoles.

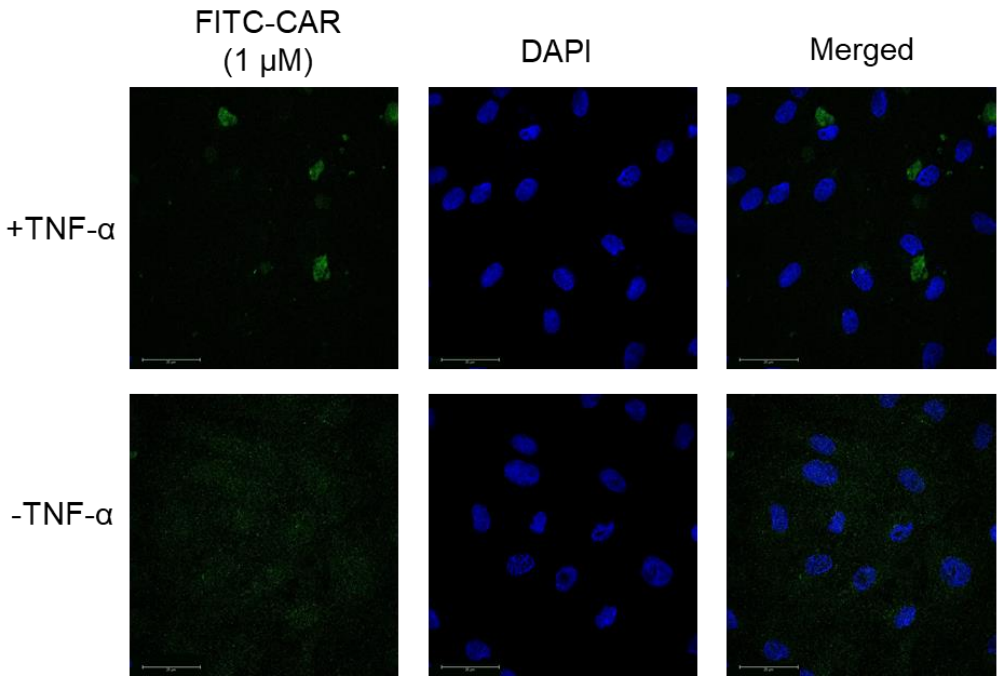

Figure 5-31. Binding of fluorescein-labelled cyclised-CARSKNKDC (FITC-CAR) **73** to human umbilical vein endothelial cells (HUVECs) was investigated at a lower concentration of FITC-CAR (1 μM). Fluorescent microscopy of HUVECs using 494 nm to measure FITC excitation and emission wavelengths of 525 nm and 495 nm emission and 358 nm and 461 nm were used to visualise DAPI-stained nuclei. Specific binding of FITC-CAR was only observed in cells treated with TNF-α. FITC-CAR appeared to be internalised but did not co-localise with DAPI.

At a lower concentration, a clear difference between FITC-CAR binding in a healthy and TNF-α induced inflamed cells was observed. Localisation is not observed in nuclear regions as seen in at 10 μM although bright regions in the near nuclear regions were observed in both. The close proximity of fluorescent emission to the nuclear region suggests internalisation, as previously reported.[452,453] The reaction was also conducted at a 10-fold lower concentration but no fluorescein emission was observed. With hindsight, more information could have been derived from the experiment by employing only half dilution.

Targeting Peptide Summary

A previously reported targeting moiety was synthesised and tested for its use in targeting large macromolecules to the lung. The ability of CAR to home specifically to cells grown in an inflammatory environment, was tested in an *in vitro* cell assay cell assay (HUVECs). The

binding studies were performed using 10 μM of CAR peptide, as conducted in the original CAR peptide literature, however binding was observed in the nucleus in the absence of TNF-α. The reaction was conducted once more at a concentration 10-fold lower which did not show specific binding without TNF- α. At the lower concentration, in the presence of TNF-α, FITC-CAR was shown to localise nuclear region, suggesting the peptide was internalised.

With the data suggesting a change in behaviour when cells were incubated in healthy cells to those in an inflammatory environment, further experiments were planned. In order to conduct a more thorough investigation in the selectivity of CAR binding, a scrambled and polymerised version were designed. Unfortunately, work on the synthesis was initiated but not completed with enough time to conduct biological assays.

5.2.2 Tryptase specific conjugate linker

Treprostinil **4** conjugation to a carrier molecule such as a polymer (or an antibody) requires a linker that is stable in circulation while being degradable in PAH diseased tissue. Linker degradation strategies often employ an enzyme that may be present at the intended site of action.[270] We therefore considered linkers that could be degraded by a proteolytic enzyme that is upregulated in the PAH lung, with minimal expression in healthy tissue. To release treprostinil it was necessary that the enzyme must cleave at either end of a peptide linker and not between two amino acids (**Figure 5-32**).

Figure 5-32. Generic tripeptide showing the terminal amine and carboxylic acid groups. Chemically, conjugation to a drug molecule can occur at either site. Enzymatic cleavage between any two amino acids will not result in drug release. Therefore, a suitable enzyme must cleave either the N- or C- terminus. The site of conjugation will be determined by the enzyme specificity. AA = amino acid, where the number denotes the order of conjugation on resin.

Tryptase and chymase are both serine proteases released from mast cells upregulated in PAH. The tryptase and chymase are released upon mast cell degranulation in response to chronic inflammation. They contribute to the inflammatory response by facilitating collagen formation and tryptase can induce pulmonary fibrosis and contribute to PAH progression.[500,501] Specific substrates of both enzymes have been identified which cleave at the carboxyl terminus. Chromogenic conjugates of the substrates are available for use to identify and quantify mast cells in tissue samples and *in vitro* assays. Upon contact of tryptase, found in the mast cells, the hydrophobic chromophore cleaves to produce a bright colour. The replacement of the chromophore for treprostinil was considered and a similar tryptase specific mechanism for treprostinil released was hypothesised.

Direct conjugation of the treprostinil acid terminus **4**, to the C-terminus of an amino acid is not possible, however a spacer would facilitate conjugation. Tryptase cleaves the amide bond at the C-terminus, therefore a spacer must possess on amine group to facilitate an amide bond to the peptide.

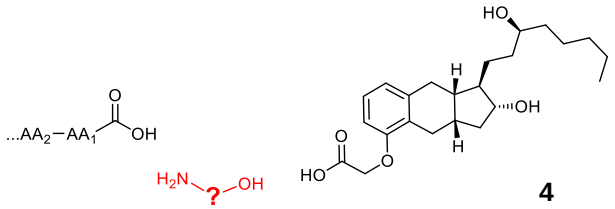

Figure 5-33. The C-terminus of a peptide linker which can form an amide which can be enzymatically cleaved, as well as the C-terminus of treprostinil **4**. It is not possible to conjugate the two moieties directly, so a spacer must be employed (labelled in red).

Conjugation to the treprostinil **4** could be achieved with either an amine or a hydroxyl, to form the amide and ester, respectively. For ease of synthesis, possessing one amine and one hydroxyl will allow for selective reactions at only on end of the molecule. However, conjugation of most simple spacers, e.g. hydroxylamine, or amine terminal triethylene glycol, will facilitate amide cleavage at the N-terminus to release an inactive esterified treprostinil.

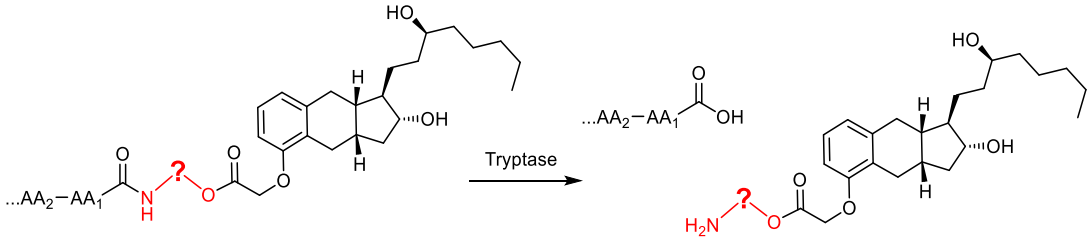

Scheme 5-17. Proposed structure of tryptase substrate-amine linker-treprostinil prodrug. Successful enzymatic cleavage by tryptase of amide bond would release the linker-treprostinil conjugate at the site of release which would still possess minimal activity until treprostinil was released.

Self-immolative linkers are able to overcome the problem of releasing an inactive drug molecule by allowing the first cleavage of tryptase mediated amide cleavage (at the C-terminus) to initiate the second cleavage of ester cleavage (at the treprostinil acid terminus) to release the active drug. Many different immolative linkers have been described in the literature (**Table 5-3**), some using aromatic conjugation to transfer electrons which causes the second cleavage and some using cyclisation techniques to cleave the ester.

Table 5-3. Different self immolative linkers available and described in the literature. Release mechanisms and typical conditions for drug release are shown. TBAF = tetra-n-butylammonium fluoride , DTT = dithiothreitol.

Self-immolative structure	Release conditions
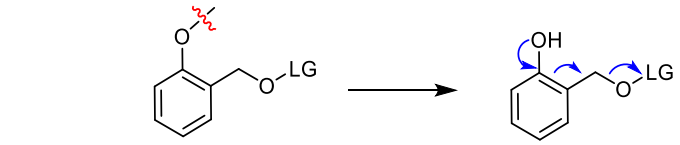	TBAF[502] Light[503]
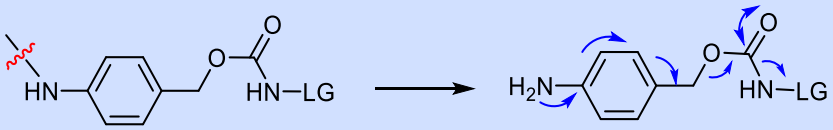	Plasmin[504] Penicillin-G-amidase[505]
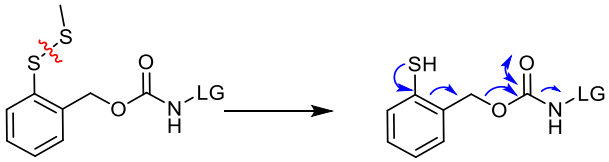	DTT[506]
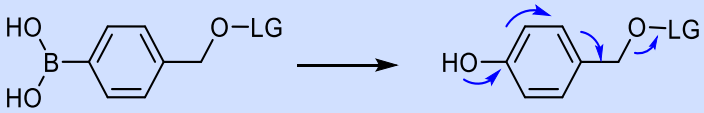	Hydrogen peroxide[507]
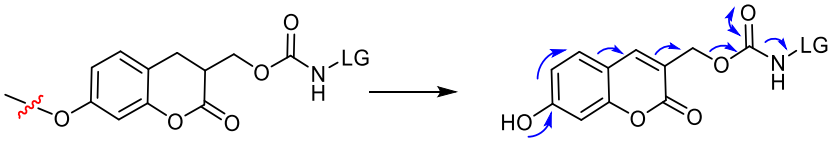	Penicillin-G-amidase[508]
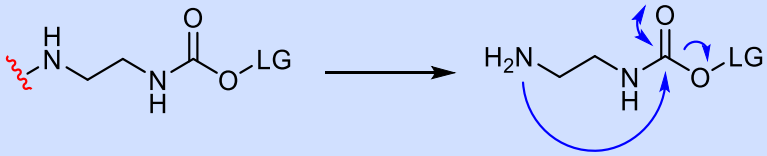	1% HCl[509510] Light[511]
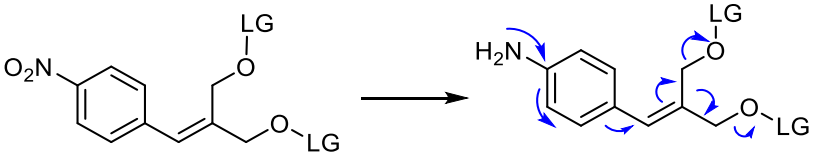	Zn/ethanoic acid[512]
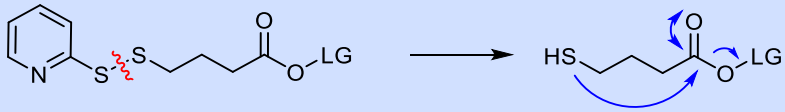	DTT[513]

To facilitate conjugation of treprostinil **4** to the C-terminus of a peptide substrate, the immolative linker, *p*ABA, was incorporated into the linker design.

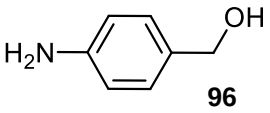

96

Figure 5-34. Structure of *para*-aminobenzyl alcohol (*p*ABA), a self-immolative linker which can employed to link two carboxylic acids together such as the C-terminal of a peptide substrate with treprostinil acid.

The amino group forms an amide bond with the enzyme substrate and an ester bond is formed with treprostinil **4**. Upon cleavage of the amide bond, electrons are transferred through the ring, forming the azaquinone, breaking the carbon-oxygen bond, releasing the treprostinil carboxylate ion.

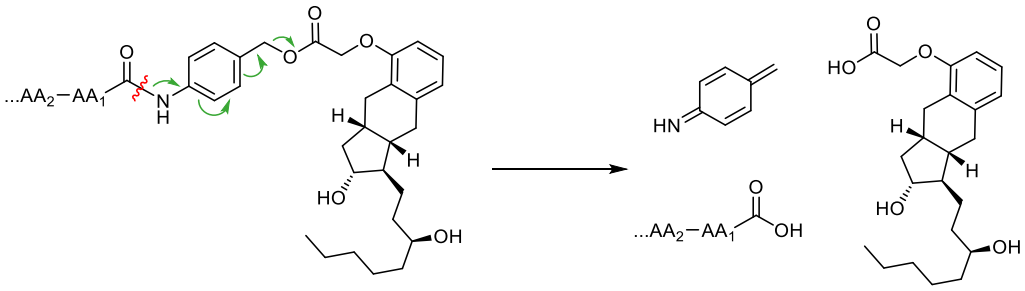

Scheme 5-18. Proposed structure of treprostinil-enzyme substrate prodrug, featuring self-immolative linker, *p*-aminobenzyl alcohol. Upon enzymatic degradation of the amide bond, electrons are transferred through the aromatic ring to release treprostinil 4.

Fluorogenic Tryptase and Chymase substrates

Peptide substrates of tryptase and chymase can be obtained from commercial suppliers (**Table 5-4.**). Based on most structures available tryptase is dependent on the C-terminal amino acid possessing a cationic side chain (i.e. lysine or arginine). The substrates are C-terminal conjugated to a fluorescent chromophore which when cleaved by their respective enzyme releases the chromophore for visualisation. The substrates are used to determine and quantify the presence of tryptase or chymase within a tissue. The substrates are expensive but could be synthesised readily by SPPS without the chromophore. The presence of the chromophore would be an ideal strategy to test the activity of tryptase as a negative control. However, as well as cost, purchasing the available substrates would not facilitate an option to test the immolative linker between the chromophore and the peptide. Furthermore, solution phase conjugation of peptide substrate to an immolative linker and then to either treprostinil or a chromophore at the C-terminus would require the amino acid side chains to be protected. The unsuccessful experience of conjugating FITC **75** to side chain protected CAR peptide **73** paired with the ease and cost efficiency of automated solid phase peptide synthesis led efforts down an in-house synthesis route. With the intention of using these substrates for a prodrug appendage, initial proof was sought that the tryptase/chymase substrates would cleave in the presence of their respective enzyme. In addition, an investigation into the relative cleavage rates when attached with the drug via a self immolative linker was planned.

Table 5-4. Commercially available peptides. AMC = 7-amido-4-trifluoromethylcoumarin. *p*NA = *para* nitrolaniline; Ac = acetyl; Tos = tosyl; Boc = tert-butyloxycarbonyl

Peptide substrates	Suppliers
H-Orn-Phe-Arg-AMC	Sigma Aldrich
Ac-Lys-Pro-Arg-AMC	Sigma Aldrich
Tos-Gly-Pro-Lys-pNa	Bachem
Z-gly-Pro-Arg-pNa	Bachem
Pyr-Pro-Arg-pNA HCl	Bachem
H-Leu-Thr-Arg-pNa	Bachem
H-D-Ile-Phe-Lys-pNA trifluoroacetate	Bachem
Boc-Val-Pro-Arg-AMC HCl	Bachem
Phe-Ser-Arg-AMC acetate	Bachem

Five substrates reported in the literature and listed as commercially available were selected to be synthesised by SPPS (below). Initially, the peptides would be conjugated to a chromophore and then would be conjugated to treprostinil *via* a self immolative linker.

Ac-Orn-Phe-Arg-OH

Z-Gly-Pro-Arg-OH

Ac-Lys-Pro-Arg-OH

H-Ala-Ala-Pro-Ile-Arg-Asn-Lys-OH

Suc-Phe-Pro-Phe-OH

Loading of chromophore onto resin

Many of the commercial substrates contained a fluorescent marker at the C-terminal to make quantification of enzymatic cleavage possible. In order to synthesise the substrates, above, on-resin, a chromophore with amino acid groups (amine and carboxyl group) was required. The amino acid derivative of the common fluorescent chromophore 7-aminocoumarin-4-acetic acid (ACA, also known as ACC) was commercially available. The Fmoc derivative **103** (Fmoc-ACA-OH) was purchased which could be loaded onto a resin using following the usual Fmoc based strategy in the presence of coupling agents. Two resins were reported in the literature, Wang and Rink amide AM, although better results were reported for Rink amide AM.[514] For this reason, as well as inefficient yields obtained using Wang resin,[515] Fmoc-ACA-OH **103** was reacted with rink amide AM resin. The loading of the batch of Rink amide resin was 0.7 mmol/g so for totally efficient loading of Fmoc-ACA-OH **103** to 100 mg of resin would result in 31 mg immobilised onto the resin. For efficient coupling, the reaction of carried out in duplicate. For each coupling, a minimum of 2 equivalent of Fmoc-ACA-OH **103** is required, therefore ~120mg of Fmoc-ACA-OH is required to achieve only 30 mg immobilised on the resin.

Table 5-5. Chromogenic substrates using 7-amino coumarin acetic acid as the chromophore which can be loaded onto the resin and facilitate peptide growth. Ac = acetyl; Z = carboxybenzyl; H = free N-terminal amine; Suc = succinic acid.

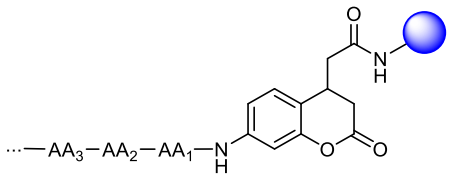

Substrate	N-terminal group	AA_7	AA_6	AA_5	AA_4	AA_3	AA_2	AA_1
97	Ac	-	-	-	-	Orn	Phe	Arg
98	Z	-	-	-	-	Gly	Pro	Arg
99	Ac	-	-	-	-	Lys	Pro	Arg
100	H	Ala	Ala	Pro	Ile	Arg	Asn	Lys
101	Suc	-	-	-	-	Phe	Pro	Phe

Loading of Fmoc-ACA **103** was initially attempted by coupling with disopropyl carbodiimide thrice, following the procedure described by the manufacturer.[516] The first coupling was erroneously conducted in DMF, which was substituted for a mix of DCM/DMF (7:3) for the following reactions. DMF has been shown to facilitate formation of the *N*-acylurea **24** in carbodiimide-mediated coupling. Colourimetric Kaiser testing for the presence of the unreactive amine produced a positive intense blue result, indicating that the coupling had not proceeded as expected.

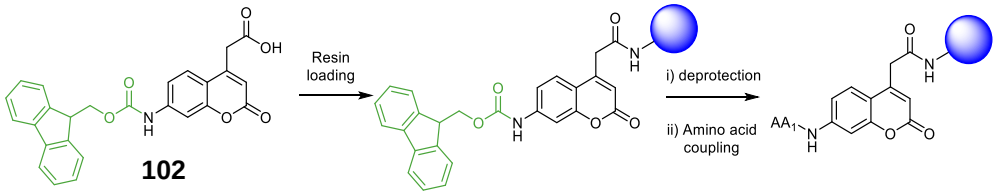

Scheme 5-19. The proposed method of employing aminocoumarin acetic acid (**103**) as a terminal chromophore amino acid.

Given the aliphatic nature of the carboxylic acid moiety of Fmoc-ACA **103**, coupling to a resin was not anticipated to be problematic. Therefore, standard SPPS coupling conditions, HBTU/DIPEA, were employed, but coupling was not successful, as determined using the Kaiser test. Further attempts with HBTU/DIPEA included the catalytic additive HOBt **27**, although Kaiser test revealed that the coupling had still not progressed.

To determine the reason for the unsuccessful resin loading, the resin and coupling reagents were investigated. A sample was taken from the failed coupling, rinsed and placed into a vessel with a simple amino acid, Fmoc-Ala-OH **146**, using the same coupling reagents (including same batches). The following morning, the coupling was deemed complete by

ninhydrin test. This provided assurance that the resin and reagents were suitable for coupling and signalled a problem with the Fmoc-ACA-OH **103**.

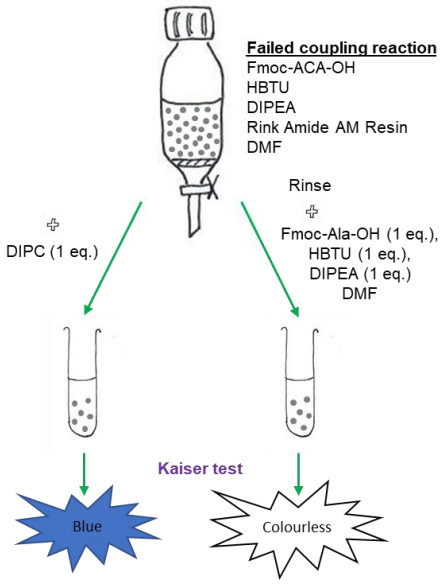

Figure 5-35. Sample reactions trialled to ascertain whether the failed coupling of Fmoc-aminocoumarin acetic acid was a result of the coupling reagents or the acid reagent. One sample was treated with additional coupling agent, diisopropylcarbodiimide (DIPC) which remained blue when a Kaiser test was performed indicating no coupling had occurred. The right-hand arm sample was rinsed with dimethylformamide (DMF) and treated to the same reagents (including the same batches of HBTU and DIPC) but with an alanine amino acid, in dimethylformamide. After 18 hours, Kaiser test revealed a negative result indicating that the coupling had occurred successful to leave no unreacted amines. HBTU = 3-[Bis(dimethylamino)methyliumyl]-3H-benzotriazol-1-oxide hexafluorophosphate; DIPEA = diisopropylethylamine

An investigation into the structure of the chromophore acid **103** was conducted. TLC showed one major spot with R_f 0.62 which was UV active but did not stain with bromocresol blue which should stain yellow in the presence of protons with pKa < 3. ^{1}H NMR indicated the presence of the expected number of protons; the aliphatic and aromatic resonances of the Fmoc group, the acidic proton. The broad singlet with chemical shift 12.8 ppm confirmed the presence of an acidic proton belonging to a carboxylic acid. However, the methylene proton was not observed in the expected region of ~2.9 ppm. A singlet was observed at 3.9 ppm but integrated to 1.5 protons instead of 2 (yellow in **Figure 5-36**).

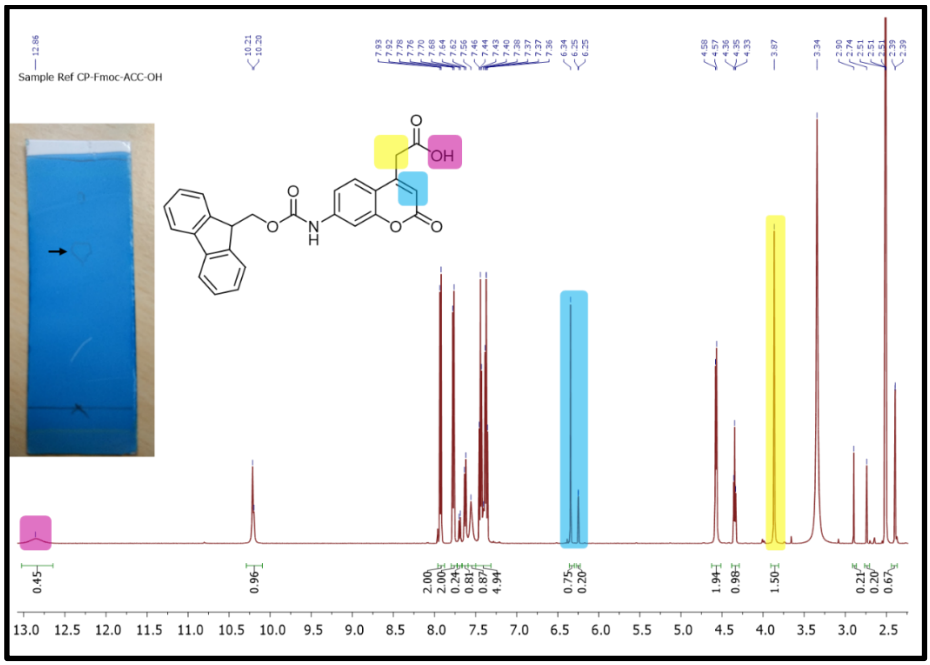

Figure 5-36. ^{1}H NMR spectrum of Fmoc-aminocoumarin acetic acid **103** (Fmoc-ACA-OH). The expected protons are present but do not integrate to the number expected from the structure. Inset image of Fmoc-ACA-OH analysed by thin layer chromatography which did not stain yellow, expected of carboxylic acid compounds.

Resonant structures of Fmoc-ACA-OH **103** are possible (**Scheme 5-20**), particularly in basic conditions (DIPEA), which would explain the reduced peak integration and the observed inactivity during coupling. Deprotonation of one of the benzyl methylene (labelled blue, **Scheme 5-20**) could explain the reduced integration as it becomes unsaturated. However, this would be accompanied with a singlet resonance found closer to the aromatic region, which was not observed.

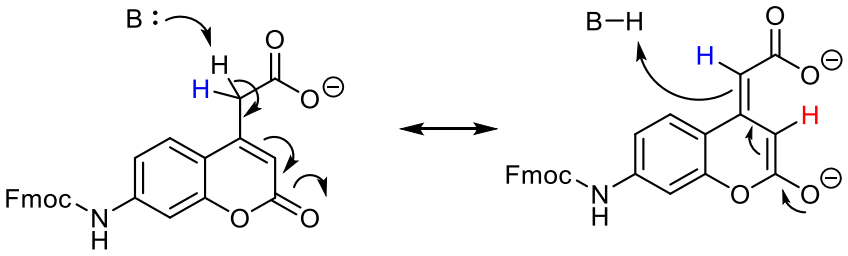

Scheme 5-20. Possible resonant forms of Fmoc-ACA-OH 103 showing the different protons which could alter the ^{1}H NMR spectrum and the structure deduced through its interpretation. The acidic proton is labelled in blue and the aromatic proton is labelled in red.

The cyclic alkene proton in the ACA adduct **103** (labelled in red, **Scheme 5-20**), would also be expected to have split into additional downfield resonances, which was also not observed.^{13}C NMR showed a short resonance at 162.2 ppm which, may represent the acidic carbonyl (**Figure 5-37**). FTIR confirmed an absorbance at 1735 cm^{-1} which represents the stretching frequency of the acid carbonyl as well as a broad absorbance at 2972 cm^{-1} which

indicates the presence of hydrogen bonding hydroxyl groups including those of a carboxyl acid. Additionally, the observed broad band in the region of 2972 nm, corresponding to the O-H bond stretch of an acid, suggested the compound to have the expected moieties.

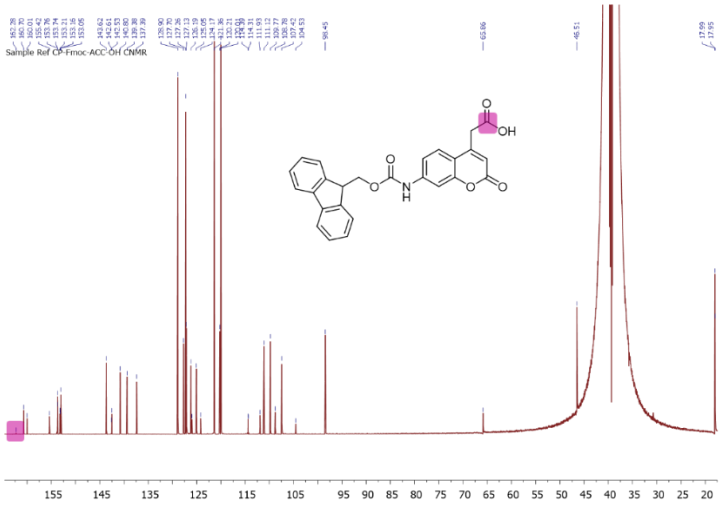

Figure 5-37. ^{13}C NMR spectrum of Fmoc-aminocoumarin acetic acid 103 (Fmoc-ACA-OH) indicating the presence of an acid carbon

To be certain the acid moiety of Fmoc-ACA-OH **103** was present, a functional test was performed by attempting to esterify the acid. Fmoc-ACA-OH **103** was stirred overnight in ethanol (with minimal DMF to aid solubilisation) in the presence of catalytic sulphuric acid (2 drops). Following a 16-hour incubation and work up into ethyl acetate, the proton NMR spectrum revealed a triplet at 1.19 ppm and a quadruplet with chemical shift 4.12 ppm, corresponding to the expected ethyl ester protons of the esterified acid (**Figure 5-38**).

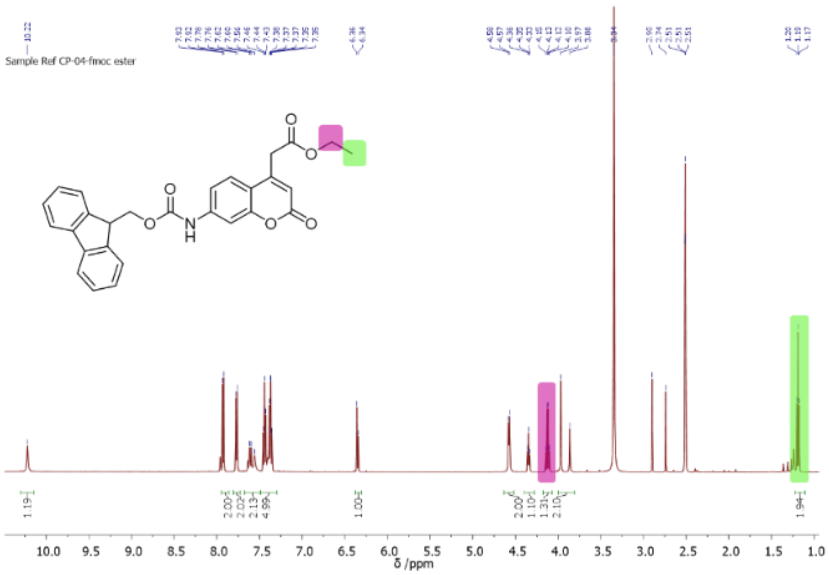

Figure 5-38. Proton NMR spectrum for the esterification product of Fluorenylmethyloxycarbonyl-7-aminocoumarin-4-acetic acid **103**, showing the correct integration for methylene and methyl protons, highlighted in pink and green

respectively. Successful esterification indicates that the acid group of chromophore **103** is present.

It was confirmed that the acid was present on Fmoc-ACA-OH **103**, which suggested that either the acid was much less active than initially expected or that a steric effect caused by the close proximity to the aromatic Fmoc-ACA **103** to the resin loading functionality was preventing successful interaction and coupling reactions. To investigate the role of steric hindrance in coupling Fmoc-ACA-OH **103** to Rink Amide AM resin, aminohexanoic acid **105** (Ahx), used a short chain spacer, was first coupled to the resin. Resin was successfully coupled to Fmoc-Ahx-OH **105** to afford the free amine Ahx-bound resin **104**. The resin bound Fmoc as deprotected and Fmoc-ACA-OH **103** was coupled using HBTU/DIPEA chemistry and left for a total of three days (**Scheme 5-21**). Reaction progression by Kaiser test revealed a blue solution, indicating negligible coupling to free amine of Ahx moiety.

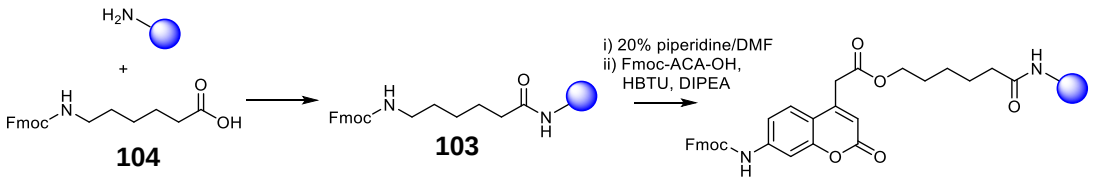

Scheme 5-21. Coupling of aminohexanoic acid **105** (Ahx) to Rink Amide AM resin to afford the resin bound Ahx **104** to reduce steric hindrance for subsequent coupling to Fmoc-aminocoumarin acetic acid **103** (Fmoc-ACA-OH) in the presence of N,N,N′,N′-Tetramethyl-O-(1H-benzotriazol-1-yl)uronium hexafluorophosphate (HBTU) and diisopropylethyl amine (DIPEA).

The reason for the unexpected low reactivity of Fmoc-ACA-OH 103 could not be determined. Synthetic efforts to make tryptase substrates **97**-**101** utilising Fmoc-ACA-OH 103 were terminated and an alternative approach was sought.

Amino acid bound fluorescent moieties

A chromophore was required to determine cleavage of the peptide substrate. Tryptase cleaves its substrates at the C-terminus which during synthesis is where the resin is attached. The obvious solution was to employ chromogenic amino acids but one such attempt was not successful. Chromogenic amino acids are expensive, so a more cost-effective solution was sought (**Figure 5-39**).

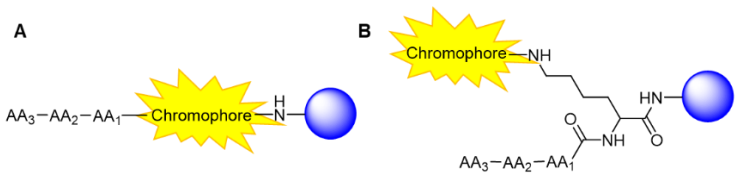

Figure 5-39. Ways considered to append a chromophore to the C-terminus of tryptase substrate sequences. A) Direct linkage of the chromophore to the resin and B) conjugation of chromophore to a lysine side chain.

Instead of direct conjugation of the chromophore to the resin from which a peptide substrate can be appended, a lysine with a chromophore attached to the side chain can be conjugated to the C-terminus (**Scheme 5-22**).

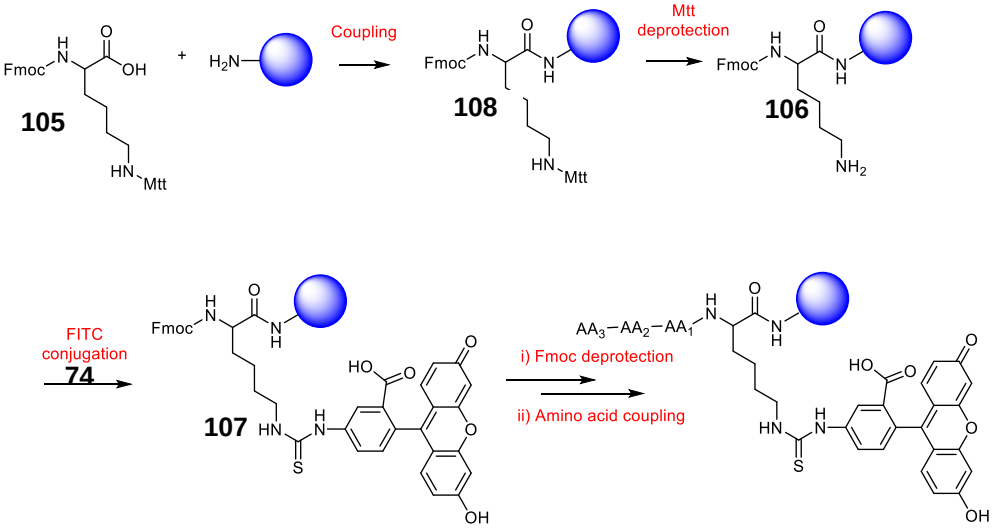

Scheme 5-22. Proposed synthesis of substrates with fluorescein isothiocyanate **75** (FITC) conjugated through the side chain of an additional lysine residue **106** to afford a resin-bound chromophore **108** to which substrates can be conjugated. Coupling of the first lysine derivative is carried out using standard coupling techniques. Lysine side chain protecting group 4-methyltrityl (Mtt) is weakly acid labile allowing for lysine deprotection without resin cleavage. The resulting side chain amine can be coupled to FITC **75**. Following fluorenylmethyloxycarbonyl deprotection of resin chromophore **108**, tryptase substrates can be synthesised.

Mtt sidechain-protected lysine **106** was linked to Rink Amide AM resin using standard HBTU/HOBt/DIPEA conditions.[517] Once complete, the lysine side chain of resin-bound lysine **109** was deprotected using TFA/TIS in DCM under an argon environment to afford the free amine derivative **107**. Removal of Mtt releases methyl trityl cation which is yellow. TIS **95** is added to the cleavage cocktail to quench the cation so over time the yellow colour fades. The resin was washed with the solution until no yellow colour was produced upon addition. FITC **75** was then coupled onto the side chain amine in the presence of DIPEA in an argon environment. The dried resin **108** was split into 5 equal portions and tryptase and chymase substrates were built onto them, incorporating in a final Fmoc deprotection step on the peptide synthesiser to liberate the N-terminal amines.

Table 5-6. Chromogenic substrates using fluorescein conjugated the side chain of a C-terminus lysine as the chromophore, allowing for immobilisation on the resin and facilitating peptide growth. Ac = acetyl; Z = carboxybenzyl; H = free N-terminal amine; Suc = succinic acid.

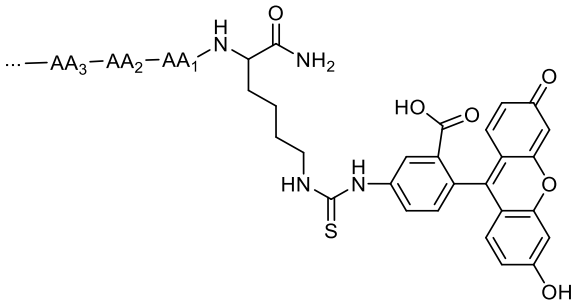

Substrate	N-terminal group	AA_7	AA_6	AA_5	AA_4	AA_3	AA_2	AA_1
109	Ac	-	-	-	-	Orn	Phe	Arg
110	Z	-	-	-	-	Gly	Pro	Arg
111	Ac	-	-	-	-	Lys	Pro	Arg
112	H	Ala	Ala	Pro	Ile	Arg	Asn	Lys
113	Suc	-	-	-	-	Phe	Pro	Phe

To replicate the substrates commercially available and thus known to be active, of the five substrate variations prepared, three required post-sequence N-terminal modifications with either acetic anhydride or succinic anhydride. The carboxylbenzyl group (Z) was added by coupling Z-glycine. Kaiser test was performed to confirm successful N-terminal capping. Peptides were then rinsed, cleaved and isolated using standard procedures.

Lysine(FITC) substrate derivatives **109**-**113** were synthesised as an alternative to the ACA derivatives attempted unsuccessfully with the immobilisation of Fmoc-ACA-OH **103**. Side chain conjugation of FITC to lysine was achieved easily without issues. Enzymatic cleavage of the C-terminal amide bond of the substrate releases the Lysine-FITC conjugate. However, no change in absorption is associated with the release making monitoring enzyme activity, and thus substrate specificity, not possible by spectroscopic methods. No changes in UV absorption occurs over time. To be able to monitor the rate of substrate cleavage, HPLC analysis would be required. In order to measure multiple time points, multiple solutions would need to be incubated with enzyme, quenched and analysed. Before committing time to the analysis, efforts were dedicated to the conjugation of treprostinil to the substrate.

Treprostinil-tryptase substrate

The substrates identified in **Table 5-4** were designed for use as a prodrug appendage to the carboxylic acid of treprostinil, thus on-resin synthesis of the substrates which could be conjugated at the C-terminus to treprostinil, was considered simultaneously (**Scheme 5-23**).

For proof of concept a simple self-immolative linker was sought and the p-aminobenzyl alcohol **97** was employed. Cleavage of the amide bond by enzymatic degradation allows the amine electrons to resonate through the aromatic ring to form the azaquinone methide and break the C-O bond, releasing the free acid of treprostinil 4.[255]

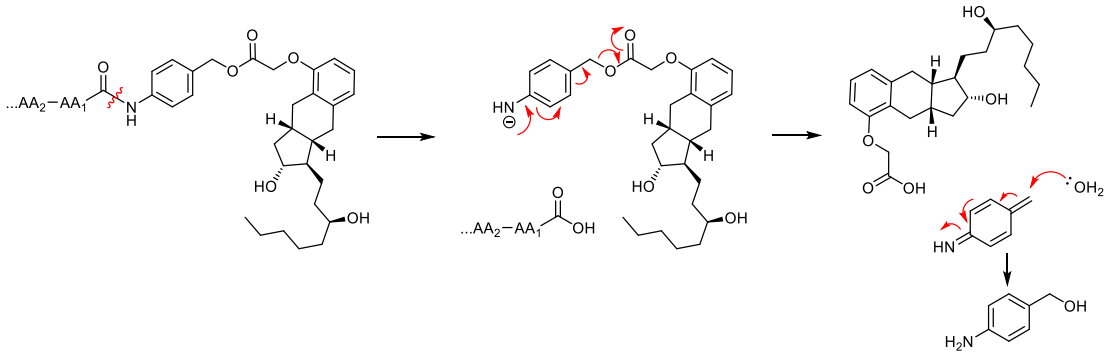

Scheme 5-23. Enzyme initiated cleavage of the amide bond causing electrons to be transferred through a resonant form which results in ester cleavage to release treprostinil **4**.

To restrict the resonance of the amine electrons into the aromatic ring, the amine must be coupled first. Amines are usually more nucleophilic than their hydroxyl counterpart, so protection of the alcohol is often not warranted. However, non-nucleophilic, weakly basic amines are more similar in pKa and reactivity to an alcohol. This results in the coupling being less readily afforded than an aliphatic amine and the requirement of hydroxyl protection to afford the correct product.

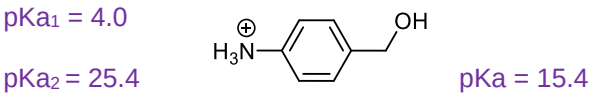

Figure 5-40. Structure of *p*-aminobenzyl alcohol **97**. Although the pKa_2 of the amine is greater than that of the alcohol, the available lone pair which can resonate into te ring, increases the electronegativity and makes it a better nucleophile.

For *p*ABA **97**, the pKa of the ammonium and alcohol are 9.4 and 15.4, respectively so the ammonium is more readily deprotonated owing to the aromatic resonance. Once the amide bond is formed and the peptide grown **116**, the reaction of the alcohol with treprostinil **4** to afford the treprostinil ester **115** can be attempted, which may or not require a deprotection step beforehand. It was noted at this point that the final structure would involve a treprostinil ester bond in the presence of free amine on the lysine side chains which may undergo substitution to cause premature release of treprostinil. Therefore, the protonated salt of the compound would need to be considered as the final compound. To support the overall concept that treprostinil could be linked to a carboxyl terminus *via* an immolative linker, the feasibility of the required steps was examined (**Scheme 5-24**).

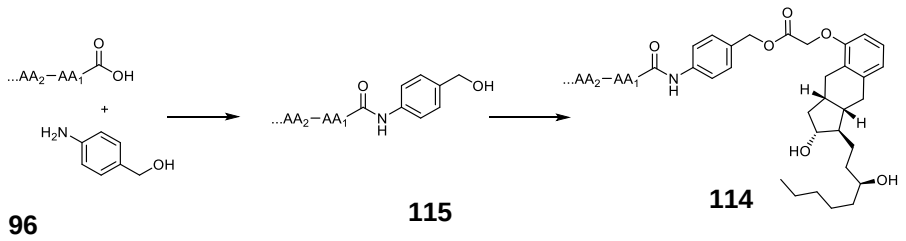

Scheme 5-24. Conjugation of *para*-aminobenzyl alcohol 97 to the carboxylic acid of a substrate peptide to form the aromatic amide 116 which can then undergo esterification of treprostinil to form the final conjugate 115.

Coupling of the aniline amine of *p*ABA **97** to a carboxylic acid was not achieved using standard coupling agents. Carbodiimide derivative EDCI **33** and the uronium based HBTU did not afford complete conversion of the amine to the amide. On-resin coupling of anilines had been reported successful by employing the effective, yet relatively expensive uronium derivative, HATU **117**.[518]

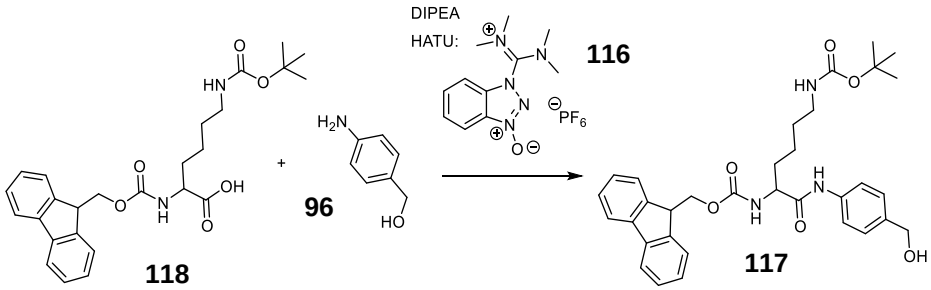

Scheme 5-25. Conjugation of para-aminobenzyl alcohol **97** to C-terminus of lysine **119** using 1-[Bis(dimethylamino)methylene]-1H-1,2,3-triazolo[4,5-b]pyridinium 3-oxid hexafluorophosphate **117** (HATU) to form the amide conjugated product **118**.

Coupling of *p*ABA **97** to Fmoc-lysine(boc)-OH **119** on a 200 mg scale, was conducted in anhydrous DMF conditions in the presence of HATU **117** and DIPEA. The reaction was monitored by TLC using ninhydrin to stain for amines. After 96 hours, a product spot was visible (Rf = 0.6) which no longer stained deep purple like the starting material but stained brown with heating, indicating the presence of an amide. ^{1}H NMR spectroscopy confirmed the desired product **118** had formed and coupling had not occurred involving the alcohol. The spectrum showed a shift in the aromatic resonance of aminobenzyl alcohol **97** from 6.97 and 6.52 ppm to 7.55 and 7.25 ppm for each aromatic pair (**Figure 5-41**). The proton of the aromatic amide is observed at 10.0 ppm. The benzyl protons neighbouring the alcohol did not show a shift indicating that the coupling had occurred at the amine terminus and not the hydroxyl terminus.

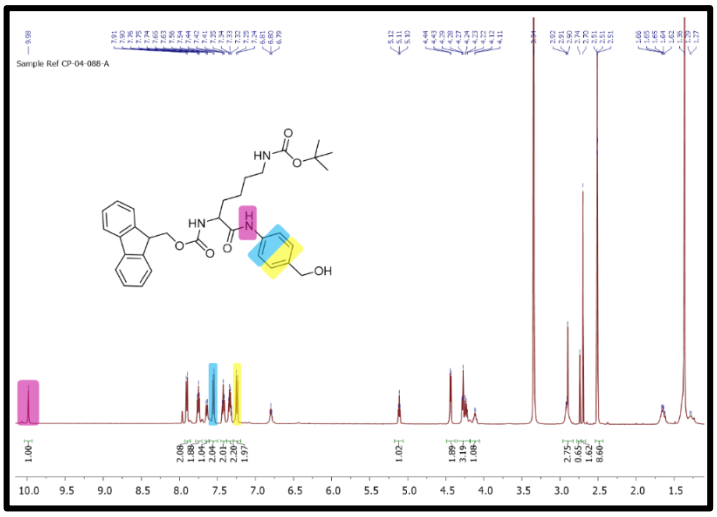

Figure 5-41. ^{1}H NMR spectrum of the successful coupling between Fmoc-Lys(Boc)-OH **119** and *p*-aminobenzyl alcohol **97** to form the amide derivative **118**.

Coupling of the free hydroxyl of the amide product **118** to the carboxyl acid of treprostinil **4** was conducted using phenoxyacetic acid **22** as a model (**Scheme 5-26**). Previous work in **chapter 3** identified CDI **36** as a suitable coupling agent for the esterification of phenoxyacetic acid **22**. However, when these conditions were used to couple phenoxyacetic acid **22** and the hydroxyl of amide product **118** no reaction was observed after 24 hours. HBTU was utilised using several different conditions. Interestingly, the addition of HOBt hydrate **29**, did not result in coupling. HOBt **29** is understood to increase the rate of reaction by acting as a nucleophilic catalyst towards the acid carbonyl, which reduces the likelihood of racemisation. The exclusion of HOBt hydrate **29** however, afforded the complete exhaustion of starting materials and formation of ester product **120**, as determined by TLC.

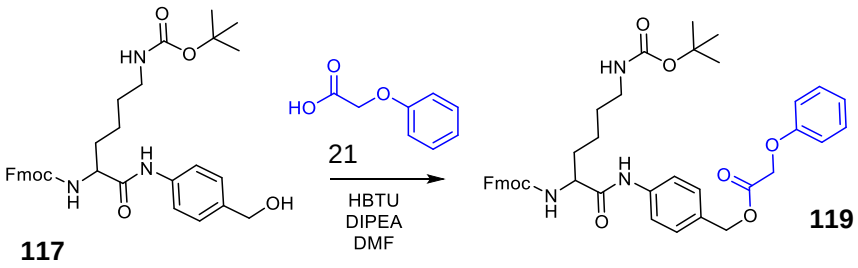

Scheme 5-26. Esterification of Fmoc-Lys(boc)-amide benzyl alcohol **118** with phenoxyacetic acid **22** in the presence of HBTU and diisopropylethyl amine (DIPEA) in dimethylformamide (DMF), to afford Fmoc-Lys(boc)-amide benzylphenoxtacetate **120**.

Isolation of this compound and subsequent ^{1}H NMR analysis (**Figure 5-42**) indicated the formation of the ester **120**. A downfield shift in resonance from 4.26 to 5.09 ppm corresponding to the benzyl protons of the pABA moiety. Additionally, a shift is observed at 4.56 ppm corresponding to the methylene resonance of phenoxyacetic ester **120** which is seen at 4.70 ppm when in the acid form, giving confidence that the coupling has occurred. HOBt **29** is an explosive compound so is often supplied as the hydrate to reduce the associated risk.[360] The

poor coupling observed when HOBt **29** was employed was unexpected and could be a result of the presence of competing water within the reaction mixture.

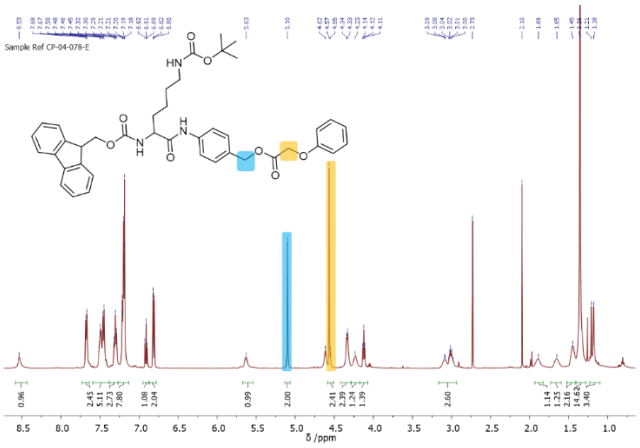

Figure 5-42. ^{1}H NMR spectrum of the esterified product **120**, formed by coupling phenoxyacetic acid **22** with the hydroxyl of Fmoc-Lys(boc)-amide benzyl alcohol **118**.

Using HBTU coupling reagent, a route to conjugate the *p*-aminobenzyl alcohol **97** self-immolative linker between the C-terminus of an amino acid and an aryl acid such as that of treprostinil **4**, has been identified.

A benefit of SPPS is the ease of synthesis and deprotection in the global resin cleavage step (cleavage of resin and all standard acid-labile side chain protecting groups). Deprotection of the side chains in solution, post-resin cleavage would allow for conjugation of treprostinil linker to the carboxylic terminus but requires removal of different side chain protecting groups. Additionally, work up of solution phase reactions has the potential for the loss of product whereas with a successful solid phase reaction, the product is immobilised on the resin and all other reagent, by products and side reactions are removed. Particularly for multistep synthetic routes, the ability to immobilise and locate the desired product at each step maximises the benefit derived from solid phase reactions.[519] Furthermore, the purification after each step for solution phase reactions is a time-consuming exercise. SPPS reactions require the use of excess reagents to force reactions to completion, although the recycling of precious reagents is possible. Therefore, conjugation of treprostinil **4** to the substrate would ideally be carried out on-resin, before the amino acid side chains have been deprotected to minimise possible side reactions.

Owing to the lack of suitable functional groups, treprostinil **4** cannot easily loaded onto a resin and facilitate peptide conjugation, which ruled out traditional resin loading techniques. To overcome this problem, a synthetic route was devised which linked the resin to the amide bond between the first and *p*-aminobenzyl alcohol **97**. Such an intermediate bound to the resin, would allow the substrate to be grown in the usual manner and render the hydroxyl of *p*-aminobenzyl alcohol **97** available to conjugate to treprostinil **4**.

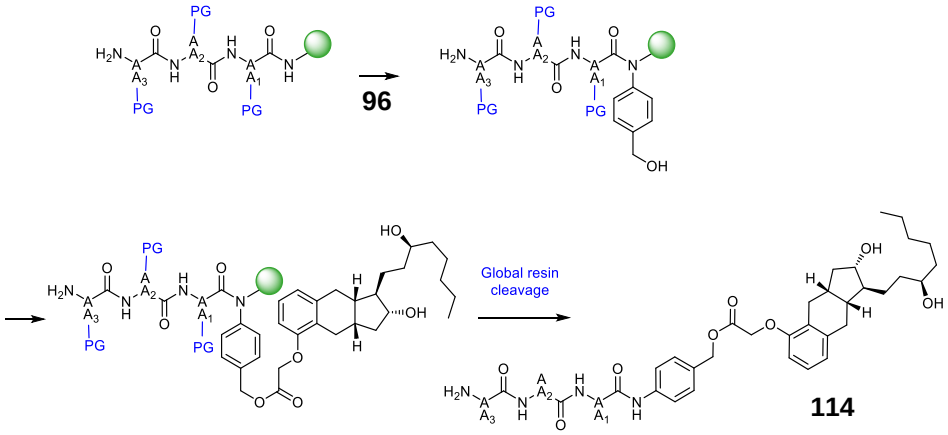

Scheme 5-27. Desired order of synthesis of treprostinil peptide prodrug **115**. Peptide is synthesised first, followed by conjugation of p-aminobenzyl alcohol **97** and then by treprostinil **4**. Cleavage and simultaneous deprotection of the amino acid side chains would result in the desired prodrug structure **115**.

In order to link the resin to the two amino acids *via* a tertiary amide such as **121**, a formyl resin was employed, and a two-step synthesis required; reductive amination followed by secondary amidation (**Scheme 5-28**).

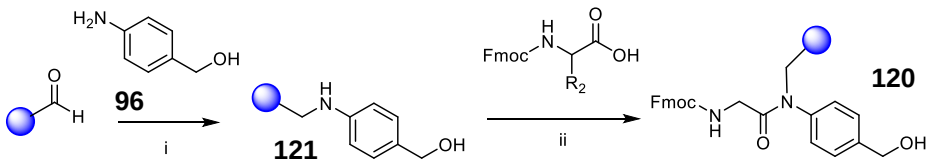

Scheme 5-28. Linking of *p*-aminobenzyl alcohol 97 and first amino acid onto formyl resin by tertiary amide link. i) Loading of *p*-aminobenzyl alcohol 97 onto formyl resin by reductive amination. ii) Coupling of secondary amine 122 to Fmoc-protected amino acid.

4-(4-Formyl-3-methoxyphenoxy)butyryl (FMPB) resin **123** is a formyl resin which facilitates loading by reductive amination. The loading of the resin is 0.52 mmol/g which means for a successful 50 mg scale reaction, a maximum of 0.025 mmol of product will be formed. The resin terminal is a resin derivative of 2,4-alkoxybenzaldehyde which after formation of the tertiary amide on-resin, is cleaved by standard TFA-mediated cleavage conditions to generate a secondary amide.

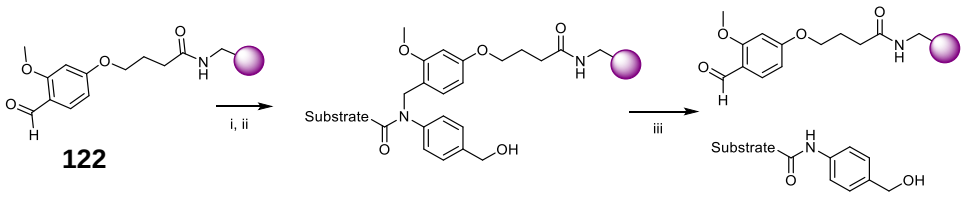

Scheme 5-29. FMPB formyl resin **123** (i) loading of amine **97** and (ii) subsequent amidation; iii) when cleaved in standard TFA-mediated conditions, the secondary amide is released from the resin.

The main drawback with SPPS is during method development, the time between running a reaction and determining its success can be slow. Additionally, the cleaving and work up

process is laborious compared to TLC used in solution phase. Therefore, a solution phase reaction was utilised to gain an understanding of the suitable reaction conditions, using methods to track the reaction progression such as TLC and NMR. Once conditions were identified, they could later be transferred to the solid phase. To mimic the FMBP resin **123** reactivity as closely as possible in the solution phase, 2,4-dimethoxybenzaldehyde **124** (DMB) was employed as the aldehyde function. With the intention of transferring optimised conditions to on-resin techniques, only solution phase reducing agent were employed (i.e. palladium, platinum and nickel were not considered).

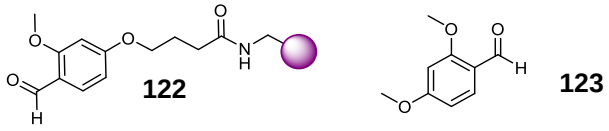

Figure 5-43. Structure of 2,4-dimethoxybenzaldehyde **124** used as a solution phase mimic of the terminal group of FMBP resin **123**.

Dissolution of a nucleophilic amine **97** in the presence of benzaldehyde **124** was expected to form the imine **125**. The instability of the imine **125** makes detection of its formation difficult. As a result, the imine formation step was not monitored, but left to react for a sufficient time and success later determined by the amine product **126** that formed after reduction. Addition of a suitable reducing agent, such as sodium borohydride or 2-methylpyridine borane complex **127**, provides a nucleophilic hydride ion which can attack the imine carbon, resulting in a secondary amine. However, reduction of the unreacted aldehyde **124** to an alcohol renders it unreactive and prevents imine formation.

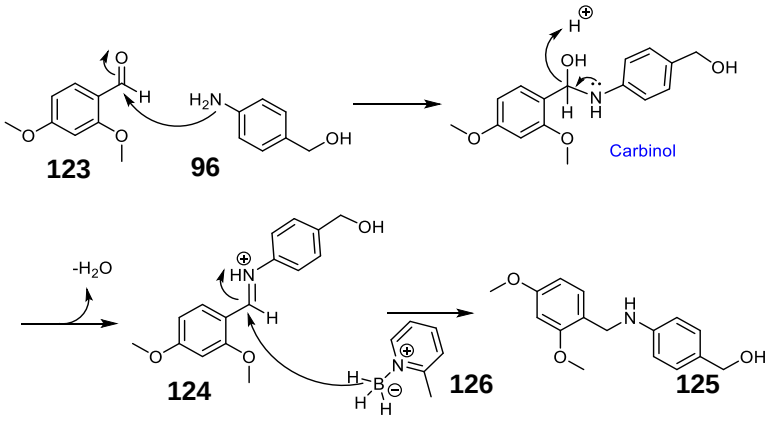

Scheme 5-30. Proposed formation of secondary amine **126** through reductive amination of 2,4-dimethoxy benzylaldehyde **124** and p-aminobenzyl alcohol **97** *via* an imine intermediate **125** which is reduced by 2-methyl pyridinium borane **127**.

DMB **124** initially underwent reaction with *p*-ABA **97** and reduced with 2-methyl borane complex **127** (**Scheme 5-30**).[520] Addition of the DMB **124**, *p*ABA **97** and the reducing agent in one step uses a direct reductive approach where the carbinol amine (labelled in blue) is

reduced, without the need for imine **125** formation.[521] However, tracking by TLC did not indicate any change in R_f values 0.6 and 0.3 for DMB **124** and pABA **97** respectively.

Reductive amination had been shown to be successful at forming the secondary amine between aromatic benzaldehyde **124** and an aniline derivative **97** using sodium borohydride and Dowex 50WD8 in THF.[522] Sodium borohydride is considered a green, environmentally friendly reducing agent which is safe and inexpensive to use. Unfortunately, it is able to reduce other functional groups including aldehydes so is often used alongside catalysts, such as Dowex which assist in the formation of imines. A reaction of DMB **124**, *p*ABA **97** and $NaBH_4$ (1:1:1) in the presence of a catalytic amount of Dowex was performed and after 15 minutes, TLC showed no trace of starting aldehyde **124** or amine **97**, as well as the appearance of a new spot indicating a reaction had progressed. The reaction was worked up by liquid phase separation and the products were separated by column chromatography. Unfortunately, only the benzyl alcohol derivative **128** was isolated (**Scheme 5-31**), suggesting the aldehyde **124** was prematurely reduced before the imine **125** formation could occur. For both the borane and sodium borohydride reduction reactions described, only 5 minutes were allowed for the imine **125** to form before addition of the reducing agent.

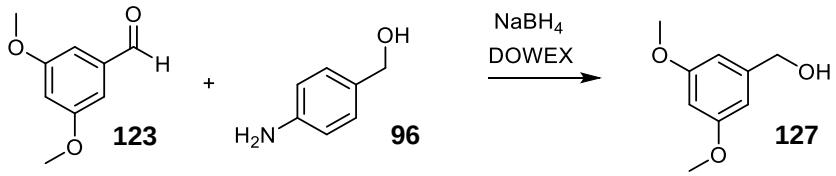

Scheme 5-31. Undesired reduction of aldehyde to form the alcohol derivative **128** when reductive amination of 2,4-dimethoxy benzylaldehyde **124** along with *p*-amino benzyl alcohol **97** in the presence of sodium borohydride **131** and Dowex resin was attempted.

Longer imine formation times were expected to facilitate successful reductive amination reactions.[521] Imine **125** formation between DMB **124** and *p*ABA **97** was allowed 2 hours to form in the presence of Dowex resin, before sodium borohydride **131** was added. However, TLC showed only the presence of starting compounds and the alcohol product **128**. The formation of the alcohol **128** suggested that the imine **125** still did not form after 2 hours. The presence of starting materials indicated that the desired stoichiometry was not achieved, likely to be a result of sodium borohydride **131** hydrolysis either during transfer to the reaction vessel or upon contact with solvent containing residual water.

Aniline derivates have been reported to undergo reductive aminations,[522] however, in the work presented, the desired secondary amine could not be achieved. The most successful and commonly employed agents were employed[521] but the evidence observed suggested that the imine did not form. Formation of the imine is hindered by the donation of the aniline lone pair into the aromatic ring which reduces the nucleophilicity of the nitrogen. The proximity of the moieties to electron dense aromatic rings contribute to steric effects and electron repulsion.

Therefore, efforts attempting to achieve reductive amination by nucleophilic addition of *p*-aminobenzyl alcohol were terminated and a route to utilise a more nucleophilic amine was sought.

The attachment of the resin mimic, 2,4-dimethoxybenzaldehyde **124**, at an amide bond was modified to attach between amino acid 1 and 2 instead of between amino acid 1 and *p*ABA **97** (**Scheme 5-32**). This would allow an imine to form more readily using a nucleophilic, primary, aliphatic amine.

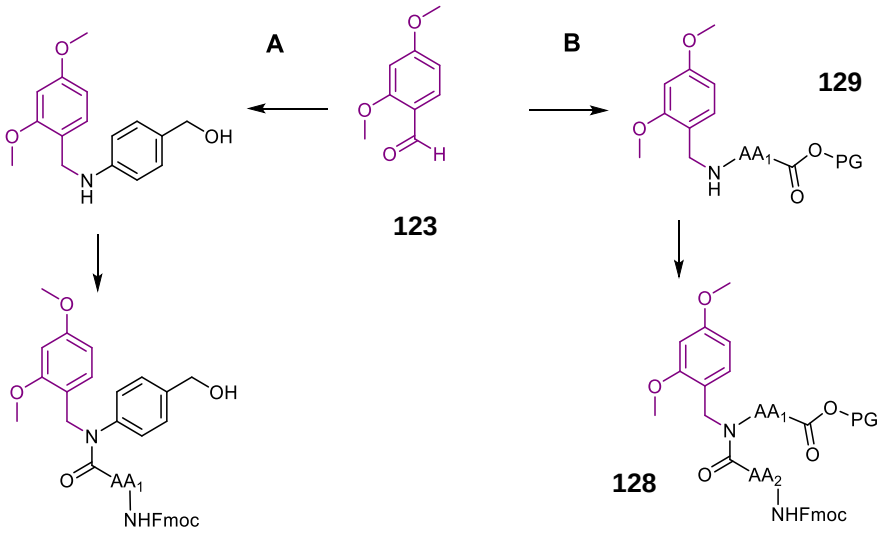

Scheme 5-32. Two proposed schemes for reductive amination of FMBP resin-mimic 2,4-dimethoxybenzaldehyde **124**. A) mimics resin linkage between *p*-aminobenzyl alcohol **97** and first amino acid (AA_1); B) mimics resin linkage between the first (AA_1) and second (AA_2) amino acids **129**.

In brief, an esterified derivative of the first amino acid is left to react with aldehyde **124** in the presence of base which forms the imine **136**. (**Scheme 5-33**). Addition of a borohydride reducing agent (eg. sodium borohydride **131**) reduces the imine **136** to the corresponding secondary amine product **130**, which can couple the next amino acid to give the tertiary amine structure **129**.

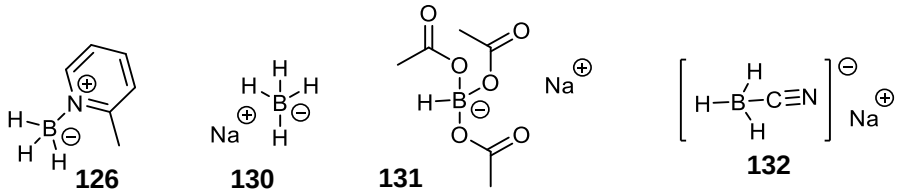

Figure 5-44. Structures of borohydride reducing agents suitable for reductive aminations; 2-methylpyridine borane complex **127**; sodium borohydride **131**; sodium triacetoxy borohydride **132**; sodium cyanoborohydride **133**. The different substituents of the borohydrides alter the reductive abilities of the borohydride.

The amino acid requires a free amine, protected side chain and a protected carboxylic acid. The carboxyl-ester derivatised amino acids were employed initially as they were commercially available. The hydrochloride salt of β-alanine ethyl ester **135** was allowed to undergo reaction

with DMB **124** for 2 hours in methanol (**Scheme 5-33**). Methanol has been shown to successfully form an imine of a primary amine quantitatively when leaving 3 hours for the aldimine to form before addition of sodium borohydride. Following conditions successfully employed by Abdel-Magid and colleagues, sodium triacetoxyborohydride **132** (STAB) was employed as a reducing agent with excess equivalents (1.4) to give the desired amine **134**.[521] The acetoxy groups in the reducing agent have an electron withdrawing effect on the boron atom resulting in a milder reducing agent than the boro-tetrahydride derivatives. STAB **132** appears to be more suitable for reductive aminations[523] although it is still effective at reducing aldehydes to alcohols.[524,525]

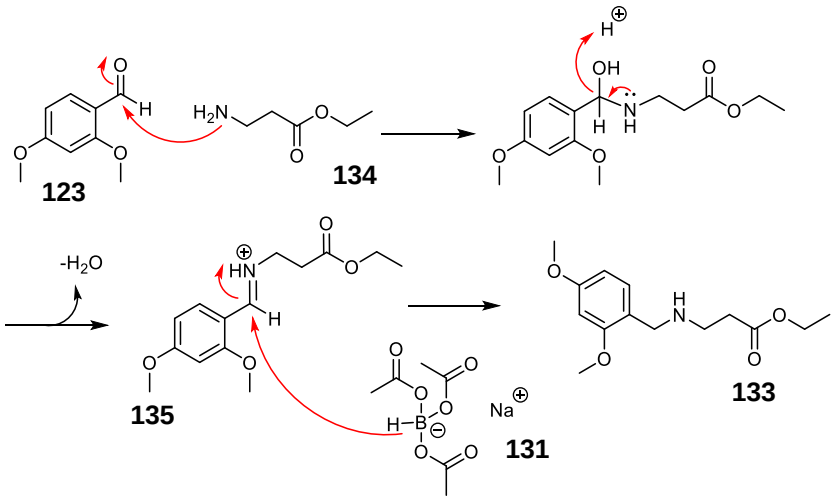

Scheme 5-33. Mechanism for reductive amination *via* imine formation between 2,4-dimethoxybenzaldehyde **124** and primary amine of β alanine ethyl ester **135**. The imine intermediate **136** is reduced by sodium triacetoxyborohydride to form secondary amine **134**.

Initially the first reductive amination attempt was conducted in standard methanol. After 4 hours, TLC indicated DMB **124** and amine **135** were still present. An additional spot was observed which stained yellow with ninhydrin, suggesting the desired secondary amine **134** had formed. Further addition of STAB **132** increased the intensity of the yellow spot but starting materials were not completely consumed and the addition of more STAB **132** (0.5 equivalents) soon produced a precipitate thought to be insoluble STAB **132**. The observed partial success of the reaction by TLC was attributed to the amine. The β-alanine ethyl ester **135** was used as the hydrochloride salt to avoid the free amine from undergoing intermolecular reaction with the ester upon storage. The protonation of the amine eliminates its ability to act as a nucleophile and prevents possible polymerisation (**Scheme 5-34**).

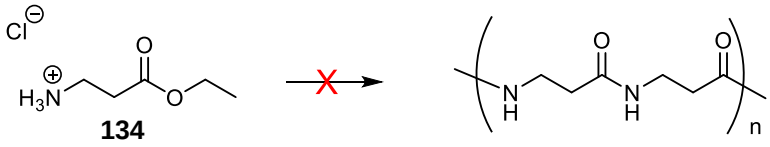

Scheme 5-34. The protonation of the primary amine of β-alanine ethyl ester 135 prevents nucleophilic substitution reactions between molecules which can potentially form dimers to polymers. Therefore, esterified amino acids are supplied as the

hydrochloride salt. The ester salt **135** has reduced nucleophile activity until the ammonium ion is neutralised.

To enable imine **136** formation, the reaction was performed using the same conditions as before but in the presence of triethylamine in slight excess (1.2 equivalents). Basic conditions are known to slow the rate of the competing reduction of the aldehyde **124** and favour formation of a secondary amine **134** when a similar reducing agent, lithium cyanoborohydride is employed.[526] Heat-activated molecular sieves (3 Å) were added to the reaction to remove the water produced upon imine **136** formation so as to drive equilibrium forward in methanol. A yellow ninhydrin stain spot was present after the first 2 hours, but starting materials were only depleted by the addition of a further 1.4 equivalents of STAB **132**. The reaction was worked up by liquid extraction between ethyl acetate and water, made aqueous by addition of sodium hydroxide. ^{1}H NMR spectroscopy of the isolated product revealed the presence of a resonance at 3.64 ppm (highlighted in purple in **Figure 5-45**), corresponding to the benzylic protons neighbouring the secondary amine in the desired product **134**.

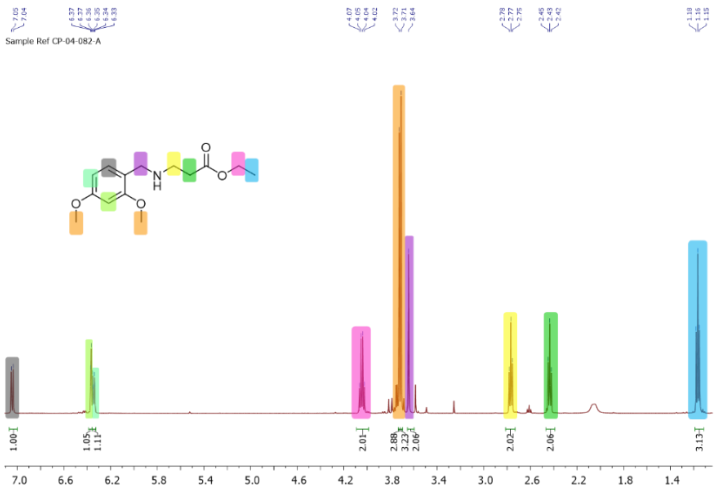

Figure 5-45. ^{1}H NMR spectrum of ethyl 3-((3,5-dimethoxybenzyl)amino)propanoate **134** following the successful solution phase reductive amination of 2,4-dimethoxy benzaldehyde **124** with β-alanine ethyl ester **135**. The presence of the reduction protons (purple) and the shift in the alanine protons neighbouring the mine (yellow) indicate the success of the reaction.

Having established reductive amination conditions in solution to afford the secondary alcohol, the reaction was repeated in the solution phase using conditions more applicable to solid phase synthesis. Firstly, the solution phase reaction was repeated using a bulkier amino acid, phenylalanine ethyl ester **137**, to better mimic the hindrance associated with reactions conducted on-resin. Secondly, methanol is not a suitable solvent for solid phase reactions as it shrinks polystyrene-based resins, thus limiting the interaction between solution phase reagents and resin-bound functional groups. Therefore, the solution phase reductive amination was attempted using phenylalanine ethyl ester **137** in DCM using the conditions previously successfully optimised (**Scheme 5-35**). After 2 hours, the reaction seemed to

progress, however complete consumption of starting materials to produce an intense yellow colour of TLC product spot was only observed after adding excess STAB **132** (2 equivalents).

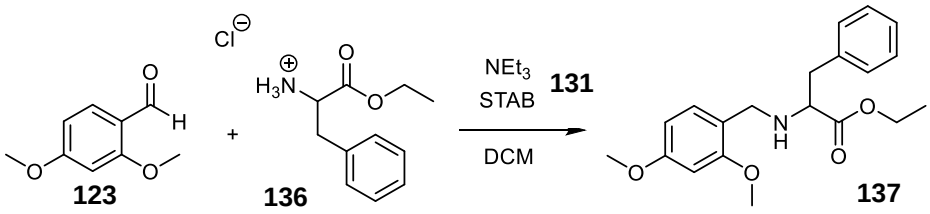

Scheme 5-35. Reductive amination between 2,4-dimethoxybenzaldehyde 124 and bulkier amino acid, phenyl alanine ethyl ester hydrochloride 137 in the presence of triethylamine (NEt_3) and sodium triacetoxyborohydride (STAB) 132 to form secondary amine 138.

The requirement for excess reducing agent could indicate a slower rate of imine formation or the hydrolysis of the reducing agent. After basic work-up into ethyl acetate, ^{1}H NMR spectroscopy indicated successful reductive amination. The presence of the phenyl group causes more restricted rotation of the bonds between the secondary amine and the dimethoxy-aromatic ring. This causes the resonance of the methylene protons (highlighted in blue in **Figure 5-46**) to split into a doublet of doublets. Furthermore, the methoxy groups also further diverge from each other as a result of the interaction, which limits the free rotation of the dimethoxy aromatic ring.

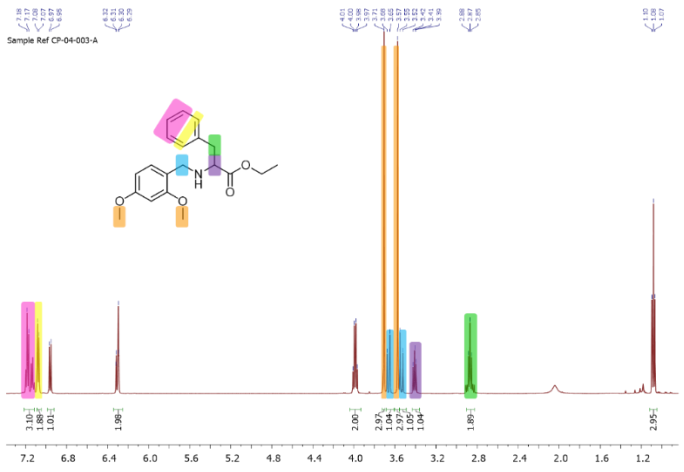

Figure 5-46. ^{1}H NMR spectrum of ethyl (3,5-dimethoxybenzyl)phenylalaninate **138** formed by reductive amination between 2,4-dimethoxy benzaldehyde **124** and phenylalanine ethyl ester **137**. Notably, the presence of the phenyl group results in the splitting of the resonances corresponding to the methoxy (orange) and the methylene groups (blue).

Reductive amination to load the first amino acid onto an aldehyde compound **124** in solution, was achieved using the mild reducing agent, STAB **132**. Product was formed in both DCM and MeOH (yielding 52% and 47%, respectively), despite the known risk of hydrolysis of STAB in methanol. DCM is known to swell polystyrene resin, so the successful reaction optimisation in

DCM will be useful in transferring these techniques to resin bound aldehydes. Reaction mixtures were easily worked up by liquid phase extraction to yield the desired secondary amine compounds.

Having identified suitable conditions for the solution phase reductive amination, the reaction conditions were then attempted for an aldehyde functionalised resin. However, the reaction does not involve free primary amines on the resin which excludes the Kaiser test for monitoring the reaction progress. To monitor the reaction a colourimetric test for the presence of an aldehyde (using the p-anisaldehyde test[527]) and a secondary amine (using the acetaldehyde test[528]) were employed.

The p-anisaldehyde test is based on its use for monitoring reactions by TLC.[529] Addition of acetaldehyde 139 causes a reaction with the resin bound secondary amine **122** forming an imine which is in a resonant form with the enamine (**Scheme 5-36**). When in its enamine form, it can undergo Michael addition with the reactive alkene of unreacted dibenzofulvene **140** (DBF) found in the matrix of polystyrene based resins or derived from Fmoc-amino acids present. This initiates a spontaneous and anionic polymerisation and causes colouration of the beads to orange/brown. For polystyrene deficient resins, Fmoc-amino acids should be added with the aldehyde **139** to form DBF **122** *in situ* and donate the reactive alkene.[528]

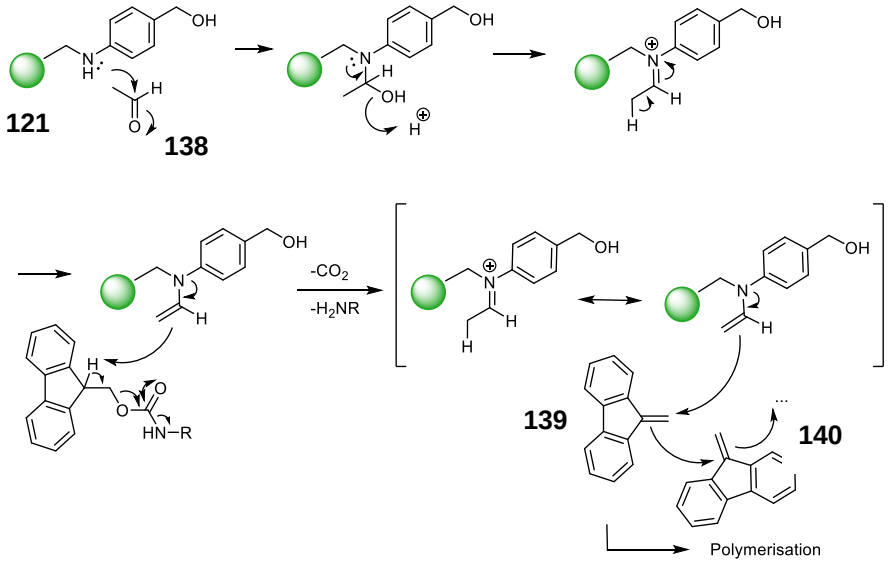

Scheme 5-36. The proposed mechanism for the acateldehyde **139** colourimetric test of secondary amines.[528] Imine formation occurs between the resin-bound secondary amine and acetaldehyde **139**. This can undergo a reaction with Fmoc groups to create a dibenzofulvene **140**, which reacts with the enamine to initiate a spontaneous anionic polymerisation turning beads orange/brown. The polymerisation ends when a proton acts as the electrophile.

The reductive amination of formyl resin **123** was carried out with β-alanine ethyl ester hydrochloride **135** neutralised with triethylamine in the presence of STAB **132** in DCM (**Scheme 5-37**). Complete dissolution of the STAB **132** reducing agent was not observed as a white precipitate remained. Resin-bound aldehyde **123** was not detected after 3 hours as determined by the beads being clear in the presence of *p*-anisaldehyde. Unfortunately, no

secondary amine **142** was detected either as the resin beads were clear in the presence of acetaldehyde **139**. These observations indicated the resin bound aldehyde **123** was reduced to an alcohol before formation of the imine had occurred. New conditions for on-resin reductive amination were thus needed.

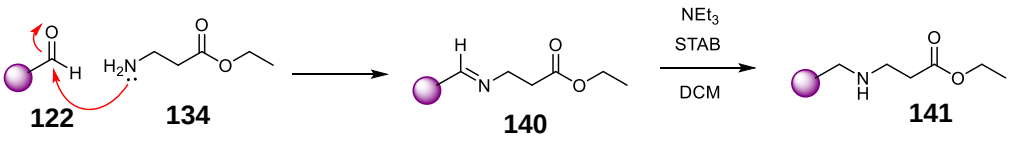

Scheme 5-37. Imine formation between an aldehyde and primary amine which is then reduced by reducing agent sodium borohydride to form the secondary amine.

To aid solubility, alternative solvents were investigated. Dichloroethane is considered the preferred solvent for reductive aminations and is recommended for reductive aminations by the suppliers of the formyl resin. Contrary to this assertion, dichloroethane would not dissolve the amino acid H-Arg(Pbf)-OMe **143**. Also recommended by the suppliers was the use of a mixture of DMF/trimethyl orthoformate (TMOF) (2:1) which did successfully dissolve H-Arg(Pbf)-OMe **143** and was thus employed.[530] The formyl resin **123** and basic arginine **143** solution was allowed 5 minutes to react before the addition of the STAB **132** solvent mixture was added. Surprisingly, aldehyde **123** was still detected after 24 hours of reaction, by production of purple coloured beads upon treatment with p-anisaldehyde. The presence of aldehyde **123** indicated that neither the reductive amination or the reduction to alcohol had occurred. To be certain of this unexpected result, the reaction was repeated once more exactly on a 50 mg scale but produced the same result, confirming the original observation.

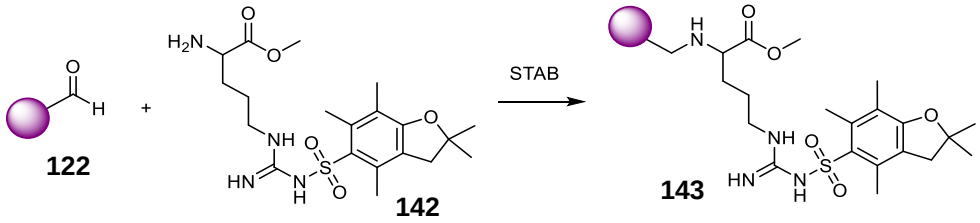

Scheme 5-38. Proposed formation of secondary amine by reductive amination of formyl resin and arginine(Pbf) methyl ester *via* imine intermediate.

The reductive amination was then attempted using 1% acetic acid/DMF solvent and sodium cyanoborohydride **133** ($NaBH_3CN$) as reducing agent.[531] Despite releasing HCN/NaCN as a by-product, $NaBH_3CN$ **133** can reduce imines at a faster rate than the reduction of aldehydes, offering a degree of selectivity for the desired secondary amine product.[532] Deprotonation of the amino acid salt is not necessary in this system as acid is added to the reaction (**Scheme 5-39**). The reaction between formyl resin **123** and H-Arg(Pfb)-OMe **143** was conducted for 3 hours to allow for imine formation before adding the $NaBH_3CN$ **133** reducing agent. Testing for the presence of resin bound aldehyde with *p*-anisaldehyde was negative after 16 hours. An aliquot of beads was then evaluated in the presence of acetaldehyde **139** which gave an

orange colour indicating the presence of a secondary amine **144**. These observations were consistent with reductive amination having occurred.

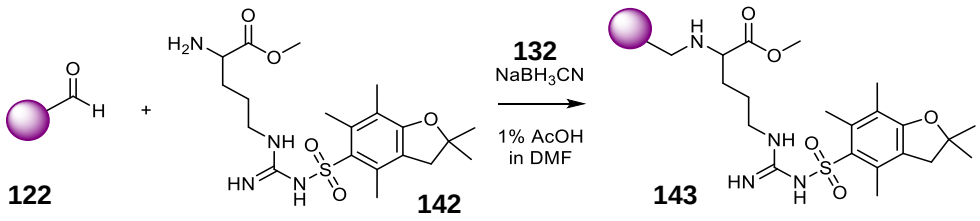

Scheme 5-39. Successful reaction conditions for the reductive amidation of 4-(4-Formyl-3-methoxyphenoxy)butyryl (FMPB) resin **123** to afford secondary amine **144** with H-Arg(Pbf)-OMe **143** in the presence of sodium cyanoborohydride **133** ($NaBH_3CN$) and 1% acetic acid (AcOH) in dimethylformamide (DMF).

Secondary amidation

Once the conditions were found to attach the first amino acid (AA_1) to the resin formyl group by reductive amination, the next step required the coupling of an Fmoc protected amino acid (AA_2) This would produce a tertiary amide at the resin bound secondary amine (**Scheme 5-40**).

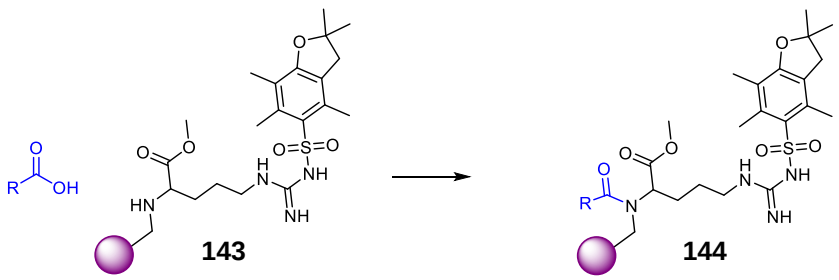

Scheme 5-40. Proposed amide coupling of secondary amine **144** to acid to form tertiary amide **145**.

The nucleophilicity of secondary amines in solution is generally greater than primary amines owing to the electron donating effects of the alkyl groups compared to hydrogen. The steric effects of secondary amines often counter-acts and sometimes significantly reduces the expected increase in activity. Although solid-phase reactions offer advantages (e.g. purification, automation), one of the biggest limitations is achieving sufficient interaction between the resin reactive group and reagents in solution. High concentrations of reagents in solvents that facilitate swelling of the resin are employed to overcome this limitation. While solid phase coupling of sterically hindered functional groups can be inhibited or incomplete, it is possible to couple a tripeptide (Ala-Thr-($X^{Me,Me}$Pro)) to a resin bound secondary amine of Gly-OMe.[531]

Several attempts to achieve tertiary amide derivatives were made in solution phase using the secondary amines, although all were unsuccessful (**Table 5-7**). Given that the conditions identified in the solution phase for the reductive amination were not successfully transferred to solid phase, solution phase optimisation of the amidation was considered unworthwhile. Therefore, attempts were made on resin without successful conditions in solution being identified the identified

Table 5-7. Unsuccessful reaction conditions employed in attempting to form the tertiary amide in solution phase. Both secondary amines formed by reductive amination were attempted to couple to Fmoc-alanine **146**. DIPEA = diisoproylethylamine, Ph = phenyl; Me = methyl; DCC = dicyclohexylcarbodiimide; DMAP = dimethylamino pyridine; DMF = dimethyl formamide; THF = tetrahydrofuran; DCM = dichloromethane; Fmoc = fluorenylmethyloxycarbonyl; Bz = benzyl.

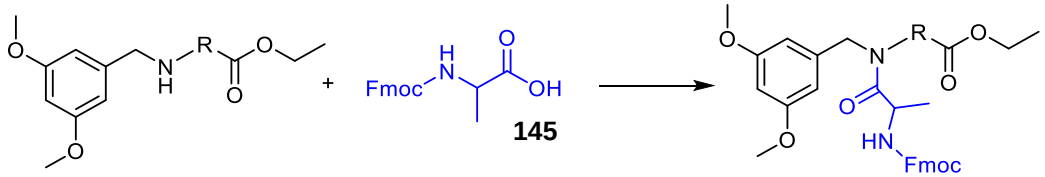

Amine	R	Reagents	Solvent	Scale /mg
138	CH(Bz)	HBTU, DIPEA, HOBt	DMF	41
138	CH(Bz)	N-methyl morpholine, ethyl Chloroformate	THF	90
134	CH_2CH_2	N-methyl morpholine, ethyl Chloroformate	DCM	59
134	CH_2CH_2	N-methyl morpholine, ethyl Chloroformate	DCM	50
138	CH(Bz)	DCC, DMAP	DCM	113

Without an optimised method for the solution phase tertiary amidation to transfer, on-resin coupling of secondary amide **145** and Fmoc-proline **147** was initially conducted following conditions reported.[531] Known for its high yielding couplings, compared to other coupling reagents, HATU **117** is often employed for coupling of hindered, basic or weakly nucleophilic amines.[533,534] To test the suggested conditions, resin-bound secondary amine **145** was coupled to Fmoc-proline **147** using *in situ* carboxyl activation by HATU **117** and DIPEA in DMF (**Scheme 5-41**). The reaction was repeated in triplicate, leaving each coupling over 16 hours to react.

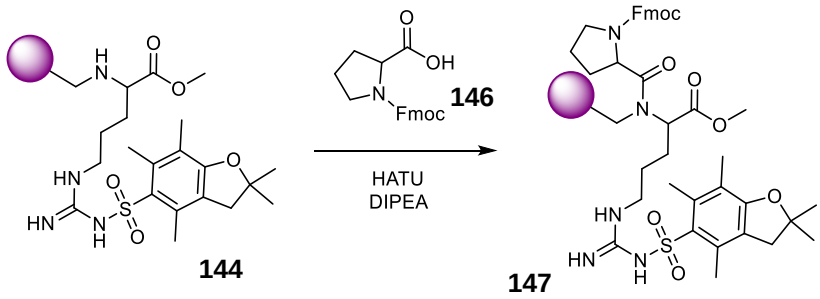

Scheme 5-41. Proposed amidation of resin-bound secondary amide **145** with fluorenylmethyloxycarbonyl proline **147**, activating the acid carbonyl with 1-[Bis(dimethylamino)methylene]-1H-1,2,3-triazolo[4,5-b]pyridinium 3-oxid hexafluorophosphate **117** (HATU) and diisopropyl ethylamine (DIPEA) to form the tertiary amide **148**.

The reaction was tracked by a colorimetric acetaldehyde **139** test for the presence of secondary amines, however, no reduction in orange colour was observed, indicating the remaining presence of secondary amine. To confirm the accuracy of the positive result given

by the acetaldehyde the solution was divided into two portions. The first was cleaved from the resin using TFA/TIS/water to afford the deprotected lysine side chain amine. The solution was re-dissolved in acetonitrile and analysed by LCMS. An impure product was observed, although the largest absorbance (44%) was attributed to the desired dipeptide **149** with $[M+H]^+$ 508 m/z. The uncoupled deprotected arginine methyl ester was also detected as the potassium salt, $[M+K]^+$ = 227 m/z.

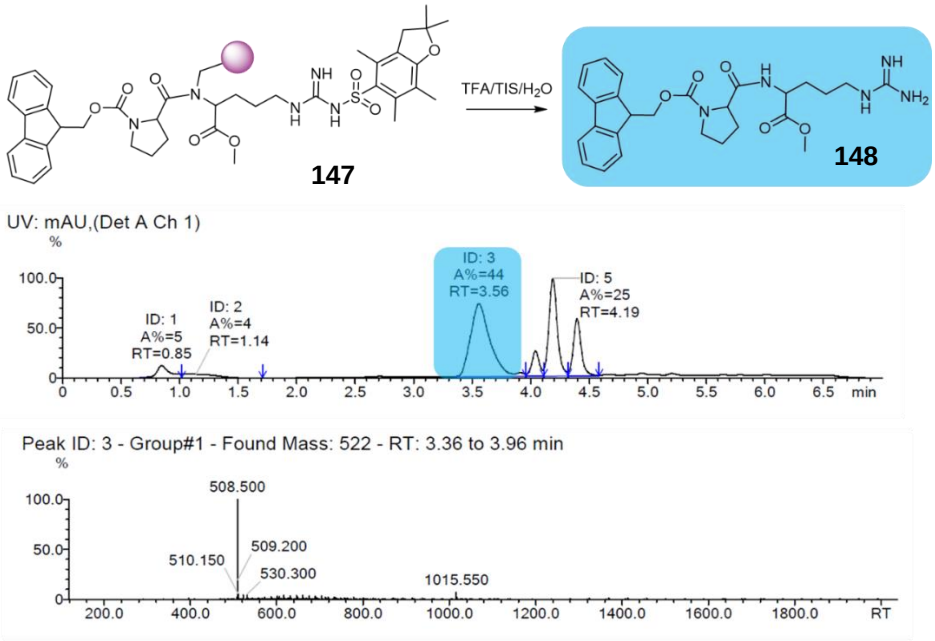

Figure 5-47. LCMS analysis of cleaved product following attempt to amidate resin-bound secondary amine of 2,2,4,6,7-pentamethyldihydrobenzofuran-5-sulfonyl arginine methyl ester **145** to Fmoc-proline **147**. 1-[Bis(dimethylamino)methylene]-1H-1,2,3-triazolo[4,5-b]pyridinium 3-oxide hexafluorophosphate **117** (HATU) was used as coupling reagent and resin cleavage was achieved using trifluoroacetic acid, tiisopropyl silane **95** and water. An absorbance was detected corresponding to the desired dipeptide **149** with $[M+H]^+$ = 508 m/z.

To the second portion, resin was treated to 10 equivalents of acetic anhydride to acetylate any remaining secondary amine (**Scheme 5-42**). Upon repeating the acetaldehyde test no colour was observed, indicating that although some desired dipeptide had formed, the acetaldehyde test result was accurate and the coupling of proline **147** to the secondary amine **145** was only partially successful.

With confidence in the acetaldehyde test, the reaction was repeated using Fmoc-phenylalanine **152** and leaving HATU **117** to react for longer to attempt to complete the coupling. After 72 hours and 3 coupling cycles, the acetaldehyde test remained positive for the presence of secondary amine **145**, indicating unsuccessful coupling.

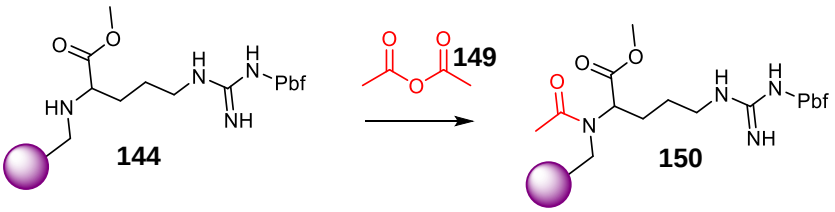

Scheme 5-42. Acetylation of any remaining secondary amine **145** with treatment of acetic anhydride **150**, to form the tertiary amide **151**, which will provide a negative control for the colourimetric test for the presence of secondary alcohols.

DIPC in the presence of a strong auxillary nucleophile, such as HOAt has been shown to give very successful amide couplings.[353] *In lieu* of the expensive HOAt, the cheaper alternative, DMAP **32** was used. Using the same 10 equivalents of DMAP **32** as previously employed for DIPEA to couple Fmoc-phenylalanine **152** to the resin-bound arginine ester **145**, no secondary amine was detected after one hour.

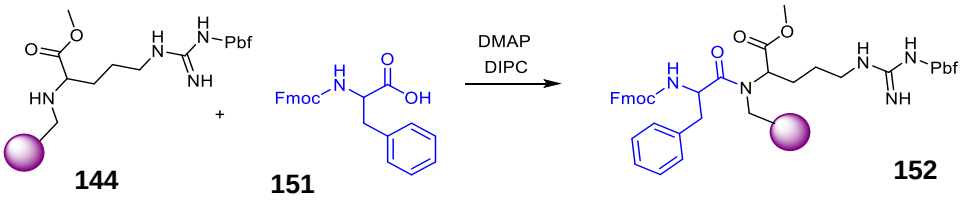

Scheme 5-43. Coupling of fluorenylmethyloxycarbonyl (Fmoc) phenyl alanine **152** to secondary amine of resin-bound arginine methyl ester **145** using diisopropyl carbodiimide (DIPC) and 10 equivalents of 4-(dimethylamino)pyridine **32** (DMAP) to form the resin-bound Fmoc-phenylalanine-arginine methyl ester dipeptide **153**.

Once the resin bound product **153** was cleaved from the resin, using standard cleavage conditions described in the methods, the isolated product was analysed by LCMS (**Figure 5-48**). The chromatogram exhibited 3 peaks, of which the larger peak, with retention time 3.6 minutes, possessed a mass of 558 m/z, corresponding to the desired Fmoc-Phe-Arg-OMe **154**. When repeated using 10 equivalents of DIPEA and a catalytic amount (0.2 equivalents) of DMAP **32**, the reaction however, did not progress after 24 hours. The use of DIPC without any base is also reported to be successful.[535] In our hands, however, the exclusion of base resulted in no reaction as detected by the acetaldehyde test for secondary amine which remained positive.

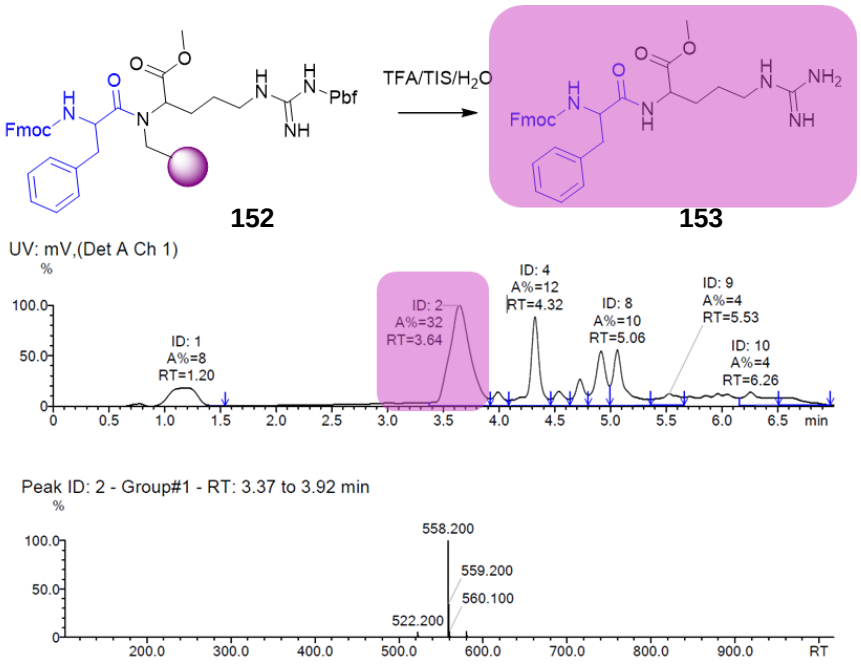

Figure 5-48. The resin-bound product expected to be fluorenylmethyloxycarbonyl (Fmoc) phenylalanine- 2,2,4,6,7-pentamethyldihydrobenzofuran-5-sulfonyl (Pbf) arginine methyl ester **153** was cleaved from the resin using trifluoroacetic acid (TFA), triisopropylsilane **95** (TIS) and water. The expected Fmoc protected dipeptide **154** was analysed by LCMS. The peak highlighted in pink, with retention time 3.6 minutes shows entirely product ion $[M+H]^+$ = 558.2 m/z.

Despite the unconventional conditions employing 10 equivalents of DMAP **32**, the reaction progressed as desired, albeit in low yield. The desired peptide made up only 32% of the total compounds analysed by UV absorbance. Unfortunately, the success of the reaction was not realised until nearing the end of the project after other methods had been pursued. With only a few days left to verify the conditions, a repeat was attempted. This required synthesising the secondary amine **134** by on resin reductive amination between β-alanine ethyl ester **135** and formyl resin **123** using the successful conditions found with sodium triacetoxyborohydride **132**. The reaction was repeated as before on a 0.058 mmol scale of formyl resin **123**. However, the aldehyde was found to be reduced as determined by no colour with the acetaldehyde **139** test and no bead colouration with the *p*-anisaldehyde test.

On-resin reductive amination and subsequent amidation has been successfully reported in the literature.[536] Although a method to achieve the reductive amination step was found and employed, the conditions were not reproducible. Furthermore, coupling of the secondary amine formed was not successful. An extensive variety of coupling agents and combinations with reaction promoters are available.[355]. Perhaps with the right combination, the desired tertiary amine might be achieved. The limitation with the reaction may also be inherently caused by the steric hindrance surrounding the secondary amine and the carboxylic acid, although the ability to form the tertiary amide Fmoc-Phe-Arg(Pbf) **153** suggests that the steric hindrance is not the limitation

The objective of this section of work was to investigate methods to achieve a tryptase substrate with a C-terminal treprostinil. The reductive amination method was prone to reduction of the aldehyde to the resin which resulted in unreproducible results. Efforts to achieve immobilisation of treprostinil and substrate on resin *via* the reductive amination were terminated and alternative approaches were considered. One option would be to link the resin to the arginine side chain (**Scheme 5-44**) as described by Hamże and colleagues,[537] however few reports have utilised this method in the literature. Furthermore, arginine side-chain immobilisation would only be an option for peptide substrates with arginine as the C-terminal amino acid.

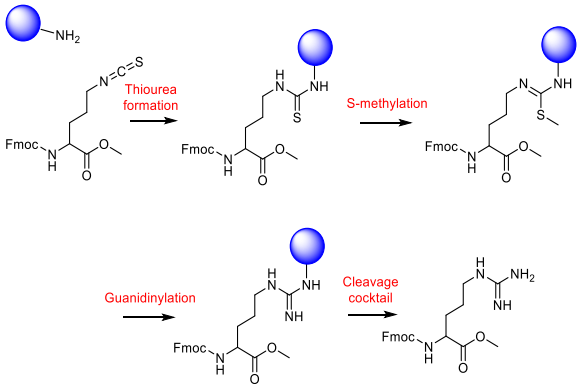

Scheme 5-44. Proposed immobilisation of arginine derivative to Rink Amide resin allowing for peptide growth at N-terminal and *p*-aminobenzyl alcohol- and treprostinil conjugation at the C-terminus. On resin conversion of the thiourea to guanidyl group on resin results in an arginine side group upon cleavage.

Another route considered was to add a side chain to the *p*-ABA group which theoretically should not interfere with immolative resonance required from drug release (**Scheme 5-45**).

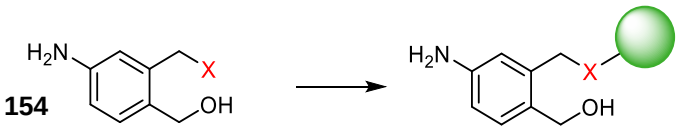

Scheme 5-45. Proposed side chain immobilisation of *p*-aminobenzyl alcohol (or derivative) on resin to facilitate conjugation of the first amino acid to the N-terminal, and the esterification to treprostinil at the hydroxyl terminal. X is any group which can link to any resin.

Side chain immobilisation of p-aminobenzyl alcohol

Immobilising the peptide-treprostinil on a resin through a side chain possessing derivative of *p*-aminobenzyl alcohol, as shown in **Scheme 5-45** was considered the most accessible method. No commercially available compounds, such as **155**, were identified. However, an acid terminal derivative could be obtained by ring opening of phthalide structure **158** (**Scheme 5-46**).

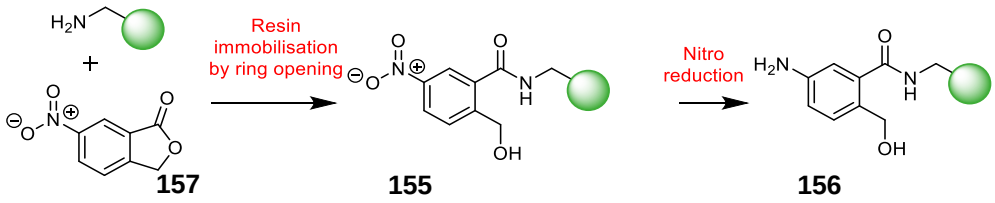

Scheme 5-46. Proposed reaction scheme for the side chain immobilisation of p-aminobenzyl alcohol, by ring opening of 4-nitrophthalide **158** and subsequent reduction of the immobilised nitro benzyl alcohol **156**. The resulting immobilised *para*-aminobenzyl alcohol **157** can facilitate both amino acid conjugation (amine terminus) and treprostinil conjugation (hydroxyl terminus).

Ring opening of the phthalide **158**, by a resin-bound amine will form an amide bond and liberate benzyl alcohol **156** (**Scheme 5-46**). Following reduction of the resin-immobilised nitro group **156** to the amine derivative **157**, an amino acid can be conjugated which can grow the peptide substrates using standard Fmoc-conjugation (**Scheme 5-47**). Treprostinil can then be conjugated to the resin-bound protected substrate through the benzyl alcohol. The enzyme substrate-treprostinil conjugate is isolated following removal from the resin.

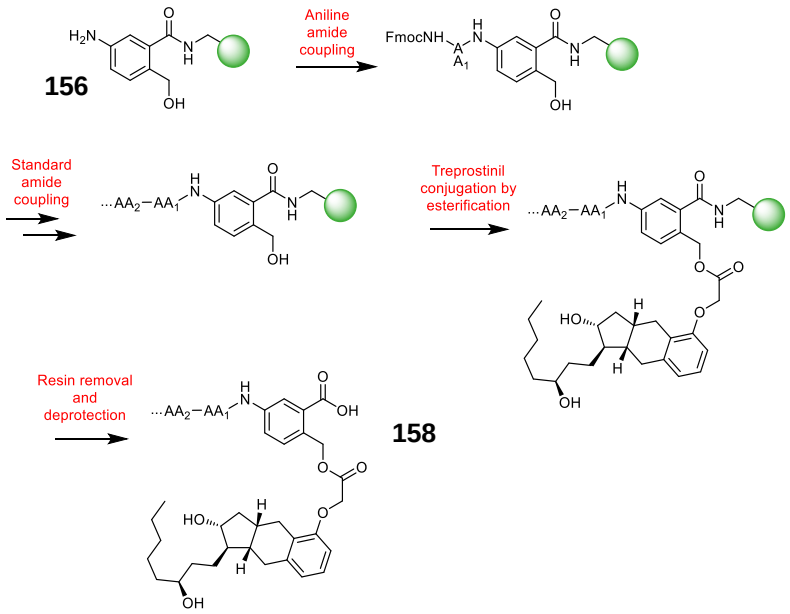

Scheme 5-47. Proposed route to conjugate peptide substrate and treprostinil **4** to the immobilised *para*-aminobenzyl alcohol **157**. Cleavage of the conjugate from the resin will liberate the desired enzyme substrate conjugate of treprostinil **159**.

In the design of the synthetic plan outlined, several potential issues or considerations were identified. First, the choice of the resin is partially determined by whether the cleaved product is desired as the free acid or the primary amide. As the design is for an enzyme substrate with a terminal hydrophobic moiety, treprostinil, it was hypothesised that preservation of as much hydrophilic character as possible would be preferred. This involves use of an alcohol terminal resin, and Wang resin was available. However, this would mean attempting a ring opening by nucleophilic substitution by an alcohol. An alcohol is less nucleophilic than an amine, so in this respect an amine terminal resin would be desired. Furthermore, with an alcohol moiety on the

resin and no primary aliphatic amine on the phthalide, detection of the successful reaction progression could not easily be determined. Given the lack of certainty surrounding the successful ring opening reaction, a desirable reaction would involve an amine which could be determined by the robust Kaiser test. Therefore, it was decided that the Wang resin would first be conjugated to Fmoc-ala-OH **146** (**Scheme 5-48**). This would result in an ester link to the resin which when cleaved would form the soluble acid. The conjugation of Wang could be easily determined by deprotection of a sample a subsequent Kaiser test. Following loading, the Fmoc can be cleaved to reveal a primary aliphatic amine which is expected to undergo nucleophilic addition of the ester to facilitate ring opening.

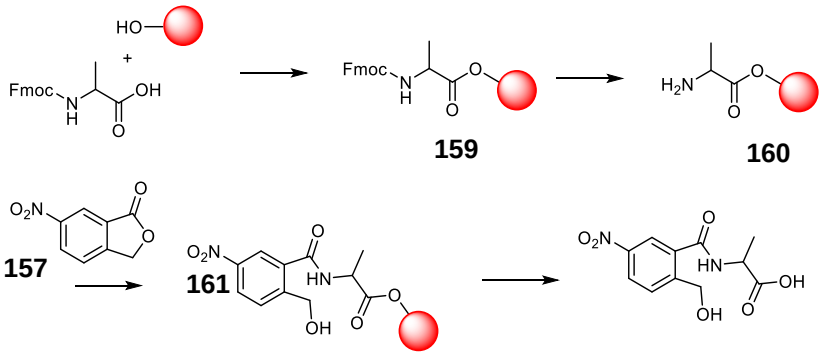

Scheme 5-48. Proposed immobilisation of *p*-amino benzyl alcohol by phthalide ring opening by amine of alanine-functionalised Wang resin **160**. The fluorenylmethyloxycarbonyl (Fmoc)-deprotected alanine **161** amine undergoes ring opening of phthalide **158** which when cleaved releases the acid derivative **162**.

Second, upon opening of the lactone ring, a benzyl alcohol is exposed but whether the alcohol requires protection whilst the peptide substrate is conjugated, was not yet determined.

Third, the nitro-phthalide compound **158** is cheaper than the corresponding amine **163** so initial attempts were made with the nitro-derivative. On-resin reduction of the nitro group to the amine is not common, but a method is described in the literature.[538] Failing that, solution phase reduction of the nitro phthalide **158** could be attempted to afford the amine-derivative **163** which could then be used on-resin (**Scheme 5-49**).

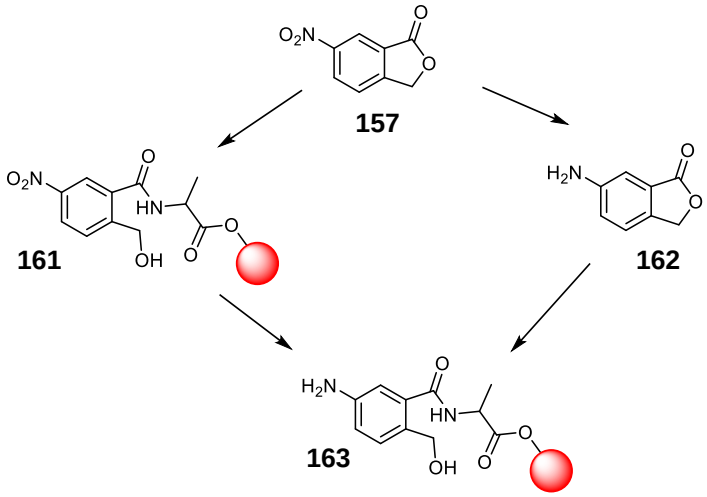

Scheme 5-49. Proposed methods to achieve the resin bound aniline derivative **164**, composing of either on-resin reduction of nitro group after resin-loading, ring opening step to form **162** or off resin reduction to form the aniline phthalide **163** and subsequent resin-loading by ring opening.

Fourth, testing the success of nitro reduction of nitro-resin **162** to the aniline derivative **164**, may or may not be determined with the Kaiser test. An alternative method of testing the reaction progression is to couple an Fmoc-amino acid to the nitro/amine group, remove the Fmoc group and check the presence of primary amine of the conjugate **165** with the Kaiser test (**Scheme 5-50**). Coupling of the aromatic amine to the C-terminal of an Fmoc-amino acid was previously determined using solution phase reagents employing HATU **117** as a suitable coupling agent.

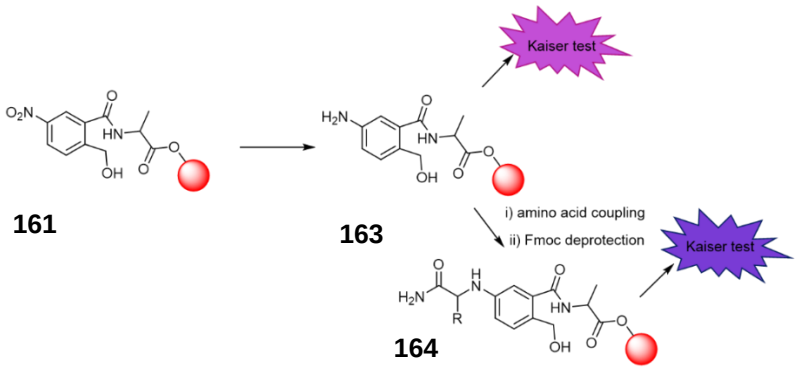

Scheme 5-50. Methods of testing progression of reduction of nitro-resin **162** on resin using colourimetric Kaiser test. Aromatic amines, such as **164**, are difficult to detect using the Kaiser test, owing to the changes in electron density. The Kaiser test can be used to determine the success of the reduction by detecting for the presence of the amine by conjugation of the aniline **164** to a second amino acid. The primary amine conjugate **165** produces a strong result using the Kaiser test.

Fifth, ester coupling conditions were previously described in **Chapter 3**, using carbonyl diimidazole **36** (CDI). Treprostinil **4** could be appended either before or after nitro reduction and peptide growth at the N-terminal (**Scheme 5-46** and **Scheme 5-47**). In considering the order of conjugation (i.e. should treprostinil be conjugated before or after the peptide has been conjugated), the bond stabilities were compared. The ester employed to conjugate treprostinil

to the conjugate is less robust than the amide bonds contained in the conjugate. Therefore, during the amino acid coupling steps, when the resin is treated with 5 equivalents of Fmoc-amino acids and coupling agent, the ester bond may be jeopardised which could potentially remove treprostinil **4** from the resin. The conjugation of treprostinil was designed to be incorporated towards the end of the synthetic. Another consideration, learning from experience in **Chapter 3**, is the potential need for treprostinil hydroxyl protection. Silylation of the alcohols and acid of treprostinil prior to conjugation at the acid terminus was shown to be partially successful in **Chapter 3** and could be employed for conjugation to the resin. Treprostinil reagent can be collected after the resin reaction to recover unreacted treprostinil.

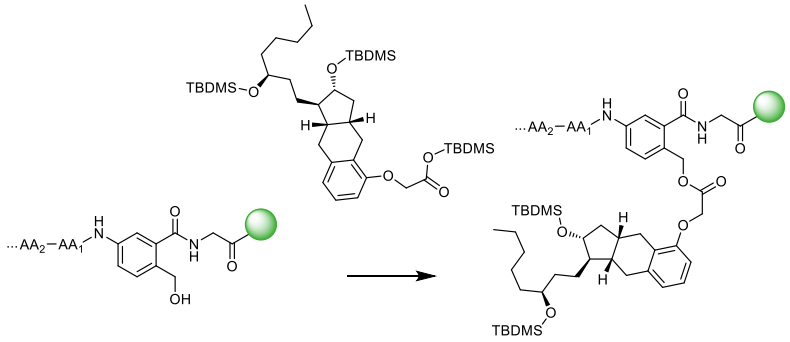

Scheme 5-51. Proposed protection of treprostinil with tertiary butyl dimethyl silyl (TBDMS) groups which will allow for esterification at the carboxyl terminus. Being acid labile, the hydroxyl TBDMS groups are expected to cleave upon resin cleavage.

Lastly, upon cleavage of the product from the resin, an ester bond requires cleavage, however the treprostinil is also linked *via* an ester. Therefore, cleavage conditions will need to be sought to selectively cleave the resin ester, whilst leaving the treprostinil ester intact (**Scheme 5-52**).

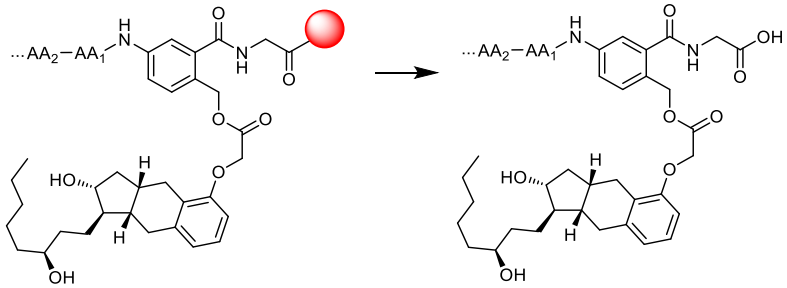

Scheme 5-52. Removal of the tryptase substrate-amidebenzylester-treprostinil conjugate from resin. The conditions employed for the ester cleavage of the wang resin must leave treprostinil ester in-tact.

Before the phthalide reduction was conducted on-resin, the reaction was attempted in solution to determine the conditions required for phthalide ring opening (**Scheme 5-53**). A carboxyl-protected β-alanine ethyl ester hydrochloride **135** was employed to mimic the role of the resin.

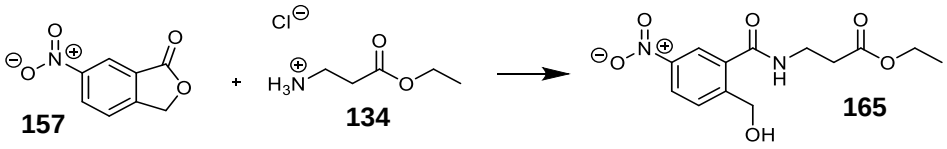

Scheme 5-53. Ring opening of 6-nitrophthalide **158** by β-alanine ethyl ester hydrochloride **135** to form the amide derivative of *para*-nitrobenzyl alcohol **166**.

Ring opening of 6-nitrophthalide **158** was carried out by nucleophilic attack of β-alanine ethyl ester hydrochloride **135** in the presence of triethylamine to neutralise the salt ammonium ion. Reagents were refluxed in ethanol at 86 ° to drive the reaction and after 3 hours the desired ring opened amide **166** was formed in 60 % yield. Analysis by ^{1}H NMR revealed a shift in the singlet resonance (highlighted in blue in **Figure 5-49**) from 5.4 to 4.8 ppm indicating the loss of ester linkage in favour of the alcohol, as well as resonance shift in triplet (highlighted in pink) from 3.4 to 3.7 ppm indicating that the amine had undergone reaction to the amide.

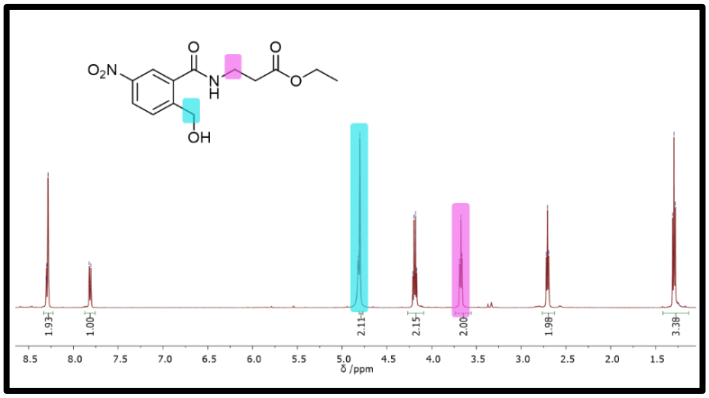

Figure 5-49. ^{1}H NMR spectrum of the amide product **166** formed through ring opening of 6-nitrophthalide **158** by nucleophilic substitution of β-alanine ethyl ester hydrochloride **135**.

To transfer the successful solution phase conditions to solid phase, Fmoc-alanine 146 was immobilised onto the resin using standard HATU **117** coupling conditions and confirmed by a negative Kaiser test. After deprotection of the Fmoc group, the resin was left to react with 6-nitrophthalide **158** in the presence of base and refluxed. The reaction was deemed complete by a negative, colourless Kaiser test.

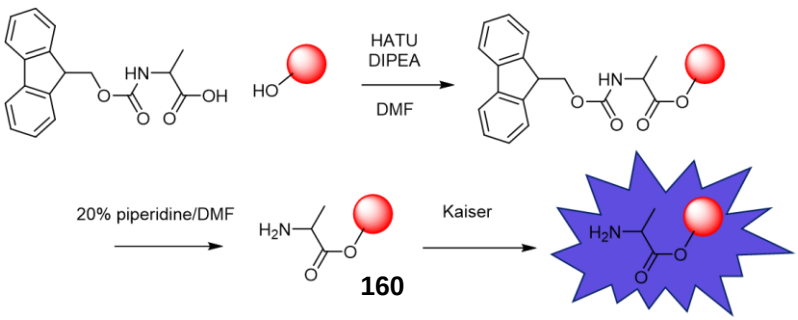

Scheme 5-54. Conjugation of fluorenylmethyloxycarbonyl (Fmoc) alanine to Wang resin employing 1-[Bis(dimethylamino)methylene]-1H-1,2,3-triazolo[4,5-b]pyridinium 3-oxide hexafluorophosphate **117** (HATU) as coupling agent with the presence of diisopropylethylamine (DIPEA) in dimethylformamide (DMF). Following the removal of

Fmoc group to produce Ala-Wang **161**, the amine can be detected using the Kaiser test to produce a blue colour.

It was considered that the reduction of the nitro- group to the corresponding amine could be avoided by repeating the solution phase reaction using the amine derivative, 6-aminophthalide **163**. Employing the same reaction conditions, 6-aminophthalide **163** was allowed to react with β-alanine ethyl ester **135**, but the ring opened, amide product **167** was not observed by TLC (**Scheme 5-55**). The nitro group of **158** has an electron withdrawing effect on the aromatic ring which through inductive effects, weakens the ester bond. The aniline amine however, donates electrons to the aromatic ring which results in a strong ester bond.

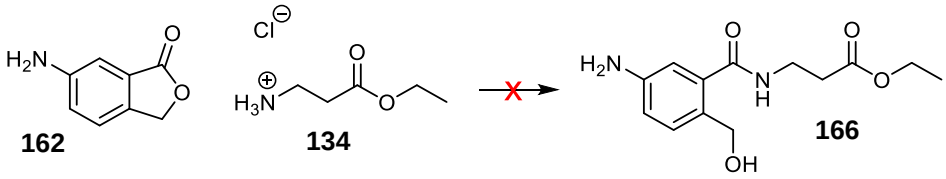

Scheme 5-55. The proposed ring opening of 6-aminophthalide **163** by amide formation with β-alanine ethyl ester **135** to form the amide derivative of *para*-aminobenzyl alcohol **167**. However, the reaction was unsuccessful.

Coupling of the aniline **163** to a carboxylic acid to form the corresponding amide was thought to remove the electron donating effect of the aniline electrons and allow for successful ring opening by nucleophilic substitution of the ester carbonyl. Using conditions previously described for the coupling of ACA alinine **97**, HATU 117 was employed to activate the carboxyl of Fmoc-Lys(Boc)-OH **169** and couple the aniline **163** in solution to form the Lysine-phthalide derivative 168. The reaction was conducted in the presence of DMAP **32** catalyst in DMF (**Scheme 5-56**).

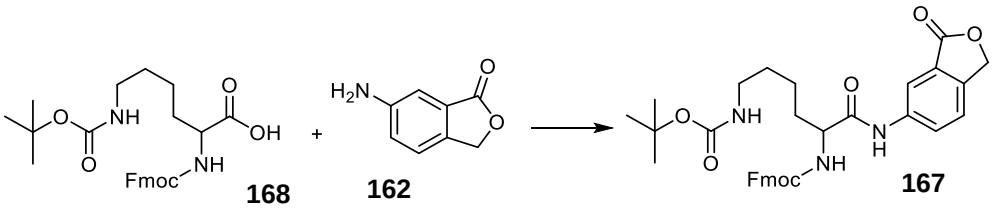

Scheme 5-56. Amidation of the aniline phthalide by coupling to fluorenylmethyloxycarbonyl (Fmoc)-lysine **169** to form the Fmoc-lysine phthalide **168**. The reaction was achieved using 1-[Bis(dimethylamino)methylene]-1H-1,2,3-triazolo[4,5-b]pyridinium 3-oxide hexafluorophosphate **117** (HATU) coupling agent and 4-(dimethylamino)pyridine **32** (DMAP) in dimethylformamide..

^{1}H NMR spectroscopy (**Figure 5-50**) confirmed a shift in the proton of the aromatic nitrogen (labelled in pink) from 5.53 to 10.4 ppm upon amidation. The lactone ring appeared to be intact by the presence of the singlet at 5.4 ppm, highlighted in blue.

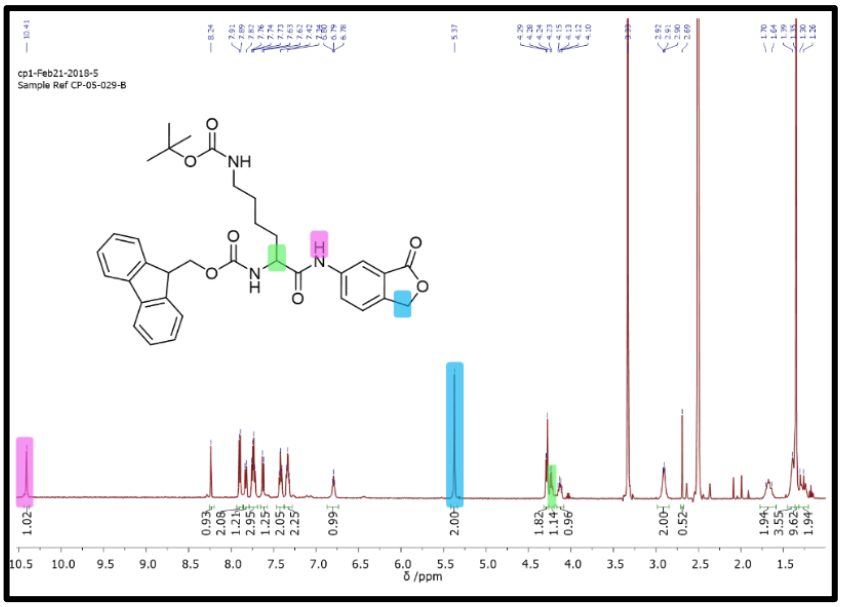

Figure 5-50. ^{1}H NMR spectrum of amide product **168** formed by amide coupling Fmoc-Lysine(Boc) **169** and 6-aminephthalide **163**. The shift in the aromatic amine (pink) as well as the lysine methine (green) confirm conjugation. The persistent methylene resonance (blue) indicated that the lactone ring is in-tact.

The aniline-amide product, Fmoc-Lys(boc) amide phthalide **168** was used to attempt ring opening on the resin. The immobilisation of the amino acid-phthalide conjugate on resin in one step was considered to be an efficient method to circumvent the requirement for an on-resin nitro reduction.

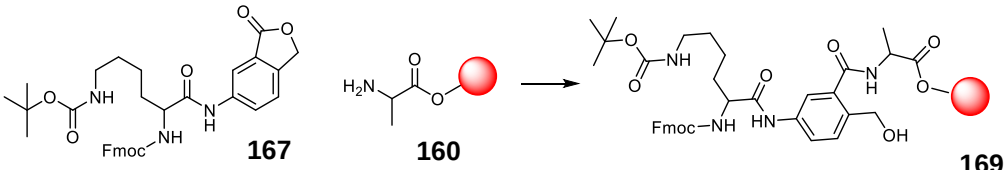

Scheme 5-57. The ring opening and simultaneous resin immobilisation of amidated phthalide **168** by nucleophilic substitution of the resin bound alanine **161**. The amide is not electron withdrawing enough to facilitate ester bond cleavage which would otherwise form the amide linked resin bound lysine amidobenzyl alcohol **170**.

Opening of the ring of Fmoc-lys-phthalide **168** lactone ring to form an amide bond on resin (**161**) was unsuccessful, using conditions found to be successful with the nitro derivative **158**. Lysine-phthalide **168** was refluxed in the presence of resin-bound alanine **161**. However, the opening of the ring was not observed by Kaiser test, in the case of the resin. The reaction was attempted in solution using tyramine **171** an unhindered amine compound to determine if the hindrance of the amine resin was preventing ring opening. Refluxing phthalide **168** with tyramine 171 in DMF at 175 °C did not afford the amide product.

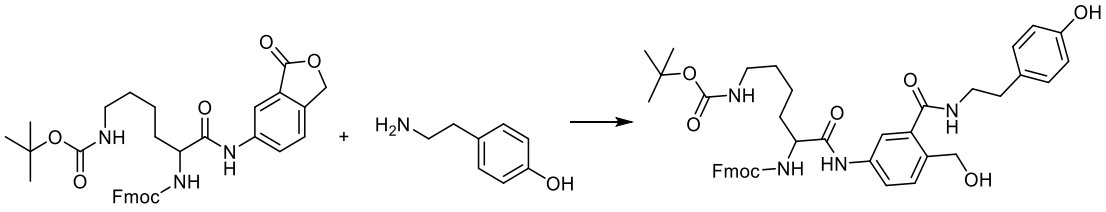

167 **170**

Scheme 5-58. Proposed ring opening of fluorenylmethyloxycarbonyl (Fmoc)Lysine phthalide **168** by tyramine **171** to form the amide derivative.

Hydrolysis of the amide phthalide **168** was attempted using lithium hydroxide ester hydrolysis conditions but the acid benzyl alcohol product was not formed (**Scheme 5-59**). The electron withdrawing effect of the aniline is not sufficiently reduced by amidation and ring opening of the nitro is the most successful route. Therefore, a route to reduce the nitro moiety on the resin was sought.

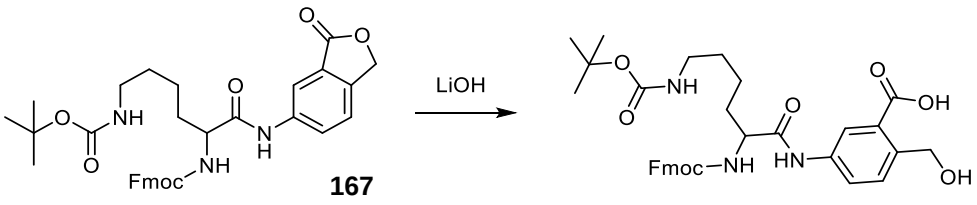

167

Scheme 5-59. Proposed hydrolysis of the amidated phthalide **168** by lithium hydroxide, to afford the acid-alcohol ring opened product. Fmoc = fluorenylmethyloxycarbonyl

A literature search only identified one method to reduce a nitro group to the amine on a solid phase reaction without metal catalysis, although the yields were not reported.[538] The reaction employed a bi-phasic solvent of DCM and water (9:1). An aqueous solution of hydrogen thiosulfate in the presence of potassium carbonate was employed as the reducing agent and a phase transfer catalyst was employed to facilitate reaction between the solvent layers. A pyridinium halide phase transfer catalyst was used by Scheuermann and colleagues[538], although n-tetrabutyl ammonium iodide was available so was used in the reaction attempt.

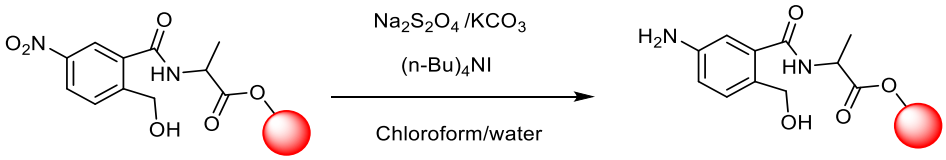

161 **163**

Scheme 5-60. The reduction of resin bound nitro **162** to achieve resin-bound amine derivative **164** modified from a reported procedure.[538] To facilitate interaction between the protic aqueous solvent and the aprotic dichloromethane, *n*-butyl ammonium iodide ((n-Bu)$_4$NI) was added as a phase transfer catalyst, instead of the viologen reported in the paper. Colourimetric montoring of the reaction was not achieved directly but was deemed successful indirectly by further conjugation.

After 24 hours a Kaiser test was carried out and a pale purple colour solution was observed. It was not certain whether the pale colour meant very few amines were present or that the aromatic amine presented that colour when treated with the Kaiser test. For this reason, it was determined that a further coupling of any amine groups followed by Fmoc deprotection step would be needed to clarify the potentially ambiguous result. Coupling of the aniline was shown

here to be successful when HATU **117** was employed and similarly previously reported on resin.[514,516,539]. Therefore, for the investigation of nitro group reduction, it was assumed that the subsequent coupling of any amines present would be complete. Coupling of a resin sample taken from the reduction reaction (**162** and/or **164**) with Fmoc-Arg(Pbf)-OH was carried out in the presence of HATU **117** and DIPEA for 12 hours. After which, a sample was taken and treated with piperidine to cleave the Fmoc group (**Scheme 5-61**). Kaiser test revealed an intense blue colour indicating the presence of a coupled primary amine.

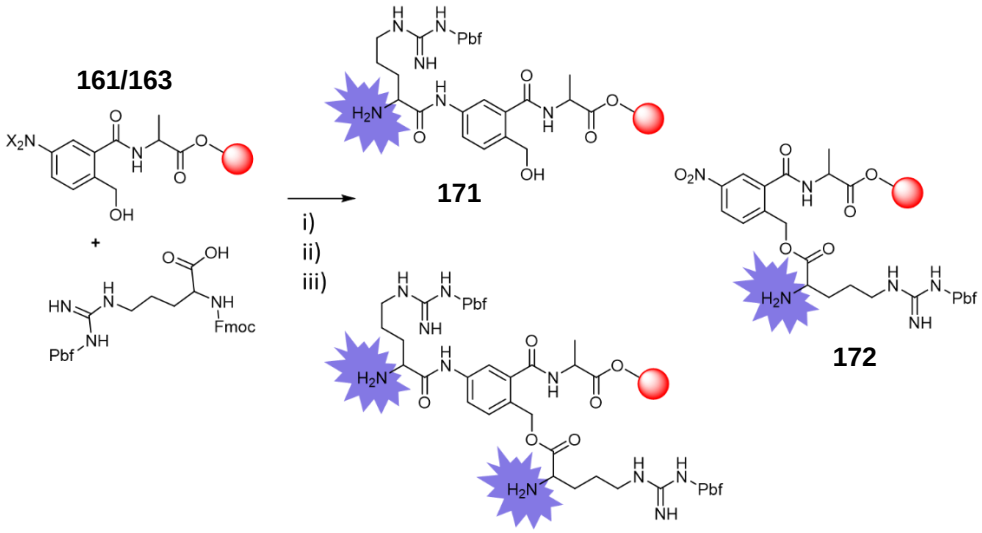

Scheme 5-61. Possible structures formed when coupling Fluorenylmethyloxycarbonyl (Fmoc) 2,2,4,6,7-Pentamethyldihydrobenzofuran-5-sulfonyl (Pbf) Arginine to a potential mixture of nitro resin **162** (X = O)and reduced aniline resin derivative **164** (X = H). Both structures produce the same positive Kaiser test; the desired amide **172** *via* the aniline derivative **164**; and ester formation by coupling *via* the hydroxyl **173**, or a mixture of both. (i) 1-[Bis(dimethylamino)methylene]-1H-1,2,3-triazolo[4,5-b]pyridinium 3-oxide hexafluorophosphate **117** (HATU), diisopropylethylamine, Fmoc-arginine(Pbf)-OH; (ii) 20% piperidine/ dimethylformamide; (iii) Kaiser test.

In the presence of the free hydroxyl of the aniline compound, 164 the coupling could have also occurred at the hydroxy terminus to produce a positive result (**Scheme 5-61**). To circumvent this possibility, the nitro derivative **162** was acetylated by treatment of acetic anhydride **150** at the hydroxy terminus to prevent unwanted hydroxyl coupling (**Scheme 5-62**). The resin was reduced using the conditions used previously, coupled to Fmoc-Ala-OH and Fmoc-deprotected. A translucent purple colour was revealed upon treatment with the Kaiser test, confirming the suspicion that phenylalanine **152** had previously coupled to the hydroxyl terminus. Furthermore, in the presence of excess Fmoc-alanine, the pale purple colour also indicated only partial reduction of the nitro group **162** to the amine derivative **164** occurred. To facilitate successful reduction of the nitro resin **162**, longer reaction times were considered.

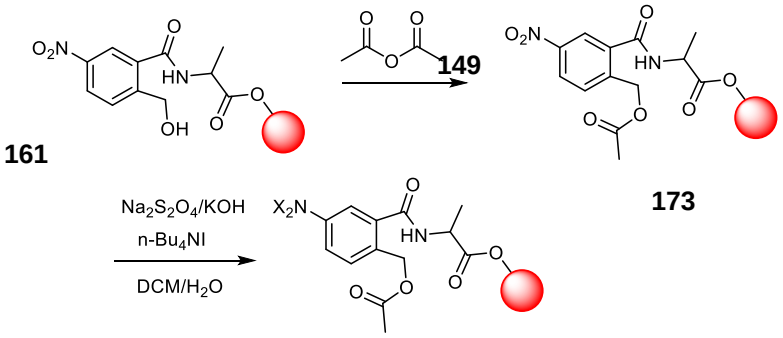

Scheme 5-62. Acetylation of the resin-bound nitro benzyl alcohol 162 using acetic anhydride 150 to prevent coupling at the hydroxyl terminus. The reduction was then attempted again. DCM = dichloromethane

The coupling at the hydroxyl terminus highlighted the need for hydroxyl protection, and for this, benzyl groups, THP and trityl groups were all considered. Tetrahydropyran and benzyl groups were attempted although a method to detect the presence of alcohols proved difficult, as described below. Protection by benzyl ether was also not ideal because of the hydrogenation removal step. Trityl protecting groups are frequently used in SPPS for the protection of cysteine side chains, because they are so are resistant to the basic conditions employed for amide coupling and Fmoc removal. Additionally, they are very sensitive to acidic conditions so can be removed selectively leaving the resin ester link and side chain protecting groups intact. Tritylation of the nitro-resin **162** was attempted using trityl chloride in a basic environment (**Scheme 5-63**). The presence or absence of the alcohol was not easily determined using a colorimetric test. The 4-toluene sulfonyl chloride - *p*-nitrobenzylpyridine (TosCl-PNBP) test often employed for alcohol detection converts the alcohol to its tosylate form which is subsequently displaced by the PNBP. Upon treatment with base, the pyridinium salt is formed which produces a strong red/purple colour.[540] Unfortunately, the preceding phthalide ring opening step results in a brown stained resin which makes subtle changes in colour to pale red/purple difficult to determine with certainty (**Figure 5-51**). Wang resin was run as a positive control and acetylated wang resin (by treatment with acetic anhydride **150**) run as a negative control.

Figure 5-51. Ambiguous result of the 4-toluene sulfonyl chloride - *p*-nitrobenzylpyridine (TosCl-PNBP) test run in parallel (a) Wang resin as positive control; (b) reaction resin when tritylating alcohol of nitro resin 162; (c) acetylated wang resin was used as a negative control.

Another method to determining the presence of hydroxyls is to use bromocresol blue.[541] The utilisation of trityl protecting groups permitted an alternative approach to test for the hydroxyl protection; to test for trityl deprotection. In the presence of 1% TFA in DCM, trityl groups are

cleaved and upon liberation of the cation a yellow colour emerges (**Scheme 5-63**). A sample of the nitro resin treated with trityl chloride was swirled in a solution of 1% TFA in dichloromethane and a yellow formed. To confirm the yellow colour is a result of the trityl cation, TIS **95** was added to quench the cation and remove the yellow colour, which indeed turned the solution colourless. This confirmed the conditions required for the tritylation of the alcohol.

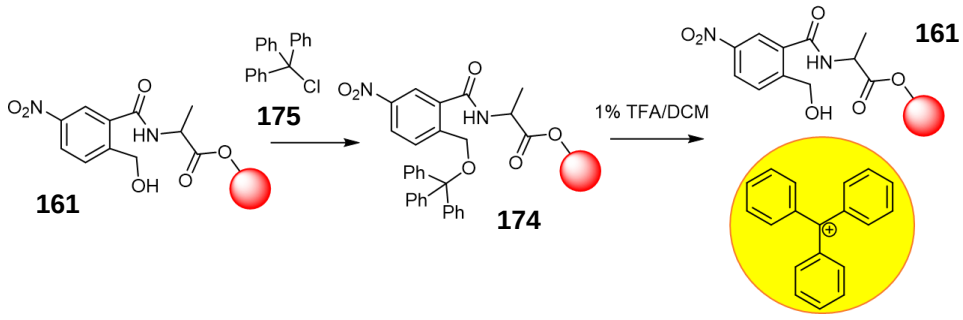

Scheme 5-63. Tritylation of resin-bound nitro benzyl alcohol **162** by treating alcohol with trityl chloride **176**. Upon treatment with mild acid, the trityl cation is formed which produces a yellow solution.

The tritylation was carried out on a larger scale (0.680 mmol), using an excess of trityl chloride. The trityl-removal step was conducted on a small sample using weak acid to confirm reaction success. The nitro group reduction step was carried out in triplicate, leaving the reaction mixture to shake for 24 hours for each cycle.

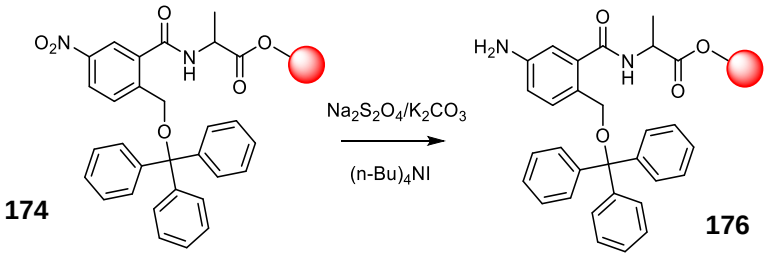

Scheme 5-64. Proposed on-resin reduction of trityl-protected immobilised nitro benzyl alcohol derivative **175** to form the aniline derivative **177**.

A test sample was taken and coupled to Fmoc-phenylalanine **152** in duplicate using HATU **117** and DIPEA. After which, the Fmoc-groups were removed and to half the sample, the Kaiser test conducted, revealing an intense blue solution, indicating successful coupling. To the remaining test sample, 1% TFA in DCM was added which immediately produce a yellow solution, confirming that the trityl groups were still intact and thus coupling had occurred through the aniline and not the hydroxyl. The intense blue solution upon Kaiser test, therefore indicates that the on-resin reduction had been successful.

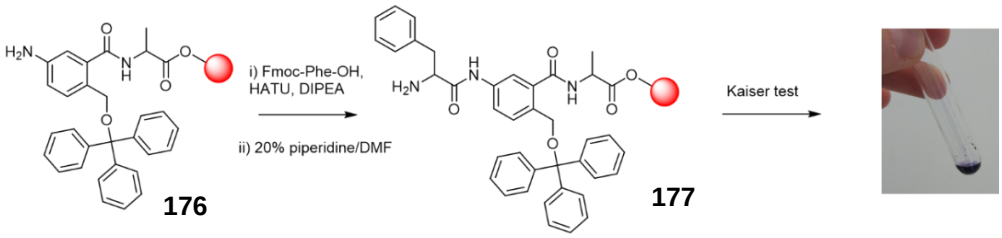

Figure 5-52. Image of Kaiser test result following coupling of fluorenylmethyloxycarbonyl alanine to reduced resin-bound amine **177** and subsequent fluorenylmethyloxycarbonyl-deprotection.

With the trityl protecting group intact and the confirmed aromatic amine of the reduced resin product **177**, the next step was to split the resin into equal protons to couple the desired first amino acid. However, the positive result occurred in the final weeks of the project, during the writing phase so the coupling of the substrates remains yet to be conducted.

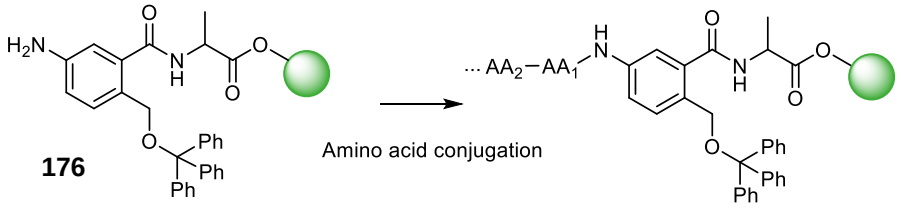

Scheme 5-65. The proposed conjugation of the amino acid sequence to the trityl-protected resin-bound aniline **177**.

When discussing the nitro-reduction mechanism employed for the on-resin reduction more closely during the work up, previously literature of biphasic reductions using sodium dithionite was consulted. The publication followed for the work reported used various pyridyl bromide viologens as phase transfer agents, to aid interaction across the biphasic interface.[538] When designing the nitro reduction described in this chapter, n-butylammonium iodide was already in possession so was employed in a similar manner, in the same sub stoichiometric quantity. Viologens also possess the ability to transfer electrons between phases.[542,543]

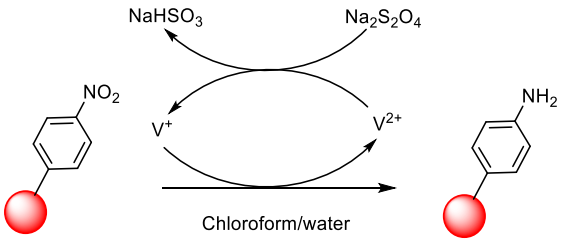

Scheme 5-66. Mechanism of the viologen (V) in the reduction of resin-bound nitro group to the aniline derivative. Viologen is both a phase transfer agent and electron transfer agent. V^+ carries the electron from the aqueous layer to the chloroform layer to donate it to the nitro, becoming V^{2+} and resulting in the aniline derivative. Replenishment of the viologen is achieved by reaction with sodium thiosulfate.

The phase transfer catalyst employed, n-butylammonium iodide does not possess known electron transferring properties, but the evidence suggests that coupling to a nucleophile other

than the hydroxyl was successful, suggesting nitro reduction to the aniline. Additionally, when n-butylammonium iodide was erroneously forgotten from the reduction reactions, coupling of an amino acid did not appear to occur, confirming a role of n-butyl ammonium iodide necessary for reduction of the nitro group. The reduction reaction took between 1 and 3 days to complete, requiring longer reaction times for larger reaction batches. For any commercial utilisation, the reaction time would need to be reduced and the use of an electron transfer agent such as the viologen phase transfer catalysts may offer a route to achieve more efficient conversion to the aniline derivative.

Resin Cleavage Conditition Testing

During the period of developing the method this far, a simultaneous investigation was carried out to consider the treprostinil-ester stability (highlighted red in **Scheme 5-67**) in the resin removal and side chain removal steps. This step would also require forming the amine salts of the terminal and lysine amines to prevent nucleophilic attack into the ester carbonyl, releasing the treprostinil prematurely.

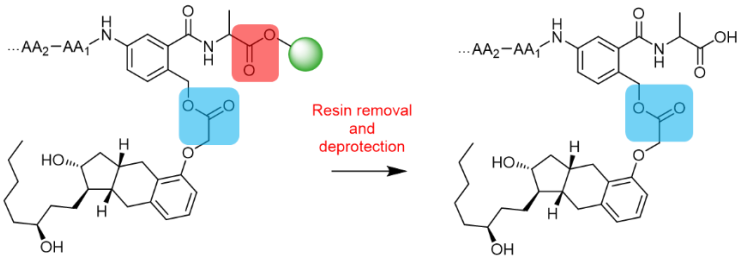

Scheme 5-67. Desired conjugate isolation upon resin cleavage which cleaves the Wang resin-linking ester (red) and leaves the treprostinil ester (blue) in-tact.

An investigation was undertaken to determine resin cleavage and side chain deprotection conditions suitable to be employed in the presence of the treprostinil ester. For this, Fmoc-lys(boc)-*p*ABA-Phenox **120** was synthesised to act as a model which could be tracked in real-time. Ester **120** was exposed to various conditions known to remove protecting groups and compounds from resins. The results are displayed in the table below.

Table 5-8. Ester stability of lysine-amidobenzyl phenoxyester is resin cleavage cocktails. TFA = trifluoroacetic acid; TIS = triisopropylsilane; DCM = dichloromethane; HCl = hydrochloric acid; HFIP = hexafluoroisopropanol, ^{1}H NMR = proton nuclear magnetic resonance.

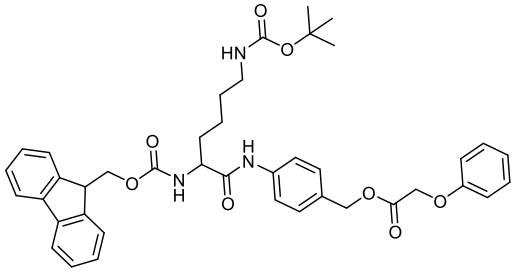

Cleavage cocktail	Time	Outcome	Analysis	Reference
TFA	2 hours	Ester cleavage	^{1}H NMR	544
TFA/TIS/H_2O (95:2.5:2.5)	2 hours	Ester cleavage	^{1}H NMR	544
1% TFA / DCM	2 hours	Ester in tact	^{1}H NMR	545
0.1 N HCl / HFIP / DCM (20%)	1.5 hours	Ester in tact	^{1}H NMR	546

The arginine-phenoxyester conjugate was unstable when exposed to standard TFA-mediated resin-cleavage conditions. The experiment was re-run without the addition of water to investigate whether the cleavage was a result of hydrolysis. ^{1}H NMR analysis of the two products showed a shift in methylene resonances corresponding to the benzyl and phenoxy moietyies. A change in both resonances suggests that the bond between them has been cleaved. When the ester conjugate was treated to milder cleavage conditions using only 1% TFA in DCM, the ester methylene remained unchanged. However, such mild cleavage conditions are inadequate in removing robust protecting groups such as the 2,2,4,6,7-pentamethyldihydrobenzofuran-5-sulfonyl (Pbf) group. Palladino and colleagues had identified a mild resin cleavage procedure which avoids TFA but is suitable to remove Pbf groups from arginine. The cleavage cocktail consists of HCl, 1,1,1,3,3,3-hexafluoroisopropanol and DCM and can remove Pbf groups in 1.5 hours. The arginine ester was treated to the cleavage solution and analysis of the crude product after 1.5 hours revealed the ester was still present. In the ^{1}H NMR sprectra (**Figure 5-53**), a resonance at 4.66 ppm corresponding to the methylene of the phenoxy moiety is shifted slightly downfield upon cleavage of the ester. Furthermore, the peak corresponding to the benzyl methylene protons is visible at 5.2 ppm when the ester bond is present. Upon ester cleavage, the protons are detected upfield of 5.2 ppm, however the number of resonances in the region prevent the exact peak being identified.

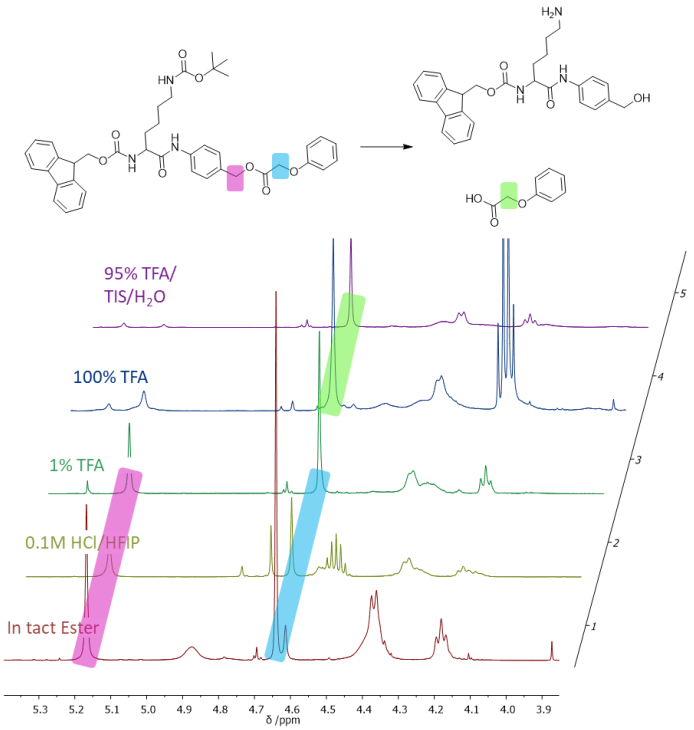

Figure 5-53. In-line ^{1}H NMR spectra of the products obtained when treating lysine-phenoxyacetate ester **125** to different resin removal conditions. A small shift in the peak corresponding to the phenoxyacetic ester methylene (shown in blue) from 4.66 to 4.70 ppm is observed upon ester cleavage (shown in green). Furthermore, the benzyl methylene resonance (shown in pink) is no longer observed at 5.2 ppm when a high proportion of trifluoroacetic acid (TFA) is employed in the mixture, indicating that the the ester is cleaved. TIS = triisopropyl silane; HCl = hydrochloric acid; HFIP = 1,1,1,3,3,3-hexafluoropropanol.

With ester-stability identified, the resin-cleavage conditions were employed to verify the sensitivity to remove peptides from Wang resin. To investigate the success of the nitro reduction of the tritylated resin-immobilised nitro benzyl alcohol by amide formation (**Scheme 5-68**), the resin-bound product **178**, was removed from the resin using HFIP.

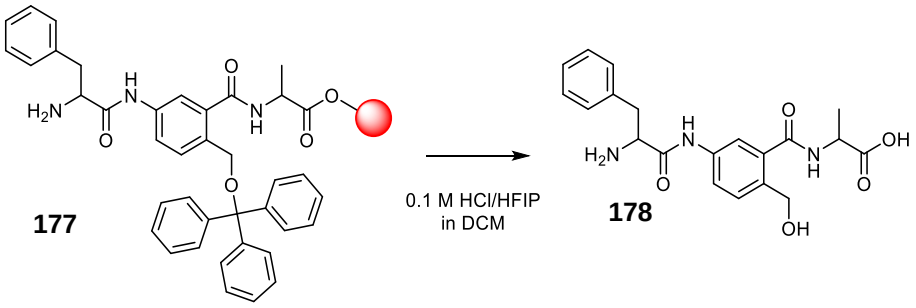

Scheme 5-68. Cleavage of expected resin-bound phenylalanide tritylbenzoyl alanine using test cleavage conditions 0.1 M hydrochloric acid and 1,1,1,3,3,3-hexafluoropropanol. The trityl group is expected to cleave simultaneously.

After 1.5 hours, the resin was filtered off and the crude filtrate dried and analysed by ^{1}H NMR spectroscopy (**Figure 5-54**). The NMR spectrum of the crude product showed peaks similar to that of the expected product. Notably, the aromatic resonances of the phenylalanine (labelled yellow in **Figure 5-54**) integrated with that of the alanine resonances (highlighted

pink) in a 2:3 ratio which indicated successful coupling. The trityl group peaks are not present, as expected, owing to the acidic cleavage conditions. The benzyl alcohol methylene protons are no longer a singlet integrating to 2 protons which indicates that coupling may be occurred at unprotected alcohol terminals or that the two protons experience two different nuclear environments which is detectable by the splitting of the NMR signal. In this case, it might be expected to observe splitting resulting from geminal coupling which is not visible in the spectra. The methine protons and the phenyl methylene protons did not produce a visible peak, although it is possible they are present under the broad resonance at 3.4 ppm. at unprotected from the did not show the peaks for the expected product.

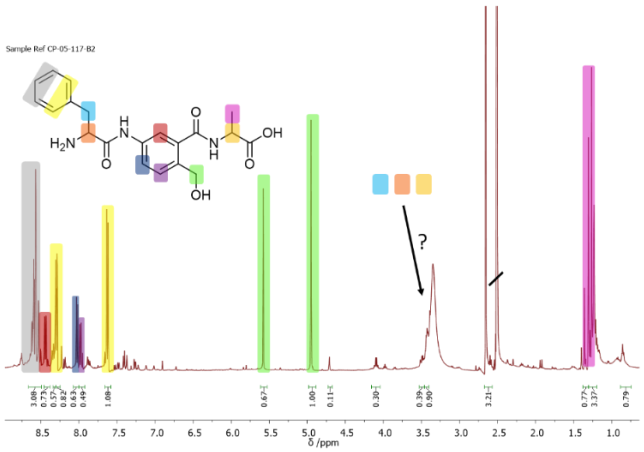

Figure 5-54. ^{1}H NMR of the product isolated from the resin removal using hexafluoro-2-propanol. The protons observed match that of the expected product although the methine and benzyl protons are either not present or found beneath the broad resonance at 3.4 ppm. Furthermore, the benzyl protons neighbouring the alcohol appear to have split into two singlets.

Cleavage from the resin using HFIP produces a product which shares ^{1}H NMR resonances with the expected product. The exact structure is not determined, owing to the lack of methine resonances. In order to be certain, a further investagtion is necessitated to confirm efficient coupling and determine resin removal efficacy. As a preliminary result, it appears that the HFIP conditions remove product from the resin which may be suitable for the removal of a treprostinil ester conjugate.

To localise the release of treprostinil in the PAH lung, the conjugation of treprostinil to an enzyme upregulated in PAH was considered. With the reported ease, scalability and reproducibility of solid phase synthesis, a method to synthesise such a conjugate on resin was considered to offer greater commercial feasibility. Achieving a tryptase or chymase substrate conjugate with treprostinil required conjugation at the N-terminus. Conjugation of treprostinil to a resin which could then facilitate peptide conjugation was not an option and therefore, a synthetic route to accommodate both resin growth and treprostinil on-resin was investigated. A route was found (**Scheme 5-69**) to immobilise a derivative of nitro-benzyl alcohol onto the resin which after hydroxyl protection and nitro reduction would facilitate a sequence of amino acid conjugation using standard coupling of Fmoc amino acid derivatives. Following hydroxyl

deprotection, treprostinil could be conjugated on resin which will facilitate an easy method to remove and recycle excess equivalents of treprostinil. Following conjugation, conditions were sought for the resin removal step which is mild enough to cleave the conjugate from the resin and cleave the side chain protecting groups but leave the treprostinil ester in-tact.

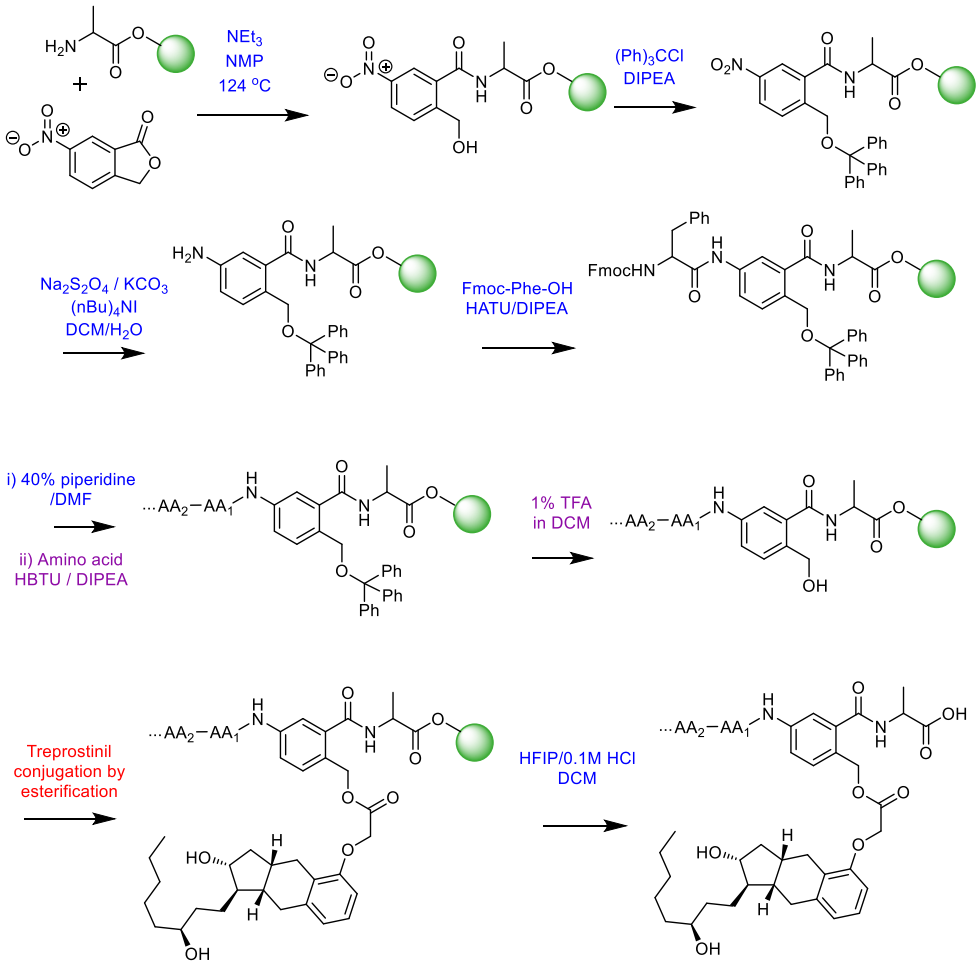

Scheme 5-69. Synthetic steps optimised to achieve the treprostinil-enzyme substrate conjugations on resin. Reaction reagents shown in blue have been shown to produce the proposed compound, whereas those in red are yet to be determined. Reactions conditions shown in green have been attempted but the reaction product ambiguous or not confirmed. Purple reaction conditions indicate conditions which have been successfully employed in other reaction within this work but not attempted on the compound shown.

Tryptase substrate summary

On resin techniques were thought to provide a clean and reproducible route to the synthesis and purification of C-terminus enzyme substrates. Methods were pursued to achieve a chromophore at the C-terminal, for proof-of-concept, and then a method to conjugate treprostinil. Conjugation to a chromophore was initially sought as a cheaper alternative to purchasing commercially available conjugates. The time taken to synthesise the conjugates was anticipated to be negligible, given the automatic programmable synthesis of the peptide. The synthesis was hindered by unresolved issues conjugating the amino-acid derivative of amino coumarin to the resin. FITC-conjugated derivatives of the substrates were synthesised by the addition of a side chain FITC-conjugated lysine derivative at the C-terminus. The

synthesis was simple and reproducable, but their degradation does not alter electromagnetic absorbance and emission properties sensitively to facilitate real time tracking of the enzymatic degradation in the presence of tryptase. Other chromophores are available which could have facilitated resin-immobilisation, but efforts were directed from reproducing commercially available compounds to the synthesis of treprostinil conjugates.

To attach the treprostinil carboxyl group and C-terminus of a peptide chain together, a self-immolative spacer, p-aminobenzyl alcohol, was incorporated into the design which was anticipated to facilitate drug release *via* a self-immolative mechanism. Immobilisation of the peptide-treprostinil conjugate on the resin was the first hurdle, as the treprostinil structure does not facilitate conjugation exclusively and orthogonally through two moieties. At first, resin-attachment between the first amino acid and spacer was attempted. Reductive amination of p-aminobenzyl alcohol was deemed too poorly nucleophilic to form the imine intermediate which could later be reduced, immobilising it onto the resin. Therefore, attaching the resin between the first and second amino acids was sought. Attachment of the first amino acid by reductive amination was successful both in solution and on-resin. The on-resin reductive amination and subsequent amidation step was difficult to monitor using the colourimetric tests available and furthermore, results were rarely reproducible.

Using a method to immobilise derivatives of benzyl alcohol onto the resin were investigated and which saw success in the ring opening of 6-nitrophthalide, both in solution and on-resin. The need to protect the hydroxyl liberated upon ring-opening was established which was achieved by tritylation. In order to facilitate peptide conjugation, the nitro-required reduction which is not commonly employed for on-resin strategies. Attempts to negate the reduction step were sought but the amine and amide derivatives employed were not electron withdrawing enough to facilitate subsequent ring opening. Despite the unconventional approach, reduction was achieved without the need for metal catalysis. The aniline product was insensitive to the Kaiser test but a method to monitor the success of the reaction was found by coupling and deprotection of a reaction sample to a fmoc-amino acid. The process is lengthier than standard colourimetic tests but provided unambiguous reaction monitoring.

The sensitivity of the ester bond achieved upon the expected treprostinil conjugation was anticipated and resin cleavage conditions were sought that would not result in ester degradation and premature treprostinil release. Resin cleavage using HCl and HFIP in DCM was found to be suitable for ester stability and resin cleavage in solution but when employed to remove a dipeptide from Wang resin, the expected dipeptide was not detected by ^{1}H NMR.

5.2.3 Chapter Summary

Polymer drug-conjugates (PDCs) of treprostinil which include a targeting moiety to increase specificity for the lung has not previously been attempted. With no prior history of PDCs in the treatment of PAH, lessons were taken from the approach applied in treating cancer. PAH and cancer have many overlapping mechanisms and features however treprostinil is not as toxic

as the cytotoxic compounds used to kill tumour cells. Therefore, treprostinil has a larger therapeutic window than cancer therapies and could better exploit the benefit of polymer drug conjugates, as a small level of off target effects will not cause the negative effects associated with cytotoxic drugs. In the design of a polymer drug conjugate, the targeting moiety and releasable linker were considered.

CAR was investigated as the targeting moiety and a route to synthesise the fluorescein-conjugated derivative was attempted first using a bespoke made CAR(Dde) moiety and then using on-resin synthesis techniques. For both pathways taken, purification required a preparative column which, after attempting alternative methods of purification, was purchased. With hindsight, the purification of the solution phase peptide could have been made easier to read the absorbances by using a different wavelength which could have been achieved by employing a diode array spectrometer. FITC-CAR was shown to localise in the near nuclear regions of cells in the presence of TNF-α. At higher concentrations FITC-CAR was also shown to bind non-specifically to the nuclei of both healthy and inflamed cells.

Substrate-specific enzymatic degradation of prostacyclins is an approach not previously attempted in the published literature. However, its successful employment in treating patients could result in the localised release and action of PM's in diseased lung tissue in PAH. Tryptase is an enzyme only found in sites of chronic inflammation, so a tryptase-specific substrate will only release drug in the PAH lung. SPPS is a useful tool for the synthesis of peptides and small molecule which allows for multiple subsequent steps to be carried out on molecule and minimises the work up. However due to the lack of certainty and analysis in each step, robust chemistries must be employed to increase the yield of desired product. Testing of the pro-drug substrates was attempted using Fmoc-ACA-OH which is designed to link to the resin allowing for simple substrate-chromophore dimers. Immobilisation onto the resin was not achieved and so Lys(FITC) C-terminal conjugations were sought. Synthesis was readily achieved but testing of the release could not readily be tracked using change in chromophore absorbance.

Immobilisation of treprostinil on a resin allows for multiple different oligopeptides to be appended to treprostinil. This work covered the on-resin conjugation of treprostinil to tryptase and chymase substrates, it is thought that the concept could be applied to oether enzyme substrates. Multiple equivalents of treprostinil are required to react with the resin, although the excess can be easily recovered. The sensitivity of the ester bond formed to conjugate treprostinil is susceptible to nucleophilic substitution so treprostinil is added to the resin last.

5.2.4 Strengths and Limitations

PAH patients receiving prostacyclin therapy are burdened by the systemic adverse events. Despite the targeted advancements in cancer therapy, polymer-drug conjugates of PMs for PAH have not reached the clinic. The synthesis, utility and biocompatibility of HPMA polymers is well established. Although a full polymer was not synthesised, the work featured in this

chapter builds ideas and synthetic strategies towards incorporation of releasable treprostinil and a targeting moiety.

Despite the homing abilities of the CAR peptide being previously reported, the 4-year period in which no further publications or patents had been published, made us sceptical about its further utility. We initially set out to confirm some preliminary observations in a different inflammation assay, which would help to determine its utility in a drug polymer for PAH. Synthesis of the FITC conjugated peptide both in solution and on-resin took longer than expected. Although a method was found for the oxidation of the thiols, previous unsuccessful oxidation attempts could have been improved by quenching the iodine with ascorbic acid.

Targeted therapies, including using CAR peptide for the treatment of PAH have been explored in the literature but this is the first reported use in a conjugated form. This work is the first attempt to incorporate an oligopeptide prodrug approach in PAH. To achieve the prodrug structures, on-resin synthesis was pursued. This was the first report of immobilising a PM on resin which allows for versatility in the peptide substrates. Ideally, immobilisation of treprostinil on the resin would feature in the initial steps, however the lack of suitable handles and the sensitivity of esters in the presence of excess amines risks severing the bond linking treprostinil to the immolative linker. On the other hand, incorporating treprostinil onto the resin last reduces the opportunity for treprostinil to be cleaved during the synthesis. The cost and complex synthesis of treprostinil prioritise its preservation.

Although efforts for the different moieties in the context of a polymeric structure were explored, incorporation of the substrate-drug moiety and the targeting peptide into a polymeric structure was not attempted.

5.3 Chapter Conclusion

In conclusion, both a targeting moiety and releasable linker for a polymer-drug conjugate for the delivery of treprostinil to the PAH lung were investigated. Synthetic routes on-resin were explored to find reproducible methods which can later be scaled.

Achieving the derired compounds on resin was not as straight-forward as expected but did achieve the cyclised FITC-CAR method when an off-resin method for oxidation of the thiols was employed. Progress was made in achieving the first on-resin conjugate of the prostanoids. Despite the error made during the nitro reduction, further coupling through a nucleophile other than the hydroxyl was observed. The opportunity to test the tryptase substrate conjugates was not reached in the time frame, so activity is yet to be determined. The synthetic method described is thought to be compatible to any substrate designed to be cleaved at the C-terminus, which opens the potential to target a variety of disease states involving proteolytic degradation.

A targeted polymer drug conjugate based on the structure described by Ringsdorf[425] (**Figure 5-1**) has not been described previously. Here, the design of a targeting moiety and release mechanism is presented and progress made on the successful synthesis.

Chapter 6. **General Discussion**

6.1 **Project Approach**

The aims of the PhD project were to investigate methods to reduce adverse events associated with treprostinil therapy for the treatment of pulmonary arterial hypertension (PAH). First the adverse events associated with treprostinil therapy versus placebo were identified from clinical trial data in the meta-analysis described in **Chapter 2**. The analysis identified drug-mediated systemic and local adverse events which varied with administration route and prostacyclin mimetic. The conclusions provided a solid clinical rationale for the strategies that are described in the subsequent chapters. The work presented in **Chapters 3-5** describe the different pro-drug strategies that were selected to examine how to reduce the adverse reactions associated with treprostinil. Many prodrug approaches were considered as described in **Chapter 1** but were not pursued due to characteristics of PAH as a medical condition or because of the inherent structure activity limitations of treprostinil as a molecule or its mode of action as an agonist.

Two strategies that were examined include the preparation and *in vitro* characterisation of N-acyl sulfonamide treprostinil (TRE-S) **21** and a polymer-drug conjugate, oligo(PEG-treprostinil acetal) **71**. A third strategy involved the design of a targeted polymer-treprostinil conjugate. Treprostinil **4** was envisaged to be conjugated to a water-soluble polymer by an enzymatically cleavable pendent chain much as is described by the Ringsdorf model. Some key conclusions from the work described in **Chapters 2-5** include:

1. Subcutaneous treprostinil is limited by site pain.
2. Treprostinil IP activity can be reduced by using N-acyl sulfonamide prodrug
3. Treprostinil is limited as a monomer for polyacetal formation.
4. Inflamed endothelial cells facilitate binding of CAR peptide, compared to healthy cells
5. A method has been determined to immobilise both a carboxylic acid containing drug and enzyme substrate onto a resin.

Preliminary work was also done for related prodrug strategies but was terminated at early initial stages. N-acyl-sulfonamide treprostinil **21** was initially intended for a polyvalent prodrug strategy so methods were examined to conjugate treprostinil via its aryl ring. Since progress to prepare the CAR targeting moiety and tryptase linker was slower than anticipated, efforts were reduced to prepare monomers and co-polymers of N-(2-hydroxylpropyl methacrylamide), which was being considered as the polymer to be used for a targeted-treprostinil conjugate.

The breadth of the strategies examined and described in this thesis was also in part a result of the uncertainty of a supply of treprostinil at the beginning of the project, which meant treprostinil-specific approaches were not immediately pursued. A supply of treprostinil was received in May 2016. While waiting for enough treprostinil to work with, attempts to pursue

the CAR-peptide and enzymatically degradable linkages employing a model drug-compound (phenoxyacetic acid) were conducted. Once the treprostinil supply (2 g) was received, the prodrug TRE-S strategy was initiated using treprostinil as sparingly as possible. Polymer-treprostinil conjugates were not attempted until it was established that enough treprostinil was left to incorporate into a polymer.

6.2 Critical analysis and future perspective

For each clinically used dosage form of treprostinil, there are different limitations, e.g. oral treprostinil exhibits fluctuating peak and trough concentrations in the blood whereas subcutaneous does not. The project primary aim was to decrease adverse events reported in the literature owing to non-specific activation of prostanoid receptors. A secondary consideration was increasing the duration of action to reduce the frequency of dosing by utilising a polymer-based approach.

Chemical conjugation of treprostinil is not the only method that can reduce adverse events associated with treprostinil treatments. Other approaches have recently been developed and have entered clinical trials, including; pre-filled 2-day disposable capsules for subcutaneous delivery;[547] implantable intravascular infusions (FDA approved),[548,549] portable, breath-powered inhalers[550] and an inhalable treprostinil lipid nanoparticle prodrug (discussed in **Chapter 3**).[136,200]

At the time of the project conception (2014), only work on a PEG-ester derivative of treprostinil investigated in the early 2000's had been published.[338,399] The 4-arm PEG derivative developed from a collaboration between UT and Ascendis had entered trials[33979] but the results were not released until 2015.[138] No other polymer or prodrug derivatives of treprostinil had been published to our knowledge. From the understanding gained from these documented works, our work was designed to extend and not duplicate understanding. Thus, ester conjugation of treprostinil was avoided, and more site-specific release mechanisms were pursued. During the last few months of the project, results of the pharmacokinetic study of an inhaled alkyl ester treprostinil prodrug delivered in a lipid nanoparticle formulation in humans[135] revealed that the adverse events experienced were similar to inhaled treprostinil, further verifying this decision.

Analysis using publicly disclosed information of the adverse event profile of treprostinil *via* the different routes of administration was necessary to determine a plausible strategy to reduce adverse events that could be addressed utilising a polymer-based approach. Flushing related to inhaled treprostinil was the most likely adverse event, followed by site pain associated with subcutaneously delivered treprostinil. Furthermore, a comparison between selexipag 6 and treprostinil demonstrated no difference in the likelihood of gastrointestinal-associated adverse events for orally administered treprostinil. The meta-analysis identified two limiting factors associated with treprostinil; (i) activation of prostanoid receptors upon subcutaneous infusion causing site pain; and (ii) a lack of specificity for the lung resulting in systemically induced

adverse events. Thus, overcoming these limitations by a prodrug approach became the aim for developing the strategies described in the experimental **Chapters 3-5**.

Treprostinil **4** is a challenging molecule to modify chemically. Early structure activity relationships published on the initial design of treprostinil were consulted but limited information on the structure activity relationships of treprostinil derivatives were accessible. A 3-month placement at UT to conduct their synthesis of treprostinil provided an invaluable opportunity to gain experience and insights about the history and development of treprostinil. Many ideas were considered for derivatising the carboxylic acid and the two hydroxyl groups of treprostinil. As described in **Chapter 3,** several reaction conditions employed to derivatise treprostinil were unsuccessful. The hydroxyls were less reactive than first thought which was further verified in **Chapter 4** by the difficulty experienced forming polyacetal bonds via a reactive vinyl ether. The secondary alcohol groups exhibited weak nucleophilicity and were not able to displace alkyl halide but were able to silylate using silyl chlorides when the acid group was protected which prevented *in situ* degradation. Acidic reaction conditions suppressed the nucleophilic nature of the secondary hydroxyls but standard benzyl protection methods using basic conditions were also unsuccessful. Efficient nucleophilic activity of the hydroxyls was achieved when the electrophile was activated with charged salts of compounds with broken aromaticity. When activating the acid for coupling reactions with carbodiimide derivatives, the alcohols were able to undergo reactions. This was deduced by the number of reaction products formed when the hydroxyls were unprotected which when protected, were not present.The difficulties in derivatising treprostinil to achieve N-acyl sulfonamide treprostinil **21** were overcome by employing a series of protecting group steps, and then circumvented using an intermediate precursor. For the treprostinil coupling, the poor nucleophilicity of methane sulfonamide was overcome by employing a coupling agent, CDI, which produced imidazole as a by-product which helped to drive the reactions.The reduced pKa of a phenolic hydroxyl compared to alkyl hydroxyls facilitated a route to alkylate the aromatic hydroxyl without employing protecting group chemistries. Ease of alkylation depended on the activity of the electrophile which is affected by acidic neighbouring protons. The use of a strong base facilitated greater reaction yields. Although the synthesis of the N-acyl sulfonamide treprostinil **4** had been independently pursued by our collaborators, the synthesis described in **Chapter 3** from the triol precursor **51** is novel and provides a means to examine further prodrug approaches. Using HPLC, no evidence of poor stability was detected in the work described in **Chapter 3**, but it was clear that limitations may exist (e.g. solubility).

Future conjugation of treprostinil reactions at the acidic group should first consider employing the triol precursor to treprostinil. The triol approach does not require protecting group strategies to be employed which potentially increases yields. Coupling of prodrug head groups which do not possess an acidic alpha proton will likely achieve greater reaction efficacy.

The N-acyl sulfonamide treprostinil prodrug approach was successful in reducing activity at the IP receptor which indicates that further investigation would be worthwhile. The enzymatic

degradation required to remove the N-acyl sulfonamide moiety was attempted several times using a microsomal assay. Optimising the analysis method using HPLC and then LCMS was challenging, and although the data started to show a coherent result towards the end of the PhD project, repeat reactions still need to be conducted and analysed to demonstrate a reproducible trend. Overall the work described in **Chapter 3** did provide for greater understanding of the reactivity of treprostinil. The N-acyl sulfonamide prodrug **21** has not yet been published, so it is hoped that once the microsome detection methods are refined, the analysis can be repeated, and results will be submitted for publication.

Compared to the polymer-based strategies, a low molecular weight prodrug approach is a simpler and possibly more scalable approach that offers more commercially viable alternatives but does not reduce systemic permeation. Should a low molecular weight prodrug approach be desired, future work should consider a synthetic route using the triol precursor **51**. The use of the triol **51** offered a method of prodrug synthesis which did not require the treprostinil derivative until the last step. As well as minimising losses associated with the protecting group strategy, a variety of derivatives could easily be synthesised using this approach. To reduce systemic prostanoid receptor agonism, a PAH-specific prodrug-cleavable moiety might be considered. An enzymatic approach may offer a method to achieve site-specific cleavage

The concept of a polymer-drug conjugate of treprostinil that would preferentially localise drug to the PAH lung still requires *in vivo* examination to determine the extent of uptake that may be possible in the diseased vasculature. The pathological changes in the PAH diseased lung may facilitate uptake of macromonomers which could result in accumulation of a polymer-drug conjugate. The endothelial damage of PAH to facilitate uptake of macromolecules into the tissue space by an enhanced permeation and retention effect clearly requires further study. Furthermore, the specificity of conjugate uptake can be enhanced by the inclusion of a selective targeting moiety, which still needs further validation.

Use of a diol-containing drug as a monomer to prepare a polyacetal that incorporates the drug in the main chain is known[401,402,416] for synthesising an acid labile, biodegradable polymer-drug conjugates. The work described in Chapter 4 shows that this approach may not apply to treprostinil as with other molecules that have been described in the literature. Treprostinil was the first molecule with secondary diols that to our knowledge has been examined for polyacetal synthesis. Although the hydroxyls are known poor nucleophiles, reaction with vinyl ethers to form acetal bonds was observed although was likely hindered by the acidic conditions employed. The preparation of the treprostinil oligoacetal **71** is still considered a viable candidate for further preclinical evaluation because an oligomeric acetal would be expected to diffuse from the hypodermis more quickly than a larger molecular weight polyacetal. Clearly there are significant *in vivo* experiments that would need to be conducted to determine efficacy. It is unfortunate that progress was hindered by a yet to determine limitation in the acid catalysed reaction conditions for preparing treprostinil containing co-polyacetals. It is possible that a base-catalysed polymerisation should be examined and compared with the

acid catalysed reaction, which may be a feasible strategy for future work. Alternatively, functionalising the treprostinil to form acetal containing monomers (e.g. diamino-diacetal treprostinil) which could then undergo a more reactive and better controlled polymerisation is another potentially successful strategy.

Since little is known about the possibility for passively targeting PAH tissue and since active targeting strategies are clinically proven (e.g. ADCs), a targeting strategy for a polymer-drug conjugate to the diseased lung was pursued. An antibody-based approach was beyond the scope of what was known at the outset of the project, so the CAR peptide was investigated as it appeared from the literature that it could be selective for PAH tissue. First a method to synthesise CAR was established which then allowed for the binding to be tested. Fmoc coupling of amino acids was achieved on resin and oxidation of the peptide in solution facilitated disulphide bond formation intramolecularly and reducing intermolecular bond formation. A preliminary study on the binding properties of CAR was conducted and CAR binding to HUVEC cells was shown to increase in the presence of TNF-α which is an inflammatory promoter. A more extensive investigation into CAR binding and the use of CAR over other targeting peptides is warranted.

Several strategies to prepare an enzymatically degradable peptide linker for treprostinil were considered. Of these, a method to conjugate treprostinil to a peptide substrate on-resin was investigated. Once established, the method could be applied to synthesise peptide linker-treprostinil adducts and could be used to prepare an optimised linker-treprostinil on large scale. Using an on-resin immobilisation method, other carboxylic acid drugs could be considered for conjugation to N-terminal enzyme substrates.

The biggest obstacle for preparing the enzyme cleavable linker for treprostinil was establishing a method to link treprostinil and the peptide to a resin. A base-mediated method wasdeveloped which first immobilised the p-aminobenzyl alcohol spacer onto the resin by nucleophilic ring opening of a phthalide ester. The reaction was facilitated by the increased electrophilicity of the carbonyl resulting from the electron withdrawing nitro group at the meta position. On-resin biphasic reduction of the nitro group was conducted to facilitate peptide coupling. . Although the amine derivative was obtained, further efforts to improve the reduction are possible by using an electron phase transfer catalyst, rather than an ion phase transfer catalyst, which may be a strategy for future studies. Nonetheless, the resin bound aryl amine was prepared, but the final conjugation of the enzyme substrate and treprostinil to the resin was not conducted owing to time limitations. The method for the final steps to make the desired peptide-treprostinil linker have been described for future work and a mild resin-cleavage method determined which preserves the treprostinil ester. It is hoped that the synthetic approach will be verified and published soon after thesis submission.

Considering the CAR targeting moiety and the enzymatically degradable peptide linker there are significant additional challenges that will need to be addressed. For example, while conjugating a CAR peptide to a polymer could result in sub-optimal binding of CAR to its target,

there may be alternatives for exploiting CAR. For example, a treprostinil-peptide linker-CAR prodrug that would localise in PAH diseased tissue could be a plausible candidate. Although such a peptide-treprostinil molecule would clear relatively quickly, it would also be expected to be less able to bind to the IP, DP_1 and EP_2 receptors may which cause pain. Treprostinil **4** release would not be expected to occur in the hypodermis, so a large dose could be given, and CAR homing would allow some of the dose to localise in the PAH disease tissue where enhanced concentrations of tryptase could release treprostinil.

As the mechanisms of PAH progression and the pharmacology of treatments become elucidated, opportunities to target multiple pathways are presented. Dual therapy for PAH is utilised and recommended which offers a way to maximise the efficacy whilst limiting the adverse events experienced. Achieving a prodrug dosage form of treprostinil which offers enhanced efficacy in the lung whilst mitigating the adverse events allows for a greater number of dual therapy combinations. As suggested in **Chapter 3**, if adverse events could be reduced then the concept of co-administering two prostacyclin mimetics working *via* different receptors (e.g. selexipag **5** and treprostinil **4**) could also be explored. Further investigation into dual combination therapy would be required but the increased tolerability of including a prodrug prostanoid receptor agonist has the potential to open more avenues for therapeutic strategies.

Chapter 7. Materials and methods

Pulmonary arterial hypertension is a chronic orphan disease with a complex mechanism and poor prognosis. Much attention has been focused on developing safe and efficacious therapies to manage disease progression, but current therapies are still dose-limited owing to adverse events. The impact of the administration route and adverse events associated with therapy on decreasing quality of life is significant. Further investigations are necessitated to improve long term therapies, but it is hoped that a polymer-drug conjugate strategy could offer a method to prevent off-target receptor interactions and increase efficacy of current drug structures.Materials and Methods

7.1 Materials

Treprostinil 4 and the treprostinil precursor, benzindine triol 51 were kindly provided by United Therapeutics Corp (Silver Spring, USA). Selexipag (Cat. No. 10010411) was purchased from Cayman Chemicals (Ann Arbor, USA.)

Phenoxyacetic acid (Cat. No. 169875000), silica (Cat. No. 419290050) for column chromatography, piperidine (Cat. No. 147181000) tyramine (Cat. No. 51-67-2) and 1,1-carbonyldiimiazole (Cat. No. 151810250) were purchased from Acros Organics (Geel, Belgium). Sodium sulfate (Cat. No. 28104.292), N-methyl-2-pyrrolidinone (Cat. No. 25675.3) and anhydrous sodium sulfate (Cat. No. 28104.292) were purchased from VWR chemicals (Radnor, USA). Sulfuric acid (Cat. No. MFCD00064589) was obtained from BDH chemicals (now VWR International).

Potassium carbonate (Cat. No. P/4080/53), acetic acid (Cat. No. 1332902) and 1M Hydrochloric acid (Cat. No. J/4320/15) were bought from Fisher Scientific (Hampton, USA). Fluorescein (Cat. No. 46955) and 3Å molecular sieves (Cat. No. 69833) were bought from Fluka (now part of Fisher Scientific).

Trifluoromethyl benzene (Cat. No. B21340), bromoacetyl bromide (Cat. No. A19580), trifluoroacetic acid (Cat. No. LO6374-AE), 6-Aminophthalide (Cat. No. A18896-02), 6-nitrophthalide (Cat. No. B20375), bromocresol (Cat. No. A17090), N-benzyloxycarbonylglycine (Cat. No. A15928), thallium trifluoroacetate (Cat. No. 43643), acetic anhydride (Cat. No, L04295), trifluoroacetic acid (Cat. No. L06374-AE) and anhydrous toluene (Cat. No. 41464) were obtained from Alfa Aesar (Haverhill, USA).

p-anisaldehyde (Cat. No. 15364) were bought from Avocado (Heysham, UK). H-Arg(Pbf)-OMe (Cat. No. E3110) was purchased from BaChem (Bubendorf, Switzerland). N-(3-Dimethylaminopropyl)-N'-ethylcarbodiimide hydrochloride (EDCI, Cat. No. AS-29855) was bought from Cambridge Biosciences (Cambridge, UK). Chloranil (Cat. No. SC-252566) was purchased from Chem Cruz (Dallas, USA). Cyclised CARSK(Dde)NK(Dde)DC was supplied by China Peptide (Hangzhou, China).

Ammonium bicarbonate (Cat. No. A6141) was purchased from Honeywell (Morris Plains, USA). 7-(9-Fluorenylmethyloxycarbonylamino)-coumarin-4-acetic acid (Cat. No. RL-1170) was purchased from Iris Biotech Gmbt (Marktredwitz, Germany). 4-(dimethylamino)pyridine (Cat. No. 8.51055), Fmoc-alanine (Cat. No. 8.52003), Fmoc-arginine(Pbf)-OH (Cat. No. 8.52067), Fmoc-Asn(trt)-OH (Cat. No. 8.52044), Fmoc-Asp(OtBu)-OH (Cat. No. 8.52005), Fmoc-Cys(Acm)-OH (Cat. No. 8.52006), Fmoc-Cys(trt)-OH (Cat. No. 8.52008), Fmoc-D-leu-OH (Cat. No. 8.52145), Fmoc-e-Ahx-OH (Cat. No. 8.52053), Fmoc-Ile-OH (Cat. No. 8.52010), Fmoc-Lys(Boc)-OH (Cat. No. 8.52012), Fmoc-Lys(mtt)-OH (Cat. No. 8.52065), Fmoc-Orn(Boc)-OH (Cat. No. 8.52015), Fmoc-Phe-OH (Cat. No. 8.52016), Fmoc-Pro-OH (Cat. No. 8.52017), Fmoc-Ser(tBu)-OH (Cat. No. 8.52019), FMPB Novagel HL (Cat. No. 8.55087), 3-[Bis(dimethylamino)methyliumyl]-3H-benzotriazol-1-oxide hexafluorophosphate (HBTU, Cat. No. 8.51006), PAL-Novasyn TG resin (Cat. No. 8.55137), Rink AM resin (Cat. No. 8.55130) and Wang resin (Cat. No. 8.55002) were purchased from Novabiochem (now Merck; Kenilworth, USA). Aluminium backed silica thin layer chromatography plates (Cat. No. 1.05554.0001) and 1M sodium hydroxide solution (Cat. No. 1.09137.1000) were obtained from Merck (Kenilworth, USA).

Magnesium oxide (Cat. No. 203718), sodium Citrate dihydrate (Cat. No. W302600), dichlorodiisopropyl silane (Cat. No. 38385), triethylene glycol divinyl ether (Cat. No. 329800), polyethylene glycol 3400 (Cat. No. 20,244-4), *para*-toluene sulfonic acid monohydrate (Cat. No. 402885), anhydrous tetrahydrofuran (Cat. No. 401757), pyridine (Cat. No. 270970), triethylamine (Cat. No. T0886), Citric acid (Cat. No. C2404), phosphate buffered saline tablet (Cat. No. P4417), magnesium sulfate (Cat. No. 208094) 2-benzyloxy-1-methylpyridinium triflate (Cat. No. 679674), Celite (Cat. No. 6858), lithium hydroxide (Cat. No 402974), methanesulfonamide (Cat. No. 64275), 1,8-diazabicyclo[5.4.0]undec-7-ene (1M in THF; Cat. No. 714852), Palladium on Carbon 5% wet (Cat. No. 205680), zinc granules (Cat. No. 31653), hydrochloric acid solutions were made from 12 M concentration solution (Cat. No. 320331), triethylene glycol mono methyl ether (Cat. No. 317292), tetrabutylammonium iodide (Cat. No. 140775), sodium hydride (60 % dispersed in mineral oil; Cat. No. 45912) 1,2-Ethanedithiol (Cat. No 2390), 1-hydroxybenzotriazole hydrate (Cat. No. 54802), 2,4-dimethoxybenzaldehyde (Cat. No. D130400), 2-methylpyridine borane complex (Cat. No. 654213), 4-(4-nitrobenzyl)pyridine (Cat. No. 73210), 4-aminobenzyl alcohol (Cat. No. 191558), acetaldehyde (Cat. No. 465380), aluminium chloride (Cat. No. 6220), anhydrous dimethylformamide (Cat. No. 227056), hydrazine hydrate (Cat. No. 225819), lithium hydroxide monohydrate (Cat. No. 402974), N,N-diisopropylcarbodiimide (Cat. No D125407), N,N-diisopropylethyl amine (Cat. No. D125806), ninhydrin (Cat. No. 26H2616), p-toluenesulfonyl chloride (Cat. No. T35955), sodium bicarbonate (Cat. No. S6014), sodium borohydride (Cat. No. 71320), sodium thiosulfate (Cat. No. 217263), sodium triacetoxyborohydride (Cat. No. 316393), tetrabutylammonium iodide (Cat. No. 140775), ethyl chloroformate (Cat. No. 185892), 1-[Bis(dimethylamino)methylene]-1H-1,2,3-triazolo[4,5-b]pyridinium 3-oxide hexafluorophosphate (HATU; Cat. No. 445460) and succinic anhydride (Cat. No. 239690),

triethylamine (Cat. No. T0886), dichoroethane (Cat. No. 28450), L-phenylalanine ethyl ester hydrochloride (Cat. No. 22070), phosphomolybdic acid solution (Cat. No. 319279), sodium cyano borohydride (Cat. No. 156159), triisopropylsilane (Cat. No. 23378), trimethylorthoformate (Cat. No. 108456), pyridine (Cat. No. 270970), β-alanine ethyl ester (Cat. No. 306142) and trityl chloride (Cat. No. 93000) were purchased from Sigma Aldrich (St. Louis, USA).

7.2 General Methods

7.2.1 Characterisation and Analysis

^{1}H and ^{13}C nuclear magnetic resonance (NMR) were determined on either a Bruker 400 MHz Avance system with Ultrashield Bruker magnet and broadband probe or Bruker 500 MHz Avance system with 500 MHz Oxford magnet and QNP cryoprobe (Billerica, USA). d^{6}- DMSO (Cat. No. DLM-10-10), $CDCl_3$ (Cat. No. DLM-7-100MS), MeOD (Cat. No. DLM-24-10), D_2O (Cat. No. DLM-4-10) were all purchased from Cambridge Isotope Laboratories Inc. (MA, USA). NMR data was analysed using Mestrenova software (version 6.0.2; Santiago de Compostela, Spain.

Infrared (IR) data were collected using a Perkin Elmer (Tokyo, Japan) Spectrum 100 FTIR spectrometer. Samples were analysed between wavelengths 650-4000 cm^{-1} at 4 cm^{-1} resolution and recorded as an average of 4 scans as percentages transmission.

High performance liquid chromatography (HPLC) was conducted on a Jasco system (Jasco Corp., Oklahoma, US) equipped with a Supelco discovery-HS C_{18} column (Cat. No. 568522U) from Sigma Aldrich and ChromNAV software (version 2.02.05; Jasco Corp). The system comprised of a UV detector (Jasco-2077), pump (Jasco-980) and autosampler (Jasco-2055). HPLC grade solvents were spiked with 0.1% trifluoroacetic acid (Cat. No. L06374, Alfa Aesar) and degassed with a stream of argon (BOC, Guilford, UK) before use.

Liquid chromatography-mass spectrometry (LC-MS) was carried out on a Shimadzu LC-MS 2020 (Kyoto, Japan). The LC comprised of a pump (Shimadzu LC-20AD), an autosampler (Shimadzu- SIL20AC HT) with loop volume 100 µL, an oven (Shimadzu CTO-20A) set at 40 ^{o}C and a UV detector (Shimadzu-SPD-20A) set to read absorbance at 220-254 nm. The MS comprised of a single quadrupole with DL temperature 250 ^{o}C and heating block at 300 ^{o}C. The nebulising gas was flowing at 1.5 L/min and the drying gas flowing at 15 l/min. The system was fitted with a Xterra MS C18 column (186000602) from Waters (Milford, USA). Flow rate was set at 1.0 mL/min with a a water and acetonitrile mobile phase, both spiked with 0.1% formic acid and run in the volume described below.

Table 7-1. Mobile phase for the 7-minute method used for the paired Shimadzu liquid chromatography – mass spectroscopy analysis. Both mobile phases were spiked with formic acid.

Time	% Water	% Acetonitrile

0	90	10
4	5	95
5	5	95
5.2	90	10
7	90	10

Automated column chromatography was carried out on a Isolera one system (Biotage, Uppsala, Sweden) equipped with SNAP cartridge (KP-Sil, 25 g). Reagent grade ethyl acetate (EA) and hexane were used.

Liquid chromatography mass spec (LCMS) grade water (Cat. No. 39253) and LCMS grade acetonitrile (Cat. No. 34967) were bought from Honeywell (Morris Plains, USA). Solvents were spiked using formic acid (Cat. No. F/1900/PB09; Fisher Scientific. Liquid chromatography-tandem mass spectrometry (LCMS/MS) comprised two systems; LC was carried out on an Agilent 1260 Infinity system (Agilent; Santa Clara, USA) equipped with a phenomenex synergi hydro column (C_{18}, 150 x 4.6, 4 µm) fitted with guard column. MS was carried out on an Aqilent triple Quad 6460 with tandem quadrupole mass spectrometer (Agilent; Santa Clara, USA). Peak intensities of characteristic ions (m/z) were measured in multiple reaction monitoring (MRM) mode. Mass spec data was analysed using Mass Hunter software (version B.06.00).

Chemical properties and drawings were made using ChemDraw from Perkin Elmer (Waltham, USA). Analysed data was plotted using GraphPad Prism (version 7.04) as mean with standard error of the mean (SEM).

7.3 Methods for Chapter 2

7.3.1 Literature search

The PRISMA and PRISMA-P checklists for systematic reviews and meta-analyses were followed.[551,552] Studies were searched for in the online databases: PubMed/Medline, Scopus, EMBASE and Cochrane library with no year limits. Highwire, Springer link, Sciencedirect and Wiley library online publisher platforms were also searched. The Key words used were; iloprost, ilomedine, ventavis, epoprostenol, Flolan, selexipag, Uptravi, beraprost, treprostinil, UT15, UT-15, UT 15, Remodulin, Tyvaso, Orenitram, Pulmonary arterial hypertension, human, patient, pulmonary arterial hypertension, pulmonary hypertension. MeSH terms used were “pulmonary hypertension” and “epoprostenol/analogs and derivatives”. When and where necessary, the RCT filters were applied. The search was conducted up until June 2016. Other meta-analyses have been released since this time[322,553] but no new trial results have been published.

7.3.2 Inclusion and exclusion criteria for meta-analysis

All trials in all years, conducted pre- and post-marketing worldwide, involving IP receptor agonists delivered in any form to adults (aged 16 years or older) for the treatment of PAH which complied to the following criteria were considered:

(1) Randomised controlled trials vs. placebo;

(2) patients with PAH who had a follow up period > 8 week;

(3) patients were diagnosed as having PAH according to the WHO/NYHA classification system. Individual case studies, open-label studies, trials in healthy volunteers, abstracts, letters or trials which had been terminated early due to safety concerns were not included.

Pulmonary hypertension (PH) was used as an umbrella term to incorporate PH of any sort including in association with other diseases. Trials which focussed exclusively on PAH secondary to a primary disease were excluded. Only randomised clinical trial studies which used PMs were included, whilst trials including other classes of PAH treatments (phosphodiesterase-5 inhibitors; PDE-5i and endothelin receptor antagonists; ERAs), without PMs, were excluded. No language limits were used.

7.3.3 Study quality and data extraction

Two reviewers independently extracted data and assessed the quality of the trials. Uncertainty and disagreement was resolved by consulting a third reviewer. The abstracts (or full text, if abstract not available) of these results were assessed against the inclusion criteria. The investigators then extracted data from the selected studies, including: author, year of publication, aim of the study, sample size, mean age, female percentage, study design. Change from baseline outcome data for treatment and control groups, including; 6MWD, Borg Score, change in quality of life scores, mortality, patients developing right ventricular heart failure, patients requiring lung transplant or rescue therapy, discontinuation due to AEs, Haemodynamic measures (i.e mixed venous saturation, right atrial pressure, heart rate and cardiac index), were collected. AEs were also reported, (site pain, flushing, jaw pain, headache, pain in extremities, diarrhoea, vomiting, arthralgia, nausea, peripheral oedema, fatigue, cough, upper respiratory tract infection and dyspnea). Analysis of all outcomes considers treatment as either monotherapy or combination therapy versus. placebo. The quality of studies (risk of bias) was assessed with Cochrane Collaboration's tool.[554] For the meta-analysis, studies were examined for *P*-values, means and standard deviations or other metrics depicting the effect of PMs on adverse event in PAH.

7.3.4 Clinical end points

The 6MWD test is a clinical measure of functional capacity, used as an indicator of disease severity in patients with pulmonary/cardiovascular impairment. Patients walk along a flat surface between two markers during a 6-minute period and the total distance recorded [555]. Discontinuation refers to patients who did not complete the trial due to intolerable adverse

events. Rescue therapy describes when patients are advised by medical professionals to abandon the study protocol to receive approved medication for the benefit of the patient's health. The death of any patient whilst enrolled in a study was recorded as a fatality.

Reports of adverse event frequency experienced during the trial period were collected. Although site pain was only applicable to parenteral administration formulations, it was included in this analysis, owing to its reported frequency and impact. No distinction was made between facial and general flushing. Data for adverse events which showed no difference in odds ratio (OR) to placebo group in the overall meta-analysis or any of the sub groups was not shown.

7.3.5 Statistical analysis

All outcomes were synthesized with a random effects model[556] which was chosen to account for differences in the treatment effects from study to study.[557] The difference of continuous variable or dichotomous data between two groups was estimated by weighted mean difference (WMD) with a two-tailed 95% confidence interval (CI) or an OR with two-tailed 95% CI, based on the Mantel-Haenszel method.[558,559] Standardised mean difference (SMD) was also used as a summary statistic for continuous outcomes. SMD values of 0.2, 0.5 and 0.8 were defined as small, moderate and large effect size respectively.[560,561] Statistical heterogeneity was assessed using Cochran's Q test, which examines the null hypothesis that all studies are evaluating the same effect.[562] Statistical significance for heterogeneity was set as $p \leqslant 0.10$. Statistic value I^2 was used to quantify the degree of heterogeneity with a score of 25, 50, and 75% representing low, moderate, and high levels of inconsistency, respectively.[563] Heterogeneity was further investigated with subgroup analysis and meta-regression. Publication bias was assessed using funnel plots and Egger's and Begg's test.[564] $P < 0.05$ was regarded as statistically significant for the outcomes. RevMan software package (Review Manager, Version 5.2, The Cochrane Collaboration, Oxford, UK) and Stata 12.0 (College Station, Texas, USA) were employed for statistical analyses.

Groups for sub group analyses were split to compare the trials firstly into the different drug types then into the different routes of administration. To investigate the effect of therapies given in the 30 days preceding trial initiation, the trials were split into three groups: those given non-PAH specific therapy including oxygen, digoxin, calcium channel blockers, anti-coagulants and diuretics, termed supportive therapy; those given non-prostanoid PAH-specific therapy including ERAs and PDE-5i; and those given prostacyclin therapy which in this case included only epoprostenol. Investigating the effect of background therapy meant dividing trials into two groups; those who were receiving other PAH-specific treatment at a stable monitored dose and those trials in which patients were not. In this case, concomitant therapies included ERAs and PDE-5is only. The other groups were not given any PAH-specific therapy on any specific dosing regimen but were treated with supportive therapies (as previously defined) when necessary.

7.4 Methods for Chapter 3

7.4.1 Synthesis

Treprostinil was synthesised during at 3-month visit to UT's laboratory in Silver Springs, Maryland, USA. The large scale synthetic rote as well as the small-scale route were followed and compaired. Details of the synthesis can be found in appendix 8.2.

Preparation of N-(methylsulfonyl)-2-phenoxyacetamide 26

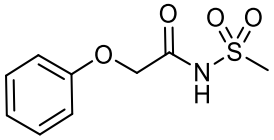

26

Phenoxyacetic acid **22** (51.0 mg, 0.335 mmol) was added to a stirred solution of *N*-(3-dimethylamino)propyl-*N'*-ethyl carbodiimide hydrochloride **34** (EDCI, 85.1 mg, 0.444 mmol) and 4-(dimethylamino)pyridine **32** (DMAP, 96.7 mg, 0.792 mmol) in anhydrous dichloromethane (1 mL). After 5 mins, methane sulfonamide **25** (31.6 mg, 0.332 mmol) was added and the solution monitored by TLC (silica, 20% Methanol/ethyl acetate, visualised with UV and phosphomolybdic acid (PMA)). After 24 hours, TLC showed the presence of a PMA-staining product spot (R_f = 0.94) paired with a decreased intensity of phenoxyacetic acid spot (R_f = 0.45). HCl (1 M, 2 mL) was added to the solution and the product was extracted with ethyl acetate (2 mL × 3). The combined organic layers were washed with brine, dried over Na_2SO_4, and the filtrate was concentrated *in vacuo* to give a white soft solid. Crude product was purified by recrystalisation from $CDCl_3$ and hexane (~2:10 mL ratio) to afford purified N-(methylsulfonyl)-2-phenoxyacetamide **26** (2.7 mg, 4% yield) as a white solid. Melting point = 131.32 °C.

^{1}H NMR δ_H (500 MHz, $CDCl_3$) 8.84 (1 H, s), 7.36 (2 H, dd, *J* 8.5, 7.5), 7.09 (1 H, t, *J* 7.4), 6.93 (2 H, d, *J* 8.1), 4.60 (2 H, s), 3.37 (3 H, s); ^{13}C NMR δ_C (126 MHz, DMSO) 168.20, 157.52, 129.51, 121.25, 114.44, 65.86, 41.14; FTIR (ATR) v /cm^{-1}: 3255(N-H), 3024-2931

(C-H), 1712 (C=O), 1600 (C-H), 1340-1329 (S=O); [M-H]- found: 228.0 m/z.

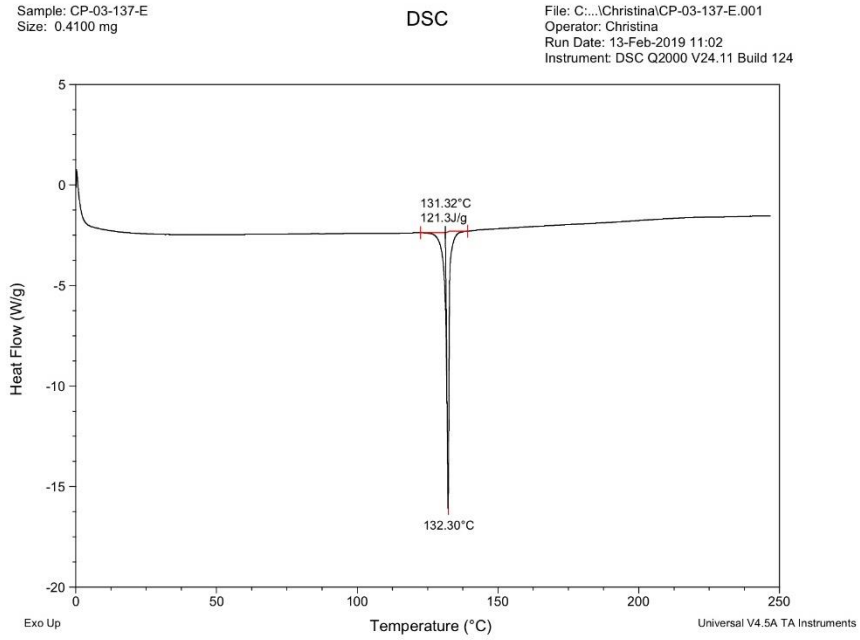

Figure 7-1. Graph showing the melting point of N-acyl sulfonamide phenoxyacetamide at 131.32 °C. The compound is stable up to 250°C.

Phenoxyacetic acid **22** (197.2 mg, 1.296 mmol) and 1,1-carbonyldiimidazole **36** (CDI, 232.2 mg, 1.432 mmol) were dissolved in anhydrous tetrahydrofuran (THF, 2 mL) in a single neck 10 mL round bottom flask fitted with a septum and the solution stirred at RT for 40 mins, then refluxed at 75 °C for 40 mins. The reaction mixture was then allowed to cool to RT over 1 hour and methane sulfonamide **25** (126.1 mg, 1.326 mmol) added. After 20 mins, 1,8-Diazabicyclo[5.4.0]undec-7-ene **31** (DBU) (1 M in THF, 222.6 µL, 1.314 mmol) was added dropwise. The solution monitored by TLC and extra CDI **36** added to drive the reaction to completion. After 5 days, the reaction was deemed complete by TLC and the solution was concentrated *in vacuo.* HCl (0.2 M, 5 mL) was added and the product extracted in DCM (3 mL × 3). The organic layers were combined and washed with NH_4Cl (1M, 3mL), dried over Na_2SO_4, and filtrate concentrated *in vacuo*. Purified product was isolated by crystallisation from $CHCl_3$ and recrystallised from cold chloroform. Crystals were dried *in vacuo* which afforded white powder **26** (7.1 mg, 2.4% yield).

^1H NMR δ_H (500 MHz, $CDCl_3$) 8.91 (1 H, s), 7.39 – 7.30 (2 H, m), 7.07 (1 H, t, *J* 7.4), 6.93 (2 H, d, *J* 8.0), 4.58 (2 H, s), 3.35 (3 H, s). ^{13}C NMR δ_C (101 MHz, $CDCl_3$) 167.56 (s), 156.37 (s), 130.03 (s), 122.96 (s), 114.70 (s), 67.16 (s), 41.68 (s). FTIR (ATR) v /cm^{-1}: 3257(N-H), 3024-2930 (C-H), 1713 (C=O), 1600 (C-H), 1341-1329 (S=O); $[M-H]^-$ Found: 228.0 m/z.

Preparation of phenoxyacetamide 39

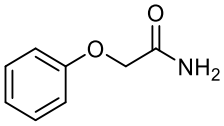

39

In a 25 mL round bottom flask purged with argon and fitted with septum, phenoxyacetic acid **22** (102.5 mg, 0.674 mmol) and triethylamine (375.6 mL, 2.995 mmol) in anhydrous THF (0.3 mL) were stirred. The solution was cooled to 0 ^{o}C in an ice bath and ethyl chloroformate (90.2 µL, 0.943 mmol) was added dropwise. After 30 minutes, aqueous ammonium chloride (1 M, 1.011 mL, 1.011 mmol) was added. The reaction was monitored by TLC (silica, 40% ethyl acetate/hexane) and visualised by UV and ninydrin. The reaction was quenched with ice cold water (8 mL) and the product extracted with ethyl acetate (2 mL × 3). Organic layers were combined, washed with brine, dried over Na_2SO_4 and solvent was removed *in vacuo* to afford primary amide **39** (84.1 mg, 83%) as pale yellow oil. TLC indicated one product spot (R_f 0.9).

^{1}H NMR (400 MHz, MeOD) δ_H 7.33 – 7.25 (2 H, m), 6.97 (1 H, d, *J* 6.6), 6.95 – 6.91 (2 H, m), 4.69 (2 H, s); ^{13}C NMR (126 MHz, MeOD) δ_C 171.05, 159.44, 130.54, 122.57, 115.64, 66.12.

Preparation of N-acylsulfonamide treprostinil via trimethyl silane treprostinil

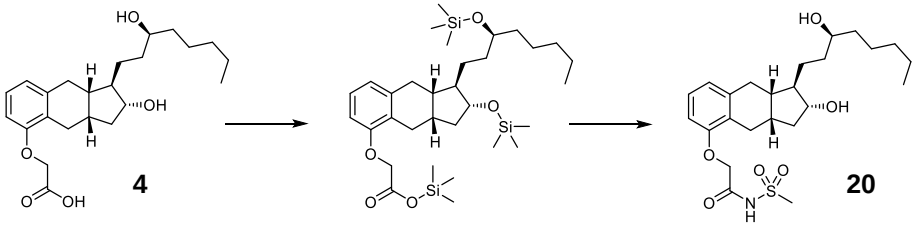

4 **20**

In a 2 mL round bottom flask purged with argon was added a solution of treprostinil 4 (50.3 mg, 0.129 mmol) in anhydrous dimethyl formamide (DMF, 1.0 mL). The solution was cooled to 0 ^{o}C in an ice bath and *N,O*-bis(trimethlsilyl)acetamide **41** (50.7 µL, 0.205 mmol) was added in two portions using a 25 µL Hamilton syringe. After 16 hours and in a separate argon-purged flask, EDCI **34** (32.7 mg, 0.171 mmol) and DMAP **32** (35.4 mg, 0.290 mmol) were dissolved in anhydrous DMF (0.9 mL). The solution was cooled to 0 ^{o}C and the treprostinil 4 solution added dropwise *via* syringe. A solution of methane sulfonamide **25** (12.2 mg, 0.128 mmol) in anhydrous DMF (0.4 mL) was added and stirred at RT for 24 hours. The solution was diluted with saturated solution of ammonium chloride (15 mL) and extracted with ethyl acetate (5 mL × 3). Combined organic layers were washed with brine, dried over Na_2SO_4 and solvent removed *in vacuo*. The residue was dissolved in methanol and purified by repeat HPLC using analytical column. Mobile phase was 10-90% acetonitrile/water over 20 minutes. Retention time = 13.3 minutes. Solvent removed from collected fractions *in vacuo* to yield 12 mg (20%) of N-acyl sulfonamide treprostinil. ^{13}C NMR was not measured but ^{1}H NMR spectrum indicated pure compound (**Figure 3-22**).

^{1}H NMR (400 MHz, MeOD) δ_H 7.07 – 6.96 (1 H, m), 6.78 (1 H, d, *J* 7.3), 6.67 (1 H, d, *J* 8.3), 4.67 (2 H, s), 3.75 (3 H, d, *J* 4.5), 3.66 – 3.55 (2 H, m), 3.49 (2 H, d, *J* 16.2), 2.80 – 2.58 (5 H, m), 2.49 (2 H, dd, *J* 14.4, 5.7), 2.26 (2 H, d, *J* 7.1), 2.13 – 1.98 (2 H, m), 1.91 (2 H, dd, *J* 12.7, 7.4), 1.69 (1 H, dd, *J* 11.4, 5.8), 1.57 (2 H, ddd, *J* 14.8, 12.4, 6.3), 1.45 (4 H, dd, *J* 17.0, 11.2), 1.39 – 0.97 (10 H, m), 0.90 (4 H, q, *J* 6.8).

Preparation of treprostinil ethyl ester 43

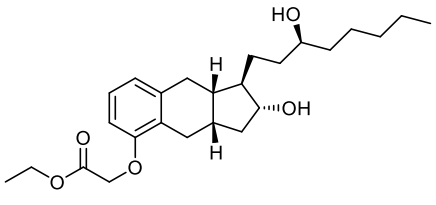

43

Ethanol (~15 mL) was dried by stirring in the presence of heat-activated 4 Å molecular sieves in an argon purged sealed 50 mL round bottom flask (RBF) for 20 minutes before allowing to settle. Ethanol was transferred via syringe fitted with a 0.22 mm syringe filter. Treprostinil 4 (495.8 mg, 1.270 mmol) was dissolved in dry absolute ethanol (9.0 mL) in a 50 mL round bottom flask and cooled to 0 ˚C with ice bath. Sulfuric acid (6.8 µL, 0.127 mmol) was then added and the solution was refluxed at 86 ˚C for 16 hours. The reaction was monitored by TLC (silica, 20% methanol/ethyl acetate, visualised by UV and PMA). Towards the end of reaction sodium sulfate was added to remove water. Once complete, the filtrate was neutralised by addition of saturated potassium carbonate solution (3 mL) and removed *in vacuo*. Crude product was dissolved in ethyl acetate (10 mL × 3) and extracted 3 times from 20% aqueous potassium carbonate solution (15 mL). Combined organic layers washed with brine and dried over sodium sulfate before solvent removal *in vacuo* to afford dry white solid **43** (472.4 mg, 88% yield).

^{1}H NMR (500 MHz, $CDCl_3$) δ_H 7.03 (t, *J* = 7.8 Hz, 1H), 6.78 (d, *J* = 7.4 Hz, 1H), 6.60 (d, *J* = 8.2 Hz, 1H), 4.58 (s, 2H), 4.22 (d, *J* = 7.1 Hz, 2H), 3.65 (dd, *J* = 14.5, 11.0 Hz, 1H), 3.53 (s, 1H), 2.88 (dd, *J* = 14.7, 6.0 Hz, 1H), 2.72 (dd, *J* = 14.3, 6.2 Hz, 1H), 2.46 (ddd, *J* = 21.1, 20.1, 12.4 Hz, 2H), 2.27 – 2.07 (m, 2H), 1.82 (t, *J* = 16.5 Hz, 1H), 1.72 – 1.57 (m, 2H), 1.56 – 1.36 (m, 5H), 1.34 – 1.19 (m, 9H), 1.14 (dd, *J* = 21.7, 10.4 Hz, 1H), 0.88 (t, *J* = 6.9 Hz, 3H). ^{13}C NMR ($CDCl_3$, 500 Hz) δ_C 169.31 (s), 154.87 (s), 141.15 (s), 127.90 (s), 126.06 (s), 121.49 (s), 109.69 (s), 77.42 (s), 72.38 (s), 66.05 (s), 61.24 (s), 52.27 (s), 41.17 (d, *J* = 8.0 Hz), 37.47 (s), 35.06 (s), 33.90 (s), 32.74 (s), 31.98 (s), 28.61 (s), 26.06 (s), 25.47 (s), 22.69 (s), 14.16 (d, *J* = 8.6 Hz). FTIR (ATR) v /cm^{-1}: 3352 (OH), 2931 (CH), 1751 (C=O ester), 1601 (Ar-H), 1179 (C-O ester). Theoretical mass = 418.6 g/mol; [M-H]- found: 417.3 m/z

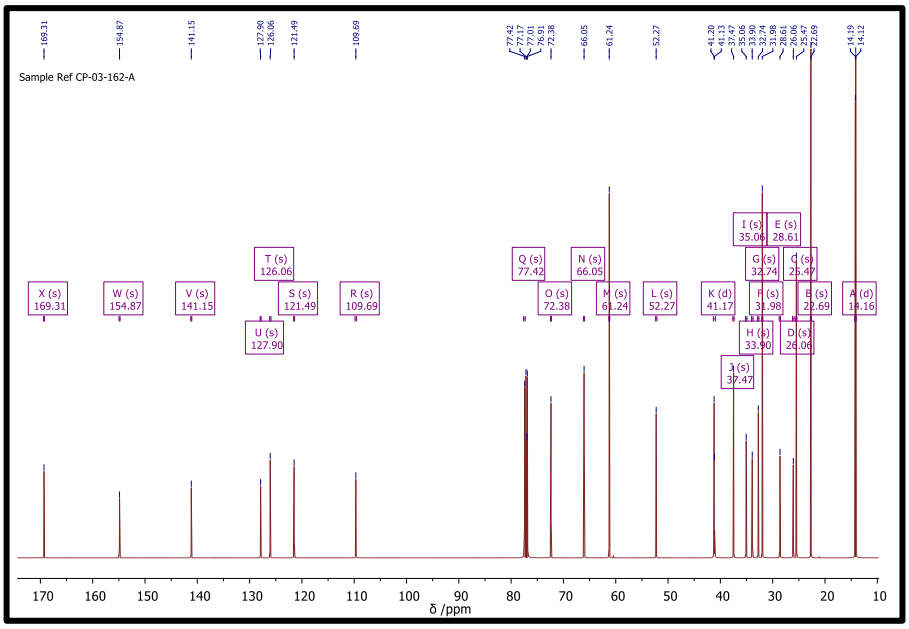

Figure 7-2. ^{13}C NMR of treprostinil ethyl ester.

Preparation of bis-benzyl treprostinil ethyl ester 44

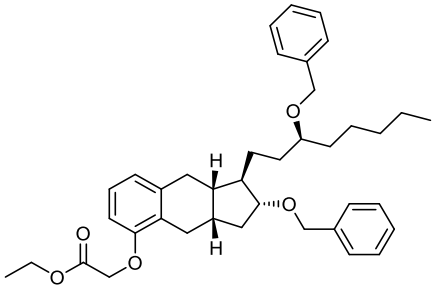

44

Magnesium oxide **47** (88.8 mg, 2.203 mmol) and 2-benzyloxy-1-methylpryridinium triflate **46** (782.2mg, 2.239 mmol) was added to a solution of treprostinil ethyl ester **43** (283.9 mg, 0.678 mmol) in trifluoromethyl benzene (6.0 mL) in an argon purged 25 mL round bottom flask fitted with septum. The solution was then heated to 83 ˚C for 16 hours. The reaction was monitored by TLC (silica, 40% ethyl acetate/hexane, developing by UV and PMA). The reaction was cooled, diluted with trifluoromethyl benzene (6 mL), filtered through celite and flushed with benzotrifuoride to remove the heterogenous magnesium oxide **47**. The solvent was removed from the filtrate *in vacuo* and the crude product purified by automated silica column (10 g, Biotage SNAP cartridge) to yield product **45** as a yellow oil (198.2 mg, 49% yield).

^{1}H NMR (500 MHz, $CDCl_3$) δ_H 7.42 – 7.16 (11 H, m), 7.03 (1 H, t, *J* 7.8), 6.76 (1 H, d, *J* 7.4), 6.60 (1 H, d, *J* 8.1), 4.58 (2 H, s), 4.54 (1 H, d, *J* 11.7), 4.49 (2 H, s), 4.40 (1 H, d, *J* 11.7), 4.23 (2 H, q, *J* 7.1), 3.51 (1 H, d, *J* 5.7), 3.38 (1 H, s), 2.93 (1 H, dd, *J* 14.8, 5.9), 2.73 (1 H, dd, *J* 14.4, 6.2), 2.53 (1 H, dd, *J* 14.8, 6.7), 2.46 (1 H, dd, *J* 14.4, 7.2), 2.29 – 2.16 (2 H, m), 1.84 (1 H, s), 1.70 (1 H, d, *J* 17.2), 1.62 (2 H, s), 1.52 (4 H, d, *J* 5.8), 1.39 (1 H, s), 1.27 (10 H, t, *J* 7.1), 0.88 (3 H, q, *J* 7.0). ^{13}C NMR (126 MHz, $CDCl_3$) δ_C 169.35 (s), 154.87 (s), 141.11 (s), 139.22

(s), 138.80 (s), 126.00 (s), 121.56 (s), 109.66 (s), 84.12 (s), 71.66 (s), 70.77 (s), 66.16 (s), 61.23 (s), 50.25 (s), 40.80 (s), 37.62 (s), 33.96 (s), 33.74 (s), 33.30 (s), 32.12 (s), 31.57 (s), 28.54 (s), 26.15 (s), 25.03 (s), 22.70 (s), 14.17 (d, *J* = 9.2 Hz). IR (ATR) v /cm^{-1}: 3183 + 3085 ((Ar)C-H), 2928 + 2858 (-C-H), 1759 (C=O), 1732, 1585 (C=C), 1453 (C-H *bend*), 1276 ((Ar)C-O-C), 1196 (C-O), 1094 (C-O-C); Theoretical mass = 598.8 g/mol; [M+H]+ found 599.3 m/z.

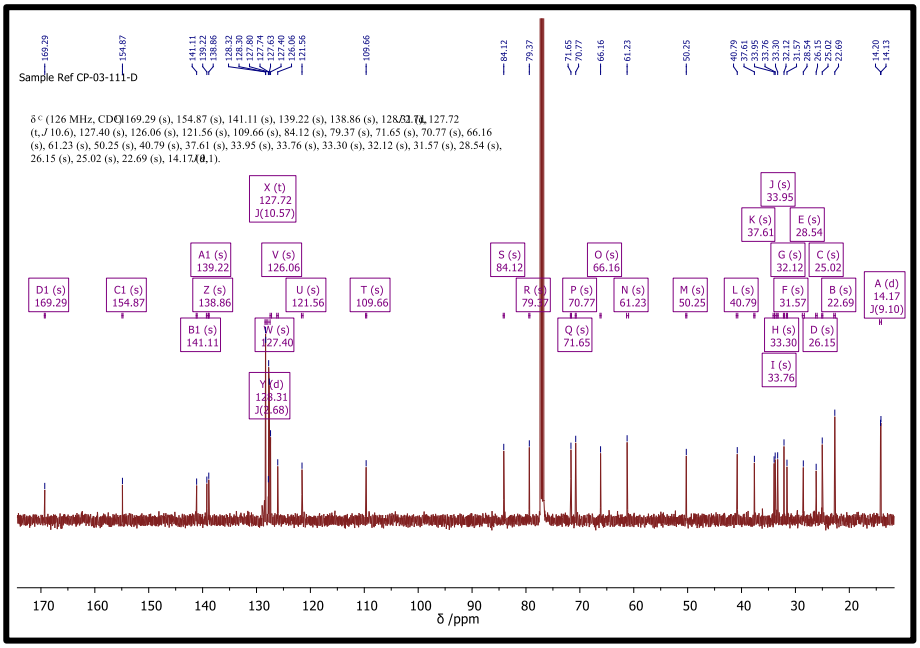

Figure 7-3. 13C NMR spectra of bis-benzyl treprostinil ethyl ester.

Preparation of bis-benzyl Treprostinil 49

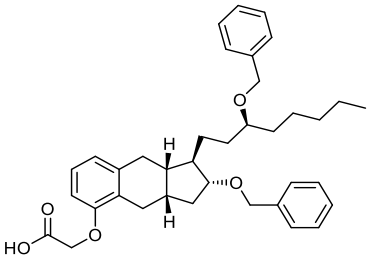

49

To a solution of bis-benzyl treprostinil ethyl ester **45** (60.4 mg, 0.101 mmol) dissolved in THF/H_2O/MeOH (4:1:1, 3.0 mL) in an argon purged 10 mL round bottom flask fitted with septum, was added lithium hydroxide (20.3 mg, 0.483 mmol) and stirred at room temperature overnight. The reaction was monitored by TLC (silica, 40% ethyl acetate/hexane, developing by UV and ninhydrin). Once complete, the reaction solvent was removed *in vacuo* and the remaining residue diluted with HCl solution to pH 2. Product was extracted with ethyl acetate (2 mL × 3). The combined organic layers were washed with brine and dried over Na_2SO_4. Solvent removed *in vacuo* to yield a pale, yellow oil **49**. (51.4 mg, 89 % yield).

^{1}H NMR (500 MHz, $CDCl_3$) δ_H 9.29 (1 H, s), 7.40 – 7.19 (10 H, m), 7.03 (1 H, t, *J* 7.8), 6.76 (1 H, d, *J* 7.4), 6.60 (1 H, d, *J* 8.2), 4.60 (2 H, d, *J* 3.2), 4.53 (1 H, d, *J* 11.7), 4.49 (2 H, s), 4.38

(1 H, d, *J* 11.7), 3.48 (1 H, dd, *J* 8.3, 5.8), 3.43 – 3.32 (1 H, m), 2.89 (1 H, dd, *J* 14.8, 5.9), 2.71 (1 H, dd, *J* 14.4, 6.2), 2.47 (2 H, ddd, *J* 32.9, 14.8, 7.0), 2.29 – 2.12 (2 H, m), 1.83 (1 H, d, *J* 8.4), 1.68 (1 H, dd, *J* 10.2, 5.3), 1.62 – 1.16 (14 H, m), 0.92 – 0.80 (3 H, m). ^{13}C NMR (126 MHz, CDCl3) δ_C 173.89 (s), 154.56 (s), 141.22 (s), 138.93 (d, J 41.2), 128.35 (d, J 2.6), 127.93 – 127.33 (m), 126.18 (s), 121.89 (s), 109.70 (s), 84.09 (s), 79.42 (s), 77.35 (s), 77.09 (s), 76.84 (s), 71.66 (s), 70.76 (s), 65.59 (s), 50.19 (s), 40.76 (s), 37.61 (s), 33.90 (s), 33.74 (s), 33.27 (s), 32.13 (s), 31.54 (s), 28.52 (s), 26.16 (s), 25.03 (s), 22.71 (s), 14.16 (s); FTIR (ATR) v /cm^{-1}: 3029 ((Ar)C-H), 2927 (-C-H), 2858 (COO-H), 1732 (C=O), 1453 (C-H *bend*), 1233 (C-O), 1204 ((Ar)C-O-C), 1113 (C-O-C). [M-H]$^-$ found: 569.3 m/z.

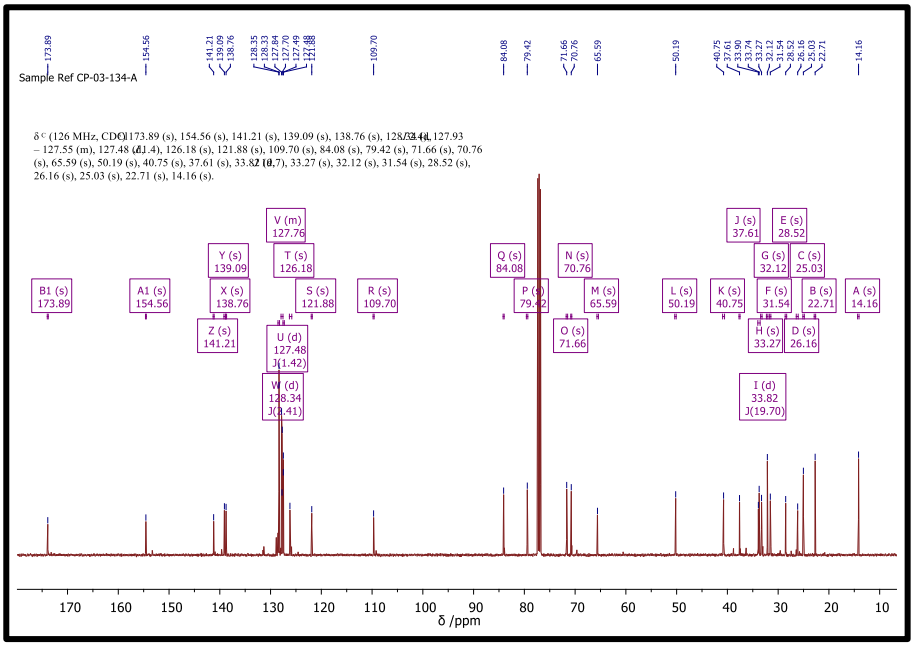

Figure 7-4. ^{13}C NMR of bis benzyl treprostinil.

Treprostinil **4** (49.7 mg, 0.127 mmol) and magnesium oxide **47** (16.6 mg, 0.412 mmol) were added to a 25 mL round bottom flask purged with argon and fitted with septum, and stirred together with trifluoromethyl benzene (5.0 mL). Once dissolved, 2-benzyloxy-1-methylpyridinium triflate **46** (143.3 mg, 0.410 mmol) was added. The suspension was refluxed at 83 °C in an oil bath for 16 hours and the reaction tracked by TLC (silica, 20% methanol/ethyl acetate, developed by UV and PMA). Reaction mix was filtered through a celite pad to remove magnesium oxide **47** and the filtrate concentrated *in vacuo*. The residue was separated between DCM (30 mL) and acidifed water (0.1M HCl, 30 mL) and further extracted with DCM (20 mL × 2). Organic layers were combined, washed with brine and dried over Na_2SO_4 before concentrating *in vacuo* to yield unpurified product as yellow cloudy gel **49** (>100% yield); ^{1}H NMR of crude mixture indicated desired product present.

^{1}H NMR δ_H (500 MHz, $CDCl_3$) 7.30 – 7.13 (10 H, m), 6.97 (1 H, t, *J* 7.9), 6.70 (1 H, d, *J* 7.3), 6.56 (1 H, d, *J* 8.2), 4.56 (1 H, d, *J* 19.1), 4.49 (1 H, s), 4.46 (1 H, s), 4.43 (2 H, s), 4.38 (1 H, s), 4.33 (1 H, d, *J* 11.7), 3.50 (1 H, d, *J* 6.6), 3.48 – 3.38 (1 H, m), 3.36 – 3.24 (1 H, m), 2.85

(1 H, dd, *J* 14.8, 5.9), 2.66 (1 H, dd, *J* 14.4, 6.1), 2.41 (2 H, ddd, *J* 32.4, 14.7, 6.8), 2.21 – 2.05 (2 H, m), 1.83 – 1.70 (2 H, m), 1.70 – 1.58 (4 H, m), 1.58 – 1.49 (4 H, m), 1.49 – 1.37 (2 H, m), 1.37 – 1.04 (m), 1.04 – 0.92 (m), 0.91 – 0.56 (m). ^{13}C NMR (126 MHz, $CDCl_3$) δ_C 127.67 – 126.92 (m), 126.92 – 126.45 (m), 126.35 (d, *J* 4.8), 78.33 (s), 76.27 (s), 76.02 (s), 75.76 (s), 69.70 (s), 36.80 – 36.06 (m), 32.68 (d, *J* 3.2), 31.74 (d, *J* 3.1), 31.00 (d, *J* 19.3), 31.23 – 28.94 (m), 28.88 – 26.71 (m), 23.97 (s), 22.04 – 21.16 (m), 18.69 (dd, *J* 6.6, 1.9), 13.78 – 12.40 (m). FTIR (ATR) v /cm^{-1}: 3029 ((Ar)C-H), 2924 (C-H), 2858 (COO-H), 1733 (C=O), 1453 (C-H *bend*), 1204 ((Ar)C-O-C), 1112 (C-O-C).Theoretical mass = 570.3 g/mol $[M+H]^+$ found: 571.3 m/z.

Preparation of Bis-benzyl-N-acyl sulphonamide treprostinil 50

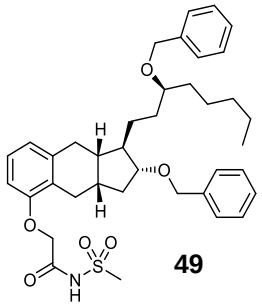

49

To a 5 mL RBF fitted with reflux condenser was added bis-benzyl treprostinil **49** (46.4 mg, 0.081 mmol) and 1,1-carbonyldiimidazole **36** (14.3mg, 0.088 mmol) in anhydrous tetrahydrofuran (1.0 mL). The solution was stirred at RT for 40 mins then refluxed at 72 °C for 30 minutes. Once cooled to RT, methanesulfonamide **25** (7.8 mg, 0.082 mmol) and DBU **31** (81 µL of 1M in THF solution, 0.081 mmol) were added and reaction stirred for 19 hours. The reaction was tracked by TLC (silica, 30% methanol/ethyl acetate, developing by UV and PMA). The reaction solvent was removed *in vacuo* and acidified water (HCl, 1M, 2 mL) added. Product extracted with ethyl acetate (1.0 mL × 3). Combined organic layers washed with brine (1.0 mL). Crude product (67.0 mg) was separated by column chromatography (silica, 14 g). Mobile phase 5 – 100 % ethyl acetate/hexane. Solvent of relevant fractions removed *in vacuo* to yield a clear oil **50** (10.8 mg, 21 % yield).

^{1}H NMR (400 MHz, $CDCl_3$) δ_H 7.32 – 7.13 (13 H, m), 7.06 – 7.00 (1 H, m), 6.79 (1 H, d, *J* 7.4), 6.59 (1 H, d, *J* 7.8), 4.50 (2 H, s), 4.47 (1 H, s), 4.43 (2 H, d, *J* 1.1), 4.36 (1 H, t, *J* 11.6), 3.51 – 3.41 (1 H, m), 3.32 (3 H, d, *J* 5.0), 3.30 (3 H, s), 2.71 (2 H, ddd, *J* 20.1, 13.2, 6.0), 2.44 (2 H, dd, *J* 14.5, 6.6), 2.26 – 2.11 (2 H, m), 1.89 – 1.76 (1 H, m), 1.71 – 1.37 (11 H, m), 1.33 – 1.08 (10 H, m), 0.82 (3 H, t, *J* 7.0); FTIR (ATR) v /cm^{-1}: 3421-2856 (C-H), 1728 (C=O), 1585 (C-H), 1454 (C-H), 1345 (S=O); [M-H]- found: 646.3 m/z.

Under an argon environment, DMAP **32** (11.1 mg, 0.091 mmol) and EDCI **34** (9.4 mg, 0.049 mmol) were stirred in in DCM (0.3 mL) an argon purged 1 mL reaction vial, fitted with septum. Bis-benzyl treprostinil **49** (20.0 mg, 0.0375mmol) was dissolved in DCM (0.6 mL) and added to the solution followed by methane sulfonamide **25** (3.9 mg, 0.041 mmol). The reaction was stirred for 4 days whilst tracking by TLC and then the solvent was removed *in vacuo*. The

residue was dissolved in HCl (0.5M, 6 mL) and then extracted in ethyl acetate (3 mL × 3), and the combined organic layers were then washed with brine and dried over Na_2SO_4. After filtration, the ethyl acetate was removed *in vacuo* and the crude oily residue purified by column chromatography (silica, 20g) using a mobile phase of 50-100% ethyl acetate/hexane to yield 11.3 mg (46% yield) of the desired product **50** as colourless oil.

^{1}H NMR (500 MHz, $CDCl_3$) δ_H 7.36 – 7.19 (46 H, m), 7.07 (4 H, t, *J* 7.8), 6.83 (3 H, d, *J* 7.4), 6.63 (3 H, d, *J* 8.2), 4.54 (8 H, d, *J* 2.6), 4.51 (3 H, s), 4.48 (6 H, d, *J* 1.6), 4.43 (2 H, s), 4.39 (4 H, d, *J* 11.6), 3.51 (5 H, dd, *J* 13.7, 8.2), 3.39 – 3.31 (14 H, m), 2.74 (7 H, ddd, *J* 23.7, 14.8, 6.0), 2.47 (9 H, dd, *J* 15.0, 6.6), 2.29 – 2.17 (9 H, m), 2.02 (2 H, s), 1.87 (5 H, dd, *J* 15.1, 7.9), 1.73 – 1.63 (5 H, m), 1.51 (28 H, ddd, *J* 19.4, 11.7, 4.1), 1.26 (50 H, dt, *J* 14.3, 5.9), 0.86 (15 H, q, *J* 6.9). **^{13}C NMR (126 MHz, $CDCl_3$) δ_C** 166.86 (s), 152.46 (s), 140.52 (s), 138.13 (s), 137.63 (s), 127.36 (dd, *J* 15.6, 2.1), 126.67 (d, *J* 5.1), 126.39 (t, *J* 10.5), 125.58 (s), 121.99 (s), 109.18 (s), 82.93 (s), 70.69 (s), 69.75 (s), 67.10 (s), 49.09 (s), 40.67 (s), 39.59 (s), 36.64 (s), 32.66 (d, *J* 9.2), 32.21 (s), 31.07 (s), 30.54 (s), 27.47 (s), 25.44 (s), 23.97 (s), 21.66 (d, *J* 2.8), 13.10 (d, *J* 2.4), -0.05 (d, *J* 11.9); FTIR (ATR) v /cm^{-1}: 2926-2558 (C-H), 1728 (C=O), 1584 (C-H), 1343 (S=O); [M-H]- found: 646.3 m/z.

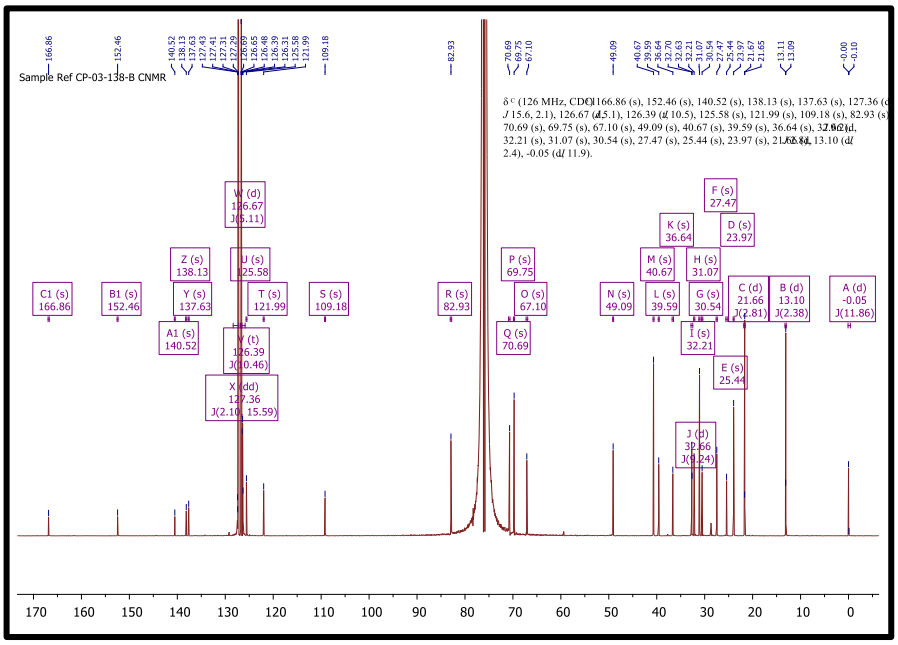

Figure 7-5. ^{13}C NMR spectrum of bis benzyl *N*-acl sulfonamide treprostinil

Preparation of N-acyl sulfonamide treprostinil 21

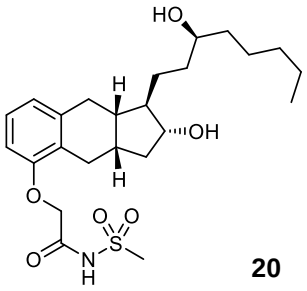

20

Into an argon purged chamber of “CO-ware” apparatus, bis-benzyl-N-acyl sulfonamide treprostinil **50** (10.8 mg, 0.017 mmol) and 5% palladium on carbon (2.9 mg, 0.357 mmol) were stirred in ethanol (3.0 mL). Into the second chamber, zinc pellets (433 mg, 6.623 mmol) were added and the chambers stoppered, and air evacuated by vacuum. *Via* syringe, HCl (4M, 3.3 mL) was added to the zinc pellets and the solutions left 16 hours, topping up zinc pellets if hydrogen evolution ceased. The reaction solution was filtered through celite to remove heterogenous catalyst, and then rinsed with ethanol. Filtrate solvent was removed *in vacuo* to produce a clear oil **21** (5.0 mg, 64 % yield).

^{1}H NMR (400 MHz, $CDCl_3$) δ_H 7.12 (1 H, t, *J* 7.8), 6.90 (1 H, d, *J* 7.4), 6.69 (1 H, d, *J* 8.2), 4.58 (2 H, s), 3.77 (2 H, dd, *J* 9.1, 6.1), 3.62 (1 H, s), 2.83 – 2.67 (2 H, m), 2.57 – 2.44 (2 H, m), 2.24 (3 H, ddd, *J* 19.0, 13.2, 6.8), 1.98 – 1.86 (2 H, m), 1.84 – 1.03 (27 H, m), 0.90 (4 H, t, *J* 6.8); **^{13}C NMR (126 MHz, $CDCl_3$) δ_C** 167.90, 153.58, 141.55, 127.41, 126.71, 123.04, 110.29, 72.63, 72.59, 68.17, 52.15, 41.72, 41.43, 41.16, 37.46, 34.92, 33.54, 32.75, 31.91, 29.72, 28.66, 26.33, 25.39, 22.66, 14.08. $[M+H]^+$ found: 468.2 m/z.

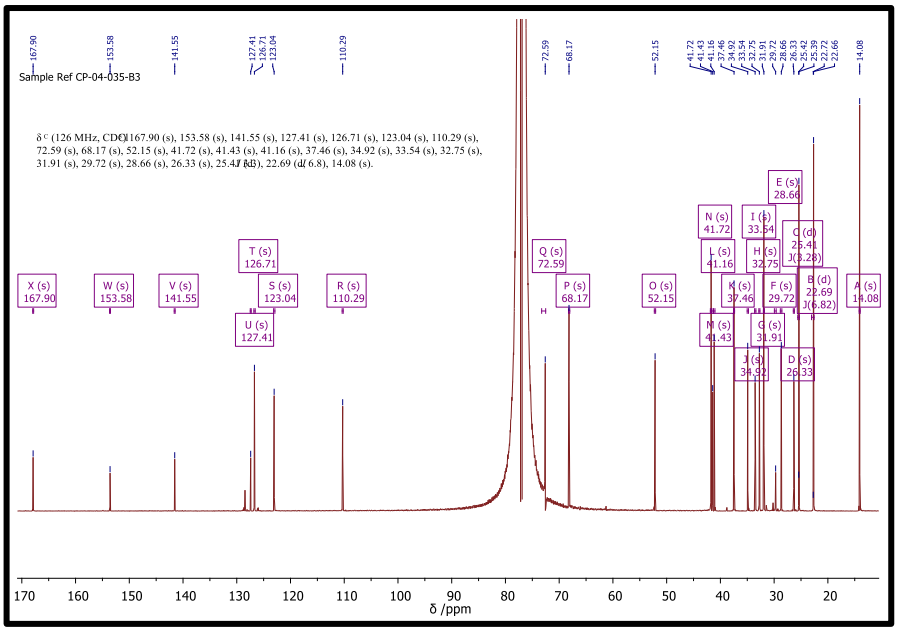

Figure 7-6. ^{13}C NMR spectra of N-acyl sulfonamide treprostinil.

Preparation of Bromoacetyl bromide – prodrug intermediate 54

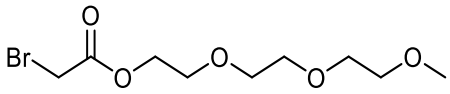

53

In a 10 mL round bottom flask purged with argon and fitted with septum, a stirred solution of triethylene glycol mono methyl ether (97.5 µL, 0.609 mmol) and triethylamine (84.9 µL, 0.609 mmol) dissolved in diethyl ether (3.0 mL) was cooled to 0 ˚C on ice. Bromoacetyl bromide **53** (58.2 µL, 0.670mmol) was added dropwise in three portions over 6 minutes. The solution was stirred at 0 °C for 15 mins and then at room temperature for 20 minutes. After which, the solvent was removed *in vacuo* and the product extracted from water in DCM (3 mL × 3). The combined organic solvents were washed with brine, dried over Na_2SO_4 and solvent was removed *in vacuo* to yield yellow oil, bromomethyl triethylene acetate **54** in 73 % yield.

^{1}H NMR (500 MHz, $CDCl_3$-*d*^{1}) δ_H 3.33 (s, 3H, OCH_3, **h**); 3.51 (t, 2H, $C\underline{H_2}OCH_3$, J = 9.3 Hz, **g**); 3.61 (dd, 6H, $CH_2OC\underline{H_2}$, J = 3.6, 11.1 Hz, **d, e, f**); 3.69 (t, 2H, $CO_2CH_2C\underline{H_2}O$, J = 4.8 Hz, **c**); 3.83 (s, 2H, $BrC\underline{H_2}$, **a**); 4.28 (t, 2H, $CO_2C\underline{H_2}CH_2$, J = 4.7 Hz, **b**). FTIR (ATR) v/cm^{-1} 2876 (C-H), 1736 (C=O), 1285 (C-O), 1098 (C-O-C). $[M+Na]^+$ found: 307.0 m/z.

Preparation of Bromo N-acyl sulfonamide – prodrug intermediate **55**

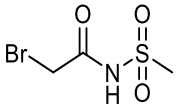

54

In an argon-purged 2-neck 50 mL RBF fitted with reflux condenser a suspension of methane sulfonamide **25** (245.2 mg, 1.215 mmol) in anhydrous toluene (7.0 mL) was stirred and bromoacetyl bromide **53** (140 µL, 1.472 mmol) was added dropwise. The reaction was refluxed at 118 °C for 5 hours in an oil bath, then cooled to crystallise from toluene. 2-bromo-N-(methylsulfonyl)acetamide **55** was recrystallised from toluene to yield clear needles (58.0 mg, 24%).

^{1}H NMR (500 MHz, δ^6-DMSO) δ_H 4.04 (s, 2H), 3.27 (s, 3H); ^{13}C NMR (126 MHz, δ^6-DMSO) δ_C 172.39 (s), 61.20 (s); FTIR (ATR) v/cm^{-1} 3163 (N-H), 3022-2942 (C-H), 1706 (C=O), 1470 (C-H), 1332 (S=O); $[M-H]^-$ found: 213.9 m/z.

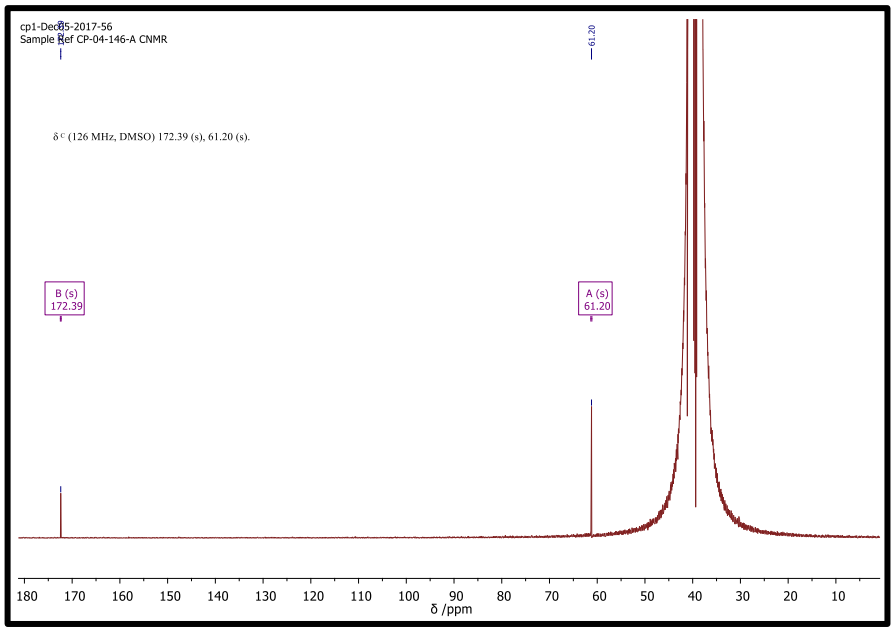

Figure 7-7. ^{13}C NMR spectrum of 2-bromo-*N*-(methylsulfonyl)acetamide.

Preparation of Triol-TEG prodrug 56

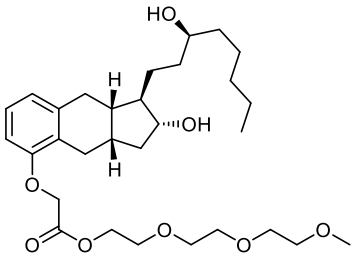

55

Bromomethyltriethylene acetate **54** (17.7 mg, 0.062 mmol), potassium carbonate (24.7 mg, 0.179 mmol), benzindene triol **51** (19.9 mg, 0.060 mmol) and tetrabutyl ammonium iodide (22.4 mg, 0.061 mmol) were stirred in acetone (4.0 mL) in a 10 mL round bottom flask fitted with reflux condenser and refluxed at 58 ˚C for 5 hours. The reaction was tracked by TLC (silica, 100% ethyl acetate, visualised by potassium permanganate), and once complete, the suspension was filtered through celite. The filtrate was condensed *in vacuo* and product isolated by column chromatography. Mobile phase used was 50 – 80% ethyl acetate in hexane. Yellow oil **56** (26.6 mg, 82% yield).

^{1}H NMR (500 MHz, $CDCl_3$) δ_H 6.99 (t, J = 7.8 Hz, 1H), 6.73 (d, J = 7.4 Hz, 1H), 6.56 (d, J = 8.2 Hz, 1H), 4.59 (s, 2H), 4.28 (td, J = 4.3, 1.9 Hz, 2H), 3.65 (t, J = 4.7 Hz, 3H), 3.61 – 3.50 (m, 7H), 3.48 (dd, J = 5.7, 3.6 Hz, 2H), 3.30 (s, 3H), 2.77 (dd, J = 14.7, 6.1 Hz, 1H), 2.67 (dd, J = 14.3, 6.2 Hz, 1H), 2.50 (dd, J = 14.8, 6.4 Hz, 1H), 2.39 (dd, J = 14.3, 6.4 Hz, 1H), 2.13 (ddd, J = 19.4, 14.9, 7.2 Hz, 2H), 1.92 – 1.70 (m, 4H), 1.63 – 1.53 (m, 2H), 1.53 – 1.42 (m, 3H), 1.42 – 1.30 (m, 4H), 1.30 – 1.14 (m, 11H), 0.83 (t, J = 6.9 Hz, 4H); ^{13}C NMR (126 MHz, $CDCl_3$) δ_C 169.26, 154.88, 141.03, 127.74, 126.12, 121.59, 109.59, 77.36, 72.58, 71.92, 70.59, 70.57, 70.53, 68.94, 65.85, 64.19, 59.07, 52.22, 41.41, 41.24, 37.43, 35.00, 33.69, 32.76, 31.93, 28.66, 25.92, 25.40, 22.67, 14.09; FTIR (ATR) v/cm^{-1} 3392 (O-H), 2924- 2857 (C-H),

1759 (C=O), 1585 (C-H), 1469 (C-H bend of TEG), 1195 (C-O ester), 1109 (C-O ether); Theoretical mass = 536.7 g/mol [M+Na]+ found = 559.3 m/z.

Preparation of N-acyl sulfonamide treprostinil 21 from triol intermediate 51

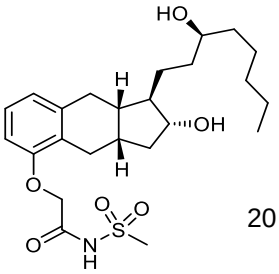

20

Over an ice bath at 0 ˚C and in an argon purged 5 mL round bottom flask fitted with septum, benzindene triol **51** (19.5 mg, 0.059 mmol) was dissolved in DMF (1.0 mL) and sodium hydride (1.4 mg, 60% in mineral oil washed in hexane, 0.059 mmol) added. After 5 minutes, 2-bromo-N-(methylsulfonyl)acetamide **55** (14.1mg, 0.0653 mmol) and the remaining sodium hydroxide (1.6 mg, 0.0675 mmol) were added. Immediately the reaction turned orange which was subsequently lost during reaction process. The reaction was tracked by TLC (silica, 100% ethyl acetate, visualised by UV and PMA), and when deemed complete the reaction was diluted with acidified water (25 mL, 0.1M HCl solution, pH 2) and the product extracted in ethyl acetate (20 mL × 3), dried over Na_2SO_4 and solvent removed *in vacuo*. Crude product was separated by column chromatography (silica) using a solvent system comprising of ethyl acetate and hexanes (50 – 100%) to yield a purified oil (5.5 mg, 20% yield).

^{1}H NMR (500 MHz, $CDCl_3$) δ_H 7.12 (t, *J* = 7.8 Hz, 1H), 6.90 (d, *J* = 7.3 Hz, 1H), 6.68 (d, *J* = 8.2 Hz, 1H), 4.58 (s, 2H), 3.77 (dd, *J* = 9.1, 3.0 Hz, 1H), 3.62 (s, 1H), 3.36 (s, 3H), 2.76 (ddd, *J* = 14.7, 6.0, 3.4 Hz, 2H), 2.50 (dt, *J* = 14.3, 5.8 Hz, 2H), 2.34 – 2.25 (m, 1H), 2.20 (dd, *J* = 12.0, 6.5 Hz, 1H), 1.95 – 1.87 (m, 1H), 1.68 – 1.62 (m, 2H), 1.56 (dd, *J* = 8.8, 4.0 Hz, 2H), 1.48 – 1.40 (m, 3H), 1.36 – 1.20 (m, 10H), 1.13 (d, *J* = 11.7 Hz, 1H), 0.92 – 0.84 (m, 4H); **^{13}C NMR (126 MHz, $CDCl_3$) δ_C** 167.92 (s), 153.59 (s), 141.50 (s), 127.42 (s), 126.70 (s), 123.03 (s), 110.29 (s), 72.58 (s), 68.17 (s), 52.15 (s), 41.70 (s), 41.42 (s), 41.15 (s), 37.46 (s), 34.92 (s), 33.54 (s), 32.74 (s), 31.91 (s), 30.97 (s), 28.66 (s), 26.33 (s), 25.39 (s), 22.66 (s), 14.08 (s).; FTIR (ATR) v /cm^{-1}: (3262 (O-H), 2926-2856 (C-H), 1722 (C=O), 1585 (C-H), 1467-1403 (C-H), 1383 (S=O); [M-H]- found: 466.2255 m/z.

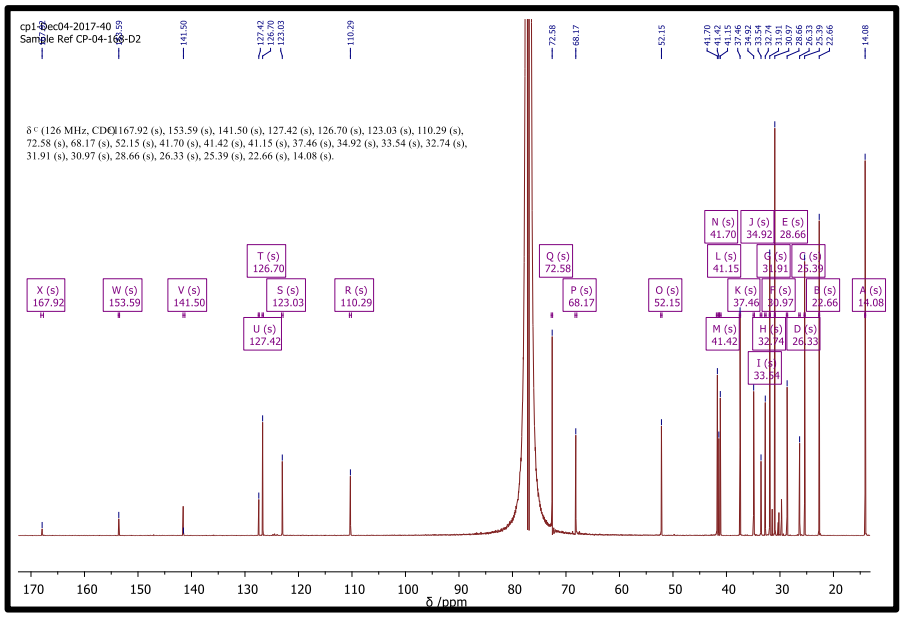

Figure 7-8. ^{13}C NMR spectrum of *N*-acyl sulfonamide treprostinil synthesised from triol intermediate.

7.4.2 Biological analysis

Cell Culture

Human embryonic kidney cells (HEK-293) cells stably transfected with the IP receptor[565] were grown from frozen in minimum essential growth medium (MEM; Cat. No. 11095080; Thermo Fisher; Waltham, USA) containing 10 % foetal bovine serum (FBS; Cat. No. 10270-106; Thermo Fisher) and 1% penicillin and streptomycin (PenStrep; Cat. No. 15070-063; Invitrogen; Carlsbad, USA).[47] Cells were cultured in a T75 flask (Cat. No. 658 170; Sigma Aldrich; St. Louis, USA) in 10 mL of warmed growth medium in a temperature and CO_2 controlled incubator at 37 ˚C and 5% CO_2. After 1 day, the medium was replaced with 15 mL of fresh medium containing 0.04 % added zeocin (Cat. No. ant-zn-1p; InvivoGen; San Diego, USA) to maintain selection of cells expressing the IP receptor. Cells were grown until reaching 80-85% confluency, with medium changed every 3-4 days.

Once confluency was reached, cells were split for further subculture. Media was removed by vacuum and cells were washed with 12 mL of warm calcium and magnesium free phosphate buffered saline solution (PBS; Cat No. 10010-015; Thermo Fisher) and then removed. 5 mL of warm 0.05% trypsin-EDTA (Cat. No. 25300054; Invitrogen) was added to lift adherence cells from the flask bottom by incubating the flask at 37 ˚C and 5% CO_2 for 1-2 mins. Once cells had become detached, growth medium (10 mL) was added to neutralise the trypsin and the cell suspension pipetted into a 50 mL falcon tube and centrifuged at 180 × g (Centrifuge 5804 R; Eppendorf; Hamburg, Germany), 21 ˚C for 5 minutes. The supernatant was removed by vacuum and the cell pellet re-suspended in fresh growth medium (4 mL). Once a homogeneous suspension of cells was obtained, cells counted were counted using an ADAM

Automated Cell Counter (Digital Bio; Seoul, Korea) according to manufacturer instructions. Thus, two aliquots (20 µL) were placed in Eppendorf vials containing either the 'T' solution (20 µL), which detects total cell numbers, or 'N' solution (20 µL) which detects all non-viable cells. Both solutions contain propidium iodide which stains the nucleus of the target cells that have been permeabilised or damaged. An aliquot (15 µL) of each mixed solution was placed onto a cell counting chip (Cat. No. AD4K-200; Cambridge Bioscience; Cambridge, UK) and loaded into the cell counter, which takes 22 fluorescent images of the cells and determines the number of cells per millimetre of cell suspension. Using the following equation, the amount of cell suspension solution and growth medium was determined to give the desired concentration.

$$n_1 \times v_1 = n_2 \times v_2$$

n_1 – number of cells required for plating

v_1 – volume of cell growth medium in which n_1 will be cultured

n_2 - concentration of cells in the total cell suspension (represented by the 20 µL aliquot)

v_2 – volume of cell suspension required for desired plating density.

Once the cell suspension had been made up according to the required density, the cells were added to either 12-well plates or a T75 flask.

Cyclic-AMP Assay

HCl (0.1M) was obtained as part of the cAMP ELISA kit (ADI-900-163) from Enzo Life Sciences, Pierce™ BCA protein assay kit (Cat. No. 23227) was obtained from Thermo Fisher Scientific, bovine serum albumin (BSA; Cat. No. A0281) was obtained from Sigma Aldrich. The Opsys MR plate-reader was from Dynex Technologies, UK. Data was analysed using GraphPad Prism Software, version 7, (CA, USA).

TRE-S (5.6 mg) was dissolved in 1 mL of 90% MeCN/H2O solution. This was used as a stock solution for all biological assays and stored at -20 °C between experiments.

For the concentration-response experiments, the cell suspension (1 mL) in MEM containing 10 % foetal bovine serum (FBS) and 1% penicillin and streptomycin (PenStrep) was added to each well of a 12-well plate (Cat. No. 734-2324; VWR; Radnor, USA) at a density of 1 x10^4 cells mL^{-1} and incubated for 48 hours at 37 °C / 5% CO_2. Following this, the growth medium was replaced with fresh growth medium (1 mL) to remove any unattached cells and incubated for a further 24 hours at 37°C / 5% CO_2. After which, drug concentrations (0.001 -1000nM) were made up into media (3 mL) and added to the respective wells in duplicate and cells incubated for 15 minutes with the IP receptor agonist (Treprostinil and N-sulfonamide treprostinil, TRE-S). When organic solvents were used in the drug stock solutions, equal final percentages of solvent (acetonitrile or DMSO) were added to the serial dilution vials to maintain consistency in all vials to achieve final amount of 0.1% solvent. The medium was removed and replaced with cold HCl (0.1 M, 250 µL) whilst the plate was resting on ice. The lysed cells were scraped and collected in 1.5 mL Eppendorf vials. Duplicate concentrations of

each drug were pooled together and centrifuged at 10 000 × g at 4 °C for 10 mins to pellet cell debris; the supernatant was transferred to new vial and frozen at -80°C until required.

Before the ELISA was carried out, the supernatant solutions were thawed. The cyclic adenosine monophosphate (cAMP) assay kit (ADI-900-163; Enzo Life Sciences; Farmingdale, USA) used a competitive binding technique, where each well was coated with a goat anti-rabbit IgG antibody. Cyclic AMP conjugated to alkaline phosphatase followed by rabbit polyclonal antibody was added to each well. The antibody binds competitively to the cAMP. The *para*-nitro phenyl phosphate substrate then reacts with the alkaline phosphatase on the cAMP conjugate, releasing a yellow colour. The 96-well plate was read at 405 nm using a Dynex Opsys MR plate-reader (Worthing, UK) where the absorbance signal was inversely proportional to the concentration of cAMP in the sample. Standard solutions of cAMP were made up with known concentrations which are used to generate a standard curve to determine levels in HEK-293-IP cells exposed to a particular IP agonist.

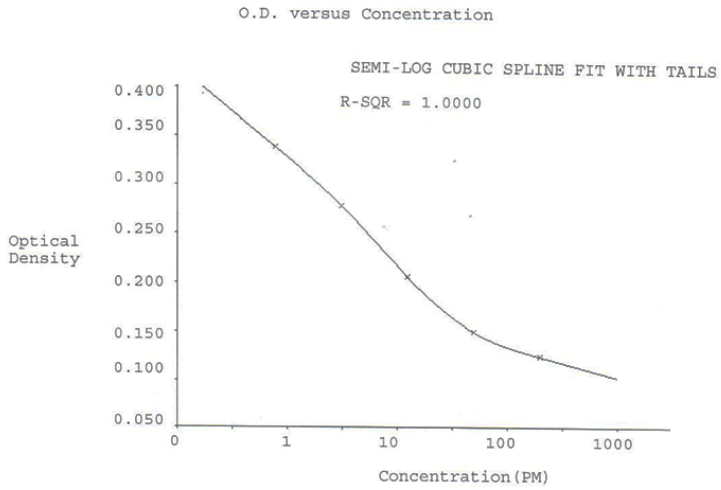

Figure 7-9. Standard curve of concentration of cAMP standards versus optical density. cAMP is measured using enzyme-linked immunosorbent assay and optical density is read at 405 nm. Curve fit uses semi-log cubic spline fit with tails.

A bovine serum albumin (BCA) protein kit was used to normalise cAMP levels against the level of protein. The assay was based on the principle that proteins reduce copper in alkaline solution (Cu^{2+} to Cu^{1+}) producing a colour change which was detected. A standard was prepared using a 1 mg / mL solution of bovine serum albumin (BSA) dissolved in distilled water. 25 µL of each sample and 200 µL of BCA working solution was added to each well and the plate placed on a microplate shaker (VWR, Radnor, USA) for 30 seconds. The plate was incubated for 30 minutes at 37°C / 5% CO_2 before being cooled to room temperature and read at 540 nm using a plate reader.

Microsomal Degradation Assay

Sterile distilled water (Cat. No. 15230-071), β- nicotinamide adenine dinucleotide phosphate disodium salt (Cat. No. 101166) and PBS tablets (Cat. No. 18912-014) were obtained from

Thermo Fisher Scientific, Selexipag (Cat. No. 10010411) was obtained from Cayman chemicals (Ann Arbor, USA). Phosphoric acid (Cat. No. 21510-4), indomethacin (Cat. No. I-7378), D-Glucose 6-phosphate disodium hydrate (Cat. No. G7250), glucose-6-phosphate dehydrogenase (Cat. No. G-4134), potassium phosphate monobasic (Cat. No. P8416) and potassium phosphate dibasic (Cat. No. 60353) were bought from Sigma Aldrich, Oasis Prime HLB plus lite SPE cartridges (Cat. No. 186005125) were bought from Waters. Papaverine (Cat. No. 207220050) was from Acros Organics, rat microsomes (Cat. No. RTMCPL) and human microsomes (Cat. No. HMMCPL) were obtained from Life Technologies (Paisley, UK), magnesium chloride (anhydrous, Cat. No. 8.14733.0100) was bought from Merck.

Potassium phosphate buffer (100 mM) was prepared using dibasic potassium phosphate and monobasic potassium phosphate. The final solution was filtered through 0.2-mm Nalgene filter flask with vacuum assistance and stored at 4 °C.

The microsome assay is often used as a measure of enzymatic degradation of a prodrug to its respective metabolite.[278,393] The final assay in each vial includes hepatic microsomes (0.4 mg/mL), regenerating system (25 mM glucose-6-phosphate, 4 units/mL glucose-6-phosphate dehydrogenase, 2.5 mM β-NADP, and 10mM mM $MgCl_2$), test compound (10μM), in potassium phosphate buffer at pH 7.4 in a final volume of 500 µL. Rat and human hepatic microsomes were obtained as a 20 mg/ mL stock solution. A solution of microsome stock suspension (193.5 µL) in the buffer solution (8.8 mL) described above was made. Sample solutions (1mM) were prepared. The selexipag solution was prepared by diluting (10 fold) the drug stock (5 µL, 10mM) in buffer solution (45 µL). TRE-S (1mM) solution was made by diluting stock (4.67 µL, 10.7 mM) in buffer (45.33 µL). Indomethacin (50 µM) was made by diluting stock (0.1 µL. 10mM) in buffer (19.9 µL). For the NADPH-regenerating system: glucose-6-phosphate (190.1 mg) was dissolved in buffer (375 µL); nicotamide adenosine diphosphate (49.2 mg) was dissolved in buffer (375 µL); anhydrous magnesium chloride (23.8 mg) was dissolved in sterile distilled water (375 µL); a stock of glucose-6-phosphate dehydrogenase (114 U, 0.6 mg) was dissolved in buffer (427.5 µL), of which 375 µL used in assay. All NADPH-generating solutions were kept on ice and immediately before use, the four solutions were added together. Portions of microsome solution (465 µL) were aliquoted into 1.5 µL vials for incubation which after the designated amount of time would be extracted. Combined NADPH-regenerating solution (30 µL) was added to each vial and the solutions vortexed then preincubated at 37 °C for 5 minutes. The assay was initiated by the addition of drug stock (5 µL) to achieve a final concentration of 10 µM for selexipag and TRE-S, and 0.5 µM for indomethacin. Solutions were vortexed and incubated for various time periods between 0 and 120 minutes. The reactions were quenched by addition of LCMS grade acetonitrile (100 µL) and vortexed. The solutions were then centrifuged at 9279 × g (Eppendorf; Hamburg, Germany) for 10 minutes at 4 °C.

Sample preparation for LCMS/MS involved filtering supernatant (500 µL) through solid phase extraction (SPE) cartridges using a 1 mL syringe to remove salts and lipids. The sample was

washed of salts by flushing through 500 µL of 5% methanol/water solution. Into a fresh vial, drug was eluted from cartridge by addition of 500 µL acetonitrile spiked with internal standard (papaverine, 1 pg/mL). Papaverine was chosen as the internal standard as it forms positive ion with mass smaller than that of any of the test compounds. Filtrate (20 µL) was analysed by LCMS/MS. The mobile phase was a fixed gradient at 55% acetonitrile/water both spiked with 0.1% formic acid. The column was operated with a fixed flow rate of 1 mL/minute at a temperature of 40 °C. Prodrug masses were identified by electrospray ionisation in positive ion mode. Multiple reaction monitoring was used for accurate ion quantification. The most abundant ion for each precursor compound was used for quantification. For all compounds; dwell was set to 200 and cell accelerator voltage was set to 7 V.

Table 7-2. Most abundant product ions of each drug used in microsome assay used for quantification of compound.

Compound	Precursor ion	Product ion	Fragmentor	Collision energy
Papaverine	340.01	324.1	130	30
Indomethacin	157.9	138.9	155	14
Selexipag	497.01	377.1	160	30
TRE-S	467.6	337.2	135	14

Stability of TRE-S in cell culture media was also carried out using the same procedure as the blood stability assay and worked up as below.

7.5 Methods for Chapter 4

7.5.1 Instrumentation

Gel permeation chromatography was carried out by size exclusion by an in-house technician. Size exclusion chromatography (SEC) was conducted with DMF as the mobile phase containing 5 mM NH_4BF_4 additive at 70 ˚C with a flow rate of 1.00 mL/min. 100 µL of polymer aliquots in DMF (5 mg/mL) were injected in a Viscotek system equipped with a refractive index (RI) detector. Poly(methyl methacrylate) (PMMA) standards were used for calibration and OMNISEC software was used to determine the average molecular weight (M_n) and index of polydispersity (PDI).

A degradation assay was carried out in an Innova 40 incubator (New Jersey) set to 37 °C. Worked up samples were analysed by High performance liquid chromatography (HPLC), on system described on page 317.

7.5.2 **Synthesis**

Poly(PEG acetal) 70

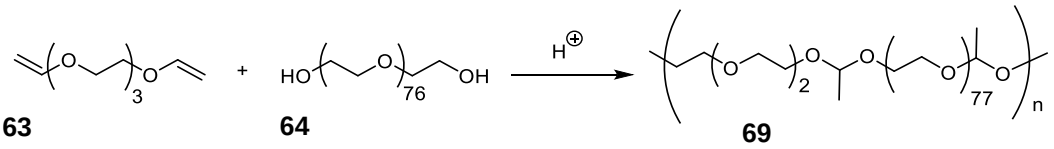

63 **64** **69**

In an argon environment, poly(ethylene glycol) 3400 **65** (3.5980 g, 1.038 mmol) and *p*-toluene sulfonic acid (5.7 mg, 0.030 mmol) were stirred together in toluene and distilled at 175 °C to remove any trace water. Once the solvent had been removed the residue was cooled to 50 °C and THF (5 mL) was added. Triethylene glycol di vinyl ether **64** (TEGDVE, 216 µL, 1.058 mmol) was added to the solution, the flask wrapped in foil and left to stir for 2 hours. Triethylamine (289 µL, 2.076 mmol) was added and the reaction solution was slowly added to cold hexane (200 mL) to precipitate polyacetal **70**. The precipitated solid material was isolated by vacuum filtration and washed with hexane, before drying under reduced pressure for 24 hours to yield (3.43 g, 92% yield) of a white solid; Average molecular weight = 48.7 kDa; PDI = 2.0; **^{1}H NMR (500 MHz, D_2O) δ_H** 7.67 (1 H, d, J 8.2), 7.36 (1 H, d, J 8.0), 6.50 (1 H, dd, J 14.3, 6.7), 4.86 (2 H, q, J 5.3), 3.87 – 3.78 (6 H, m), 3.76 – 3.57 (331 H, m), 3.56 – 3.48 (3 H, m), 1.33 (6 H, d, J 5.4).

Oligo(PEG-treprostinil acetal) 71

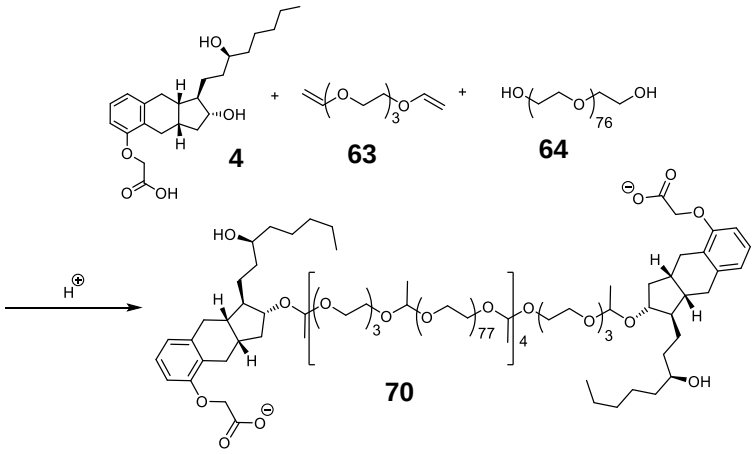

4 **63** **64**

70

In a RBF (25 mL) under argon, a solution of PEG 3400 **65** (874.5 mg, 0.257 mmol) and *p*TSA (7.4 mg, 0.039 mmol) were stirred in 8 mL toluene. Water was removed by azeotropic distillation of toluene by heating to 175 °C. Once a majority of toluene was removed and the residue cooled to below 50 °C, treprostinil **4** (100.5 mg, 0.257 mmol) in THF (3 mL) was added followed by dropwise addition of TEGDVE **64** (106.2 µL, 0.520 mmol). The reaction mixture was stirred in darkness for 3 hours and then precipitated into hexane. Triethylamine (178.5 µL, 1.281 mmol) was added to the reaction mixture midway through the precipitation step. The precipitate collected by vacuum filtration and then dried under vacuum for 24 hours, affording oligo(PEG-treprostinil acetal) **71** as a solid (0.8574 g, 80% yield.) Average molecular weight = 17.4 kDa; PDI = 1.8 kDa; **^{1}H NMR (500 MHz, D_2O) δ_H** 7.67 (1 H, d, *J* 8.2), 7.35 (1 H, d, *J* 8.1),

7.14 (1 H, d, *J* 7.8), 6.89 (1 H, d, *J* 7.2), 6.75 (1 H, d, *J* 8.2), 4.89 – 4.83 (2 H, m), 4.45 (2 H, s), 3.86 – 3.75 (15 H, m), 3.74 – 3.58 (1431 H, m), 3.56 – 3.51 (9 H, m), 2.68 (3 H, q, *J* 7.2), 2.58 (1 H, dd, *J* 13.1, 6.6), 2.50 (1 H, dd, *J* 13.1, 4.6), 2.38 (2 H, s), 2.32 – 2.24 (1 H, m), 2.24 – 2.18 (1 H, m), 2.18 – 2.08 (1 H, m), 2.00 – 1.92 (1 H, m), 1.92 – 1.84 (1 H, m), 1.81 – 1.73 (1 H, m), 1.65 (1 H, s), 1.33 (14 H, d, *J* 5.3), 0.85 (3 H, t, *J* 6.5).

Oligo(treprostinil ethyl ester-PEG acetal) 72

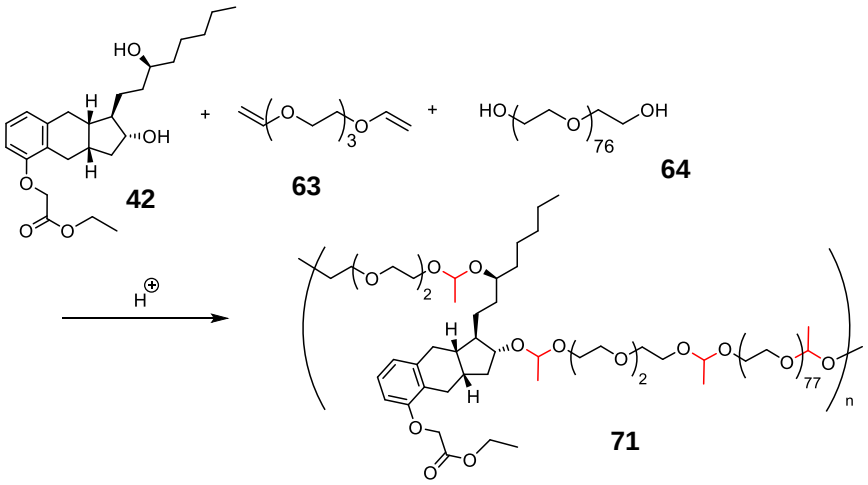

Using a Dean Stark condenser, PEG 3400 **65** (436.3 mg, 0.1283 mmol) and *p*TSA (0.7 mg, 3.8 µmol) were dissolved in toluene (8 mL) and heated to 175 °C in an argon environment whilst stirring for 1 hour. Once all toluene had been removed, treprostinil ethyl ester **43** (51.2 mg, 0.1223 mmol) and THF (6 mL) were added. The reaction flask was wrapped in foil and TEGDVE **64** (54 µL, 0.2670 mmol) added dropwise. After 3.5 hours, the reaction was quenched by addition of triethylamine (8.9 µL, 0.0639 mmol) and then precipitated into hexane (400 mL). The precipitate collected by vacuum filtration, washed with cold hexane and dried under vacuum to yield a white solid (0.3795 g, 81% yield.) Average molecular weight = 7.0 kDa; PDI = 1.1; **^{1}H NMR (500 MHz, D_2O) δ $_H$** 7.58 (1 H, d, *J* 8.2), 7.27 (1 H, d, *J* 8.0), 7.06 (1 H, t, *J* 7.8), 6.80 (1 H, d, *J* 7.5), 6.66 (1 H, d, *J* 8.4), 6.42 (2 H, dd, *J* 14.3, 6.8), 4.77 (4 H, q, *J* 5.4), 4.36 (2 H, s), 4.24 (2 H, dd, *J* 14.3, 2.2), 4.05 (2 H, dd, *J* 6.7, 2.2), 3.82 (5 H, dd, *J* 5.4, 3.3), 3.74 (33 H, dd, *J* 5.3, 3.5), 3.71 – 3.48 (5006 H, m), 3.48 – 3.27 (44 H, m), 2.72 – 2.63 (2 H, m), 2.57 (2 H, q, *J* 7.3), 2.46 (1 H, d, *J* 6.1), 2.41 (1 H, dd, *J* 14.5, 5.8), 2.29 (2 H, s), 2.20 (1 H, d, *J* 7.5), 2.09 – 1.97 (1 H, m), 1.85 (1 H, s), 1.56 (1 H, s), 1.44 (1 H, d, *J* 19.4), 1.33 (2 H, d, *J* 11.1), 1.24 (12 H, d, *J* 5.4), 1.08 (4 H, dd, *J* 12.0, 4.9), 0.96 (3 H, t, *J* 7.3).

Poly(silyl PEG)

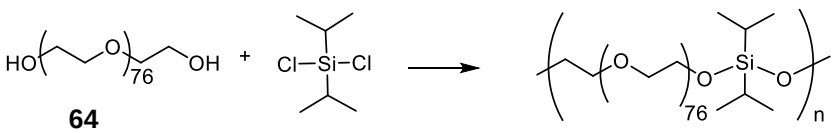

In an oven dried, argon purged RBF (25 mL), PEG 3400 **65** (996.7 mg, 0.2931 mmol) was dried by azeotropic removal of toluene (50mL) *in vacuo*. Once toluene had been removed,

THF (12 mL) and pyridine (47.0 µL, 0.5835 mmol) were added and heated slightly to solubilise. Whilst stirring vigorously, dichlorodiisopropyl silane (46.0 µL, 0.2549 mmol) was added dropwise. The solution was stirred for 16 hours. The cloudy reaction mixture was precipitated into hexane and the precipitate collected by vacuum filtration. After drying under vacuum, a white powder was afforded (0.9262 g) Average molecular weight = 10.7 kDa; PDI = 1.06. Polymerisation was unsuccessful.

Poly(silyl PEG treprostinil)

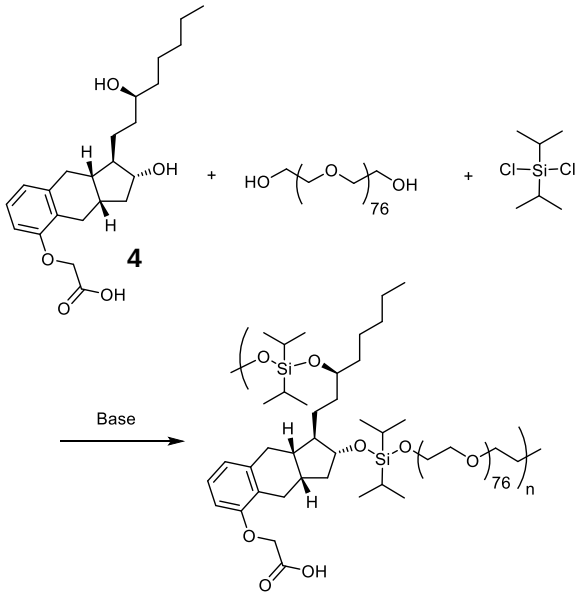

PEG 3400 **65** (435.4 mg, 0.1281 mmol) was dried by azeotropic removal of toluene from an argon-purged 25 mL RBF, *in vacuo*. The dried residue was dissolved in anhydrous THF aided by heating to 40 °C and pyridine (52.0 µL, 0.6468 mmol) added. Treprostinil **4** (50.0 mg, 0.1280 mmol) was added, followed by dropwise addition of dichloroisopropyl silane (46.2 µL, 0.2560 mmol). The solution stirred for 16 hours and precipitated into hexane. Precipitate collected and dried over partial pressure to afford white powder (0.409 g,) although polymerisation was unsuccessful.

7.5.3 **Degradation Assay**

PBS buffers were made at pH 7.4, 6.6, by dissolution of a PBS tablet in deionised water (200 mL). Citrate buffer was made by addition of citric acid solution (0.11 M, 82 mL) and sodium citrate solution (0.11 M, 18 mL). All pH measurements were taken using a Hanna HI 2210 pH meter (Rhode Island, US) and adjustments were made by dropwise addition of standard HCl (0.1 M) or NaOH (0.1M). Oligo(PEG-Treprostinil acetal) solutions were made by dissolving the sample in buffers at 5 mg/mL or 2.5 mg/mL. Immediately upon oligomer dissolution, the solutions were vortexed and aliquoted into 200 µL samples. The aliquots were incubated at 37 °C and at predefined time points, the solutions were extracted using ethyl acetate. Briefly, treprostinil was extracted into EA (3 × 200 µL) and the combined EA layers washed with brine (200 µL). Trace water was removed from the organic layer by filtration through a layer of

$MgSO_4$ and cotton wool. The filter was flushed with EA (200 µL) and the filtrate dried over a stream of air. Once dried, the residue was reconstituted in a 200 µL acetonitrile solution with 1 mg/mL phenoxyacetic acid as an internal standard. HPLC samples were frozen until analysis.

A 1 mg/mL stock solution of treprostinil was prepared in the same solution of MeCN spiked with phenoxyacetic acid as samples. Treprostinil calibrants were prepared by 2-fold serial dilution using spiked MeCN as solvent. Samples were analysed by HPLC in duplicate.

HPLC analysis was conducted using a Supelco Discovery HS RP-C_{18} column (Cat. No. 567209-U). Water and acetonitrile spiked with 0.1 % TFA comprised the liquid phase. A gradient was run from 40% to 90% MeCN over 8 minutes. An injection volume of 20 µL and a flow rate of 1 mL/minute were used and treprostinil was detected by UV (217 nm).

HPLC analysis was calculated as a ratio between internal standard with retention time 3.6 minutes and treprostinil concentration with retention time 7.1 minutes. Ratios for calibration standards were plotted measuring regression. Ratios of samples with unknown concentrations were converted into concentrations (mg/mL) using the linear equation. To compensate for the different aliquot and extraction volumes, the concentration calculated was divided by the relevant dilution factor.

Degradation analysis by GPC was conducted on a separate sample (200 µL) for each time point. At predefined time points (0, 1, 2, 4, 6, 24 hours), one sample was analysed by HPLC as before and the other was flash frozen in an acetone/dry ice bath, stored at -20 °C and lyophilised for 24 hours. The samples were then prepared for GPC as described on page 338 .Methods for Chapter 5

7.6 Methods for Chapter 5

7.6.1 General on-resin techniques

Peptides were synthesised by automated solid phase peptide synthesis (SPPS) using a Biotage Syro (Uppsala, Sweden). Each coupling was carried out in duplicate and 5 equivalents of the Fmoc-amino acid were added. Coupling was carried out in peptide grade dimethylformamide (DMF) by N,N,N′,N′-Tetramethyl-O-(1H-benzotriazol-1-yl)uronium hexafluorophosphate (HBTU, 5 eq) in the presence of diisopropyl ethylamine (DIPEA, 10 eq). After duplicate coupling the Fmoc-amine was deprotected by reaction with piperidine (40%).

Number of moles for each repeat reaction were calculated using the following equation.

$$No.Moles = Resin\ loading\ \left(\frac{mmol}{g}\right) * resin\ weight\ (g)$$

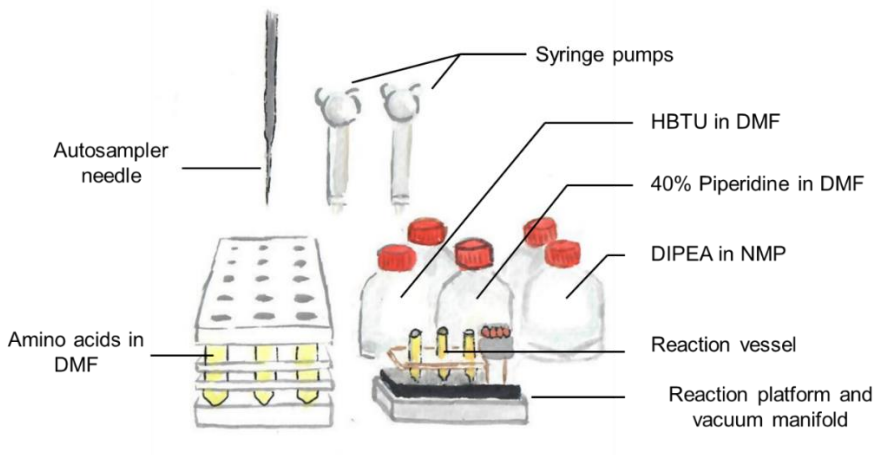

Figure 7-10. Image of automated solid phase peptide synthesiser used to make amino build amino acid sequences on resin matrices. Solutions of coupling 3-[Bis(dimethylamino)methyliumyl]-3H-benzotriazol-1-oxide hexafluorophosphate (HBTU), piperidine and individual amino acids are made up individually in dimethylformamide (DMF). Diisopropylethylamine (DIPEA) is dissolved in *N*-methylpyrrolidinone (NMP). Each pre-programmed amino acid sequence is synthesised in the respective reaction vessel which is loaded with swollen resin. The needle collects the correct amount of each solution and dispenses them in the reaction vessel. The vessel is vortexed for 3 minutes for each coupling and each coupling is conducted twice.

Resin drying and removal

Unless otherwise stated, before different reaction steps (coupling, cyclisation, resin removal), resins were rinsed with DMF (6x 3 mL) to rinse any remaining unreacted compounds. Dichloromethane (DCM, 6x 3 mL) was used to rinse DMF and 50% DCM/MeOH (6x 3 mL) was used to help the resin shrink. The resin was subsequently dried in a vacuum desiccator overnight.

Unless otherwise stated, compounds were removed from resin by the addition of a solution containing 95% trifluoroacetic acid (TFA), 2.5% triisopropyl silane 95 (TIS) and 2.5% water.[544] The solution was left to sit for 2 hours with the occasional swirling of the reaction mixture. The resin was removed by filtration through a sinter funnel, rinsing with further TFA. The filtrate was condensed but not dried *in vacuo* and the product was precipitated by the addition of ice-cold diethyl ether. The precipitate was collected on a sinter, washed further with diethyl ether, dissolved in a suitable solvent (95% aqueous acetic acid or water) and filtrate collected in a RBF. The collected filtrates were lyophilised using one of three options; for acidic solutions a Heto Powerdry LL1500 freeze dryer (Thermo Fisher, US) was used; for aqueous solutions, the solvent was removed using a Virtis Advantage freeze dryer (-60 ^{o}C environment with shelf temperature -20 ^{o}C), when neither of these were available, a freeze dryer was made using a rotary evaporator (Buchi Rotavapor R-200; Flawil, Switzerland) set to no rotation. The sample was cooled in salt ice bath (-12 ^{o}C), the vapour cooled with ice finger (-78 ^{o}C) and system depressurised with a vacuum pump.

HPLC – Analytical and preparative

Analytical reverse phase high performance liquid chromatography (RP-HPLC) was carried out as described before in the general methods, page 317). UV detector measured absorbances at 217 nm (amide bond detection), 254 nm (aromatic detection) and 495 nm (fluorescein detection). Unless stated otherwise, samples were analysed using an aqueous mobile phase of increasing acetonitrile (10% - 60%) over 22 minutes. The total analysis time was 30 minutes.

Preparative HPLC was carried out on a Jasco system (Jasco Corp., Oklahoma, US) comprised of a pump (Jasco-980), a 2 mL loop volume autosampler (Jasco AS-1555), and a single wavelength UV detector (Jasco-1570) set to 217 nm. The system was equipped with a reverse phase column Supelco Discovery HS C_{18} column, (25 cm x 2.1 cm, 5 µm; Cat. No. 568543-U) purchased from Sigma Aldrich UK and ChromNAV software (version 2.02.05, Jasco Corp). The mobile phase consisted of 0.1% TFA (Cat. No. L06374) buffered water with increasing TFA-buffered (0.1%) acetonitrile concentration (10% - 60%) over 90 minutes. The total analysis time was 120 minutes.

Purification by automated column chromatography was carried out on a Biotage system as described in Chapter 3. The system was fitted with a Reveleris C18 cartridge (4 g or 12 g, Cat. No. 145152990; Buchi; Flawil, Switzerland). A mobile phase of acetonitrile and water, in a gradient as described below, was run at 6 mL/min.

Table 7-3. Mobile phase used for automated chromatography system. Using column volumes to measure the solvent allowed for the same method to be applied exactly, irrespective of the column cartridge size used.

Column Volumes	% Acetonitrile	% Water
2	5	95
20	5 – 40	95 – 60
3	40	60

Kaiser test for primary amines

The Kaiser test consists of three solutions and was used to determine the presence of primary alcohols on resin.[566]

Solution 1: Ninhydrin (5 g) was dissolved in ethanol (100 mL)

Solution 2: Liquid phenol (80 g) was mixed with ethanol (20 mL)

Solution 3: Potassium cyanide (0.001 M, aqueous, 2 mL) was mixed with pyridine (98 mL)

To prepare the resin, a sample of resin beads (~10 beads) was removed from the reaction, placed on a sinter under partial pressure, and washed in the following order; DMF (3 mL) to rid any solution phase reagents, DCM (3 mL) to rinse away DMF traces, and DCM/MeOH (50%, 3 mL) to shrink the resin. After drying the resin for 2 minutes on the sinter under reduced pressure, the beads were transferred into a soda tube. The Kaiser test was performed by addition of the following solutions *via* glass pipette in the order described; solution 1 (1 drop),

solution 2 (2 drops) and solution 3 (1 drop). The solution gentle agitated and heated to 110 °C for 3-5 minutes. An intense blue solution with blue beads was positive and indicated primary amines were present. A colourless or faintly coloured solution with pale beads indicated that no primary amines are present. A dark blue solution with pale beads indicates that the coupling was nearly complete.

P-anisaldehyde test for aldehydes

The presence of aldehydes was determined using a *p*-anisaldehyde solution.[527] Ethanol (4.4 mL), sulfuric acid (0.45 mL), acetic acid (50 µL) and *p*-anisaldehyde (127.5 µL) were stirred together and stored at 4 °C for up to 5 days. To test for aldehydes, a small sample of resin was washed with DMF (3 mL), DCM (3 mL) and a 50% solution of DCM/MeOH (3 mL). Once dried under partial pressure for a couple of minutes the beads were transferred to a soda tube and the test solution (~300 mL) was added. The solution was heated to 110 °C for 4 minutes in a heated block and the colour change was interpreted. In the absence of aldehydes, no change in bead colour was observed. In the presence of aldehydes, the beads turn purple/red.

Acetaldehyde test for secondary amines

The presence of secondary amines was determined using the acetaldehyde test. A solution of 2% acetaldehyde **139** in DMF and NMP (1 mL) was mixed together. Sample resin (10-20 beads) was washed with DMF prior to testing and placed in a soda tube. 2-3 drops of the testing solution were added and after 10 minutes the colour noted. The presence of secondary amines turned the beads red and no colour change was observed in their absence.

4-toluene sulfonyl chloride – p-nitrobenzylpyridine (TosCl-PNBP) test for alcohols

Detection of alcohol was determined using the TosCl-PNBP test[567,568] which was comprised of three different solutions.

Solution 1: *p*-toluenesulfonyl chloride in toluene (0.12M)
Solution 2: *p*-nitrobenzylpyridine in toluene (0.30M)
Solution 3: Piperidine 10% (v/v) in chloroform

A sample of test resin was washed with DMF (3 mL) and DCM (6 mL). As a suspension in DCM, approximately 10 beads were pipetted onto a sheet of silica. Once dry, 1 drop of solution 1 followed by a drop of solution 2 was added to the beads. The silica plate was heated from beneath using a heat gun for 1 minute or until a yellow colour had appeared and disappeared again. A drop of solution 3 was then added. The presence of hydroxyls was indicated by a purple colouration to the beads which appeared pink when concentrations were low. The absence of alcohols and phenols resulted in no colour change. Samples were run alongside control tests; using Wang resin as a positive control and acetylated Wang resin as a negative control.

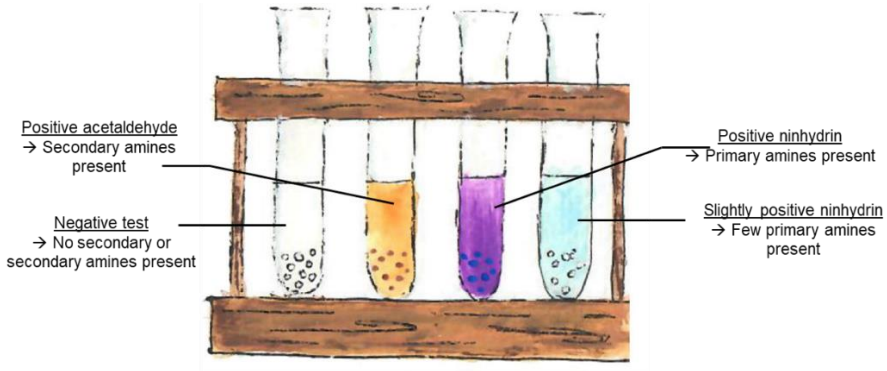

Figure 7-11. Depiction of results of colourimetirc resin tests for amines. Beads produced no colour when no groups are present, became purple when primary amines were present and exposed to ninhydrin. A very pale blue colour indicated very few amines were present. Orange solution and brown/red beads indicated the presence of secondary amines.

7.6.2 Synthesis

FITC-CARSKNKDC synthesis

In solution CAR peptide conjugation

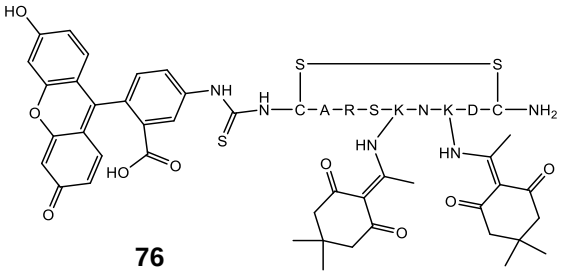

76

A solution of DIPEA (155 µL, 122.1 µL) in anhydrous DMF (2.5 mL) was added to disulfide-cyclised CARSK(Dde)NK(Dde)DC-NH_2 **74** (50 mg, 37 µmol) and fluoroscein isothiocyanate **75** (FITC, 19.2 mg, 48 µmol) in an argon purged flask. The flask was wrapped in foil and left stirring at RT for 16 hours and monitored by reverse phase thin layer chromatography (RP-TLC). DMF was removed by passing a stream of air over the solution and redissolving the residue in THF. The precipitate was filtered off and the filtrate dried down. HPLC retention time of FITC-peptide **77** = 13.7 minutes; R_f = 0.56. Peptide FITC conjugation was conducted following previous procedures:[569]

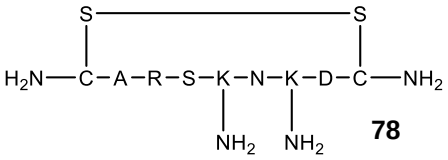

78

Disulfide-cyclised H-CARSK(Dde)NK(Dde)DC 74 (2mg, 1.5 µmol) was dissolved in DMF (50 µL) and hydrazine hydrate **78** (2 µL) added. After 10 minutes, RP-TLC was run in 50% MeCN/H_2O by drying a sample of reaction solution. The dried solution was analysed by HPLC in water; retention time = 8.2 minutes; R_f = 0.5;

^{1}H NMR (400 MHz, MeOD) δ 8.18 – 8.13 (1 H, m), 8.07 (1 H, s), 8.02 (1 H, s), 8.00 (1 H, s), 7.97 (3 H, s), 6.69 (1 H, d, J 7.4), 6.54 (1 H, d, J 8.6), 4.93 (1 H, s), 4.90 (1 H, s), 4.89 – 4.78 (242 H, m), 4.76 (1 H, s), 4.70 (1 H, s), 4.69 (1 H, s), 4.56 (1 H, dd, J 8.8, 4.9), 4.49 (1 H, d, J 7.1), 4.36 (1 H, dd, J 14.3, 6.8), 4.31 (1 H, t, J 4.4), 4.24 – 4.18 (1 H, m), 4.14 (1 H, s), 3.95 (1 H, dd, J 11.2, 4.3), 3.84 (1 H, dd, J 11.1, 4.5), 3.50 – 3.47 (1 H, m), 3.35 (1 H, s), 3.34 – 3.29 (111 H, m), 3.29 (1 H, s), 3.24 (2 H, dd, J 9.4, 4.0), 3.13 (1 H, dt, J 3.3, 1.7), 3.03 (1 H, d, J 3.7), 2.99 (1 H, s), 2.95 (3 H, t, J 7.2), 2.90 (1 H, d, J 0.5), 2.86 (2 H, d, J 0.6), 2.80 (2 H, d, J 6.6), 2.78 (1 H, d, J 5.0), 2.76 – 2.73 (1 H, m), 2.70 (4 H, s), 2.66 (1 H, s), 2.62 (1 H, s), 2.55 (1 H, d, J 6.4), 2.52 – 2.49 (1 H, m), 2.45 (6 H, s), 2.42 (1 H, s), 2.40 (1 H, d, J 5.8), 2.34 (5 H, d, J 2.2), 2.14 (1 H, s), 2.10 (1 H, s), 2.04 (1 H, s), 1.98 (1 H, d, J 5.4), 1.91 (4 H, dt, J 23.3, 9.1), 1.68 (4 H, s), 1.48 (3 H, d, J 7.0), 1.43 (2 H, d, J 7.0), 1.29 (1 H, s), 1.09 (12 H, s), 1.07 (1 H, d, J 3.5), 1.05 (1 H, s), 1.02 (1 H, s).

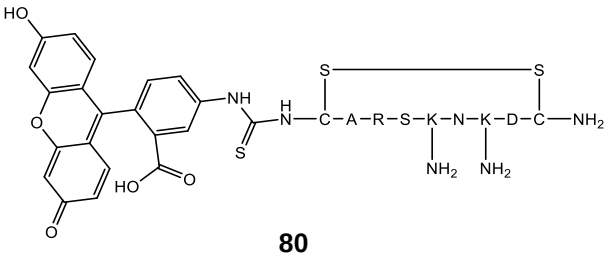

80

To a solution of crude disulfide-cyclised FITC-XCARSK(Dde)NK(Dde)DC-NH_2 **77** (3.7 μL) in THF (0.5 mL) was added hydrazine hydrate 78 (10 μL, 0.174 mmol). The reaction was tracked by HPLC using a solvent gradient of 25-50% acetonitrile over 15 minutes then the 50% acetonitrile was maintained for a further 15 minutes. UV detection was carried out at 220 nm. HPLC trace showed two sharp absorbances; one at 15.1 minutes expected to be product and another at 20.9 minutes indicating an excess of FITC.

On resin CAR synthesis

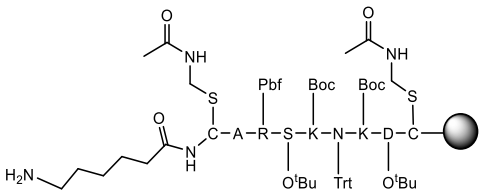

83

H-Ahx-Cys(Acm)-Ala-Arg(Pbf)-Ser(O^{t}Bu)-Lys(Boc)-Asn(Trt)-Lys(Boc)-Asp(O^{t}Bu)-Cys(Acm) **84** was synthesised by automated solid phase peptide synthesis. Peptides were grown on PAL Novasyn resin (Barany's aminomethyl-dimethoxyphenoxyvaleric acid linker attached to NovaSyn® TentaGel® resin,100 mg) in quintuplet. The loading of the batch was 0.22 mmol/g, therefore each vial possessed 0.022 mmol of reactive amines.

Table 7-4. Amounts of reagents required for automated solid phase peptide synthesis of CARSKNKDC peptide on PAL NovaSyn® resin using Fmoc chemistry and employing Fmoc-Cys(Acm) as the thiol protecting group.

Code	Compound	Mol	Amount	Solvent	Vol of solvent
C	Fmoc-Cys(Acm)-OH	414.5	0.476 g	DMF	16.37 mL
A	Fmoc-Ala-OH	311.3	0.184 g	DMF	8.47 mL
R	Fmoc-Arg(Pbf)-OH	648.8	0.384 g	DMF	8.32 mL
S	Fmoc-Ser(OtBu)-OH	383.4	0.227 g	DMF	8.43 mL
K	Fmoc-Lys(Boc)-OH	468.2	0.538 g	DMF	16.26 mL
N	Fmoc-Asn(Trt)-OH	597.8	0.353 g	DMF	8.36 mL
D	Fmoc-Asp(OtBu)-OH	411.5	0.243 g	DMF	8.42 mL
X	Fmoc-Ahx-OH	353.4	0.209 g	DMF	8.45 mL
	HBTU	379.3	2.235 g	DMF	88.21 mL
	DIPEA	129.3	2.01 mL	NMP	40.99 mL
	Piperidine	85.15	38.4 mL	DMF	57.60 mL

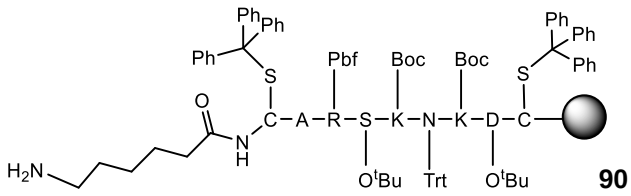

90

H-Ahx-Cys(Trt)-Ala-Arg(Pbf)-Ser(O^{t}Bu)-Lys(Boc)-Asn(Trt)-Lys(Boc)-Asp(O^{t}Bu)-Cys(Trt) **91** was synthesised on PAL Novasyn resin (100 mg) in duplicate. Resin loading was 0.22 mmol/g, therefore each vial possessed 0.022 mmol of reactive amines.

Table 7-5. Amounts of reagents required for SPPS of CAR peptide using Cys(Trt).

Code	Compound	Mol wt (g/mol)	Amount	Solvent	Total vol of solvent (mL)
C	Fmoc-Cys(Trt)-OH	585.7	0.286 g	DMF	6.89
A	Fmoc-Ala-OH	311.3	0.081 g	DMF	3.74
R	Fmoc-Arg(Pbf)-OH	648.8	0.169 g	DMF	3.67
S	Fmoc-Ser(OtBu)-OH	383.4	0.100 g	DMF	3.373
K	Fmoc-Lys(Boc)-OH	468.2	0.229 g	DMF	6.91
N	Fmoc-Asn(Trt)-OH	597.8	0.156 g	DMF	3.67
D	Fmoc-Asp(OtBu)-OH	411.5	0.108 g	DMF	3.72
X	Fmoc-Ahx-OH	353.4	0.092 g	DMF	3.74
	HBTU	379.3	0.983 g	DMF	38.81
	DIPEA	129.3	0.89 mL	NMP	18.11
	Piperidine	85.15	16.8 mL	DMF	25.2

The last step included a fluorenylmethyloxycarbonyl protecting group (Fmoc)-deprotection step, which rendered the amine reactive for further conjugation reactions.

On resin FITC-conjugation

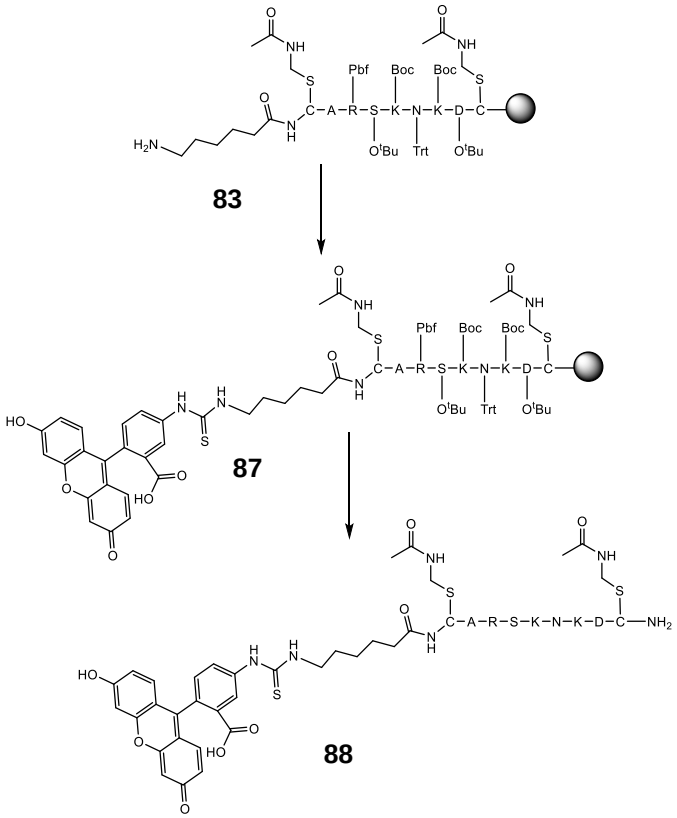

H-Ahx-Cys(Acm)-Ala-Arg(Pbf)-Ser(O^{t}Bu)-Lys(Boc)-Asn(Trt)-Lys(Boc)-Asp(O^{t}Bu)-Cys(Acm) – PAL Novasyn resin **88** (0.0044 mmol) was allowed to swell in DCM for 1.5 hours before washing with DMF (3 × 3 mL) and purging the vessel with Argon. A solution of FITC **75** (6.9 mg, 0.0176 mmol) in anhydrous DMF (1 mL) was added followed by DIPEA (1.23 µL, 0.0070 mmol). The solution was covered in foil and shaken for 3 hours. The reaction was monitored by Kaiser test which returned positive. The resin was washed with DMF (3 × 6 mL), DCM (3 × 6 mL), 50% DCM/MeOH (3 × 6 mL) and dried in a vacuum desiccator overnight. Peptide **89** was removed from the resin using the standard procedure and isolated by preparative HPLC to yield 15.7 mg, 43% yield, 71% column recovery, HPLC retention time = 10.2 minutes; Rf value = 0.4 (acetonitrile/aqueous HCl)

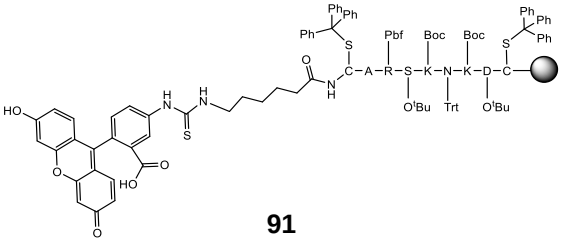

H-Ahx-Cys(Trt)-Ala-Arg(Pbf)-Ser(O^{t}Bu)-Lys(Boc)-Asn(Trt)-Lys(Boc)-Asp(O^{t}Bu)-Cys(Trt) – PAL Novasyn resin **91** (0.022 mmol) was swollen in DMF (2 mL) for 45 minutes. The syringe vessel was purged with argon and the solvent replaced with a solution of fluorescein

isothiocyanate **75** (34.7 mg, 0.089 mmol) in anhydrous DMF (2 mL). DIPEA (6.3 µL, 0.036 mmol) was added and the reaction covered in foil and shaken for 3 hours. The reaction was tracked using the Kaiser test which produced a positive result. The resin was washed and dried using the standard method and carried forward to the next reaction.

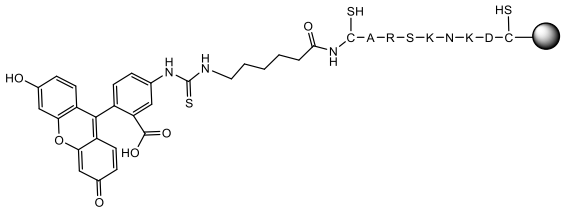

FITC-CAR resin **92** was cleaved in a cocktail of TFA (1.88 mL), H_2O (50 µL), 1,2-ethanedithiol (50µL) and TIS 95 (50 µL) which removed side chain protecting groups. The precipitated peptide was dissolved in deionised water before lyophilisation. Peptide yield was 28.9 mg, (86%); HPLC was conducted using the method described on page 342. The uncyclised peak was observed after 14.2 minutes but the cyclised product was also observed at 10.05 minutes so the peptide was taken forward for cysteine cyclisation without further analysis.

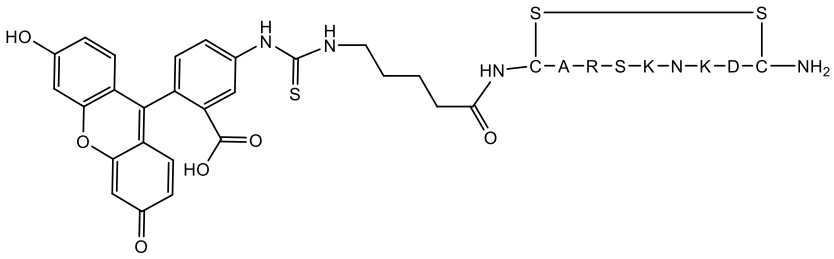

Table 7-6. Unsuccessful cyclisation conditions used to form the disulfide bond between cysteine thiols. DIPEA = diisopropylethylamine; DMF = dimethylformamide. **72**

Compound	Scale (mmol)	Reaction medium	Cyclisation conditions	Outcome
88	0.022	On-resin in DMF	Iodine (0.219 mmol), DIPEA (2 eq.)	Analysed by HPLC (40:60 MeCN/H_2O, isocratic) to show many peaks. LCMS (standard method) identified the expected ion 520.8 m/z
88	0.0044	On-resin in DMF	Thallium trifluoroacetate (0.0066 mmol)	Analysed by HPLC (standard procedure) to show two prominent peaks amoung many impurities.
92	0.0022	On-resin in DMF	Iodine (0.038 mmol)	Analysed by HPLC (standard method) to show multiple peaks.
92	0.0022	On-resin in DMF	Iodine (0.017 mmol) DIPEA (0.017 mmol)	Analysed by HPLC (standard method) to show multiple peaks.

In solution cyclisation

FITC-Ahx-Cys(SH)-Ala-Arg-Ser-Lys-Asn-Lys-Asp-Cys(SH)-NH_2 **94** (16.2 mg, 0.022 mmol) was dissolved in a deaerated aqueous solution of ammonium bicarbonate (0.1M, 32.4 mL). The solution was wrapped in foil and stirred at RT for 1 hour. The reaction was tracked by HPLC using the general method described on page 342 and the reaction stopped by removal of solvent and salt *in vacuo*. The elutogram showed a single resonance after 10.05 minutes. Preparative HPLC of the peptide afforded a 6% yield (2.1 mg). Theoretical mass = 1523.6 g/mol; $[M+2H]^+$ = 763.3 m/z;

Tryptase substrate prodrug

ACC-different couplings

Table 7-7. Unsuccessful reaction conditions to attempt to load Fmoc-ACA-OH onto resin. DIPC = diisopropylcarbodiimide; HOBt = hydroxybenzotriazole hydrate; DCM = dichloromethane; DMF = dimethylformamide; HBTU = N,N,N′,N′-Tetramethyl-O-(1H-benzotriazol-1-yl)uronium hexafluorophosphate; DIPEA = diisoproylethylamine.

Compound	Scale	Resin	Reaction conditions	Outcome
103	0.0168 mmol	Rink amide AM (0.0084 mmol)	DIPC (0.0168 mmol), HOBt (0.0168 mmol) in DCM/DMF (7:3; 1 mL). 18 hours total.[533]	Kaiser test remained intense blue indicating no coupling.
103	0.700 mmol	Rink amide AM (0.35 mmol)	HBTU (0.7 mmol) and DIPEA (1.4 mmol) in DMF (1.3 mL). 30 hours total. [539]	Kaiser test remained intense blue indicating no coupling.
103	0.071 mmol	**104** (0.035 mmol)	HBTU (0.069 mmol, DIPEA (0.144 mmol), in DMF (1 mL). 72 hours total.	Kaiser test remained intense blue indicating no coupling.

FITC-Lys couplings

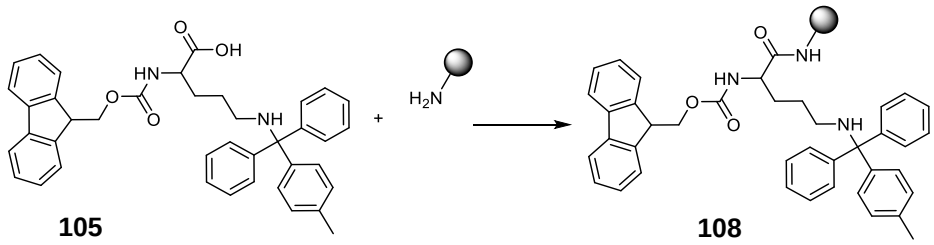

105 **108**

Rink amide AM resin (401.0 mg, 0.281 mmol) was swollen and deprotected using standard procedures. Fmoc-Lys(mtt)-OH **106** (437.4 mg, 0.700 mmol), HBTU (265.4 mg, 0.700 mmol) and DIPEA (243.8 mg, 1.400 mmol) were dissolved in DMF (2.5 mL) and added to the resin. After 1 hour, the reagents were refreshed, including HOBt **29** (107.2 mg, 0.700 mmol). After a further 3 hours, the Kaiser test was performed revealing a faint purple solution indicating successful reaction coupling, affording resin-bound lysine **109.**

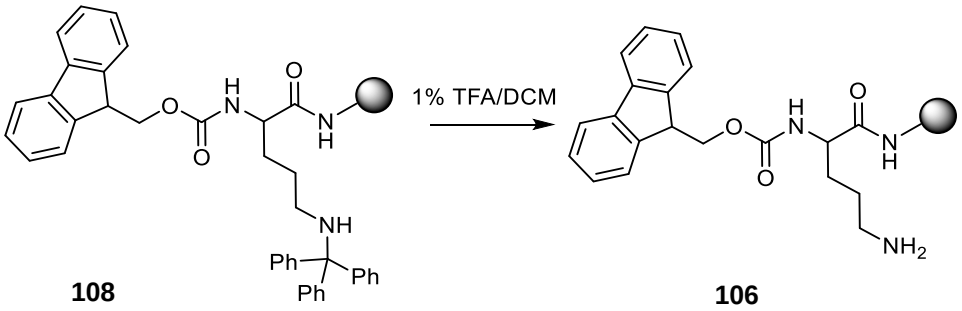

Fmoc-Lys(mtt)-Rink amide AM resin **109** (0.281 mmol) was swollen in DCM (3 mL) in an argon environment for 40 minutes. The solution was removed, and system purged by an argon balloon. A solution (5 mL) of TFA (0.7 mL), DCM (49 mL) and TIS 95 (2.5 mL) was added to the resin and stirred for 2 minutes before removing the solution by positive pressure of argon. This reaction was repeated 10 more times until no yellow colouration was created upon addition. Resin-bound lysine amine **107** was rinsed with DCM and dried in a desiccator overnight.

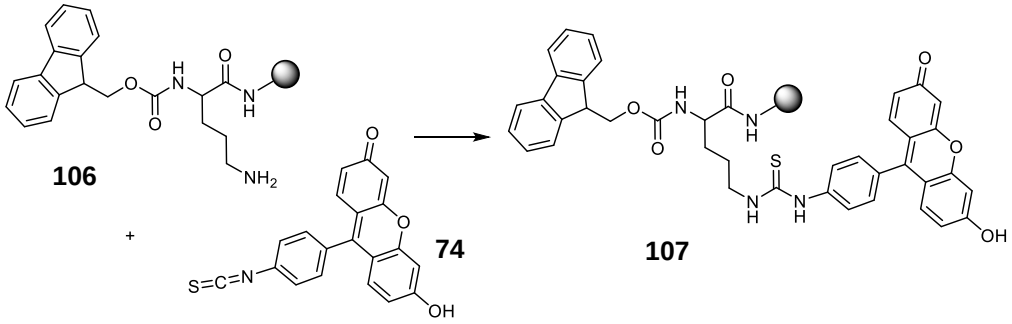

Fmoc-Lys-Rink amide AM resin **107** (0.281 mmol) was swollen using the standard procedure. The system was purged with argon and a solution of FITC **75** (436.8 mg, 1.122 mmol) and DIPEA (78 µL, 0.448 mmol) in anhydrous DMF (8 mL) was added. The solution was wrapped in foil and left shaking for 4 hours. No colour produced with the Kaiser test indicated coupling was complete. FITC conjugate **108** was rinsed with DMF, DCM and 50% DCM/MeOH before drying under vacuum overnight.

The following Lys(FITC)-terminated peptide substrates were synthesised in parallel by automated peptide synthesis. Fmoc-Lys(FITC)-bound Rink amide AM resin 108 was used to grow the peptides by using the reagents described in the table below. Each reaction vessel contained 0.056 mmol, by theoretical calculation (0.280 mmol of total Lys(FITC)-Resin split between 5 reaction vessels). Couplings were carried in duplicate and Fmoc groups were removed with 40% piperidine/DMF.

Ac-Orn-Phe-Arg-Lys(FITC)-Resin

Z-Gly-Pro-Arg-Lys(FITC)-Resin

Ac-Lys-Pro-Arg-Lys(FITC)-Resin

H-Ala-Ala-Pro-Ile-Arg-Asn-Lys-Lys(FITC)-Resin

Suc-Phe-Pro-Phe-Lys(FITC)-Resin

Table 7-8. Quantities of each amino acid and coupling reagents required for the automated sysnthesis of tryptase substrates on resin using an automated spolid phase peptide synthesiser. Mol. Wt – molecular weight. DMF = dimethylformamide; NMP = N-methyl pyrrolidinone; DIPEA – diisopropylethylamine.

Amino acid code	Compound	Mol wt (g/mol)	Amount	Solvent	Total vol of solvent (mL)
A	Fmoc-Ala-OH	311.3	0.212 g	DMF	3.75
F	Fmoc-Phe-OH	387.4	0.380 g	DMF	5.31
I	Fmoc-Ile-OH	353.4	0.136	DMF	2.10
K	Fmoc-Lys(Boc)-OH	468.2	0.320	DMF	3.64
N	Fmoc-Asn(Trt)-OH	597.8	0.230	DMF	2.04
P	Fmoc-Pro-OH	337.4	0.419	DMF	6.79
R	Fmoc-Arg(Pbf)-OH	648.8	0.806	DMF	6.50
Orn	Fmoc-Orn(Boc)-OH	454.5	0.175	DMF	2.08
G	Z-Gly-OH	209.2	0.081	DMF	2.14
	HBTU	379.3	2.378	DMF	35.72
	DIPEA	129.3	2.13 mL	NMP	15.77
	Piperidine	85.15	19.60	DMF	29.40

The programmed sequence finished with a deprotection reaction rendering the terminal amines free. Peptides H-Ala-Ala-Pro-Ile-Arg-Asn-Lys-Lys(FITC)-Resin and Z-Gly-Pro-Arg-Lys(FITC)-Resin were rinsed, dried, cleaved and isolated using standard procedures, yielding 75.1 mg and 50.9 mg, of modified peptide, respectively. The remaining peptides were left in their DMF swollen states for subsequent amine capping.

A solution of acetic anhydride **150** (211.2 µL, 1.12 mmol) and DIPEA (390.2 µL, 2.24 mmol) in DMF (6 mL) was stirred together and split in two. The first portion was added to H-Orn-Phe-Arg-Lys(FITC)-Resin and left to stir for 30 minutes and the reaction repeated. The Kaiser test returned negative, so the resin was rinsed, dried, cleaved and isolated using standard conditions, yielding 56.9 mg of isolated peptide. The second portion of acetic anhydride solution was added to H-Lys-Pro-Arg-Lys(FITC)-Resin and left to reaction for 30 minutes before repeating the reaction. The peptide was isolated using standard drying and resin removal procedures to yield 54.2 mg.

A solution of succinic anhydride (57.3 mg, 0.573 mmol), HOBt **29** (85.9 mg, 0.560 mmol) and DIPEA (97.5 µL, 0.560 mmol) in DMF (3 mL) was added to H-Phe-Pro-Phe-Lys(FITC)-Resin and left to react for 3 minutes. The reaction was repeated without addition of HOBt. The reaction was rinsed, dried, cleaved and isolated using standard procedure to yield 61.7mg of glassy residue.

109) Ac-Orn-Phe-Arg-Lys(FITC)-OH

110) Z-Gly-Pro-Arg-Lys(FITC)-OH

111) Ac-Lys-Pro-Arg-Lys(FITC)-OH

112) H-Ala-Ala-Pro-Ile-Arg-Asn-Lys-Lys(FITC)-OH

113) Suc-Phe-Pro-Phe-Lys(FITC)-OH

Off-resin reductive amination

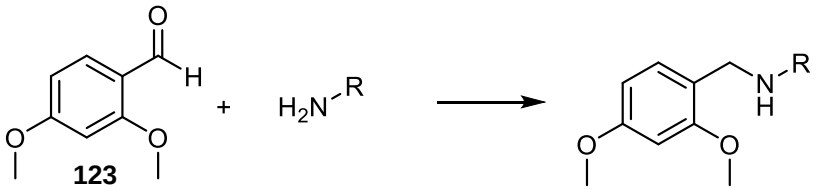

Reductive amination reactions were attempted between 2,4-dimethoxybenzaldehyde **124** (DMB) and amine derivatives in solution with a variety of reducing agents (**Table 7-9**). Typically, the aldehyde and amine were stirred together, in the presence of base (or additive if used), for between 5 minutes – 3 hours before adding the reducing agent.

Table 7-9. Conditions used for reductive aminations. DMB = 2,4-dimethoxybenzaldehyde; PMHS = polymethylhydrosiloxane; *p*ABA = *para*-aminobenzyl alcohol; STAB – sodium triacetoxyborohydride MeOH = methanol, NEt_3 = triethylamine; EtOH = ethanol; THF = tetrahydrofuran; DCM = dichloromethane. **Bold** indicates successful reaction conditions.

Aldehyde derivative	Amine derivative	Reducing agent	Additives	Solvent	Reaction time	Ref
DMB (**124**) 70.3 mg 0.423 mmol	*p*ABA (**97**) 50.1 mg 0.407 mmol	Methyl pyridine borane (**127**) 52.2 mg 0.487 mmol	-	MeOH 2 mL	20 mins	[520]
DMB (**124**) 50.2 mg 0.301 mmol	*p*ABA (**97**) 37.1 mg 0.301 mmol	$NaBH_4$ (**131**) 11.9 mg 0.315 mmol	Dowex 172 mg 0.301 mmol	THF 1 mL	15 mins	[522]
DMB (**124**) 50.2 mg 0.301 mmol	*p*ABA (**97**) 37.6 mg 0.305 mmol	$NaBH_4$ (**131**) 12.2 mg 0.322 mmol	Dowex 172 mg 0.301 mmol	THF 1 mL	1 hour	[522]
DMB (**124**) 50.0 mg 0.300 mmol	**Phe-OEt (137)** 69.5 mg 0.303 mmol	**STAB (132)** 89.3 mg 0.421 mmol	**NEt_3** 50.3 µL 0.361 mmol	DCM 1.5 mL	20 minutes	[521]
DMB (**124**) 150.9 mg, 0.908 mmol	**β-Ala-OEt (135)** 138.4 mg, 0.901 mmol	**STAB (**132**)** 381.3 mg, 1.799 mmol	**NEt_3** 150 µL 1.805 mmol	DCM 3 mL	16 hours	[521]
DMB (**124**) 149.5 mg 0.900 mmol	β-Ala-OEt (**135**) 147.1 mg 0.958 mmol	STAB (**132**) 307.0 mg 1.448 mmol	-	MeOH 9 mL	4 hours	[521]
DMB (**124**) 151.7 mg, 0.913 mmol	**β-Ala-OEt** (**135**) 147.1 mg, 0.958 mmol	**STAB (132)** 307.2 mg, 1.449 mmol	**NEt_3** 133 µL 0.957 mmol	MeOH 9 mL	16 hours	[521]

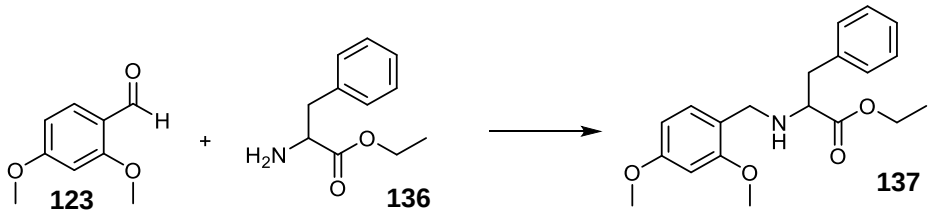

2,4-dimethoxybenzaldehyde **124** (DMB, 50.0 mg, 0.300 mmol), phenylalanine ethyl ester **137** (69.5 mg, 0.303 mmol) and NEt_3 (50.3 µL, 0.361 mmol) were dissolved in DCM (1.5 mL) and stirred for 2 hours. Heat activated 3Å molecular sieves were added and the solution stirred for a further 3 hours before sodium triacetoxyborohydride **132** (STAB, 89.3 mg, 0.421 mmol) was added. After 16 hours additional STAB (93.0 mg, 0.439 mg) was added and the reaction deemed complete after 4 hours by TLC (silica, 30 % ethyl acetate/hexane, UV and ninhydrin visualisation). Molecular sieves were removed by filtration and the filtrate solvent removed *in vacuo*. $NaHCO_3$ (1M, 3 mL) was added to the residue and extracted with ethyl acetate (3 × 3 mL). The combined organic layer was washed with brine, dried over Na_2SO_4 and the solvent removed *in vacuo* to yield product 138 (40.7 mg, 39% yield).

^{1}H NMR (500 MHz, $CDCl_3$) δ_H 7.18 (2 H, d, *J* 7.8), 7.08 (2 H, d, *J* 7.0), 6.96 (1 H, d, *J* 7.9), 6.30 (2 H, dd, *J* 11.3, 2.3), 3.99 (2 H, q, *J* 7.1), 3.71 (3 H, s), 3.66 (1 H, d, *J* 13.3), 3.57 (3 H, s), 3.54 (1 H, d, *J* 13.3), 3.41 (1 H, t, *J* 7.2), 2.87 (2 H, t, *J* 7.3), 1.08 (3 H, t, *J* 7.1). Insufficient sample for ^{13}C NMR analysis.

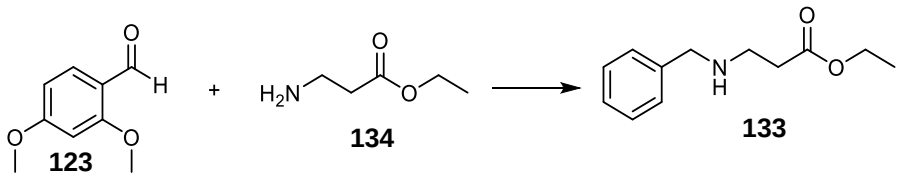

DMB **124** (151.7 mg, 0.913 mmol), β-Ala-OEt **135** (147.1 mg, 0.958 mmol) and NEt_3 (133 µL, 0.957 mmol) were dissolved in MeOH (9 mL) in the presence of activated 3Å molecular sieves. The solution was stirred for 2.5 hours before adding STAB **132** (307.2 mg, 1.449 mmol) and further stirred for 16 hours. The reaction was monitored by TLC (silica, 50% MeOH/ethyl acetate, UV and ninhydrin visualisation). The solvent was removed *in vacuo*, and the residue dissolved in EA (10 mL) and 0.1M NaOH (10 mL). Product was extracted a further 2 times. Organic layers were combined and washed with brine, dried over Na_2SO_4 and concentrated *in vacuo*. Secondary amine (**134**) was afforded (113.3 mg, 47% yield).

^{1}H NMR (500 MHz, $CDCl_3$) δ_H 7.04 (1 H, d, *J* 8.1), 6.37 (1 H, d, *J* 2.2), 6.34 (1 H, dd, *J* 8.1, 2.3), 4.04 (2 H, q, *J* 7.1), 3.72 (3 H, s), 3.71 (3 H, s), 3.64 (2 H, s), 2.77 (2 H, t, *J* 6.7), 2.43 (2 H, t, *J* 6.6), 1.16 (3 H, t, *J* 7.1). Insufficient sample for ^{13}C NMR analysis.

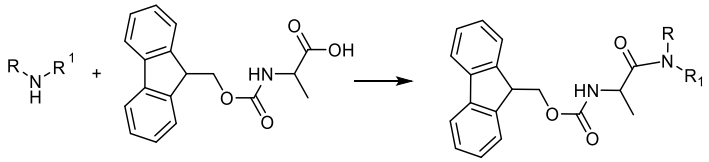

137 **145**

Table 7-10. Unsuccessful reaction conditions used for the amidation between an Fmoc-Ala-OH and a secondary amine. DMF = dimethylformamide; DCM = dichloromethane; THF = tetrahydrofuran; HBTU =N,N,N′,N′-Tetramethyl-O-(1H-benzotriazol-1-yl)uronium hexafluorophosphate ; DIPEA = diisoproylethylamine; HOBt = 1-Hydroxybenzotriazole hydrate; DCC = dicyclohexylcarbodiimide; DMAP = dimethylaminopyridine; NMM = N-methylmorpholine; TLC = thin layer chromatography.

Secondary amine	Scale	Solvent	Coupling conditions	Outcome
138	0.119 mmol	DMF (1.2 mL)	HBTU (0.142 mmol), DIPEA (0.284 mmol), HOBt (0.074 mmol). 72 hours total.	No change in TLC. Only starting materials observed.
134	0.424 mmol	DCM (5 mL)	DCC (0.638 mmol), DMAP (0.044 mmol), 0 °C. 16 hours total	No change in TLC. Only starting materials observed.
138	0.262 mmol	THF (1 mL)	Fmoc-Ala-OH (0.218 mmol), and NMM (0.194 mmol) at -10°C before **138** added. Refluxed for 16 hours.	TLC indicated new product spot but when worked up appeared to be Fmoc-cleaved Ala-OH.

On resin reductive amination

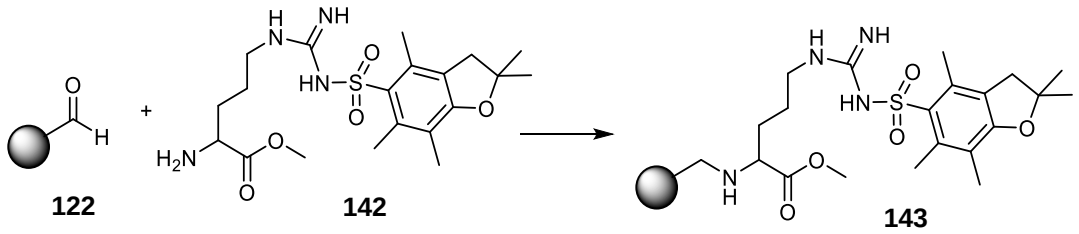

122 **142** **143**

Typically, FMPB AM resin **123** was swollen in solvent for 1.5 hours before addition of H-Arg(Pbf)-OMe.HCl **143** (10 equivalents) and base (10 equivalents) if used. The reaction was pre-reacted before addition of the reducing agent. Reaction was monitored by colorimetric p-anisaldehyde test and acetaldehyde test.

Table 7-11. Conditions employed for reductive amination of FMBP resin **123** by arginine (Pbf) methyl ester **143**. STAB = sodium triacetoxyborohydride **132**; DIPEA = diisopropylethylamine; DCE = dichloroethane; TMOF = trimethyl orthoformate; DMF = dimethylformamide; DCM = dichloromethane.

Reducing agent	Additive	Solvent	Pre-reaction time /mins	Time /hours	Reference
STAB	-	DCE/TMOF (2:1)	240	16	[534]
STAB	DIPEA	TMOF/DMF (2:1)	5	1.5	[534]
STAB	DIPEA	TMOF/DMF (2:1)	240	16	[534]

STAB	-	DMF	240	2	
STAB	DIPEA	DCM	90	3	off-resin method

In an argon environment, FMPB AM resin **123** (53 mg, 0.027 mmol) was swollen in anhydrous DMF for 1 hour. The solvent was removed by argon balloon and replaced with a 1% acetic acid/DMF solution (3 mL) of H-Arg(Pbf)-OMe **143** (130.8 mg, 0.274 mmol). The resin suspension was shaken for 3 hours before the addition of $NaBH_3CN$ **133** (18 mg, 0.280 mmol). The reaction was shaken for 16 hours. *P*-anidaldehyde test produced colourless beads suggesting aldehyde has been consumed. Secondary amide test using acetaldehyde returned beads orange indicating successful reductive amination. Secondary amine **144** was rinsed with DMF (9 mL), 10% DIPEA in DMF (9 mL) and DCM (9 mL).

On resin amidation of secondary amine

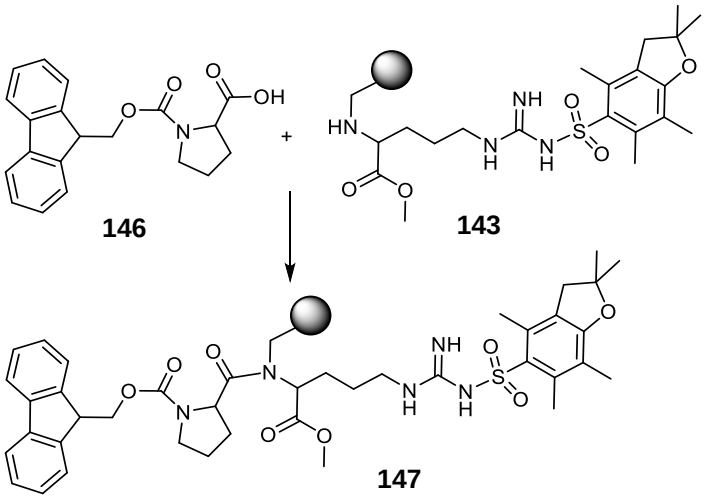

FMPB AM resin-Arg(Pbf)-OMe **144** (0.052 mmol) was swollen in DCM for 1 hour and replaced with a solution of HATU **117** (100 mg, 0.260 mmol), Fmoc-Pro-OH **147** (87.6 mg, 0.260 mmol) and DIPEA (90.6 µL, 0.520 mmol) in a solution of DMF/DCM (1:5, 3.5 mL) and left to react for 16 hours. The reagents were refreshed and left to react for a further 20 hours. The resin **148** was rinsed, dried and cleaved using standard procedures, excluding the precipitation step in diethyl ether and instead, the filtrate was diluted with acetic acid and lyophilised. The sample was analysed by LCMS using the method described on page 317; retention time = 3.56; peak area = 44%; Theoretical mass = 507 g/mol $[M+H]^+$ found: 508 m/z

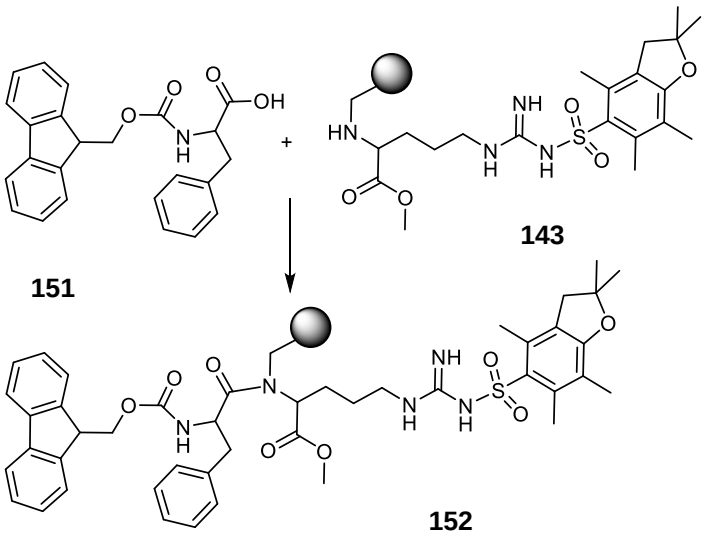

Table 7-12. Unsuccessful coupling of on-resin secondary amine to acid. HATU = 1-[Bis(dimethylamino)methylene]-1H-1,2,3-triazolo[4,5-b]pyridinium 3-oxid hexafluorophosphate; DIPEA = diisopropyl ethylamine; DIPC = Diisopropylcarbodiimide; DCM = dicloromethane; NMP = *N*-methylpyrrolidinone.

Resin	Conditions	Outcome
144 (0.014 mmol)	Fmoc-phe-OH (0.069 mmol), HATU (0.068), DIPEA (0.135 mmol) in DMF (2 mL) for 1 hour and repeated. Total of 72 hours.	Beads remained orange/brown with acetaldehyde test, indicating secondary amine did not undergo coupling.
144 (0.057 mmol)	Fmoc-Phe-OH (0.285 mmol), DIPC (0.285 mmol) and DMAP (0.025 mmol) in DCM (5 mL). Repeated after 2 hours. Total of 5 hours.	Acetaldehyde test returned beads orange indicating unsuccessful coupling
144 (0.057 mmol)	Fmoc-Phe-OH (0.285 mmol), DIPC (0.142 mmol) in DCM/NMP (95:5, 2 mL). 16 hours total. [570]	Acetaldehyde test returned beads positive indicating the secondary amine had not undergone coupling reaction

FMPB AM resin-Arg(Pbf)-OMe **144** (0.0135 mmol) still swollen from previous reaction was rinsed with DCM (3 × 12 mL). A solution of Fmoc-Phe-OH **152** (26.6 mg, 0.069 mmol), DIPC (11 µL, 0.070 mmol) and DMAP **32** (17.1 mg, 0.140 mmol) in DCM (2 mL) was added to the resin. After 2 hours shaking the, acetaldehyde test returned colourless beads. Resin **153** was rinsed, dried and cleaved using standard condition. Dipeptide **154** was extracted in EA from water and analysed by LCMS; Retention time = 3.64; Peak Area = 32%, indicating partial reaction success but not complete. $[M+H]^+$ found: 558 m/z.

Phthalide ring opening for resin-immobilisation

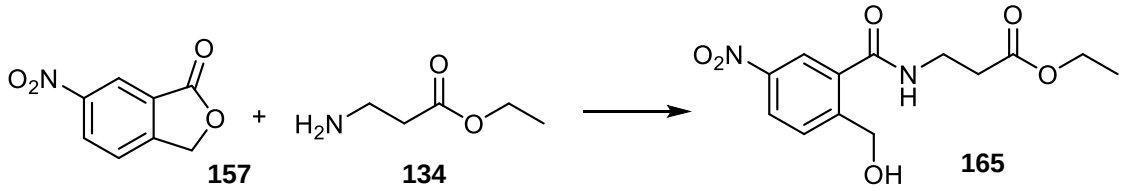

6-Nitrophthalide **158** (1.00 g, 5.581 mmol), β-alanine ethyl ester hydrochloride **135** (1.72 g, 11.182 mmol) and NEt_3 (1.6 mL, 11.165 mmol) were dissolved in ethanol (6 mL) and refluxed at 86 °C. The reaction was tracked by TLC (silica, 40% EA/hex, developed by UV and PMA) and after 3 hours the reaction was deemed complete. Solvent was removed *in vacuo* and the product extracted in DCM (3 × 30 mL) from acidified water (0.01M HCl, 50 mL). Combined organic layers were washed with brine, dried over Na_2SO_4 and concentrated *in vacuo*. Crystallisation was carried out by dissolving in the minimum amount of ethanol, heated with a heat gun, and the maximum amount of water before precipitation. After 16 hours crystals were washed with water, redissolved in methanol and concentrated in vacuo to afford ring opened amide **166** (1.00 g, 60% yield). Method for phthalide ring opening modified from reference:[571]

^{1}H NMR (500 MHz, MeOD) δ_H 8.29 (2 H, d, *J* 8.0), 7.81 (1 H, d, *J* 8.3), 4.80 (2 H, s), 4.19 (2 H, q, *J* 7.1), 3.67 (2 H, t, *J* 6.6), 2.71 (2 H, t, *J* 6.6), 1.29 (3 H, t, *J* 7.2); **^{13}C NMR (126 MHz, MeOD)** δ_C 173.49 (s), 169.62 (s), 148.66 (s), 148.04 (s), 136.94 (s), 130.15 (s), 126.00 (s), 123.65 (s), 62.53 (s), 61.97 (s), 37.10 (s), 34.87 (s), 14.70 (s).

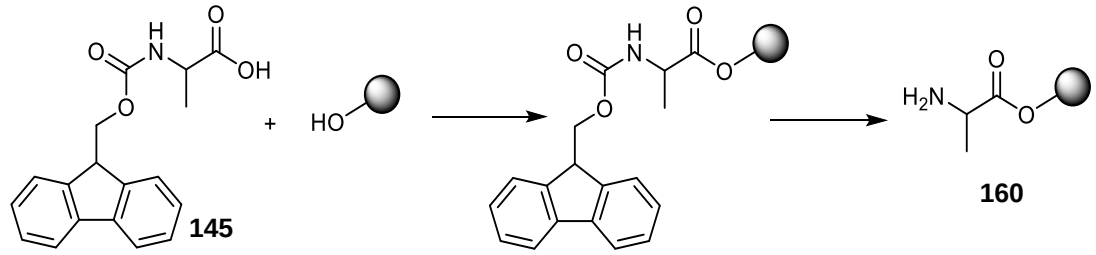

Wang resin (1.00 g, 1.142 mmol) was swollen in DCM for 1.5 hours and rinsed with DMF (4 x 4 mL). A solution of Fmoc-Ala-OH **146** (889.0 mg, 2.855 mmol), HBTU (1.08 g, 2.855 mmol), HOBt **29** (437.1 mg, 2.855 mmol) and DIPEA (994.4 µL, 5.709 mmol) in DMF (8 mL) was added to the resin and shaken for 16 hours. After which, the resin was rinsed with DMF and fresh reagents were added. After 4 hours, a few beads were taken, and Fmoc-deprotected using a standard procedure. The Kaiser test revealed an intense blue solution and beads. The remaining resin **161** was washed with DMF (15 mL), DCM (15 mL) and 50% DCM/MeOH (15 mL) and dried under vacuum.

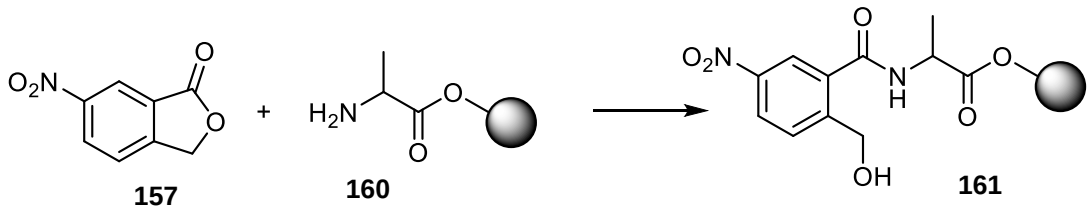

157 **160** **161**

Fmoc-Ala-Wang resin **161** (230.9 mg, 0.175 mmol) was swollen in *N*-Methyl-2- pyrrolidinone (NMP) for 16 hours and rinsed with DMF. The resin was Fmoc-deprotected using standard procedure and once confirmed by Kaiser test was rinsed with NMP. After transferal into a 50 mL RBF, a solution of 6-nitrophthalide **158** (63.0 mg, 0.352 mmol) in NMP (15 mL) was added. The suspension was refluxed at 124 °C without stirring for 7 hours then stirred at RT for 16 hours. After a positive Kaiser test, NEt_3 (12.2 µL, 0.088 mmol) was added and the suspension refluxed for a further 7 hours. After 48 hours of sitting at RT, the suspension refluxed for a further 8 hours at higher temperature, 142 °C. Kaiser test indicated synthesis of **162** successful. Resin washed with DMF (10 mL), DCM (10 mL) and 50% DCM/MeOH (10 mL) and dried in vacuum desiccator.

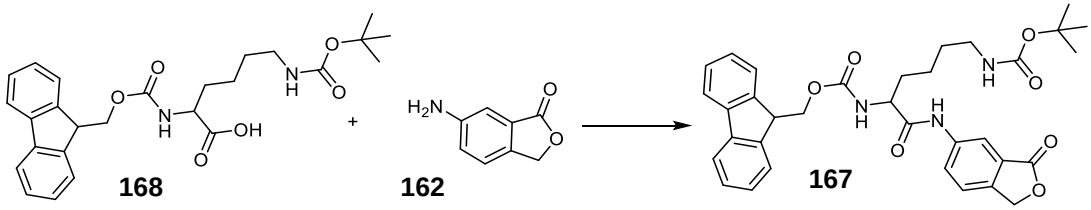

168 **162** **167**

In an argon purged RBF, Fmoc-Lys(Boc)-OH **169** (250.3 mg, 0.534 mmol), HATU 117 (197.3 mg, 0.519 mmol) and DIPEA (163.4 µL, 0.938 mmol) were stirred together in DMF (5 mL). After 40 minutes a catalytic amount of DMAP **32** (3 mg) was added, followed by 6-aminophthalide **163** (70.1 mg, 0.470 mmol) and left to stir at RT for 18 hours. TLC (silica, 100% EA, developed by UV and ninhydrin) was used to track reaction progress which showed consumption of starting materials and presence of a new product. The solution was diluted in acidified water (50 mL) and extracted with EA (3 × 25 mL). Combined organic layers were washed with brine, dried over Na_2SO_4 and concentrated *in vacuo* to afford a cream powder. Purification was carried out by column chromatography (silica, 40 g), and using a solvent gradient EA/hex (10-60%). The column was loaded using dry loading technique, dissolving sample in minimum tetrahydrofuran (THF) adding silica and drying then *in vacuo*. **168** was afforded as a cream powder (163.8 mg, 58% yield).

^{1}H NMR (500 MHz, DMSO) δ_H 10.41 (1 H, s), 8.24 (1 H, s), 7.90 (2 H, d, *J* 7.6), 7.83 (1 H, d, *J* 8.3), 7.74 (3 H, dd, *J* 13.1, 7.2), 7.62 (1 H, d, *J* 8.3), 7.42 (2 H, t, *J* 7.5), 7.33 (2 H, t, *J* 9.1), 6.79 (1 H, t, *J* 5.7), 5.37 (2 H, s), 4.29 (2 H, d, *J* 6.9), 4.24 (1 H, d, *J* 6.7), 4.13 (1 H, dd, *J* 14.5, 8.6), 2.96 – 2.83 (2 H, m), 1.67 (2 H, d, *J* 32.7), 1.39 (3 H, s), 1.35 (11 H, s), 1.28 (2 H, d, *J* 19.9). **^{13}C NMR (126 MHz, DMSO)** δ_C 171.70 (s), 170.57 (s), 156.12 (s), 155.54 (s), 143.79 (d, J 8.0), 141.80 (s), 140.69 (s), 139.61 – 139.50 (m), 127.61 (s), 127.03 (s), 125.36 (d, J

16.9), 123.34 (s), 120.09 (d, J 2.3), 114.17 (s), 77.30 (s), 69.77 (s), 65.63 (s), 55.48 (s), 46.62 (s), 31.34 (s), 29.20 (s), 28.22 (s), 22.95 (s).

Table 7-13. Unsuccessful reaction conditions for the opening of amide-phthalide **168**. NEt_3 = triethylamine; DCM = dichloromethane; *N*-methylpyrrolidinone; RT = room temperature; $AlCl_3$ = aluminium trichloride; DCE = dichloroethane; TLC = thin layer chromatography.

Nucleophile	Scale	Conditions	Outcome
NH_2-Ala-Wang resin **161**	0.116 mmol	Lysine-phthalide (0.232 mmol), NEt_3 (0.127 mmol) in DCM at 40 °C for 16 hours	Kaiser test produced intense blue colour indicting unsuccessful coupling.
NH_2-Ala-Wang resin **161**	0.038 mmol	Lysine phthalide (0.057 mmol) in NMP (1 mL), refluxed at 123 °C, for 6 hours then left at RT for 16 hours. (heating repeated for 2 days.	Kaiser test turned intense blue indicating no coupling.
Tyramine **171**	0.083 mmol	$AlCl_3$ (0.108 mmol) in DCE at 0°C added, followed by lysine-phthalide (0.033 mmol) in DMF (2.5 mL). 18 hours.[572]	TLC showed no change in R_f values
Lithium hydroxide	0.043 mmol	Mixed with lysine phthalide (0.025 mmol) in THF/water/methanol (4:1:1, 4 mL). Left at RT for 6 hours and refluxed at 60°C for 2 hours.	Solution turned from clear to yellow but only starting materials observed by TLC.

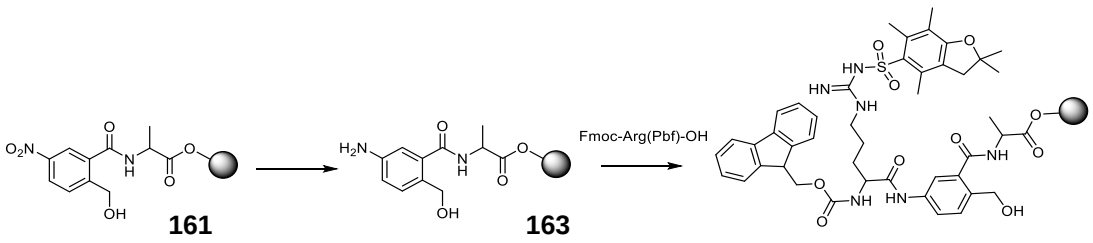

161 **163**

Resin-bound nitrobenzyl alcohol **162** (50.0 mg, 0.046 mmol) was swollen in DCM, rinsed and suspended in fresh DCM (3600 µL). A solution of 0.5 M $Na_2O_4S_2$ (87.1 mg) and K_2CO_3 (69.1 mg) in water (1 mL) was made and 400 µL added to the resin. Tetrabutylammonium iodide (<1 mg) was added and the suspension shaken for 16 hours. After which, the resin was rinsed with DCM then DMF. A solution of Fmoc-Arg(Pbf)-OH (149.4 mg, 0.230 mmol), HATU **117** (87.5 mg, 0.230 mmol) and DIPEA (80.1 µL, 0.460 mmol) in DMF (3 mL) was added to the resin. After 18 hours, reagents were refreshed and left for a further 3 hours. A sample was taken and Fmoc-deprotected using standard procedure. The Kaiser test revealed an intense blue colour to the solution and beads. A repeat of the reaction in the presence of the acetylated benzyl alcohol did not produce the result, suggesting the original Kaiser result described here was a false positive. The resin was rinsed and dried in a vacuum desiccator. On-resin reduction was conducted following a previously reported method, exchanging the phase

transfer catalyst:[538] The conjugation of the aniline formed was conducted following a previous method reported for aniline amidation.[514]

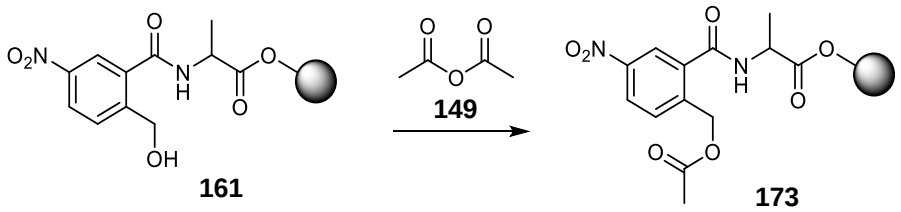

Resin-bound nitrobenzyl alcohol **162** was swollen in DCM for 16 hours and rinsed with DMF. Acetic anhdrydride **150** (14.5 µL, 0.152 mmol) in DMF (1.5 mL) was added to the resin followed by pyridine (12 µL, 0.151 mmol). The solution was left for 30 minutes and rinsed with DMF then DCM, before carrying on to the reduction step.

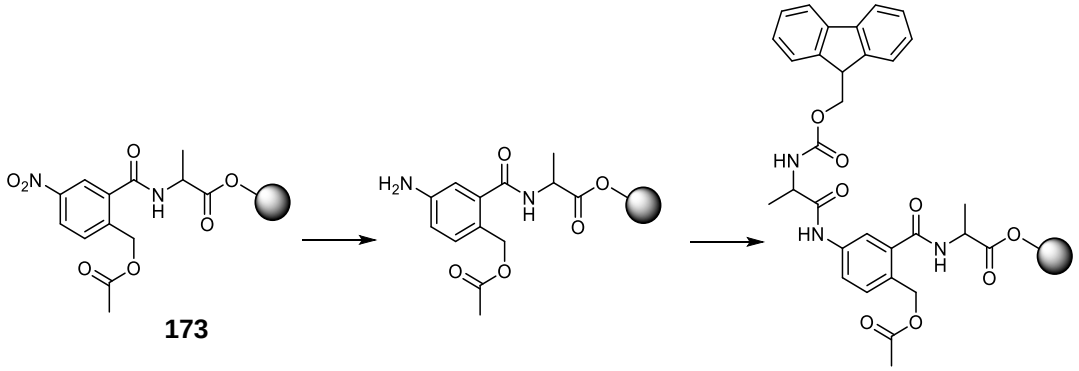

Sodium dithionite and potassium carbonate solution, made at a previous step (200 µL) was added to acetylated nitro resin **174** in DCM (1800 µL) followed by a catalytic amount of tetrabutylammonium iodide (<1 mg). The biphasic solution was shaken for 16 hours and reagents refreshed, shaken for a further 18 hours and rinsed with DMF. A solution of Fmoc-Ala-OH **146** (9.6 mg, 0.031 mmol), HATU **117** (11.8 mg, 0.031 mmol) and DIPEA (10.8 µL, 0.062 mmol) in DMF (2 mL) was added and the suspension shaken for 18 hours. Reagents were refreshed and left for a further 20 hours. A sample was taken, rinsed and Fmoc-deprotected using a standard procedure. The Kaiser test revealed a pale purple colour of the beads and solution.

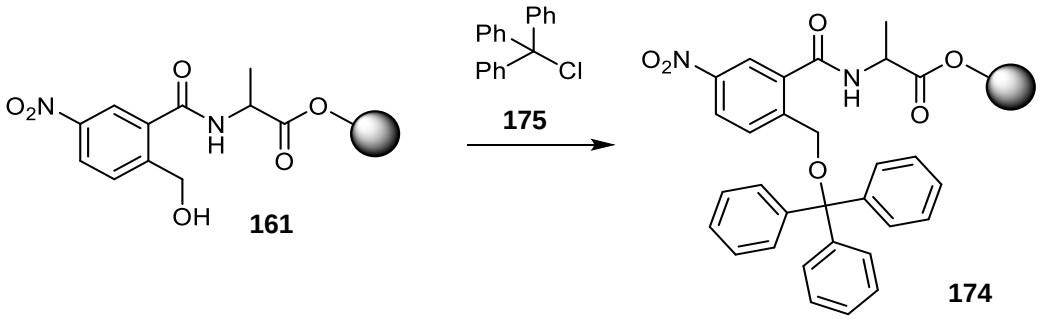

Resin-bound nitrobenzyl alcohol **162** (50.0 mg, 0.046 mmol) was swollen in DCM and rinsed before suspended in anhydrous DCM (2 mL) in an argon environment. A solution of trityl chloride **176** (64.3 mg, 0.231 mmol), triethylamine (51.3 µL, 0.368 mmol) and a catalytic

amount of DMAP **32** (<1 mg) in anhydrous DCM (1 mL) was added. The suspension was shaken for 18 hours. A sample of beads were treated and assessed by the TosCl-PNBP test, but the orange colour of the beads made the presence of a purple colour to the bead difficult to judge. Instead, a sample of resin was taken and rinsed with DMF then DCM. Beads were then transferred to a soda tube and a few drops of 1% TFA/DCM solution added. An intense yellow colour was seen immediately indicating the release of trityl groups. Addition of the trityl-scavenging compound, TIS **95** (2-3 drops) removed the yellow. Remaining tritylated resin **177** was rinsed in DMF, DCM and 50% DCM/MeOH and dried in a vacuum desiccator. Tritylation was previously reported.[573,574]

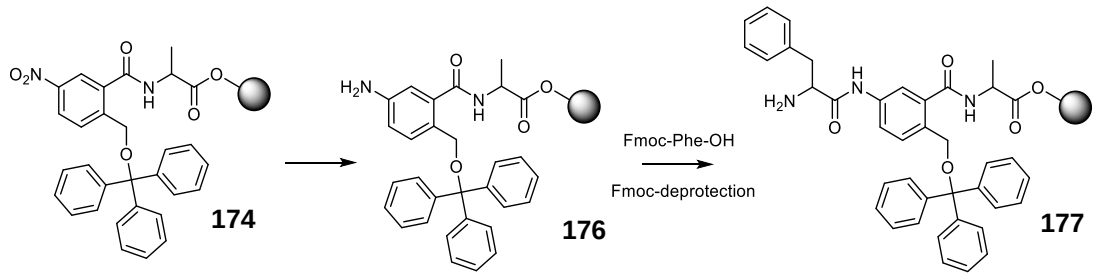

174 **176** **177**

Resin **175** (0.142 mmol) was swollen in DCM and rinsed before addition of fresh DCM (1800 µL), an aqueous solution of 0.5 M potassium carbonate and sodium thiosulfate (200 µL) and tetra-*n*-butyl ammonium iodide (6.3 mg, 0.017 mmol).[538] The reaction mixture was shaken for 3 days before the reaction progression was checked. The Kaiser test was employed but did not show any purple tint. The resin was washed with DCM and DMF. A sample of resin was removed and to it, a solution of Fmoc-Phe-OH **152** (278 mg, 0.716 mmol), HATU **117** (271 mg, 0.713 mmol) and DMAP **32** (170.2 mg, 1.393 mmol) in DMF (1.5 mL) was added. Reagents were refreshed after 3 hours and shaken for a further 3 hours. A sample of resin was taken, deprotected using the standard procedure and analysed by the Kaiser test. The beads returned intense blue. Upon treatment of a second conjugated-resin sample with 1% TFA in DCM a yellow solution was observed The Fmoc-deprotected conjugated resin **178** was then dried for 24 hours under vacuum

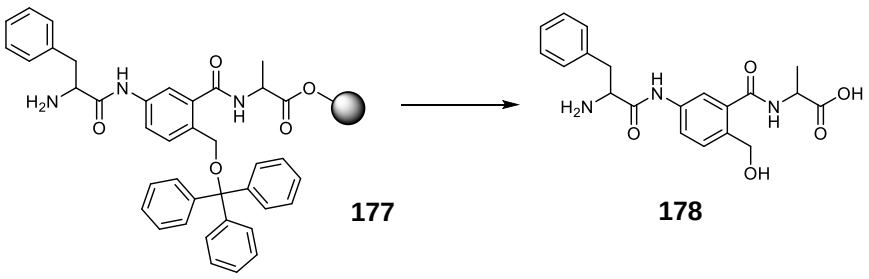

177 **178**

The Fmoc-deprotected Phe-conjugated resin **178** removed by treatment with a solution of hexafluoro-2-propanol (HFIP, 80 µL), TIS **95** (50 µL), dichloromethane (200 µL) and conc. HCl (2 drops) for 1.5 hours.[546] After which, resin filtered off and washed with DCM. Filtrate

collected, and solvent removed by rotary evaporation.**^{1}H NMR (500 MHz, DMSO)** δ_H 13.49 (1 H, s), 8.62 (1 H, d, *J* 2.1), 8.59 (2 H, d, *J* 2.5), 8.57 (2 H, d, *J* 2.5), 8.53 (1 H, d, *J* 1.8), 8.50 (1 H, d, *J* 2.2), 8.44 (1 H, dd, *J* 8.7, 2.5), 8.34 (1 H, dd, *J* 8.4, 2.1), 8.30 (2 H, dd, *J* 8.4, 2.5), 8.02 (1 H, d, *J* 8.6), 7.98 (1 H, d, *J* 8.6), 7.63 (2 H, d, *J* 8.5), 7.45 – 7.34 (1 H, m), 5.58 (1 H, s), 4.95 (2 H, s), 4.71 (1 H, s), 4.10 (1 H, d, *J* 7.1), 3.53 – 3.46 (1 H, m), 3.46 – 3.40 (2 H, m), 3.39 (2 H, s), 2.66 (7 H, s), 1.29 (10 H, dd, *J* 41.7, 21.7).

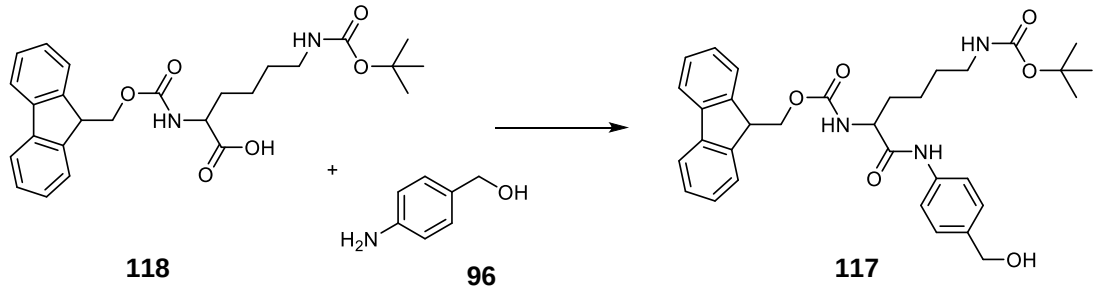

118 **96** **117**

Table 7-14. Unsuccessful reaction conditions employed to attempt to form an amide between the alanine of *p*-amino benzyl alcohol **97** and the acid of Fluorenylmethyloxycarbonyl (Fmoc) and tertiary-butyloxy carbonyl (boc) protected lysine **119.** ECDI = N-(3-Dimethylaminopropyl)-N′-ethylcarbodiimide hydrochloride; HBTU = 3-[Bis(dimethylamino)methyliumyl]-3H-benzotriazol-1-oxide hexafluorophosphate; HOBT.H_2O = hydroxybenzotriazole hydrate; NEt_3 = triethylamine; DMF = dimethylformamide.

Coupling agent	Additive	Solvent	Scale	Reference
EDCI	$HOBt.H_2O$	DMF	74 mg	[575]
EDCI	$HOBt.H_2O$	DMF	100 mg	[575]
HBTU	NEt_3	DMF	209 mg	[576]

In a RBF (5 mL), purged with argon, Fmoc-Lysine(Boc)-OH **119** (209.4 mg, 0.447 mmol), HATU **117** (169.8 mg, 0.447 mmol) and DIPEA (77.8 µL, 0.447 mmol) were dissolved in anhydrous DMF (1.8 mL). The solution turned pale yellow and a solution of *p*-aminobenzylalcohol **97** (50.4 mg, 0.409 mmol) in DMF (0.7 mL) was added. The reaction was left to stir for 18 hours and the reaction tracked by TLC (silica, 100% ethyl acetate, visualised by UV and ninhydrin). An absence of red-staining from p-aminobenzylalcohol was noted together with the presence of an additional product spot (R_f = 0.51) which stained brown with excessive heating. The reaction mixture was diluted with acidified water (0.1M HCl, 10 mL) and extracted with excess ethyl acetate (3 × 8 mL). Organic layers were combined, washed with brine (10 mL), dried over Na_2SO_4 and the solvent removed *in vacuo* and then under vacuum. A crude yellow powder was afforded (352.2 mg, >100% yield). Fmoc-Lys(Boc)-OH present determined by ^{1}H NMR (10%).

^{1}H NMR (500 MHz, DMSO) δ_H 9.98 (1 H, s), 8.77 (1 H, dd, *J* 4.3, 1.1), 8.54 (1 H, dd, *J* 8.4, 1.2), 7.96 (1 H, s), 7.90 (2 H, d, *J* 7.5), 7.77 – 7.71 (2 H, m), 7.63 (1 H, d, *J* 8.0), 7.57 – 7.49 (2 H, m), 7.43 (2 H, t, *J* 7.3), 7.34 (2 H, dd, *J* 12.7, 6.9), 7.24 (2 H, d, *J* 8.4), 6.80 (1 H, t, *J* 5.4), 5.11 (1 H, t, *J* 5.6), 4.44 (2 H, d, *J* 5.2), 4.32 – 4.26 (2 H, m), 4.26 – 4.19 (1 H, m), 4.16 – 4.07 (1 H, m), 2.96 – 2.85 (4 H, m), 1.74 – 1.56 (2 H, m), 1.37 (12 H, d, *J* 4.4), 1.26 (2 H, dd, *J* 14.2, 7.0).

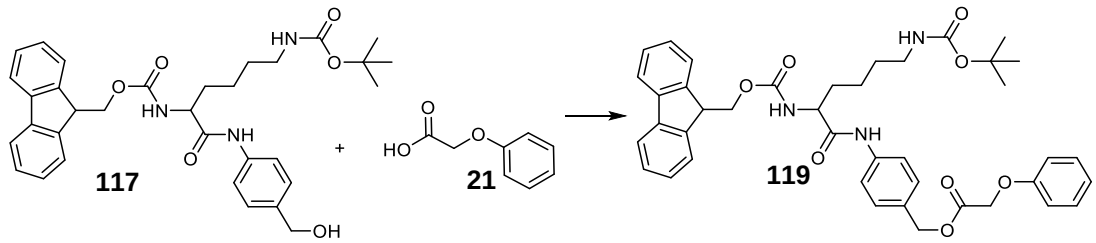

Into an argon purged 5 mL RBF charged with (9H-fluoren-9-yl)methyl tert-butyl (6-((4-(hydroxymethyl)phenyl)amino)-6-oxohexane-1,5-diyl)dicarbamate **118** (50.2 mg, 0.087 mmol), was added a solution of phenoxyacetic acid **22** (12.1 mg, 0.079 mmol), DIPEA (27.6 µL, 0.159 mmol) and HBTU (33.4 mg, 0.088 mmol) in DMF (1 mL). The reaction was left for 5 days and monitored by TLC (silica, 80% ethyl acetate/hexane, visualised by UV and PMA). The solution diluted with HCl acid (0.1M, 8 mL) and extracted with ethyl acetate (3 mL × 6 mL). Organic layers were combined, washed with saturated sodium bicarbonate solution (8 mL) then brine (8 mL), dried over Na_2SO_4 and solvent removed *in vacuo*. Crude product **120** (17.8 mg, 32% yield).

^{1}H NMR (500 MHz, $CDCl_3$) δ_H 8.53 (1 H, s), 7.67 (3 H, d, *J* 7.4), 7.47 (5 H, dd, *J* 17.5, 7.2), 7.30 (3 H, t, *J* 7.3), 7.27 – 7.13 (8 H, m), 6.91 (1 H, t, *J* 7.4), 6.81 (2 H, d, *J* 7.9), 5.63 (1 H, s), 5.10 (2 H, s), 4.62 (1 H, s), 4.57 (2 H, s), 4.34 (2 H, d, *J* 6.3), 4.23 (1 H, s), 4.12 (1 H, t, *J* 6.8), 3.08 (1 H, d, *J* 5.6), 3.05 – 2.95 (2 H, m), 1.89 (1 H, s), 1.65 (1 H, s), 1.45 (2 H, s), 1.36 (15 H, s), 1.20 (3 H, d, *J* 14.5).

HFIP resin cleavage investigation.

Ester-protecting conditions for the cleavage of peptide resin from resin were investigated. Lysine-benzyl-phenoxy ester **120** was used as a test model and was subjected to several resin cleavage methods to ascertain which would retain the ester bond.

Table 7-15. Resin and protecting group cleavage cocktails for testing stability of ester. TFA = trifluoroacetic acid; TIS = triisopropylsilane; DCM = dichloromethane; HCl = hydrochloric acid; HFIP = hexafluoroisopropanol, ^{1}H NMR = proton nuclear magnetic resonance.

Cleavage cocktail	Time	Reference
TFA	2 hours	[544]
TFA/TIS/H_2O (95:2.5:2.5)	2 hours	[544]
1% TFA / DCM	2 hours	[545]
0.1 N HCl / HFIP / DCM (20%)	1.5 hours	[546]

In all cases, a sample of model conjugate **120** (~20 mg, 28 µmol) was dissolved into corresponding cleavage cocktail (1 mL) and left stirring for the time recommended for resin cleavage (**Table 7-15**). At the designated time point, TFA was removed *in vacuo* and the solution redissolved in deuterated chloroform ($CDCl_3$) and analysed by ^{1}H NMR without work up.

7.6.3 Biological testing

Cell Culture

Human umbilical vein endothelial cells (HUVECs) cells were thawed at 37 ^oC and grown from frozen in Endothelial growth medium kit (EGM; Cat. No. C-22110; PromoCell Gmbh; Heidelberg, Germany). The media contained; fetal calf serum (0.02 ml/mL, Endothelial cell growth supplement (4 µL/mL), recombinant human epidermal growth factor (0.1 ng/mL), recombinant human basic fibroblast growth factor (1ng/mL), heparin (90 µg/mL) and hydrocorticone 1µg/mL. Cells were incubated at 37 ^oC in a humidified environment with 5% CO_2 for 24 hours to allow cells to adhere to the flask. Afterwhich, media was replaced every 2-3 days until cells reached 80% confluency.

Binding Assay

Once confluency was reached, cells were split for further subculture. Media was removed by vacuum and cells were washed with 12 mL of warm calcium and magnesium free phosphate

buffered saline solution (PBS; Cat No. 10010-015; Thermo Fisher) and then removed. 5 mL of warm 0.05% trypsin-EDTA (Cat. No. 25300054; Invitrogen) was added to lift adherence cells from the flask bottom by incubating the flask at 37 ˚C and 5% CO_2 for 1-2 mins. Once cells had become detached, growth medium (10 mL) was added to neutralise the trypsin and the cell suspension pipetted into a 50 mL falcon tube and centrifuged at 180 × g (Centrifuge 5804 R; Eppendorf; Hamburg, Germany), 21 ˚C for 5 minutes. The supernatant was removed by vacuum and the cell pellet re-suspended in fresh growth medium (4 mL). Once a homogeneous suspension of cells was obtained, cells counted were counted using an ADAM Automated Cell Counter (Digital Bio; Seoul, Korea), as previously described

Cells were seeded onto 8-well chamber slides at 10,000 cells per slide in 1 mL of media. The cells were grown to 70% confluency in approximately 24 hours. FITC-CAR (1.5 mg, 0.98 µmol) was dissolved in sterile water (0.98 mL) and vortexed to dissolve. FITC-CAR solution (1 mM) was stored at -80 ºC until required. Two solutions were made;

Non-inflammatory control: FITC-CAR (20 µL) in endothelial cell media (1980 µL) to achieve a final concentration of 10 µM

Pro-inflammatory test solution: FITC-CAR (20 µL) in endothelial cell media (1980 µL) with the addition of tumour necrosis factor alpha (TNF- α, 10 µg/mL, 2 µL) with final concentration 10 ng/mL.

When cells were deemed confluent, media was removed and replaced with either of the above solutions (1 mL). Lower dilutions were carried out by 1 in 10 dilutions of original solutions in EC media. All reactions were run in duplicate.

The cells were treated for 24 hours, after which the media was removed, and the cells washed with PBS solution. After drying, cells were treated with 4% paraformaldehyde (PFA, 500 µL, Sigma Aldrich) for 20 minutes and washed with PBS (3x 1mL). The chamber walls were removed to leave the fixed cells on a glass slide. A solution of 4',6-diamidino-2-phenylindole (DAPI) was added to the cells to stain the nuclei and after 3-4 minutes of air drying, a cover slip was placed on the cells and sealed with nail varnish. Cells were stored at -20 °C until analysis Fluorescence was visualised within 48 hours of cell fixing, using a confocal microscope (Leica TCS SPE; Wetzlar, Germany). Following previous studies, excitation and emission wavelengths of 525 nm and 495 nm were used for fluorescein, and 358 nm and 461 nm were used for DAPI.[452]

Bibliography

1. Gaine SP, Rubin LJ. Primary pulmonary hypertension. *Lancet*. 1998;352(9129):719-725. doi:10.1016/S0140-6736(98)02111-4
2. Simonneau G, Gatzoulis MA, Adatia I, et al. Updated clinical classification of pulmonary hypertension. *J Am Coll Cardiol*. 2013;62(25 Suppl):D34-41. doi:10.1016/j.jacc.2013.10.029
3. Farber HW, Loscalzo J. Pulmonary arterial hypertension. *N Engl J Med*. 2004;351(16):1655-1665. doi:10.1056/NEJMra035488
4. Rabinovitch M. Molecular pathogenesis of pulmonary arterial hypertension. *J Clin Invest*. 2008;118(7):2372-2379. doi:10.1172/JCI33452
5. Yang Wang K. The Changing Landscape of Pulmonary Arterial Hypertension in 21st Century. *Acta Cardiol Sin*. 2017;33(5):510-513. doi:10.6515/ACS20170810A
6. Hoeper MM, Gibbs JSR. The changing landscape of pulmonary arterial hypertension and implications for patient care. *Eur Respir Rev*. 2014;23:450-457. doi:10.1183/09059180.00007814
7. Strange G, Gabbay E, Kermeen F, et al. Time from symptoms to definitive diagnosis of idiopathic pulmonary arterial hypertension: The delay study. *Pulm Circ*. 2013;3(1):89-94. doi:10.4103/2045-8932.109919
8. Vachiéry J-L, Yerly P, Huez S. How to detect disease progression in pulmonary arterial hypertension. *Eur Respir Rev*. 2012;21(123):40-47. doi:10.1183/09059180.00009011
9. Galie N, Humbert M, Vachiery JL, et al. 2015 ESC/ERS Guidelines for the diagnosis and treatment of pulmonary hypertension. *Eur Respir J*. 2015;46(4):903-975.
10. Budhiraja R, Tuder RM, Hassoun PM. Endothelial dysfunction in pulmonary hypertension. *Circulation*. 2004;109(2):159-165. doi:10.1161/01.CIR.0000102381.57477.50
11. Paulin R, Courboulin A, Barrier M, Bonnet S. From oncoproteins/tumor suppressors to microRNAs, the newest therapeutic targets for pulmonary arterial hypertension. *J Mol Med*. 2011;89(11):1089-1101. doi:10.1007/s00109-011-0788-5
12. Morrell NW, Adnot S, Archer SL, et al. Cellular and molecular basis of pulmonary arterial hypertension. *J Am Coll Cardiol*. 2009;54(1 Suppl):S20-31. doi:10.1016/j.jacc.2009.04.018
13. Shimoda LA, Laurie SS. Vascular remodeling in pulmonary hypertension. *J Mol Med (Berl)*. 2013;91(3):297-309. doi:10.1007/s00109-013-0998-0
14. Voelkel NF, Gomez-Arroyo J. The Role of Vascular Endothelial Growth Factor in Pulmonary Arterial Hypertension. The Angiogenesis Paradox. *Am J Respir Cell Mol Biol*. 2014;51(4):474-484. doi:10.1165/rcmb.2014-0045TR
15. Tuder RM, Marecki JC, Richter A, Fijalkowska I, Flores S. Pathology of pulmonary hypertension. *Clin Chest Med*. 2007;28(1):23-42, vii. doi:10.1016/j.ccm.2006.11.010
16. Rabinovitch M. Pathobiology of Pulmonary Hypertension. *Annu Rev Pathol Mech Dis*.

2007;2(1):369-399. doi:10.1146/annurev.pathol.2.010506.092033

17. Pietra GG, Edwards WD, Kay JM, et al. Histopathology of primary pulmonary hypertension. A qualitative and quantitative study of pulmonary blood vessels from 58 patients in the National Heart, Lung, and Blood Institute, Primary Pulmonary Hypertension Registry. *Circulation*. 1989;80(5):1198-1206.
18. Eduardo Morales-Blanhir J, Eduardo Carmona-Rubio A, de Jesus Rosas-Romero M, Vergara de Marquez GS, Adolfo Arbo-Oze-de-Morvil G. Pulmonary arterial hypertension, a rare entity. *Rev Investig Clin*. 2014;66(1):65-78.
19. Rabinovitch M. Pathobiology of Pulmonary Hypertension. *Annu Rev Pathol Mech Dis*. 2007;2(1):369-399. doi:10.1146/annurev.pathol.2.010506.092033
20. Vlodavsky I, Ilan N, Naggi A, Casu B. Heparanase: structure, biological functions, and inhibition by heparin-derived mimetics of heparan sulfate. *Curr Pharm Des*. 2007;13(20):2057-2073.
21. Farha S, Asosingh K, Comhair SA, et al. Mast cell number, phenotype, and function in human pulmonary arterial hypertension. *Pulm Circ*. 2012;2(2):220. doi:10.4103/2045-8932.97609
22. Maxová H, Novotná J, Vajner L, et al. In Vitro Hypoxia Increases Production of Matrix Metalloproteinases and Tryptase in Isolated Rat Lung Mast Cells. *Physiol Res*. 2008;57:903-910.
23. Bartelds B, van Loon RLE, Mohaupt S, et al. Mast cell inhibition improves pulmonary vascular remodeling in pulmonary hypertension. *Chest*. 2012;141(3):651-660. doi:10.1378/chest.11-0663
24. Virk H, Arthur G, Bradding P. Mast cells and their activation in lung disease. *Transl Res*. 2016;174:60-76. doi:10.1016/J.TRSL.2016.01.005
25. Breitling S. The mast Cell - B cell axis in lung vascular remodelling and pulmonary hypertension. 2016.
26. Kosanovic D, Dahal BK, Peters DM, et al. Histological Characterization of Mast Cell Chymase in Patients with Pulmonary Hypertension and Chronic Obstructive Pulmonary Disease. *Pulm Circ*. 2014;4(1):128-136. doi:10.1086/675642
27. Hunt LW, Colby T V., Weiler DA, Sur S, Butterfield JH. Immunofluorescent Staining for Mast Cells in Idiopathic Pulmonary Fibrosis: Quantification and Evidence for Extracellular Release of Mast Cell Tryptase. *Mayo Clin Proc*. 1992;67(10):941-948. doi:10.1016/S0025-6196(12)60924-0
28. Andersson CK, Andersson-Sjöland A, Mori M, et al. Activated MCTC mast cells infiltrate diseased lung areas in cystic fibrosis and idiopathic pulmonary fibrosis. *Respir Res*. 2011;12(1):139. doi:10.1186/1465-9921-12-139
29. Clapp LH, Patel J. The mechanistic basis for prostacyclin action in pulmonary hypertension. *Int J Respir Care*. 2010;6(1):27-33.
30. Metz M, Grimbaldeston MA, Nakae S, Piliponsky AM, Tsai M, Galli SJ. Mast cells in the promotion and limitation of chronic inflammation. *Immunol Rev*. 2007;217(1):304-

328. doi:10.1111/j.1600-065X.2007.00520.x

31. Mitani Y, Ueda M, Maruyama K, et al. Mast cell chymase in pulmonary hypertension. *Thorax*. 1999;54(1):88-90. doi:10.1136/THX.54.1.88
32. Hamada H, Terai M, Kimura H, Hirano K, Oana S, Niimi H. Increased Expression of Mast Cell Chymase in the Lungs of Patients with Congenital Heart Disease Associated with Early Pulmonary Vascular Disease. *Am J Respir Crit Care Med*. 1999;160(4):1303-1308. doi:10.1164/ajrccm.160.4.9810058
33. Heath D, Yacoub M. Lung mast cells in plexogenic pulmonary arteriopathy. *J Clin Pathol*. 1991;44(12):1003-1006.
34. Dahal BK, Kosanovic D, Kaulen C, et al. Involvement of mast cells in monocrotaline-induced pulmonary hypertension in rats. *Respir Res*. 2011;12(1):60. doi:10.1186/1465-9921-12-60
35. Price LC, Wort SJ, Perros F, et al. Inflammation in pulmonary arterial hypertension. *Chest*. 2012;141(1):210-221. doi:10.1378/chest.11-0793
36. Bartelds B, Loon RLE va., Mohaupt S, et al. Mast Cell Inhibition Improves Pulmonary Vascular Remodeling in Pulmonary Hypertension. *Chest*. 2012;141(3):651-660. doi:10.1378/CHEST.11-0663
37. Hoffmann J, Yin J, Kukucka M, et al. Mast cells promote lung vascular remodelling in pulmonary hypertension. *Eur Respir J*. 2011;37(6):1400-1410. doi:10.1183/09031936.00043310
38. Luitel H, Sydykov A, Schymura Y, et al. Pressure overload leads to an increased accumulation and activity of mast cells in the right ventricle. *Physiol Rep*. 2017;5(6):e13146. doi:10.14814/phy2.13146
39. Vajner L, Vytásek R, Lachmanová V, et al. Acute and chronic hypoxia as well as 7-day recovery from chronic hypoxia affects the distribution of pulmonary mast cells and their MMP-13 expression in rats. *Int J Exp Pathol*. 2006;87(5):383-391. doi:10.1111/j.1365-2613.2006.00493.x
40. Miyata M, Sakuma F, Ito M, Ohira H, Sato Y, Kasukawa R. Athymic nude rats develop severe pulmonary hypertension following monocrotaline administration. *Int Arch Allergy Immunol*. 2000;121(3):246-252. doi:24324
41. Banasová A, Maxová H, Hampl V, et al. Prevention of mast cell degranulation by disodium cromoglycate attenuates the development of hypoxic pulmonary hypertension in rats exposed to chronic hypoxia. *Respiration*. 2008;76(1):102-107. doi:10.1159/000121410
42. Hassoun PM, Mouthon L, Barberà JA, et al. Inflammation, Growth Factors, and Pulmonary Vascular Remodeling. *J Am Coll Cardiol*. 2009;54(1):S10-S19. doi:10.1016/J.JACC.2009.04.006
43. Maxová H, Bacáková L, Eckhardt A, et al. Growth of vascular smooth muscle cells on collagen I exposed to RBL-2H3 mastocytoma cells. *Cell Physiol Biochem*. 2010;25(6):615-622. doi:10.1159/000315080

44. Bradding P, Pejler G. The controversial role of mast cells in fibrosis. *Immunol Rev*. 2018;282(1):198-231. doi:10.1111/imr.12626
45. Boucherat O, Vitry G, Trinh I, Paulin R, Provencher S, Bonnet S. The cancer theory of pulmonary arterial hypertension. *Pulm Circ*. 2017;7(2):285-299. doi:10.1177/2045893217701438
46. Hanahan D, Weinberg RA. Hallmarks of cancer: the next generation. *Cell*. 2011;144(5):646-674. doi:10.1016/j.cell.2011.02.013
47. Falcetti E, Hall SM, Phillips PG, et al. Smooth Muscle Proliferation and Role of the Prostacyclin (IP) Receptor in Idiopathic Pulmonary Arterial Hypertension. *Am J Respir Crit Care Med*. 2010;182(9):1161-1170. doi:10.1164/rccm.201001-0011OC
48. Hulter HN, Krapf R. Interrelationships among hypoxia-inducible factor biology and acid-base equilibrium. *Semin Nephrol*. 2006;26(6):454-465. doi:10.1016/j.semnephrol.2006.10.006
49. Paulin R, Michelakis ED. The Metabolic Theory of Pulmonary Arterial Hypertension. *Circ Res*. 2014;115(1):148-164. doi:10.1161/CIRCRESAHA.115.301130
50. Kellum JA, Song M, Li J. Science review: Extracellular acidosis and the immune response: clinical and physiologic implications. *Crit Care*. 2004;8(5):331. doi:10.1186/cc2900
51. Yildiz P. Molecular mechanisms of pulmonary hypertension. *Clin Chim Acta*. 2009;403(1–2):9-16. doi:http://dx.doi.org/10.1016/j.cca.2009.01.018
52. Lang IM, Gaine SP. Recent advances in targeting the prostacyclin pathway in pulmonary arterial hypertension. *Eur Respir Rev*. 2015;24(138):630-641.
53. Chester AH, Yacoub MH. The role of endothelin-1 in pulmonary arterial hypertension. *Glob Cardiol Sci Pract*. 2014;(2) (no pa(29).
54. Giaid A, Yanagisawa M, Langleben D, et al. Expression of Endothelin-1 in the Lungs of Patients with Pulmonary Hypertension. *N Engl J Med*. 1993;328(24):1732-1739. doi:10.1056/NEJM199306173282402
55. Durante W. Role of arginase in vessel wall remodeling. *Front Immunol*. 2013;4:111. doi:10.3389/fimmu.2013.00111
56. Maarsingh H, Pera T, Meurs H. Arginase and pulmonary diseases. *Naunyn Schmiedebergs Arch Pharmacol*. 2008;378(2):171-184. doi:10.1007/s00210-008-0286-7
57. Klinger JR, Kadowitz PJ. The Nitric Oxide Pathway in Pulmonary Vascular Disease. *Am J Cardiol*. 2017;120(8):S71-S79. doi:10.1016/J.AMJCARD.2017.06.012
58. Galie N, Ghofrani HA, Torbicki A, et al. Sildenafil citrate therapy for pulmonary arterial hypertension. *N Engl J Med*. 2005;353(20):2148-2157. doi:10.1056/NEJMoa050010
59. Henrie AM, Nawarskas JJ, Anderson JR. Clinical utility of tadalafil in the treatment of pulmonary arterial hypertension: An evidence-based review. *Core Evid*. 2015;10:99-108.
60. He C-J, Chen S-J, Wang J, Zhu C-Y, Yin Y-H. Efficacy and safety of phosphodiesterase

type-5 inhibitors for pulmonary arterial hypertension: A meta-analysis focusing on 6MWD. *Pulm Pharmacol Ther*. 2015;32:24-28. doi:10.1016/j.pupt.2015.03.002

61. Vane J, Corin R. Prostacyclin: A Vascular Mediator. *Eur J Vasc Endovasc Surg*. 2003;26(6):571-578. doi:10.1016/S1078-5884(03)00385-X
62. Clapp LH, Gurung R. The mechanistic basis of prostacyclin and its stable analogues in pulmonary arterial hypertension: Role of membrane versus nuclear receptors. *Prostaglandins Other Lipid Mediat*. 2015;120:56-71. doi:10.1016/j.prostaglandins.2015.04.007
63. Christman BW, McPherson CD, Newman J, et al. An Imbalance between the Excretion of Thromboxane and Prostacyclin Metabolites in Pulmonary Hypertension. *N Engl J Med*. 1992;327:70-75.
64. Tuder RM, Cool CD, Geraci MW, et al. Prostacyclin Synthase Expression Is Decreased in Lungs from Patients with Severe Pulmonary Hypertension. *Am J Respir Crit Care Med*. 1999;159(6):1925-1932. doi:10.1164/ajrccm.159.6.9804054
65. Tahara N, Kai H, Niiyama H, et al. Repeated Gene Transfer of Naked Prostacyclin Synthase Plasmid into Skeletal Muscles Attenuates Monocrotaline-Induced Pulmonary Hypertension and Prolongs Survival in Rats. *Hum Gene Ther*. 2004;15(12):1270-1278. doi:10.1089/hum.2004.15.1270
66. Rollins K, Laliberte K, Gotzkowsky K, Wade M, Mottola D. Overview of the Drug-Drug Interaction Potential with Treprostinil. In: *American Thoracic Society International Conference Meetings Abstracts*. San Diego; 2009:B55.
67. Safdar Z. Treatment of pulmonary arterial hypertension: the role of prostacyclin and prostaglandin analogs. *Respir Med*. 2011;105(6):818-827. doi:10.1016/j.rmed.2010.12.018
68. GlaxoSmithKline. *Flolan*. Research Triangle Park, NC; 2015.
69. Ryerson CJ, Nayar S, Swiston JR, Sin DD. Pharmacotherapy in pulmonary arterial hypertension: a systematic review and meta-analysis. *Respir Res*. 2010;11(1):12. doi:10.1186/1465-9921-11-12
70. VELETRI (epoprostenol) [package insert]. South San Francisco, CA: Actelion Pharmaceuticals US, Inc. (accessed 29 July 2018).
71. Davis H, Harley C, Proudlove G. *Epoprostenol: Important Information about Change in Formulation of Flolan*.; 2016.
72. Kingman M, Archer-Chicko C, Bartlett M, Beckmann J, Hohsfield R, Lombardi S. Management of prostacyclin side effects in adult patients with pulmonary arterial hypertension. *Pulm Circ*. 2017;7(3):598-608. doi:10.1177/2045893217719250
73. Buckley MS, Feldman JP. *Inhaled Epoprostenol for the Treatment of Pulmonary Arterial Hypertension in Critically Ill Adults*. doi:10.1592/phco.30.7.728
74. Haché M, Denault A, Bélisle S, et al. Inhaled epoprostenol (prostacyclin) and pulmonary hypertension before cardiac surgery. *J Thorac Cardiovasc Surg*. 2003;125(3):642-649. doi:10.1067/MTC.2003.107

75. De Wet CJ, Affleck DG, Jacobsohn E, et al. Inhaled prostacyclin is safe, effective, and affordable in patients with pulmonary hypertension, right heart dysfunction, and refractory hypoxemia after cardiothoracic surgery. *J Thorac Cardiovasc Surg*. 2004;127(4):1058-1067. doi:10.1016/j.jtcvs.2003.11.035

76. Ventola CL. The nanomedicine revolution: part 2: current and future clinical applications. *P T*. 2012;37(10):582-591.

77. Gupta N, Al-Saikhan FI, Patel B, Rashid J, Ahsan F. Fasudil and SOD packaged in peptide-studded-liposomes: Properties, pharmacokinetics and ex-vivo targeting to isolated perfused rat lungs. *Int J Pharm*. 2015;488(1-2):33-43. doi:10.1016/j.ijpharm.2015.04.031

78. Jain P, Leitinger G, Leber R, et al. Liposomal nanoparticles encapsulating iloprost exhibit enhanced vasodilation in pulmonary arteries. *Int J Nanomedicine*. 2014;Volume 9(1):3249. doi:10.2147/IJN.S63190

79. Hershel U, Rau H, Lessman T, et al. Carrier-linked treprostinil prodrugs for treating or preventing pulmonary hypertension. 2013.

80. Leifer F, Omiatek D, Malinin V, et al. Prolonged activity of inhaled treprostinil prodrug nanoparticles in a rat model of pulmonary arterial hypertension. *Eur Respir J*. 2014;44(Suppl_58):P2356-.

81. Wade M, Baker FJ, Roscigno R, et al. Pharmacokinetics of treprostinil sodium administered by 28-day chronic continuous subcutaneous infusion. *J Clin Pharmacol*. 2004;44(5):503-509. doi:10.1177/0091270004264638

82. Research Triangle Park, United Therapeutics, MA U. Remodulin [insert package]. https://www.remodulin.com/downloads/remodulin-prescribinginformation.pdf. Accessed November 1, 2015.

83. Skoro-Sajer N, Lang I, Naeije R. Treprostinil for pulmonary hypertension. *Vasc Health Risk Manag*. 2008;4(3):507-513.

84. Gotzkowsky SK, Dingemanse J, Lai A, Mottola D, Laliberte K. Lack of a pharmacokinetic interaction between oral treprostinil and bosentan in healthy adult volunteers. *J Clin Pharmacol*. 2010;50(7):829-834. doi:10.1177/0091270009351173

85. Whittle BJ, Silverstein AM, Mottola DM, Clapp LH. Binding and activity of the prostacyclin receptor (IP) agonists, treprostinil and iloprost, at human prostanoid receptors: treprostinil is a potent DP1 and EP2 agonist. *Biochem Pharmacol*. 2012;84(1):68-75. doi:10.1016/j.bcp.2012.03.012

86. Vachiéry JL, Hill N, Zwicke D, Barst R, Blackburn S, Naeije R. Transitioning from IV epoprostenol to subcutaneous treprostinil in pulmonary arterial hypertension. *Chest*. 2002;121(5):1561-1565. doi:10.1378/chest.121.5.1561

87. Schilz RJ, Rubenfire M, McLaughlin V V, et al. Transition from epoprostenol to treprostinil in pulmonary arterial hypertension: a controlled trial. *Chest*. 2006;27(3):622. doi:10.1378/chest.06-2118

88. Laliberte K, Arneson C, Jeffs R, Hunt T, Wade M. Pharmacokinetics and steady-state

bioequivalence of treprostinil sodium (Remodulin) administered by the intravenous and subcutaneous route to normal volunteers. *J Cardiovasc Pharmacol*. 2004;44(2):209-214.

89. Simonneau G, Barst RJ, Galie N, et al. Continuous subcutaneous infusion of treprostinil, a prostacyclin analogue, in patients with pulmonary arterial hypertension: a double-blind, randomized, placebo-controlled trial. *Am J Respir Crit Care Med*. 2002;165(6):800-804. doi:10.1164/ajrccm.165.6.2106079
90. Oudiz RJ, Farber HW. Dosing considerations in the use of intravenous prostanoids in pulmonary arterial hypertension: An experience-based review. *Am Heart J*. 2009;157(4):625-635. doi:10.1016/j.ahj.2008.10.029
91. Ditrick D, Longo L. *Treprostinil Inhalation*.; 2010.
92. Borghardt JM, Kloft C, Sharma A. Inhaled Therapy in Respiratory Disease: The Complex Interplay of Pulmonary Kinetic Processes. *Can Respir J*. 2018;2018:1-11. doi:10.1155/2018/2732017
93. European Medicines Agency. *Ventavis - Scientific Discussion*. London; 2004.
94. Tissot C, Beghetti M. Review of inhaled iloprost for the control of pulmonary artery hypertension in children. *Vasc Heal Risk Manag*. 2009;5:325-331.
95. Ewert R, Gläser S, Bollmann T, Schäper C. Inhaled iloprost for therapy in pulmonary arterial hypertension. *Expert Rev Respir Med*. 2011;5(2):145-152. doi:10.1586/ers.11.14
96. Olschewski H, Rohde B, Behr J, et al. Pharmacodynamics and Pharmacokinetics of Inhaled Iloprost, Aerosolized by Three Different Devices, in Severe Pulmonary Hypertension. *Chest*. 2003;124(4):1294-1304. doi:http://dx.doi.org/10.1378/chest.124.4.1294
97. Krause W, Krais T. Pharmacokinetics and pharmacodynamics of the prostacyclin analogue iloprost in man. *Eur J Clin Pharmacol*. 1986;30(1):61-68. doi:10.1007/BF00614197
98. Oudiz RJ, Farber HW. Dosing considerations in the use of intravenous prostanoids in pulmonary arterial hypertension: An experience-based review. *Am Heart J*. 2009;157(4):625-635. doi:10.1016/j.ahj.2008.10.029
99. Olschewski H, Simonneau G, Galie N, et al. Inhaled iloprost for severe pulmonary hypertension. *N Engl J Med*. 2002;347(5):322-329. doi:10.1056/NEJMoa020204
100. Gessler T, Schmehl T, Hoeper MM, et al. Ultrasonic versus jet nebulization of iloprost in severe pulmonary hypertension. *Eur Respir J*. 2001;17:14-19.
101. Hirata T, Narumiya S. Prostanoid Receptors. *Chem Rev*. 2011;111(10):6209-6230. doi:10.1021/cr200010h
102. United Therapeutics Corp. *Tyvaso (Treprostinil) Prescribing Information*. Research triangle park, NC; 2009.
103. Voswinckel R, Ghofrani HA, Grimminger F, Seeger W, Olschewski H. Inhaled treprostinil [corrected] for treatment of chronic pulmonary arterial hypertension. *Ann*

Intern Med. 2006;144(2):149-150.

104. McLaughlin V V, Benza RL, Rubin LJ, et al. Addition of inhaled treprostinil to oral therapy for pulmonary arterial hypertension: a randomized controlled clinical trial. *J Am Coll Cardiol*. 2010;55(18):1915-1922. doi:10.1016/j.jacc.2010.01.027
105. Voswinckel R, Enke B, Reichenberger F, et al. Favorable effects of inhaled treprostinil in severe pulmonary hypertension: results from randomized controlled pilot studies. *J Am Coll Cardiol*. 2006;48(8):1672-1681. doi:10.1016/j.jacc.2006.06.062
106. Billington CK, Ojo OO, Penn RB, Itod S. cAMP Regulation of Airway Smooth Muscle Function. *Pulm Pharmacol Ther*. 2013;26(1):112-120.
107. Gessler T, Seeger W, Schmehl T. The potential for inhaled treprostinil in the treatment of pulmonary arterial hypertension. *Ther Adv Respir Dis*. 2011;5(3):195-206. doi:10.1177/1753465810397693
108. Kumar P, Thudium E, Nelsen A. A comprehensive Review of Treprostinil Pharmoacokinetics via four routes of adminsitration. *Clin Pharmacokinet*. 2016;55:1495-1505.
109. Enderby CY, Soukup M, Al Omari M, Zeiger T, Burger C. Transition from intravenous or subcutaneous prostacyclin therapy to inhaled treprostinil in patients with pulmonary arterial hypertension: A retrospective case series. *J Clin Pharm Ther*. 2014;39(5):496-500.
110. De Jesus Perez VA, Rosenzweig E, Rubin LJ, et al. Safety and efficacy of transition from systemic prostanoids to inhaled treprostinil in pulmonary arterial hypertension. *Am J Cardiol*. 2012;110(10):1546-1550. doi:10.1016/j.amjcard.2012.07.012
111. Simonneau G, Galie N, Humbert H, et al. Effects of beraprost sodium, an oral prostacyclin analogue, in patients with pulmonary arterial hypertension: A randomised, double-blind, placebo-controlled trial. *J Am Coll Cardiol*. 2002;39(9):1496-1502. doi:10.1016/S0735-1097(02)01786-2
112. Barst RJ, McGoon M, McLaughlin V, et al. Beraprost therapy for pulmonary arterial hypertension. *J Am Coll Cardiol*. 2003;41(12):2119-2125. doi:10.1016/S0735-1097(03)00463-7
113. European Medicines Agency. *Uptravi (Selexipag): Summary of Product Characteristics*. London; 2016.
114. Asaki T, Hamamoto T, Sugiyama Y, Kuwano K, Kuwabara K, Niwa T. Structure–activity relationship study on the 6-membered heteroaromatic ring system of diphenylpyrazine-type prostacyclin receptor agonists. *Bioorg Med Chem Lett*. 2007;17(23):6588-6592. doi:http://dx.doi.org/10.1016/j.bmcl.2007.09.066
115. Nakamura A, Yamada T, Asaki T. Synthesis and evaluation of N-acylsulfonamide and N-acylsulfonylurea prodrugs of a prostacyclin receptor agonist. *Bioorg Med Chem*. 2007;15(24):7720-7725. doi:10.1016/j.bmc.2007.08.052
116. Scott LJ. Niraparib: First Global Approval. *Drugs*. 2017;77(9):1029-1034. doi:10.1007/s40265-017-0752-y

117. Skoro-Sajer N, Lang IM. Selexipag for the treatment of pulmonary arterial hypertension. *Expert Opin Pharmacother*. 2014;15(3):429-436. doi:10.1517/14656566.2014.876007

118. Paramothayan NS, Lasserson TJ, Wells AU, Walters EH. Prostacyclin for pulmonary hypertension. *Cochrane database Syst Rev*. 2003;(2):CD002994-CD002994.

119. Nakanishi N. 2009 ESC/ERS Pulmonary Hypertension Guidelines and Connective Tissue Disease. *Allergol Int*. 2011;60(4):419-424. doi:http://dx.doi.org/10.2332/allergolint.11-RAI-0362

120. Gomberg-Maitland M, Preston IR. Prostacyclin therapy for pulmonary arterial hypertension: new directions. *Semin Respir Crit Care Med*. 2005;26(4):394-401. doi:10.1055/s-2005-916154

121. Jones A, Wang-Smith L, Pham T, Laliberte K. Pharmacokinetics of 3 times a day dosing of oral treprostinil in healthy volunteers. *J Cardiovasc Pharmacol*. 2014;63(3):227-232. doi:10.1097/FJC.0000000000000039

122. Jones A, Wang-Smith L, Pham T, Laliberte K. Pharmacokinetics of 3 Times a Day Dosing of Oral Treprostinil in Healthy Volunteers. *J Cardiovasc Pharmacol Ô*. 2014;63:227-232.

123. Lang I, Gomez-Sanchez M, Kneussl M, et al. Efficacy of Long-term Subcutaneous Treprostinil Sodium Therapy in Pulmonary Hypertension. *Chest*. 2006;129(6):1636-1643. doi:10.1378/CHEST.129.6.1636

124. Libri V, Gibbs JSR, Pinato DJ, et al. Capsaicin 8% patch for treprostinil subcutaneous infusion site pain in pulmonary hypertension patients. *Br J Anaesth*. 2014;112(2):337-347. doi:10.1093/bja/aet308

125. Fukushima S, Miyagawa S, Sakai Y, Sawa Y. A sustained-release drug-delivery system of synthetic prostacyclin agonist, ONO-1301SR: a new reagent to enhance cardiac tissue salvage and/or regeneration in the damaged heart. *Heart Fail Rev*. 2015;20(4):401-413. doi:10.1007/s10741-015-9477-8

126. Skoro-Sajer N, Lang IM. Selexipag for the treatment of pulmonary arterial hypertension. *Expert Opin Pharmacother*. 2014;15(3):429-436. doi:10.1517/14656566.2014.876007

127. Tapson VF, Jing Z-C, Xu K-F, et al. Oral treprostinil for the treatment of pulmonary arterial hypertension in patients receiving background endothelin receptor antagonist and phosphodiesterase type 5 inhibitor therapy (the FREEDOM-C2 study): a randomized controlled trial. *Chest*. 2013;144(3):952-958. doi:10.1378/chest.12-2875

128. McLaughlin V V, Benza RL, Rubin LJ, et al. Addition of inhaled treprostinil to oral therapy for pulmonary arterial hypertension: a randomized controlled clinical trial. *J Am Coll Cardiol*. 2010;55(18):1915-1922. doi:10.1016/j.jacc.2010.01.027

129. Ishihara T, Takahashi M, Higaki M, Takenaga M, Mizushima T, Mizushima Y. Prolonging the In Vivo Residence Time of Prostaglandin E1 with Biodegradable Nanoparticles. *Pharm Res*. 2008;25(7):1686-1695. doi:10.1007/s11095-008-9549-8

130. Takeda M, Maeda T, Ishihara T, et al. Synthesis of Prostaglandin E1 Phosphate Derivatives and Their Encapsulation in Biodegradable Nanoparticles. *Pharm Res*. 2009;26(7):1792-1800. doi:10.1007/s11095-009-9891-5
131. Ishihara T, Hayashi E, Yamamoto S, et al. Encapsulation of beraprost sodium in nanoparticles: analysis of sustained release properties, targeting abilities and pharmacological activities in animal models of pulmonary arterial hypertension. *J Control Release*. 2015;197:97-104. doi:10.1016/j.jconrel.2014.10.029
132. Malinin V, Li Z, Chapman R, et al. Treprostinil pharmacokinetics in rats are extended using inhaled prodrug formulations. *Eur Respir J*. 2014;44(Suppl_58):P2367-.
133. Omiatek D, Leifer F, Malinin V, et al. Incorporation into lipid nanoparticles extends the duration of activity of treprostinil in an acute hypoxia rat model of pulmonary arterial hypertension. *Eur Respir J*. 2014;44(Suppl_58):P2357-.
134. Chapman RW, Li Z, Corboz MR, et al. Inhaled hexadecyl-treprostinil provides pulmonary vasodilator activity at significantly lower plasma concentrations than infused treprostinil. *Pulm Pharmacol Ther*. 2018;49:104-111. doi:10.1016/J.PUPT.2018.02.002
135. Han D, Fernandez C, Sullivan E, et al. Single dose pharmacokinetics of C16TR for Inhalation (INS1009) vs treprostinil inhalation solution. In: *4.3 Pulmonary Circulation and Pulmonary Vascular Diseases*. Vol 48. European Respiratory Society; 2016:PA2398. doi:10.1183/13993003.congress-2016.PA2398
136. Han D, Fernandez C, Sullivan E, et al. Safety and pharmacokinetics study of a single ascending dose of C16TR for inhalation (INS1009). In: *4.3 Pulmonary Circulation and Pulmonary Vascular Diseases*. Vol 48. European Respiratory Society; 2016:PA2403. doi:10.1183/13993003.congress-2016.PA2403
137. United Therapeutics. Dose Escalation, MTD, Safety and PK Study of a Single Dose SC Injection of TransCon PEG Treprostinil in Healthy Male Volunteers. NIH ClinicalTrials. https://clinicaltrials.gov/ct2/show/NCT02149095. Published 2014. Accessed April 20, 2018.
138. Ascendis Pharma A/S. Ascendis Pharma A/S Announces Results of Phase 1 Study of TransCon Treprostinil. Press Release. https://www.prnewswire.com/news-releases/ascendis-pharma-as-announces-results-of-phase-1-study-of-transcon-treprostinil-300073527.html. Published 2015. Accessed April 20, 2018.
139. Adams DH, Whittaker VP. The characterization of the esterases of human plasma. *Biochem J*. 1949;44(1):62-70.
140. Vahlquist B. On the esterase activity of human blood plasma. *Skand Arch Physiol*. 1935;72(2):133-160. doi:https://doi.org/10.1111/j.1748-1716.1935.tb00418.x
141. Vachiéry J-L, Naeije R. Treprostinil for pulmonary hypertension. *Expert Rev Cardiovasc Ther*. 2014;2(2):183-191.
142. Patel J, Shen L, Hall S, et al. Prostanoid EP2 Receptors Are Up-Regulated in Human Pulmonary Arterial Hypertension: A Key Anti-Proliferative Target for Treprostinil in

Smooth Muscle Cells. *Int J Mol Sci*. 2018;19(8):2372. doi:10.3390/ijms19082372

143. Falcetti E, Flavell DM, Staels B, Tinker A, Haworth SG, Clapp LH. IP receptor-dependent activation of PPARγ by stable prostacyclin analogues. *Biochem Biophys Res Commun*. 2007;360(4):821-827. doi:10.1016/J.BBRC.2007.06.135
144. Orie NN, Clapp LH. Role of prostanoid IP and EP receptors in mediating vasorelaxant responses to PGI2 analogues in rat tail artery: Evidence for Gi/o modulation via EP3 receptors. *Eur J Pharmacol*. 2011;654(3):258-265. doi:10.1016/j.ejphar.2010.12.005
145. Whittle BJR, Moncada S. 6 Antithrombotic Assessment and Clinical Potential of Prostacyclin Analogues. *Prog Med Chem*. 1985;21:237-279. doi:10.1016/S0079-6468(08)70411-9
146. Kingman MS, Tankersley MA, Lombardi S, Spence S, Torres F, Chin KS. Prostacyclin administration errors in pulmonary arterial hypertension patients admitted to hospitals in the United States: a national survey. *J Hear Lung Transpl*. 2010;29(8):841-846. doi:10.1016/j.healun.2010.03.008
147. Tiwari G, Tiwari R, Sriwastawa B, et al. Drug delivery systems: An updated review. *Int J Pharm Investig*. 2012;2(1):2-11. doi:10.4103/2230-973X.96920
148. Huttunen KM, Raunio H, Rautio J. Prodrugs--from serendipity to rational design. *Pharmacol Rev*. 2011;63(3):750-771. doi:10.1124/pr.110.003459
149. Müller CE. Prodrug Approaches for Enhancing the Bioavailability of Drugs with Low Solubility. *Chem Biodivers*. 2009;6(11):2071-2083. doi:10.1002/cbdv.200900114
150. Pozarowska D. Safety and tolerability of tafluprost in treatment of elevated intraocular pressure in open-angle glaucoma and ocular hypertension. *Clin Ophthalmol*. 2010;4:1229-1236. doi:10.2147/OPTH.S6369
151. Ksander GM, Ghai RD, deJesus R, et al. Dicarboxylic acid dipeptide neutral endopeptidase inhibitors. *J Med Chem*. 1995;38(10):1689-1700.
152. Elliott EL, Ferdous AJ, Kaufman MJ, et al. Boronate ester compounds and pharmaceutical compositions thereof. Nič M, Jirát J, Košata B, Jenkins A, McNaught A, eds. August 2014. doi:10.1351/goldbook
153. Trochine A, Creek DJ, Faral-Tello P, Barrett MP, Robello C. Benznidazole Biotransformation and Multiple Targets in Trypanosoma cruzi Revealed by Metabolomics. Pollastri MP, ed. *PLoS Negl Trop Dis*. 2014;8(5):e2844. doi:10.1371/journal.pntd.0002844
154. Goldstein DS. L-Dihydroxyphenylserine (L-DOPS): A Norepinephrine Prodrug. *Cardiovasc Drug Rev*. 2006;24(3-4):189-203. doi:10.1111/j.1527-3466.2006.00189.x
155. Vera-Cabrera L, Gonzalez E, Rendon A, et al. In vitro activities of DA-7157 and DA-7218 against Mycobacterium tuberculosis and Nocardia brasiliensis. *Antimicrob Agents Chemother*. 2006;50(9):3170-3172. doi:10.1128/AAC.00571-06
156. Wiggins JB, Rajapakse R. Balsalazide: a novel 5-aminosalicylate prodrug for the treatment of active ulcerative colitis. *Expert Opin Drug Metab Toxicol*. 2009;5(10):1279-1284. doi:10.1517/17425250903206996

157. Morello CM. Pharmacokinetics and pharmacodynamics of insulin analogs in special populations with type 2 diabetes mellitus. *Int J Gen Med*. 2011;4:827-835.
158. Sleep D. Albumin and its application in drug delivery. *Expert Opin Drug Deliv*. 2015;12(5):793-812.
159. Li X, Chen D, Wang G, Lu Y. Study of interaction between human serum albumin and three antioxidants: ascorbic acid, α-tocopherol, and proanthocyanidins. *Eur J Med Chem*. 2013;70:22-36. doi:10.1016/j.ejmech.2013.09.033
160. Nishina K, Unno T, Uno Y, et al. Efficient in vivo delivery of siRNA to the liver by conjugation of alpha-tocopherol. *Mol Ther*. 2008;16(4):734-740. doi:10.1038/mt.2008.14
161. Masereeuw R, Russel FGM. Mechanisms and clinical implications of renal drug excretion *. *Drug Metab Rev*. 2001;33(3-4):299-351. doi:10.1081/DMR-120000654
162. Veronese FM, Morpurgo M. Bioconjugation in pharmaceutical chemistry. *Farm*. 1999;54(8):497-516. doi:10.1016/S0014-827X(99)00066-X
163. Ulbrich K, Šubr V, Strohalm J, Plocová D, Jelínková M, Říhová B. Polymeric drugs based on conjugates of synthetic and natural macromolecules: I. Synthesis and physico-chemical characterisation. *J Control Release*. 2000;64(1):63-79. doi:10.1016/S0168-3659(99)00141-8
164. Dragojevic S, Ryu J, Raucher D, Dragojevic S, Ryu JS, Raucher D. Polymer-Based Prodrugs: Improving Tumor Targeting and the Solubility of Small Molecule Drugs in Cancer Therapy. *Molecules*. 2015;20(12):21750-21769. doi:10.3390/molecules201219804
165. Larson N, Ghandehari H. Polymeric conjugates for drug delivery. *Chem Mater*. 2012;24(5):840-853. doi:10.1021/cm2031569
166. Duncan R, Vicent MJ. Polymer therapeutics-prospects for 21st century: The end of the beginning. *Adv Drug Deliv Rev*. 2013;65(1):60-70. doi:10.1016/J.ADDR.2012.08.012
167. Srichana T, Suwandecha T. Polyethylene Glycol in Clinical Application and PEGylated Drugs. In: *Biodegradable Polymers in Clinical Use and Clinical Development*. Hoboken, NJ, USA: John Wiley & Sons, Inc.; 2011:451-493. doi:10.1002/9781118015810.ch13
168. Ivens IA, Achanzar W, Baumann A, et al. PEGylated Biopharmaceuticals. *Toxicol Pathol*. 2015;43(7):959-983. doi:10.1177/0192623315591171
169. Wang Y-S, Youngster S, Grace M, Bausch J, Bordens R, Wyss DF. Structural and biological characterization of pegylated recombinant interferon alpha-2b and its therapeutic implications. *Adv Drug Deliv Rev*. 2002;54(4):547-570. doi:10.1016/S0169-409X(02)00027-3
170. Glue P, Fang JWS, Rouzier-Panis R, et al. Pegylated interferon-α2b: Pharmacokinetics, pharmacodynamics, safety, and preliminary efficacy data. *Clin Pharmacol Ther*. 2000;68(5):556-567. doi:10.1067/mcp.2000.110973
171. Jørgensen KE, Møller J V. Use of flexible polymers as probes of glomerular pore size. *Am J Physiol*. 1979;236(2):F103-11. doi:10.1152/ajprenal.1979.236.2.F103

172. Ringsdorf H. Structure and properties of pharmacologically active polymers. *J Polym Sci Polym Symp*. 1975;51(1):135-153. doi:10.1002/polc.5070510111
173. Greco F, Vicent MJ, Gee S, et al. Investigating the mechanism of enhanced cytotoxicity of HPMA copolymer-Dox-AGM in breast cancer cells. *J Control Release*. 2007;117(1):28-39. doi:10.1016/j.jconrel.2006.10.012
174. Duncan R. Polymer therapeutics at a crossroads? Finding the path for improved translation in the twenty-first century. *J Drug Target*. 2017;25(9-10):759-780. doi:10.1080/1061186X.2017.1358729
175. Greish K. Enhanced Permeability and Retention (EPR) Effect for Anticancer Nanomedicine Drug Targeting. In: Humana Press; 2010:25-37. doi:10.1007/978-1-60761-609-2_3
176. Fang J, Nakamura H, Maeda H. The EPR effect: Unique features of tumor blood vessels for drug delivery, factors involved, and limitations and augmentation of the effect. *Adv Drug Deliv Rev*. 2011;63(3):136-151. doi:10.1016/J.ADDR.2010.04.009
177. Maeda H. Polymer therapeutics and the EPR effect. *J Drug Target*. 2017;25(9-10):781-785. doi:10.1080/1061186X.2017.1365878
178. Torchilin VP. Drug targeting. *Eur J Pharm Sci*. 2000;11:S81-S91. doi:10.1016/S0928-0987(00)00166-4
179. Stylianopoulos T. EPR-effect: utilizing size-dependent nanoparticle delivery to solid tumors. *Ther Deliv*. 2013;4(4):421-423. doi:10.4155/tde.13.8
180. Segura-Ibarra V, Wu S, Hassan N, et al. Nanotherapeutics for Treatment of Pulmonary Arterial Hypertension. *Front Physiol*. 2018;9:890. doi:10.3389/fphys.2018.00890
181. Durymanov M, Kamaletdinova T, Lehmann SE, Reineke J. Exploiting passive nanomedicine accumulation at sites of enhanced vascular permeability for non-cancerous applications. *J Control Release*. 2017;261:10-22. doi:10.1016/J.JCONREL.2017.06.013
182. Duncan R, Gac-Breton S, Keane R, et al. Polymer–drug conjugates, PDEPT and PELT: basic principles for design and transfer from the laboratory to clinic. *J Control Release*. 2001;74(1-3):135-146.
183. Doppalapudi S, Jain A, Domb AJ, Khan W. Biodegradable polymers for targeted delivery of anti-cancer drugs. *Expert Opin Drug Deliv*. 2016;13(6):891-909. doi:10.1517/17425247.2016.1156671
184. Pang X, Yang X, Zhai G. Polymer-drug conjugates: recent progress on administration routes. *Expert Opin Drug Deliv*. 2014;11(7):1075-1086. doi:10.1517/17425247.2014.912779
185. Greco F, Vicent MJ. Polymer-drug conjugates: current status and future trends. *Front Biosci*. 2008;13(13):2744. doi:10.2741/2882
186. Pelegri-O'Day EM, Lin E-W, Maynard HD. Therapeutic protein-polymer conjugates: advancing beyond PEGylation. *J Am Chem Soc*. 2014;136(41):14323-14332. doi:10.1021/ja504390x

187. Zhao H, Rubio B, Sapra P, et al. Novel Prodrugs of SN38 Using Multiarm Poly(ethylene glycol) Linkers. *Bioconjug Chem*. 2008;19(4):849-859. doi:10.1021/bc700333s
188. Lee JY, Bae KH, Kim JS, Nam YS, Park TG. Intracellular delivery of paclitaxel using oil-free, shell cross-linked HSA – Multi-armed PEG nanocapsules. *Biomaterials*. 2011;32(33):8635-8644. doi:10.1016/J.BIOMATERIALS.2011.07.063
189. Prencipe G, Tabakman SM, Welsher K, et al. PEG Branched Polymer for Functionalization of Nanomaterials with Ultralong Blood Circulation. *J Am Chem Soc*. 2009;131(13):4783-4787. doi:10.1021/ja809086q
190. Yang Q, Lai SK. Anti-PEG immunity: emergence, characteristics, and unaddressed questions. *Wiley Interdiscip Rev Nanomedicine Nanobiotechnology*. 2015;7(5):655-677. doi:10.1002/wnan.1339
191. Zhang P, Sun F, Liu S, Jiang S. Anti-PEG antibodies in the clinic: Current issues and beyond PEGylation. *J Control Release*. 2016;244(Pt B):184-193. doi:10.1016/j.jconrel.2016.06.040
192. Hamad I, Hunter AC, Szebeni J, Moghimi SM. Poly(ethylene glycol)s generate complement activation products in human serum through increased alternative pathway turnover and a MASP-2-dependent process. *Mol Immunol*. 2008;46(2):225-232. doi:10.1016/J.MOLIMM.2008.08.276
193. Swierczewska M, Leec KC, Lee S. What is the future of PEGylated therapies? *Expert Opin Emerg Drugs*. 2015;20(4):531-536.
194. Venditto VJ, Simanek EE. Cancer therapies utilizing the camptothecins: a review of the in vivo literature. *Mol Pharm*. 2010;7(2):307-349. doi:10.1021/mp900243b
195. Schluep T, Cheng J, Khin KT, Davis ME. Pharmacokinetics and biodistribution of the camptothecin-polymer conjugate IT-101 in rats and tumor-bearing mice. *Cancer Chemother Pharmacol*. 2006;57(5):654-662. doi:10.1007/s00280-005-0091-7
196. Cheng J, Khin KT, Davis ME. Antitumor Activity of β-Cyclodextrin Polymer−Camptothecin Conjugates. *Mol Pharm*. 2004;1(3):183-193. doi:10.1021/mp049966y
197. Svenson S, Wolfgang M, Hwang J, Ryan J, Eliasof S. Preclinical to clinical development of the novel camptothecin nanopharmaceutical CRLX101. *J Control Release*. 2011;153(1):49-55. doi:10.1016/j.jconrel.2011.03.007
198. Lang IM, Gaine SP. Recent advances in targeting the prostacyclin pathway in pulmonary arterial hypertension. *Eur Respir Rev*. 2015;24(138).
199. Gentile MA, Chatburn RL, McLeary T, Prat G, Tonnelier J, Lefevre M. Inhaled medical gases: more to breathe than oxygen. *Respir Care*. 2011;56(9):1341-57; discussion 1357-9. doi:10.4187/respcare.01442
200. Corboz MR, Zhang J, LaSala D, et al. Therapeutic administration of inhaled INS1009, a treprostinil prodrug formulation, inhibits bleomycin-induced pulmonary fibrosis in rats. *Pulm Pharmacol Ther*. 2018;49:95-103. doi:10.1016/J.PUPT.2018.01.012
201. Loira-Pastoriza C, Todoroff J, Vanbever R. Delivery strategies for sustained drug

release in the lungs. *Adv Drug Deliv Rev*. 2014;75:81-91. doi:10.1016/j.addr.2014.05.017

202. Todoroff J, Vanbever R. Fate of nanomedicines in the lungs. *Curr Opin Colloid Interface Sci*. 2011;16(3):246-254. doi:10.1016/j.cocis.2011.03.001
203. Gupta V, Davis M, Hope-Weeks LJ, Ahsan F. PLGA microparticles encapsulating prostaglandin E1-hydroxypropyl-β-cyclodextrin (PGE1-HPβCD) complex for the treatment of pulmonary arterial hypertension (PAH). *Pharm Res*. 2011;28(7):1733-1749. doi:10.1007/s11095-011-0409-6
204. Hoet PH, Brüske-Hohlfeld I, Salata O V. Nanoparticles – known and unknown health risks. *J Nanobiotechnology*. 2004;2(1):12. doi:10.1186/1477-3155-2-12
205. Sun Q, Tan D, Ze Y, et al. Pulmotoxicological effects caused by long-term titanium dioxide nanoparticles exposure in mice. *J Hazard Mater*. 2012;235-236:47-53. doi:10.1016/J.JHAZMAT.2012.05.072
206. Wang P, Nie X, Wang Y, et al. Multiwall Carbon Nanotubes Mediate Macrophage Activation and Promote Pulmonary Fibrosis Through TGF-β/Smad Signaling Pathway. *Small*. 2013;9(22):3799-3811. doi:10.1002/smll.201300607
207. Shvedova AA, Kisin E, Murray AR, et al. Inhalation vs. aspiration of single-walled carbon nanotubes in C57BL/6 mice: inflammation, fibrosis, oxidative stress, and mutagenesis. *Am J Physiol Lung Cell Mol Physiol*. 2008;295(4):L552-65. doi:10.1152/ajplung.90287.2008
208. Strebhardt K, Ullrich A. Paul Ehrlich's magic bullet concept: 100 years of progress. *Nat Rev Cancer*. 2008;8(6):473-480. doi:10.1038/nrc2394
209. Bouchard H, Viskov C, Garcia-Echeverria C. Antibody-drug conjugates—a new wave of cancer drugs. *Bioorg Med Chem Lett*. 2014;24(23):5357-5363. doi:10.1016/j.bmcl.2014.10.021
210. Sassoon I, Blanc V. Antibody–Drug Conjugate (ADC) Clinical Pipeline: A Review. In: Humana Press, Totowa, NJ; 2013:1-27. doi:10.1007/978-1-62703-541-5_1
211. Moskowitz CH, Nademanee A, Masszi T, et al. Brentuximab vedotin as consolidation therapy after autologous stem-cell transplantation in patients with Hodgkin's lymphoma at risk of relapse or progression (AETHERA): a randomised, double-blind, placebo-controlled, phase 3 trial. *Lancet (London, England)*. 2015;385(9980):1853-1862. doi:10.1016/S0140-6736(15)60165-9
212. Thomas X. Profile of inotuzumab ozogamicin and its potential in the treatment of acute lymphoblastic leukemia. *Blood Lymphat Cancer Targets Ther*. 2014;4:1. doi:10.2147/BLCTT.S49048
213. Norsworthy KJ, Ko C-W, Lee JE, et al. FDA Approval Summary: Mylotarg for Treatment of Patients with Relapsed or Refractory CD33-Positive Acute Myeloid Leukemia. *Oncologist*. April 2018:theoncologist.2017-0604. doi:10.1634/theoncologist.2017-0604
214. Peddi PF, Hurvitz SA. Trastuzumab emtansine: the first targeted chemotherapy for treatment of breast cancer. *Future Oncol*. 2013;9(3):319-326. doi:10.2217/fon.13.7

215. Sapra P, Stein R, Pickett J, et al. Anti-CD74 Antibody-Doxorubicin Conjugate, IMMU-110, in a Human Multiple Myeloma Xenograft and in Monkeys. *Clin Cancer Res*. 2005;11(14):5257-5264. doi:10.1158/1078-0432.CCR-05-0204
216. Socinski MA, Kaye FJ, Spigel DR, et al. Phase 1/2 Study of the CD56-Targeting Antibody-Drug Conjugate Lorvotuzumab Mertansine (IMGN901) in Combination With Carboplatin/Etoposide in Small-Cell Lung Cancer Patients With Extensive-Stage Disease. *Clin Lung Cancer*. 2017;18(1):68-76.e2. doi:10.1016/j.cllc.2016.09.002
217. Cardoso MM, Peça IN, Roque ACA. Antibody-conjugated nanoparticles for therapeutic applications. *Curr Med Chem*. 2012;19(19):3103-3127.
218. Teicher BA, Chari RVJ. Antibody conjugate therapeutics: challenges and potential. *Clin Cancer Res*. 2011;17(20):6389-6397. doi:10.1158/1078-0432.CCR-11-1417
219. Vezina HE, Cotreau M, Han TH, Gupta M. Antibody-Drug Conjugates as Cancer Therapeutics: Past, Present, and Future. *J Clin Pharmacol*. 2017;57:S11-S25. doi:10.1002/jcph.981
220. Badescu G, Bryant P, Bird M, et al. Bridging Disulfides for Stable and Defined Antibody Drug Conjugates. *Bioconjug Chem*. 2014;25(6):1124-1136. doi:10.1021/bc500148x
221. Frka-Petesic B, Zanchi D, Martin N, Carayon S, Huille S, Tribet C. Aggregation of Antibody Drug Conjugates at Room Temperature: SAXS and Light Scattering Evidence for Colloidal Instability of a Specific Subpopulation. *Langmuir*. 2016;32(19):4848-4861. doi:10.1021/acs.langmuir.6b00653
222. Agarwal P, Bertozzi CR. Site-specific antibody-drug conjugates: the nexus of bioorthogonal chemistry, protein engineering, and drug development. *Bioconjug Chem*. 2015;26(2):176-192. doi:10.1021/bc5004982
223. Khalili H, Godwin A, Choi J, Lever R, Brocchini S. Comparative Binding of Disulfide-Bridged PEG-Fabs. *Bioconjug Chem*. 2012;23(11):2262-2277. doi:10.1021/bc300372r
224. Trepel M, Grifman M, Weitzman MD, Pasqualini R. Molecular adaptors for vascular-targeted adenoviral gene delivery. *Hum Gene Ther*. 2000;11(14):1971-1981. doi:10.1089/10430340050143408
225. Blankart CR, Stargardt T, Schreyogg J. Availability of and access to orphan drugs: an international comparison of pharmaceutical treatments for pulmonary arterial hypertension, Fabry disease, hereditary angioedema and chronic myeloid leukaemia. *Pharmacoeconomics*. 2011;29(1):63-82. doi:10.2165/11539190-000000000-00000
226. Desogus A, Burioni R, Ingianni A, Bugli F, Pompei R, Fadda G. Production and Characterization of a Human Recombinant Monoclonal Fab Fragment Specific for Influenza A Viruses. *Clin Diagn Lab Immunol*. 2003;10(4):680-685.
227. Ruoslahti E. Vascular zip codes in angiogenesis and metastasis. *Biochem Soc Trans*. 2004;32(Pt3):397-402. doi:10.1042/BST0320397
228. Järvinen TAH, May U, Prince S. Systemically Administered, Target Organ-Specific Therapies for Regenerative Medicine. *Int J Mol Sci*. 2015;16(10):23556-23571. doi:10.3390/ijms161023556

229. Le Joncour V, Laakkonen P. Seek & Destroy, use of targeting peptides for cancer detection and drug delivery. *Bioorg Med Chem*. 2018;26(10):2797-2806. doi:10.1016/J.BMC.2017.08.052

230. Baumann A, Tuerck D, Prabhu S, Dickmann L, Sims J. Pharmacokinetics, metabolism and distribution of PEGs and PEGylated proteins: quo vadis? *Drug Discov Today*. 2014;19(10):1623-1631. doi:10.1016/J.DRUDIS.2014.06.002

231. Johnson RN, Kopečková P, Kopeček J. Biological Activity of Anti-CD20 Multivalent HPMA Copolymer-Fab' Conjugates. *Biomacromolecules*. 2012;13(3):727-735. doi:10.1021/bm201656k

232. Lee T-Y, Lin C-T, Kuo S-Y, Chang D-K, Wu H-C. Peptide-mediated targeting to tumor blood vessels of lung cancer for drug delivery. *Cancer Res*. 2007;67(22):10958-10965. doi:10.1158/0008-5472.CAN-07-2233

233. Shamay Y, Paulin D, Ashkenasy G, David A. E-selectin binding peptide-polymer-drug conjugates and their selective cytotoxicity against vascular endothelial cells. *Biomaterials*. 2009;30(32):6460-6468. doi:10.1016/j.biomaterials.2009.08.013

234. Pan H, Kopečková P, Wang D, Yang J, Miller S, Kopeček J. Water-soluble HPMA copolymer—prostaglandin E $_1$ conjugates containing a cathepsin K sensitive spacer. *J Drug Target*. 2006;14(6):425-435. doi:10.1080/10611860600834219

235. Liu J, Liu J, Chu L, et al. Novel peptide-dendrimer conjugates as drug carriers for targeting nonsmall cell lung cancer. *Int J Nanomedicine*. 2010;6:59-69. doi:10.2147/IJN.S14601

236. Escárcega RO, Baker NC, Lipinski MJ, et al. Current application and bioavailability of drug-eluting stents. *Expert Opin Drug Deliv*. April 2014.

237. Abizaid A, Costa JR. New drug-eluting stents: an overview on biodegradable and polymer-free next-generation stent systems. *Circ Cardiovasc Interv*. 2010;3(4):384-393. doi:10.1161/CIRCINTERVENTIONS.109.891192

238. Lüscher TF, Steffel J, Eberli FR, et al. Drug-eluting stent and coronary thrombosis: biological mechanisms and clinical implications. *Circulation*. 2007;115(8):1051-1058. doi:10.1161/CIRCULATIONAHA.106.675934

239. Hsiao H-M, Chiu Y-H, Wu T-Y, Shen J-K, Lee T-Y. Effects of through-hole drug reservoirs on key clinical attributes for drug-eluting depot stent. *Med Eng Phys*. 2013;35(7):884-897. doi:10.1016/j.medengphy.2012.08.021

240. Sammel AM, Chen D, Jepson N. New generation coronary stent technology--is the future biodegradable? *Heart Lung Circ*. 2013;22(7):495-506. doi:10.1016/j.hlc.2013.02.008

241. D'Souza AJM, Topp EM. Release from polymeric prodrugs: linkages and their degradation. *J Pharm Sci*. 2004;93(8):1962-1979. doi:10.1002/jps.20096

242. Binauld S, Stenzel MH. Acid-degradable polymers for drug delivery: a decade of innovation. *Chem Commun (Camb)*. 2013;49(21):2082-2102. doi:10.1039/c2cc36589h

243. Greenwald RB, Pendri A, Conover CD, et al. Drug delivery systems employing 1,4- or

1,6-elimination: poly(ethylene glycol) prodrugs of amine-containing compounds. *J Med Chem*. 1999;42(18):3657-3667. doi:10.1021/jm990166e

244. Firestone RA, Willner D, Hofstead SJ, et al. Synthesis and antitumor activity of the immunoconjugate BR96-Dox. *J Control Release*. 1996;39:251-259.
245. Lu J, Jiang F, Lu A, Zhang G. Linkers Having a Crucial Role in Antibody-Drug Conjugates. *Int J Mol Sci*. 2016;17(4):561. doi:10.3390/ijms17040561
246. Masson C, Garinot M, Mignet N, et al. pH-sensitive PEG lipids containing orthoester linkers: new potential tools for nonviral gene delivery. *J Control Release*. 2004;99(3):423-434. doi:10.1016/J.JCONREL.2004.07.016
247. Gillies ER, Goodwin AP, Fréchet JMJ. Acetals as pH-sensitive linkages for drug delivery. *Bioconjug Chem*. 15(6):1254-1263. doi:10.1021/bc049853x
248. Hervault A, Dunn AE, Lim M, et al. Doxorubicin loaded dual pH- and thermo-responsive magnetic nanocarrier for combined magnetic hyperthermia and targeted controlled drug delivery applications. *Nanoscale*. 2016;8(24):12152-12161. doi:10.1039/C5NR07773G
249. Du C, Deng D, Shan L, et al. A pH-sensitive doxorubicin prodrug based on folate-conjugated BSA for tumor-targeted drug delivery. *Biomaterials*. 2013;34(12):3087-3097. doi:10.1016/J.BIOMATERIALS.2013.01.041
250. Finniss MC, Chu KS, Bowerman CJ, Luft JC, Haroon ZA, DeSimone JM. A versatile acid-labile linker for antibody–drug conjugates. *Medchemcomm*. 2014;5(9):1355. doi:10.1039/C4MD00150H
251. Sproule BJ, Phillipson EA, Couves CM, Brownlee RT. Acute pulmonary hypertension in idiopathic lactic acidosis. *Can Med Assoc J*. 1966;94(3):141-143.
252. Park HI, Turk BE, Gerkema FE, Cantley LC, Sang Q-XA. Peptide substrate specificities and protein cleavage sites of human endometase/matrilysin-2/matrix metalloproteinase-26. *J Biol Chem*. 2002;277(38):35168-35175. doi:10.1074/jbc.M205071200
253. Alouane A, Labruère R, Le Saux T, Schmidt F, Jullien L. Self-Immolative Spacers: Kinetic Aspects, Structure-Property Relationships, and Applications. *Angew Chemie Int Ed*. 2015;54(26):n/a-n/a. doi:10.1002/anie.201500088
254. Jin H, Lu J, Wu X. Development of a new enzyme-responsive self-immolative spacer conjugate applicable to the controlled drug release. *Bioorg Med Chem*. 2012;20(11):3465-3469. doi:10.1016/j.bmc.2012.04.012
255. Blencowe CA, Russell AT, Greco F, Hayes W, Thornthwaite DW. Self-immolative linkers in polymeric delivery systems. *Polym Chem*. 2011;2(4):773-790. doi:10.1039/C0PY00324G
256. Gordon EJ, Sanders WJ, Kiessling LL. Synthetic ligands point to cell surface strategies. *Nature*. 1998;392(6671):30-31. doi:10.1038/32073
257. Vance D, Shah M, Joshi A, Kane RS. Polyvalency: A promising strategy for drug design. *Biotechnol Bioeng*. 2008;101(3):429-434. doi:10.1002/bit.22056

258. Mourez M, Kane RS, Mogridge J, et al. Designing a polyvalent inhibitor of anthrax toxin. *Nat Biotechnol*. 2001;19(10):958-961. doi:10.1038/nbt1001-958

259. Hill NS, Preston IR, Roberts KE. Inhaled Therapies for Pulmonary Hypertension. *Respir Care*. 2015;60(6):794-805. doi:10.4187/respcare.03927

260. Channick RN, Voswinckel R, Rubin LJ. Inhaled treprostinil: a therapeutic review. *Drug Des Devel Ther*. 2012;6:19-28. doi:10.2147/DDDT.S19281

261. Raina A, Coons JC, Kanwar M, Murali S, Sokos G, Benza RL. Transitioning from parenteral treprostinil to inhaled treprostinil in patients with pulmonary arterial hypertension. *Pulm Circ*. 2013;3(1):116-120. doi:10.4103/2045-8932.109926

262. Gessler T, Seeger W, Schmehl T. The potential for inhaled treprostinil in the treatment of pulmonary arterial hypertension. *Ther Adv Respir Dis*. 2011;5(3):195-206. doi:10.1177/1753465810397693

263. Lu X, Zhu T, Chen C, Liu Y. Right or left: the role of nanoparticles in pulmonary diseases. *Int J Mol Sci*. 2014;15(10):17577-17600. doi:10.3390/ijms151017577

264. Hwang J, Chun K-J, Lee DS, et al. Extraction of a Fully Deployed Coronary Stent during Retrieval of Another Dislodged Stent. *Korean Circ J*. 2016;46(6):862-865. doi:10.4070/kcj.2016.46.6.862

265. Miele E, Spinelli GP, Miele E, Tomao F, Tomao S. Albumin-bound formulation of paclitaxel (Abraxane ABI-007) in the treatment of breast cancer. *Int J Nanomedicine*. 2009;4:99-105.

266. Food and Drug administration. *Remodulin ® (Treprostinil Sodium) Injection*. Research Triangle Park, NC; 2008.

267. Petrak K. Essential properties of drug-targeting delivery systems. *Drug Discov Today*. 2005;10(23-24):1667-1673. doi:10.1016/S1359-6446(05)03698-6

268. Tolcher AW. Antibody drug conjugates: lessons from 20 years of clinical experience. *Ann Oncol*. 2016;27(12):2168-2172. doi:10.1093/annonc/mdw424

269. Rautio J, Meanwell NA, Di L, Hageman MJ. The expanding role of prodrugs in contemporary drug design and development. *Nat Rev Drug Discov*. 2018;17(8):559-587. doi:10.1038/nrd.2018.46

270. Fejerskov B, Zelikin AN, Scheeren H, Haisma H, Pinedo H. Substrate Mediated Enzyme Prodrug Therapy. Bansal V, ed. *PLoS One*. 2012;7(11):e49619. doi:10.1371/journal.pone.0049619

271. Chazova I, Loyd JE, Zhdanov VS, Newman JH, Belenkov Y, Meyrick B. Pulmonary artery adventitial changes and venous involvement in primary pulmonary hypertension. *Am J Pathol*. 1995;146(2):389-397.

272. Falcetti E, Hall SM, Phillips PG, et al. Smooth muscle proliferation and role of the prostacyclin (IP) receptor in idiopathic pulmonary arterial hypertension. *Am J Respir Crit Care Med*. 2010;182(9):1161-1170. doi:10.1164/rccm.201001-0011OC

273. Badesch DB, McLaughlin V V, Delcroix M, et al. Prostanoid therapy for pulmonary arterial hypertension. *J Am Coll Cardiol*. 2004;43(12 Suppl S):56s-61s.

doi:10.1016/j.jacc.2004.02.036

274. Orie NN, Ledwozyw A, Williams DJ, Whittle BJ, Clapp LH. Differential actions of the prostacyclin analogues treprostinil and iloprost and the selexipag metabolite, MRE-269 (ACT-333679) in rat small pulmonary arteries and veins. *Prostaglandins Other Lipid Mediat*. 2013;106:1-7. doi:http://dx.doi.org/10.1016/j.prostaglandins.2013.07.003
275. Falcetti E, Hall SM, Phillips PG, et al. Smooth muscle proliferation and role of the prostacyclin (IP) receptor in idiopathic pulmonary arterial hypertension. *Am J Respir Crit Care Med*. 2010;182(9):1161-1170. doi:10.1164/rccm.201001-0011OC
276. Clapp LH, Finney P, Turcato S, Tran S, Rubin LJ, Tinker A. Differential effects of stable prostacyclin analogs on smooth muscle proliferation and cyclic AMP generation in human pulmonary artery. *Am J Respir Cell Mol Biol*. 2002;26(2):194-201. doi:10.1165/ajrcmb.26.2.4695
277. Lai Y-J, Pullamsetti SS, Dony E, et al. Role of the prostanoid EP4 receptor in iloprost-mediated vasodilatation in pulmonary hypertension. *Am J Respir Crit Care Med*. 2008;178(2):188-196. doi:10.1164/rccm.200710-1519OC
278. Kuwano K, Hashino A, Asaki T, et al. 2-{4- (5,6-diphenylpyrazin-2-yl)(isopropyl)amino butoxy}-N(methylsulfony l)acetamide (NS-304), an orally available and long-acting prostacyclin receptor agonist prodrug. *J Pharmacol Exp Ther*. 2007;322(3):1181-1188. doi:10.1124/jpet.107.124248
279. Liu Q-Q, Jing Z-C. The limits of oral therapy in pulmonary arterial hypertension management. *Ther Clin Risk Manag*. 2015;11:1731-1741. doi:10.2147/TCRM.S49026
280. Whittle BJ, Silverstein AM, Mottola DM, Clapp LH. Binding and activity of the prostacyclin receptor (IP) agonists, treprostinil and iloprost, at human prostanoid receptors: treprostinil is a potent DP1 and EP2 agonist. *Biochem Pharmacol*. 2012;84(1):68-75. doi:10.1016/j.bcp.2012.03.012
281. Asaki T, Kuwano K, Morrison K, Gatfield J, Hamamoto T, Clozel M. Selexipag: An Oral and Selective IP Prostacyclin Receptor Agonist for the Treatment of Pulmonary Arterial Hypertension. *J Med Chem*. 2015;58(18):7128-7137. doi:10.1021/acs.jmedchem.5b00698
282. Narumiya S, Sugimoto Y, Ushikubi F, Conclusions VI. Prostanoid Receptors : Structures , Properties , and Functions. *Physiol Rev*. 1999;79(4):1193-1227.
283. Sitbon O, Channick R, Chin KM, et al. Selexipag for the Treatment of Pulmonary Arterial Hypertension. *N Engl J Med*. 2015;373(26):2522-2533. doi:10.1056/NEJMoa1503184
284. Walpole SC, Prieto-Merino D, Edwards P, Cleland J, Stevens G, Roberts I. The weight of nations: an estimation of adult human biomass. *BMC Public Health*. 2012;12(1):439. doi:10.1186/1471-2458-12-439
285. United Therapeutics Corp. *Full Prescibing Information: Orenitram (TM) Extended Release Tablets for Oral Administration*. Research Triangle Park; 2013.
286. Beraprost pharmacology. DrugBank Database.

https://www.drugbank.ca/drugs/DB05229. Published 2007. Accessed July 1, 2017.

287. Davis FA. *Flolan (Epoprostenol)*. Philadelphia; 2015.
288. McLaughlin V V, Gaine SP, Barst RJ, et al. Efficacy and safety of treprostinil: an epoprostenol analog for primary pulmonary hypertension. *J Cardiovasc Pharmacol*. 2003;41(2):293-299.
289. Schilz RJ, Rubenfire M, McLaughlin V V, et al. Transition from epoprostenol to treprostinil in pulmonary arterial hypertension: a controlled trial [Abstract]. *Chest*. 2006;27(3):622. doi:10.1378/chest.06-2118
290. Hiremath J, Thanikachalam S, Parikh K, et al. Exercise improvement and plasma biomarker changes with intravenous treprostinil therapy for pulmonary arterial hypertension: a placebo-controlled trial. *J Heart Lung Transplant*. 2010;29(2):137-149. doi:10.1016/j.healun.2009.09.005
291. Jing Z-C, Parikh K, Pulido T, et al. Efficacy and Safety of Oral Treprostinil Monotherapy for the Treatment of Pulmonary Arterial Hypertension: A Randomized, Controlled Trial. *Circulation*. 2013;127(5):624-633. doi:10.1161/CIRCULATIONAHA.112.124388
292. Simonneau G, Galie N, Humbert H, et al. Effects of beraprost sodium, an oral prostacyclin analogue, in patients with pulmonary arterial hypertension: A randomised, double-blind, placebo-controlled trial [abstract]. *J Am Coll Cardiol*. 2002;39(9):1496-1502. doi:10.1016/S0735-1097(02)01786-2
293. McLaughlin V V, Oudiz RJ, Frost A, et al. Randomized study of adding inhaled iloprost to existing bosentan in pulmonary arterial hypertension. *Am J Respir Crit Care Med*. 2006;174(11):1257-1263. doi:10.1164/rccm.200603-358OC
294. Tapson VF, Torres F, Kermeen F, et al. Oral treprostinil for the treatment of pulmonary arterial hypertension in patients on background endothelin receptor antagonist and/or phosphodiesterase type 5 inhibitor therapy (the FREEDOM-C study): a randomized controlled trial. *Chest*. 2012;142(6):1383-1390. doi:10.1378/chest.11-2212
295. Simonneau G, Torbicki A, Hoeper MM, et al. Selexipag: An oral, selective prostacyclin receptor agonist for the treatment of pulmonary arterial hypertension. *Eur Respir J*. 2012;40(4):874-880. doi:10.1183/09031936.00137511
296. Olschewski H, Simonneau G, Galie N, et al. Inhaled iloprost for severe pulmonary hypertension. *N Engl J Med*. 2002;347(5):322-329. doi:10.1056/NEJMoa020204
297. Rubin LJ, Mendoza J, Hood M, et al. Treatment of Primary Pulmonary Hypertension with Continuous Intravenous Prostacyclin (Epoprostenol). *Ann Intern Med*. 1990;112(7):485. doi:10.7326/0003-4819-112-7-485
298. McLaughlin V V, Gaine SP, Barst RJ, et al. Efficacy and safety of treprostinil: An Epoprostenol analog for primary pulmonary hypertension. *J Cardiovasc Pharmacol*. 2003;41(2):293-299. doi:10.1097/00005344-200302000-00019
299. Mathier MA, McDevitt S, Saggar R. Subcutaneous treprostinil in pulmonary arterial hypertension: Practical considerations. *J Hear Lung Transpl*. 2010;29(11):1210-1217. doi:10.1016/j.healun.2010.06.013

300. Hoeper MM, Gall H, Seyfarth HJ, et al. Long-term outcome with intravenous iloprost in pulmonary arterial hypertension. *Eur Respir J*. 2009;34(1):132-137. doi:10.1183/09031936.00130408

301. Kamanna VS, Ganji SH, Kashyap ML. The mechanism and mitigation of niacin-induced flushing. *Int J Clin Pract*. 2009;63(9):1369-1377. doi:10.1111/j.1742-1241.2009.02099.x

302. Hohjoh H, Inazumi T, Tsuchiya S, Sugimoto Y. Prostanoid receptors and acute inflammation in skin. *Biochimie*. 2014;107:78-81. doi:10.1016/j.biochi.2014.08.010

303. Cheng K, Wu T-J, Wu KK, et al. Antagonism of the prostaglandin D2 receptor 1 suppresses nicotinic acid-induced vasodilation in mice and humans. *Proc Natl Acad Sci U S A*. 2006;103(17):6682-6687. doi:10.1073/pnas.0601574103

304. Kabashima K, Nagamachi M, Honda T, et al. Prostaglandin E2 is required for ultraviolet B-induced skin inflammation via EP2 and EP4 receptors. *Lab Investig*. 2007;87(1):49-55. doi:10.1038/labinvest.3700491

305. Hohjoh H, Inazumi T, Tsuchiya S, Sugimoto Y. Prostanoid receptors and acute inflammation in skin. *Biochimie*. 2014;107:78-81. doi:10.1016/j.biochi.2014.08.010

306. Corboz MR, Li Z, Malinin V, et al. Preclinical Pharmacology and Pharmacokinetics of Inhaled Hexadecyl-Treprostinil (C16TR), a Pulmonary Vasodilator Prodrug. *J Pharmacol Exp Ther*. 2017;363(3):348-357. doi:10.1124/jpet.117.242099

307. Kurzyna M, Małaczyńska-Rajpold K, Koteja A, et al. An implantable pump Lenus pro® in the treatment of pulmonary arterial hypertension with intravenous treprostinil. *BMC Pulm Med*. 2017;17(1):162. doi:10.1186/s12890-017-0474-7

308. Coghlan JG, Channick R, Chin K, et al. Targeting the Prostacyclin Pathway with Selexipag in Patients with Pulmonary Arterial Hypertension Receiving Double Combination Therapy: Insights from the Randomized Controlled GRIPHON Study. *Am J Cardiovasc Drugs*. 2018;18(1):37-47. doi:10.1007/s40256-017-0262-z

309. Lajoie A-C, Bonnet S, Provencher S. Combination therapy in pulmonary arterial hypertension: recent accomplishments and future challenges. *Pulm Circ*. 2017;7(2):312-325. doi:10.1177/2045893217710639

310. Lajoie AC, Lauziere G, Lega J-C, et al. Combination therapy versus monotherapy for pulmonary arterial hypertension: a meta-analysis. *Lancet Respir Med*. 2016;4(4):291-305. doi:10.1016/s2213-2600(16)00027-8

311. Zhang H, Li X, Huang J, Li H, Su Z, Wang J. Comparative Efficacy and Safety of Prostacyclin Analogs for Pulmonary Arterial Hypertension: A Network Meta-Analysis. *Medicine (Baltimore)*. 2016;95(4):e2575. doi:10.1097/MD.0000000000002575

312. Gaine S, Simonneau G. The need to move from 6-minute walk distance to outcome trials in pulmonary arterial hypertension. *Eur Respir Rev*. 2013;22(130):487-494. doi:10.1183/09059180.00006213

313. Savarese G, Paolillo S, Costanzo P, et al. Do changes of 6-minute walk distance predict clinical events in patients with pulmonary arterial hypertension?: A meta-

analysis of 22 randomized trials. *J Am Coll Cardiol*. 2012;60(13):1192-1201. doi:10.1016/j.jacc.2012.01.083

314. Ryerson CJ, Nayar S, Swiston JR, Sin DD. Pharmacotherapy in pulmonary arterial hypertension: a systematic review and meta-analysis. *Respir Res*. 2010;11. doi:10.1186/1465-9921-11-12
315. Xing X-Q, Han B, Wu X-W, Xiao Y, Wu S-J. Efficacy and safety of prostacyclins therapy in pulmonary arterial hypertension: A meta-analysis. *African J Pharm Pharmacol*. 2011;5(20):2199-2208. doi:10.5897/ajpp11.188
316. Mathai SC, Puhan MA, Lam D, Wise RA. The minimal important difference in the 6-minute walk test for patients with pulmonary arterial hypertension. *Am J Respir Crit Care Med*. 2012;186(5):428-433. doi:10.1164/rccm.201203-0480OC
317. Gabler NB, French B, Strom BL, et al. Validation of 6-minute walk distance as a surrogate end point in pulmonary arterial hypertension trials. *Circulation*. 2012;126(3):349-356. doi:10.1161/CIRCULATIONAHA.112.105890
318. Demir R, Kucukoglu MS. Six-minute walk test in pulmonary arterial hypertension. *Anatol J Cardiol*. 2015;15(3):249-254. doi:10.5152/akd.2015.5834
319. Benza RL, Gomberg-Maitland M, Naeije R, Arneson CP, Lang IM. Prognostic factors associated with increased survival in patients with pulmonary arterial hypertension treated with subcutaneous treprostinil in randomized, placebo-controlled trials. *J Hear Lung Transplant*. 2011;30(9):982-989. doi:10.1016/j.healun.2011.03.011
320. Fritz JS, Blair C, Oudiz RJ, et al. Baseline and Follow-up 6-Min Walk Distance and Brain Natriuretic Peptide Predict 2-Year Mortality in Pulmonary Arterial Hypertension. *Chest*. 2013;143(2):315-323. doi:10.1378/chest.12-0270
321. Zamanian RT, Levine DJ, Bourge RC, et al. An observational study of inhaled-treprostinil respiratory-related safety in patients with pulmonary arterial hypertension. *Pulm Circ*. 2016;6(3):329-337. doi:10.1086/688059
322. Gao X-F, Zhang J-J, Jiang X-M, et al. Targeted drugs for pulmonary arterial hypertension: a network meta-analysis of 32 randomized clinical trials. *Patient Prefer Adherence*. 2017;11:871-885. doi:10.2147/PPA.S133288
323. Liu H, Chen X, Li J, et al. Efficacy and safety of PAH-specific therapy in pulmonary arterial hypertension: a meta-analysis of randomized clinical trials. *Chest*. 2916;150(2):353-366. doi:http://dx.doi.org/10.1016/j.chest.2016.03.031
324. Zhang H, Li X, Huang J, Li H, Su Z, Wang J. Comparative efficacy and safety of prostacyclin analogs for pulmonary arterial hypertension: A network meta-Analysis. *Med (United States)*. 2016;95(4):e2575. doi:10.1097/MD.0000000000002575
325. He G, Massarella J, Ward P. Clinical Pharmacokinetics of the Prodrug Oseltamivir and its Active Metabolite Ro 64-0802. *Clin Pharmacokinet*. 1999;37(6):471-484. doi:10.2165/00003088-199937060-00003
326. Rasheed A, Kumar CKA, Mishra A. Synthesis, hydrolysis studies and phamacodynamic profiles of amide prodrugs of dexibuprofen with amino acids. *J*

Enzyme Inhib Med Chem. 2011;26(5):688-695. doi:10.3109/14756366.2010.548327

327. Nicholas JA, Boster AL, Imitola J, O'Connell C, Racke MK. Design of oral agents for the management of multiple sclerosis: benefit and risk assessment for dimethyl fumarate. *Drug Des Devel Ther*. 2014;8:897-908. doi:10.2147/DDDT.S50962
328. Leu Y-L, Roffler SR, Chern J-W. Design and Synthesis of Water-Soluble Glucuronide Derivatives of Camptothecin for Cancer Prodrug Monotherapy and Antibody-Directed Enzyme Prodrug Therapy (ADEPT). *J Med Chem*. 1999;42(18):3623-3628. doi:10.1021/JM990124Q
329. Mulholland PJ, Ferry DR, Anderson D, et al. Pre-clinical and clinical study of QC12, a water-soluble, pro-drug of quercetin. *Ann Oncol*. 2001;12(2):245-248. doi:10.1023/A:1008372017097
330. Diane E. Gingrich †, Dandu R. Reddy †, Mohamed A. Iqbal †, et al. A New Class of Potent Vascular Endothelial Growth Factor Receptor Tyrosine Kinase Inhibitors: Structure−Activity Relationships for a Series of 9-Alkoxymethyl-12-(3-hydroxypropyl)indeno[2,1-a]pyrrolo[3,4-c]carbazole-5-ones and the Identification of CEP-5214 and Its Dimethylglycine Ester Prodrug Clinical Candidate CEP-7055. 2003. doi:10.1021/JM0301641
331. Marathe PH, Kamath A V., Zhang Y, D'Arienzo C, Bhide R, Fargnoli J. Preclinical pharmacokinetics and in vitro metabolism of brivanib (BMS-540215), a potent VEGFR2 inhibitor and its alanine ester prodrug brivanib alaninate. *Cancer Chemother Pharmacol*. 2009;65(1):55-66. doi:10.1007/s00280-009-1002-0
332. Chan OH, Schmid HL, Stilgenbauer LA, Howson W, Horwell DC, Stewart BH. Evaluation of a Targeted Prodrug Strategy to Enhance Oral Absorption of Poorly Water-Soluble Compounds. *Pharm Res*. 1998;15(7):1012-1018. doi:10.1023/A:1011969808907
333. Ermer JC, Pennick M, Frick G. Lisdexamfetamine Dimesylate: Prodrug Delivery, Amphetamine Exposure and Duration of Efficacy. *Clin Drug Investig*. 2016;36(5):341-356. doi:10.1007/s40261-015-0354-y
334. Lee SH, Gupta MK, Bang JB, Bae H, Sung H-J. Current progress in Reactive Oxygen Species (ROS)-Responsive materials for biomedical applications. *Adv Healthc Mater*. 2013;2(6):908-915.
335. Stella VJ. Prodrugs: Some Thoughts and Current Issues. *J Pharm Sci*. 2010;99(12):4755-4765. doi:10.1002/JPS.22205
336. Chapman RW, Malinin V, Konicek D, et al. Effect of a Lipid Nanoparticle Prodrug Formulation of Treprostinil on the Cough Reflex in Guinea Pigs. In: *American Thoracic Society International Conference Meetings Abstracts*. Denver; 2017:A52.
337. Leifer FG, Konicek D, Li Z, et al. Prolonged Pharmacokinetic Profile of a Prodrug Lipid Nanoparticle Formulation of Treprostinil in Dogs. *Am J Resp Crit Care Med*. 2015;191.
338. Emery CJ, Lal H, Marriott HM, et al. Pulmonary vasodilation by airway delivered prostacyclin analogues, UT-15 & pegylated UT-15. *Thorax*. 2000;55(Suppl 3):A161.

339. United Therapeutics Corps. United Therapeutics Announces Collaboration With Ascendis Pharma To Develop Self-Injectable Treprostinil For Pulmonary Arterial Hypertension | United Therapeutics Corporation. http://ir.unither.com/news-releases/news-release-details/united-therapeutics-announces-collaboration-ascendis-pharma. Published 2012. Accessed April 20, 2018.

340. Stitham J, Stojanovic A, Merenick BL, O'Hara KA, Hwa J. The unique ligand-binding pocket for the human prostacyclin receptor. Site-directed mutagenesis and molecular modeling. *J Biol Chem*. 2003;278(6):4250-4257. doi:10.1074/jbc.M207420200

341. Stitham J, Arehart EJ, Gleim SR, Douville KL, Hwa J. Human prostacyclin receptor structure and function from naturally-occurring and synthetic mutations. *Prostaglandins Other Lipid Mediat*. 2007;82(1-4):95-108. doi:10.1016/j.prostaglandins.2006.05.010

342. Batra H, Guo L. Process of making prostacyclin compounds with linker thiol and pegylated forms. March 2014.

343. Corsair Pharma. Velocity Pharmaceutical Development - We Build Drugs, Not Companies.™. http://www.vpd.net/PFC/Corsair_VPD-380.html. Published 2017. Accessed April 20, 2018.

344. Skonberg C, Olsen J, Madsen KG, Hansen SH, Grillo MP. Metabolic activation of carboxylic acids. *Expert Opin Drug Metab Toxicol*. 2008;4(4):425-438. doi:10.1517/17425255.4.4.425

345. Olsen J, Li C, Skonberg C, et al. Studies on the metabolism of tolmetin to the chemically reactive acyl-coenzyme A thioester intermediate in rats. *Drug Metab Dispos*. 2007;35(5):758-764. doi:10.1124/dmd.106.013334

346. Ammazzalorso A, De Filippis B, Giampietro L, Amoroso R. N-acylsulfonamides: Synthetic routes and biological potential in medicinal chemistry. *Chem Biol Drug Des*. 2017;90(6):1094-1105. doi:10.1111/cbdd.13043

347. Battu S, Pottabathini V. Hydrolytic Degradation Study of Lansoprazole, Identification, Isolation and Characterisation of Base Degradation Product. *Am J Anal Chem*. 2015;06(02):145-155. doi:10.4236/ajac.2015.62013

348. Gong J, Eley T, He B, et al. Characterization of ADME properties of [^{14}C]asunaprevir (BMS-650032) in humans. *Xenobiotica*. 2016;46(1):52-64. doi:10.3109/00498254.2015.1048487

349. Kaufmann P, Okubo K, Bruderer S, et al. Pharmacokinetics and Tolerability of the Novel Oral Prostacyclin IP Receptor Agonist Selexipag. *Am J Cardiovasc Drugs*. 2015;15(3):195-203. doi:10.1007/s40256-015-0117-4

350. European Medicines Agency. *Uptravi: Assessment Report*. London; 2016.

351. Persico FJ, Pritchard JF, Fisher MC, Yorgey K, Wong S, Carson J. Effect of tolmetin glycine amide (McN-4366), a prodrug of tolmetin sodium, on adjuvant arthritis in the rat. *J Pharmacol Exp Ther*. 1988;247(3).

352. Kingman M, Archer-Chicko C, Bartlett M, Beckmann J, Hohsfield R, Lombardi S. Management of prostacyclin side effects in adult patients with pulmonary arterial

hypertension. *Pulm Circ*. 2017;7(3):598-608. doi:10.1177/2045893217719250

353. Valeur E, Bradley M. Amide bond formation: beyond the myth of coupling reagents. *Chem Soc Rev*. 2009;38(2):606-631. doi:10.1039/B701677H
354. Moriarty RM, Rani N, Enache LA, et al. The intramolecular asymmetric Pauson-Khand cyclization as a novel and general stereoselective route to benzindene prostacyclins: synthesis of UT-15 (treprostinil). *J Org Chem*. 2004;69(6):1890-1902. doi:10.1021/jo0347720
355. El-Faham A, Albericio F. Peptide Coupling Reagents, More than a Letter Soup. *Chem Rev*. 2011;111(11):6557-6602. doi:10.1021/cr100048w
356. Lehr P, Winiski A. 1-Benzenesulfonyl-1H-indole derivatives as inhibitors of CCR9 activity. 2008.
357. Montalbetti CAGN, Falque V. Amide bond formation and peptide coupling. *Tetrahedron*. 2005;61(46):10827-10852. doi:10.1016/j.tet.2005.08.031
358. Asaki T, Hamamoto T, Sugiyama Y, Kuwano K, Kuwabara K. Structure–activity studies on diphenylpyrazine derivatives: A novel class of prostacyclin receptor agonists. *Bioorg Med Chem*. 2007;15(21):6692-6704. doi:http://dx.doi.org/10.1016/j.bmc.2007.08.010
359. Lorion MM, Duarte FJS, Calhorda MJ, Oble J, Poli G. Opening the Way to Catalytic Aminopalladation/Proxicyclic Dehydropalladation: Access to Methylidene γ-Lactams. *Org Lett*. 2016;18(5):1020-1023. doi:10.1021/acs.orglett.6b00143
360. Wehrstedt KD, Wandrey PA, Heitkamp D. Explosive properties of 1-hydroxybenzotriazoles. *J Hazard Mater*. 2005;126(1-3):1-7. doi:10.1016/J.JHAZMAT.2005.05.044
361. Larrivée-Aboussafy C, Jones BP, Price KE, et al. DBU Catalysis of N,N′-Carbonyldiimidazole-Mediated Amidations. doi:10.1021/ol9026599
362. Huang S, Connolly PJ, Lin R, Emanuel S, Middleton SA. Synthesis and evaluation of N-acyl sulfonamides as potential prodrugs of cyclin-dependent kinase inhibitor JNJ-7706621. *Bioorg Med Chem Lett*. 2006;16(14):3639-3641. doi:10.1016/J.BMCL.2006.04.071
363. Asaki T, Hamamoto T, Sugiyama Y, Kuwano K, Kuwabara K. Structure–activity studies on diphenylpyrazine derivatives: A novel class of prostacyclin receptor agonists. *Bioorg Med Chem*. 2007;15(21):6692-6704. doi:10.1016/j.bmc.2007.08.010
364. Woodman EK, Chaffey JGK, Hopes PA, Hose DRJ, Gilday JP. *N,N '*-Carbonyldiimidazole-Mediated Amide Coupling: Significant Rate Enhancement Achieved by Acid Catalysis with Imidazole·HCl. *Org Process Res Dev*. 2009;13(1):106-113. doi:10.1021/op800226b
365. Noguchi T, Sekine M, Yokoo Y, Jung S, Imai N. Convenient Preparation of Primary Amides via Activation of Carboxylic Acids with Ethyl Chloroformate and Triethylamine under Mild Conditions. *Chem Lett*. 2013;42(6):580-582. doi:10.1246/cl.130096
366. Bordwell FG, Bartmess JE, Hautala JA. Alkyl effects on equilibrium acidities of carbon acids in protic and dipolar aprotic media and the gas phase. *J Org Chem*.

1978;43(16):3095-3101. doi:10.1021/jo00410a001

367. Han D, Wang B, Jin H, Wang H, Chen M. Design, synthesis and CoMFA studies of OEA derivatives as FAAH inhibitors. *Med Chem Res*. 2017;26(11):2951-2966. doi:10.1007/s00044-017-1995-6
368. Pasha MA, Khan R-R, Shrivatsa N. N-Sulfonylation of amines, imides, amides and anilides using p-TsCl in presence of atomized sodium in EtOH–THF under sonic condition. *Ultrason Sonochem*. 2015;26:15-21. doi:10.1016/J.ULTSONCH.2015.01.018
369. Green TW, Wuts PGM. *Protective Groups in Organic Synthesis*. New York: Wiley-Interscience; 1999.
370. Sprogoe K, Rau H, Hersel U, Wegge T, Keil O, Zettler J. Sustained release composition of prostacyclin for treatment or prevention of pulmonary hypertension andischemic diseases. February 2013.
371. Baker W, Van Veldhuizen J. Inhaled carbaprostacyclin and prostacylin prodrugs for the treatment of pulmonary arterial hypertension. December 2009.
372. Shorr R, Rothblatt M, Bentley, Michael D, Zhao X. Prostaglandin compounds, compositions and methods of treating peripheral vascular disease and pulmonary hypertension. October 2000.
373. Patschinski P, Zhang C, Zipse H. The Lewis Base-Catalyzed Silylation of Alcohols—A Mechanistic Analysis. *J Org Chem*. 2014;79(17):8348-8357. doi:10.1021/jo5016568
374. Eckenberg P, Groth U, Huhn T, Richter N, Schmeck C. A useful application of benzyl trichloroacetimidate for the benzylation of alcohols. *Tetrahedron*. 1993;49(8):1619-1624. doi:10.1016/S0040-4020(01)80349-5
375. Skaanderup PR, Poulsen CS, Hyldtoft L, Jørgensen MR, Madsen R. Regioselective Conversion of Primary Alcohols into Iodides in Unprotected Methyl Furanosides and Pyranosides. *Synthesis (Stuttg)*. 2002;2002(12):1721-1727. doi:10.1055/s-2002-33641
376. Pehlivan L, Métay E, Delbrayelle D, Mignani G, Lemaire M. Synthesis of 3-Substituted Tetrahydrofuran and 4-Substituted Tetrahydropyran Derivatives by Cyclization of Dicarboxylic Acids with InBr3/TMDS. *European J Org Chem*. 2012;2012(25):4689-4693. doi:10.1002/ejoc.201200727
377. Yoshida M, Sekioka N, Izumikawa M, et al. Total Synthesis and Structure Elucidation of JBIR-39: A Linear Hexapeptide Possessing Piperazic Acid and γ-Hydroxypiperazic Acid Residues. *Chem - A Eur J*. 2015;21(7):3031-3041. doi:10.1002/chem.201406020
378. Lopez SS, Dudley GB. Convenient method for preparing benzyl ethers and esters using 2-benzyloxypyridine. *Beilstein J Org Chem*. 2008;4:44. doi:10.3762/bjoc.4.44
379. Tlais SF, Lam H, House SE, Dudley GB. New Strategies for Protecting Group Chemistry: Synthesis, Reactivity, and Indirect Oxidative Cleavage of *para* -Siletanylbenzyl Ethers. *J Org Chem*. 2009;74(5):1876-1885. doi:10.1021/jo802229p
380. Poon KW, House SE, Dudley GB. A Bench-Stable Organic Salt for the Benzylation of

Alcohols. *Synlett*. 2005;2005(20):3142-3144. doi:10.1055/s-2005-921898

381. Pereira CL, Chen Y-H, McDonald FE. Total Synthesis of the Sphingolipid Biosynthesis Inhibitor Fumonisin B $_1$. *J Am Chem Soc*. 2009;131(17):6066-6067. doi:10.1021/ja9009265
382. Lopez SS, Dudley GB. Convenient method for preparing benzyl ethers and esters using 2-benzyloxypyridine. *Beilstein J Org Chem*. 2008;4(1):44. doi:10.3762/bjoc.4.44
383. Ogawa A, Curran DP. Benzotrifluoride: A Useful Alternative Solvent for Organic Reactions Currently Conducted in Dichloromethane and Related Solvents. *J Org Chem*. 1997;62(3):450-451. doi:10.1021/JO9620324
384. Pelletier JC, Hesson DP. A Mild Preparation of Amino Acid N-Acylsulfonamides. *Synlett*. 1995;1995(11):1141-1142. doi:10.1055/s-1995-5219
385. Sarma S Das, Pahari P, Hazarika S, Hazarika P, Borah MJ, Konwar D. Aluminium chloride hexahydrate: an efficient and versatile reagent in organic synthesis. *Arkivoc*. 2013;2013(1):243. doi:10.3998/ark.5550190.p007.863
386. Burwell RL. The Cleavage of Ethers. *Chem Rev*. 1954;54(4):615-685. doi:10.1021/cr60170a003
387. Kokotos G, Feuerherm AJ, Barbayianni E, et al. Inhibition of Group IVA Cytosolic Phospholipase A $_2$ by Thiazolyl Ketones in Vitro, ex Vivo, and in Vivo. *J Med Chem*. 2014;57(18):7523-7535. doi:10.1021/jm500192s
388. Batra H, Moriarty RM. Novel process for the stereoselective synthesis of the drug remodulin (Treprostinil, UT-15) using an intramolecular asymmetric catalytic Pauson-Khand cyclization. *Abstr Pap Am Chem Soc*. 2003;225(1-2):291-MEDI 291.
389. Oslund RC, Cermak N, Gelb MH. Highly Specific and Broadly Potent Inhibitors of Mammalian Secreted Phospholipases A $_2$. *J Med Chem*. 2008;51(15):4708-4714. doi:10.1021/jm800422v
390. Kuwano K, Hashino A, Asaki T, et al. 2-[4-[(5,6-Diphenylpyrazin-2-yl)(isopropyl)amino]butoxy]-N-(methylsulfonyl)acetamide (NS-304), an Orally Available and Long-Acting Prostacyclin Receptor Agonist Prodrug. *J Pharmacol Exp Ther*. 2007;322(3):1181-1188. doi:10.1124/jpet.107.124248
391. Yan K, Gao L-N, Cui Y-L, Zhang Y, Zhou X. The cyclic AMP signaling pathway: Exploring targets for successful drug discovery (Review). *Mol Med Rep*. 2016;13(5):3715-3723. doi:10.3892/mmr.2016.5005
392. Kuwano K, Hashino A, Asaki T, et al. 2-{4-[(5,6-Diphenylpyrazin-2-yl)(isopropyl)amino]butoxy}-N-(methylsulfonyl) acetamide (NS-304), an orally available and long-acting prostacyclin receptor agonist prodrug. *J Pharmacol Exp Ther*. 2007;322(3):1181-1188. doi:10.1124/jpet.107.124248
393. Ackley DC, Rockich KT, Baker TR. Metabolic Stability Assessed by Liver Microsomes and Hepatocytes. In: *Optimization in Drug Discovery*. Totowa, NJ: Humana Press; 2004:151-162. doi:10.1385/1-59259-800-5:151
394. Richardson SJ, Bai A, Kulkarni AA, Moghaddam MF. Efficiency in Drug Discovery:

Liver S9 Fraction Assay As a Screen for Metabolic Stability. *Drug Metab Lett*. 2016;10(2):83-90. doi:10.2174/1872312810666160223121836

395. Tangen O, Jonsson J, Orrenius S. Isolation of rat liver microsomes by gel filtration. *Anal Biochem*. 1973;54(2):597-603. doi:10.1016/0003-2697(73)90392-8
396. Nakajima M, Inoue T, Shimada N, Tokudome S, Yamamoto T, Kuroiwa Y. Cytochrome P450 2C9 Catalyzes IndomethacinO-Demethylation in Human Liver Microsomes. *Drug Metab Dispos*. 1998;26(3).
397. Clozel M, Beharry K, Aranda J V. Indomethacin Metabolism in Liver Microsomes during Postnatal Development in the Rat. *Neonatology*. 1986;50(2):83-90. doi:10.1159/000242572
398. Mathier MA, McDevitt S, Saggar R, al. et. Subcutaneous treprostinil in pulmonary arterial hypertension: Practical considerations. *J Heart Lung Transplant*. 2010;29(11):1210-1217. doi:10.1016/j.healun.2010.06.013
399. CJ E, H L, HM M, et al. Pulmonary vasodilation by airway delivered UT-15, a PGI2 analogue: prolongation by PEGylation [abstract]. *Am J Respir Crit Care*. 2001;163:A540.
400. Heller J, Barr J, Ng SY, Abdellauoi KS, Gurny R. Poly(ortho esters): synthesis, characterization, properties and uses. *Adv Drug Deliv Rev*. 2002;54(7):1015-1039. doi:10.1016/S0169-409X(02)00055-8
401. Samanta S, De Silva CC, Leophairatana P, Koberstein JT. Main-chain polyacetal conjugates with HIF-1 inhibitors: temperature-responsive, pH-degradable drug delivery vehicles. *J Mater Chem B*. 2018;6(4):666-674. doi:10.1039/C7TB01417A
402. Vicent MJ, Tomlinson R, Brocchini S, Duncan R. Polyacetal-diethylstilboestrol: A Polymeric Drug Designed for pH-triggered Activation. *J Drug Target*. 2004;12(8):491-501. doi:10.1080/10611860400011885
403. Tomlinson R, Heller J, Brocchini S, Duncan R. Polyacetal−Doxorubicin Conjugates Designed for pH-Dependent Degradation. *Bioconjug Chem*. 2003;14(6):1096-1106. doi:10.1021/BC030028A
404. Heller J, Penhale DWH, Helwing RF. Preparation of polyacetals by the reaction of divinyl ethers and polyols. *J Polym Sci Polym Lett Ed*. 1980;18(4):293-297. doi:10.1002/pol.1980.130180410
405. Tomlinson R, Klee M, Garrett S, Heller J, Ruth Duncan A, Steve Brocchini. Pendent Chain Functionalized Polyacetals That Display pH-Dependent Degradation: A Platform for the Development of Novel Polymer Therapeutics. *Macromolecules*. 2001;35(2):473-480. doi:10.1021/MA0108867
406. Hunter AC, Moghimi SM. Therapeutic synthetic polymers: a game of Russian roulette? *Drug Discov Today*. 2002;7(19):998-1001. doi:10.1016/S1359-6446(02)02444-3
407. D'souza AA, Shegokar R. Polyethylene glycol (PEG): a versatile polymer for pharmaceutical applications. *Expert Opin Drug Deliv*. 2016;13(9):1257-1275. doi:10.1080/17425247.2016.1182485

408. Patnaik A, Papadopoulos KP, Tolcher AW, et al. Phase I dose-escalation study of EZN-2208 (PEG-SN38), a novel conjugate of poly(ethylene) glycol and SN38, administered weekly in patients with advanced cancer. *Cancer Chemother Pharmacol*. 2013;71(6):1499-1506. doi:10.1007/s00280-013-2149-2

409. Walsh MD, Hanna SK, Sen J, et al. Pharmacokinetics and antitumor efficacy of XMT-1001, a novel, polymeric topoisomerase I inhibitor, in mice bearing HT-29 human colon carcinoma xenografts. *Clin Cancer Res*. 2012;18(9):2591-2602. doi:10.1158/1078-0432.CCR-11-1554

410. Leppert W, Woron J. The role of naloxegol in the management of opioid-induced bowel dysfunction. *Therap Adv Gastroenterol*. 2016;9(5):736-746. doi:10.1177/1756283X16648869

411. Webster R, Didier E, Harris P, et al. PEGylated proteins: evaluation of their safety in the absence of definitive metabolism studies. *Drug Metab Dispos*. 2007;35(1):9-16. doi:10.1124/dmd.106.012419

412. Phillipson EA, Sproule BJ. The Clinical Significance of Elevated Blood Lactate. *Can Med Assoc J*. 1965;92(26):1334-1338.

413. Geldart A, Vitali S, Touma M, Aorons E, Christou H. The effect of acidosis on pulmonary vascular smooth muscle cell metabolic response to hypoxia: implications for Pulmonary Hypertension | The FASEB Journal. *FASEB J*. 2011;25(1).

414. Tomlinson R, Klee M, Garrett S, Heller J, Duncan R, Brocchini S. Pendent Chain Functionalized Polyacetals That Display pH-Dependent Degradation: A Platform for the Development of Novel Polymer Therapeutics. *Macromolecules*. 2001;35(2):473-480. doi:10.1021/MA0108867

415. Hashimoto T, Ishizuka K, Umehara A, Kodaira T. Synthesis of polyacetals with various main-chain structures by the self-polyaddition of vinyl ethers with a hydroxyl function. *J Polym Sci Part A Polym Chem*. 2002;40(22):4053-4064. doi:10.1002/pola.10490

416. Paramonov SE, Bachelder EM, Beaudette TT, et al. Fully Acid-Degradable Biocompatible Polyacetal Microparticles for Drug Delivery. *Bioconjug Chem*. 2008;19(4):911-919. doi:10.1021/bc7004472

417. Lieber CS. Metabolic effects of acetaldehyde. *Biochem Soc Trans*. 1988;16(3):241-247. doi:10.1042/BST0160241

418. Wickramasinghe SN, Hasan R, Pearson JD. A possible acetaldehyde-mediated cardioprotective mechanism. *Alcohol Alcohol*. 1996;31(3):309-311. doi:10.1093/oxfordjournals.alcalc.a008154

419. European Medicines Agency. *Withdrawal Assessment Report for Tyvaso*. London; 2009.

420. Plyduang T, Armiñán A, Movellan J, England RM, Wiwattanapatapee R, Vicent MJ. Polyacetal-Based Combination Therapy for the Treatment of Prostate Cancer. *Macromol Rapid Commun*. July 2018:1800265. doi:10.1002/marc.201800265

421. Miyashita M, Yoshikoshi A, Grieco PA. Pyridinium p-toluenesulfonate. A mild and

efficient catalyst for the tetrahydropyranylation of alcohols. *J Org Chem*. 1977;42(23):3772-3774. doi:10.1021/jo00443a038

422. Gaikwad VL, Bhatia MS. Polymers influencing transportability profile of drug. *Saudi Pharm J*. 2013;21(4):327-335. doi:10.1016/j.jsps.2012.10.003
423. Godwin A, Bolina K, Clochard M, et al. New strategies for polymer development in pharmaceutical science - a short review. *J Pharm Pharmacol*. 2001;53(9):1175-1184. doi:10.1211/0022357011776612
424. Haverstick K, Fleming A, Mark Saltzman W. Conjugation to increase treatment volume during local therapy: a case study with PEGylated camptothecin. *Bioconjug Chem*. 2007;18(6):2115-2121. doi:10.1021/bc700214h
425. Ringsdorf H. Structure and properties of pharmacologically active polymers. *J Polym Sci Polym Symp*. 2007;51(1):135-153. doi:10.1002/polc.5070510111
426. Feng Y, Zhu Z, Chen W, Prabakaran P, Lin K, Dimitrov DS. Conjugates of Small Molecule Drugs with Antibodies and Other Proteins. *Biomedicines*. 2014;2(1):1-13. doi:10.3390/biomedicines2010001
427. Tuder RM, Chacon M, Alger L, et al. Expression of angiogenesis-related molecules in plexiform lesions in severe pulmonary hypertension: evidence for a process of disordered angiogenesis. *J Pathol*. 2001;195(3):367-374. doi:10.1002/path.953
428. Geiger R, Berger RMF, Hess J, Bogers AJJC, Sharma HS, Mooi WJ. Enhanced expression of vascular endothelial growth factor in pulmonary plexogenic arteriopathy due to congenital heart disease. *J Pathol*. 2000;191(2):202-207. doi:10.1002/(SICI)1096-9896(200006)191:2<202::AID-PATH608>3.0.CO;2-D
429. Partovian C, Ladoux A, Eddahibi S, et al. Cardiac and lung VEGF mRNA expression in chronically hypoxic and monocrotaline-treated rats. *Chest*. 1998;114(1 Suppl):45S-46S. doi:10.1378/CHEST.114.1_SUPPLEMENT.45S-A
430. Partovian C, Adnot S, Eddahibi S, et al. Heart and lung VEGF mRNA expression in rats with monocrotaline- or hypoxia-induced pulmonary hypertension. *Am J Physiol Circ Physiol*. 1998;275(6):H1948-H1956. doi:10.1152/ajpheart.1998.275.6.H1948
431. Cramer T, Yamanishi Y, Clausen BE, et al. HIF-1 alpha is essential for myeloid cell-mediated inflammation. *Cell*. 2003;112(5):645-657.
432. Jantsch J, Chakravortty D, Turza N, et al. Hypoxia and hypoxia-inducible factor-1 alpha modulate lipopolysaccharide-induced dendritic cell activation and function. *J Immunol*. 2008;180(7):4697-4705. doi:10.4049/JIMMUNOL.180.7.4697
433. McNamee EN, Korns Johnson D, Homann D, Clambey ET. Hypoxia and hypoxia-inducible factors as regulators of T cell development, differentiation, and function. *Immunol Res*. 2013;55(1-3):58-70. doi:10.1007/s12026-012-8349-8
434. Sakamaki F, Kyotani S, Nagaya N, et al. Increased plasma P-selectin and decreased thrombomodulin in pulmonary arterial hypertension were improved by continuous prostacyclin therapy. *Circulation*. 2000;102(22):2720-2725.
435. Palma C, Bellarosa D, Nardelli F, Mannori G, Manzini S. Constitutive expression of E-

and P-selectin cognate ligands in human endothelial cells. *Mediators Inflamm*. 1998;7(3):211-215. doi:10.1080/09629359891153

436. Schweitzer KM, Dräger AM, van der Valk P, et al. Constitutive expression of E-selectin and vascular cell adhesion molecule-1 on endothelial cells of hematopoietic tissues. *Am J Pathol*. 1996;148(1):165-175.
437. Levy M, Bonnet D, Mauge L, Celermajer DS, Gaussem P, Smadja DM. Circulating Endothelial Cells in Refractory Pulmonary Hypertension in Children: Markers of Treatment Efficacy and Clinical Worsening. *PLoS One*. 2013;8 (6) (no(e65114).
438. Cella G, Bellotto F, Tona F, et al. Plasma Markers of Endothelial Dysfunction in Pulmonary Hypertension. *Chest*. 2001;120(4):1226-1230. doi:10.1378/CHEST.120.4.1226
439. Farha S, Asosingh K, Xu W, et al. Hypoxia-inducible factors in human pulmonary arterial hypertension: a link to the intrinsic myeloid abnormalities. *Blood*. 2011;117(13):3485-3493. doi:10.1182/blood-2010-09-306357
440. Oguz MM, Oguz AD, Sanli C, Cevik A. Serum levels of soluble ICAM-1 in children with pulmonary artery hypertension. *Texas Hear Inst J*. 2014;41(2):159-164. doi:10.14503/THIJ-12-3012
441. Lawson C, Wolf S. ICAM-1 signaling in endothelial cells. *Pharmalogical reports*. 2009;61:22-32.
442. Schermuly RT, Ghofrani HA, Wilkins MR, Grimminger F. Mechanisms of disease: pulmonary arterial hypertension. *Nat Rev Cardiol*. 2011;8(8):443-455. doi:10.1038/nrcardio.2011.87
443. Smadja DM, Mauge L, Sanchez O, et al. Distinct patterns of circulating endothelial cells in pulmonary hypertension. *Eur Respir J*. 2010;36(6):1284-1293. doi:10.1183/09031936.00130809
444. Hargett L, O'Neill K, Yarbrough T, Bauer N. Circulating microparticles from pulmonary arterial hypertension stimulate ICAM-1 and E-selectin expression in pulmonary artery endothelial cells. In: *Physiology*. Vol 27. FASEB; 2014:1090.6. doi:10.1007/s10409-011-0511-3
445. Firer MA, Gellerman G. Targeted drug delivery for cancer therapy: the other side of antibodies. *J Hematol Oncol*. 2012;5:70. doi:10.1186/1756-8722-5-70
446. Kovtun Y V., Goldmacher VS. Cell killing by antibody–drug conjugates. *Cancer Lett*. 2007;255(2):232-240. doi:10.1016/J.CANLET.2007.04.010
447. Lau JL, Dunn MK. Therapeutic peptides: Historical perspectives, current development trends, and future directions. *Bioorg Med Chem*. 2018;26(10):2700-2707. doi:10.1016/J.BMC.2017.06.052
448. Tang S-C, Kumthekar P, Brenner AJ, et al. ANG1005, a novel peptide-paclitaxel conjugate crosses the BBB and shows activity in patients with recurrent CNS metastasis from breast cancer, results from a phase II clinical study. *Ann Oncol*. 2016;27(suppl_6). doi:10.1093/annonc/mdw367.02

449. Kurzrock R, Gabrail N, Chandhasin C, et al. Safety, pharmacokinetics, and activity of GRN1005, a novel conjugate of angiopep-2, a peptide facilitating brain penetration, and paclitaxel, in patients with advanced solid tumors. *Mol Cancer Ther*. 2012;11(2):308-316. doi:10.1158/1535-7163.MCT-11-0566

450. Vrettos EI, Mező G, Tzakos AG. On the design principles of peptide-drug conjugates for targeted drug delivery to the malignant tumor site. *Beilstein J Org Chem*. 2018;14:930-954. doi:10.3762/bjoc.14.80

451. Shamay Y, Raviv L, Golan M, Voronov E, Apte RN, David A. Inhibition of primary and metastatic tumors in mice by E-selectin-targeted polymer–drug conjugates. *J Control Release*. 2015;217:102-112. doi:10.1016/J.JCONREL.2015.08.029

452. Järvinen TAH, Ruoslahti E. Molecular changes in the vasculature of injured tissues. *Am J Pathol*. 2007;171(2):702-711. doi:10.2353/ajpath.2007.061251

453. Urakami T, Järvinen TAH, Toba M, et al. Peptide-directed highly selective targeting of pulmonary arterial hypertension. *Am J Pathol*. 2011;178(6):2489-2495. doi:10.1016/j.ajpath.2011.02.032

454. VBS pharmaceuticals. CAR peptide technology. http://vascularbiosciences.com/products-services/vbs-pharmaceuticals/technology/. Published 2015. Accessed October 19, 2015.

455. Mann D. Hypothesized Mechanism Of Action And Putative Receptor For The Pulmonary Hypertensive Homing Peptide CARSKNKDC (CAR) (ATS Journals). *Am Thorac Soc Int Conf Meet Abstr*. 2013;A52.

456. Toba M, Alzoubi A, O'Neill K, et al. A novel vascular homing peptide strategy to selectively enhance pulmonary drug efficacy in pulmonary arterial hypertension. *Am J Pathol*. 2014;184(2):369-375. doi:10.1016/j.ajpath.2013.10.008

457. Gupta N, Patel B, Nahar K, Ahsan F. Cell permeable peptide conjugated nanoerythrosomes of fasudil prolong pulmonary arterial vasodilation in PAH rats. *Eur J Pharm Biopharm*. 2014;88(3):1046-1055. doi:10.1016/j.ejpb.2014.10.012

458. Nahar K, Absar S, Gupta N, et al. Peptide-coated liposomal fasudil enhances site specific vasodilation in pulmonary arterial hypertension. *Mol Pharm*. 2014;11(12):4374-4384. doi:10.1021/mp500456k

459. Jain N, Smith SW, Ghone S, Tomczuk B. Current ADC Linker Chemistry. *Pharm Res*. 2015;32(11):3526-3540. doi:10.1007/s11095-015-1657-7

460. Filipovska A, Rackham O. Specialization from synthesis: How ribosome diversity can customize protein function. *FEBS Lett*. 2013;587(8):1189-1197. doi:10.1016/J.FEBSLET.2013.02.032

461. Suzuki T, Yamazaki T, Yazaki Y. The role of the natriuretic peptides in the cardiovascular system. *Cardiovasc Res*. 2001;51(3):489-494. doi:10.1016/S0008-6363(01)00238-3

462. Klein JD. Corin: an ANP protease that may regulate sodium reabsorption in nephrotic syndrome. *Kidney Int*. 2010;78(7):635-637. doi:10.1038/ki.2010.223

463. Spichalska B, Lesner A, Wysocka M, et al. The influence of substrate peptide length on human beta-tryptase specificity. *J Pept Sci*. 2008;14(8):917-923. doi:10.1002/psc.1026

464. Manafi M. Fluorogenic and chromogenic enzyme substrates in culture media and identification tests. *Int J Food Microbiol*. 1996;31(1-3):45-58. doi:10.1016/0168-1605(96)00963-4

465. Maxová H, Herget J, Vízek M. Lung mast cells and hypoxic pulmonary hypertension. *Physiol Res*. 2012;61(1):1-11.

466. Hallgren J, Pejler G. Biology of mast cell tryptase. An inflammatory mediator. *FEBS J*. 2006;273(9):1871-1895. doi:10.1111/j.1742-4658.2006.05211.x

467. Khan NM, Kapahi H, Kumar S, Bhardwaj TR, Arora S, Mishra N. Role of polymer–drug conjugates in organ-specific delivery systems. *J Drug Target*. 2015;23(5):387-416. doi:10.3109/1061186X.2015.1016436

468. Perrino E, Steiner M, Krall N, et al. Curative properties of noninternalizing antibody-drug conjugates based on maytansinoids. *Cancer Res*. 2014;74(9):2569-2578. doi:10.1158/0008-5472.CAN-13-2990

469. Gébleux R, Stringhini M, Casanova R, Soltermann A, Neri D. Non-internalizing antibody-drug conjugates display potent anti-cancer activity upon proteolytic release of monomethyl auristatin E in the subendothelial extracellular matrix. *Int J Cancer*. 2017;140(7):1670-1679. doi:10.1002/ijc.30569

470. Subr V, Strohalm J, Ulbrich K, Duncan R, Hume IC. Polymers containing enzymatically degradable bonds, XII. Effect of spacer structure on the rate of release of daunomycin and adriamycin from poly [N-(2-hydroxypropyl)-methacrylamide] copolymer drag carriers in vitro and antitumour activity measured in vivo. *J Control Release*. 1992;18(2):123-132. doi:10.1016/0168-3659(92)90181-P

471. Pauli J, Licha K, Berkemeyer J, et al. New Fluorescent Labels with Tunable Hydrophilicity for the Rational Design of Bright Optical Probes for Molecular Imaging. *Bioconjug Chem*. 2013;24(7):1174-1185. doi:10.1021/bc4000349

472. Hermanson GT, Hermanson GT. (Strept)avidin–Biotin Systems. *Bioconjugate Tech*. January 2013:465-505. doi:10.1016/B978-0-12-382239-0.00011-X

473. Bogdanowich-Knipp SJ, Chakrabarti S, Siahaan TJ, Williams TD, Dillman RK. Solution stability of linear vs. cyclic RGD peptides. *J Pept Res*. 1999;53(5):530-541. doi:10.1034/j.1399-3011.1999.00052.x

474. Augustyns K, Kraas W, Jung G. Investigation on the stability of the Dde protecting group used in peptide synthesis: migration to an unprotected lysine1. *J Pept Res*. 2009;51(2):127-133. doi:10.1111/j.1399-3011.1998.tb00630.x

475. Wilhelm RR, Srinivasan A, Schmidt MA. Evaluation of ivDde as a quasi-orthogonal protecting group for Fmoc solid-phase peptide synthesis. In: *Peptides for the New Millennium*. Dordrecht: Kluwer Academic Publishers; :58-59. doi:10.1007/0-306-46881-6_19

476. Zheng Y, Ji S, Czerwinski A, Valenzuela F, Pennington M, Liu S. FITC-Conjugated Cyclic RGD Peptides as Fluorescent Probes for Staining Integrin $\alpha_v\beta_3$ /$\alpha_v\beta_5$ in Tumor Tissues. *Bioconjug Chem*. 2014;25(11):1925-1941. doi:10.1021/bc500452y

477. Juan Jose Díaz-Mochón, Laurent Bialy and, Bradley* M. Full Orthogonality between Dde and Fmoc: The Direct Synthesis of PNA−Peptide Conjugates. 2004. doi:10.1021/OL049905Y

478. Behrendt R, White P, Offer J. Advances in Fmoc solid-phase peptide synthesis. *J Pept Sci*. 2016;22(1):4-27. doi:10.1002/psc.2836

479. Laakkonen P, Akerman ME, Biliran H, et al. Antitumor activity of a homing peptide that targets tumor lymphatics and tumor cells. *Proc Natl Acad Sci U S A*. 2004;101(25):9381-9386. doi:10.1073/pnas.0403317101

480. Jullian M, Hernandez A, Maurras A, et al. N-terminus FITC labeling of peptides on solid support: the truth behind the spacer. *Tetrahedron Lett*. 2009;50(3):260-263. doi:10.1016/J.TETLET.2008.10.141

481. Tsonopoulos C, Coulson DM, Inman LB. Ionization constants of water pollutants. *J Chem Eng Data*. 1976;21(2):190-193. doi:10.1021/je60069a008

482. Poole LB. The basics of thiols and cysteines in redox biology and chemistry. *Free Radic Biol Med*. 2015;80:148-157. doi:10.1016/j.freeradbiomed.2014.11.013

483. Kamber B, Hartmann A, Eisler K, et al. The Synthesis of Cystine Peptides by Iodine Oxidation ofS-Trityl-cysteine andS-Acetamidomethyl-cysteine Peptides. *Helv Chim Acta*. 1980;63(4):899-915. doi:10.1002/hlca.19800630418

484. Lamthanh H, Virelizier H, Frayssinhes D. Side reaction of S-to-N acetamidomethyl shift during disulfide bond formation by iodine oxidation of S-acetamidomethyl-cysteine in a glutamine-containing peptide. *Pept Res*. 8(6):316-320.

485. Nishino N, Mihara H, Izumi N, Fujimoto T, Ando S, Ohba M. Disulfide cyclization of protected peptide assembled on oxime resin. *Tetrahedron Lett*. 1993;34(8):1295-1298. doi:10.1016/S0040-4039(00)91778-7

486. Albericio F, Hammer RP, García-Echeverría C, et al. Cyclization of disulfide-containing peptides in solid-phase synthesis. *Int J Pept Protein Res*. 1991;37(5):402-413.

487. Wang X-Y, Wang Q, Huang X-Y, Wang T, Yu X-Q. Synthesis of small cyclic peptides containing disulfide bonds. *Arkivoc*. 2006;2006(11):148. doi:10.3998/ark.5550190.0007.b14

488. Popa C, Netea MG, van Riel PLCM, van der Meer JWM, Stalenhoef AFH. The role of TNF-alpha in chronic inflammatory conditions, intermediary metabolism, and cardiovascular risk. *J Lipid Res*. 2007;48(4):751-762. doi:10.1194/jlr.R600021-JLR200

489. Bradley J. TNF-mediated inflammatory disease. *J Pathol*. 2008;214(2):149-160. doi:10.1002/path.2287

490. Kim CW, Song H, Kumar S, et al. Anti-inflammatory and antiatherogenic role of BMP receptor II in endothelial cells. *Arterioscler Thromb Vasc Biol*. 2013;33(6):1350-1359. doi:10.1161/ATVBAHA.112.300287

491. Li X, Wang H, Yang C, Zhang X, Han D, Wang H. Fluoxetine inhibited extracellular matrix of pulmonary artery and inflammation of lungs in monocrotaline-treated rats. *Acta Pharmacol Sin*. 2011;32(2):217-222. doi:10.1038/aps.2010.187

492. Soon E, Holmes AM, Treacy CM, et al. Elevated levels of inflammatory cytokines predict survival in idiopathic and familial pulmonary arterial hypertension. *Circulation*. 2010;122(9):920-927. doi:10.1161/CIRCULATIONAHA.109.933762

493. Itoh T, Nagaya N, Ishibashi-Ueda H, et al. Increased plasma monocyte chemoattractant protein-1 level in idiopathic pulmonary arterial hypertension. *Respirology*. 2006;11(2):158-163. doi:10.1111/j.1440-1843.2006.00821.x

494. Fujita M, Shannon JM, Irvin CG, et al. Overexpression of tumor necrosis factor-α produces an increase in lung volumes and pulmonary hypertension. *Am J Physiol Cell Mol Physiol*. 2001;280(1):L39-L49. doi:10.1152/ajplung.2001.280.1.L39

495. Zhang L, Lu J, Li M, Wang Q, Zeng X. Preventive and remedial application of etanercept attenuate monocrotaline-induced pulmonary arterial hypertension. *Int J Rheum Dis*. 2016;19(2):192-198. doi:10.1111/1756-185X.12304

496. Hurst LA, Dunmore BJ, Long L, et al. TNFα drives pulmonary arterial hypertension by suppressing the BMP type-II receptor and altering NOTCH signalling. *Nat Commun*. 2017;8:14079. doi:10.1038/ncomms14079

497. Price LC, Caramori G, Perros F, et al. Nuclear factor κ-B is activated in the pulmonary vessels of patients with end-stage idiopathic pulmonary arterial hypertension. *PLoS One*. 2013;8(10):e75415. doi:10.1371/journal.pone.0075415

498. Esposito E, Cuzzocrea S. TNF-Alpha as a Therapeutic Target in Inflammatory Diseases, Ischemia- Reperfusion Injury and Trauma. *Curr Med Chem*. 2009;16(24):3152-3167. doi:10.2174/092986709788803024

499. Wang Q, Zuo X, Wang Y, Xie W, Wang H, Zhang M. Monocrotaline-induced pulmonary arterial hypertension is attenuated by TNF-α antagonists via the suppression of TNF-α expression and NF-κB pathway in rats. *Vascul Pharmacol*. 2013;58(1-2):71-77. doi:10.1016/J.VPH.2012.07.006

500. Kofford MW, Schwartz LB, Schechter NM, Yager DR, Diegelmann RF, Graham MF. Cleavage of type I procollagen by human mast cell chymase initiates collagen fibril formation and generates a unique carboxyl-terminal propeptide. *J Biol Chem*. 1997;272(11):7127-7131.

501. Cairns JA. Mast cell tryptase and its role in tissue remodelling. *Clin Exp Allergy*. 1998;28(12):1460-1463. doi:10.1046/j.1365-2222.1998.00467.x

502. Lee HY, Jiang X, Lee D. Kinetics of Self-Immolation: Faster Signal Relay over a Longer Linear Distance? *Org Lett*. 2009;11(10):2065-2068. doi:10.1021/ol900433g

503. Alouane A, Labruère R, Le Saux T, et al. Light Activation for the Versatile and Accurate Kinetic Analysis of Disassembly of Self-Immolative Spacers. *Chem - A Eur J*. 2013;19(35):11717-11724. doi:10.1002/chem.201301298

504. de Groot FMH, Loos WJ, Koekkoek R, et al. Elongated Multiple Electronic Cascade

and Cyclization Spacer Systems in Activatible Anticancer Prodrugs for Enhanced Drug Release. 2001. doi:10.1021/JO0158884

505. Erez R, Shabat D. The azaquinone-methide elimination: comparison study of 1,6- and 1,4-eliminations under physiological conditions. *Org Biomol Chem*. 2008;6(15):2669. doi:10.1039/b808198k
506. Senter PD, Pearce WE, Greenfield RS. Development of a drug-release strategy based on the reductive fragmentation of benzyl carbamate disulfides. *J Org Chem*. 1990;55(9):2975-2978. doi:10.1021/jo00296a082
507. Avital-Shmilovici M, Shabat D. Dendritic chain reaction: Responsive release of hydrogen peroxide upon generation and enzymatic oxidation of methanol. *Bioorg Med Chem*. 2010;18(11):3643-3647. doi:10.1016/J.BMC.2010.02.038
508. Weinstain R, Segal E, Satchi-Fainaro R, Shabat D. Real-time monitoring of drug release. *Chem Commun*. 2010;46(4):553-555. doi:10.1039/B919329D
509. DeWit MA, Gillies ER. Design, synthesis, and cyclization of 4-aminobutyric acid derivatives: potential candidates as self-immolative spacers. *Org Biomol Chem*. 2011;9(6):1846. doi:10.1039/c0ob00890g
510. DeWit MA, Gillies ER. A Cascade Biodegradable Polymer Based on Alternating Cyclization and Elimination Reactions. *J Am Chem Soc*. 2009;131(51):18327-18334. doi:10.1021/ja905343x
511. de Gracia Lux C, McFearin CL, Joshi-Barr S, Sankaranarayanan J, Fomina N, Almutairi A. A Single UV or Near IR Triggering Event Leads to Polymer Degradation into Small Molecules. *ACS Macro Lett*. 2012;1(7):922-926. doi:10.1021/mz3002403
512. de Groot FMH, Albrecht C, Koekkoek R, Beusker PH, Scheeren HW. “Cascade-Release Dendrimers” Liberate All End Groups upon a Single Triggering Event in the Dendritic Core. *Angew Chemie Int Ed*. 2003;42(37):4490-4494. doi:10.1002/anie.200351942
513. Dewit MA, Beaton A, Gillies ER. A reduction sensitive cascade biodegradable linear polymer. *J Polym Sci Part A Polym Chem*. 2010;48(18):3977-3985. doi:10.1002/pola.24180
514. Zhu Q, Li DB, Uttamchandani M, Yao SQ. Facile synthesis of 7-amino-4-carbamoylmethylcoumarin (ACC)-containing solid supports and Their corresponding fluorogenic protease substrates. *Bioorg Med Chem Lett*. 2003;13(6):1033-1036. doi:10.1016/S0960-894X(03)00087-8
515. Lu G, Mojsov S, Tam JP, Merrifield RB. Improved synthesis of 4-alkoxybenzyl alcohol resin. *J Org Chem*. 1981;46(17):3433-3436. doi:10.1021/jo00330a009
516. Harris JL, Backes BJ, Leonetti F, Mahrus S, Ellman JA, Craik CS. Rapid and general profiling of protease specificity by using combinatorial fluorogenic substrate libraries. *Proc Natl Acad Sci U S A*. 2000;97(14):7754-7759. doi:10.1073/pnas.140132697
517. Fields CG, Lloyd DH, Macdonald RL, Otteson KM, Noble RL. HBTU activation for automated Fmoc solid-phase peptide synthesis. *Pept Res*. 4(2):95-101.

518. Zhu Q, Li DB, Uttamchandani M, Yao SQ. Facile synthesis of 7-amino-4-carbamoylmethylcoumarin (ACC)-containing solid supports and Their corresponding fluorogenic protease substrates. *Bioorg Med Chem Lett*. 2003;13(6):1033-1036. doi:10.1016/S0960-894X(03)00087-8

519. Fields GB, Fields GB. Introduction to peptide synthesis. *Curr Protoc protein Sci*. 2002;Chapter 18:Unit 18.1. doi:10.1002/0471140864.ps1801s26

520. Long K, Edwards TA, Wilson AJ. Microwave assisted solid phase synthesis of highly functionalized N-alkylated oligobenzamide α-helix mimetics. *Bioorg Med Chem*. 2013;21(14):4034-4040. doi:10.1016/j.bmc.2012.09.053

521. Ahmed F. Abdel-Magid *, Kenneth G. Carson, Bruce D. Harris, Cynthia A. Maryanoff and, Shah RD. Reductive Amination of Aldehydes and Ketones with Sodium Triacetoxyborohydride. Studies on Direct and Indirect Reductive Amination Procedures1. 1996. doi:10.1021/JO960057X

522. Sociedad Química de México. D, Sepehraddin F. *Revista de La Sociedad Química de México.* Vol 58. Sociedad Química de México; 2014.

523. Gribble GW, Nutaitis CF. Sodium borohydride in carboxylic acid media. A review of the synthetic utility of acyloxyborohydrides. *Org Prep Proced Int*. 1985;17(4-5):317-384. doi:10.1080/00304948509355522

524. Gribble GW, Ferguson DC. Reactions of sodium borohydride in acidic media. Selective reduction of aldehydes with sodium triacetoxyborohydride. *J Chem Soc Chem Commun*. 1975;0(13):535. doi:10.1039/c39750000535

525. Nutaitis CF, Gribble GW. Chemoselective reduction of aldehydes with tetra-n-butylammonium triacetoxyborohydride. *Tetrahedron Lett*. 1983;24(40):4287-4290. doi:10.1016/S0040-4039(00)88322-7

526. Borch RF, Durst HD. Lithium cyanohydridoborate, a versatile new reagent. *J Am Chem Soc*. 1969;91(14):3996-3997. doi:10.1021/ja01042a078

527. Vázquez J, Albericio F. A useful and sensitive color test to monitor aldehydes on solid-phase. *Tetrahedron Lett*. 2001;42(38):6691-6693. doi:10.1016/S0040-4039(01)01372-7

528. Boas U, Mirsharghi S. Color Test for Selective Detection of Secondary Amines on Resin and in Solution. *Org Lett*. 2014;16(22):5918-5921. doi:10.1021/ol502936d

529. Gaggini F, Porcheddu A, Reginato G, Rodriquez M, Taddei A. Colorimetric Tools for Solid-Phase Organic Synthesis. *J Comb Chem,*. 2004;6(5):805-810. doi:10.1021/CC049963A

530. Merck Millipore. Application 2-9. In: *Novabiochem Peptide Synthesis*. ; 2014:2.40.

531. Merck Millipore. Method 2-15: Reductive amination of formyl resins. In: *Novabiochem Peptide Synthesis*. ; 2014:2.40.

532. Lane C. Sodium Cyanoborohydride - A Highly Selective Reducing Agent for Organic Functional Groups. *Synthesis (Stuttg)*. 1975;03:135-146. doi:10.1055/s-1975-23685

533. Maly DJ, Leonetti F, Backes BJ, et al. Expedient Solid-Phase Synthesis of Fluorogenic

Protease Substrates Using the 7-Amino-4-carbamoylmethylcoumarin (ACC) Fluorophore. *J Org ChemOrg Chem*. 2002;67(3):910-915. doi:10.1021/JO016140O

534. Merck Millipore. Novabiochem Peptide Sythesis. In: Merck KGaA; 2014:2.40 Method 2-15.
535. Mirsharghi S, Knudsen KD, Bagherifam S, Nyström B, Boas U. Preparation and self-assembly of amphiphilic polylysine dendrons. *New J Chem*. 2016;40(4):3597-3611. doi:10.1039/C5NJ02690C
536. Ede NJ, Ang KH, James IW, Bray AM. Incorporation of 2-hydroxy-4-methoxybenzyl protection during peptide synthesis via reductive alkylation on the solid phase. *Tetrahedron Lett*. 1996;37(50):9097-9100. doi:10.1016/S0040-4039(96)02095-3
537. Abdallah Hamzé, Jean Martinez and, Hernandez* J-F. Solid-Phase Synthesis of Arginine-Containing Peptides and Fluorogenic Substrates Using a Side-Chain Anchoring Approach. 2004. doi:10.1021/JO048792T
538. Scheuerman RA, Tumelty D. The reduction of aromatic nitro groups on solid supports using sodium hydrosulfite (Na2S2O4). *Tetrahedron Lett*. 2000;41(34):6531-6535. doi:10.1016/S0040-4039(00)00959-X
539. Poreba M, Mihelic M, Krai P, et al. Unnatural amino acids increase activity and specificity of synthetic substrates for human and malarial cathepsin C. *Amino Acids*. 2014;46(4):931-943. doi:10.1007/s00726-013-1654-2
540. Kuisle O, Lolo M, Quiñoá E, Riguera R. Monitoring the solid-phase synthesis of depsides and depsipeptides. A color test for hydroxyl groups linked to a resin. *Tetrahedron*. 1999;55(51):14807-14812. doi:10.1016/S0040-4020(99)00945-X
541. Bunin BA, Bunin BA. Combinatorial solid-phase synthesis. In: *The Combinatorial Index*. Elsevier; 1998:77-212. doi:10.1016/B978-012141340-8/50005-1
542. Park KK, Oh CH, Joung WK. Sodium dithionite reduction of nitroarenes using viologen as an electron phase-transfer catalyst. *Tetrahedron Lett*. 1993;34(46):7445-7446. doi:10.1016/S0040-4039(00)60148-X
543. Park KK, Oh CH, Sim W-J. Chemoselective Reduction of Nitroarenes and Nitroalkanes by Sodium Dithionite Using Octylviologen as an Electron Transfer Catalyst. *J Org Chem*. 1995;60(19):6202-6204. doi:10.1021/jo00124a043
544. Merck Millipore. 3.8 Fmoc resin cleavage and deprotection. In: *Novabiochem Peptide Synthesis*. ; 2014:3.29.
545. Merck Millipore. Method 3-30. In: *Novabiochem Peptide Synthesis*. ; 2014:3.30.
546. Palladino P, Stetsenko DA. New TFA-Free Cleavage and Final Deprotection in Fmoc Solid-Phase Peptide Synthesis: Dilute HCl in Fluoro Alcohol. *Org Lett*. 2012;14(24):6346-6349. doi:10.1021/ol303124r
547. SteadyMed Therapeutics Inc. SteadyMed Trevyent. https://www.steadymed.com/portfolio/trevyent. Accessed September 21, 2018.
548. Morris M, Phares K, Zaccardelli D, Ujhelyi MR. A novel catheter system for totally implantable intravenous drug therapy: assessment of catheter function and patency

with trepostinil therapy. *J Vasc Access*. 2008;9(1):20-27.

549. Medtronic Plc. Medtronic Receives FDA Approval for Implantable System for Remodulin® to Treat Patients with Pulmonary Arterial Hypertension. GlobeNewswire. https://globenewswire.com/news-release/2018/07/31/1544416/0/en/Medtronic-Receives-FDA-Approval-for-Implantable-System-for-Remodulin-to-Treat-Patients-with-Pulmonary-Arterial-Hypertension.html. Published 2018. Accessed September 21, 2018.
550. MannKind Corp. MannKind Successfully Completes Phase 1 Trial of Treprostinil Technosphere for Pulmonary Arterial Hypertension Advancing Development to Next Phase. http://investors.mannkindcorp.com/news-releases/news-release-details/mannkind-successfully-completes-phase-1-trial-treprostinil. Published 2018. Accessed September 21, 2018.
551. Moher D, Liberati A, Tetzlaff J, Altman DG. Preferred Reporting Items for Systematic Reviews and Meta-Analyses: The PRISMA Statement. *Ann Intern Med*. 2009;151(4):264. doi:10.7326/0003-4819-151-4-200908180-00135
552. Moher D, Shamseer L, Clarke M, et al. Preferred reporting items for systematic review and meta-analysis protocols (PRISMA-P) 2015 statement. *Syst Rev*. 2015;4(1):1. doi:10.1186/2046-4053-4-1
553. Liu H-L, Chen X-Y, Li J-R, et al. Efficacy and Safety of Pulmonary Arterial Hypertension-specific Therapy in Pulmonary Arterial Hypertension: A Meta-analysis of Randomized Controlled Trials. *Chest*. 2016;150(2):353-366. doi:10.1016/j.chest.2016.03.031
554. Deeks JJ, Higgins JP, Altman DG. Analysing Data and Undertaking Meta-Analyses. In: *Cochrane Handbook for Systematic Reviews of Interventions*. Chichester, UK: John Wiley & Sons, Ltd; :243-296. doi:10.1002/9780470712184.ch9
555. ATS Statement: Guidelines for the Six-Minute Walk Test. *Am J Respir Crit Care Med*. 2002;166(1):111-117. doi:10.1164/ajrccm.166.1.at1102
556. DerSimonian R, Laird N. Meta-analysis in clinical trials. *Control Clin Trials*. 1986;7(3):177-188. doi:10.1016/0197-2456(86)90046-2
557. Riley RD, Higgins JPT, Deeks JJ. Interpretation of random effects meta-analyses. *BMJ*. 2011;342:d549. doi:10.1136/BMJ.D549
558. Greenland S, Robins JM. Estimation of a common effect parameter from sparse follow-up data. *Biometrics*. 1985;41(1):55-68.
559. Mantel N, Haenszel W. Statistical Aspects of the Analysis of Data From Retrospective Studies of Disease. *JNCI J Natl Cancer Inst*. 1959;22(4):719-748. doi:10.1093/jnci/22.4.719
560. Faraone S V. Interpreting Estimates of Treatment Effects: Implications for Managed Care. *Pharm Ther*. 2008;33(12):700.
561. Cohen J. *Statistical Power Analysis for the Behavioral Sciences*. 2nd ed. Hillsdale, N.J.: L. Erlbaum Associates; 1988.

562. Higgins JPT, Thompson SG, Deeks JJ, Altman DG. Measuring inconsistency in meta-analyses. *BMJ*. 2003;327(7414):557-560. doi:10.1136/bmj.327.7414.557

563. Higgins JPT, Thompson SG. Quantifying heterogeneity in a meta-analysis. *Stat Med*. 2002;21(11):1539-1558. doi:10.1002/sim.1186

564. Fragkos KC, Tsagris M, Frangos CC. Publication Bias in Meta-Analysis: Confidence Intervals for Rosenthal's Fail-Safe Number. *Int Sch Res Not*. 2014;2014:825383. doi:10.1155/2014/825383

565. Falcetti E, Flavell DM, Staels B, Tinker A, Haworth SG, Clapp LH. IP receptor-dependent activation of PPARgamma by stable prostacyclin analogues. *Biochem Biophys Res Commun*. 2007;360(4):821-827. doi:10.1016/j.bbrc.2007.06.135

566. Kaiser E, Colescott RL, Bossinger CD, Cook PI. Color test for detection of free terminal amino groups in the solid-phase synthesis of peptides. *Anal Biochem*. 1970;34(2):595-598. doi:10.1016/0003-2697(70)90146-6

567. Vázquez J, Qushair G, Albericio F. Qualitative Colorimetric Tests for Solid Phase Synthesis. *Methods Enzymol*. 2003;369:21-35. doi:10.1016/S0076-6879(03)69002-6

568. Christensen T, Eriksson A, Thornell L-E. A Qualitative Test for Monitoring Coupling Completeness in Solid Phase Peptide Synthesis Using Chloranil. *Acta Chem Scand*. 1979;33b:763-766. doi:10.3891/acta.chem.scand.33b-0763

569. Shabab M, Arnold MFF, Penterman J, et al. Disulfide cross-linking influences symbiotic activities of nodule peptide NCR247. *Proc Natl Acad Sci U S A*. 2016;113(36):10157-10162. doi:10.1073/pnas.1610724113

570. Mirsharghi S, Knudsen KD, Bagherifam S, Nyström B, Boas U. Preparation and self-assembly of amphiphilic polylysine dendrons. *New J Chem*. 2016;40(4):3597-3611. doi:10.1039/C5NJ02690C

571. Südkamp B, Meise W. Zur Aminolyse von Phthaliden. *Arch Pharm (Weinheim)*. 1985;318(7):640-648. doi:10.1002/ardp.19853180713

572. Lesimple P, Bigg DCH. Aluminum Chloride Mediated Aminolysis of Lactones: A General Method for the Preparation of ω-Hydroxyalkylamides. *Synthesis (Stuttg)*. 1991;1991(04):306-308. doi:10.1055/s-1991-26451

573. Maltese M. Reductive Demercuration in Deprotection of Trityl Thioethers, Trityl Amines, and Trityl Ethers. 2001. doi:10.1021/JO0156971

574. Yus M, Behloul C, Guijarro D. Detritylation Procedure under Non-Acidic Conditions: Naphthalene Catalysed- Reductive Cleavage of Trityl Ethers. *Synthesis (Stuttg)*. 2003;2003(14):2179-2184. doi:10.1055/s-2003-41057

575. Di Marzo V, Ligresti A, Morera E, Nalli M, Ortar G. The anandamide membrane transporter. Structure–activity relationships of anandamide and oleoylethanolamine analogs with phenyl rings in the polar head group region. *Bioorg Med Chem*. 2004;12(19):5161-5169. doi:10.1016/J.BMC.2004.07.026

576. He S, Dong G, Wang Z, et al. Discovery of Novel Multiacting Topoisomerase I/II and Histone Deacetylase Inhibitors. *ACS Med Chem Lett*. 2015;6(3):239-243.

doi:10.1021/ml500327q

577. KHARASCH MS, WEINHOUSE S. GRIGNARD REAGENTS—THEIR REDUCING ACTION AND RATES OF ADDITION *. *J Org Chem*. 1936;01(2):209-230. doi:10.1021/jo01231a011

Chapter 8. **Appendix**

8.1 **Meta-Analysis**

Table 8-1. Adverse events associated with treprostinil

AE	Overall OR	p-value	No. studies	Oral	Inhaled	IV	SC
Any event	**10.3** (1.1-92.8) 51%, 0.128	0.038	3	26.2 5.1, 135.4 0%,	-	0.7 0.1, 17.7 -	-
Site pain	**8.7** 1.6, 45.9 79%, 0.003	0.011	4	-	-	0.7 0.2, 3.6 -	17.5 11.1, 27.4 0%
Flushing	4.4 2.7, 7.1 30% 0.222	< 0.0001	5	4.6 3.2, 6.6 0%	20.6 2.7, 157.9 -	-	1.3 0.2, 7.4 -
Jaw Pain	4.0 2.9, 5.6 0%, 0.421	< 0.0001	7	4.9 3.3, 7.4 0%	1.3 0.4, 4.3 -	11.0 0.6, 204.7 -	3.1 1.6, 6.2 0%
Headache	3.3 1.6-6.8 88%, 0.0001	0.001	7	6.5 3.4, 12.4 77%	-	6.0 1.1, 31.5 -	1.5 0.8, 2.8 59%
Pain in extremity	3.3 2.2, 4.9 0%, 0.412	< 0.0001	5	3.1 2.0, 4.8 7%	-	13.0 1.5, 112.3 -	1.9 0.2, 22.2 -
Diarrhoea	2.7 1.9, 3.9 47%, 0.079	< 0.0001	7	3.6 2.7, 4.9 0%	1.3 0.5, 3.3 -	6.5 0.4, 57.0 -	1.8 1.2, 2.9 0%
Vomiting	2.6 1.1, 6.1 79%, 0.0001	0.024	7	2.9 0.9, 9.5 90%	-	6.0 1.1, 31.5 -	1.2 0.5, 3.1 12%
Peripheral Oedema	2.1 1.2, 3.8 18%, 0.297	0.013	3	1.6 0.8, 3.0 0%	-	-	3.8 1.5, 9.6 -
Nausea	2.0 1.3, 3.0 63%, 0.012	0.002	7	3.0 2.2, 4.0 8%	2.0 0.9, 4.1 -	1.1 0.3, 4.3 -	0.8 0.2, 3.7 65%
Dizziness	1.2 0.9, 1.6 0%, 0.625	0.172	7	1.3 0.7, 2.2 53%	1.2 0.6, 2.4 -	1.1 0.2, 5.2	1.1 0.6, 2.1 0%

						-	
Upper respiratory tract infection	1.0 0.6, 1.7 0%, 0.486	0.923	4	1.1 0.6, 2.1 0%	0.7 0.3, 1.7 -	-	3.9 0.4, 41.3 -
Insomnia	2.4 0.8, 7.4 0%, 0.919	0.131	3	3.0 0.6, 2.1 0%	-	2.0 0.2, 19.8 -	1.7 0.2, 19.4 -
Abdominal pain	1.2 0.6, 2.4 0%, 0.693	0.579	3	1.3 0.6, 13.6 -	-	-	0.5 0.1, 10.0 -
Arthalgia	1.7 0.9, 3.4 0%, 0.628	0.129	3	1.7 0.9, 3.4, 0%	-	-	-
Fatigue	1.3 0.9, 1.9 0%, 0.726	0.159	4	1.5 1.0, 2.2 0%	0.9 0.4, 2.1 -	-	-
Palpitations	0.7 0.2, 2.4 72%, 0.028	0.595	3	1.0 0.2, 4.2 79%	0.3 0.1, 1.4 -	-	-
Chest pain	1.0 0.5, 2.0 3%, 0.357	0.948	3	0.9 0.4, 2.2 -	0.9 0.5, 6.6 -	0.4 0.1, 2.3 -	-
Dyspnoea	1.1 0.5, 2.5 59%, 0.046	0.830	5	1.1 0.2, 6.9 87%	0.7 0.3, 1.7 -	1.8 0.3, 10.2 -	1.2 0.1, 15.3 -
Cough	1.5 0.6, 3.9 68%, 0.042	0.372	3	0.8 0.3, 1.9 -	2.8 1.7, 4.9	1.3 0.3, 6.0 -	-

8.2 Treprostinil Synthesis

8.2.1 Methods

Synthesis of Chiral benzylalkynol

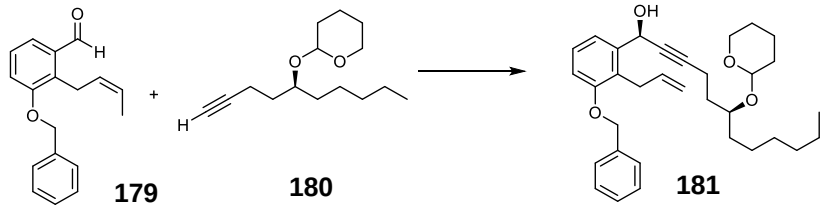

179 **180** **181**

Alkyne coupling with aldehyde in the presence of (+)-N-Methylephridrine: A solution of N-methylephedrine (1.06 g 5.94 mmol) in anhydrous toluene (7.5 mL) and triethylamine (0.83 mL, 5.94 mmol) were added to a flask charged with dried zinc triflate (2.19 g, 5.94 mmol) and the solution was left stirring at RT under argon for 80 minutes. A solution of anhydrous (S)-1-decyn-O-tetrahydropyran-2-yl-1-ol 181 (1.42 g, 5.94 mmol) in anhydrous toluene (1.25 mL) was added to the orange solution and after a further 25 minutes, 3-benzyl-2-allyl benzaldehyde 180 (0.5062 g, 1.98 mmol) dissolved in toluene (1.25 mL) was also added. After 21.5 hrs, the reaction was monitored by TLC (ethyl acetate/Hexane 1:4) and quenched by addition of water (7 mL). Ethyl acetate (5 mL) was added and the two layers separated. The aqueous layer was extracted with ethyl acetate and the organic layer washed with brine (5 mL) and saturated ammonium chloride solution (2 × 5 mL). The organic layers were combined, dried over Na_2SO_4 and the solvent removed *in vacuo* to yield a dark orange viscous liquid. The crude product was chromatographed on silica gel column using a gradient of ethyl acetate in hexane (2-10%) to yield an orange viscous liquid 182 (0.53 g, 55% yield). ^{1}H NMR (300 MHz, $CDCl_3$) 7.41-7.38 (m, 6H), 7.26 (s, 1H), 6.91 (d, 1H), 6.07-5.98 (m, 1H), 5.64 (d, 1H), 5.08 (s, 2H), 5.00 (d, 2H), 3.89-3.88 (m, 1H), 3.72-3.67 (m, 3H), 3.48-3.44 (m, 1H), 2.40 (q, 2H), 2.29 (t, 1H), 1.77-1.26 (m, 17H), 0.88 (t, 3H); ^{13}C NMR (300 MHz, $CDCl_3$) 156.8, 140.9, 137.1, 128.6, 127.9, 127.4, 127.2, 119.6, 115.0, 112.0, 98.0, 97.3, 75.4, 70.3, 62.9, 62.2, 35.3, 34.0, 33.5, 32.1, 31.2, 29.8, 25.6, 24.8, 22.7, 20.0, 15.6, 15.0, 14.2; IR 3401.3 (O-H), 2930.1 (C-H), 2858.6 (C-H), 1584.1 (C=C). Purity was determined by HPLC analysis (98% de).

Alkyne coupling with aldehyde in the presence of (1S, 2S)-3-(t-butyldimethylsilyloxy)-2-N,N-dimethylamino-1-(p-nitrophenyl)propan-1-ol: To a solution of dry zinc triflate (10.8 g, 29.73 mmol) in anhydrous THF (20 mL) under argon at 30 °C was added a solution of (1S, 2S)-3-(t-butyldimethylsilyloxy)-2-N,N-dimethylamino-1-(p-nitrophenyl)propan-1-ol (10.55 g, 29.73 mmol) in THF (10 mL), then triethylamine (4.14 mL, 2.73 mmol). (S)-1-decyn-O-tetrahydropyran-2-yl-1-ol 181 (7.10 g, 29.73 mmol) were added and the heat reduced to RT. Then 3-benzyl-2-allyl benzaldehyde 180 (0.51 g, 1.98 mmol) was added and the reaction stirred at RT for 44 hours and monitored by TLC (ethyl acetate/hexanes 1:4). The solution was quenched by addition of saturated ammonium chloride solution (20 mL) and the product was extracted with ethyl acetate (4 × 40 mL) until colourless. The combined organic layers were

washed with H_20 (2 × 30mL) and brine (12 mL), dried over Na_2SO_4 and the solvent removed *in vacuo*. The crude product was chromatographed by silica gel column using a gradient of ethyl acetate and hexanes (2-10%) to yield an orange viscous liquid 182 (4.98 g, 51.3%). ^{1}H NMR (300 MHz, $CDCl_3$) 7.46-7.27 (m, 5H), 7.22 (td, 1H), 6.91 (d, 1H), 6.10-5.94 (m, 1H), 5.64 (d, 1H), 5.08 (s, 2H), 5.4-4.9 (m, 2H), 4.69-4.62 (m, 1H), 3.94-3.88 (m, 1H), 3.78-3.54 (m, 3H), 3.52-3.40 (m, 1H), 2.46 (m, 3H), 1.86-1.63 (m, 4H), 1.63-1.40 (m, 5H),1.40-1.18 (m, 6H), 0.87 (t, 3H); ^{13}C NMR (300 MHz, $CDCl_3$) 156.8, 140.9, 137.4, 137.1, 128.6, 127.9, 127.4, 127.2, 119.5, 115.0, 112.0, 98.0, 97.3, 87.5, 87.1, 75.9, 75.4, 70.3, 62.8, 62.2, 35.0, 34.0, 33.5, 32.5, 32.1, 31.2, 29.8, 25.6, 25.4, 24.8, 22.7, 20.0, 15.6, 15.0, 14.2; IR 3391 (O-H), 2930 (C-H), 2859 (C-H); Purity was determined by HPLC (96% *de*).

Synthesis of racemic benzylalkynol

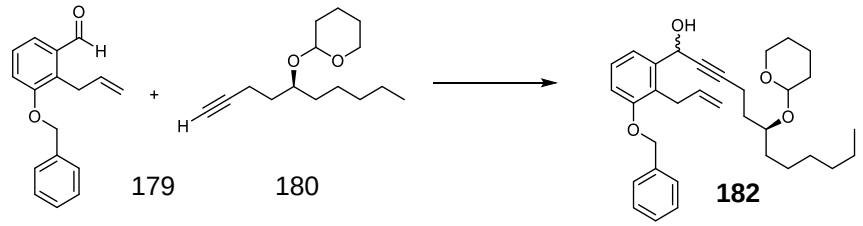

179 180 **182**

Racemic alkyne coupling with aldehyde: Ethylmagnesium bromide (19.8 mL, 19.8 mmol) was added drop-wise to a stirring solution of (S)-1-decyn-O-tetrahydropyran-2-yl-1-ol 181 (5.00 g, 20.79 mmol) in anhydrous THF (20 mL) under argon and stirred for 90 minutes. The reaction was cooled to 0-10 °C and a solution of 3-benzyloxy-2-allyl benzaldehyde 180 (5.00 g, 19.8 mmol) in anhydrous THF (15 mL) was added drop-wise over 30 minutes. The reaction was monitored by TLC (ethyl acetate/hexane 1:4) and after 29 hours the reaction quenched by addition of saturated ammonium chloride (2 mL) to form granules and stirred for 10 minutes. The precipitate was filtered, the filtrate dried over Na_2SO_4 and the solvent removed in vacuo. The crude product was chromatographed by silica gel column to yield racemic benzyl alkynol 183 (6.99 g, 72%). ^{1}H NMR (300 MHz, $CDCl_3$) δ_H 7.43-7.27 (m, 7H), 7.25-7.16 (td, 2H), 6.90 (d, 1H), 6.10-5.93 (m, 1H), 5.64 (d, 1H), 5.07 (s, 2H), 5.04-4.9 (m, 2H), 4.73-4.59 (m, 1H), 3.96-3.81 (m, 1H), 3.80-3.62 (m 3H), 3.61-3.54 (m, 1H), 3.54-3.39 (m, 1H), 2.44-2.36 (t, 1H), 2.36-2.24 (m, 2H), 1.90-1.17 (m, 21H), 0.93-0.80 (t, 3H). ^{13}C NMR (300 MHz, $CDCl_3$) δ_C 157, 141, 137.4, 137.0, 128.7, 128.0, 127.5, 127.0, 126.5, 119.5, 115.0, 112.0, 98.0, 97.0, 87.0, 70.0, 62.5, 62.0, 35.0, 34.0, 33.5, 32.5, 32.0, 31.0, 29.5, 25.5, 24.5, 22.5, 20.0, 14.0. IR 3398 (O-H), 2930 (C-H), 2859 (C-H), 1582 (C=C). Theoretical mass = 490.3 g/mol. $[M+Na]^+$ Found = 513.7 m/z. Purified by HPLC revealing diasteroisomers.

Synthesis of aryl alkyne ketone

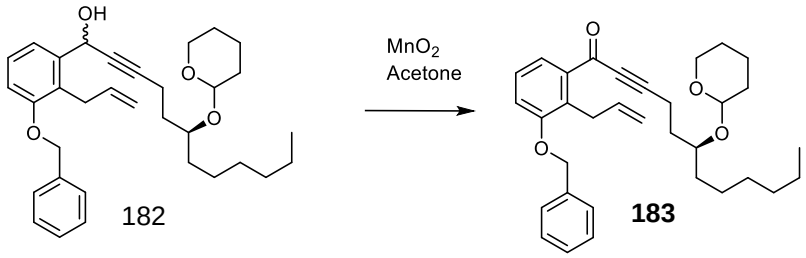

Alkyne alcohol oxidation of benzyl alkynol: Manganese (IV) oxide (1.23 g, 14.19 mmol) was added to a solution of racemic benzylalkynol 183 (0.12 g, 0.252 mmol) in acetone (10 mL) and the solution stirred at RT for 20 hours. The reaction was monitored by TLC (ethyl acetate/hexane 1:4). The reaction mixture was filtered through Celite® and the filtrate solvent removed *in vacuo* to afford aryl alkyne ketone 184 (0.11 g, 87%). ^{1}H NMR (300 MHz, $CDCl_3$) δ_H 7.75 (t, 1H), 7.54 (m, 9H), 7.20-7.03 (d, 1H), 6.12-5.90 (m, 1H), 5.11 (d, 2H), 5.02 (d, 1H), 4.98-4.89 (m, 2H), 4.70-4.58 (m, 1H), 3.95-3.80 (m, 3H), 3.80-3.68 (m, 1H), 2.66-2.56 (td, 1H), 2.51 (t, 1H), 2.18 (s, 1H), 1.94-1.18 (m, 18H), 0.88 (t, 3H); ^{13}C NMR (300 MHz, $CDCl_3$) δ_C 180.1, 136.9, 131.0, 128.7, 128.0, 127.2, 126.8, 124.8, 123.0, 116.3, 116.2,3, 115.1, 98.7, 97.9, 96.1, 95.5, 81.8, 77.2, 76.8, 70.6, 63.2, 53.9, 40.0, 33.7, 32.1, 31.8, 31.3, 30.1, 25.5, 25.2, 22.7, 20.3, 15.9, 15.1, 14.2; IR 3070 (C-H), 2930 (C-H), 2859 (C-H), 2213 (C≡C), 1644 (C=O).

Synthesis of chiral benzylalkynol

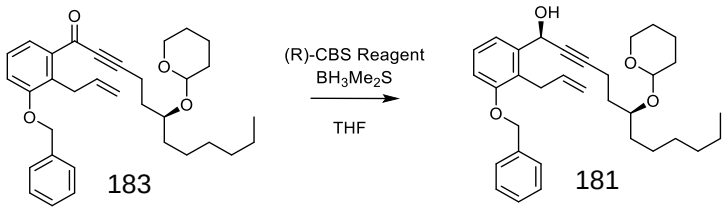

CBS reduction of aryl alkynyl ketone: To a solution of aryl alkyne ketone 184 (0.10 g, 0.205 mmol) in anhydrous THF (2 mL) was added CBS reagent in toluene (1M) (0.25 mL, 0.246 mmol), drop-wise under argon at RT. After 15 minutes, the solution was cooled to -30 °C by acetone/dry ice bath and the borane dimethyl sulfide complex in toluene (2M) (0.15 mL, 0.307 mmol) was added drop-wise. After 3.5 hours at -30 °C, the reaction was brought up to -20 °C for 1 hour. The reaction was monitored by TLC (ethyl acetate/hexane 1:4) and the reaction cooled back to -40 °C and quenched by drop-wise addition of methanol (0.18 mL). The reaction was allowed to reach 0 °C before ammonium chloride (0.7 mL) and ethyl acetate (2 mL) added. The product was extracted from the aqueous phase and the organic layer washed with ammonium chloride (5 mL), water (2 × 5 mL) and brine (5 mL), dried over Na_2SO_4 and the solvent removed in vacuo. The crude product was chromatographed through silica gel column in Ethyl acetate/hexanes (2-10%) which afforded the chiral benzylalkynol 182 (0.03 g, 30%). ^{1}H NMR (300 MHz, $CDCl_3$) δ_H 7.48-7.28 (m, 5H), 7.20 (t, 1H), 7.03 (d, 1H), 6.91 (d, 1H), 6.11-5.94 (m, 1H), 4.99 (dt, 2H), 4.93 (q, 1H), 4.70 (d, 2H), 3.57 (d, 2H), 1.65-1.52 (m, 2H), 1.25 (s,

3H); ^{13}C NMR (300 MHz, $CDCl_3$) δ_C 156.8, 140.8, 137.1, 128.6, 127.8, 127.2, 119.6, 115.0, 112.0, 98.0, 76.7, 75.9, 70.3, 62.9, 35.2, 33.9, 32.7, 32.1, 31.2, 29.8, 25.6, 24.8, 22.7, 20.0, 15.0, 14.2; IR 3398 (O-H), 2928 (C-H), 2857 (C-H); Purity was determined by HPLC (94% de).

Synthesis of Benzyl alkynyl t-butyldimethylsilyl ether

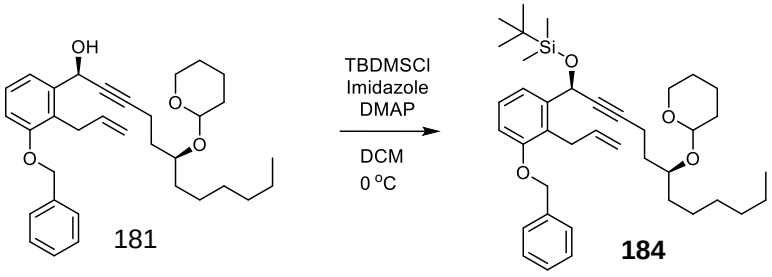

181 **184**

Silylation of benzylalkynol: To a solution of chiral benzylalkynol 182 (4.50 g, 9.17mmol) in anhydrous dichloromethane under argon was added imidazole (0.75 g, 11.004 mmol) and dimethylaminopyridine **32** (0.23 g, 1.832 mmol) and stirred. Once dissolved, the solution was cooled to 0 °C and t-butyldimethylsilyl chloride (1.66 g 11.004 mmol) was added. The reaction was monitored by TLC (ethyl acetate/hexane 1:4) and after 22 hours was quenched by addition of H_2O (15 mL). The aqueous layer was extracted with DCM (3 × 10mL) and the organic layers combined and washed with brine (15 mL) then dried over Na_2SO_4 and the solvent removed *in vacuo*. The crude product was purified by silica gel column chromatography using ethyl acetate in hexanes (1-5%) which afforded a viscous liquid product 185 (1.30 g, 24%). ^{1}H NMR (300 MHz, $CDCl_3$) 7.48-7.26 (m, 5H), 7.20 (td, 1H), 6.87 (d, 1H), 6.07-5.90 (m, 1H), 5.60 (s, 1H), 5.08 (s, 2H), 5.02-4.9 (m, 2H), 4.59 (dt, 1H), 3.95-3.80 (m, 1H), 3.74-3.56 (m, 2H), 3.50-3.38 (m, 1H), 2.37-2.27 (m, 1H), 2.23 (t, 1H), 1.86-1.62 (m, 4H), 1.62-1.41 (m, 6H), 1.39-1.20 (m, 6H), 0.91 (s, 10H), 0.11 (d, 6H).

Synthesis of t-butyldimethylsilyl tricyclic enone

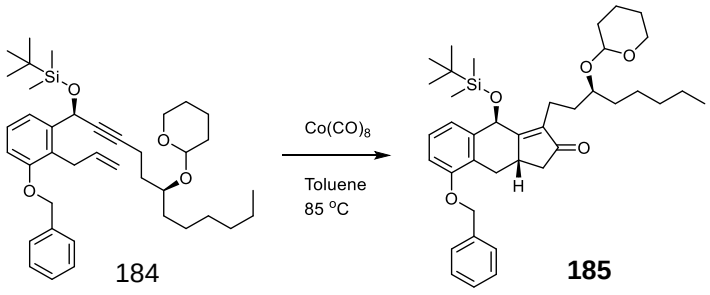

184 **185**

Stoichiometric Pauson-Khand cyclisation: To a solution of benzyl alkynyl t-butyldimethylsilyl ether 185 (2.44 g, 4.028 mmol) in toluene, was added octacarbonyl dicobalt (1.38 g, 4.028 mmol) and the brown solution stirred for 48 hours. The reaction was monitored by TLC in (ethyl acetate in hexane 1:9) The reaction mixture was filtered through Celite®, rinsed with ethyl acetate and solvent removed *in vacuo*. The crude product was chromatographed on silica gel column using a gradient of ethyl acetate in hexanes (2-6%) to give pure cyclic enone 186 (1.07 g, 42%). ^{1}H NMR (300 MHz, $CDCl_3$) δ_H 7.45-7.38 (t, 8H),

7.38-7.3 (m, 1H), 7.24-7.17 (m, 1H), 6.93 (m, 1H), 6.84 (q, 1H), 5.60 (s, 1H), 5.48 (s, 0.5H), 5.30 (s, 0.5H), 5.05 (s, 0.5H), 4.54-4.48 (dt, 1H), 3.91-3.71 (m, 1H), 3.65-3.43 (m, 2H), 3.43-3.29 (m, 2H), 2.69 (dd, 1H), 2.53-2.42 (m, 1H), 2.41-2.10 (m, 2H), 2.04 (s, 1H), 1.83-1.78 (m, 1H), 1.74-1.39 (m, 9H), 1.36-1.14 (m, 7H), 0.90-0.83 (m, 3H), 0.81 (s, 8H), 0.17 (s, 2H), 0.13 (s, 1H), 0.08 (d, 3H); ^{13}C NMR (300 MHz, $CDCl_3$) δ_C 210.0, 172.7, 156.2, 137.4, 137.1, 128.6, 127.9, 127.4, 122.5, 110.5, 98.0, 97.3, 77.5, 77.2, 76.7, 70.2, 65.6, 62.9, 42.4, 34.0, 33.3, 32.2, 32.1, 25.8, 22.7, 22.5, 20.0, 19.5, 14.4, 14.0; IR 2927 (C-H), 2855 (C-H), 1702 (C=O), 1584 (C=C). Theoretical mass = 646.4 g/mol. Mass found: $[M+Na]^+$ = 655.8 m/z. Purification and analysis by HPLC rendered the pure compound (90% *de*).

Catalytic Pauson-Khand cyclisation using carbon monoxide: To a solution of benzyl alkynyl t-butyldimethylsilyl ether 185 (0.21 g, 0.34 mmol) in 1,2-dimethoxyethane, was added octacarbonyl dicobalt (0.02 g, 0.0341 mmol) in an argon atmosphere. The system was purged with CO gas and stirred for 17 hours at RT. The reaction was then refluxed at 60 °C for 24 hours. The reaction was monitored by TLC in (ethyl acetate in hexane 1:4). The solvent was removed in vacuo and purified by silica gel column chromatography in ethyl acetate/hexane (2-6%) to give pure cyclic enone 186 (0.12 g, 58%). ^{1}H NMR (300 MHz, $CDCl_3$) δ_H 7.45-7.29 (m, 5H), 7.23-7.17 (m, 1H), 6.93 (q, 1H), 6.84 (q, 1H), 5.60 (s, 1H), 5.48 (s, 1H), 5.05 (s, 2H), 4.51 (dt, 1H), 3.90-3.81 (m, 1H), 3.80-3.71 (m, 1H), 3.68-3.44 (m, 2H), 3.43-3.28 (m, 2H), 2.69 (dd, 1H), 2.55-2.11 (m, 4H), 1.92-1.73 (m, 1H), 1.73-1.11 (m, 20H), 0.91-0.76 (m, 12H), 0.15 (d, 3H), 0.09 (d, 3H); ^{13}C NMR (300 MHz, $CDCl_3$) δ_C 172.7, 156.1, 138.7, 137.4, 128.7, 128.0, 127.3, 125.5, 122.4, 110.6, 97.9, 70.0, 65.3, 62.9, 42.3, 33.8, 33.7, 32.2, 31.5, 25.7, 25.6, 25.3, 24.8, 22.7, 18.2, 14.1; IR 2928 (C-H), 2855 (C-H), 1702 (C=O), 1584 (C=C); Theoretical mass = 646.4 g/mol. Mass found: $[M+Na]^+$ = 655.8 m/z. Purity was determined by HPLC (90% de).

Synthesis of tricyclic ketone

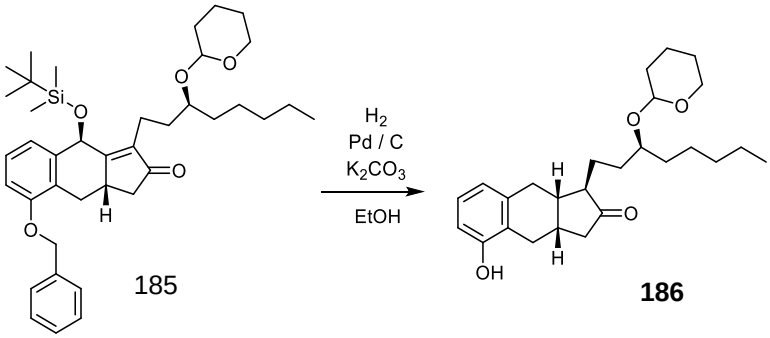

Hydrogenation of cyclic enone: To a solution of pure *t*-butyldimethylsilyl tricyclic enone 186 (2.07g, 3.2mmol) in ethanol (8 mL) was added potassium carbonate (0.20 g, 10% wt./wt. of cyclic enone). Once purged with argon, palladium on activated carbon was added and the system purged with hydrogen then stirred at RT for 20 hours. The reaction was monitored by TLC (ethyl acetate/hexane 1:4) and IR (peak shift from 1702 to 1732 cm^{-1}). The reaction mixture was filtered through Celite® and the solvent removed from the filtrate *in vacuo*. The

crude product was combined with the crude products of two other batches and chromatographed together through silica gel column using solvent gradient ethyl acetate in hexanes (2-14%) to yield the tricyclic ketone product 187 (0.92 g, 43% of combined theoretical yields). ^{1}H NMR (300 MHz, $CDCl_3$) δ_H 7.06-6.94 (m, 1H), 6.71 (q, 1H), 6.63 (d, 1H), 4.98-4.87 (m, 1H), 4.71-4.57 (dm, 1H), 3.98-3.80 (m, 1H), 3.70-3.55 (m, 1H), 3.55-3.40 (m, 1H), 3.08-2.89 (m, 2H), 2.78-2.26 (m, 5H), 2.25-2.12 (dt, 1H), 2.01-1.16 (m, 24H) ^{13}C NMR (300 MHz, $CDCl_3$) δ_C 220.3, 153.9, 152.8, 136.6, 126.4, 122.4, 112.6, 98.1, 97.4, 63.1, 58.2, 51.7, 45.3, 38.9, 35.0, 32.2, 31.9, 30.6 25.7, 22.7, 19.9, 14.1; IR 3365 (O-H), 2927 (C-H), 2855 (C-H), 1732 (C=O), 1590 (C=C), Purity was confirmed by HPLC (94%).

Synthesis of tricyclic diol

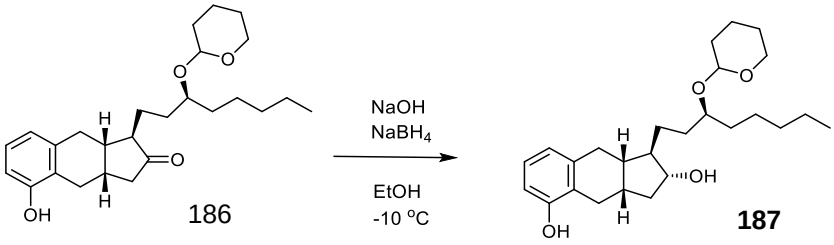

186 **187**

Reduction of tricyclic ketone: To a solution of tricyclic ketone 187 (0.11g, 0.26 mmol) in ethanol (2 mL) at -10 °C was added dropwise a solution of sodium hydroxide (0.10 g, 0.10 mmol) in H_2O (1mL). The solution was kept at -10 °C and after 30 minutes sodium borohydride (0.02 g, 0.54 mmol) was added in 5 portions and the solution allowed to reach RT. The reaction was monitored by TLC (ethyl acetate/hexanes 2:5 silica). Additional $NaBH_4$ (10%) was added to push the reaction to completion which was reached after 2 hours. The reaction was quenched by addition of saturated ammonium chloride solution (1 mL) and the solvent removed *in vacuo*. To the remaining solution was added H_2O (2mL) and extracted with t-butylmethyl ether (3 × 2 mL). The organic layers were combined and washed with H_2O (2 × 2 mL) and brine (3 mL), dried over Na_2SO_4 and the solvent removed *in vacuo*. The tricyclic diol 188 (0.11 g, 94%) was obtained. ^{1}H NMR (300 MHz, $CDCl_3$) δ_H 6.93 (t, 1H), 6.78-6.55 (m, 2H), 4.65 (dt, 1H), 4.00-3.85 (m, 1H), 3.80-3.57 (m, 2H), 3.57-3.42 (m, 1H), 2.79 (dd, 2H), 2.41 (m, 2H), 2.31-2.03 (m, 2H), 1.98-1.02 (m, 25H), 0.88 (t, 3H); ^{13}C NMR (300 MHz, $CDCl_3$) δ_C 153.2, 140.9, 126.2, 124.9, 113.1, 98.7, 97.6, 77.6, 73.3, 63.7, 62.7, 52.2, 49.5, 41.2, 40.8, 34.9, 33.7, 32.9, 32.2, 31.2, 27.1, 25.5, 22.8, 19.9, 14.2; IR 3332 (O-H), 2927 (C-H), 2857 (C-H), 1589 (C-H); Theoretical mass = 416.3 g/mol. $[M+Na]^+$ found by LCMS: 439.7. Purity was determined by HPLC (94%).

Synthesis of tricyclic triol

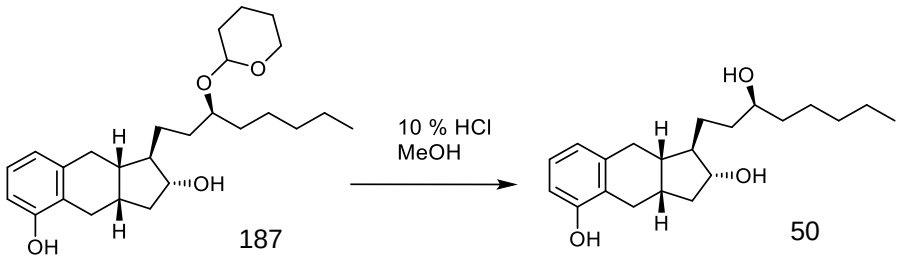

THP cleavage to triol: To a solution of tricyclic diol 188 (0.10 g, 0.252 mmol) in methanol (2.5 mL) was added dropwise HCl (10%, 3 mL) and the solution stirred at RT. The reaction was monitored by TLC (ethyl acetate/hexane 1:1) and after 4 hours, the reaction was quenched with saturated sodium bicarbonate solution until the pH reached 7-8. Methanol was removed in vacuo and the remaining aqueous solution was extracted with ethyl acetate (2 × 10 mL). The organic layers were combined and washed with H_2O (2 × 5 mL) and brine (7 mL), dried over Na_2SO_4 and the solvent removed in vacuo to yield tricyclic triol 51 (0.07 g, 86%). ^{1}H NMR (300 MHz, $CDCl_3$) δ_H 6.92 (t, 1H), 6.70-6.57 (q, 2H), 3.71-3.46 (m, 2H), 2,73-2.52 (qn, 2H), 2.41 (td, 2H), 2.26-1.94 (m, 2H), 1.91-1.73 (m, 1H), 1.69-0.97 (m, 15H), 0.89 (t, 3H); ^{13}C NMR (300 MHz, $CDCl_3$) δ_C 153.1, 140.8, 126.2, 125.0, 120.2, 113.4, 72.8, 60.6, 51.9, 41.1, 40.9, 37.4, 35.0, 33.7, 32.8, 32.0, 28.6, 26.0, 25.5, 22.8, 14.2; IR 3298 (O-H), 2924 (C-H), 2855 (C-H), 1588 (C=O); Purity was analysed by HPLC (92% de).

Synthesis of benzindene nitrile

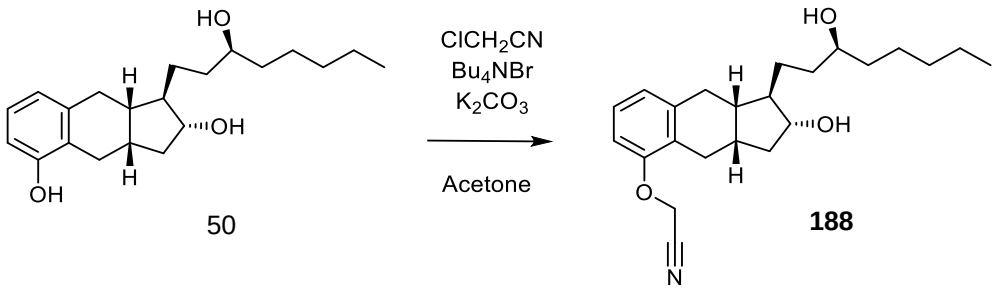

Alkylation of tricyclic triol by chloroacetonitrile: To a solution of tricyclic triol 51 (0.07 g, 0.205 mmol) in acetone (3 mL) under argon was added chloroacetonitrile (0.06 g, 0.820 mmol), tetrabutylammonium bromide (0.01 g, 0.018mmol) and powdered potassium carbonate (0.17 g, 1.23 mmol). The mixture was stirred at RT for 36 hours and the reaction monitored by TLC (alumina plate, 5% MeOH/DCM). The reaction was filtered through Celite® and the solvent removed from filtrate *in vacuo*. The crude product was chromatographed though silica gel column using ethyl acetate in hexanes (10-45%). TLC were carried out in 80% ethyl acetate/hexane. The benzindene nitrile product 189 was obtained (0.12 g, 150%). ^{1}H NMR (300 MHz, $CDCl_3$) δ_C 7.13 (t, 1H), 6.90 (d, 1H), 6.81 (d, 1H), 4.75 (s, 2H), 3.80-3.67 (m, 1H), 3.67-3.52 (m, 1H), 2.48 (qn, 2H), 2.33-2.10 (m, 2H), 2.04 (s, 2H), 1.94-1.05 (m, 21H), 0.89 (t, 3H); ^{13}C NMR (300 MHz, $CDCl_3$) 153.8, 141.6, 128.4, 126.6, 123.1, 115.5, 110.5, 72.6, 60.5, 54.5, 52.3, 41.4, 41.2, 37.5, 35.0, 33.7, 32.8, 32.0, 28.7, 26.0, 25.5, 22.7, 14.2; IR 3328 (O-

H), 2926 (C-H), 2856 (C-H), 1732 (C≡N), 1236 (C-O). Chiral purity determined by HPLC (90% *de*).

Synthesis of treprostinil

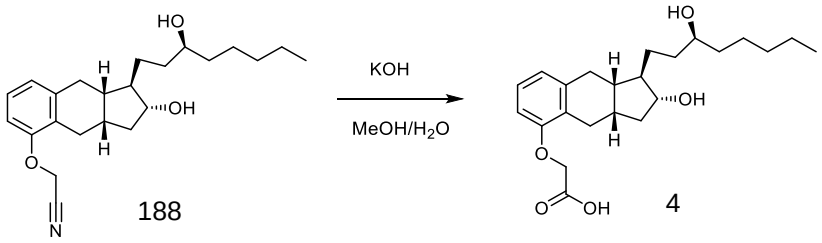

Hydrolysis of benzindene: To a solution of tricyclic nitrile 189 (0.12 g, 0.313 mmol) in MeOH (3 mL) was added potassium hydroxide (0.10 g, 1.25 mmol) in H_2O (0.5 mL) and the reaction heated to 80 °C under reflux for 48 hours. The reaction was monitored using TLC (7:3 ethyl acetate/hexane. The solvent was removed *in vacuo* and the remaining solution extracted with t-butylmethyl ether (3 × 2 mL). HCl (10%, 2 mL) was added to pH 2 and ethyl acetate (10 mL) added. The organic layer was washed with H_2O (8 mL) and brine (8 mL) then dried over Na_2SO_4 and solvent removed *in vacuo* to yield treprostinil 4 (0.07 g, 55%). ^{1}H NMR (300 MHz, MeOD) 7.04 (t, 1H), 6.73 (dd, 2H), 4.62 (s, 2H), 3.66-3.40 (dm, 2H), 2.81-2.56 (m, 3H), 2.47 (dd, 1H), 2.34-2.15 (m, 1H), 1.25-1.96 (m, 1H), 1.96-1.80 (m, 1H), 1.80-1.02 (m, 16H), 1.90 (t, 3H);^{13}C NMR (300 MHz, MeOD) 155.2, 140.9, 127.4, 125.9, 121.1, 109.4, 76.3, 71.6, 65.2, 51.3, 41.0, 40.7, 37.0, 34.8, 33.3, 32.8, 31.9, 28.3, 27.6, 25.3, 25.2, 22.5, 13.2; IR 3310 (O-H), 2925 (C-H), 2856 (C-H), 1729 (C=O); Theoretical mass = 390.5 g/mol. $[M+Na]^+$ found by LCMS: 413.6 m/z. Purity was analysed by HPLC (96% *de*).

8.2.2 **Discussion**

Treprostinil **4** was successfully synthesised during a 3-month internship with United Therapeutics & Lung Biotechnology at their headquarters in Silver Springs, Maryland, USA (**Scheme 70**). The purpose of this endeavour was to gain an appreciation of the synthetic routes used on a commercial level and to investigate common intermediates which could be modified for conjugation. Two methods used by United Therapeutics for both large, FDA approved (route i)[354] and small scale production (route ii) of alkyne addition to aldehyde were followed and their diastereomeric purity compared between the alternative steps and overall isolated product. The FDA approved synthesis includes the use of a tetrahydropyran protected side chain in the first synthetic step which is racemic and sensitive to degradation which limits synthetic options and also causes problems in the diastereomeric purity of all intermediates. However, FDA approval would need to be re-submitted to change the protecting group used so alternative protecting groups have not been introduced into the synthesis route used to make the clinical product. Although modification of an intermediate is possible and could potentially open up different synthesis and various modifications, the production of the intermediate chosen would take a considerable amount of time, taking the project in a different direction than intended. Additionally, a certain amount of purified treprostinil has been pledged

towards the project saving time and money. This route may be revisited if the other options selected involving modification of final treprostinil are unsuccessful. Characterisation data was not permitted off UT's site but as all compounds are known, a comparison of the compounds synthesised was conducted against published (where possible) and in-house data.

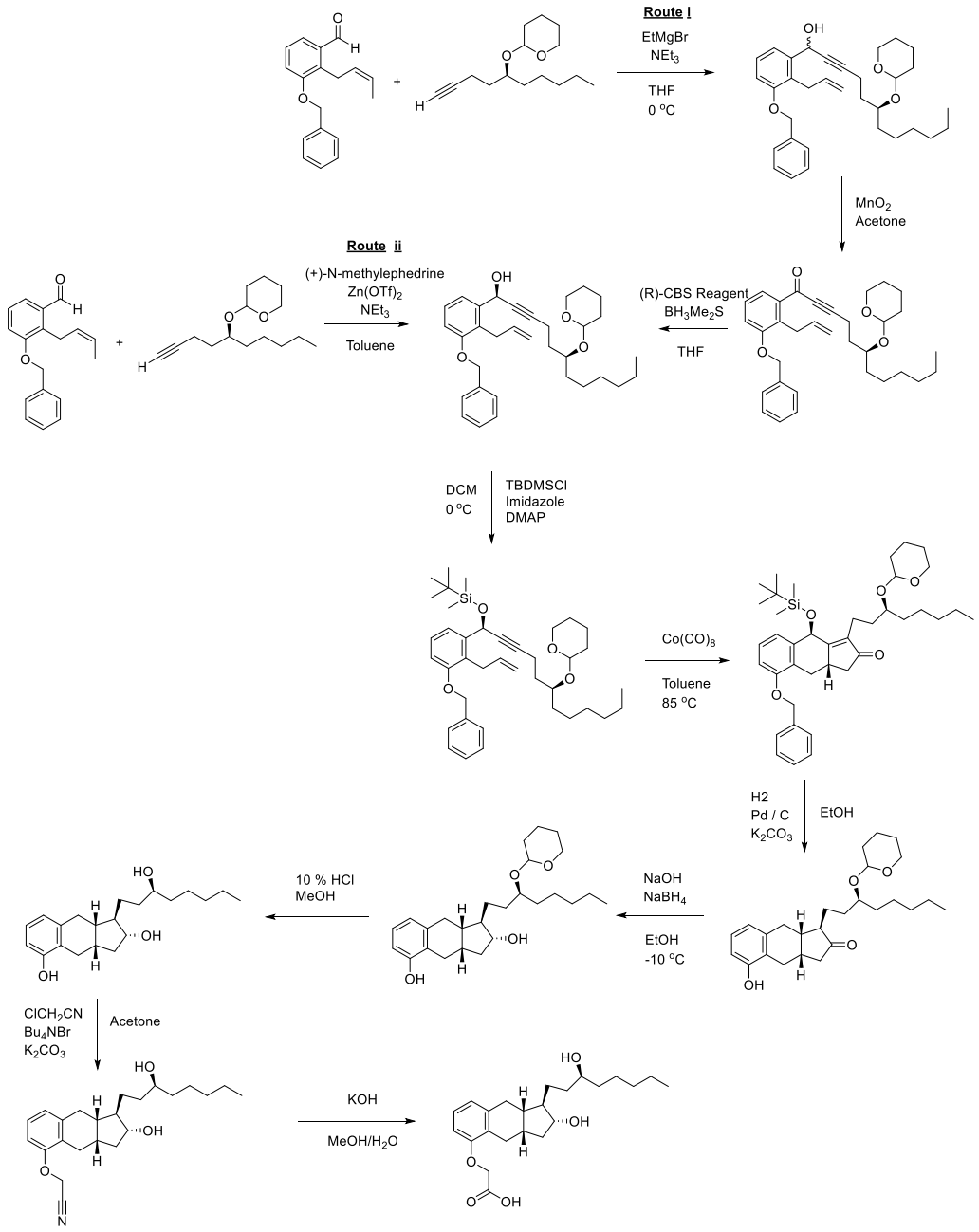

Scheme 70. Synthetic Scheme for Treprostinil using chiral and non-chiral reagents for the addition of the alkyne to aldehyde.

Treprostinil was prepared following the reactions shown in **Scheme 70**. Benzyl alkynyl alcohol (**182**) was afforded from the addition of 3-benzyloxy-2-allyl benzaldehyde (**180**) and (S)-1-decyn-O-tetrahydropyran-2-yl-1-ol (**181**) by two different methods; racemically and stereoselectively. The racemic Grignard reaction was conducted in the presence of

ethylmagnesium bromide to form the alkyne Grignard. This underwent nucleophilic addition to the aldehyde 180 to form the racemic alcohol (**183**) in 72% yield. This benzyl alkynyl alcohol (183) was oxidized by MnO_2 to afford aryl alkyne ketone (**184**) in 87% yield which was then stereoselectively reduced in the presence of borane dimethyl sulphide complex and (R)-2-methyl-CBS-oxazaborolidine to afford chiral benzylalkynyl alcohol (**182**) in 30% yield with chiral purity of 94 % de. Alternatively, the stereoselective reduction forms the desired product in one step which avoids the need to oxidise and reduce and can be carried out using two different chiral agents, both of which were undertaken. The first was carried out in the presence of zinc triflate and (+)-N-methylephedrine. Zinc triflate ($Zn(OTf)_2$) coordinates to the alkyne in a similar manner to the Grignard rendering it more active towards the aldehyde and the methylephedrine, a chiral molecule itself, coordinates to the aldehyde oxygen *via* hydrogen bonding by the oxygen and nitrogen lone pairs and uses the phenyl group to direct the alkyne addition to the Re face with 98% *de*. Due to the cost and restricted supply of (+)-N-methylephedrine, a second chiral reagent can be used, (1S, 2S)-3-(*t*-butyldimethylsilyloxy)-2-N,N-dimethylamino-1-(*p*-nitrophenyl)propan-1-ol. The reaction is carried out similar as that as before, with zinc triflate, but using THF in place of toluene. The reaction required a longer period to reach completion and gave the desired product with 96% *de*. Both of the products were identified using ^{1}H NMR spectroscopy with the presence of the resonance at δ 5.6 corresponding to the proton adjacent to the newly formed alcohol, as well as the aromatic proton resonance shift from δ 7.2 to δ 6.9.

Before cyclisation, the alcohol (**182**) was protected by reaction with tertiary-butyldimethylsilyl chloride (TBDMSCl) in the presence of imidazole and dimethyl aminopyridine (DMAP), to form the silyl ether (**185**) in 42 % yield. The Pauson-Khand cyclisation of (**185**) requires the use of octacarbonyl dicobalt and occurs by complexation to the alkyne and alkene which facilitates cyclic electron transfer with the donation and incorporation of a carbonyl ligand to form the tricylic enone (**186**). This can either be carried out in in stoichiometric amounts of cobalt complex or in a catalytic quantity regenerating the catalyst using carbon monoxide gas. Both methods were investigated. The silyl ether acts as an important directing group as the bulky moiety blocks complexation on the upper face of the molecule and preferentially forms the 5-membered ring with S configuration. The first reaction used a catalytic amount of octacarbonyl dicobalt (0.1 equivalents) in a carbon monoxide atmosphere at 60 °C to afford the tricyclic enone (**186**) in 58 % yield. The alternative uses a stoichiometric amount of octacarbonyl dicobalt (1 equivalent) in an argon environment at 80 °C to afford the same product in 94 % yield. Despite giving a better yield, the cost of the cobalt complex limits the use of the stoichiometric method in scaled up production.

Both products are identifiable by IR spectroscopy with the observance of the absorbance at 1702 cm^{-1} corresponding to the enone carbonyl. In ^{1}H NMR spectroscopy, the absence of the characteristic proton resonance at δ 5.9 which corresponds to the non-terminal alkene proton of the product is also a clear indicator that cyclisation has taken place. The conformational restriction imposed by cyclisation results in the splitting of the resonance at δ 5.6

corresponding to the proton adjacent to the alcohol. The presence of the THP group results in two diastereomers which are more distinguishable when the molecules loose conformational freedom, hence the splitting was not observed in the benzyl alkynyl (**181**) precursor. The reduction of t-butyldimethyl silyl ether and enone as well as the cleavage of the benzyl protecting group was conducted in a one-step reaction in the presence of potassium carbonate, over palladium carbon in a hydrogen environment for afford (**187**). The reaction was carried out several times on different scales and the crude products combined and chromatographed together to afford the tricyclic ketone (**187**) in 44% yield. The benzyl group cleavage and silyl ether reduction are relatively fast compared to the enone reduction which alters the polarity of the molecule and makes the reaction appear complete by TLC. The R_f value for the de-silylated and de-benzylated enone and the desired ketone are indistinguishable by TLC so for this reason, the reaction of monitored by IR spectroscopy. The IR absorption corresponding to the carbonyl will change from enone resonance (1702 cm^{-1}) to ketone resonance, (1732 cm^{-1}). The ketone was reduced to the corresponding secondary alcohol in the presence of sodium hydroxide and sodium borohydride to afford the tricyclic diol (**188**) in 94% yield. This was determined by the absence of the absorbance of the carbonyl bond at 1732 cm^{-1} by IR spectroscopy. The tetrahydropyran group was cleaved in acid to yield triol (**51**) at 86% which was proven by the absence of the racemic proton resonances at δ 4.6 and 4.7. The THP cleavage also resulted in an observed upfield peak shift from δ 3.9 to δ 3.6 corresponding to the proton adjacent to the newly formed alcohol. The triol (**51**) was alkylated by chloroacetonitrile in the presence of tetrabutylammonium bromide (Bu_4NBr) and potassium chloride to give benzindene nitrile (**189**). The carbon- chlorine bond is stronger than the corresponding bromide bond so the addition of tetrabutylammonium bromide serves to displace the chloride on the chloroacetonitrile which increases the rate of alkylation. The bond formation was confirmed by ^1H NMR with the presence of the OCH_2CN proton resonance at δ 4.7 which had shifted from δ 3.5 in the chloroacetonitrile reagent. The CN bond stretch was not observed in the expected nitrile region (2260 – 2220 cm^{-1}) due to the inductive effect of the resonant oxygen. The benzindene nitrile (189) was hydrolyzed by potassium hydroxide in aqueous methanol to afford crystalline treprostinil (4) in 55% yield which was characterized by ^1H NMR, ^{13}C NMR, IR, purity by HPLC (96% *de*). The hydrolysis was confirmed by the presence of the IR absorbance corresponding to the carboxylic acid carbonyl at 1728 cm^{-1}. A summary of the synthesis and the stereochemical outcomes is given in **Table 8-2**.

Table 8-2. Summary of the scales, diasteromeric outcomes, and conditions of the synthetic routes used to obtain treprostinil 2.PKC = pauson-Kahn cyclisation; RT= room temperature;

<table>
<tr><th colspan="2">Racemic</th><th colspan="2">Stereoselective</th></tr>
<tr><td>Alkyne coupling with grignard THF:
5 g scale.
EtMgBr
Refluxed at RT → 60 °C for 29 hrs
25 % impurity by NMR.
86% de.</td><td>Alkyne coupling with grignard in diethyl ether:
0.5 g scale.
EtMgBr
Refluxed at RT → 40 °C for 3.5 hrs. <4 % impurity by NMR.</td><td>Alkyne coupling:
0.5g scale.
Zinc triflate and (+)-N-methylephidrine employed to give 98% de.</td><td>Alkyne coupling: 5g scale.
Zinc triflate and (1S, 2S)-3-(t-butyl dimethylsilyloxy)-2-N,N-dimethylamino-1-(p-nitrophenyl) propan-1-ol
96% de.</td></tr>
<tr><td colspan="2">Oxidation (from THF reaction):
0.1 g scale. Oxidation by MnO_2 at RT</td><td colspan="2"></td></tr>
<tr><td colspan="2">Chiral CBS reduction:
CBS reagent in presence of borane complex.
Ar atmosphere at -30 °C.
94% de</td><td colspan="2"></td></tr>
<tr><td colspan="4">Protection by TBDMS group:
DMAP with imidazole and tertiary-butyldimethylsilyl chloride.</td></tr>
<tr><td colspan="2">Catalytic PKC:
0.2 g scale.
0.1 eq. $Co_2(CO)_8$ in CO atmosphere at 60 °C for 24 hours. 58% yield.</td><td colspan="2">Stoichiometric PKC:
0.2 g scale.
1 eq. $Co_2(CO)_8$ in Ar atmosphere at RT→80 °C for 24 hours. 55% yield.</td></tr>
<tr><td colspan="4">Hydrogenation:
Pd catalyzed in hydrogen atmosphere at RT.</td></tr>
<tr><td colspan="4">Reduction:
Ketone reduction by sodium borohydride.</td></tr>
<tr><td colspan="4">THP hydrolysis:
Reflux in presence of excess 10 % HCl.</td></tr>
<tr><td colspan="4">Alkylation:
Selective alkylation of phenol using chloroacetonitrile.</td></tr>
<tr><td colspan="4">Hydrolysis:
Base catalyzed hydrolysis in excess KOH. 96% de.</td></tr>
</table>

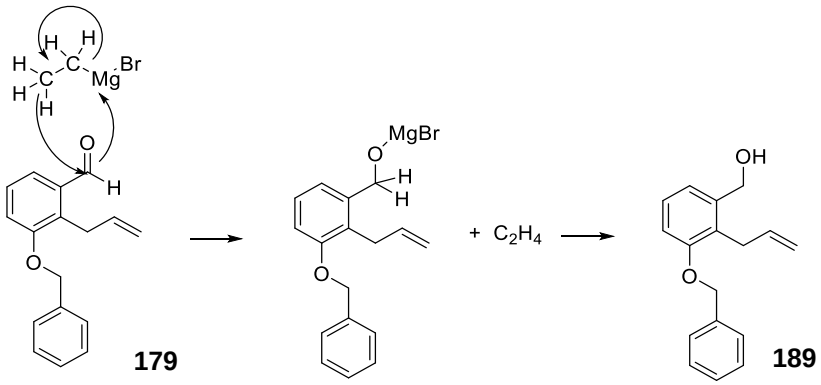

Scheme 71. Reduction during the Grignard reaction to produce the alcohol impurity **190**.

When carrying out the Grignard addition to afford **183**, it was noticed that two spots on the TLC formed as the product. They were not easily separated on silica gel column and when looking back at previous experiments of this type, it was also the case, but had not been investigated. The crude product was carried forward to the oxidation step where it appeared by TLC that only one product had formed as there was only one spot, however, ^{1}H NMR spectra showed the presence of an aldehyde proton which had previously been attributed to starting material (**180**). Upon stereoselective reduction, two spots were again identified which led us to believe that an unidentified side product was forming. A small amount was isolated of each of the spots and it was determined that the lower spot was an unexpected benzyl alcohol derivative (**190**) present at 25%. Literature reports known competition of the outcomes of a Grignard to aldehyde reaction[577]; addition (desired in this case) and self-reduction (undesired) which forms the benzyl alcohol product (**Scheme 71**). Further reading identified the solvent and temperature to be a major factor in the relative outcomes of the reaction. The reaction was carried out in both THF (current procedure) and diethyl ether.

Table 8-3. A comparison of the percentage of impurity **190** formed in the each of the different reaction conditions.

Reaction	Impurity
0.5 g scale in THF at RT	25 %
0.5 g scale in diethyl ether at RT	3.9 %
0.5 g scale in diethyl ether, refluxing at 40 °C	3.6 %

The percentage impurity, detected by ^{1}H NMR spectroscopy, from the reaction carried out in THF at room temperature was 25% however, the same reaction in diethyl ether showed only 3.9% of the self-reducing product. The same reaction in diethyl ether was carried out whilst refluxing at 40 °C however the increased temperature made negligible difference with 3.6% impurity. The low boiling point (and therefore refluxing temperature) of diethyl ether means that the refluxing temperature is similar to room temperature so perhaps the effect of temperature would be more pronounced using THF. However, the investigation was deemed complete as the impurity had been isolated and a method to reduce it had been determined.

8.3 Polyvalent Synthesis

A polyvalent approach takes inspiration from nature to amplify a binding effect by binding multiple moieties to a surface simultaneously. When an antibody binds to its respective antigen on a cell surface there can be an effector function where the antibody Fc recruits other cells, generally from the immune system, to evoke a biological response. The more antibody bound to the antigen, the more Fc is present and the stronger can be the effector function. Additionally, bacteria interact with cell surfaces using polyvalent interactions to gain entry. A polyvalent approach has been used to enhance an anthrax toxin inhibitor which consists of a liposome covered in inhibitor ligands. The polyvalent inhibitor extended clearance time and blocked anthrax toxin action more potently than free inhibitor.[258] Polyvalency has potential for the therapeutic activation of cell surface receptors.[257]

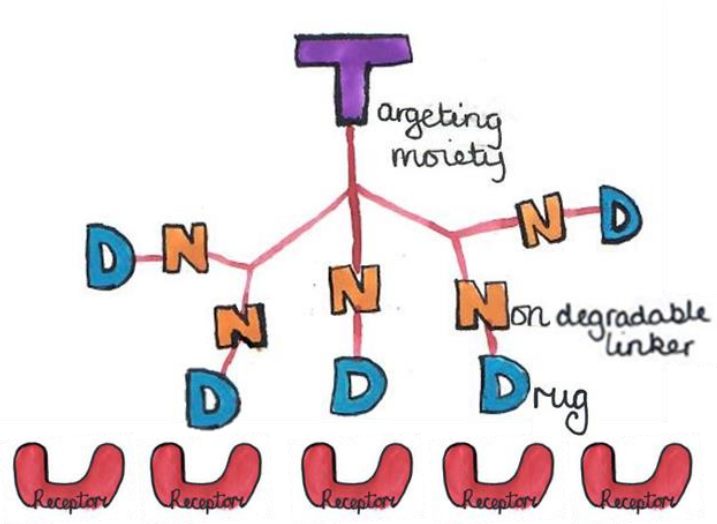

Figure 8-1. Structure of a polyvalent approach which possesses multiple non-cleavable drug molecules on the same structure. The drugs are conjugated without the intention of release as a polyvalent approach requires the drug structures to be active upon conjugation. As the first drug ligand bind to the receptor, other ligands are in close proximity to other receptors which uses a co-operative binding effect in increase lreceptor activation. A targeting moiety can be employed to localise receptor binding.

The prostanoid receptors (IP, EP_2, DP_1) are present on endothelial cells, smooth muscle cells (which infiltrate the vascular lumen in PAH) and platelets. Once in the blood stream, treprostinil has exposure to the target receptors, which may present an opportunity to achieve receptor activation using a polyvalent approach.

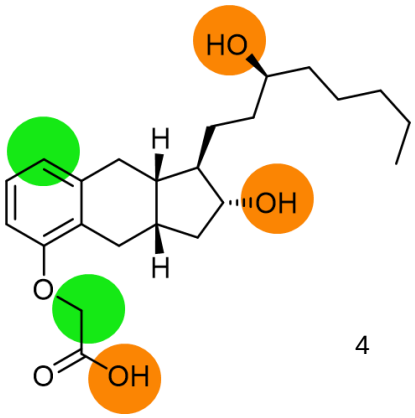

4

Figure 8-2. Modifiable atoms in the treprostinil 4 structure. Modifiable atoms required for receptor binding are labelled in orange, and those in green are atoms which are not known to interact with the binding pocket.

A structure possessing multiple treprostinil molecules which are active at the IP, EP_2 and DP_1 receptors can be envisaged. A polyvalent strategy is complex for treprostinil **4** because (i) of the injection site toxicity displayed by treprostinil **4** and (ii) the need for the carboxylic acid and two hydroxyl groups on treprostinil **4** for activity (**Figure 8-2**). If the treprostinil acid and hydroxyls cannot be used to make a polyvalent treprostinil construct, then it would be necessary to conjugate treprostinil **4** at one of its aliphatic or aromatic carbons (**Figure 8-2**). Nonetheless it is possible to imagine a polyvalent treprostinil conjugate using a prodrug variant of the conjugated treprostinil (**Figure 8-3**). For example, a polyvalent treprostinil construct could contain multiple copies of treprostinil 4 bound to a polymer where either the carboxylic acid or hydroxyls on treprostinil **4** are derivatised with a labile moiety to mask the conjugated treprostinil 4 during injection.

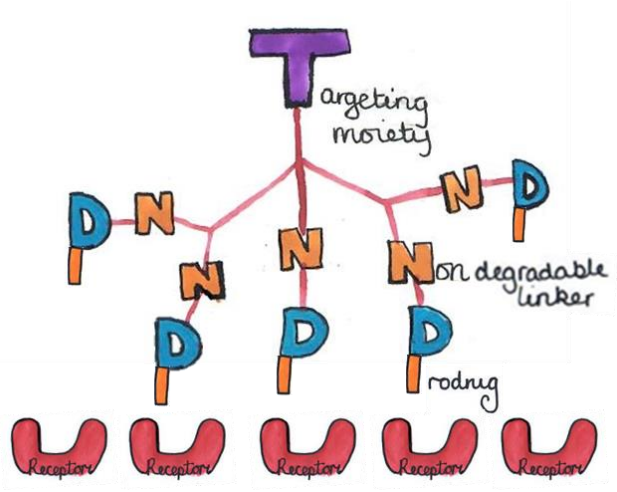

Figure 8-3. Depiction of a polyvalent approach which requires prodrug moieties to prevent receptor activity in other organs. The prodrug would require deprotection in the disease tissue to localise the receptor activity. A targeting moiety could be utilised to enhance localisation in the pulmonary vessels.

There are many limitations of a polyvalent strategy using treprostinil which include, multi-step synthesis, the need for prodrug activation, the risk that a polyvalent treprostinil 4 would not

display higher potency or enhanced PK properties. Conjugating a drug to a polymer via a covalent bond to an aromatic or aliphatic carbon on the drug is not a conventional strategy and could pose challenges for scaling the synthesis. Nonetheless, preliminary experiments were conducted with treprostinil 4 to determine if a polyvalent strategy might be possible.

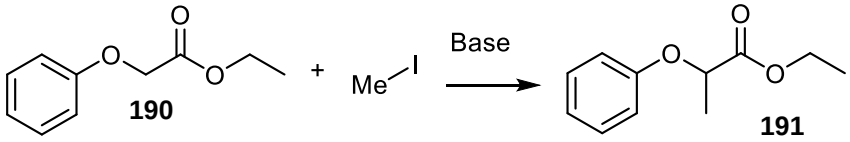

Scheme 8-72. Proposed methylation of the methylene carbon of ethyl-2-phenoxyacetate **191** in the presence of base to afford methylated ether **192**.

Initial reactions focused on the derivatisation of phenoxy model *via* the methylene carbon (**Scheme 8-72**). The pKa of the methylene protons is lower than other carbon-protons which may facilitate a route to derivatise using alkyl halide and strong base. To prevent alkylation of the acid group, the first attempts were to methylate the methylene proton of ethyl-2-phenoxyacetate **191** (50 mg) with methyl iodide in the presence of lithium diisopropylamide (1 equivalent) which has a pKa of 36. The reactions were conducted in THF at -78 °C using a dry ice/acetone bath. TLC monitoring did not show change over time. The reactions were repeated several times unsuccessfully before attempting with milder potassium tertiary butoxide (pKa ~17). After 24 hours, a slight shift in the TLC spot from starting material was observed so the reaction was worked up and the residue analysed by ^{1}H NMR. The spectra showed starting material and no methylation of the methylene carbon, as shown in **Figure 8-4**.

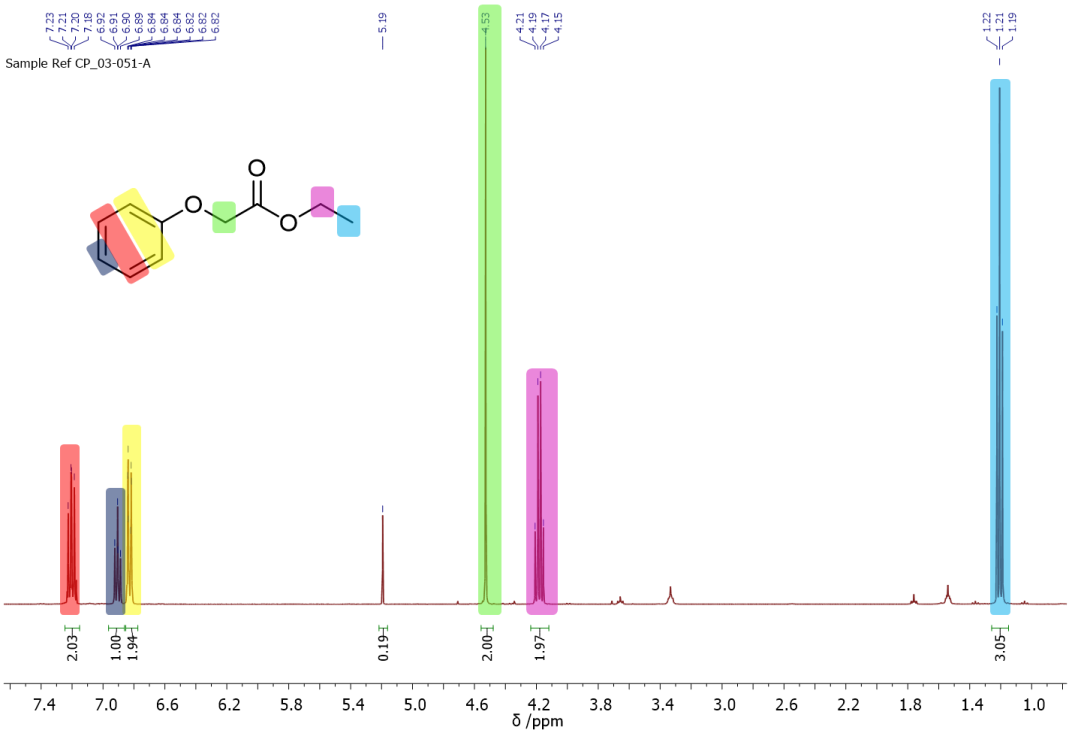

Figure 8-4. The ^{1}H NMR spectrum obtained following attempts to methylate at the methylene carbon using methyl iodide. Only the presence of starting ester was indicated.

The more robust ester group, tertiary butoxide was employed by reaction of phenoxyacetic acid with di-tert-butylcarbonate in tert-butyl alcohol as solvent. The tert-butyl ester product was treated with methyl iodide and lithium diisopropylamide as before but following work up in ethyl acetate, only starting ester was isolated as determined by ^{1}H NMR. The added bulky groups may have prevented the alkylation of the methylene however, a similar result was found with the ethyl ester, suggesting that the methylene possess poor reactivity. The alkylated product did not seem to be as accessible as possible and the derivatisation of the phenol to achieve the alkylated product would be a better route (**Scheme 8-73**). Phenol could be employed for the model reaction but treprostinil triol had not yet been donated. Therefore, efforts to achieve the alkylation methylene derivative were terminated.

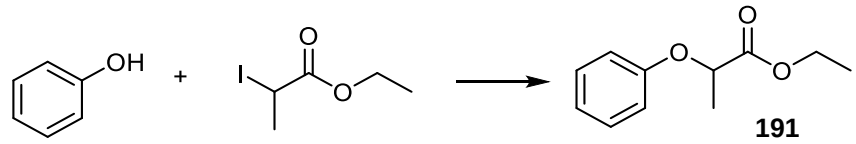

Scheme 8-73. Suggested method to alkylate the methylene by reaction of phenol derivative. Displacement of the iodine would result in the same desired product **192** but starting with a phenol derivative instead of the acid.

Alternative to the methylene derivatisation, the aromatic protons can also in principle be derivatised. A Friedel Crafts acylation of the benzene ring was considered. The oxygen of the phenoxy group has an electron donating effect on the aromatic ring which facilitates derivatisation at the ortho and para positions. Only one ortho position is available and is likely hindered by the acid moiety. Therefore, it was expected that derivatisation would occur at the para position **193** (**Scheme 8-74**). Formation of a carbon-carbon bond by a Friedel Crafts type reaction can be modified to form the acylated or alkylated product. Alkylation would form a simple carbon-carbon bond to the benzindene ring, which is an electron donating group. The electron donation further activates the ring which results in additional alkylation at the ortho positions. To avoid unwanted activity, a Friedel Crafts reaction can form an acylated product which results in the addition of an electron withdrawing group which de-activates the ring and prevents further acylation. Subsequent reduction of the carbonyl results in the alkyl derivative (**Scheme 8-74**).

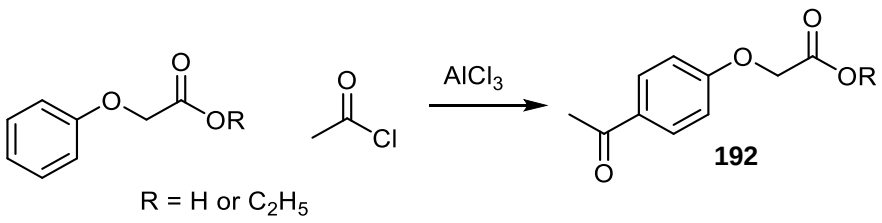

Scheme 8-74. Proposed Friedel Crafts acylation of phenoxy acid derivatives at the para position. Nucleophilic substitution of the aromatic electrons into the acid chloride carbonyl displaces the chloride with the assistance of the aluminium chloride.

Ethyl-2-phenoxyacetate **191** was used as a model in a preliminary attempt to acylate the aromatic ring. It was assumed that the treatment with one equivalent of acetal chloride would

preferentially form the para-derivatised product **193** over the ortho products owing to the steric hindrance provided by the acid group. Ethyl-2-phenylacetate (100 mg) was treated to crushed aluminium chloride (2 equivalents) in dichloromethane and acetyl chloride (1.5 equivalents) was slowly added. Monitoring by TLC in 40% ethyl acetate/hexane showed no presence of ester starting material but upon work-up no product was observed. Several repeats were conducted, increasing the amount of aluminium chloride and using carbon disulfide as solvent. Reaction of the acid **22** and the addition of a refluxing step (70 °C) for 5 hours produced the expected product 193 (**Figure 8-5**).

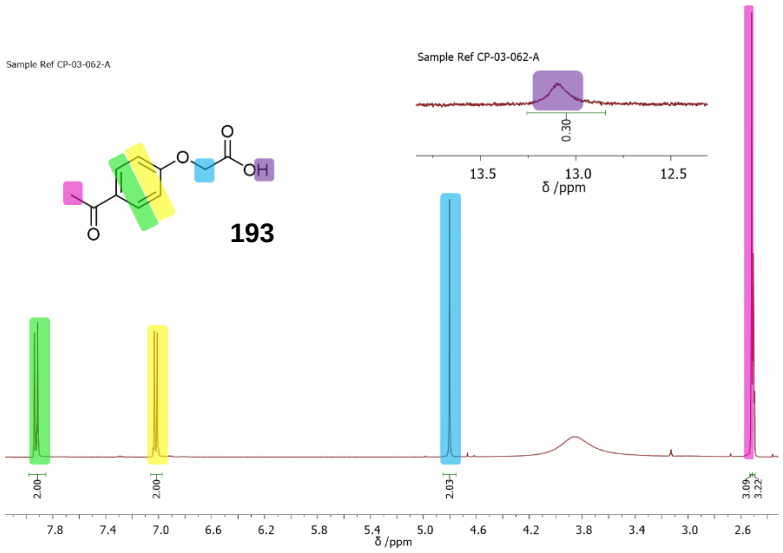

Figure 8-5. ^{1}H NMR spectra of the acylated phenoxyacetic acid 193 by Friedel Crafts acylation. Phenoxyacetic acid 22 (100 mg) was left to react with aluminium chloride (3 equivalents) in carbon disulfide before the addition of acetyl chloride (1.2 equivalents). The reaction solution was refluxed for 5 hours. A change in the aromatic protons indicated substitution of the para position and the singlet of the acetyl group was present with integral 3.

Following a successful acylation of the model compound, the reaction was repeated using a halide acid with a reactive handle suitable for further conjugation. Ethyl-2-phenoxyacetate **191** was treated with bromoacetyl bromide **53** in the presence of aluminium chloride. Addition of reagents with cooling was conducted as before which was followed by 5 hours of heating to 70 °C. TLC monitoring indicated the absence of ester starting material **191** and subsequent work up gave the desired product **195** (**Figure 8-6**).

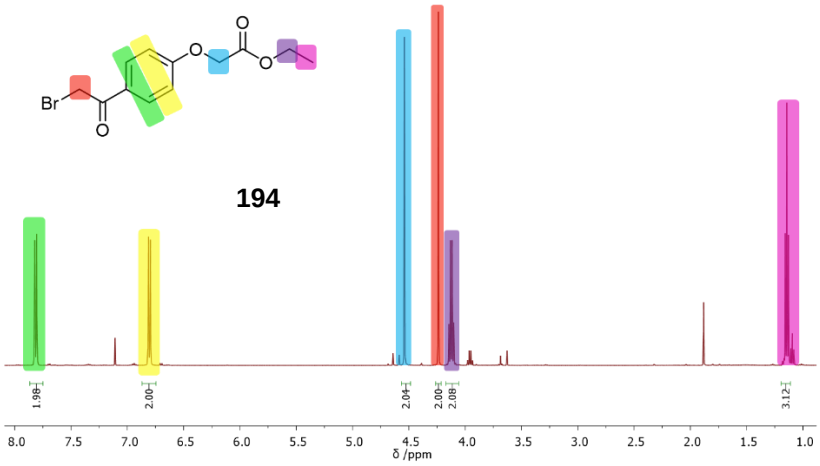

Figure 8-6. ^{1}H NMR of the bromoacetylated phenoxyacetate derivative **195** following Freidel Crafts acylation. A reaction at the para position of the aromatic ring was indicated by the symmetrical remaining aromatic resonances (green and yellow). The presence of the bromo methylene peak (red) integrates exactly with the other peaks suggesting the reaction occurred as desired.

The reduction of the acyl group of bromo product **195** was successfully attempted on a 50 mg scale using triethyl silane (3 equivalents) and a catalytic amount of trifluoroacetic acid. The reaction was heated to 70 °C in ethyl acetate for 4 hours which afforded the desired alkylated product **196** (**Figure 8-7**).

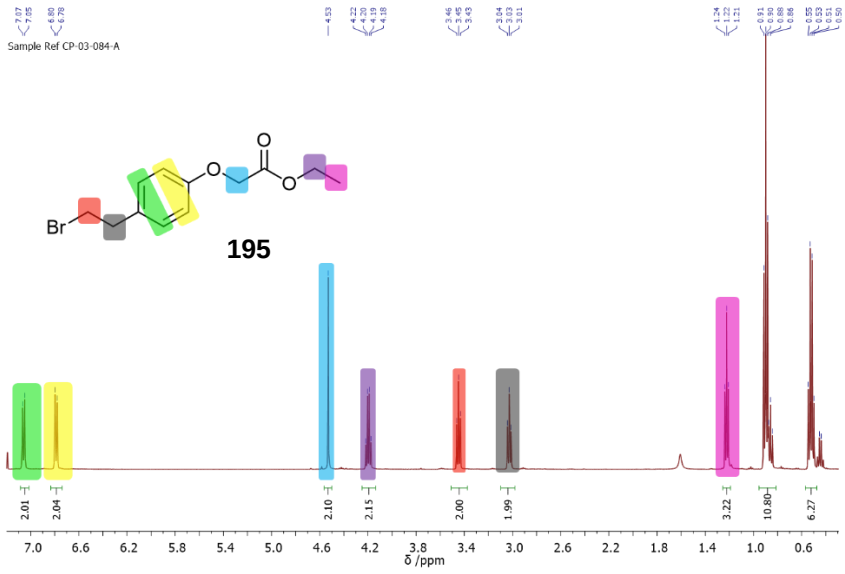

Figure 8-7. ^{1}H NMR spectra of the acyl reduction product 196. Reaction was deemed successful by the upfield shift and splitting of the protons neighbouring the bromide (red) and the presence of two additional resonances where the acyl group once was (grey).

Following success with ethyl-2-phenoxyacetate, the reaction was attempted using treprostinil. Experience gained from the work described Chapter 3 on the interference of the alcohol and

acid groups led the decision to test the acylation reaction on the protected bis-benzyl ester treprostinil (**Scheme 8-75**).

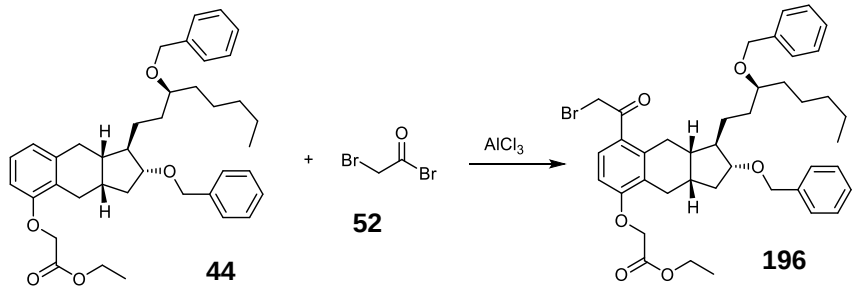

Scheme 8-75. Expected acylation of bis-benzyl treprostinil ethyl ester **45** in the presence of bromoacetyl bromide **53** and aluminium chloride.

The acylation reaction was conducted on a 15 mg scale of treprostinil derivative in DCM. Reagents were added whilst cooling to -78 °C and reaction solution was heated to 70 °C. After 16 hours, TLC showed multiple products, including starting treprostinil derivative **45**. The reaction was worked up by ethyl acetate/aqueous separation and the crude product was analysed by ^{1}H NMR. The resulting NMR spectrum showed no difference in the treprostinil benzindene aromatic resonances. Unfortunately the benzyl aromatics that were part of the hydroxyl protection groups were not observed, indicating that the reaction conditions had cleaved the protecting group benzyl ethers. Additional aromatic resonances were seen downfield in a small proportion as a pair of doublets which suggested that acylation had occurred on the benzyl groups. For future investigations, a more robust hydroxyl protecting group will require employment.

Ultimately the polyvalent approach will result in treprostinil **4** as the active ingredient being required to have a modified structure. Whilst forming a carbon-carbon bond to link treprostinil on a macromolecule remains challenging, the activity of treprostinil when conjugated at the chosen points also remains unknown. Initial efforts were undertaken to understand the structure activity relationship (SAR) of treprostinil further were considered. An *in-silico* approach was investigated using previous literature on the IP receptor SAR which described the following points as significant for IP receptor binding; carboxylic acid charge pairing to an arginine side chain; hydrogen bonding of the hydroxyls to serine and threonine derivatives; and a hydrophobic interaction between the alkyl chain and a hydrophobic pocket.

A model of the IP receptor has been investigated before, but to replicate the binding pocket, the homology model using a rhodopsin receptor required reconstructing. In addition, the activity of treprostinil at the EP_2 receptor is established as therapeutically beneficial so replicating the IP receptor binding may not be entirely relevant given the wider context of treprostinil binding.

Although work on the treprostinil derivatisation and *in silico* binding was initiated, the work was not continued owing to the complexity of the polyvalent approach and the lack of accessible information including to act as a base from which a structure can be designed. Beyond the

challenges in synthesising a prodrug polyvalent molecule that could become active, testing the sustained activity of the molecule was also considered to be challenging. The extent of the challenges paired with the minimal information suggesting a polyvalent approach might be promising, efforts were terminated and were focussed on the pro-drug approaches described in **Chapters 3-5**.